A Study of T Cell Receptor Usage in Allergic Asthma and Analysis of a Humanised T Cell Receptor Transgenic Model of Immunity to Allergen

A thesis submitted for the degree of Doctor of Philosophy by

Tracey Elizabeth Pollard

at Imperial College, London

Lung Immunology Group,
National Heart and Lung Institute,
Faculty of Medicine,
Sir Alexander Fleming Building,
South Kensington campus,
Imperial College,
London
SW7 2AZ

Supervisors:

Dr Rosemary J. Boyton
Prof. Daniel M. Altmann

June 2009

Abstract

It has been previously shown that the length of complementarity-determining region 3 (CDR3) loops of a T-cell receptor (TCR) may determine T-cell phenotype, with elongated CDR3s being favoured in T helper-type 2 (Th2) cells. Here, in a human system of Th2-mediated allergic asthma, TCR CDR3 usage has been studied in T-cell lines derived from Human Leukocyte Antigen (HLA)-DR1-positive, cat-allergic asthmatic subjects, and generated against peptide 4, a T-cell epitope of the major cat allergen Fel d 1. Populations of T-cells expanded that expressed particular TCRs carrying elongated CDR3α or β loops. A system was developed to transduce the immortalised TCR-negative murine thymoma line BW7 with the human TCR genes identified here and also murine Th1 and Th2 associated TCR genes identified from previous work in our laboratory to allow further study of the influence of TCR structure on T-cell phenotype. A TCR/MHC class II transgenic model of allergic asthma has been developed by others in our laboratory. As part of the initial characterisation of this model, to establish if the TCR was expressed, the impact of the presence of the TCR transgenes on thymic selection and the expression of costimulatory molecules was studied. A block at the double negative stage in thymocyte development is seen as well as differences in expression of the costimulatory molecules CD44, CD62L, ICOS and OX40. Allergic inflammatory lung disease was induced in this model using a sensitisation and challenge protocol with Fel d 1 and cat dander, and changes usually associated with an asthma phenotype studied. Increased airway hyperreactivity, eosinophilic lung influx, raised serum IgE, Th2-associated cytokines in BAL and lung, mild lung inflammation and increased mucus secretion in the airways were observed, all changes that would be expected in a good model of allergic asthma.

Statement of declaration

I performed all of the experiments and data analysis contained in this thesis except where otherwise stated in the text.

Tracey Pollard
2009

Acknowledgments

I would like to thank my supervisor Rosemary Boyton for all her help and support, for her guidance and ideas throughout the course of my project, for her help and suggestions when I was having difficulties, and for her encouragement and advice throughout my time working in her lab. I am very grateful to her for providing me with this project as well as such a friendly and welcoming environment in which to work. I would also like to thank my co-supervisor Danny Altmann for his guidance throughout my PhD, particularly for all his help and suggestions when I encountered difficulties in my work, and for giving up his time to help me, particularly during my writing up.

I would like to thank Catherine Reynolds for her help and advice throughout my time in the lab. In particular, I thank her for her advice in designing the Southern strategy for the P4TCRTg mice and her help with the allergic disease induction experiments - doing lung inflations, sectioning frozen lung, differential cell counting, inflammation and mucus scoring, and helping me with measuring Penh. Thank you to Kate Choy for doing resistance/compliance measurements and Eleanor Raynsford for doing differential cell counts and for her help with the disease induction experiments. Thanks to Xiaoming Cheng for devising the PCR strategy to determine correct splicing of TCR genes in the P4TCRTg mice, and for all her help in setting up the disease induction experimental model used here. Thanks to Rebecca Beavil for supplying our lab with recombinant Fel d 1, and Laboratorios Leti for supplying us with cat dander extract for use in these experiments. Last but not least, I am extremely grateful to the CBS staff for their care of the animals used in these experiments.

Thank you to Alexander Annenkov for help setting up the retroviral transduction system used here, Diane Mathis and Christophe Benoist for supplying the pTcass TCR expression vectors and Hongyan Wang for her much-appreciated advice and help with this system. Thanks also to Julian Dyson for supplying me with EcoPhoenix cells.

Many thanks to Mark Larché for supplying human HLA-DR1-restricted peptide 4-specific T-cell lines for the TCR CDR3 analysis, and to Adrienne Verhoef and Betty Lo for their help growing the lines. Thank you also to Julia Llewellyn-Hughes and her colleagues at the Natural History Museum sequencing facility for carrying out DNA sequencing.

Finally, I would like to thank Catherine, Eleanor and Xiaoming for being good friends and colleagues to me, and making the experience a really enjoyable one. Also, thank you to Charis for her support and for not minding when my thesis seemingly took over the flat whilst I was writing up! Thanks also to my parents for worrying about me! Without the support of these people I don't think I'd have made it this far...

Table of contents

		Page number
	Title page	1
	Abstract	2
	Statement of declaration	3
	Acknowledgments	4
	Table of contents	5
	List of figures	16
	List of tables	25
	List of abbreviations	27
	List of appendices	37
Chapter 1	Introduction	40
1.1	Clinical and epidemiological aspects of allergic asthma	40
1.1.1	Prevalence of allergic asthma	40
1.1.2	The 'hygiene hypothesis'	40
1.1.3	The clinical manifestations of asthma	42
1.2	Immune mechanisms of allergic asthma	43
1.2.1	Antigen-presenting cells (dendritic cells) in allergic asthma	43
1.2.2	Immunoglobulin E in allergic asthma	45
1.2.3	Mast cells in allergic asthma	46
1.2.4	Eosinophils in allergic asthma	47
1.2.5	Basophils in allergic asthma	48
1.2.6	Neutrophils in allergic asthma	49
1.2.7	Invariant natural killer T (iNKT) cells in allergic asthma	50
1.2.8	$CD8^+$ T-cells (cytotoxic T-cells) in allergic asthma	52
1.2.9	The role of T helper type 17 (Th17) cells in allergic asthma	55
1.2.10	The role of Th1 cells in allergic asthma	56

1.2.11	The role of regulatory T-cells (Tregs) in allergic asthma	59
1.2.12	The role of Th2 cells in allergic asthma	61
1.3	Mouse models of allergic asthma	64
1.3.1	The principles of molecular cloning and their use in animal models of disease	64
1.3.2	The use of animals in human disease modelling	66
1.3.3	The use of ovalbumin (OVA) as an allergen in mouse models of allergic asthma	69
1.3.4	Adoptive transfer of OVA-pulsed APCs or OVA-specific T-cells as a means of inducing allergic airway disease in mice	72
1.3.5	Use of the OVA model in investigating disease pathogenesis in allergic asthma	73
1.3.6	The use of house dust mite allergens in a mouse model of allergic asthma	76
1.3.7	Uses of the HDM mouse model of allergic asthma to investigate lung remodelling processes	79
1.3.8	Other uses of the HDM mouse model of allergic asthma	81
1.3.9	Other mouse models of allergic asthma	81
1.3.10	TCR transgenic models of allergic asthma	82
1.3.11	Human T-cell responses in allergic asthma caused by the major allergen in cat dander, Fel d 1	87
1.4	T-cell receptor structure	90
1.4.1	Identification of the T-cell antigen receptor (TCR)	90
1.4.2	The interaction between TCR, peptide and MHC molecule	91
1.4.3	T-cell receptor structure	92
1.4.4	V(D)J recombination and T-cell receptor diversity	92
1.5	T-cell development in the thymus	95
1.5.1	Precursor entry into the thymus and the earliest stages of T-cell development	95
1.5.2	TCRα gene rearrangement	97

1.5.3	Positive and negative selection	97
1.5.4	The CD4 vs. CD8 lineage decision	99
1.6	T-cell signalling, activation and differentiation	99
1.6.1	Proposed mechanisms of TCR triggering	99
1.6.2	T-cell signalling through the TCR	101
1.6.3	The immunological synapse	104
1.6.4	The signalling pathways involved in differentiation of naive T helper cells into effector T helper lineages	106
1.6.5	Factors affecting the differentiation of naive T-cells into effector phenotypes upon antigen stimulation	108
1.6.6	The serial triggering model	112
1.6.7	The role of TCR structure in determining the affinity of the interaction with peptide-MHC	113
1.6.8	Clonotypic expansion of T-cells in response to antigen stimulation and functional maturation of the T-cell response	115
1.6.9	Can TCR structure influence the fate of a naive T helper cell upon stimulation with antigen?	117
1.7	Aims of this thesis	121
Chapter 2	Materials and Methods	122
2.1	Molecular biology techniques	122
2.1.1	Human TCR CDR3 analysis	122
2.1.1.1	RNA isolation from human T-cell lines	122
2.1.1.2	cDNA preparation from human T-cell RNA	122
2.1.1.3	Polymerase chain reaction (PCR)	123
2.1.2	Cloning of TCRα and β chains into MFG and pTcass expression vectors	123
2.1.2.1	RNA isolation from murine T-cells	126
2.1.2.2	cDNA preparation from murine T-cell RNA	126
2.1.2.3	PCR using high-fidelity DNA polymerase	127
2.1.3	General DNA cloning techniques	127
2.1.3.1	Preparation of competent cells	127

2.1.3.2	Restriction digests	128
2.1.3.3	Oligonucleotide preparation	129
2.1.3.4	Nuclease treatment	129
2.1.3.5	Cloning ligations	129
2.1.3.6	TA cloning ligations	130
2.1.3.7	*E.coli* transformation	130
2.1.3.8	Plasmid DNA preparation	131
2.1.3.9	Sequence analysis	131
2.2	Genotyping of P4 TCR/DR1/ABO transgenic mice	132
2.2.1	Genomic DNA extraction from tail tips	132
2.2.2	Genotyping by PCR	132
2.2.3	Collection, preparation and staining of tailbleed samples for phenotyping by flow cytometry	132
2.2.4	Genotyping by Southern analysis	133
2.2.4.1	Southern (DNA) blotting	133
2.2.4.2	Probe production	134
2.2.4.3	Hybridisation of DIG-labelled probe to the DNA blot	134
2.2.4.4	Detection of probe binding to membrane	135
2.3	Tissue culture and transduction techniques	135
2.3.1	Culture of adherent cell lines EcoPhoenix, PT67 and NIH3T3	135
2.3.2	Reselection of PT67 cells	136
2.3.3	Culture of non-adherent cell lines BW7 and CTLL-2	136
2.3.4	Retroviral transduction	137
2.3.4.1	Retroviral transfection of packaging cell line EcoPhoenix	137
2.3.4.2	Infection of secondary packaging line PT67 with retroviral supernatant	137
2.3.4.3	Infection of adherent target cell line NIH3T3 with retroviral supernatant	138
2.3.4.4.	Infection of non-adherent target cell line BW7 with retroviral supernatant	138
2.3.4.5	Principles of flow cytometry	139

2.3.5	Transfection of non-adherent target cell line BW7 with TCR expression vectors using the Amaxa Nucleofector™ electroporation system	140
2.3.6	Analysis of cell death by flow cytometry using propidium iodide	140
2.3.7	Measurement of IL-2 production in transduced BW7 cells using the CTLL-2 assay	141
2.4	Induction of allergic asthma in a murine model using Fel d 1	141
2.4.1	Sensitisation with Fel d 1	141
2.4.2	Challenge with cat dander extract	142
2.4.3	Measurement of lung function – Penh	142
2.4.4	Measurement of lung function – resistance and compliance	143
2.4.5	Collection of BAL fluid and cytospin preparation	143
2.4.6	Collection of serum for measurement of total serum [IgE]	143
2.4.7	Lung inflation for histological analysis	144
2.4.8	Disaggregation of cells from lung tissue and cytospin preparation	144
2.4.9	Staining of cytospins for differential cell count analysis	144
2.4.10	Differential cell counting	145
2.4.11	Lung tissue homogenisation	145
2.4.12	Measurement of total [IgE] in serum by ELISA	145
2.4.13	Measurement of cytokine concentrations in BAL fluid and lung homogenate by ELISA	146
2.4.14	Preparation of lung sections and staining with haematoxylin and eosin for histological analysis	147
2.4.15	Inflammation scoring system (for haematoxylin and eosin stained slides)	148
2.4.16	Preparation of lung sections and staining with periodic acid-Schiff's reagent (PAS reagent) for histological analysis	148

2.4.17	Scoring of mucus-producing cells (for PAS reagent stained slides)	149
2.5	Analysis of costimulatory molecule expression in P4/DR1/ABO TCR transgenic mice	149
2.5.1	Isolation of splenocytes for flow cytometric analysis and RNA isolation	149
2.5.2	Isolation of thymocytes for flow cytometric analysis	149
2.5.3	Staining of cells with fluorescently-conjugated antibodies for flow cytometric analysis	150
2.6	Statistical analysis	150
Chapter 3	TCR CDR3 analysis of cat allergic asthmatic patients and a transduction system to express TCRs of interest in the TCR-negative murine thymoma line BW7	152
3.1	TCR CDR3 analysis in a cat allergic asthmatic individuals	152
3.1.1	Overview	152
3.1.2	TCRα chain and CDR3 usage in human peptide 4 specific, DR1-restricted T-cell lines	155
3.1.3	TCRβ chain and CDR3 usage in human peptide 4-specific, DR1-restricted T-cell lines	160
3.1.4	Summary	166
3.2	Preparation of TCR expression constructs for the transduction of the cell line BW7	171
3.2.1	Preparation of TCR expression constructs for use in a retroviral transduction system	173
3.2.1.1	Transfer of genes encoding TCR α and β chains from the PLP_{56-70}-specific murine T-cell clones A10(2) and D3(3) into the retroviral expression vector MFG	175
3.2.1.1.1	Vector modifications	175
3.2.1.1.2	Transfer of TCRα chains from T-cell clones A10(2) and D3(3) into the vector MFG	178

3.2.1.1.3	Transfer of TCRβ chains from T-cell clones A10(2) and D3(3) into the vector MFG	186
3.2.1.2	Transfer of genes encoding dominant TCR α and β chains from the peptide 4-specific human T-cell line CIR010 into the retroviral expression vector MFG	196
3.2.1.2.1	Transfer of the dominant TCRα chain from human T-cell line CIR010 into MFG	196
3.2.1.2.2	Combination of the dominant recombined TCRα V-J segment from the human T-cell line CIR010 with a murine TCRα C region and transfer into MFG	196
3.2.1.2.3	Combination of the dominant recombined TCRβ V-J segment from the human T-cell line CIR010 with a murine TCRβ C region and transfer into MFG	205
3.2.2	Preparation of TCR expression constructs for use in the Amaxa transduction system	210
3.2.2.1	Overview of the Amaxa Nucleofector system and TCR expression vectors	210
3.2.2.2	Transfer of genes encoding TCR α and β chains from the PLP_{56-70}-specific murine T-cell clone A10(2) into the pTcass TCR expression vectors	211
3.2.2.2.1	Transfer of TCRα chain 5-D4 from the T-cell clone A10(2) into the vector pTαcass	211
3.2.2.2.2	Transfer of TCRα chain 7-D3 from the T-cell clone A10(2) into the vector pTαcass	216
3.2.2.2.3	Transfer of the TCRβ chain from the T-cell clone A10(2) into the vector pTβcass	216
3.2.2.3	Transfer of genes encoding TCR α and β chains from the PLP_{56-70}-specific murine T-cell clone D3(3) into the pTcass TCR expression vectors	225
3.2.2.3.1	Transfer of the TCRα chain from T-cell clone D3(3) into vector pTαcass	225
3.2.2.3.2	Transfer of the TCRβ chain from T-cell clone D3(3) into vector pTβcass	225

3.2.2.4	Transfer of genes encoding the dominant TCR α and β chains from the human peptide 4-specific T-cell line CIR010 into the pTcass TCR expression vectors	234
3.2.2.4.1	Transfer of the TCRα chain from T-cell line CIR010 into vector pTαcass	234
3.2.2.4.2	Transfer of the TCRβ chain from T-cell line CIR010 into vector pTβcass	234
3.2.3	Summary	243
3.3	Transduction of the TCR-negative murine thymoma line BW7 with TCR	244
3.3.1	Retroviral transduction of BW7 with TCR	244
3.3.1.1	Overview of the retroviral transduction system	244
3.3.1.2	Retroviral vectors	247
3.3.1.3	Optimisation of the system using eGFP	247
3.3.1.4	Retroviral transduction of line BW7 with genes encoding the TCR from the PLP_{56-70}-specific murine T-cell clone D3(3)	255
3.3.1.5	Use of a modified retroviral transduction protocol to transducer the line BW7 with genes encoding the TCRs from the PLP_{56-70}-specific murine T-cell clones A10(2) and D3(3)	262
3.3.1.6	Measurement of TCR expression using the IL-2-dependent cell line CTLL-2	271
3.3.2	Transduction of BW7 with TCR genes using the Amaxa Nucleofector system	273
3.3.2.1	Principles of the Amaxa Nucleofector system	273
3.3.2.2	Use of the Amaxa system to transfect BW7 with GFP	274
3.3.2.3	Use of the Amaxa system to transfect BW7 with the TCR from PLP_{56-70}-specific murine T-cell clone D3(3)	276
3.3.3	Summary	278
3.4	**Discussion**	279

Chapter 4	Induction of allergic inflammation in the lung and analysis of T-cell costimulatory molecule expression in P4 TCR/DR1/ABO transgenic mouse lines 4 and 16	289
4.1	Characterisation of P4 TCR/DR1/ABO transgenic mice	289
4.1.1	Overview	289
4.1.2	PCR genotyping identifies P4 TCR/DR1/ABO transgenic mice	289
4.1.3	FACS phenotyping of P4 TCR/DR1/ABO transgenic mouse lines confirms murine MHC class II knockout status	292
4.1.4	Southern analysis confirms the presence of TCR transgenes in the genomic DNA of P4 TCR/DR1/ABO transgenic mice	294
4.1.5	mRNA products of the TCR transgenes in P4 TCR/DR1/ABO transgenic mice are correctly spliced	296
4.2	Induction of allergic inflammation in the lung of P4 TCR/DR1/ABO transgenic mice using Fel d 1	299
4.2.1	Overview	299
4.2.2	Disease induction with Fel d 1 induces increased airway hyperreactivity and bronchoconstriction in response to methacholine challenge	301
4.2.2.1	Lung function data from the line 4 experiment	301
4.2.2.2	Lung function data from the line 16 experiment	304
4.2.3	Differential cell counts in BAL fluid and disaggregated lung tissue of Fel d 1-treated mice showed a substantial eosinophilic influx into the lungs	306
4.2.3.1	Differential cell counts in BAL fluid from line 4 and line 16 experiments	306
4.2.3.2	Differential cell counts in disaggregated lung tissue from line 4 and line 16 experiments	308

4.2.4	Fel d 1 treatment induced a significant increase in serum total IgE	308
4.2.5	Levels of the Th2-type cytokines IL-4, IL-5 and IL-13 were increased in BAL fluid in response to treatment with Fel d 1 when using the lower dose challenge protocol	310
4.2.6	The amount of IL-4, IL-5 and IL-13 in lung tissue homogenate supernatant following disease induction	310
4.2.7	Histological analysis of frozen lung sections shows inflammation in the lungs of Fel d 1-treated mice	314
4.2.8	Histological analysis of frozen lung sections shows goblet cell hyperplasia and mucus production in the lungs of Fel d 1-treated mice	317
4.2.9	Summary of findings	319
4.3	Analysis of T-cell costimulatory molecule expression in P4 TCR/DR1/ABO transgenic mice	320
4.3.1	Overview	320
4.3.2	A block in thymocyte development is seen at the double negative (DN) stage in P4 TCR/DR1/ABO transgenic mice	322
4.3.3	Expression of CD44 on DN thymocytes is decreased in P4 TCR/DR1/ABO transgenic mice	324
4.3.4	Expression of CD62L on thymocyte subsets is generally increased in P4 TCR/DR1/ABO transgenic mice from line 16	327
4.3.5	There is a small increase in expression of OX40 on cells of the DN thymocyte subset in line 4 and line 16 TCR/DR1/ABO transgenic mice	329
4.3.6	Expression of ICOS in P4 TCR/DR1/ABO transgenic mice is significantly decreased on the DN, CD4 SP and CD8 SP thymocyte subsets in comparison to DR1/ABO transgenic control mice	331

4.3.7	Expression of T-cell costimulatory molecules CD69, CD3, CD54 and CD25 on thymocytes in P4 TCR/DR1/ABO transgenic mice is similar to the expression seen in DR1/ABO transgenic controls	334
4.3.8	Expression of the T-cell costimulatory molecules CD69, CD3, CD54, CD25, CD44 and CD62L on freshly-isolated splenocytes in P4 TCR/DR1/ABO transgenic mice is similar to the expression seen in DR1/ABO transgenic control mice	340
4.3.9	Expression of the T-cell costimulatory molecules OX40 and its ligand OX40L and ICOS on freshly-isolated splenocytes in P4 TCR/DR1/ABO transgenic mice is similar to the expression seen in DR1/ABO transgenic control mice	345
4.3.10	Summary of findings	348
4.4	**Discussion**	351
Chapter 5	**Summary**	359
	Bibliography	369
	Appendices	428

List of figures

		Page number
Figure 1.1	Downstream T-cell signalling pathways that are activated upon TCR binding to peptide-MHC	103
Figure 1.2	Characterisation of the TCRs expressed by PLP 56-70-specific T-cell clones A10(2) and D3(3) (see reference 622)	120
Figure 2.1	MFG(eGFP)	125
Figure 3.1	Outline of the strategy used to investigate TCR usage in HLA-DR-1 restricted T-cell lines against peptide 4	153
Figure 3.2	Agarose gel pictures at different stages of the human TCR analysis	154
Figure 3.3	Expansion of T-cells with specific TCRα (A) and TCRβ (B) CDR3 regions in an HLA-DR1-restricted T-cell line, CIR014, after one restimulation with peptide 4	167
Figure 3.4	Expansion of T-cells with specific TCRα (A) and TCRβ CDR3 (B) regions in an HLA-DR1-restricted T-cell line, B1, at its 3rd restimulation with peptide 4	168
Figure 3.5	Expansion of TCRα (A) and TCRβ (B) chains expressed in the HLA-DR1-restricted T-cell line CIR010 at its fourth restimulation with peptide 4	169
Figure 3.6	pQCXIP(eGFP)	174
Figure 3.7	The cloning strategy designed to move TCRα chains for clones A10(2) (chains 5-D4 and 7-D3) and D3(3) from the vector pQC into MFG.	176
Figure 3.8	Gel images showing stages of the cloning strategy followed to modify the vectors MFG and pBluescriptII to allow cloning of the TCR chains from murine T cell clones A10(2) and D3(3) and the dominant TCR from the human T cell line CIR010 into MFG from pQC	177
Figure 3.9	Orientation of TCR chains in MFG using PCR	179

Figure 3.10	Gel images of the stages involved in moving the TCRα chain 5-D4 of murine clone A10(2) into MFG	180
Figure 3.11	Final construct map of TCR α chain 5-D4 from the murine Th1-type T cell clone A10(2) in the retroviral vector MFG	181
Figure 3.12	Gel images of the stages involved in moving the TCR α chain 7-D3 of murine clone A10(2) into MFG	182
Figure 3.13	Final construct map of TCR α chain 7-D3 from the murine Th1-type T cell clone A10(2) in the retroviral vector MFG	183
Figure 3.14	Gel images of the stages involved in moving the TCR α chain of murine clone D3(3) into MFG	184
Figure 3.15	Final construct map of the TCR α chain from the murine Th2-type T cell clone D3(3) in the retroviral vector MFG	185
Figure 3.16	A schematic diagram showing the cloning strategy designed to move TCR β chains for clones A10(2) and D3(3) from the vector pQC into MFG.	187
Figure 3.17	Cloning strategy designed to mutate the Cβ region of TCR chain βA10(2)	188
Figure 3.18	Gel images of the stages involved in moving the TCR β chain from the murine T cell clone A10(2) into MFG including correcting a mutation in the Cβ region	189
Figure 3.19	Amino acid sequence of the TCR β chain (TRBV 14 TRBJ 2-7 TRBC 1) from the murine T cell clone A10(2) cloned into retroviral vector MFG	190
Figure 3.20	Final construct map of the TCR β chain from the murine Th1-type T cell clone A10(2) in the retroviral vector MFG	191
Figure 3.21	Cloning strategy designed to mutate the Cβ region of TCR chain βD3(3)	192
Figure 3.22	Gel images of the stages involved in moving the TCR β chain from the murine T cell clone D3(3) into MFG including correcting a mutation in the Cβ region	193
Figure 3.23	Amino acid sequence of the TCR β chain (TRBV 2 TRBJ 2-5 TRBC 1) from the murine T cell clone D3(3) cloned into retroviral vector MFG	194

Figure 3.24	Final construct map of the TCR β chain from the murine Th2-type T cell clone D3(3) in the retroviral vector MFG	195
Figure 3.25	Cloning strategy designed to transfer the dominant TCR α chain from the human T cell line CIR010 into the retroviral vector MFG	197
Figure 3.26	Gel images of the stages involved in moving the dominant TCR α chain of human T cell line CIR010 into the retroviral vector MFG	198
Figure 3.27	Final construct map of the dominant TCR α chain from the human T cell line CIR010 in the retroviral vector MFG	199
Figure 3.28	Cloning strategy designed to combine the VJ region from the dominant TCR α chain from the human T cell line CIR010 with a murine TCR Cα region in the retroviral vector MFG	200
Figure 3.29	Gel images of the stages involved in moving the variable region (VJ) of the dominant TCRα chain of human T cell line CIR010 combined with a murine constant region (C) into MFG	203
Figure 3.30	Final construct map of the dominant TCR α chain (combined with a murine Cα region) from the human T cell line CIR010 in the retroviral vector MFG	204
Figure 3.31	Cloning strategy designed to combine the VJ region from the dominant TCR β chain from the human T cell line CIR010 with a murine TCR Cβ region in the retroviral vector MFG	206
Figure 3.32	Gel images of the stages involved in moving the variable region (VJ) of the dominant TCR β chain of the human T cell line CIR010 combined with a murine constant region (C) into MFG	208
Figure 3.33	Final construct map of the dominant TCR β chain (combined with a murine Cβ region) from the human T cell line CIR010 in the retroviral vector MFG	209

Figure 3.34	Cloning strategy designeded to move the TCR α chain (VJ region plus intronic sequence) from the mouse Th1-type T cell clone A10(2) 5-D4 into the TCR expression vector pTαcass	212
Figure 3.35	Gel images of the stages involved in moving the rearranged VJ region from the TCR α chain from murine T cell clone A10(2) 5-D4 combined with intronic sequence immediately downstream of the J region terminus into the TCR expression vector pTαcass	214
Figure 3.36	Final construct map showing the insertion of the TCR α chain 5-D4 from the Th1-type murine T cell clone A10(2) into the TCR expression vector pTαcass	215
Figure 3.37	Cloning strategy designed to move the TCR α chain (VJ region plus intronic sequence) from the mouse Th1-type T cell clone A10(2) 7-D3 into the TCR expression vector pTαcass	217
Figure 3.38	Gel images of the stages involved in moving the rearranged VJ region from the TCR α chain of murine T cell clone A10(2) 7-D3 combined with intronic sequence immediately downstream of the J region terminus into the TCR expression vector pTαcass	219
Figure 3.39	Final construct map showing the insertion of the TCR α chain 7-D3 from the Th1-type murine T cell clone A10(2) into the TCR expression vector pTαcass	220
Figure 3.40	Cloning strategy designed to move the TCR β chain (VJ region plus intronic sequence) from the mouse Th1-type T cell clone A10(2) into the TCR expression vector pTβcass	221
Figure 3.41	Gel images of the stages involved in moving the rearranged VJ region from the TCR β chain of murine T cell clone A10(2) combined with intronic sequence immediately downstream of the J region terminus into the TCR expression vector pTβcass	223

Figure 3.42 Final construct map showing the insertion of the TCR β chain from the Th1-type murine T cell clone A10(2) into the TCR expression vector pTβcass 224

Figure 3.43 Cloning strategy designed to move the TCR α chain (VJ region plus intronic sequence) from the mouse Th2-type T cell clone D3(3) into the TCR expression vector pTαcass 226

Figure 3.44 Gel images of the stages involved in moving the rearranged VJ region from the TCR α chain from murine T cell clone D3(3) combined with intronic sequence immediately downstream of the J region terminus into the TCR expression vector pTαcass 228

Figure 3.45 Final construct map showing the insertion of the TCR α chain from the Th2-type murine T cell clone D3(3) into the TCR expression vector pTαcass 229

Figure 3.46 Cloning strategy designed to move the TCR β chain (VJ region plus intronic sequence) from the mouse Th2-type T cell clone D3(3) into the TCR expression vector pTβcass 230

Figure 3.47 Gel images of the stages involved in moving the rearranged VJ region from the TCR β chain of murine T cell clone D3(3) combined with intronic sequence immediately downstream of the J region terminus into the TCR expression vector pTβcass 232

Figure 3.48 Final construct map showing the insertion of the TCR β chain from the Th2-type murine T cell clone D3(3) into the TCR expression vector pTβcass 233

Figure 3.49 Cloning strategy designed to move the dominant TCR α chain (VJ region plus intronic sequence) from the human T cell line CIR010 into the TCR expression vector pTαcass 235

Figure 3.50 Gel images of the stages involved in moving the rearranged VJ region from the dominant TCR α chain from human T cell line CIR010 combined with intronic sequence immediately downstream of the J region terminus into the TCR expression vector pTαcass 237

Figure 3.51	Final construct map showing the insertion of the dominant TCR α chain from the human T cell line CIR010 into the TCR expression vector pTαcass	238
Figure 3.52	Cloning strategy designed to move the dominant TCR β chain (VJ region plus intronic sequence) from the human T cell line CIR010 into the TCR expression vector pTβcass	239
Figure 3.53	Gel images of the stages involved in moving the rearranged VJ region from the dominant TCRβ chain from human T cell line CIR010 combined with intronic sequence immediately downstream of the J region terminus into the TCR expression vector pTβcass	241
Figure 3.54	Final construct map showing the insertion of the dominant TCR β chain from the human T cell line CIR010 into the TCR expression vector pTβcass	242
Figure 3.55	Outline of the basis of the Phoenix retroviral transduction system	245
Figure 3.56	Transduction of the target lines BW7 and NIH3T3 with the gene for eGFP encoded in the plasmid pQC using retroviral supernatant harvested from the EcoPhoenix packaging cell line or the PT67 packaging cell line	250
Figure 3.57	Transduction of the target lines BW7 and NIH3T3 with the gene for eGFP encoded in either plasmid pQC or plasmid MFG using retroviral supernatant harvested from the EcoPhoenix packaging cell line or the PT67 packaging cell line	251
Figure 3.58	eGFP expression in NIH3T3 cells transduced according to the optimised retroviral transduction system outlined in Table 3.9	253
Figure 3.59	Expression of TCR D3(3) on transduced BW7	256
Figure 3.60	Analysis of TCR D3(3) expression in clones derived from the D3(3) transduced BW7 line	258
Figure 3.61	Characterisation of the disparate BW7 populations defined on the basis of their light scattering properties	259

Figure 3.62	eGFP expression in disparate populations of transduced BW7 cells	261
Figure 3.63	eGFP expression in NIH3T3 and BW7 cells transduced according to the modified retroviral transduction system outlined in Table 3.11	264
Figure 3.64	Expression of the TCR D3(3) in transduced BW7 cells	266
Figure 3.65	Expression of the TCRs A10(2) 5-D4 and A10(2) 7-D3 in transduced BW7 cells	267
Figure 3.66	Comparison of specific anti-Vβ antibody staining with isotype controls in TCR-transduced and untransduced BW7	269
Figure 3.67	Gel images of the PCR products obtained when analysing D3(3) and A10(2) 7-D3 TCR-transduced BW7 cells for the presence of specific TCRα chain	270
Figure 3.68	Proliferation of the IL-2 dependent CTLL-2 line in supernatant derived from retrovirally-transduced BW7 lines expressing TCRs from the PLP_{56-70}-specific murine T-cell clones A10(2) and D3(3) that had been stimulated with PLP_{56-70} peptide	272
Figure 3.69	GFP expression in BW7 cells transduced with the vector pmaxGFP using the Amaxa Nucleofector system	275
Figure 3.70	Specific anti-Vβ 4-FITC staining to assess TCR D3(3) expression in BW7 transduced using the Amaxa Nucleofector	277
Figure 4.1	Genotyping PCRs to identify P4 TCR/DR1/ABO transgenic mice in lines 4 and 16	291
Figure 4.2	Phenotyping FACS to show mouse MHC class II knockout status of P4 TCR/DR1/ABO transgenic mice in lines 4 and 16	293
Figure 4.3	Southern analysis of the P4 TCR/DR1/ABO transgenic line 4	295
Figure 4.4	PCRs to identify correct splicing of the TCR mRNA gene products to remove intronic sequence in P4 TCR/DR1/ABO transgenic mice in lines 4 and 16	297

Figure 4.5	The disease induction protocol used to induce allergic lung inflammation in the P4 TCR/DR1/ABO transgenic lines 4 and 16	300
Figure 4.6	Lung function parameter measurements in response to methacholine provocation in the line 4 Fel d 1 disease induction experiment	303
Figure 4.7	Lung function parameter measurements in response to methacholine provocation in the line 16 Fel d 1 disease induction experiment	305
Figure 4.8	Differential cell counts in BAL fluid and lung tissue in the Fel d 1 disease induction experiments in TCR P4 lines 4 and 16	307
Figure 4.9	Total serum IgE production in the Fel d 1 disease induction experiments in TCR P4/DR1/ABO lines 4 and 16	309
Figure 4.10	Th2-associated cytokines in the BAL fluid of line 4 P4 TCR/DR1/ABO transgenic mice and DR1/ABO transgenic mice after Fel d 1 sensitisation/cat dander challenge	311
Figure 4.11	Production of Th2-associated cytokines in the BAL fluid of line 16 P4 TCR/DR1/ABO transgenic mice and DR1/ABO transgenic mice after Fel d 1 sensitisation/cat dander challenge	312
Figure 4.12	Th1- and Th2-associated cytokines in the lung tissue of line 4 and line 16 P4 TCR/DR1/ABO transgenic and DR1/ABO transgenic mice after Fel d 1 sensitisation/cat dander challenge	313
Figure 4.13	Inflammation scores obtained from H&E-stained sections of inflated lung from line 4 and line 16 P4 TCR/DR1/ABO transgenic and DR1/ABO transgenic mice	315
Figure 4.14	Haematoxylin and eosin stained sections used for scoring lung inflammation in line 16 P4 TCR/DR1/ABO mice	316
Figure 4.15	PAS stained (and haematoxylin counter-stained) sections used for scoring goblet cell hyperplasia and mucus production in line 16 P4 TCR/DR1/ABO mice	318

Figure 4.16	Analysis of CD4 vs. CD8 staining on thymocytes from P4 TCR/DR1/ABO transgenic mice	323
Figure 4.17	CD44 expression on thymocyte subsets in P4 TCR/DR1/ABO transgenic mice	325
Figure 4.18	CD62L expression on thymocyte subsets in P4 TCR/DR1/ABO transgenic mice	328
Figure 4.19	OX40 expression on thymocyte subsets in P4 TCR/DR1/ABO transgenic mice	330
Figure 4.20	ICOS expression on thymocyte subsets in P4 TCR/DR1/ABO transgenic mice	332
Figure 4.21	Gating used for analysis of expression of T-cell co-stimulatory molecules on thymocytes from P4 TCR/DR1/ABO transgenic mice by flow cytometry	335
Figure 4.22	Gating used for analysis of co-stimulatory molecule expression on splenocytes from P4 TCR/DR1/ABO transgenic mice by flow cytometry	341
Figure 4.23	Gating used for analysis of expression of late activation-associated T-cell co-stimulatory molecules on splenocytes from P4 TCR/DR1/ABO transgenic mice by flow cytometry	346

List of tables

		Page number
Table 3.1	TCRα sequences obtained from TCR CDR3 analysis of HLA-DR1-restricted, peptide 4-specific T-cell line CIR014 at its first restimulation with peptide 4	156
Table 3.2	TCRα sequences obtained from TCR CDR3 analysis of HLA-DR1-restricted, peptide 4-specific T-cell line B1 at its third restimulation with peptide 4	157
Table 3.3	TCRα sequences obtained from TCR CDR3 analysis of HLA-DR1-restricted, peptide 4-specific T-cell line CIR010 at its third restimulation with peptide 4	158
Table 3.4	TCRβ sequences obtained from TCR CDR3 analysis of HLA-DR1-restricted, peptide 4-specific T-cell line CIR014 at its first restimulation with peptide 4	161
Table 3.5	TCRβ sequences obtained from clonotypic analysis of HLA-DR1-restricted, peptide 4-specific T-cell line B1 at its third restimulation with peptide 4	162
Table 3.6	TCRβ sequences obtained from clonotypic analysis of HLA-DR1-restricted, peptide 4-specific T-cell line CIR010 at its third restimulation with peptide 4	163
Table 3.7	α and β expansions of the three lines CIR014, B1 and CIR010 with their related CDR3 amino acid sequences	170
Table 3.8	Packaging cell line types	246
Table 3.9	A simple representation of the retroviral system being tested	248
Table 3.10	The protocol used to transduce the target line BW7 with the D3(3) TCR	254
Table 3.11	The modified protocol used to transduce the target line BW7 with the D3(3) and A10(2) TCRs	263
Table 4.1	Group numbers used in the Fel d 1 disease induction experiments	302

Table 4.2 Expression of T-cell costimulatory molecules on thymocytes from P4 TCR/DR1/ABO transgenic mice 336

Table 4.3 Expression of T-cell costimulatory molecules on splenocytes from P4 TCR/DR1/ABO transgenic mice 342

Table 4.4 Expression of the late activation-associated T-cell costimulatory molecules OX40, ICOS and OX40L on splenocytes from P4 TCR/DR1/ABO transgenic mice 347

Table 4.5 The differences identified in levels of expression of costimulatory molecules at the cell surface of thymocyte subsets between P4 TCR/DR1/ABO transgenic mice from lines 4 and 16 and DR1/ABO transgenic control mice by flow cytometry. 350

List of abbreviations used

°C	degrees Centigrade
2-ME	β-mercaptoethanol
^3H	tritium
A	alanine
ADAP	adhesion and degranulation promoting adaptor protein
AHR	airway hyperreactivity
Aire	autoimmune regulator
AMV	avian myeloblastosis virus
AP-1	activated protein-1
APC	antigen-presenting cell
APL	altered peptide ligand
ASM	airway smooth muscle
ATP	adenosine triphosphate
BAL	bronchoalveolar lavage
BALF	bronchoalveolar lavage fluid
Bcl-2	B cell CLL/lymphoma-2
Bcl-X_L	Basal cell lymphoma-extra large
BHR	bronchial hyperreactivity
bp	base pair
BSA	bovine serum albumin
C	cysteine
C region	constant region
Ca^{2+}	calcium ion
$CaCl_2$	calcium chloride
CCL	CC-chemokine ligand
Cat. no.	catalogue number
CCR	CC-chemokine receptor
CD	cluster of differentiation
cDNA	complementary DNA
CDR	complementarity-determining region
C_{dyn}	dynamic compliance
CFA	complete Freund's adjuvant
Ci	Curie

CLP	common lymphoid progenitor
cm	centimetre
CMV	cytomegalovirus
CNS	central nervous system
CO_2	carbon dioxide
ConA	concanavalin A
COPD	chronic obstructive pulmonary disease
CRTH2	chemoattractant receptor homologous molecule expressed on Th2 cells
Csk	C-terminal Src kinase
cSMAC	central supramolecular activation cluster
CSPD	disodium 3-chloro-3-(methoxyspiro{1,2-dioxetane-3,2'-(5'-chloro) tricyclo [3.3.1.1] decan}-4-yl) phenyl phosphate
cTEC	cortical thymic epithelial cell
CTL	cytotoxic T lymphocyte
CTLA-4	cytotoxic T lymphocyte antigen-4
CXCL	CXC chemokine ligand
Cys LT	cysteinyl leukotriene
D	aspartic acid/aspartate
d	day
D region	diversity region
dC	deoxycytosine
DC	dendritic cell
DC1	dendritic cell type 1
DC2	dendritic cell type 2
dCTP	deoxycytosine triphosphate
dG	deoxyguanosine
dGTP	deoxyguanosine triphosphate
dH_2O	deionised water
DIG	digoxygenin
DMEM	Dulbecco's Modified Eagle's Medium
DN	double negative
DNA	deoxyribonucleic acid
DNA-PK	DNA-dependent protein kinase
DNA-PKcs	DNA-dependent protein kinase catalytic subunit
DNase	deoxyribonuclease

dNTP	deoxynucleotide triphosphate
DP	double positive
DP1	prostaglandin D_2 receptor
dsRNA	double-stranded RNA
dT	deoxythymidine
DTE	dithioerythritol
DTT	dithiothreitol
dTTP	deoxythymidine triphosphate
dU	deoxyuridine
dUTP	deoxyuridine triphosphate
E	glutamic acid/glutamate
EAE	experimental autoimmune encephalomyelitis
EAR	early asthmatic response
EB	eosinophilic bronchitis
EBV	Epstein-Barr virus
E. coli	*Escherichia coli*
EDTA	ethylenediamminetetraacetic acid
eGFP	enhanced green fluorescent protein
ELISA	enzyme-linked immunosorbent assay
env	viral envelope protein/gene
ERK	extracellular signal-related kinase
f	forward primer
F	phenylalanine
FACS	fluorescence associated cell sorting
FcεRI	high-affinity receptor for IgE
FcεRII	low-affinity receptor for IgE
FEV_1	forced expiratory volume in 1 second
FITC	fluorescein isothiocyanate
FL-1	green fluorescent channel
FL-2	red fluorescent channel
Foxp3	forkhead box p3
FSC	forward scatter
G	glycine
g	gram
g	gravitational constant

GADS	Grb2-related adaptor downstream of Shc
gag	viral group antigen protein/gene
GATA-3	GATA-binding protein-3
gDNA	genomic DNA
GEM	glycosphingolipid-enriched microdomain
GFP	green fluorescent protein
Grb2	growth factor receptor-bound protein 2
H	histidine
h	hour
HAT	hypoxanthine, aminopterin, thymidine
HBS	HEPES-buffered saline
HBSS	Hanks' buffered saline solution
HCl	hydrochloric acid
HDM	house dust mite
HEPES	4-(2-hydroxyethyl)-1-piperazineethanesulphonic acid
HEV	high endothelial venule
HLA	human leukocyte antigen
HT	hypoxanthine, thymidine
I	isoleucine
i.n.	intranasal
i.p.	intraperitoneal
ICAM-1	intracellular adhesion molecule-1 (CD54)
ICOS	inducible costimulator
Id3	inhibitor of DNA binding protein-3
IFN-	interferon
IFN-γR	IFN-γ receptor
Ig	immunoglobulin
IgE	immunoglobulin isotype E
IgG	immunoglobulin isotype G
IgG1	immunoglobulin isotype G1
IgG2a	immunoglobulin isotype G2a
IgG2b	immunoglobulin isotype G2b
IgG4	immunoglobulin isotype G4
IGIF	IFN-γ inducing factor
IgM	immunoglobulin isotype M

IL-	interleukin
IL-2Rα	IL-2 receptor α chain (CD25)
IL-4R	IL-4 receptor
IL-5R	IL-5 receptor
IL-12Rβ	IL-12 receptor β chain
IL-13R	IL-13 receptor
IL-18Rα	IL-18 receptor α chain
IMGT	Immunogenetics
IMS	industrial methylated spirit
iNKT	invariant natural killer T
$InsP_3$	inositol 1,4,5-trisphosphate
IPTG	isopropyl β-D-1-thiogalactopyranoside
IRES	internal ribosomal entry site
IS	immunological synapse
ITAM	immunoreceptor tyrosine activation motif
Itk	IL-2-inducible T-cell kinase
J region	joining region
JAK	Janus kinase
K	lysine
k	kilo
K-S	kinetic segregation
kb	kilobase
KCl	potassium chloride
kD	kiloDalton
KO	knockout
L	leucine
l	litre
lacZ	β-galactosidase gene
LAR	late asthmatic response
LAT	linker of activated T-cells
LB	Luria-Bertani
Lck	leukocyte-specific protein tyrosine kinase
LCMV	lymphocytic choriomeningitis virus
LFA-1	lymphocyte function-associated antigen-1
LM	littermate

LPS	lipopolysaccharide
LT	leukotriene
μ	micro
μm	micrometre
m	milli
M	methionine
M	molar
MAPK	mitogen activated protein kinase
Mb	megabase
MBP	major basic protein
MCS	multiple cloning site
mDC	myeloid dendritic cell
MES	4-morpholineethanesulfonic acid
MFI	mean fluorescence intensity
$MgCl_2$	magnesium chloride
$MgSO_4$	magnesium sulphate
MHC	major histocompatibility complex
MMP	matrix metalloproteinase
MOG	myelin oligodendrocyte glycoprotein
MoMuLV	Moloney murine leukaemia virus
mRNA	messenger RNA
MSV	Moloney sarcoma virus
mTEC	medullary thymic epithelial cell
MUC5AC	mucin gene 5AC
MUC5B	mucin gene 5B
mut	mutation
N	asparagine
n	nano
N region	non-germline encoded region
NaCl	sodium chloride
Neo^r	neomycin resistance gene
NFAT	nuclear factor of activated T-cells
NF-κB	nuclear factor-κB
NH_4	ammonium
$(NH_4)_2SO_4$	ammonium sulphate

NHEJ	non-homologous end joining
NK	natural killer
NOD	non-obese diabetic
NOD.E	non-obese diabetic transgenically expressing H-2E
nTreg	natural regulatory T-cell
O. C. T.	Optimal Cutting Temperature
OD	optical density
OD_{600}	optical density at 600 nm
ori	origin
OVA	ovalbumin
OX40L	OX40-ligand
p	pico
P	proline
ψ^+	viral packaging signal
P4	peptide 4 of Fel d 1
P4 TCR	TCR specific for peptide 4 of Fel d 1
P region	palindromic region
PAG	phosphoprotein associated with GEMs
PAMP	pathogen-associated molecular pattern
PAS reagent	periodic acid-Schiff's reagent
PBMC	peripheral blood mononuclear cell
PBS	phosphate buffered saline
pBSII	pBluescript II
PCC	pigeon cytochrome c
PCR	polymerase chain reaction
pDC	plasmacytoid dendritic cell
PE	phycoerythrin
PE-Cy5	phycoerythrin-Cy5
PEG	polyethylene glycol
Penh	enhanced pause
PG	prostaglandin
PGD_2	prostaglandin D_2
Pgp-1	phagocytic glycoprotein-1 (CD44)
PI	propidium iodide

PKC	protein kinase C
PLC	phospholipase C
PLP	proteolipoprotein
pol	viral polymerase protein/gene
polyG	polydeoxyguanosine triphosphate
pSMAC	peripheral supramolecular activation cluster
pTα	pre-TCRα chain
Q	glutamine
R	arginine
r	reverse primer
RAG	recombination activating gene
ref.	reference
R_L	pulmonary resistance
RNA	ribonucleic acid
RNase	ribonuclease
RORγ	retinoic acid orphan receptor-γ
RORγt	retinoic acid orphan receptor-γ t
rpm	revolutions per minute
rRNA	ribosomal RNA
RSS	recombination signal sequence
RSV	respiratory syncytial virus
S	serine
s.d.	standard deviation
SCF	stem cell factor
SCID	severe combined immunodeficiency
SDS	sodium dodecyl sulphate
SEM	standard error of the mean
SH2	Src homology domain 2
SHP-1	SH2-domain-containing protein tyrosine phosphatase-1
SHP-2	SH2-domain-containing protein tyrosine phosphatase-2
SIT	SH2-interacting transmembrane adaptor protein
SIT	specific immunotherapy
SKAP-55	Src kinase associated phosphoprotein of 55 kDa
SLP-76	Src homology domain 2-containing leukocyte protein of 76 kDa
SMAC	supramolecular activation cluster

S. mansoni	*Schistosoma mansoni*
SP	single positive
Stat	signal transducer and activator of transcription
Sos	son of sevenless
SSC	saline sodium citrate
SSC	side scatter
Syk	spleen tyrosine kinase
T	threonine
TAE	Tris-acetate-EDTA
TAP-1	transporter 1, ATP binding cassette, sub-family B
T-bet	T-box expressed in T cells
Tc2	T cytotoxic type 2
TCR	T-cell receptor
TdT	terminal deoxynucleotidyl transferase
TE	Tris-EDTA
temp.	temperature
Tg	transgenic
TGF	transforming growth factor
Th1	T helper type 1
Th2	T helper type 2
Th3	T helper type 3
Th17	T helper type 17
TLR	Toll-like receptor
TNF	tumour necrosis factor
Tr1	T regulatory type 1
TRAC	T cell receptor α constant gene
TRAJ	T cell receptor α joining gene
TRAV	T cell receptor α variable gene
TRBC	T cell receptor β constant gene
TRBD	T cell receptor β diversity gene
TRBJ	T cell receptor β joining gene
TRBV	T cell receptor β variable gene
Treg	regulatory T-cell
Tyk2	tyrosine kinase 2
U	unit

UV	ultraviolet
V	valine
V region	variable region
VEGF	vascular endothelial growth factor
VSV	vesicular stomatitis virus
W	tryptophan
X-gal	5-bromo-4-chloro-3-indolyl β-D-galactopyranoside
XLF	XRCC4-like factor
XRCC4	X-ray repair complementing defective repair in Chinese hamster cells-4
Y	tyrosine
ZAP-70	ζ-associated protein kinase of 70 kDa
Zbtb7b	zinc finger and BTB domain containing 7B
$ZnSO_4$	zinc sulphate

List of appendices

		Page number
Appendix 1	Stock solutions and buffers	428
Appendix 2	PCR conditions, primers and restriction enzymes for TCR CDR3 analysis in the HLA-DR1-restricted human T-cell lines grown in response to peptide 4 of Fel d 1	433
Appendix 3	PCR conditions, primers and linkers used in MFG cloning strategies	434
Appendix 4	PCR conditions, primers and linkers used in pTcass cloning strategies	436
Appendix 5	Restriction enzymes and digests used in MFG and pTcass cloning strategies	439
Appendix 6	PCR conditions and primers, fluorescently-labelled FACS antibodies and restriction enzymes for Southern hybridisations used in genotyping the P4 TCR/DR1/ABO transgenic mouse lines	442
Appendix 7	Fluorescently-labelled antibodies used in FACS analysis of potentially-transduced BW7 lines	444
Appendix 8	Differential cell phenotyping of Wright-Giemsa stained cytospins	445
Appendix 9	Antibodies and standards used in ELISAs	446
Appendix 10	Fluorescently-labelled antibodies used in FACS analysis of mice from P4 TCR/DR1/ABO transgenic lines 4 and 16	447
Appendix 11	pCR®2.1 – vector map and multiple cloning site	448
Appendix 12	pBluescriptII - vector map and multiple cloning site	449
Appendix 13	Amino acid sequence of the TCR α chain (TRAV 5-D4 TRAJ 13 TRAC) from the murine T cell clone A10(2) (chain 5-D4) cloned into retroviral vector MFG	450
Appendix 14	Amino acid sequence of the TCR α chain (TRAV 7-D3 TRAJ 15 TRAC) from the murine T cell clone A10(2) (chain 7-D3) cloned into retroviral vector MFG	451

Appendix 15	Amino acid sequence of the TCR α chain (TRAV 7-D4 TRAJ 26-like TRAC) from the murine T cell clone D3(3) cloned into retroviral vector MFG	452
Appendix 16	Amino acid sequence of the TCRβ chain (TRBV 14 TRBJ 2-7 TRBC 1) from the murine T cell clone A10(2) cloned into retroviral vector MFG	453
Appendix 17	Amino acid sequence of the TCRβ chain (TRBV 2 TRBJ 2-5 TRBC 1) from the murine T cell clone D3(3) cloned into retroviral vector MFG	454
Appendix 18	Amino acid sequence of the dominant TCR α chain (TRAV 8-4 TRAJ 32 TRAC) from the human T cell line CIR010 cloned into retroviral vector MFG	455
Appendix 19	Amino acid sequence of the dominant TCR α chain (TRAV 8-4 TRAJ 32) from the human T cell line CIR010 joined to a murine C region (murine TRAC 1) cloned into retroviral vector MFG	456
Appendix 20	Amino acid sequence of the dominant TCR β chain (TRBV 6-1 TRBJ 1-1) from the human T cell line CIR010 joined to a murine C region (murine TRBC 1) cloned into retroviral vector MFG	457
Appendix 21	pUC19 – vector diagram and multiple cloning site	458
Appendix 22	Amino acid sequence of one of the two TCR α chains (TRAV 5-D4 TRAJ 13) from the murine T cell clone A10(2) cloned into the TCR cassette vector pTαcass	459
Appendix 23	Amino acid sequence of one of the two TCR α chains (TRAV 7-D3 TRAJ 15) from the murine T cell clone A10(2) cloned into the TCR cassette vector pTαcass	460
Appendix 24	Amino acid sequence of the TCR β chain (TRBV 14 TRBJ 2-7) from the murine T cell clone A10(2) cloned into the TCR cassette vector pTβcass	461
Appendix 25	Amino acid sequence of the TCR α chain (TRAV 7-D4 TRAJ 26-like) from the murine T cell clone D3(3) cloned into the TCR cassette vector pTαcass	462

Appendix 26	Amino acid sequence of the TCR β chain (TRBV 2 TRBJ 2-5) from the murine T cell clone D3(3) cloned into the TCR cassette vector pTβcass	463
Appendix 27	Amino acid sequence of the dominant TCR α chain (TRAV 8-4 TRAJ 32) from the human T cell line CIR010 cloned into the TCR cassette vector pTαcass	464
Appendix 28	Amino acid sequence of the dominant TCR β chain (TRBV 6-1 TRBJ 1-1) from the human T cell line CIR010 cloned into the TCR cassette vector pTβcass	465
Appendix 29	pmaxGFP - vector diagram	466
Appendix 30	DNA coding sequences for the P4 TCR α and β chains	467

1. Introduction

1.1 Clinical and epidemiological aspects of allergic asthma

1.1.1 Prevalence of allergic asthma

Allergic asthma is a significant cause of morbidity and mortality in developed countries. In the U.K., the incidence of wheeze and diagnosis of asthma in children has increased from 1964 to 2004, correlating with an increase in hospital admissions for asthma over the same time frame (1). Mortality due to asthma increased sharply during the 1960s and to a lesser extent in the 1970s (1). Corresponding trends have also been seen in other developed countries such as Australia (2). In more recent years, this trend appears to have lessened - a worldwide study of the prevalence of asthma in children suggested that the occurrence of asthma in children from developed countries decreased from 1995-2005 (3, 4) whilst the occurrence of asthma in developing countries increased over the same period (3). Overall, therefore, the worldwide prevalence of asthma is still increasing.

1.1.2 The 'hygiene hypothesis'

An inverse correlation between incidence of allergic rhinitis and increasing family size (5) led to the suggestion that development of allergic disease could be prevented by exposure to infectious agents at a young age, e.g. through contact with older siblings. The concurrent trends of decreasing family size and increasing standards of hygiene and health care in developed countries were proposed to have decreased the exposure of young children to infection, thus increasing their risk of allergy. A number of studies provided epidemiological evidence in support of this hypothesis suggesting that children from a rural background, in particular those brought up in a farming environment, were protected against the development of allergic sensitisation and hay fever (6) as well as allergic asthma. Increased protection was linked both to increased exposure to livestock (7) and drinking unpasteurised milk produced on the farm during early childhood (8), suggesting that exposure to microbial compounds could protect against development of allergic disease. Lipopolysaccharide (LPS), a component of some bacterial cell walls (9), and other microbial products such as CpG

oligonucleotides (10) were later shown to prevent allergic disease in murine models, suggesting that the protective effect of microbial products may be mediated through their interaction with innate immune receptors such as Toll-like receptors (TLRs). Support came from studies showing that expression of TLR2 messenger RNA (mRNA) was increased in the children of farmers (11) and that polymorphisms in the TLR2 gene (12) and the CD14 gene, a coreceptor for TLR4 (the LPS receptor) (13), have been associated with increased risk of allergy. A more recent study showed lower expression of TLR4 on $CD4^+$ T-cells in allergic asthmatics compared with T-cells from normal controls (14). Bacterial strains associated with cowsheds reduced allergic disease in sensitised mice and promoted the development of human dendritic cells (DC) *in vitro* that promoted a T helper type 1 (Th1) T-cell response (15), which is associated with production of the cytokine interferon-γ (IFN-γ) (16). This suggested that protection was due to the promotion of Th1-associated immunity over T helper type 2 (Th2) immunity, characterised by production of the cytokine interleukin-4 (IL-4) (16) and which is strongly associated with the development of atopy (17) and allergic asthma (18).

Evidence against a simple Th1/Th2 version of the hygiene hypothesis includes the presence of a concurrent increase in Th1-mediated autoimmune diseases such as diabetes (19) alongside the increase in Th2-mediated allergic disease, suggesting that a more general immune dysregulation may be the basis of the hygiene hypothesis. In addition, chronic helminth infection is protective against the development of allergy and atopy (20). Helminth infections are associated with 'modified' Th2-mediated immunity and not Th1-mediated immunity (21). In mouse models of human autoimmune disease (22, 23), helminth infection protects against the development of disease, suggesting that the hygiene hypothesis also applies to autoimmune disease. There are conflicting results from studies investigating the effect of LPS on allergic disease with some suggesting that LPS is protective (9) whilst others showed that it has no effect and can even act to potentiate allergic disease (24, 25). Infection with agents that induce a Th1-mediated immune response such as certain viruses, e.g. influenza A, do not protect against allergic disease but instead exacerbate the associated inflammation (26). These findings suggest that the hygiene hypothesis applies to both Th2-mediated allergic disease and Th1-mediated autoimmune disease, with reduced exposure to infectious agents during early life causing immune dysregulation that leads to development of these diseases.

1.1.3 The clinical manifestations of asthma

Allergic asthma occurs as a result of an inappropriate immune response to an inhaled harmless substance such as grass or tree pollen, house dust mite or cat dander (27). A distinct subgroup of asthmatic patients present with a form of the disease unrelated to atopy or allergy which is associated with neutrophilic airway inflammation rather than the eosinophilic inflammation associated with allergic asthma (28). The proportion of asthmatic patients with non-eosinophilic asthma is approximately 50% (29) and possible causes include exposure to bacterial endotoxin, air pollution, ozone or viral infection (30). Asthma is a chronic inflammatory disease of the lower airways characterised by bronchial hyperreactivity (BHR), mucus hypersecretion and progressive lung damage and remodelling due to persistent inflammation causing reversible airway obstruction. This manifests itself as wheeze, cough, shortness of breath and in some cases severe bronchoconstriction (an 'asthma attack') (31). The disease is mainly treated through use of inhaled anti-inflammatory corticosteroids and bronchodilators (β_2 agonists) which control the symptoms of asthma but do not cure the disease (32), and which are less effective in the treatment of neutrophilic asthma (33, 34). Another treatment for allergic asthma is specific immunotherapy (SIT) - this involves exposure to high doses of allergen extract with the aim of inducing tolerance to allergen (35). It has been shown to have clinical efficacy (36) but there are safety implications due to the potential for the induction of asthmatic episodes and anaphylaxis (37).

A typical asthmatic episode is biphasic - within minutes of exposure to allergen an immediate type hypersensitivity reaction (early asthmatic reaction or EAR) occurs, causing bronchoconstriction and a decrease in lung function (27). This resolves within a short time and is followed 2-6 hours later by the late asthmatic reaction (LAR), characterised by more prolonged but less severe bronchoconstriction (38) and which usually resolves within 24 hours.

1.2 Immune mechanisms of allergic asthma

1.2.1 Antigen-presenting cells (dendritic cells) in allergic asthma

Initial exposure to allergen in the airways can lead to sensitisation in pro-asthmatic lungs. DC are the most potent antigen-presenting cells (APC) in the lung and are thought to play an important role in the development and ongoing pathogenesis of allergic asthma - intraepithelial DC isolated from allergic asthmatic patients promoted the activation of autologous $CD4^+$ T-cells to produce mediators associated with a Th2 response, namely interleukin-4 (IL-4) and IL-5 (39). Allergen is taken up by DC which form a contiguous network of cells in the respiratory epithelium (shown in immunohistochemical analysis of both rat (40) and human (41) airway sections) and which are capable of presenting inhaled antigens to T-cells *in vivo* (reviewed in 42). DC and other APC present allergens, like other antigens, in the form of short peptides bound to major histocompatibility complex (MHC) molecules which can then be recognised by a T-cell bearing a T-cell receptor (TCR) whose structure has specificity for the peptide-MHC complex and which can lead to T-cell activation (reviewed in 43, and discussed in greater detail in Section 1.4). DC numbers in the bronchial mucosa of patients with allergic asthma are greater than those in non-asthmatic controls (44). The number of myeloid DC (mDC, surface phenotype human leukocyte antigen (HLA)-DR^+ $CD11c^+$ $CD1c^+$) in the peripheral circulation of allergic asthmatic patients rapidly decreased from baseline levels upon allergen challenge in the lung, and were still below baseline 24 hours post-challenge (45). A previous study (46) investigated the recruitment of mDC to the bronchial mucosa in asthmatic patients and showed that numbers increased within 4-5 hours of allergen challenge. Taken together, this suggests that upon allergen challenge, mDC from the periphery are rapidly recruited to the bronchial mucosa where they activate T-cells and mediate asthma pathogenesis. Investigation of antigen presentation in rat lung showed that upon uptake of inhaled antigen, DC from the airways migrate to the regional lymph nodes within 24 hours of allergen exposure and upregulate their antigen-presenting capabilities for up to 7 days (47). Antigen-specific T-cells could be isolated from the lymph node after this primary sensitisation and a secondary challenge elicited an antigen-specific immune response in the airways, characterised primarily by inflammation around blood vessels in the lung. This suggests that lung DC are the antigen-presenting cells involved in the development

of T-cell-mediated immune responses in the lung, although this has not been demonstrated in human lung.

Both mDC and plasmacytoid DC (pDC, surface phenotype HLA-DR$^+$ CD123$^+$) numbers in bronchoalveolar lavage fluid (BALF) increase after allergen challenge, pDC to a greater extent than mDC (48), suggesting a role for pDC in asthma pathogenesis. The role of pDC in allergic asthma in humans is unclear - in allergic rhinitis, pDC in the nasal mucosa activate T-cells *in vitro* and promote development of a Th2 response from both naïve and memory T-cells (49). However, Jahnsen et al. (46) reported that no pDC were present in the bronchial mucosa after allergen challenge and pDC have been shown to prevent development of an allergic asthmatic response in mice (50).

Studies of the function of DC in animal models of allergic lung inflammation have shown that the presence of a low dose of LPS, signalling through TLR4, was required at the time of sensitisation to induce allergic pulmonary inflammation through induction of a Th2-mediated response in the local lymph nodes by LPS-activated DC (51). This phenomenon did not occur if sensitisation occurred in the absence of LPS or the presence of a high dose of LPS, when a Th1 response was induced in the lung instead, suggesting that the lung microenvironment at the time of antigen encounter is important in determining the nature of the response elicited. The induction of a Th2-type T-cell response by exposure to allergen is dependent upon signalling through the CD28-B7 costimulatory pathway - blocking this pathway using cytotoxic T-lymphocyte antigen-4-immunoglobulin (CTLA-4-Ig) abolished the induction of Th2-mediated allergic inflammation (52). The required costimulatory signal is supplied by DC as mice deficient in B7-1/B7-2 (CD80/CD86) on DC only are unable to induce Th2-mediated responses to allergen (53). A study (54) using a mouse model of allergic asthma demonstrated that mDC were able to induce sensitivity to inhaled allergen. DC isolated from bone marrow and pulsed with allergen migrated to regional lymph nodes and subsequent challenge with aerosolised allergen induced recruitment of activated T-cells, eosinophils and neutrophils to the lung. Recruited CD4$^+$ T-cells predominantly secreted IL-4 and IL-5. Analysis of sectioned lung showed eosinophilic infiltrates around bronchioles and blood vessels and hyperplasia of mucus-producing goblet cells in the airways, all of which is consistent with an allergic asthmatic phenotype.

1.2.2 Immunoglobulin E in allergic asthma

Immunoglobulin E (IgE) is the least abundant of the antibody isotypes with a normal concentration in the blood of ~150 ng/ml (55). IgE is believed to be involved in the immune response against parasites such as helminths and *Schistosomonas mansoni* (56). Parasitic infections induce a Th2-mediated response including production of IL-4 (57) which induces isotype switching in antigen-specific B-cells to produce IgE (58). Elevated levels of circulating IgE are also associated with allergic asthma (59) as asthmatic patients have significantly higher levels of serum IgE than non-asthmatic controls. After local allergen challenge, levels of allergen-specific IgE are increased in BALF in asthmatic patients (60). High serum levels of IgE in childhood have also been associated with development of asthma and/or atopy in later life (61). Levels of IgE receptors expressed at the cell surface of relevant cells are up-regulated in asthma; expression of the high-affinity receptor for IgE (FcεRI), expressed by mast cells, DC, macrophages and eosinophils is increased in asthma (62), whilst the low affinity receptor for IgE (FcεRII) is expressed on B-cells and is also up-regulated in asthma (63).

IL-4 secreted by allergen-specific Th2 cells induces class switching in allergen-specific B-cells in the local lymph nodes to produce IgE and migrate to the airways (58). The induction of class switching in allergen-specific B-cells has been shown to occur in the bronchial mucosa of patients with asthma (64). Class switching to IgE is antagonised by IFN-γ (65) and can be induced by the Th2-associated cytokine IL-13 through a mechanism believed to be analogous to that of IL-4 (66). Secreted IgE binds to its receptors and primes cells for activation (in most cases via secretion of pro-inflammatory mediators) upon further exposure to allergen. IL-4 (67) and IL-13 (68) upregulate surface expression of FcεRI on tissue-resident mast cells. Levels of FcεRI on basophils (and mast cells) are believed to correlate with the circulating concentration of IgE itself with the interaction between IgE and FcεRI causing its up-regulation at the cell surface (69). This is further supported by the discovery that treatment of allergic patients with anti-IgE (omalizumab) down-regulates expression of FcεRI on basophils (70). Omalizumab also down-regulates expression of FcεRI on DC (71). Antigen presentation of allergen captured by IgE bound to FcεRI on the surface of DC proceeds more efficiently than other methods of antigen processing and could act to increase the

frequency of T-cell activation by allergen-primed DC leading to a worsening of disease with subsequent allergen exposure (72).

1.2.3 Mast cells in allergic asthma

Re-exposure to antigen in a sensitised asthmatic individual causes an immediate hypersensitivity response, the EAR, as described previously. Allergen-specific IgE molecules bind to FcεRI on mast cells and when cross-linked by allergen (i.e. at least two IgE molecules bound to FcεRI and specific for different epitopes of the same allergen bind the allergen simultaneously) trigger signalling cascades via immunoreceptor tyrosine activation motif (ITAM) domains in the cytoplasmic portion of the receptor (73). The tyrosine kinases Lyn and Syk (74) phosphorylate ITAMs and initiate activation of the mast cell via a pathway involving protein kinase C (PKC)-θ (75). Activation causes degranulation and release of pre-formed pro-inflammatory mediators, including histamine, cysteinyl leukotrienes (Cys-LTs), prostaglandins (PG) and thromboxanes, which act to induce the immediate bronchoconstriction characteristic of the EAR (76). Activation also induces *de novo* synthesis of further CysLTs, PG (especially prostaglandin D_2, or PGD_2), IL-4, IL-5 and IL-13 (76). These newly synthesised molecules may play a number of roles in development of the LAR - they may directly mediate further bronchoconstriction, they may recruit other inflammatory cell types to the lung e.g. IL-5 recruits and activates eosinophils or they may recruit and promote activation of antigen-specific Th2 cells. Cys-LTs are potent bronchoconstrictors, enhance mucus secretion, vascular permeability and vasoconstriction in the lungs and are also a potent chemoattractant for eosinophils, acting through their receptors CysLT1 and CysLT2 (77). PGD_2, acting through its receptors DP1 (PGD_2 receptor) and CRTH2 (chemoattractant receptor homologous molecule expressed on Th2 cells), mediates recruitment of eosinophils, basophils and Th2 cells. Through CRTH2, it promotes the development of Th2 cells in the lung and their production of IL-4, IL-5 and IL-13 and the activation and degranulation of eosinophils and basophils. Signalling of PGD_2 through DP1 may exert anti-inflammatory effects and antagonise its effects on leukocytes through CRTH2 (78). The Th2 cytokines produced by mast cells and Th2 cells induced by the action of PGD_2 have many roles in the pathogenesis of asthma, many of them synonymous with the actions of the CysLTs and PGD_2 and will be discussed in more detail in Section 1.2.12.

The mast cell has recently been postulated to act as the central mediator of airway hyperreactivity (AHR) with evidence from a number of studies (79, 80) investigating the association between mast cells and the smooth muscle cells of the airways. Subjects with allergic asthma and eosinophilic bronchitis (EB), a disease characterised by eosinophilic infiltration into the lungs but with no associated BHR, were compared (79). The major difference between these two groups was an increase in the number of mast cells associated with airway smooth muscle (ASM) bundles in the airways of asthmatic subjects compared to both normal subjects and EB subjects where mast cell numbers were similar. Further comparison of subjects with allergic asthma and EB showed that both diseases were characterised by an increase in ASM mass, basement membrane thickening and collagen deposition in the airways (80). The lack of AHR seen in EB therefore suggests that airway remodelling is dissociated from AHR development. Mast cells in the asthmatic lung associated with ASM secrete IL-4 and IL-13 (81) and human lung mast cells up-regulate the IL-13 receptor (IL-13R) in asthma (68). IL-13 can also synergise with stem cell factor (SCF) to increase mast cell proliferation, FcεRI expression and histamine production (68). IL-13 is crucial for the development of AHR (82) - its production by mast cells associated with ASM further supports the theory that mast cells mediate AHR.

1.2.4 Eosinophils in allergic asthma

Allergic asthma is characterised by the presence of large eosinophilic infiltrates in lung tissue, BALF and blood (83) of which an increased number are activated in asthmatic patients and by an increase in eosinophil progenitors in the bone marrow of allergic asthmatic patients (84). Eosinophils migrate to the lungs in response to IL-5 and the eotaxins which selectively regulate migration of eosinophils into tissues (85) and which bind to the IL-5 receptor (IL-5R) and CC-chemokine receptor-3 (CCR3) respectively (86). IL-5, produced by allergen-specific T-cells, is an important signal for the expansion and mobilisation of eosinophils from bone marrow and their traffic into the lung (87) whilst eotaxin production is induced in lung epithelial cells and ASM cells by the actions of the Th2 cytokines IL-9 (88) and IL-13 (89). Eosinophils are activated by IL-5 and eotaxin-1 produced after exposure to allergen and secrete pro-inflammatory molecules such as major basic protein, eosinophil cationic protein and eosinophil peroxidase in pre-formed granules, all of which cause progressive tissue damage and inflammation in the lungs (90). Eosinophils can process and present allergen antigens to

primed T-cells in the regional lymph nodes and promote their Th2-associated functions (91) but they are incapable of mediating activation of naïve T-cells (92). A role in lung remodelling and repair in response to tissue injury induced by inflammation caused by allergen exposure has been suggested for eosinophils. Eosinophils are a major producer of transforming growth factor-β (TGF-β) (93) and vascular endothelial growth factor (VEGF) (94) which are implicated in tissue remodelling processes (95, 96). A number of studies in mice support this theory; tissue remodelling is diminished upon induction of disease in mice in which the eosinophil lineage is deleted (97). Induction of allergic disease in the IL-5 knockout mouse led to decreased lung eosinophilia, lung fibrosis, collagen deposition, ASM thickening and TGF-β production in the lung (98, 99), whilst induction of the same model in a transgenic mouse which overexpressed IL-5 caused increased lung fibrosis (99).

The LAR is associated with increased BALF eosinophilia in allergic asthmatic patients (100) but the role of eosinophils in the development of the LAR is uncertain. Use of an IL-5 blocking antibody in clinical trials to treat asthma decreased lung eosinophilia but had no effect on LAR induction (101). The antibody was only partially effective at removing eosinophils from the lung; the remaining eosinophils may be sufficient to maintain their role in asthma pathogenesis (102).

1.2.5 Basophils in allergic asthma

The role of basophils in the pathogenesis of allergic asthma is not as well-defined as for other immune system cells such as mast cells for several reasons. Their relative infrequency in the periphery (less than 1% of all leukocytes) and the lack of basophil specific antibodies until recently led to difficulty in their isolation from peripheral blood and in addition, mouse models of allergic asthma placed a greater emphasis on the functionally similar mast cell (103). A model of nematode infection, *Nippostrongylus brasiliensis*, in the rat showed that blood basophilia and associated IL-4 induction led to parasite clearance, suggesting a role for basophils in anti-parasite immunity (104), although the importance of basophils in protective immunity in humans is less well-defined. Basophils are implicated in disease pathogenesis of allergic asthma; there are increased numbers of basophils in the peripheral circulation (105) and lung (106) of asthmatic subjects compared to non-asthmatic controls. Investigation of both sputum (107) and bronchial biopsy tissue (108) from asthmatic subjects showed that basophil

numbers increase in the lung after allergen challenge and analysis of lung tissue showed increased numbers of basophils in fatal asthma (109).

Basophils are predominantly found in the periphery and are recruited to sites of inflammation such as the allergic lung through chemotaxis via, for example, the action of PGD_2 on CRTH2 (110) or eotaxin on CCR3 (111). IL-3 is important in the rapid expansion of basophils in response to infection but is not required for normal development as IL-3 knockout mice have normal baseline numbers of basophils (112). IL-3, predominantly produced by Th2 cells, can also induce IL-4 production in basophils via signalling through FcεRI (113). FcεRI triggering through cross-linking of allergen-specific IgE on basophils leads to degranulation, the release of histamine and pre-formed IL-4 (in contrast to mast cells) and the *de novo* synthesis of IL-13 and IL-4 (114). This initial burst of IL-4 upon activation could play an important role in the development of the Th2-dominated environment seen in allergic asthma, supported by the finding that basophils promote the development of Th2 responses when cultured *in vitro* with antigen-stimulated naïve T-cells (115). *In vitro* culture of mast cells or basophils with B-cells showed that only basophils could induce class-switching in B-cells to produce IgE, thought to be at least partially due to the higher levels of IL-4 and IL-13 secreted by the basophils in response to activation compared with the mast cells (116). These findings raise questions about the relative importance of basophils and other innate immune system effector cells such as mast cells in the development of allergic asthmatic disease in humans.

1.2.6 Neutrophils in allergic asthma

As described previously, there are two distinct types of asthma: the predominantly eosinophilic allergic asthma and the predominantly neutrophilic non-allergic asthma, in which IL-8 is believed to be a key mediator. However, lung neutrophilia is also associated with severe allergic asthma. There are increased neutrophil numbers in BALF and bronchial biopsies from severe, corticosteroid-treated, symptomatic asthmatics compared with those from mild, corticosteroid-treated, controlled asthmatics (117). Neutrophil numbers in induced sputum and bronchial biopsies correlate with a measure of chronic asthma severity, forced expiratory volume in 1 second, or FEV_1 (118). Neutrophils are steroid-resistant (119) hence it has been postulated that the lack of effect of corticosteroids in the treatment of severe asthma may be due to their failure

to control neutrophilic inflammation; conversely, it has been suggested that the presence of neutrophils in severe asthma may be caused by corticosteroid treatment as they inhibit neutrophil apoptosis (120).

Epithelial cells in the lung produce IL-8 (CXC chemokine ligand-8 or CXCL8) (121), a major chemotactic factor for neutrophils which is also the most potent activator of neutrophils (122). The number of IL-8 $mRNA^+$ cells in the bronchial epithelium is increased in moderate to severe asthma although IL-8 levels in the submucosa from the same subjects were decreased (123). Activated neutrophils produce a number of pro-inflammatory mediators: some are stored in pre-formed granules, such as the enzymes myeloperoxidase, elastase and gelatinase, whilst others are synthesised upon activation, such as leukotriene B_4 (LTB_4), reactive oxygen species, IL-9 (124) and TGFβ. IL-9 promotes mucus production in the lungs (125) and goblet cell hyperplasia (126) and also upregulates IL-8 production by polymorphonuclear neutrophils (127). TGFβ production by neutrophils, which is upregulated in neutrophils from asthmatic subjects compared with controls (128), is implicated in lung remodelling; its production by neutrophils suggests they may have a potential role in the development of lung remodelling. Neutrophils in the lung are the main source of matrix metalloproteinase-9 (MMP-9) which promotes angiogenesis and is implicated in the development of ASM cell hyperplasia (129).

1.2.7 Invariant natural killer T (iNKT) cells in allergic asthma

Invariant natural killer T (iNKT) cells recognise and respond to glycolipid antigens bound to the non-classical MHC class I molecule CD1d (130). They express the natural killer (NK) cell marker CD161 (131) and an invariant αβ TCR (in humans composed of a TCRα chain comprising variable (V) region Vα24 and joining (J) region JαQ paired with a TCRβ chain including Vβ11) (132). They are subdivided on the basis of CD4 and CD8 expression and cytokine secretion upon activation via TCR signalling through CD1d. CD1d is expressed upon epithelial cells (133) and cells of the immune system (B-cells, T-cells and monocytes) (134). $CD4^+$ iNKT cells secrete either IL-4 and IL-13 upon activation or IFN-γ, whilst $CD4^-CD8^-$ iNKT cells secrete only IFN-γ (135). A third subset of iNKT cells, $CD8^+$ iNKT cells, secrete IFN-γ upon activation (136). iNKT cells may bridge the innate and adaptive immune responses - their rapid release of cytokines upon activation may drive the development of adaptive immune responses (137).

The role of iNKT cells in allergic asthma was suggested from work in iNKT cell knockout mice (138). Allergic disease was induced using ovalbumin (OVA) but induction of AHR in response to methacholine was abolished and IgE production and lung eosinophilia were down-regulated, despite the presence of a normal Th2-mediated allergen-specific response. Adoptive transfer of wild-type iNKT cells into the lungs restored disease phenotype, suggesting that iNKT cells are essential for the development of allergic lung disease. Adoptive transfer of iNKT cells isolated from IL-4 and IL-13 double-knockout mice did not restore the asthmatic phenotype, implicating the IL-4- and IL-13-producing $CD4^+$ iNKT cells in this process. Activation of iNKT cells with α-galactosylceramide induces development of AHR without allergen sensitisation (139) even in the absence of conventional $CD4^+$ T-cells.

Whilst the importance of iNKT cells in mouse models of allergic asthma suggested that these cells might play a similar role in the human disease, elucidation of the importance of iNKT cells in human asthma has not been straightforward. Comparison of iNKT cell numbers in BALF and bronchial biopsy samples from asthmatic subjects, patients with sarcoidosis (a Th1-mediated lung disease) and normal control subjects found that approximately 60% of all $CD3^+CD4^+$ cells also stained with a CD1d tetramer loaded with α-galactosylceramide in asthmatic patients, compared with less than 2% of cells in patients with sarcoidosis and normal control subjects (140), suggesting that iNKT cells play an important role in human disease pathogenesis. The basic finding of this study, that iNKT cell numbers are increased in the asthmatic lung, has been confirmed but no other study has found such a large proportion of iNKT cells in the lung. Children with asthma had a small but significant increase in iNKT cells in BALF (using CD1d tetramer staining), from 0% to ~0.4%, a much less dramatic increase (141). Another study detected an increase in iNKT cell number in induced sputum only in severe asthmatic patients, where ~14% of cells were iNKT cells, compared with 2-3% in mild asthmatics and normal controls (142). iNKT cells were defined in this study as $CD3^+$ $CD56^+$. Numbers of $CD4^+CD56^+$ cells were much lower (less than 1%) and did not differ significantly between the groups. These studies, in conjunction with the murine studies, suggest that iNKT cells are involved in asthma pathogenesis. Other studies have failed to see increases in iNKT cell number in asthma. Use of the human invariant TCRα chain-specific antibody 6B11 with a Vβ11-specific antibody showed that at most 2.1% of BALF lymphocytes were iNKT cells (143). Analysis of iNKT cell numbers (detected by use of CD1d tetramers, 6B11 antibody, and Vα24- and Vβ11-specific

antibodies) in asthmatic (both mild and severe) patients, patients with chronic obstructive pulmonary disease (COPD) and normal controls corroborated these findings, as less than 2% of cells obtained from any subject were iNKT cells (144). In other studies corroborating these findings (145,146), no difference was seen in iNKT cell number between asthmatics and normal controls, and numbers of iNKT cells in BALF for both groups were less than 1% of total cells. Currently, there are no studies in the literature investigating the actual role or importance of iNKT cells in disease mechanisms of human allergic asthma and there is no definitive proof they are required for the development of allergic asthma in humans.

1.2.8 $CD8^+$ T cells (cytotoxic T-cells) in allergic asthma

$CD8^+$ T cells, or cytotoxic T-cells (CTL) are associated with antiviral and antitumour immunity, responding to peptide antigens presented by MHC class I molecules expressed at the surface of all cells (147). A role for $CD8^+$ T-cells in asthma was suggested through study of occupational asthma caused by exposure to toluene diisocyanate (148). This form of asthma shares many features with allergic asthma, including the induction of both an EAR and LAR through exposure to the causative agent. Analysis of peripheral blood before and at several time points after challenge with toluene diisocyanate showed a significant increase in the number of $CD8^+$ T-cells up to 48 hours after challenge, corresponding with eosinophilic influx into the blood, in contrast to the $CD4^+$ T-cell mediated response seen in allergic asthma. Further studies in allergic asthmatic subjects have suggested a role for $CD8^+$ T-cells in allergic asthma, but there is conflicting evidence as to their exact role. Two studies investigated TCR usage in T-cells isolated from BALF before and after allergen challenge. Analysis of TCR usage in $CD4^+$ and $CD8^+$ T-cells by reverse transcriptase polymerase chain reaction (RT-PCR) before and after challenge in allergic asthmatic subjects sensitive to ragweed pollen showed expanded populations of $CD4^+$ and $CD8^+$ T-cells expressing the same TCR Vα or Vβ regions, and in one case showed an expanded population of $CD8^+$ T-cells bearing the same TCR (149). Analysis of $CD4^+$ and $CD8^+$ T-cells by flow cytometry using antibodies specific for particular TCR Vα or Vβ regions showed expansions of certain Vα and Vβ regions in the population of $CD8^+$ T-cells after allergen challenge (150). These studies show that $CD8^+$ T-cells can recognise and respond to allergen-based antigens presented by MHC class I molecules and may have a role in allergic asthma. $CD8^+$ T-cell lines derived from allergic asthmatic subjects

secreted increased quantities of IL-5 compared to both atopic and non-atopic non-asthmatic control subjects (151), indicating that $CD8^+$ T-cells can potentially generate Th2-mediated allergic disease in the lung. A study of non-specific stimulation of peripheral blood $CD8^+$ T-cells isolated from allergic asthmatic subjects in the presence and absence of IL-4 showed that in the presence of IL-4, $CD8^+$ T-cells secreted increased levels of IL-5 and IL-13 (152); this suggests that during respiratory system viral infections, the IL-4-rich environment in an allergic asthmatic lung could prime activated virus-specific $CD8^+$ T-cells to produce IL-5 and IL-13. These mediators can then go on to mediate allergic inflammation and AHR and thus underlie the capacity of respiratory viral infections to exacerbate asthma.

$CD8^+$ T-cells may play a role in suppression of allergic asthma (153). Analysis of cytotoxic mediator production by peripheral blood $CD8^+$ T-cells in allergic asthmatic subjects and non-asthmatic controls showed that numbers of granzyme B- and perforin-positive $CD8^+$ T-cells, indicative of a more differentiated phenotype, were reduced in allergic asthma compared to controls. This reduction also negatively correlated with serum levels of IgE, suggesting that these more highly differentiated $CD8^+$ effector T-cells may suppress and control development of allergic disease.

Evidence from animal models of allergic asthma supports both viewpoints. A mouse model of lung infection (lymphocytic choriomeninigitis virus - LCMV) in the context of allergen (OVA) sensitisation was used to analyse responses of virus-specific $CD8^+$ T-cells in allergic asthma (154). Challenge of wild-type OVA-sensitised mice *in vivo* with intranasally administered LCMV induced significant lung eosinophilia. $CD8^+$ T-cells isolated from the lungs of these mice and stimulated non-specifically with anti-CD3 secreted IL-5 in contrast to cells from non-sensitised mice which secreted IFN-γ. A similar system in LCMV-peptide-specific TCR transgenic mice showed similar $CD8^+$ T-cell responses. This suggests that the lung environment induced by OVA sensitisation primes virus-specific T-cells to produce IL-5 upon activation by viral infection. Activating $CD8^+$ T-cells isolated from the lungs of LCMV TCR-transgenic mice with peptide in the presence of IL-4 led to IL-5 secretion and not IFN-γ; this was reversed in T-cells stimulated in the absence of IL-4. Induction of allergic disease in the lungs of CD8 knockout mice through OVA sensitisation and challenge produced a lesser phenotype, characterised by lower AHR, eosinophilia and BALF IL-13 than in sensitised wild-type mice (155). The phenotype was restored in the knockout mice by

adoptive transfer of wild-type effector $CD8^+$ T-cells, which accumulated in the lung and produced IL-13. Sensitisation and challenge of a $CD8^+$ OVA-specific TCR transgenic mouse with OVA did not induce the AHR, eosinophilia, increase in Th2 cytokine secretion or mucus hypersecretion usually associated with allergic asthma unless mice were adoptively transferred with IL-4^+ $CD4^+$ T-cells prior to sensitisation, where all the features of an allergic asthmatic phenotype were seen and IL-13^+ $CD8^+$ T-cells could be isolated from the lung (156). IL-4 produced by $CD4^+$ T-cells may be required for the induction of IL-13 production by $CD8^+$ T-cells; in the absence of IL-4, allergen-specific $CD8^+$ T-cells may suppress development of allergic disease. The previous studies support a role for $CD8^+$ T-cells in development of allergic inflammation and AHR in the lung, but suggest that IL-4 is required at the time of activation to induce a Th2 cytokine-producing subset of $CD8^+$ T-cells (sometimes referred to as Tc2 cells) that exacerbates disease.

Other studies support the theory that $CD8^+$ T-cells suppress allergic responses in the lung. OVA sensitisation of a 'low IgE responder' strain of rats caused expansion of OVA-specific IFN-γ-producing $CD8^+$ T-cells which suppressed the development of Th2 cells and thus IgE production, inducing 'tolerance' to OVA in the lung (157). Depletion of $CD8^+$ T-cells during OVA sensitisation caused a decrease in IFN-γ levels and a corresponding increase in IL-4 and IgE production, a phenomenon reversed upon reconstitution with OVA-specific $CD8^+$ T-cells at a later time point (158). Allergen-specific $CD8^+$ T-cells were shown to suppress IgE production and development of an asthmatic phenotype by production of the Th1-promoting cytokine IL-12 (159), whilst IL-18 produced by allergen-specific $CD8^+$ T-cells synergises with IL-12 to promote the development of an IFN-γ-driven response to allergen over a Th2-mediated allergic response (160).

Evidence from both mouse and human studies suggest that the default function of allergen-specific $CD8^+$ T-cells may be to suppress Th2-mediated allergic responses and that these cells are defective in allergic asthmatic subjects. However, in the context of allergic asthma i.e. an IL-4-rich, Th2-promoting environment, $CD8^+$ T-cells activated by viral infection may be skewed towards production of Th2 cytokines, promoting exacerbations of the pre-existing allergic disease.

1.2.9 The role of T helper type 17 (Th17) cells in allergic asthma

Th17 cells are a recently described subset of $CD4^+$ T-cells distinct from Th1 and Th2 cells characterised by production of the pro-inflammatory cytokine IL-17 (161, 162). Th17 cells (or IL-17) have been implicated in human disease, including autoimmune diseases such as multiple sclerosis and tumorigenesis (163). There are several studies implicating Th17 cells in allergic asthma pathogenesis. IL-17 levels are increased in BALF and induced sputum of asthmatic airways with expression localised to T-cells and eosinophils (164). Bronchial fibroblasts isolated from the lungs of asthmatic and normal subjects and cultured *in vitro* with IL-17 produce the pro-fibrotic cytokines IL-6 and IL-1β, suggesting that Th17 cells could be involved in lung remodelling. IL-17 levels in induced sputum were linked to AHR in both asthma and COPD (165). Another study found that IL-17 was produced upon non-specific activation *in vitro* of peripheral blood lymphocytes from both normal and allergic asthmatic subjects, but upon activation with specific allergen, IL-17 was only produced by cells from allergic asthmatics (166), indicating the presence of allergen-specific Th17 cells in the blood of allergic asthmatics. IL-17 has been shown to have an effect on structural cells of the lung *in vitro*: cultures of human ASM cells with IL-17A induced production of eotaxin-1 (167) and in conjunction with IL-1β, IL-17 induced production of IL-8 from the smooth muscle cells (168). In conjunction with tumour necrosis factor α (TNFα), IL-17 stimulates IL-8 and IL-6 secretion from cultured lung epithelial cells (169). Neutrophilia is more associated with severe asthma and a study investigating levels of IL-17 in bronchial biopsies from allergic asthmatics showed that levels were higher in subjects with moderate to severe asthma compared with either mild asthmatic or normal control subjects (170). IL-17A and IL-8 levels were increased in the sputum of asthmatics and their levels correlated with each other and with the numbers of neutrophils in the lung (171). The ability of IL-17 to upregulate IL-8 production in the lung and thus induce lung neutrophilia suggest that IL-17 may be involved in the development of more severe asthma. IL-17 (partly in conjunction with IL-6) upregulates the mucin genes MUC5AC and MUC5B on lung epithelial cells *in vitro*, suggesting a potential role for Th17 cells in mucus hypersecretion (172).

1.2.10 The role of Th1 cells in allergic asthma

Th1 cells produce IFN-γ, function *in vivo* in cellular immunity by promoting responses to infection with virus or other intracellular pathogens and have been implicated in some autoimmune diseases (173). Th1 cells secrete mediators that antagonise development of Th2 cells (174), leading to the proposal that Th1 cells may protect against asthma development through downregulation of Th2-mediated responses. Studies investigating this theory have produced conflicting evidence as to whether Th1 responses protect against or whether they play a role in the development and/or exacerbation of allergic asthma.

Administration of recombinant IFN-γ to the lungs was investigated as a therapy for mild atopic asthma (175). Treatment increased levels of free IFN-γ in the BALF of patients but had no effect on clinical outcome, nor did it increase lung inflammation despite its pro-inflammatory properties. The lack of efficacy of IFN-γ in treating asthma suggested that Th1 cells did not have a particular role in asthma; however, an association between levels of IFN-γ production from activated peripheral blood mononuclear cells (PBMCs) *in vitro* and asthma severity was seen in a cohort of children (176); decreased production correlated with increased disease severity, suggesting that IFN-γ production may be defective in allergic asthma and the extent of this defect may influence disease prognosis. A study of infants investigating the increased incidence of asthma development after acute bronchiolitis identified reduced IFN-γ production in response to IL-2 at the time of bronchiolitis as a risk factor for later development of asthma – infants producing higher levels of IFN-γ were less likely to have developed impaired lung function when examined ~5 months later (177). Numbers of IFN-γ^+ $CD4^+$ and $CD8^+$ T-cells in peripheral blood were lower in children with atopic asthma and not those with non-atopic asthma when compared to healthy controls (178). IFN-γ production was inversely correlated with the extent of lung eosinophilia and AHR, suggesting that IFN-γ and thus Th1 cells may protect against development of asthmatic disease. *In vitro* culture of PBMCs with IFN-γ inhibited allergen-specific proliferative responses in PBMCs from allergic asthmatic subjects through upregulation of Fas/Fas ligand expression and induction of apoptosis in these cells (179). This could be a mechanism by which IFN-γ can control development of allergic disease *in vivo;* the defect in IFN-γ production seen in allergic asthma prevents effective functioning of this pathway, allowing allergen-specific T-cells to persist and mediate disease development.

Monocytes from peripheral blood of allergic asthmatic and healthy control subjects were differentiated into mature DC *in vitro* and DC from allergic asthmatic subjects expressed higher levels of the costimulatory molecule CD86 and secreted lower levels of IL-12 as well as lower levels of the anti-inflammatory cytokine IL-10 (180). Priming naïve T-cells with allergen using these DC induced secretion of higher levels of IL-4 from cells primed by DC derived from allergic asthmatic subjects. The differences in the DC isolated from asthmatic subjects when compared to healthy controls may underlie the promotion of Th2-mediated responses in allergic asthma.

Data from mouse models of allergic asthma support the theory that Th1 cells may be protective in allergic asthma. Lung eosinophilia and T-cell capacity to exhibit a Th2 response was prolonged and induction of allergen-specific IgE was increased in IFN-γ receptor (IFN-γR) knockout mice, which cannot respond to IFN-γ, compared with wild-type mice after induction of allergic inflammation, suggesting that IFN-γ signalling may act to resolve lung inflammation caused by allergen (181). Adoptive transfer of allergen-specific Th2 cells into the lungs of wild-type mice followed by activation through exposure to allergen induced an inflammatory phenotype in the lungs, characterised by lung eosinophilia, AHR and mucus hypersecretion (182). Transfer of Th1 and Th2 cells simultaneously reduced both lung eosinophilia and mucus production, suggesting that Th1 cells may regulate asthma pathology through an IFN-γ dependent mechanism, as these protective effects were not seen in IFN-γR knockout mice (182). Adoptive transfer of Th2 cells alone in a rat model of allergic asthma increased IL-4 expression in the lungs and induced an asthmatic phenotype (AHR and eosinophilia); co-transfer of Th1 and Th2 cells reversed this phenotype, most likely through the effects of IFN-γ, as transfer of Th1 cells alone increased IFN-γ expression in the lungs (183). Th1-mediated stimulation of antigen presentation by lung macrophages induced a Th1- and IFN-γ-mediated response in the lung that inhibited development of Th2-mediated allergic inflammation, possibly via a mechanism inherent to lung macrophages, a mechanism by which allergic disease may be prevented in healthy individuals (184). Expression of T-box expressed in T-cells (T-bet) (a Th1 lineage-specific transcription factor) is decreased in the airways of allergic asthmatic subjects (185) suggesting that the ability of these subjects to induce a protective lung Th1 response to allergen may be impaired. T-bet knockout mice spontaneously develop an allergic asthma-like phenotype in the absence of allergen sensitisation or challenge, suggesting that induction of Th1-mediated immune responses in $CD4^+$ T-cells by T-bet

may be important in protecting against allergic asthma (185). IFN-γ regulates mucous cell metaplasia induced by allergen exposure in a mouse model of allergic asthma by inducing apoptosis of proliferating bronchial epithelial cells, a phenomenon blocked by IL-13 and therefore likely to be impaired in the allergic asthmatic lung (186). IFN-γ was shown *in vitro* to inhibit IL-5-mediated traffic of eosinophils (187), which could be protective against allergic asthma development *in vivo*. A study investigating the ability of TLR4 ligands such as LPS, which promote Th1-mediated immune responses, to modulate allergic disease induction in a mouse model of allergic asthma found that TLR4 agonists prevented development of allergic disease if present at the time of allergen sensitisation (188).

There is also evidence, mostly from mouse models of disease, suggesting that Th1 cells may have a role in asthma pathogenesis and that they may not always protect against allergic disease. Adoptive transfer of OVA-specific Th2 cells into both OVA-sensitised immunocompromised severe combined immunodeficiency (SCID) mice (which lack the ability to mount adaptive immune responses) and into OVA-sensitised wild-type mice induced an allergic asthmatic phenotype, characterised by AHR and eosinophilic inflammation (189). Transfer of OVA-specific Th1 cells into the same mice induced lymphocytic lung inflammation; when transferred simultaneously with Th2 cells, they did not prevent development of the asthmatic phenotype but instead exacerbated it, suggesting Th1-associated mediators were exacerbating the inflammatory response rather than abrogating it. A similar phenomenon was seen after OVA challenge when transferring OVA-specific Th1, Th2, or mixed Th1/Th2 cells into unsensitised wild-type mice (190). In this model, adoptive transfer of Th2 cells alone induced minimal inflammation; a characteristic asthmatic response was only seen when Th1 and Th2 cells were transferred simultaneously. Respiratory viral infections such as influenza exacerbate allergic asthma through promotion of both Th1 and Th2-mediated responses (26). Pulmonary DC isolated from the lungs of these mice after viral clearance and resolution of acute allergic inflammation were transferred into naïve mice and conferred an increase in allergic disease severity upon sensitisation and challenge with allergen, suggesting that viral activation of Th1 cells in the lungs positively regulates Th2-mediated asthmatic responses, at least partly through modulating pulmonary DC. Induction of allergic inflammation in IFN-γ knockout mice in which IFN-γ was constitutively expressed in the lungs under control of a lung-specific gene promoter (to remove any effects of systemic IFN-γ) (191) showed that local IFN-γ increased IL-5

and IL-13 levels and lung eosinophilia and decreased AHR and specific IgE production in comparison to both wild-type and IFN-γ knockout mice. A recent study (192) investigated the effects of a viral 'danger' signal, double-stranded ribonucleic acid (dsRNA) which signals through TLR3 at different doses on sensitisation to inhaled allergen. High and low doses of dsRNA induced lung inflammation; low dose dsRNA induced increased IL-4 production during sensitisation, whilst high dose dsRNA induced increased production of IFN-γ. Inflammation was not induced in TLR3 knockout mice, low dose dsRNA did not induce inflammation in either IL-13 or IL-4 knockout mice and high dose dsRNA did not induce inflammation in IFN-γ knockout mice, suggesting that the two doses of dsRNA induced inflammation via different pathways, hence exposure to allergen during viral infection could induce an asthmatic response through both Th1- and Th2-mediated pathways.

There is evidence both for and against the hypothesis that Th1 cells protect against allergic asthma. It may be that in healthy individuals, Th1 responses in the lung to inhaled allergens protect against asthma and these mechanisms are defective in allergic asthmatic subjects, allowing the Th2-mediated disease to develop unhindered. Once allergic disease has become established, Th1 responses, such as those induced by respiratory viral infection, may exacerbate the asthmatic response to inhaled allergen through production of pro-inflammatory mediators that synergise with mediators produced by allergen-specific Th2 cells, causing a worsening of disease.

1.2.11 The role of regulatory T cells (Tregs) in allergic asthma

Tregs are a specific subset of T-cells that control immune responses including autoimmune reactions to self antigens and responses to exogenous antigens including allergens. There are several types of Treg, such as natural T regulatory cells (nTregs) and inducible or adaptive Tregs, including the T regulatory type 1 (Tr1) cells and T helper type 3 (Th3) cells. Natural Tregs develop in Hassall's corpuscles of the thymus as part of the T-cell repertoire (193) although they may also be induced in the periphery from memory T-cells (194). They express the surface molecules CD4 and CD25 and the Treg lineage-specific transcription factor forkhead box p3 (Foxp3) (195, 196). $CD8^{+}CD28^{-}$ Tregs have also been described in humans (197) and mice (198). Natural Tregs suppress immune responses via several mechanisms including secretion of anti-inflammatory cytokines (IL-10 and TGF-β), and through cell-cell contact via CTLA-4

(an inhibitory member of the CD28 superfamily) (199). Adaptive Tregs are induced in the periphery from naïve T-cells. Tr1 cells are induced through an IL-10-dependent mechanism and produce high levels of IL-10 and TGF-β (200), whilst Th3 cells are induced through oral exposure to antigen and produce high levels of TGF-β (201).

Human studies have suggested that Treg function is impaired in allergic asthmatic disease. $CD4^+$ $CD25^+$ T-cells were isolated from peripheral blood and stimulated with allergen; Tregs from both allergic asthmatic and healthy subjects could suppress proliferation and production of Th1 and Th2 cytokines from autologous allergen-specific $CD4^+$ $CD25^-$ T-cells (202). However, Tregs from a number of the allergic asthmatic subjects could not suppress allergen-specific proliferation or Th2 cytokine production whilst retaining the ability to suppress IFN-γ production, suggesting a potential defect in Treg function in some allergic asthmatic subjects. The balance between allergen-specific Th2 cells and induced allergen-specific Tr1 cells may determine the response to allergen exposure, as Tr1 cells are the dominant allergen-specific T-cell population in healthy subjects whilst allergen-specific Th2 cells dominate in allergic asthmatic subjects (203). $CD4^+$ $CD25^+$ T-cells from healthy atopic subjects show decreased ability to suppress the allergen-specific proliferative response of autologous $CD4^+$ $CD25^-$ T-cells compared to those from healthy non-atopic subjects, and this ability decreases even further in $CD4^+$ $CD25^+$ T-cells from allergic rhinitic subjects during the pollen season (204). This supports the theory that an imbalance between Th2 and Treg cells may underlie development of allergic asthma and suggests that Treg function is impaired in atopic subjects. A study comparing the suppressive ability of Tregs from birch pollen allergic subjects in and out of the pollen season showed that outside of the pollen season, Tregs from allergic subjects could suppress T-cell proliferation and production of Th1 and Th2 cytokines to a similar degree as Tregs from non-atopic subjects (205); however, during the pollen season, the ability of Tregs from allergic subjects to suppress the production of IL-13 and IL-5 diminished significantly whilst suppression of IFN-γ production was retained, suggesting an impairment in Treg function during the pollen season. Glucocorticoids may treat asthma, at least in part, by boosting the ability of Tregs to suppress the Th2-mediated mechanisms underlying allergic asthma (206, 207). Specific immunotherapy increases the numbers of competent $CD4^+$ $CD25^+$ Treg cells, thus increasing suppression of the allergic response and tolerance to allergen (208, 209). TNF-α may inhibit Treg function in allergic asthma as it downregulates Foxp3 expression in Tregs *in vitro* and decreases

their suppressive capacity (210). Administration of anti-TNF-α to cultured Tregs from allergic asthmatic subjects increased Foxp3 expression and suppressive capacity. TNF-α is overexpressed in the airways of allergic asthmatic subjects and several of its biological functions may exacerbate asthmatic disease (211). The ability of anti-TNF-α to not only antagonise these functions but also to increase Treg functional capacity may underlie its efficacy in treating asthma.

1.2.12 The role of Th2 cells in allergic asthma

It is now widely accepted that allergic asthma is a disease mediated primarily by the actions of cytokines produced by Th2 cells, such as IL-4 (16), IL-5 (212), IL-9 (213) and IL-13 (214, 66). There is evidence from human studies that $CD4^+$ Th2 cells are the central mediators of allergic asthma. Analysis of T-cell activation and cytokine production in BALF of allergic asthmatics after allergen challenge showed that $CD4^+$ T-cell activation occurred in the absence of appreciable $CD8^+$ T-cell activation and there was an increase in the number of IL-4 and IL-5 $mRNA^+$ BALF cells, which were predominantly T-cells (215). Increase in these cytokines correlated with eosinophil number in BALF after challenge, suggesting that cytokines produced by activated Th2 cells mediate events in the LAR such as eosinophilic influx into the lungs. Spontaneous IL-5 production without allergen stimulation is increased in BALF cells and PBMCs from both atopic and non-atopic asthmatic groups compared to atopic and non-atopic control groups and correlates with lung eosinophilia and airway narrowing (216). Upon allergen stimulation, both atopic groups (asthmatic and non-asthmatic) responded to a similar extent in terms of T-cell activation, but the increase in IL-5 production was greater from both BALF cells and PBMCs in the atopic asthmatic group. Analysis of cytokine production from BALF cells taken after specific allergen challenge in allergic asthmatic subjects showed increased levels of IL-13 and decreased levels of IFN-γ compared with baseline (217). T-cell clones derived after diluent challenge produced IL-13, IL-4 and IFN-γ, whilst those derived after allergen challenge secreted IL-3, IL-4, IL-5 and IL-13, suggesting that allergen challenge in allergic asthmatic subjects induces a strong Th2-mediated response. Expression levels of T-bet and the Th2 lineage-specific transcription factors GATA-binding protein 3 (GATA-3) and c-maf increased in BALF T-cells after allergen challenge in allergic asthmatic subjects (218). Expression of c-maf correlated with the number of $IL\text{-}4^+$ $CD4^+$ T-cells in BALF and the amount of IL-5 secreted into BALF. $IFN\text{-}\gamma^+$ T-cell numbers decreased in response to

allergen challenge, suggesting the induction of a dominant Th2-mediated response upon allergen exposure in allergic asthmatic subjects.

There is also evidence suggesting a role for allergen-specific T-cells in induction of the LAR. The LAR was previously shown to depend upon allergen-specific IgE (219), but a later study demonstrated that the LAR was IgE-independent in asthmatic patients sensitive to house dust mite allergen (220). Intradermal challenge of asthmatic patients with peptide derivatives of the major cat allergen Fel d 1 showed that an LAR could be induced without a preceding EAR (221). A similar result was seen when challenge with peptide occurred via inhalation (222). Such peptides cannot cross-link IgE on the surface of mast cells due to their short length (less than 20 amino acids) suggesting IgE is not necessary for LAR induction. As the response to peptide challenge was dependent upon presentation by MHC class II molecules, this suggested that the LAR was mediated by allergen-specific T-cells. Allergic asthmatic patients were analysed for T-cell activity and BHR in response to inhaled Fel d 1-derived peptides (223); in those patients who responded to peptide challenge (i.e. a LAR was induced), there was an increase in $CD4^+$ T-cell number in BALF and bronchoscopy sections, whilst numbers of other inflammatory cell types remained constant.

Levels of Th2 cytokines are increased in the airways of allergic asthmatic subjects. Levels of IL-4 in exhaled breath condensate are significantly higher in children with untreated allergic asthma than either normal control subjects or children with steroid-controlled asthma (224). Levels of IL-5 mRNA in the cells of BALF and bronchial biopsy specimens are increased in patients with allergic asthma compared to normal controls, with more than 70% of the mRNA signals originating from $CD4^+$ and $CD8^+$ T-cells, predominantly from in $CD4^+$ cells (18). Levels of IL-9 mRNA are elevated in the airways of allergic asthmatic subjects compared with healthy controls even under baseline conditions (225). Baseline levels of IL-9 are low in allergic asthmatic and normal control subjects but after challenge, IL-9 levels (mRNA and protein) increase in the allergic asthmatic group and correlate with the percentage of eosinophils in BALF (226). Lymphocytes are the primary source of IL-9 and the correlation with eosinophil number suggests that IL-9 may play an important role in the LAR. Numbers of IL-13 $mRNA^+$ cells are increased in the bronchial mucosa of both atopic and non-atopic asthmatics compared with atopic and non-atopic non-asthmatics (227), and levels of IL-13 mRNA are related to numbers of eosinophils in the bronchial mucosa.

Evidence from mouse models of allergic asthma supports the role of Th2 cells in asthma. Lack of signal transducer and activator of transcription-6 (Stat-6) expression, a transcription factor involved in signalling through the IL-4 pathway, prevents the differentiation of activated T-cells into Th2 cells and the production of IgE from B-cells (228, 229). Stat-6 knockout mice do not develop AHR, mucus hypersecretion or show increased IgE production in response to allergic sensitisation, and there is less eosinophilia than in wild-type mice (230). Inhibition of Th2 development in these mice prevents development of allergic disease, suggesting the development of allergic disease in this mouse model is Th2 cell-dependent. $CD4^+$ T-cell-depleting monoclonal antibodies inhibit the development of AHR, eosinophilia, IgE production, IL-13 and TGF-β secretion, goblet cell hyperplasia and lung fibrosis in a mouse model of allergic asthma (231). Depletion of $CD8^+$ T-cells had no effect on disease.

Activated allergen-specific Th2 cells in sensitised individuals secrete IL-4, IL-5, IL-9 and IL-13 and through these cytokines mediate allergic asthma pathogenesis. IL-4 induces class-switching in allergen-specific B-cells to produce IgE, which primes tissue-resident mast cells and basophils recruited from the periphery for activation upon subsequent re-exposure to allergen (58). It is also required for the development of a Th2-mediated response to antigen (232) and promotes differentiation of newly-activated T-cells into Th2 cells (233), thus increasing polarisation of the lung environment towards a Th2 phenotype, favouring continuing pathogenesis of the disease. The IL-4 receptor shares a common subunit with the IL-13 receptor (234) which may explain why many of the functions of IL-4 and IL-13 overlap.

IL-5 induces migration, differentiation and survival of eosinophils in the lung. IL-5 induces eosinophil differentiation from haematopoietic precursors in culture and promotes their survival (235), migration into the airways (236) and activation (237). During sensitisation to allergen, IL-5 production causes airway eosinophilia (238), priming the lungs with an inflammatory cell which becomes activated upon subsequent allergen challenge, as described in section 1.2.4.

In vitro cultures of human lung mast cells indicate that IL-9 production by Th2 cells acts in conjunction with the mast cell growth factor, stem cell factor (SCF), to induce proliferation, expansion, survival (239) and differentiation into mature effector cells (240). It may induce mucus hypersecretion in the lung during tissue repair (241). IL-9

induces differentiation of human bronchial epithelial cells into mucus-secreting goblet cells *in vitro*, both in the context of tissue repair and when cells are not fully differentiated. As constant tissue injury and repair processes are a feature of allergic asthma, IL-9 may promote mucus hypersecretion.

IL-13 induces class switching in allergen-specific B-cells to produce IgE and IgG4 using a mechanism similar to, but not dependent upon, IL-4 (66). It is critical to the development of allergic airway inflammation and AHR in mouse models of allergic asthma – blocking IL-13 using a soluble IL-13-receptor molecule attenuated the allergen-induced asthmatic phenotype, shown as decreased AHR, lung inflammation, lung eosinophilia and goblet cell hyperplasia (242). Administration of exogenous IL-13 causes an asthmatic phenotype independently of T-cell activation, but the IL-4R (shared by IL-4 and IL-13) is required for disease induction. Another study used the same method of blocking IL-13 but also analysed the effect of IL-13 blockade on levels of allergen-specific IgE (243). As IL-13 blockade occurred after allergen sensitisation, its lack of effect is possibly due to IgE production having already occurred, supported by the finding that administration of exogenous IL-13 to unprimed mice induces an increase in IgE production. Human ASM cells express receptors and respond to IL-4 and IL-13, as shown by phosphorylation of downstream molecules such as Stat-6 and the mitogen-activated protein kinase (MAPK) extracellular-signal related kinase (ERK) (244). IL-4 and IL-13 caused phosphorylation of these proteins at different times, suggesting that they use different mechanisms to signal in ASM cells. IL-13 reduces ASM cell responsiveness to the β2-agonist isoproterenol, whilst IL-4 has no effect, indicating a potential underlying mechanism for the effects of IL-13 on mediating AHR (244).

1.3 Mouse models of allergic asthma

1.3.1 The principles of molecular cloning and their use in animal models of disease

Recombinant DNA technology has revolutionised the study of DNA and the genes encoded within it by providing simple techniques through which they can be analysed, identified and manipulated. Restriction endonucleases (restriction enzymes) are produced by bacteria, each strain producing one or more unique enzymes, as a defence

against infection with bacteriophages (245). The enzymes cut DNA at specific palindromic sites (creating blunt or overhanging 'sticky' ends) within the sequence, destroying the genetic material of invading viruses (the bacterium's own DNA is methylated to protect it from degradation). The discovery of DNA polymerase in *E.coli* (246) and the observation that DNA can re-anneal after being denatured into single strands by heating (247) provided a way of replicating DNA *in vitro,* through use of an appropriate primer (248). Such primers can be synthesised chemically or through use of the polymerase chain reaction (PCR) (249). The finding that viral and bacterial plasmid vectors can be used to massively amplify specific sequences of DNA (250), inserted by digestion with restriction enzyme and ligation using the bacterial enzyme DNA ligase (251), led to the routine use of DNA cloning in the study of genetics. DNA from an organism is digested into small fragments using a particular restriction enzyme before ligating these fragments into a vector digested using the same enzyme. Vectors are transferred into target bacteria either via viral infection or through transformation (use of calcium chloride and heat shock to temporarily permeabilise bacterial cell walls to DNA) (252). Due to the presence of antibiotic resistance genes in the vectors (253), only successfully transformed bacteria will be able to grow on agar containing this antibiotic, thus only those bacteria carrying a DNA sequence of interest should form colonies (bacteria transformed with empty vectors will also form colonies but can be distinguished if inserted DNA sequences disrupt a reporter gene e.g. β-galactosidase in the plasmid – expression of this gene can then be detected through use of a colorimetric substrate; colonies containing empty plasmids will appear coloured). This produces DNA libraries - similar libraries can be constructed from mRNA products of a cell using the viral enzyme reverse transcriptase to convert the mRNA into complementary DNA (cDNA) (254). These libraries are used in a variety of ways; for example, use of labelled DNA probes can locate genes of interest on chromosomal DNA (or cDNA), allowing further characterisation of the gene (255). Probes were initially derived from the amino acid sequence of proteins using the genetic code (256) and with the advent of robust DNA sequencing methods (257), from DNA sequences themselves. This allowed, for example, the identification of genes related to one already known or conserved genes in other species (258) and often aided in the study of diseases caused by gene mutations, such as cystic fibrosis (259). Cloning techniques have also been instrumental in sequencing entire genomes from particular organisms, including humans (260).

DNA cloning techniques have proved crucial in the field of DNA engineering. These techniques allow researchers to manipulate DNA to produce new recombinant sequences allowing improved study of genes and products and the regulation of transcription and translation. Use of restriction enzymes allows the combination of gene segments that would not otherwise exist, allowing use of reporter genes (e.g. green fluorescent protein) to monitor gene expression under different conditions and in different cell types (261) and to aid in the identification of gene promoter and repressor regions (262). Gene sequences can be altered by site-directed mutagenesis, e.g. using PCR primers which change the sequence of a gene at one or more base pairs (263), and use of expression vectors (264) to express the mutated products (or products of any gene) in cells allows investigation into the function of the resulting protein. Expression vectors can also be used to produce large quantities of protein encoded by a particular gene allowing easier characterisation of protein structure and interaction.

Another powerful use for DNA cloning techniques is in the generation of transgenic organisms (265). Transgenesis can be used to overexpress a particular protein to determine its effect in excess (99), to express a mutant form of a protein to determine its function (266) or in some cases to 'knock out' expression of a particular gene to assess the effect of its absence (98). Such organisms can be particularly useful in the study of human disease where transgenic expression of the gene or genes (mutant or otherwise) thought to be involved in disease pathogenesis can be used to more accurately model the disease in an *in vivo* setting (98, 99).

1.3.2 The use of animals in human disease modelling

To fully characterise and study the aetiology of human diseases, it is necessary to carry out studies in an *in vivo* system or to study organ and tissue systems further *in vitro*. As these studies would be unethical in humans, animal models of disease have been created to allow disease to be studied in detail. For animal models to be useful, accurate models of human disease, it is preferable that they share the same pathways of initiation and pathogenesis. Such models can be generated in many ways dependent upon the disease being modelled. For example, models of viral infection involve exposing the animal to the same pathogen as causes disease in humans, usually by the same route and analysing the disease induced, which, in a successful model, mimics the disease as it occurs in humans. A number of these models exist, such as influenza infection models

(267) and models of respiratory syncytial virus (RSV) infection (268). Use of such models has allowed researchers to identify underlying mechanisms of pathogenesis and the immune responses raised against such pathogens (267, 268, 269) as well as the effect of co-infection with more than one pathogen, e.g. concurrent influenza and bacterial infections (270). Other models of infectious disease include models of malaria (271) and *Schistosoma mansoni* infection (272).

Other diseases are modelled using chemical or physical means to induce a disease phenotype in animals, for those diseases where the underlying cause is not an infectious agent, such as epilepsy, where injection of kainic acid into the hippocampus of mice induces a disease syndrome similar to temporal lobe epilepsy in humans (273). Such a model has allowed testing of anti-epileptic therapies for efficacy (274) as well as helping to identify mechanisms leading to disease development (275). Models of ischaemic stroke have been developed using direct surgical occlusion of cerebral arteries, giving a phenotype which is close to that seen in human stroke (276). Whilst not modelling the route of disease induction exactly, these models still give useful information as to the underlying disease mechanisms and lead to better understanding of the disease and the potential for developing effective therapies.

Animal models have also been used to extensively study those diseases caused by dysregulation of the immune system, such as allergic and autoimmune diseases. The most widely used model of allergic asthma is the OVA model which will be described in more detail in Sections 1.3.3-1.3.5. An example of an autoimmune disease, where a failure of the adaptive immune response to recognise self antigens as self leads to destruction of particular tissues, which has been modelled in animals is multiple sclerosis (as experimental autoimmune encephalomyelitis, or EAE) (277, 278). These original models involved systemic injection of mice with an antigen involved in the induction of disease (allergen protein for allergic asthma, the self-antigens myelin basic protein or proteolipoprotein for EAE), as these diseases do not occur naturally in mice. Such immunisation led to the induction of syndromes similar to the disease in humans, despite lacking a similar mode of induction. In the case of EAE, a disease phenotype involving progressively severe loss of limb function and paralysis, inflammation of the CNS, nerve demyelination and axonal loss, similar to the pathology seen in multiple sclerosis, was induced. Such models have been instrumental in identifying the mechanisms at work in these diseases, and provide a means of finding targets for

therapeutic intervention. An example of a naturally-occurring mouse model of autoimmune disease is the non-obese diabetic (NOD) mouse, which develops spontaneous type I diabetes with many of the features of the human disease, including the presence of autoreactive T-cells and B-cells and islet-specific autoantibodies which shows similar genetic linkages to those seen in humans (279). This strain has been widely used to study the human disease and develop potential therapies.

As well as the use of wild-type animals in the creation of models of human disease, the advent of transgenic technology (265) has allowed further study into mechanisms underlying disease pathogenesis in a number of ways. The ability to genetically manipulate animals (usually rodent) to induce specific mutations or to overexpress or knock out expression of certain genes in a controlled fashion allows the impact of various proteins and genes on disease phenotype to be examined and may lead to the production of refined models of disease. Examples of the use of such transgenic animals in the study of allergic asthma will be discussed in Section 1.3.5, with reference to transgenic mice either overexpressing or lacking expression of the Th2 cytokines IL-4, IL-5, IL-9 and IL-13. Another example of the use of transgenic mice to produce an improved model of disease is the use of humanised TCR transgenic mice in EAE (280, 281, 282, 283). Such mice express a human TCR isolated through analysis of T-cell lines derived from human MS patients and the human MHC class II molecule expressed by the patient which is known to present peptide epitopes from the autoantigen responsible for causing the disease. These mice provide improved models of disease; in some cases, the mice develop EAE spontaneously with a very similar progression of disease to the human MS (282, 283).

As described previously, the study of disease in humans is difficult due to ethical and logistical constraints; those investigations that can be carried out are limited in scope. Most studies of allergic asthma in humans have been limited to *in vitro* culture of PBMCs or cells taken from bronchial biopsies or BALF, or histochemical analysis of sections of human lung tissue. Such studies give information of a limited nature; histological analysis gives a view of a single instant in time, whilst *in vitro* cultures lack the complicated interplay of mediators and other cell types found *in vivo*. Animal models of allergic asthma have been widely used to more closely study the interactions and disease mechanisms that lead to the development of allergic asthma in humans. Whilst models have been developed using animals such as the guinea pig (284) or rat

(285), most current models have been developed in the mouse, for several reasons. Their small size, ease of housing and the ability to breed large numbers of mice makes them ideal for use; the commercial availability of inbred strains with defined immunological properties and genetic similarity allow experiments to be well controlled. There are also a greater number of reagents, such as monoclonal antibodies or soluble cytokine receptors, available for use in mice than for any other species, and the technology available for transgenesis and gene knockdown is more advanced in mice than other species.

1.3.3 The use of ovalbumin (OVA) as an allergen in mouse models of allergic asthma

Initial protocols to develop allergic asthmatic-like disease in mice involved two intraperitoneal sensitisation injections of OVA adsorbed onto aluminium hydroxide (alum) approximately 5 days apart (286, 287). Sensitisation was followed by aerosol challenge with nebulised OVA 12 days after the first injection, and Garlisi et al. (249) also re-challenged 1, 2 or 3 weeks later. Kung et al. (286) found significant airway and BALF eosinophilia in OVA-challenged mice 24 hours post-challenge which persisted for up to 10 days. Elevated levels of serum IgE, mucus hypersecretion in the airways, epithelial damage and submucosal oedema were also features of this model, all of which are consistent with human allergic asthma. Garlisi et al. (287) showed similar findings after one challenge with OVA aerosol. They investigated T-cell influx into BALF after one challenge, showing an increase in cell numbers, predominantly $CD4^+$ T-cells, persisting for up to one week after challenge. Th2-type cytokine mRNA levels (IL-4 and IL-5) in lung tissue were also increased after one challenge, with no corresponding increase in IFN-γ. Lung function changes 24 hours after challenge in response to acetylcholine showed an increase in BHR in OVA-challenged C57BL/6 X DBA/2 (B6D2F1) male mice. When mice were re-challenged after 1 week, lung inflammation was greater in terms of eosinophil and T-cell influx. A large influx of predominantly $CD4^+$ T-cells with an activated memory phenotype ($CD44^+ CD45RB^{low}$) was seen up to 3 days after the second challenge after which T-cell numbers declined to the same level as that after only one challenge. Higher levels of IL-4 and IL-5 mRNA were also seen, and responsiveness to acetylcholine was increased. There were no noticeable changes in extent of epithelial damage or mucus hypersecretion. The phenotype induced in the mice by the protocols above, of eosinophilic and lymphocytic inflammation in the lung,

increased levels of serum IgE and BALF Th2-type cytokines, lung epithelial damage and mucus hypersecretion, along with an increase in BHR, is consistent with human disease. A different model involved sensitising male Balb/c mice with intraperitoneal injections of OVA in saline, and challenging 4 weeks later with aerosolised OVA (288). Some features of allergic asthma were seen, such as increases in total and OVA-specific serum IgE, an increase in mucosal exudation of macromolecules into BALF and increased numbers of degranulated mast cells in the lung. A bronchoconstrictive response within 15 minutes of challenge was also seen, similar to the EAR in humans. Lung function was measured 12 and 24 hours after challenge and showed an increase in responsiveness to methacholine. This model did not elicit any inflammatory cell influx into the lungs and BALF, and only small mononuclear cell infiltrates were seen in the lungs of some OVA-challenged mice. As such, models using alum as an adjuvant for sensitisation have predominated.

Other models have used different routes and methods of allergen sensitisation to induce disease that more faithfully mimics development of disease in humans. One of the main criticisms of the original models is use of alum as no such adjuvant is required for human sensitisation and because alum may increase non-specific Th2-mediated responses to antigen (289), hence could be driving an artificial response in the lungs of antigen-alum sensitised mice. Initial experiments without use of alum as an adjuvant failed to induce lung inflammation (288), but later studies generated an allergic inflammatory response in the lungs of sensitised mice without use of an adjuvant. A model in Balb/c mice, requiring intraperitoneal sensitisation with OVA solubilised in saline solution and one intranasal challenge with OVA induced an allergic asthmatic-like disease phenotype characterised by an increase in AHR, serum IgE and IgG1, BALF eosinophilia, upregulated production of IL-4, IL-5 and IL-13 in BALF and mucus hypersecretion in the airways (230). A novel model used subcutaneous implants of heat-coagulated hen's egg white as a source of allergen in Balb/c x A/J mice to model persistent allergen exposure (290). Challenge with intratracheal OVA 14 days later induced an asthma-like phenotype in the lung, characterised by eosinophilic and lymphocytic influx into lung tissue and BALF persisting for up to 3 weeks after challenge, mucus hypersecretion and the suggestion of bronchoconstriction in the airways from histological analysis.

Whilst these models have identified a number of pathways and mediators important in

asthma, they have been criticised as not being accurate models of human disease. One criticism is that the method and route of sensitisation is not the same as for humans, where sensitisation occurs via exposure to low doses of allergen in the airways with challenge occurring via the same route. Sensitisation using low dose OVA aerosols in mice induces unresponsiveness to further allergen challenge (291). Another criticism of some models is their lack of a chronic phase; most of the original models induced an acute form of disease which lacked the hallmarks of chronic disease seen in humans, in particular, lung remodelling. A study addressing these issues investigated the importance of mouse strain on development of allergic asthma-like disease. Sensitisation and challenge occurred via repeated intranasal administration of OVA to mice 3 times a week for 4, 8 or 12 weeks. Disease was induced by this method in one strain only, A/J (292). At all time points of analysis in A/J mice, OVA exposure induced a massive influx of eosinophils into the lung, an increase in serum IgE, increased inflammatory infiltrates into the lung mucosa, goblet cell hyperplasia and increased mucus secretion, increased secretion of IL-4, IL-5 and IL-13 into BALF and local lymph nodes and increased AHR. This model showed signs of lung remodelling in response to chronic challenge with allergen, such as increased collagen deposition in the basement membrane, thickening of airway walls and ASM layer and an increase in BALF TGF-β levels. This model demonstrates allergen sensitisation and challenge through a similar route to that believed to occur in humans and induction of chronic disease by repeated allergen exposure leading to lung remodelling. It also demonstrates that the strain of mouse used can have a significant impact on the extent of disease induction; no disease was induced using this protocol in Balb/c or C57BL/6 mice.

A model of chronic disease induction has been developed in Balb/c mice, involving sensitisation through intraperitoneal injection of OVA adsorbed onto alum, followed by challenge with aerosolised OVA for 3 days/week for up to 8 weeks (293). Increasing duration of exposure to OVA challenge increased the extent of disease, characterised by increasing serum levels of total and OVA-specific IgE, increasing tracheal and airway eosinophilic and lymphocytic inflammation, increased AHR in response to methacholine, increasing goblet cell hyperplasia, subepithelial fibrosis in the airways and epithelial thickening in the trachea accompanied by increased collagen deposition beneath the epithelium. The latter features are characteristic of lung remodelling. Another protocol of chronic allergic airway disease induction was developed in Balb/c mice, involving sensitisation through two intraperitoneal injections with OVA

solubilised in saline, followed by challenge on two consecutive days with aerosolised OVA one week later (294). Mice were allowed to recover from the induced acute disease and then re-challenged with aerosolised OVA at time points from 3-18 months after initial sensitisation, allowing both acute and chronic disease induction to be modelled and analysed. Analysis of disease induction after the acute phase of the protocol showed a typical disease phenotype i.e. infiltration of eosinophils and lymphocytes into BALF and peribronchial and perivascular spaces, goblet cell hyperplasia and mucus hypersecretion, increased serum IgE and increased AHR. These responses were greater in magnitude upon re-challenge at all time points analysed except for AHR, which remained increased to the same extent at all time points, and mucus production, which peaked when re-challenge occurred 3 months after initial sensitisation. When re-challenge with OVA occurred nearly 18 months after original induction of acute allergic airway disease, *in vitro* stimulation of splenocytes and mediastinal lymph node cells with OVA induced production of high levels of IL-4 and IL-5, suggesting the presence of a pool of long-lived antigen-specific memory T-cells in this model. T-cells isolated from the lung nearly two years after OVA sensitisation had a memory phenotype ($CD44^+$ $CD45RB^{low}$ $CD62L^{low}$ $CD25^{low}$), suggesting that T-cell memory persists in the lungs of mice that have recovered from acute allergic airway disease. Whilst this model induced a chronic form of allergic airway disease, there was no analysis of the effects on phenomena associated with chronic disease, such as lung remodelling.

1.3.4 Adoptive transfer of OVA-pulsed APCs or OVA-specific T-cells as a means of inducing allergic airway disease in mice

A number of studies have investigated the ability of DC pulsed with OVA *in vitro* to act as APC and induce disease pathology in the lung when transferred into naïve mice. Intratracheal administration of OVA-pulsed DC followed two weeks later by challenge on seven consecutive days with aerosolised OVA induced significant eosinophilic and lymphocytic (predominantly $CD4^+$ T-cells) infiltration into BALF, peribronchial and perivascular eosinophil-rich inflammatory infiltrates, goblet cell hyperplasia and mucus hypersecretion (54). Levels of IL-4 and IL-5 were increased in BALF and mediastinal lymph nodes, predominantly localised to $CD4^+$ T-cells.

Others have investigated the ability of adoptively transferred OVA-specific $CD4^+$ T-

cells to induce disease in naïve recipients upon challenge with OVA. Splenocytes were isolated from unsensitised mice and cultured for 3 days in the presence of OVA before transfer into naïve recipients. (295). After a single challenge with aerosolised OVA 3 days later, a disease phenotype indicative of allergic airway disease was induced, comprising eosinophilic and lymphocytic influx into BALF, an increase in IL-5 secretion into BALF and an increase in serum IgE. The effect of transferred cells on lung eosinophilia was dose-dependent and mediated by $CD4^+$ T-cells with an activated memory phenotype ($CD4^{high}$ $CD62L^{low}$ $CD25^+$); depletion of cells with this phenotype before transfer abolished eosinophilia and IL-5 production. A similar protocol adoptively transferred purified cultures of OVA-specific T-cells differentiated *in vitro* into Th1 or Th2-type cells (296). T-cells were originally isolated from a strain of mice, DO11.10, that transgenically express a TCR specific for a particular epitope of the ovalbumin protein, $OVA_{323-339}$ (297). $CD4^+$ T-cells isolated from the spleens of DO11.10 mice and cultured in the presence of $OVA_{323-339}$ and either Th1- or Th2-polarising cytokines produced Th1 and Th2 OVA-specific T-cell cultures which were transferred into recipient naïve wild type Balb/c mice, followed by challenge on consecutive days for 7-10 days starting 1 day after transfer. Transfer of OVA-specific Th2 cells induced moderate lung inflammation, primarily eosinophilic with some lymphocyte infiltration and increased mucus production upon challenge, consistent with an allergic asthma-like phenotype. Transfer of OVA-specific Th1 cells induced moderate, predominantly neutrophilic, lung inflammation and no mucus production upon challenge. T-cells of both types trafficked to the lungs and the draining lymph node.

1.3.5 Use of the OVA model in investigating disease pathogenesis in allergic asthma

The various models of allergic asthma using ovalbumin as a model allergen have allowed investigation into the mechanisms and mediators governing the development and exacerbation of allergic asthma. Work in human studies and mouse models has identified certain molecules and cell types which are implicated in causing or worsening of the disease. The OVA model allows further studies into the mode of action of these mediators, either through the ability to study or modulate their function in an *in vivo* system, or, often more informatively, through the ability to genetically manipulate mice to either overexpress or delete expression of a gene. It is possible to control the

expression of certain molecules so that they are only expressed in certain parts of the body or only at certain times, for example when the animals are treated with a substance that switches on or off expression of a gene. Entire cell lineages can be deleted through deletion of a specific gene crucial to their differentiation or development. The effect of the overexpression or absence of each mediator on the disease phenotype (e.g. it may worsen, abolish or cause no change to the phenotype) can give further insight into the processes mediated by the cell or molecule. Many such experiments have been carried out using the OVA model, investigating the causes behind many of the characteristic hallmarks of asthma, such as AHR, lung inflammation and airway remodelling. Examples of these experiments are described below as an illustration of the use of animal models of human disease to elucidate disease mechanisms and identify therapeutic targets.

The OVA models have been extremely informative in elucidating the role of Th2 cytokines in allergic asthma; many of the findings described in Section 1.2.12 were discovered using these models. Additional experiments in cytokine gene knockout and transgenic mice have added to this knowledge. The lack of disease induction by OVA sensitisation seen in IL-$4^{-/-}$ (298) and IL-$5^{-/-}$ (299) mice highlights the importance of these cytokines in allergic lung disease; disease phenotype was restored in IL-$5^{-/-}$ mice by adoptive transfer of wild-type OVA-specific Th2 cells (238) or viral expression of IL-5 (299). Blocking both IL-4 and IL-5 in the OVA model in Balb/c mice was required to abolish all features of allergic asthma (300). Induction of allergic airway disease using OVA in IL-$9^{-/-}$ mice was relatively unaffected by the lack of IL-9 (301), despite the efficacy of an IL-9 blocking antibody during sensitisation in decreasing the development of allergic airway disease (302). Differences in methodology or strains (C57BL/6 x DBA/2 (302), Balb/c (301)) may explain this discrepancy. IL-$13^{-/-}$ mice fail to develop AHR in response to OVA sensitisation and challenge, but other characteristics of allergic airway disease such as lung eosinophilia, elevated serum IgE and increased production of IL-4 and IL-5 in the lung remain (82). Administration of recombinant IL-13 early in the sensitisation phase could reconstitute the AHR response. Blocking IL-13 function using a soluble IL-13R molecule attenuated induction of disease by OVA sensitisation (242, 243). The effects on disease induction by OVA of gene depletion of IL-13 was compared with gene depletion of four major Th2-associated cytokines (IL-4/5/9/$13^{-/-}$) (303). Whilst AHR, ASM hyperplasia and increase in serum OVA-specific IgE were abolished in both strains, goblet cell hyperplasia and

lung eosinophilia were completely abolished in the quadruple knockout mice but only partially attenuated in IL-13$^{-/-}$ mice, suggesting that some allergic disease features are dependent upon IL-13, whilst others also require action of at least one other Th2-related cytokine. Transgenic overexpression of lung-specific IL-5 (304), IL-9 (305, 306) and IL-13 (307) induces a phenotype similar to allergic disease (AHR, lung eosinophilia, goblet cell hyperplasia, increased serum IgE and Th2 cytokine expression in the lung, and some features of lung remodelling) without any requirement for allergen sensitisation, indicating that it is the actions of these cytokines that induce many features of allergic lung disease in these models.

The OVA model has been used to track changes ocurring during a LAR (308). Mice were intraperitoneally sensitised with OVA and challenged with OVA aerosol, before being allowed to recover for 10 days. Mice were then provoked by nebulisation with high dose OVA and changes in lung function were monitored over the next several hours. A decrease in lung function was observed beginning about 90 minutes after provocation and persisting for up to 6 hours, peaking at approximately 4 hours, similar to the LAR seen in humans. Changes in the lung corresponding to the decrease in lung function were investigated; a significant influx of lymphocytes and eosinophils into BALF was seen, increasing up to 24 hours after provocation, followed by a sharp decrease in cell number at 48 hours. Significant mucus secretion was seen in lung sections taken 6 hours after provocation at the end of the observed late phase response. Cytokine levels in BALF and serum were analysed at various time points – a general increase in concentration of the Th2-type cytokines was seen up to 6 hours in BALF before a gradual decline to 48 hours, with no change in IFN-γ; IL-13 levels in serum increased gradually up to 24 hours and then declined whilst a sharper increase was seen in IL-5 levels up to 6 hours, after which levels declined more gradually. Levels of serum IL-4 and IFN-γ were not significantly changed by provocation. Expression of Th2 cytokines in lung tissue was significantly increased 6 hours post-provocation. The role of T-cells in the induction of the late phase response was investigated by treating OVA-sensitised and challenged recovered mice with CD4 or CD8 depleting antibodies. Depletion of CD4^{+} T-cells abolished the late-phase response indicating that CD4^{+} T-cells are responsible for induction and mediation of the late phase response in this model of allergic asthma.

The advent of chronic disease induction protocols using OVA has allowed investigation into the underlying mechanisms and mediators involved in airway remodelling, thought to be induced in humans by chronic exposure to allergen. The role of the pro-fibrotic cytokine TGF-β has been investigated in chronic models of disease to ascertain its role in the development of allergic airway disease. Administration of an anti-TGF-β monoclonal antibody to mice in which allergic airway disease had already been induced by OVA sensitisation and challenge at the same time as further challenges with allergen prevented deposition of extracellular matrix material in the peribronchiolar regions, ASM cell proliferation and mucus production from goblet cells, but had no effect on airway inflammation or Th2-type cytokine production established during the acute phase of the protocol (309). This implicated TGF-β in the development of lung remodelling in chronic allergic airway disease. Thickening of lung epithelium, ASM hyperplasia and pulmonary fibrosis can make airway walls stiffer and more prone to hyperreactivity, suggesting a role for TGF-β in mediating AHR. Levels of the TGF-β1 isoform increased in BALF after OVA sensitisation and challenge, peaking approximately 7 days after the initial challenge, and being primarily produced by airway epithelial cells (310). Administration of anti-TGF-β1 had no effect on eosinophilic lung inflammation in OVA-sensitised and challenged mice; production of IL-4 and IL-13 was enhanced in the absence of TGF-β1. Blocking TGF-β1 function decreased deposition of subepithelial collagen and lessened airway remodelling, but increased AHR. This suggests that whilst TGF-β1 is involved in development of lung remodelling in allergic airway disease, it may also suppress development of AHR induced by allergen exposure, ameliorating the clinical signs of allergic asthma and therefore antagonising TGF-β signalling as a means of asthma therapy may not be advisable as it could lead to worsening lung function.

1.3.6 The use of house dust mite allergens in a mouse model of allergic asthma

A criticism of using ovalbumin as a model allergen in mice is that humans do not become sensitised to it, hence it is irrelevant to the development of allergic asthma in humans. Models using an allergen known to cause allergic asthma in humans have been developed, many making use of house dust mite (HDM) allergens, particularly the major allergen from *Dermatophagoides pteronyssinus*, Der p 1.

A number of protocols are used to induce allergic airway disease in mice using HDM extract or Der p 1 protein. Protocols were developed along the same lines as the original OVA protocols, using intraperitoneal sensitisation with HDM extract followed by airway challenge with HDM extract. Sensitisation in one of these protocols occurred with HDM extract in complete Freund's adjuvant (CFA), a stimulator of cell-mediated immunity, and also involved intraperitoneal injection of pertussis toxin to stimulate an enhanced IgE response to allergen (311). This was followed by challenge once a week for seven weeks with intranasally-administered HDM extract and induced a phenotype consistent with human allergic asthma, namely induction of an inflammatory response in the lungs, primarily eosinophilic and lymphocytic and an increase in serum HDM-specific IgE. An increase in HDM-specific proliferation was seen in T-cells isolated from draining lymph nodes 10 days after the last sensitisation injection. Another protocol administered Der p 1 adsorbed onto alum intraperitoneally at high, medium or low dose protein, followed 2 weeks later by intranasal challenge with high, medium or low dose Der p 1 protein, after which disease induction was analysed (312). Disease induction was evident using even low doses of Der p 1; induction was most efficient with either high or low dose Der p 1 and was characterised by the presence of predominantly eosinophilic alveolar and peribronchial cell infiltrates, and increased Der p 1-specific IgE levels. Mucus production was marked, often totally obstructing some airways. These features are characteristic of allergic asthma.

Adoptive transfer of PBMCs from HDM-allergic patients into SCID mice, followed by challenge with aerosolised HDM extract led to development of significant AHR and markedly increased serum levels of total and HDM-specific human IgE in response to challenge compared with mice receiving cells from non-allergic subjects (313). Immunohistochemical analysis of lung sections identified human $CD45^+$ cells in the perivascular and peribronchial areas in the 'allergic' SCID mice; these cells were not seen in the lungs of 'non-allergic' mice. Although no obvious lung eosinophilia was seen in either group, levels of IL-5 in BALF of the 'allergic' mice was greatly increased compared with 'non-allergic' mice. Therefore, adoptive transfer of PBMCs from human HDM-allergic subjects into SCID mice sensitises these mice to HDM, and an allergic airway disease phenotype can be induced by airway challenge with HDM allergen.

Intranasal sensitisation and challenge protocols have been developed in mice using HDM allergens to induce allergic airway disease. Unlike in OVA models, use of

intranasally-administered HDM extract for sensitisation is effective in priming mice to develop allergic airway disease in response to further airway exposure to allergen. An acute protocol for the induction of allergic airway disease using HDM allergen involved exposing Balb/c mice to intranasally-administered HDM extract for 10 consecutive days. Mice were allowed to recover fully, before a recall response was induced by challenging for 3 days with further intranasal HDM extract (314). Mice in which the recall response was not induced showed induction of allergic airway disease - eosinophilic and lymphocytic infiltrate into the lungs, increased serum levels of IgE and IgG1 and development of AHR in response to methacholine. There was an approximately 20-fold increase in the number of activated ($CD69^+$) $CD8^+$ T-cells in the lung compared with naïve mice as well as an approximately 50-fold increase in the number of activated ($CD69^+$) $CD4^+$ T-cells, of which a majority also expressed the putative Th2 marker T1/ST2. Cultures of splenocytes from sensitised mice with HDM extract secreted increased levels of IL-4, IL-5 and IL-13; mRNA levels for these cytokines were increased in the lung. Responses after recall challenge were generally greater, particularly in the numbers of cells infiltrating the lung. Induction of chronic disease by intranasal sensitisation and challenge has also been demonstrated (315). Chronic allergic airway disease was induced in mice exposed to intranasally-administered HDM extract for five consecutive days a week followed by two rest days for up to seven weeks, characterised by influx of predominantly eosinophilic and lymphocytic cells into the lungs after three weeks. Cell numbers stayed constant until the end of allergen administration. Expression of markers of activated Th2 cells such as inducible costimulator (ICOS) and T1/ST2 were increased on T-cells isolated from the lungs of challenged mice. T-cells cultured *in vitro* with HDM extract proliferated and secreted increased levels of IL-5 and IL-13 from one week of allergen exposure. Total IgE levels increased from three weeks of exposure and total IgG1 levels were significantly increased at five weeks. AHR was significantly increased from baseline after five weeks of allergen exposure. Analysis of lung sections indicated the presence of severe eosinophilic perivascular and peribronchial inflammation after five weeks of allergen exposure accompanied by development of features of remodelling, including mucus hypersecretion, increased subepithelial collagen deposition and increased ASM actin levels. After seven weeks of allergen exposure, mice were left to recover and analysed for signs of persistent inflammation or remodelling. Inflammation resolved within two weeks of cessation of allergen exposure, but remodelling was present nine weeks later, suggesting that the induced changes were permanent. Increased AHR in

response to methacholine also persisted after allergen exposure stopped, as did the capacity of lung T-cells to secrete increased levels of Th2 cytokines after *in vitro* challenge with HDM extract. Nine weeks after the last exposure to allergen, rechallenge with HDM induced eosinophilic lung inflammation and increased further the capacity of lung T-cells to secrete Th2 cytokines upon HDM allergen stimulation, suggesting that a chronic persistent disease phenotype had been induced.

1.3.7 Uses of the HDM mouse model of allergic asthma to investigate lung remodelling processes

The HDM model of allergic asthma described previously demonstrated that chronic and persistent changes could be elicited in the airways of mice challenged repeatedly with intranasally-administered HDM allergen. This is in contrast to the models developed using ovalbumin, where a more acute and transitory phenotype is usually induced. The HDM model, utilising an allergen that is clinically relevant in humans, therefore induces a disease phenotype in mice that is more similar to the disease occurring in humans. The HDM model has been used to investigate mechanisms underlying chronic features of the disease, such as vascular remodelling. A study investigated the relationship between development of AHR and other features of allergic airway disease using a chronic model of HDM challenge (316). Early development of AHR was associated with inflammatory cell infiltration into the lungs, whereas more sustained and persistent increases in reactivity and maximum respiratory system resistance were seen after clearance of lung inflammation and were associated with increased collagen deposition in the lung, features which persisted for at least four weeks after the last exposure to allergen. The AHR seen in allergic asthma may have more than one underlying cause and be linked to both acute lung inflammation and aspects of chronic remodelling. Another study used a chronic disease protocol, challenging Balb/c mice intranasally with HDM extract five days a week for either seven or twenty weeks, and investigated the extent of vascular remodelling induced (317). Both protocols induced persistent airway inflammation; inflammation was predominantly eosinophilic after seven weeks of challenge, with a greater proportion of neutrophils seen after twenty weeks. Proliferation of endothelial cells and vascular smooth muscle cells was increased after both seven and twenty weeks of HDM administration, with a higher level of proliferation of endothelial cells in bronchial-associated vessels seen after twenty weeks of challenge. A significant increase in total smooth muscle area was also seen after

twenty weeks. Myofibroblast numbers around bronchial-associated vessels were increased after both seven and twenty week protocols. Perivascular collagen was significantly increased after seven weeks of challenge with HDM extract; after twenty weeks total collagen levels in bronchial areas were also significantly increased. All aspects of collagen deposition were more pronounced after twenty weeks of challenge. The study also analysed these features four weeks after the last exposure to HDM extract to investigate the persistence of these changes in the absence of allergen challenge. With the exception of collagen levels, all features had significantly decreased or returned to baseline levels within four weeks of cessation of allergen exposure. Collagen levels showed little or no change four weeks after challenge. This model therefore induces a vascular remodelling phenotype similar to that seen in human disease, but in contrast to airway remodelling (thickening of the basement membrane, increased ASM mass) which appears to be permanent in the lungs, some aspects of vascular remodelling may be reversible in the absence of allergen.

Blocking TGF-β in the HDM model using both continuous and intermittent exposure protocols was analysed (318). In the continuous protocol, mice were exposed intranasally to HDM extract five days a week for five weeks, whilst in the intermittent exposure protocol, mice were exposed intranasally to HDM extract for ten days, allowed to rest for thirty days, after which cycles of HDM exposure for three days followed by twelve days of rest were administered up to six times. Both protocols induced Th2-mediated allergic airway disease; partial resolution was seen during each rest period in the intermittent protocol. Numbers of cells infiltrating the lungs in the continuous protocol increased with increasing duration of exposure, as did TGF-β levels and activity. Administration of anti-TGF-β antibody on alternate days during the HDM exposure protocol from day 14 of the protocol decreased TGF-β activity in BALF, but had no effect on airway remodelling as it did not prevent or reverse collagen deposition, production of smooth muscle actin, goblet cell hyperplasia or mucus hypersecretion. Similar results were seen when anti-TGF-β was administered earlier in the protocol (day 4), and when anti-TGF-β was administered during re-challenge in the intermittent protocol. Anti-TGF-β treatment exacerbated Th2-mediated lung inflammatory events, in particular causing an increase in lung eosinophilia, serum IgE levels and AHR, as well as the production of Th2 cytokines, suggesting that TGF-β may be involved in the regulation of inflammatory events in allergic airway disease but not in the regulation of airway remodelling events.

1.3.8 Other uses of the HDM mouse model of allergic asthma

A number of studies have investigated antigen-specific T-cell responses in the HDM model of allergic asthma. Splenocytes isolated from HDM sensitised and challenged mice and cultured *in vitro* with Der p 1 proliferated to a greater extent than splenocytes isolated from naïve mice i.e. proliferation was allergen-specific (312). Splenocytes isolated from sensitised but unchallenged mice proliferated to an even greater extent than those from sensitised and challenged mice, perhaps an indication of allergen-specific T-cells having trafficked to the lung from the spleen in the challenged mice. T-cells isolated from the draining (inguinal, popliteal and periaortic) lymph nodes of mice immunised with intraperitoneal HDM extract and challenged intranasally proliferated in response to HDM extract stimulation *in vitro* (311). Allergen-specific T-cell hybridoma clones generated from these cultures were analysed in terms of TCR usage and a restricted repertoire was demonstrated. T-cell clones predominantly expressed TCRα chains comprising Vα8 Jα32, and TCRβ chains comprising Vβ6 Jβ2.3, suggesting the presence of a dominant expansion of T-cells bearing a particular HDM-specific TCR.

The HDM model of allergic asthma has been used in a number of studies to investigate the efficacy and mechanism of action of potential therapeutic agents, such as corticosteroids e.g. prednisolone and dexamethasone in treating allergic asthma (319). They were effective in preventing and reversing the influx of inflammatory cells into the lung and at high dose could downregulate IL-13 production in the lung. Administration of anti-TNF-α in this model decreased AHR in response to methacholine, decreased numbers of inflammatory cells infiltrating the lung and reduced mucus secretion in the lung, supporting the use of anti-TNF-α therapy in allergic asthma (320), despite it also appearing to lead to up-regulation of Th2-type cytokines. It also downregulated eotaxin levels in the lung, providing a potential mechanism through which it could mediate its anti-inflammatory effects.

1.3.9 Other mouse models of allergic asthma

Mouse models of allergic asthma have been developed using other allergens, although none are as widely used as the OVA or HDM models. Examples include a model of cow's milk allergy using β-lactoglobulin (321). Mice were sensitised through intraperitoneal injection of β-lactoglobulin adsorbed onto alum, and challenged

intratracheally 24 days later. This elicited a response characterised by an EAR, where BALF levels of histamine increased within minutes of challenge and a LAR 24 hours after challenge, characterised by AHR, lung eosinophilia, increased levels of BALF IL-4 and IL-5, plasma exudation and increased mucus secretion, providing a model of allergic asthma using a clinically relevant allergen. Another clinically relevant mouse model of allergic asthma has been developed using cockroach allergens, a significant cause of allergic asthma in children living in inner city areas (322). Intraperitoneal sensitisation with house dust extract followed by airway challenge with either house dust extract or the major cockroach allergen, Bla g 2, induced a phenotype characteristic of allergic asthma, comprising eosinophilic and lymphocytic infiltrate into the lungs and BALF, increased levels of eotaxin expression in the lung and significantly increased AHR. The ability of purified Bla g 2 to induce this phenotype after sensitisation with house dust extract suggests that the response induced is due to sensitisation to cockroach allergens present in the extract. Intranasal administration of ragweed extract to mice induced Th2-mediated sensitisation to ragweed in these mice (323). The phenotype induced was relatively mild - minor inflammation was seen in the lung and modest clinical symptoms such as laboured breathing after administration and sneezing was seen; stimulation of splenocytes from exposed animals with ragweed extract induced moderate levels of Th2 cytokine production. This may be a useful model of mild allergic asthma. A mouse model of latex allergy has also been developed - intraperitoneal sensitisation with the main allergen of latex extract, Hev b 1, followed by intratracheal challenge starting from day 24, provoked a Th2-mediated pulmonary response typified by lung eosinophilia, increased secretion of IL-5 into BALF, mucus hypersecretion by airway epithelial cells and an increase in serum levels of allergen-specific IgE, of a similar magnitude to that induced by administration of OVA by the same protocol (324).

1.3.10 TCR transgenic models of allergic asthma

Using OVA as a model allergen in all but one strain of wild-type mice requires systemic sensitisation before challenge via the airways. Using HDM as a model allergen, it is possible to induce allergic airway disease in wild-type mice when all allergen exposure occurs via the airways. The protocols involved in disease induction via this method require repeated frequent exposure to allergen over a prolonged period of time to induce disease. The use of a TCR transgenic mouse model, in which a significant proportion of

T-cells bear an allergen-specific receptor, may make disease induction more straightforward and similar to the way in which allergic asthmatic disease is induced in humans.

An ovalbumin-specific murine TCR transgenic mouse line, DO11.10 (297) has been generated and investigated for its use as a model of allergic asthma. The transgenically-expressed TCR is specific for the epitope $OVA_{323-339}$ bound to MHC class II H-2^d (325). Studies investigating disease induction in DO11.10 mice used protocols based on inhalational challenge with whole OVA aerosol. Challenge of naïve DO11.10 mice with repeated OVA aerosol led to transcription of IL-4 mRNA in lung tissue, and an apparent progressive decrease in IFN-γ transcription (326). When lung T-cells or peripheral lymph node cells from challenged mice were cultured with OVA protein, transcription of IL-4, IFN-γ and TNFα was seen. An increase in eosinophil numbers was also seen in BALF and lung tissue after OVA challenge; cell numbers increased with number of challenges. The numbers of transgenic TCR-expressing T-cells showed only a small increase when challenged and when cultured *in vitro* with OVA, increasing challenges were shown to have a greater inhibitory effect on T-cell proliferation and IL-2 production. This inhibitory effect was not seen in spleen or lymph node T-cells. A response with some features of allergic disease is induced in DO11.10 mice through challenge via the airways without systemic immunisation with OVA protein. The effects of OVA aerosol exposure on naïve DO11.10 mice compared with OVA-sensitised wild-type mice of a similar strain (327) showed that a single OVA aerosol exposure caused a large increase in BALF neutrophils 6 hours post-challenge which returned to baseline a week later. A small increase in BALF eosinophils was also seen 24 hours after exposure which persisted a week later. Lymphocytes in BALF also increased by 6 hours, and increased up to 96 hours after challenge; levels were still high one week after challenge. This contrasted with wild-type mice, where pronounced BALF eosinophilia was seen, accompanied by a much lesser neutrophilia. A single OVA challenge induced increased mucus secretion in both sensitised wild-type and naïve DO11.10 mice. Levels of IL-4 and IL-13 decreased upon aerosol exposure in DO11.10 mice whilst levels of IFN-γ increased markedly, directly opposite to the effects seen in wild-type sensitised mice. Total serum IgE in DO11.10 mice was unchanged after OVA challenge, again in contrast to wild-type sensitised mice, where IgE levels markedly increased both with and without challenge. Treatment of DO11.10 mice before OVA challenge with anti-IFN-γ caused significant lung eosinophilia,

suggesting that IFN-γ was inhibiting development of a Th2 response to allergen; blocking of $CD4^+$ T-cell function with an anti-CD4 antibody inhibited the effects seen in DO11.10 mice upon OVA challenge. Whilst multiple airway challenges with OVA induced significant AHR in sensitised wild type mice, no such effect was seen in DO11.10 mice. The response to OVA aerosol challenge in DO11.10 mice has features of both Th1 and Th2 mediated responses, some of which are reminiscent of allergic asthma. In contrast to this finding, another study exposing naïve DO11.10 mice to OVA aerosol challenge showed an increase in AHR in response to three challenges but no accompanying eosinophil influx into the lungs or increase in serum IgE (328). Lung inflammation was seen, but was composed primarily of T-cells with an activated phenotype ($CD69^+$). Cultured OVA-specific lung T-cells isolated from OVA-challenged mice secreted increased levels of IL-4, IL-5 and IL-13 upon stimulation with OVA.

As discussed in Section 1.3.4, OVA-specific T-cells have also been used in adoptive transfer experiments into naïve mice. DO11.10 OVA-specific Th2 cells (differentiated *in vitro*) were transferred into naïve wild-type mice and these mice were then challenged with OVA (296). The phenotype induced was moderate, comprising lung eosinophilia and increased mucus secretion, but reminiscent of allergic asthma. Induction of the allergic-type phenotype by transferred Th2 cells was dependent upon their IL-4 production, as transfer of Th2-polarised OVA-specific T-cells from $IL\text{-}4^{-/-}$ mice did not induce this phenotype. Analysis of lung tissue and BALF from these mice demonstrated that $IL\text{-}4^{-/-}$ T-cells were not recruited into the lung, and thus were unable to mediate development of an allergic disease phenotype. TNF-α administration overcame this deficit, and $IL\text{-}4^{-/-}$ OVA-specific Th2-type T-cells recruited to the lung through TNF-α mediated lung eosinophilia and mucus hypersecretion as normal. Another study used a similar adoptive transfer protocol of Th1- and Th2-polarised DO11.10 T-cells into naïve mice followed by repeated aerosol challenge (326). OVA challenge increased numbers of DO11.10 T-cells in the lung compared with mice which had received DO11.10 cells but were not challenged with OVA. Lung T-cells isolated from mice adoptively transferred with either Th1-type or Th2-type T-cells showed markedly reduced proliferative responses and IL-2 production after aerosol challenge, unlike spleen and lymph node-isolated T-cells, where no effect was seen. IL-4 production by lung T-cells from mice transferred with Th2 cells was unaffected. Inhibition of proliferation was caused by interstitial macrophages in the lung - removal of these cells from total lung mononuclear cell populations before culture restored

OVA-specific proliferation. This suggests that allergen-specific T-cells do not proliferate in the lungs in response to allergen challenge but are instead recruited to the lung. A recent study used adoptive transfer protocols to investigate the effects of allergen-specific Th17-type T-cells in the development of allergic airway disease (329). Th2- and Th17-type DO11.10 T-cells were generated *in vitro* and adoptively transferred into naïve Balb/c SCID mice. OVA challenge of mice receiving Th2 cells induced a typical allergic asthma-like phenotype and AHR which could be attenuated by administration of dexamethasone. OVA challenge of mice receiving Th17 cells induced IL-17-dependent lung neutrophilia, increased IL-17 and keratinocyte chemoattractant (KC) (murine homologue of human IL-8) production and AHR, all of which were unaffected by dexamethasone. These findings support the hypothesis that Th17 cells may be involved in development of non-eosinophilic asthma and severe, steroid-resistant asthma.

A murine TCR transgenic mouse line expressing a receptor specific for an immunodominant epitope of the house dust mite allergen, Der p 1, has also been generated and evaluated for its use as a model of allergic asthma (330). The TCR was identified from a murine T-cell hybridoma, 1AD2, that responds to Der p $1_{110\text{-}131}$, an epitope shown to be immunodominant in human allergic asthmatics (331), as well as in mice of the H-2^b haplotype, such as the C57BL/6 strain, onto which transgenic founders were backcrossed. The relevant TCRα and TCRβ genes were cloned from cDNA from the 1AD2 hybridoma line, inserted into a construct containing the entire human CD2 promoter (a T-cell specific promoter) region and injected into oocytes for the generation of TCR transgenic mice. Transgenic TCR genes were identified in founders using PCR to amplify the transgenic gene products. Expression of the transgenic TCRβ gene was assessed through flow cytometry – 2% to 12% of T-cells were found to express the transgenic TCR. TCR transgenic mice, backcrossed onto C57BL/6J mice for five generations, and non-transgenic C57BL/6 control mice, were challenged twice five days apart by intratracheal administration of Der p 1 protein or saline. Splenocytes and draining lymph node cells were cultured with either Der p 1 protein or Der p $1_{110\text{-}131}$ peptide and proliferative responses were assayed. Splenocytes from TCR transgenic mice responded to protein and peptide irrespective of whether they had been challenged with Der p 1, and IL-4 production increased in these cells upon *in vitro* stimulation with allergen or peptide. Control mice did not respond under any conditions tested. Cells isolated from draining lymph nodes of TCR transgenic mice responded to a much lesser

extent in response to protein and peptide than splenocytes, and only when mice had been challenged with Der p 1. Again, no response was elicited in control mice. The difference in responses between spleen and lymph node cells was suggested to be due to the tolerogenic environment present in the lung that inhibits T-cell activation unless overcome by a high dose challenge with antigen. Such a tolerogenic environment is not present in the spleen hence splenocytes responded to stimulation as normal. Analysis of lung histology in TCR transgenic mice after Der p 1 challenge showed induced inflammation in the lung, mostly limited to perivascular and peribronchial areas, predominantly composed of lymphocytes and granulocytes, a response not seen in Der p 1 challenged control mice. Differential counts of BALF cells and measurement of eosinophil peroxidase activity in lung tissue suggested that eosinophil and lymphocyte numbers were increased in the lungs of Der p 1-challenged, TCR transgenic mice. Immunohistochemical analysis indicated that 40% of infiltrating mononuclear cells in the lung were $CD3^+$ T-cells, and there was also an increase in infiltrating B-cells. Mucus production was increased in TCR transgenic mice after Der p 1 challenge compared with saline. This model may have some use as a model of allergic asthma involving induction of a disease-like phenotype in response to airway challenge with allergen without prior systemic sensitisation. It provides a physiologically relevant model of human disease induction and can be used to investigate immunological mechanisms underlying disease pathogenesis and regulation, and may be useful for testing potential immunotherapeutic strategies.

As allergic asthma is a disease mediated by allergen-specific T-cells, there would be much value in the development of a humanised mouse model, comprising the entire human MHC class II molecule-allergen epitope-TCR interaction, to allow study of the disease and testing of potential therapies in a relevant human context. To make such a mouse, a well-defined interaction known to be active in human disease is required. Studies have been carried out investigating T-cell responses to particular allergens as a means of developing T-cell-directed immunotherapy strategies. One example of such a system which has been characterised is the response to the major allergen in cat dander, Fel d 1.

1.3.11 Human T-cell responses in allergic asthma caused by the major allergen in cat dander, Fel d 1

Specific responses to Fel d 1, a member of the secretoglobin family found in cat dander extracts, account for approximately 90% of all allergic reactions to cats (332). Fel d 1 is a 35 kD tetrameric protein, formed of two heterodimers composed of chain 1 and chain 2 (333). Most T-cell recognition of Fel d 1 is limited to chain 1 of the protein (334). Intradermal administration of three short (16-17 amino acid), overlapping peptides derived from chain 1 to cat-allergic asthmatic subjects induced LARs in 9/40 patients (221). EARs were not induced in any patient due to the peptides' lack of secondary structure preventing recognition by allergen-specific IgE. Pre-challenge PBMCs from patients were cultured with each of the peptides and each patient mounted a response to at least one peptide but no patient responded to all three. Of the nine patients who developed a LAR after challenge, four expressed HLA-DRB1*13, suggesting that DR13 is capable of presenting one or more of the peptides tested. FC1P 3 (KALPVVLENARILKCNV) and HLA-DR1 induced a proliferative response and IL-5 secretion from $DR13^+$ and $DR1^+$ T-cells, whilst FC1P 2 (EQVAQYKALPVVLENA) presented by human fibroblast lines transfected with human HLA-DR4 induced these responses from $DR4^+$ T-cells. The MHC restriction of certain peptides in inducing T-cell responses *in vitro* suggests that induction of the LAR is T-cell mediated. MHC class II restriction of T-cell responses to allergen-derived peptides has been reported for the birch pollen allergen Bet v 1 (335), the grass pollen allergen Phl p 1 (336), and the bee venom allergen Api m 1 (337). Repeated intradermal challenge with the same peptides within 2-6 weeks in patients in whom a LAR was induced did not induce a LAR, suggesting induction of tolerance. When challenge was repeated after 12 months, a LAR of the same magnitude as that initially induced was seen, suggesting that hyporesponsiveness was transient. A mixture of short, overlapping peptides spanning the whole of both chains 1 and 2 of Fel d 1 (to increase the likelihood of exposing patients to a peptide presented by the MHC class II molecules they express) was injected intradermally into cat-sensitive allergic asthmatic patients, and those who developed a LAR were re-challenged 3 days-68 weeks later (338). Hyporesponsiveness increased gradually up to 2 weeks after initial exposure, with no LAR being induced between 2-8 weeks after initial challenge. After 8 weeks, re-challenge was associated with a gradual return of responsiveness, which was of original magnitude after 40 weeks. A single injection of peptides decreased *in vitro* T-cell proliferation and IL-4,

IL-13 and IFN-γ secretion in response to stimulation with both peptides and whole cat dander extract, suggesting that bronchial hyporesponsiveness was due to inhibition of allergic T-cell responses. Inhalation of allergen-derived peptides induces tolerance to whole allergen in mice (339) hence the ability of inhaled Fel d 1-derived peptides to induce tolerance to cat allergen was investigated (340). Initial exposure to peptides by inhalation induced a LAR without a preceding EAR, associated with sputum eosinophilia and increased sputum concentration of CysLTs. Repeated challenge induced a LAR of a similar magnitude indicating that inhalational exposure to peptides in humans does not induce tolerance. LARs induced by inhalation of Fel d 1-derived peptides were associated with an increase in activated $CD3^+CD4^+$ T-cell numbers in lung tissue (223).

A double-blinded clinical trial of Fel d 1 peptides as an immunotherapeutic agent involved intradermal injection of peptides into cat-sensitive allergic asthmatic patients over a course of 2 weeks, with an increasing dose of peptide given at each injection (341). If an injection induced a LAR, the next injections used the same dose of peptide until no LAR was induced. Patients were challenged intradermally with whole cat dander extract and Fel d 1 at two later time points, the first 2-8 weeks after administration of peptides, and the second between 3 and 9 months after administration of peptides; early and late phase cutaneous reactions were monitored. Late phase responses to Fel d 1 were significantly reduced at both challenges, but the early response was only significantly reduced at the second challenge. A significant decrease in the size of the late phase response to whole cat dander extract was also seen at both time points. Proliferation of T-cells *in vitro* was significantly decreased after the first challenge compared with pre-trial T-cell responses and secretion of IL-4, IFN-γ and IL-13 significantly decreased at both time points. IL-10 secretion was significantly increased from pre-trial levels at both time points, being highest after the first challenge. This suggested that Fel d 1-derived peptides corresponding to T-cell epitopes of the allergen could induce tolerance to allergen, possibly through induction of an IL-10-mediated anti-inflammatory response. A regime of intradermal Fel d 1-derived peptide immunotherapy given at 2-weekly intervals for 12 weeks significantly decreased the magnitude of the induced LAR to whole cat dander extract (342), indicating a change in a clinically relevant parameter, supporting their potential use in the treatment of allergy. Comparison of *in vitro* T-cell responses to cat allergen before and after peptide immunotherapy showed down-regulation of proliferative responses and IL-13 secretion

but these changes were not related to an increase in suppression by $CD4^+$ $CD25^+$ Tregs, suggesting that induction of conventional Tregs did not underlie tolerance induction (343). Comparison of the cutaneous response to whole cat allergen challenge before and after intradermal peptide immunotherapy showed a significant increase in the number of $CD4^+$ $CD25^+$ IFN-γ^+ T-cells in biopsies taken after immunotherapy, corresponding with the lack of cutaneous late phase response seen after whole cat allergen challenge (344). This suggested that tolerance induction through peptide immunotherapy might be caused by recruitment of IFN-γ-producing Th1 cells and not Tregs to the site of challenge. Intradermal peptide immunotherapy was shown to down-regulate IL-5 production and proliferation of allergen-specific T-cells *in vitro* and to possibly increase IL-10 production (345). $CD4^+$ T-cells isolated from PBMCs taken after peptide immunotherapy suppressed allergen-specific proliferation of non-$CD4^+$ PBMCs, suggesting that peptide immunotherapy induces a Treg population that mediates allergen hyporesponsiveness.

Difficulty in determining mechanisms underlying tolerance induction highlights the usefulness of humanised mouse models of allergic asthma. More information about tolerance may be gained from *in vivo* studies than is possible from *in vitro* studies in humans. Elucidation of mechanisms underlying allergic asthma in general may also be obtained from a mouse model engineered to express a human disease-associated interaction, and such a model would be useful in testing potential therapies for safety and efficacy before their use in humans. The discovery of specific T-cell epitopes in Fel d 1 as well as the MHC class II restrictions of these epitopes led to the development of a human TCR transgenic model of allergic asthma by postdoctoral research associates in the Boyton laboratory (Dr. Carol Pridgeon, Dr. Alexander Annenkov, Dr. Catherine Reynolds and Dr. Xiaoming Cheng), funded by Asthma UK. At the time of writing, this model has not been reported in the literature. HLA-DRB1*01-restricted T-cell lines were derived from $DR1^+$ cat-sensitive allergic asthmatic patients, and grown in response to a peptide epitope of Fel d 1 known to be presented by DR1 (peptide 4, FCP1 3 in 221). After several restimulations with peptide to expand allergen-specific T-cells, TCR sequence clonotypic analysis of the lines was carried out. One particular TCR was predominantly expressed. The TCRα and TCRβ chains (TRAV 36-DV7 TRAJ 32 TRAC and TRBV 9 TRBJ 2-7 TRBC 2 as identified by the IMGT database) were cloned into the T-cell specific pTαcass and pTβcass expression vectors (346) and used to create humanised TCR transgenic mice. Two lines, line 4 and line 16, were generated

and crossed onto an HLA-DR1 transgenic background to create humanised transgenic lines containing both a peptide 4-specific human TCR and the MHC class II molecule to which its response is restricted.

1.4 T-cell receptor structure

1.4.1 Identification of the T-cell antigen receptor (TCR)

The two major T-cell subsets, helper T-cells and cytotoxic T-cells (described originally in 347) respond to molecules expressed on the surface of other cells encoded by the major histocompatibility complex; cytotoxic T-cells respond to antigen and those MHC molecules expressed on all cells, encoded in mice in the H2-K and H2-B regions (348) and in humans in the HLA-A and HLA-B regions (349) of the MHC (class I), whilst helper T-cells respond to antigen and MHC molecules expressed only on certain cells of the immune system (APC such as macrophages) encoded in mice by the H2-A region and in humans by the HLA-DP, -DQ and –DR regions of the MHC (class II) (349, 350). The receptors on T-cells were initially defined biochemically with antibodies, using a monoclonal antibody specific for an antigen of a murine T-cell lymphoma (351). This antigen was specific to the lymphoma and not found in cells isolated from normal mouse spleen or thymus and was identified as a glycoprotein composed of two disulphide-bonded subunits (39 kilodalton (kD) and 41 kD molecular weight). Further analysis of such proteins isolated by specific monoclonal antibodies through tryptic fingerprint analysis showed that these proteins contained regions that were both constant and variable between receptors (352). The key conceptual breakthrough came when a gene encoding the receptor protein was isolated from the polysomal mRNA fraction of a T-cell hybridoma through hybridisation with a B-cell cDNA library (353). The remaining mRNA species showed T-cell specific expression and one particular species was shown to be somatically rearranged in T-cells but not B-cells, suggesting that this was the T-cell receptor gene. Chromosomal mapping studies identified the gene loci for the human TCRα genes as chromosome 14 (354) and the human TCRβ genes as chromosome 7 (355). Similar studies placed the murine TCRα genes on chromosome 14 (356) and the TCRβ genes on chromosome 6 (357). The αβ TCR is expressed at the cell surface in association with the CD3 complex (CD3γε, δε and ζζ subunits) which is required for the correct assembly of the TCR and signalling upon antigen recognition (358). MHC class II-restricted helper T-cells are associated with

another cell surface molecule, CD4 (OKT4 in 359), involved in stabilising the interaction between TCR and MHC molecule in T helper cells (CD4 is referred to as L3T4 in 360). A similar phenomenon has been observed for CD8 and cytotoxic T-cells (T8 in 361, CD8 in 362). The presence of T helper cells is required for optimal cytolytic effector function of cytotoxic T-cells (363) and antibody production from B-cells (359).

1.4.2 The interaction between TCR, peptide and MHC molecule

APC such as macrophages and DC present antigen in the form of a short peptide determinant bound to cell-surface MHC class I or class II molecules (364, 365). In humans, the MHC (known as HLA) is located on chromosome 6 and is approximately 7.6 megabases (Mb) in size (366). The HLA-A, -B, -DP, -DQ and -DR loci are highly polymorphic – according to the IMGT (Immunogenetics)/HLA database, there are currently 2,215 class I alleles and 986 class II alleles known to be expressed in humans (367). Class I molecules are composed of a larger 'heavy' polymorphic α chain (α1/α2/α3 domains) complexed with a smaller 'light' invariant β_2-microglobulin chain (368), whilst class II molecules comprise a dimer of polymorphic α (α1/α2) and β (β1/β2) chains (369, 370). Despite their dissimilar subunit composition, crystal structures of MHC class I molecule HLA-A2 (371) and MHC class II molecule HLA-DR1 (372) show that they have a similar structure; domains α1 and α2 of HLA-DR1 correspond to domain α1 and the β2 microglobulin domain of HLA-A2, whilst domains β1 and β2 of HLA-DR1 correspond to domains α2 and α3 of HLA-A2. The peptide-binding site is located at the most membrane distal portion of the protein in both class I and class II molecules, formed of α1/α2 domains for class I and α1/β1 domains for class II molecules. The peptide-binding site has a 'floor' composed of an eight-stranded antiparallel β-sheet, with α-helical 'sides' surrounding a cleft into which the peptide epitope binds (373 - HLA-A2, 374 - HLA-DR1). The residues of the MHC molecules in this domain which potentially contact the peptide are the most polymorphic residues of the molecule, thus increasing within a population the number of peptide antigens that can be presented to T-cell scanning (375). Crystal structures of TCR-peptide-MHC molecule complexes have been determined for both MHC class I e.g. HLA-A2/Tax viral peptide/TCR A6 (373), and class II molecules e.g. HLA-DR1/HA influenza peptide/TCR HA1.7 (376), suggesting a similar diagonal mode of docking of the TCR onto the peptide-MHC complex. Contact occurs through flexible loops on the TCR known as complementarity-determining regions, and the whole of the peptide and a

significant proportion of the MHC surface are hidden by the interaction. Whether this mode of docking is universal to all TCR-peptide-MHC complexes is unknown; other crystal structures have suggested that the angle of rotation of the TCR upon the peptide-MHC complex may range from 32° to 87° (377).

1.4.3 T-cell receptor structure

According to the IMGT database (378), the human TCRα gene locus on chromosome 14 spans 1000 kilobases (kb) and contains 54 TRAV (Vα) gene segments, 61 TRAJ (Jα) segments and 1 unique TRAC (Cα) region. The human TCRβ gene locus on chromosome 7 spans 620 kb, and contains 64-67 TRBV (Vβ) segments, 2 TRBD or diversity (Dβ) segments, 14 TRBJ (Jβ) segments and 2 TRBC (Cβ) segments. The segments are separated by intronic sequence that is removed during recombination events in the thymus during T-cell development, leading to the production of a functional and unique TCR, as discussed further in Section 1.5. A functional αβ TCR comprises successfully rearranged TCRα and TCRβ chains. Each TCRα chain is made up of a variable region composed of a Vα segment spliced to a Jα segment, which in turn is spliced to a constant region (Cα segment). Each TCRβ chain comprises a variable region made up of spliced Vβ, Dβ and Jβ segments which are then spliced to a constant region (Cβ segment). The peptide-MHC molecule contacts in the TCR are residues found in the variable portion of the protein in the most variable regions, the complementarity-determining regions (CDR) 1, 2 and 3. CDR1 and CDR2 are germline-encoded and are primarily thought to mediate contact with the MHC molecule (379), whilst CDR3 is found at the junction between V and J segments (V, D and J in TCRβ chains) and is thought to primarily contact the bound peptide antigen (380), although all three CDRs can contact either peptide or MHC molecule. The CDR3 is the most hypervariable part of the TCR – the joining of V segment to J segment is not always exact, and base pairs can be inserted or deleted from this junction through non-homologous end joining (NHEJ) during recombination (see section 1.4.4).

1.4.4 V(D)J recombination and T-cell receptor diversity

V(D)J recombination is a process unique to lymphocytes, occurring in both T-cells and B-cells producing populations that carry within them a wide range of specificities for antigen (381). Joining of different V, D and J gene segments in multiple combinations,

each giving rise to a unique receptor, causes variation within the TCR repertoire of an individual known as combinatorial diversity. This process generates the TCR in T-cells (and the antibody in B-cells). Recombination in these cells follows a similar pattern and is confined to the TCR and immunoglobulin (Ig) genes of the two lineages – rearrangement of TCR genes only occurs in T-cells and rearrangement of Ig genes only occurs in B-cells (382). Rearrangement has a strictly regulated order, with the rearrangement of TCRβ genes (heavy chain Ig genes in B-cells) occurring before rearrangement of TCRα (Ig light chain) genes (383, 384). Allelic exclusion is seen – rearrangement of TCRβ/Ig heavy chain genes occurs on both alleles but correct rearrangement of the segments on one allele leads to its expression at the cell surface in conjunction with a surrogate TCRα chain/light chain and prevents further rearrangement at the other allele. This avoids development of lymphocytes with specificity for more than one antigen, where there is a likelihood of one receptor being self-reactive and leading to autoimmunity (385). Expression of a rearranged TCRβ/Ig heavy chain at the surface provides signals for the further development of the T/B-cell progenitor and ultimately to rearrangement at the TCRα/Ig light chain loci. Recombination at both TCRα and TCRβ loci involves the same recombination machinery, the recombination-activating gene (RAG) complex, composed of RAG-1 (386) and RAG-2 (387) which has a similar mode of action to transposases and viral integrases (388).

Each gene segment is flanked on either side by a recombination signal sequence (RSS), consisting of a conserved palindromic heptamer and an AT-rich nonamer separated by a non-conserved spacer region of either 12 (12-RSS) or 23 base pairs (23-RSS) (389). The 12/23 rule states that gene segments flanked by 12-RSSs may only combine with those flanked by 23-RSSs and vice versa (390, 391). In the TCRβ locus, V regions are flanked by 23-RSSs, J regions by 12-RSSs, whilst the D regions are flanked by 5'-12-RSSs and 3'-23-RSSs, allowing only V-to-D or D-to-J rearrangements – although direct V-to-J recombination is theoretically possible, it is not seen, a phenomenon known as the beyond 12/23 rule (392). Rearrangement of D-to-J and V-to-D segments occurs sequentially with V to D combination occurring only upon successful D to J rearrangement (393).

The RAG complex induces single-strand breaks between the gene segment and RSS 3' of the upstream segment and 5' of the downstream segment (394). Conversion to double-strand breaks occurs through attack on the 5' non-coding strand by the 3'

hydroxyl group on the coding strand, forming a closed hairpin loop adjacent to the gene segment and blunt 5' phosphorylated ends on the RSS segment (395). The RAG complex holds the strands in position (396), so that joining of the segments can be mediated by proteins involved in DNA repair; in this context they are referred to as NHEJ proteins. RSS ends are joined precisely resulting in an excised loop. Joining of gene segments is less precise; nucleotides can be added or removed before joining occurs (397). NHEJ proteins recruited to the RAG complex after the formation of double-strand breaks include components of the DNA-dependent protein kinase (DNA-PK) – the Ku complex, Ku70 (398) and Ku80 (399), and the DNA-PK catalytic subunit (DNA-PKcs). The Ku complex is necessary for joining coding regions and RSS ends to form a signal loop that is excised from the chromosome whilst DNA-PKcs is required only for joining of coding regions (400). Another protein required for gene segment joining is Artemis, the mutation of which in humans causes severe combined immunodeficiency – Artemis may mediate opening of the hairpin loop (401). *In vitro* studies suggest that Artemis may form a complex with DNA-PKcs. Phosphorylation of Artemis by DNA-PKcs induces endonuclease activity which opens the hairpin loop (401). Loop opening can occur at the apex of the loop or to one side or the other, forming overhanging ends which if filled in and not removed form palindromic (or P) regions (397). Additional nucleotides can be added to the ends by terminal deoxynucleotidyl transferase (TdT) forming an N region unique to the receptor which is not germline-encoded (402, 403). Nucleotides can also be removed from the opened ends further increasing diversity of sequence at this point. This junction between V, (D) and J segments encodes the CDR3 described previously as the region of the receptor which determines antigen specificity. The ability to induce further diversity here (known as junctional diversity) increases the capacity of the TCR repertoire to recognise and respond to the vast array of antigens it may encounter (404).

Other NHEJ proteins involved in the joining reaction include X-ray repair complementing defective repair in Chinese hamster cells 4 (XRCC4) (405) and DNA ligase IV (406). An XRCC4-DNA ligase IV complex mediates joining of gene segment and RSS ends although the enzymatic mechanisms underlying this process remain unknown (407). XRCC4 is involved in DNA repair and may recruit polynucleotide kinase to the end joining complex (408), facilitating end processing for correct joining by DNA ligase IV (409). Correct joining forms a functional TCR chain if the modified V-J/V-D-J junction allows in-frame readthrough (397). Production of successfully

rearranged TCRβ and TCRα chains and their expression at the cell surface as a complete receptor signals to the cell to proceed to the next phase of development in the thymus.

1.5 T-cell development in the thymus

The TCR repertoire of an individual is selected in the thymus to recognise and respond to a wide variety of foreign antigens whilst lacking self-reactivity. The lower limit of the naïve peripheral αβ TCR repertoire in humans is approximately 2.5 x 10^7 different specificities (410); the corresponding figure for the mouse is approximately 2 x 10^6 (411). The estimated number of potential TCR molecules capable of being produced by V(D)J recombination is thought to be 10^{12}-10^{15}, but most combinations will produce a TCR unable to recognise self-MHC molecules or a TCR too strongly specific for self peptide-MHC complexes. During transit through the thymus, developing T-cells rearrange their TCR genes. If rearrangement is successful, the surface-expressed TCR is assayed for its potential to recognise foreign antigen in the context of self-MHC molecules whilst lacking significant self-reactivity. Cells bearing receptors that do not fulfil these requirements are deleted before they reach the periphery, allowing only those cells bearing receptors of the required specificity (a small proportion of the total cells) to mature and emigrate from the thymus.

1.5.1 Precursor entry into the thymus and the earliest stages of T-cell development

The earliest T-cell progenitors migrate into the thymus at the cortico-medullary junction (412) and are derived from haematopoietic stem cells (413). They express high levels of CD44, which is thought to home them to the thymus (Pgp-1 in 414). Cells entering the thymus can develop into other cell types e.g. γδ T-cells (which express a TCR composed of γ and δ chains) (415) or iNKT cells.

Thymocytes are defined by their expression of the TCR-associated coreceptors, CD4 and CD8. At their earliest developmental stage, they express neither coreceptor and are known as double negative (DN, $CD4^-CD8^-$) cells. They are divided into further subpopulations DN1 to DN4, based on expression of the cell surface molecules CD44 and CD25 (416): DN1, the earliest subset developmentally, phenotype $CD44^+CD25^-$,

DN2 ($CD44^+CD25^+$), DN3 ($CD44^-CD25^+$) and DN4 ($CD44^-CD25^-$). As the cells progress from DN1 to DN4, their ability to repopulate a thymocyte-depleted thymus decreases, indicating their commitment to development along the T-cell lineage pathway.

The first stage of V(D)J recombination, rearrangement of TCRβ chains, occurs at the DN3 stage (383). Thymocytes in mice deficient in RAG gene expression fail to develop beyond the DN phase (417, 418) as they cannot initiate recombination. This suggests the existence of a checkpoint requiring a fully rearranged TCRβ chain to be expressed at the cell surface before progression to the next phase of development. Transgenic expression of a rearranged TCRβ chain in RAG-deficient thymocytes allows them to pass this checkpoint (419). RAG depletion arrests thymocyte development specifically at the DN3 stage, as does disruption of the TCRβ gene locus. Deletion or disruption of the TCRα locus has no effect on DN thymocyte development, consistent with the observation that TCRα gene rearrangement occurs in the the next stage of development where thymocytes express both CD4 and CD8 and are termed double positive (DP) cells (420).

The correctly rearranged TCRβ chain is expressed at the cell surface of DN3 thymocytes in complex with the invariant pre-TCRα (pTα) chain, forming the pre-TCR (421). There is little homology between the pre-TCRα and any TCRα gene (422). A significant block in thymocyte development at the DN stage is seen in $pT\alpha^{-/-}$ mice suggesting that the pre-TCR is required to progress to the DP stage (423). The pTα chain is not merely a surrogate for the TCRα chain – transgenic expression of a correctly rearranged TCRα chain at the time of β-selection interferes with normal progression through the checkpoint (424), suggesting that the pre-TCR transmits a unique signal allowing progression past the checkpoint. The induction of a noticeable block in thymocyte development at this stage has been documented in a number of αβ TCR transgenic mice and indicates that transgenic TCR expression is occurring (425). Mutation of the cytoplasmic tail of the pTα chain abolished the ability of the pre-TCR to mediate progression of DN thymocytes into the DP stage (426), suggesting that pre-TCR signalling is required for αβ T-cell development. Cells in which gene rearrangement fails to produce a correctly-rearranged TCRβ gene (or a correctly rearranged γδ TCR) undergo apoptosis (427) as they cannot pass the β-selection checkpoint.

1.5.2 TCRα gene rearrangement

Thymocytes which have passed the β-selection checkpoint undergo several rounds of proliferation and upregulate expression of CD4 and CD8, becoming DP ($CD4^+$ $CD8^+$) thymocytes (428). Most thymocytes (approximately 80-85%) are DP thymocytes. Of these, approximately 20% are rapidly-dividing blast cells undergoing TCRα gene rearrangement. The remaining 80% are small, non-proliferating thymocytes expressing TCR undergoing positive and negative selection (429). Signalling through the pre-TCR initiates rearrangement at the TCRα gene locus (384). Upon productive rearrangement of a TCRα chain, it is expressed at the surface in complex with the rearranged TCRβ chain, displacing the pTα chain (430).

TCRα rearrangement is not subject to allelic exclusion (420). Both TCR^- and TCR^+ DP thymocytes express RAG-1 and are therefore undergoing recombination. In cultured TCR transgenic DP thymocytes, subsequent analysis of TCR chain expression showed that approximately 25% of cells did not express the transgenic TCRα chain, suggesting that rearrangement at the TCRα locus continues after initial expression of a functional αβ TCR, and that newly-rearranged TCRα chains can replace the transgenic TCRα chain. The lack of allelic exclusion at the TCRα locus maximises the potential of a developing thymocyte to express a self-tolerant TCR which can recognise self-MHC and is likely to recognise foreign antigen. T-cells expressing two TCRα chains in conjunction with one TCRβ chain have been observed in the periphery (431). New productively-rearranged TCRα chains are expressed in conjunction with TCRβ until cells are selected (positively or negatively), all gene segments have been used in unproductive rearrangements or the cell has received signals to undergo apoptosis known as 'death by neglect'.

1.5.3 Positive and negative selection

DP thymocytes expressing a correctly-rearranged αβTCR undergo positive and negative selection (432). Positive selection identifies those thymocytes with a low affinity for self peptide-MHC complexes (and therefore potentially high affinity for foreign peptide-MHC complexes) and signals for their survival and maturation. Negative selection identifies those thymocytes that are autoreactive and signals for their deletion by apoptosis (433). Most DP thymocytes are deleted, either through negative

selection (5-10% of thymocytes) or, for the majority of cells, because they fail to produce a functional TCR or produce one with no affinity for peptide-MHC and so do not receive the necessary signals for survival. Only 1-5% of DP thymocytes are positively selected and mature into peripheral T-cells (432).

DP thymocytes progress from the cortex into the medulla, interacting with thymic stromal cells as they do so. Positive selection is mediated by cortical epithelial cells (434), whilst negative selection occurs in both the cortex and as the cells progress into the medulla, suggesting that the two processes occur independently (435, 436). In TCR transgenic mice on the appropriate MHC class I background, injection with specific peptide causes deletion of TCR transgenic thymocytes (437). In the absence of peptide, TCR transgenic thymocytes were positively selected and developed as normal, indicating that interaction between TCR and peptide-MHC is required for correct negative selection. Mice homozygous for a mutation which disrupts functional cell surface expression of MHC class I molecules lack mature $CD8^+$ T-cells whilst other T-cell subsets develop normally, suggesting that positive selection of $CD8^+$ T-cell precursors from DP thymocytes depends upon interaction with peptide-MHC class I complexes (438), thus the same interaction between the TCR of a developing thymocyte and a self-peptide/MHC complex expressed on thymic stromal cells mediates both positive and negative selection. Expression of a transcription factor, autoimmune regulator (Aire), in medullary thymic epithelial cells (mTECs), suggests that an important component of negative selection occurs in the medulla (439). Aire promotes expression of proteins in mTECs from other tissues of the body, which are processed and presented as peptides in complex with MHC molecules; developing thymocytes are tested against self antigens that they would not otherwise encounter in the thymus and those that are self-reactive are deleted before they reach the periphery (440). The ability of the same TCR-peptide-MHC interaction to mediate both positive and negative selection may be based on differential avidity of the interactions. Interactions above a certain threshold lead to negative selection due to their intrinsic self-reactivity, whilst interactions with avidity below this threshold would lead to positive selection (441). Avidity is related to intrinsic affinity of TCR for a particular peptide-MHC complex and the number of TCR-peptide-MHC interactions at the thymocyte surface; the greater the number of engaged TCRs, the higher the avidity. Lower avidity interactions that initiate positive selection recognise the basic structure of a self-peptide-MHC complex without being overly specific and thus are likely to lack overt self-reactivity.

1.5.4 The CD4 vs. CD8 lineage decision

Positively-selected thymocytes receive signals to survive and proliferate and proceed to the single positive (SP) stage of development (442). Here, thymocytes downregulate expression of either CD4 or CD8 and develop along the helper (CD4 associated) or cytotoxic (CD8 associated) lineage, depending upon the MHC-restriction of the TCR they express. This ensures that the complete TCR (αβTCR, CD3 and co-receptor)-peptide-MHC interaction will be at its most stable, as CD4 and CD8 contact MHC class II and I molecules respectively and stabilise the overall complex. It is therefore important that thymocytes retain expression of the correct co-receptor. Thymocytes are thought to be directed into the correct lineage through a 'strength of signal' model where the strength and/or duration of the signal through the TCR determines lineage fate (443). All positively-selected thymocytes initially down-regulate expression of CD8, forming a $CD4^{high}$ $CD8^{low}$ subpopulation (444). A decrease in or cessation of signalling at this point then signals for development into a $CD8^{+}$ T-cell, whilst continuation of signalling signals for development into a $CD4^{+}$ T-cell. Thymocytes which have down-regulated expression of the correct co-receptor in accordance with the specificity of their TCR mature into peripheral T-cell precursors in the medulla before emigrating from the thymus into the periphery as naive T-cells (445).

1.6 T-cell signalling, activation and differentiation

1.6.1 Proposed mechanisms of TCR triggering

The mechanism by which interaction with foreign peptide-MHC complex triggers signalling within the T-cell is still largely unknown. Several mechanisms have been proposed to explain how the signal is transduced across the plasma membrane. *Conformational change models* suggest that TCR binding to foreign peptide-MHC induces a conformational change within the TCR-CD3 complex, transducing a signal across the plasma membrane which is then propagated inside the T-cell. This can account for the ability of very low levels of foreign peptide-MHC to trigger signalling, as one complex could theoretically trigger one TCR to activate the T-cell (446). The TCR-CD3 complex can undergo conformational change in the absence of phosphorylation events i.e prior to TCR signalling, such as binding of adaptor protein Nck to CD3ε upon TCR-peptide-MHC binding (447). CD3ζ subunits can undergo

conformational change rendering them more susceptible to phosphorylation (448). However, in a TCR repertoire with huge structural diversity and many different modes of peptide-MHC binding, induction of the same conformational change in each TCR-peptide-MHC interaction seems unlikely (377). Bearing in mind the constraints placed upon the interaction by TCR variability, there are possible changes that could occur, such as a change in orientation of one TCR-CD3 complex with respect to another - this would require TCRs to exist as dimers in the membrane (446), and there is evidence of multimeric organisation (449), but the basic TCR-CD3 unit appears to be monovalent. Alternative conformational changes include change in orientation of TCRαβ to CD3 within one complex, or change in orientation of the TCR-CD3 complex with respect to the membrane - peptide-MHC binding could exert pulling, pushing or twisting forces on the TCR, changing the orientation of the TCR to CD3 or TCR-CD3 to the membrane (446); there is little evidence supporting or disproving these possibilities.

The *TCR oligomerisation model* is based on the observation that TCR-specific antibodies and peptide-MHC oligomers cause aggregation of TCR molecules and can initiate signalling. Bringing TCRs into close proximity may allow signalling to proceed as their aggregation causes aggregation of TCR-associated signalling molecules (446). However, foreign peptide-MHC complexes are present at very low density on APC cell surfaces, and might be unable to mediate such large-scale aggregation. Also, a single foreign peptide-MHC complex can induce triggering of TCR signalling, an observation incompatible with this mechanism (450). Another aggregation-based model requires the TCR to associate with its coreceptor for correct triggering (the *coreceptor heterodimer model*). CD4 and CD8 are associated with the protein tyrosine kinase Lck (451), which is important for signal propagation, and this heterodimerisation would bring Lck into close contact with its target (ITAMs in the TCR-CD3 complex), facilitating triggering, but TCR triggering can occur in the absence of either coreceptor (452). The *pseudodimer model* suggests that self and foreign peptide-MHC complexes bind TCR in concert, forming a pseudodimer that triggers signalling, based on the observation that covalently-linked self peptide-MHC/foreign peptide-MHC heterodimers trigger signalling (453). TCR binds a foreign peptide-MHC complex for which it is specific, before a second TCR, associated with coreceptor, dimerises with the first and binds self-peptide MHC. Self peptide-MHC complexes are present at the APC surface in high concentration, so dimerisation would be efficient and provides an explanation as to how

a single foreign peptide-MHC can trigger signalling. There is currently no evidence that peptide-MHC complexes form such dimers at the APC surface.

The *kinetic segregation model* suggests that TCR-peptide-MHC binding forms regions of close membrane contact (~15 nm apart) excluding proteins with large extracellular domains (454), such as the protein phosphatase CD45 which can down-regulate signalling mediated by phosphorylation e.g. TCR signalling. These regions would trap the TCR-CD3 complex in close contact with molecules such as Lck, prolonging signalling through the TCR in the absence of phosphatase activity. CD45 is excluded from regions of TCR signalling (455) and removal of its large extracellular domains inhibits TCR triggering (456). Engineered elongation of the peptide-MHC complex, increasing the distance between the two membranes, prevents efficient exclusion of CD45 from the TCR signalling region and interferes with correct TCR signalling (457). However, there is no evidence that segregation is actually required for triggering.

Both clustering and conformational change within the CD3 subunits have been suggested to be required for TCR triggering (458). Multimeric forms of peptide-MHC complexes triggered efficient T-cell signalling by bringing TCR-CD3 complexes into close association and forcing a particular geometry upon the interaction that induced conformational change in the CD3 subunits and propagated downstream signalling events. This model requires peptide-MHC complexes to form dimers at cell surfaces; evidence of this has not been found.

1.6.2 T-cell signalling through the TCR

The interaction between a TCR, its associated coreceptor and peptide-MHC causes their aggregation into higher order structures known as supramolecular activation clusters (SMACs) (459). This brings the Lck associated with CD4 and CD8 intracellular regions (451) into close proximity with the TCR-CD3 complex. All CD3 subunits contain at least one ITAM (consensus sequence YXX(L/I)X_{6-8}YXX(L/I), Y indicates tyrosine, L is leucine, I is isoleucine and X is any amino acid) and TCRζ subunits contain three (460). Lck phosphorylates tyrosine residues in these motifs providing binding sites for ζ-activated protein of 70 kDA (ZAP-70) through its Src homology 2 (SH2) domain (461). Recruited ZAP-70 is phosphorylated by Lck, activating its protein kinase function (462). ZAP-70 and Lck phosphorylate tyrosine residues within the membrane-

associated scaffold (adaptor) protein, linker of activated T-cells (LAT) (463) which allows the assembly of a large signalling complex comprised of both scaffold and signalling proteins, as outlined in Figure 1.1. Growth factor receptor-bound protein 2 (Grb2) binds to LAT (464) and initiates signalling through MAPK cascades (465), ultimately leading to nuclear translocation of the transcription factor activator protein 1 (Ap-1) (466). Grb2-related adaptor downstream of Shc (GADS) (464) facilitates binding between LAT and the cytoplasmic adaptor protein SH2-domain-containing leukocyte protein of 76 kDa (SLP-76) (467). GADS promotes interaction between SLP-76 and adhesion and degranulating promoting adaptor protein (ADAP) (468) which initiates signalling promoting cell adhesion (469). SLP-76 binds Vav1 (470), a guanine nucleotide exchange factor, which is involved in the control of cytoskeleton rearrangement in response to peptide-MHC engagement by the TCR (471) as well as being involved in the activation of calcium signalling pathways, MAPK cascades (472) and phospholipase Cγ (PLCγ1) signalling (473). PLCγ1 binds LAT and SLP-76 (464), which targets it to the plasma membrane and its substrate, the lipid phosphatidylinositol 4,5-bisphosphate, where is catalyses its degradation into diacylglycerol (DAG) and inositol 1,4,5-trisphosphate ($InsP_3$) (474). Phosphorylation of IL-2-inducible T-cell kinase (Itk) enhances PLCγ1 activation (475). DAG activates PKC-θ which mediates phosphorylation of the transcription factor NF-κB allowing its translocation into the nucleus (476). $InsP_3$ induces release of Ca^{2+} ions from the endoplasmic reticulum into the cytoplasm (477), increasing intracellular Ca^{2+} concentration and activating the calcium-dependent phosphatase calcineurin, which phosphorylates nuclear factor of activated T-cells (NFAT) and allows its nuclear translocation (478, 479). Along with Ap-1 and NF-κB, NFAT initiates transcription of genes involved in T-cell activation, proliferation and differentiation. The exact composition of the T-cell signalling complex is unknown - differing recruitment of proteins and thus differential signalling may be important in determining cell phenotype upon activation.

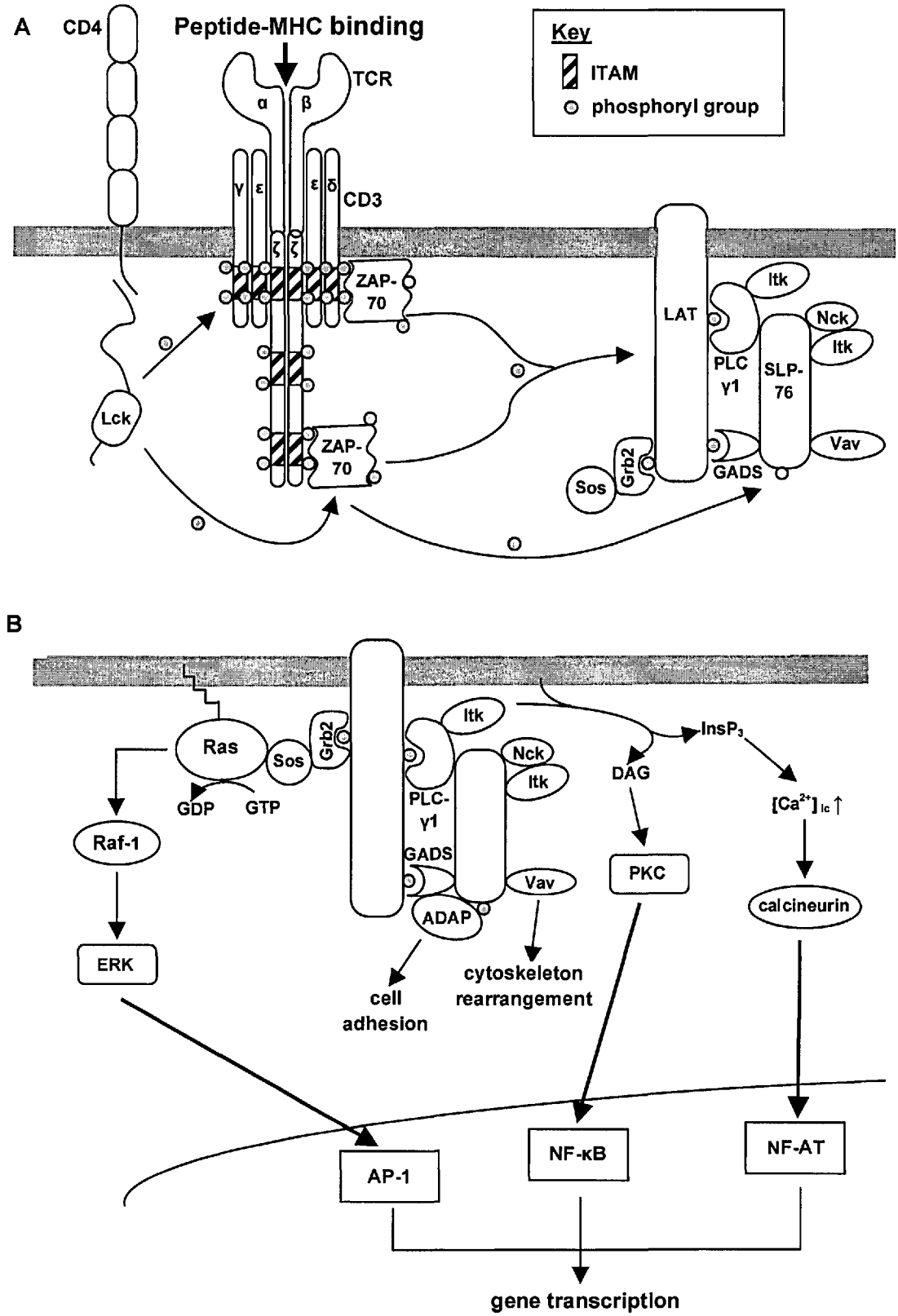


Figure 1.1 Downstream T-cell signalling pathways that are activated upon TCR binding to peptide-MHC. See section 1.6.2 for a detailed discussion of these pathways. A shows the initial recruitment of kinase and adaptor molecules to the engaged TCR. B shows the initiation of downstream signalling by these molecules. Adapted from refs. 469, 480 and 481.

T-cell signalling is also negatively regulated. Lck is controlled through phosphorylation by C-terminal Src kinase (Csk) which deactivates its kinase function (482). Csk is the main negatively-regulating kinase and is tethered to the membrane through association with the membrane scaffold protein PAG (phosphoprotein associated with GEMs (glycosphingolipid-enriched microdomains)) which is constitutively phosphorylated in resting T-cells (483). TCR triggering causes CD45 to dephosphorylate PAG, dissociating Csk from the membrane (483) allowing CD45 to dephosphorylate and activate Lck (484). CD45 may also negatively regulate Lck activity, controlling its activity in resting T-cells or down-regulating its activation after T-cell signalling (485).

1.6.3 The immunological synapse

The immunological synapse is formed at the interface between APC and T-cell where reorganisation of membrane molecules and the cytoskeleton is seen, as defined by Blanchard and Hivroz (486) although similar synapses are also formed between CD4+ T-cells and B-cells, CTLs and their target cells and by other cells in the immune system such as NK cells (487). The immunological synapse was originally visualised using fluorescence imaging as having a 'bull's eye'-like organisation (459), with a smaller central supramolecular cluster (cSMAC) containing TCR and associated signalling molecules such as CD3 and PKC-θ surrounded by a peripheral supramolecular cluster (pSMAC) containing the integrin lymphocyte function-associated antigen-1 (LFA-1) and talin. This structure has been seen in both *in vitro* (459) and *in vivo* (488) systems. Further studies have localised other TCR signalling associated molecules such as Lck (489), ZAP70 and LAT (490) and CD28 (491) within the cSMAC. It has been shown that phosphatases such as CD45 and CD43 and other molecules with large extracellular domains are excluded from the synapse (492, 493). This 'bull's eye' structure forms within 30 minutes of initial engagement of TCR with pMHC (459) and can persist for many hours.

The formation of the immunological synapse was originally thought to be necessary for the co-ordination of T-cell signalling, (494) but there is evidence suggesting that TCR signalling is initiated before the synapse forms (495) and that signalling may be largely terminated by the time the synapse forms; it may be involved in the down-regulation of signalling through internalisation of TCRs in this region (496). That formation of the immunological synapse is not necessary for TCR signalling to occur is also suggested

by the observations that signalling occurs in the absence of this structure in human CD4+ T-cell lines (486) and during the interaction between thymocytes and the thymic stroma during T-cell development, where small clusters of signalling TCR-CD3 complexes are formed all over the thymocyte/APC contact (497).

Formation of the immunological synapse is initiated by the development of small clusters of signalling TCR-pMHC complexes, and the cSMAC structure develops within 5-10 minutes of this interaction when the pMHC contains antigenic peptide for which the TCR is specific (498). The cSMAC initially forms as clusters of LFA-1 molecules surrounded by a peripheral ring of TCR-pMHC; this arrangement inverts to form the typical 'bull's-eye' within 5 minutes (494). TCR signalling is initiated in small microclusters outside the cSMAC (499) which are continuously transported to the cSMAC, where signalling is then terminated. Without this continuous movement of TCR microclusters into the cSMAC region signalling through the TCR is not sustained (500, 501).

The function of the immunological synapse is unclear, particularly in view of the observation that TCR signalling and T-cell activation can occur in the absence of its formation (495). It may mediate downregulation of signalling through internalisation of the TCR signalling complexes (496) to prevent unrestrained signalling. The function of the synapse may be determined by the strength of the signal through the TCR – CTLA-4 is recruited to the synapse in proportion to the strength of signalling through the TCR where it acts to inhibit signalling events i.e. a stronger signal recruits more CTLA-4 than a weaker signal (502). Thus, through CTLA-4, the immunological synapse may modulate TCR signalling by preventing excessive signalling from a stronger TCR-pMHC interaction whilst not affecting signalling from a weaker interaction. CTLA-4 may also counteract the activating signals through CD28, which is also recruited to the synapse (491), suggesting that the overall function of the immunological synapse is to modulate signalling depending on the strength of the TCR-pMHC interaction. An alternative suggestion for the function of the synapse is to act as a directed route for the delivery of various chemical modulators, such as release of cytolytic granules from CTLs to their target cell (503) or the directed secretion of cytokines from T-cells e.g. secretion of IL-4 or IFN-γ from CD4+ T-cells to B-cells to induce their differentiation into mature antibody-secreting B-cells (504).

1.6.4 The signalling pathways involved in differentiation of naive T helper cells into effector T helper lineages

Upon activation through peptide-MHC engagement of the TCR and subsequent signalling, naive T helper cells proliferate and differentiate into one of several effector subsets. The subset a given cell will differentiate into depends upon a number of factors present at the time of its activation, and these factors will be discussed in more detail later. Each cell lineage has a distinct pathway of development involving interaction of specific cytokines, receptors, signalling cascades and transcription factors which co-operate to induce the appropriate phenotype.

Th1 cells: As described in Section 1.2.10, Th1 cells are characterised by production of IFN-γ (16) and are mediators of cellular immunity. Development of a TCR-peptide-MHC stimulated naive $CD4^+$ T-cell into a Th1 cell is mediated primarily through action of the transcription factor T-bet (505). T-bet expression is induced by IFN-γ (506); binding of IFN-γ to its receptor on the cell surface induces signalling through the receptor-associated tyrosine kinases Janus kinase (JAK) 1 and JAK2 and their downstream effector Stat1 (507). Upon activation, Stat1 initiates transcription of T-bet (508) which in turn induces expression of the *Ifng* gene locus (505) and the inducible chain of the IL-12 receptor, IL-12Rβ, making the T-cells responsive to IL-12 (509). IL-12 has a twofold function in the differentiation of naive Th cells into Th1 cells: it is produced by activated macrophages (510) and DC (511) upon their exposure to viral antigen and induces IFN-γ production from other cells of the innate immune system, such as NK cells (512). It is this IFN-γ which is believed to initiate signalling in the naive T-cell. Up-regulation of the IL-12 receptor through IFN-γ signalling makes T-cells responsive to IL-12. The IL-12 receptor signals through JAK2 and tyrosine kinase (Tyk) 2 (513) and Stat3/Stat4 (514) to potentiate production of IFN-γ (515) and up-regulate IL-18Rα chain expression (516). IL-18 synergises with IL-12 to induce IFN-γ production in dedicated Th1 cells (517). Both IL-27 and type I interferons such as IFN-α can induce IFN-γ production in T-cells (518).

Th2 cells: As described in Section 1.2.12, Th2 cells are characterised by production of cytokines such as IL-4 (16), IL-5 (212) and IL-13 (214). They direct humoral adaptive immune responses and are implicated in the development of allergic disease. Differentiation of a naive T-cell into a Th2 cell is primarily controlled by the

transcription factor GATA-3 (519). Binding of IL-4 to its receptor on the cell surface activates JAK1/JAK3 and they transduce the signal into the nucleus through phosphorylation of Stat6 (520, 521). Stat6 binds to the GATA-3 gene, up-regulating its expression (228). GATA-3 directs IL-4 synthesis (522) and is crucial for production of other Th2-type cytokines (522) as well as autoactivating its own transcription, thus reinforcing differentiation along the Th2 pathway through positive feedback (523). The source of exogenous IL-4 that initiates Th2 differentiation is currently unknown. Mast cells (76), human eosinophils (524) and NKT cells (135) can produce IL-4 and may be the source of IL-4 required. IL-4 transcription is also induced by c-Maf (525) but c-Maf does not regulate expression of other Th2 cytokine genes (526). IL-2 signalling via Stat5 (527) is important in Th2 differentiation (528); lack of IL-2 causes a significant decrease in levels of IL-4 secreted by developing Th2 cells. This pathway is independent of signalling via the IL-4/Stat6 pathway, as IL-4 production is induced by IL-2 in $Stat6^{-/-}$ and $IL\text{-}4R^{-/-}$ mice (527). GATA-3 and Stat5 bind the IL-4 gene locus at different sites and have a synergistic effect on IL-4 production (527, 528, 529). The apparent lack of requirement for exogenous IL-4 in IL-2/Stat5 signalling and its importance in the early production of IL-4 in developing Th2 cells suggests that this pathway may also be independent of GATA-3. However, lack of IL-4 production and Th2 differentiation in conditional $GATA\text{-}3^{-/-}$ mice suggest GATA-3 is crucial for the early production of IL-4 (522). It is expressed at basal levels in all naive T-cells, and this basal level is enough to facilitate the effects of IL-2 and Stat5 on IL-4 production (522).

Th17 cells: As described in Section 1.2.9, Th17 cells are distinct from both Th1 and Th2 cells and characterised by production of IL-17 (161, 162). They are thought to play a role in local tissue inflammation and have been implicated in autoimmunity (163). Less is known about their development than their Th1/Th2 counterparts but their differentiation is thought to be primarily controlled by the transcription factor RORγt (530). In mice, IL-6 and TGF-β are required to initiate Th17 cell development (531). In the absence of IL-6, TGF-β directs development along the Treg developmental pathway (532). TNF-α and IL-1β are capable of augmenting the differentiation process (531); in humans, it is IL-1β that is necessary for Th17 differentiation with no absolute requirement for IL-6 or TGF-β (533). IL-6 may initiate Th17 differentiation by signalling through interaction of its receptor, gp130, with Stat3 (534). Signalling through this pathway is required for RORγt expression and subsequent Th17

differentiation. IL-23, a member of the IL-12 gene family, stimulates memory Th17 cells and may support stabilisation of the Th17 phenotype in a similar manner to the reinforcement of the Th1 phenotype by IL-12 (535).

1.6.5 Factors affecting the differentiation of naive T-cells into effector phenotypes upon antigen stimulation

Several factors may influence which effector phenotype an antigen-stimulated naive T-cell differentiates into, including cytokine environment at the time of activation, type of APC, antigen dose, co-stimulation during stimulation and strength and duration of signalling through the TCR, which is influenced by TCR affinity for its cognate peptide-MHC.

Cytokine environment: Differentiation of a naive T-cell into an effector cell can be determined by cytokines present in the environment of the cell when it is activated. These cytokines promote differentiation of one particular phenotype but also actively suppress development of other phenotypes. IFN-γ and IL-12 signal to naive T-cells to develop along the Th1 pathway and inhibit IL-4 and IL-17 production and therefore Th2 (536, 537) and Th17 differentiation (161, 162). The master regulator of Th1 differentiation, T-bet, induces expression of Th1-specific genes (505) and interferes with binding of GATA-3 to the IL-4 gene cluster (538). IL-4 has a similar effect on the Th1 pathway, inhibiting its function (539) and also that of the Th17 pathway (161, 162). GATA-3 blocks transcription from Th1-specific genes: ectopic expression of GATA-3 in developing Th1 cells reprogrammes them into Th2 cells by increasing IL-4 and IL-5 production and blocking production of IFN-γ and T-bet (540). How IL-4 and IFN-γ and their associated transcription factors interfere with Th17 cell differentiation is less clear, but Th17 differentiation *in vitro* only occurs in the absence of both cytokines (161, 162).

The immunological synapse may underlie the ability of Th1 and Th2 polarising cytokines to govern the differentiation of naive T helper cells into Th1 or Th2 cells (541). Analysis of the IS in the minutes immediately following engagement of peptide-MHC by TCR under neutral (i.e. no polarising cytokines) conditions showed co-localization of the IFN-γR with TCR into the IS and subsequent development of these cells into Th1 cells. This pathway was more active in T-cells from the 'Th1-like'

C57BL/6 strain of mice and less active in T-cells from the 'Th2-like' Balb/c strain, where less co-localisation of the IFN-γR was seen upon TCR engagement. IL-4 prevented this co-localisation through a Stat6-dependent mechanism and instead directed cells along the Th2 developmental pathway. A later study showed that Th1 development was mediated by Stat1 signalling through the IFN-γR, and that IL-4R signalling (i.e. when IL-4 was present) antagonised the recruitment of Stat1 to the IFN-γR (542). In addition, in T-cells where Th1 development was deficient or Th2 development was constitutive the IL-4R was recruited into the synapse instead of the IFN-γR. This suggests that the recruitment of IFN-γR to the synapse upon TCR engagement under normal conditions may be a default occurrence and therefore Th1 differentiation may be the default pathway of development for naive T helper cells in the absence of the overriding Th2-promoting cytokine IL-4.

Cytokine environment is probably the most important factor in determining T-cell phenotype upon activation by antigen but development of Th1 and Th2 responses have been observed in the absence of their polarising cytokines (515, 543, 544). This suggests that other cytokines may also drive Th1/Th2 differentiation e.g. IL-13 for Th2 cells (545) or that other factors can also drive differentiation in the absence of a definitive cytokine signal.

Role of the antigen-presenting cell: The APC e.g. DC that interacts with a naïve T helper cell provides three signals required for correct activation and differentiation. Signal 1 is provided by the peptide-MHC complex that interacts with the TCR, whilst signal 2 is provided through interaction of the constitutively-expressed T-cell costimulatory molecule CD28 with its ligand, CD80 or CD86, on the DC surface (546). Signal 3, either in the form of a soluble mediator e.g. IL-12, or membrane protein e.g. OX40L, may then provide an additional signal indicating which differentiation pathway to follow (547).

DC reside in tissues and mucosal areas where they constantly sample their surroundings for pathogens, becoming activated in response to 'danger' signals such as specific pathogen-associated molecular patterns (PAMPs) (547). PAMPS include dsRNA, a sign of viral infection and components of bacterial/fungal cell walls, such as LPS or zymosan. They interact with TLRs on the DC surface and activate them (548). The nature of the 'danger' signal induces maturation of the DC - signalling through TLR3

(dsRNA) (549) or TLR4 (*E.coli* LPS) (550) induces differentiation into a DC1-type cell which produces IL-12 and promotes Th1 differentiation. Signalling through TLR2 (zymosan (551)) initiates differentiation into a DC2-type cell, which does not produce IL-12 and hence promotes Th2 responses. DC1 maturation is induced by IFN-γ (552) whilst DC2 maturation is linked to PGE_2 (553). Site of antigen exposure may determine the response - gut mucosal DC preferentially induce Th2 responses to antigen which are overridden by high levels of IFN-γ (554), whilst even in a strain of mice which typically favours Th1 responses (C57BL/6), antigen exposure in the lung induces predominantly Th2-type responses (555), suggesting that DC environment may condition them to induce one type of immunity over another.

Co-stimulation at the time of activation: Interaction of the costimulatory molecule CD28 with its ligands, CD80 and CD86, on APC is crucial for the development of Th effector cells in the absence of IL-2 (546); if IL-2 is present, costimulation through CD28 may only be required for the induction of Th2 responses (556). T-cell responses in a $CD28^{-/-}$ TCR transgenic mouse suggest that costimulation via CD28 is required for development of Th2-mediated primary responses (557). CD86 may direct development of Th2 cells from naive precursors (558, 559); other studies suggest that CD80 and CD86 costimulation may both result in Th1 or Th2 responses (560) and Th2 responses can be elicited in the absence of either molecule (561). CD86 costimulation may mediate Th17 responses in antigen-induced arthritis whilst CD80 costimulation in this model may downregulate development of Th2 responses (562).

OX40 is up-regulated on T-cells within 48 hours of activation and interaction with its ligand OX40L on APC may promote IL-4 production and Th2 differentiation (563). The CD28 family member ICOS, which functions similarly to CD28 but is up-regulated only upon T-cell activation may favour Th2 cell development (564). Absence of CD4 signalling may be detrimental to Th2 cell development (565) whilst signalling through CD4 may inhibit development of Th1 responses (566). Interaction of lymphocyte function-associated antigen-1 (LFA-1) with its ligand CD54 on APC inhibits Th2 cell development and may be important for development of Th1 responses (567). The influence of these molecules on Th1/Th2 differentiation may be linked to antigen dose. The ability of CD4 and LFA-1 to affect development of Th2 responses is dose-dependent whilst OX40 and CD28 can promote Th1 as well as Th2 responses depending on the dose of antigen (568).

Effect of antigen dose/concentration: In vivo priming of mice with a particular peptide antigen showed that immunisation with an increased dose of antigen which induces Th2 differentiation at a lower dose switches the phenotype of primed T-cells to Th1 (569). A peptide derived from keyhole limpet haemocyanin induced a Th2 phenotype at a low dose (2μg) but the phenotype switched to Th1 at a higher dose (50μg) (570). T-cells from the peripheral blood of allergic subjects grown in culture in the presence of antigen differentiated into Th2-type cells if the dose was less than 0.01 μg/ml but differentiated into Th1-type cells if the dose increased to between 10-30 μg/ml (571). Naive T-cells from a TCR transgenic mouse specific for a moth cytochrome c peptide could differentiate into Th1 or Th2 cells upon stimulation with this peptide, dependent on the dose of peptide administered; at doses between 0.05 μg/ml and 50 μg/ml, a Th1-type phenotype dominated, whereas at doses below 0.005 μg/ml, a Th2-type response dominated (572). A conflicting result was achieved using a different TCR transgenic system (573), where naive OVA-specific TCR transgenic T-cells grown in response to specific peptide showed Th1 responses at intermediate doses (0.3 μM to ~10 μM) whilst above 10 μM and below 0.03 μM, Th2 responses were induced. The study using cytochrome c-specific T-cells may not have assessed doses high enough to see Th2 cell development and the intermediate dose range that induced Th1 differentiation in OVA-specific T-cells may correlate with the 'high' dose assayed using moth cytochrome c.

Strength and duration of TCR signalling: The ability of differing doses of antigen to promote differentiation along different pathways led to the suggestion that the strength of signal received by the cell could influence development. Low doses of antigen would restrict availability of peptide-MHC complexes resulting in a lower intensity signal than when peptide-MHC complexes are plentiful, which would occur with high doses of peptide (574). Use of peptide variants known as altered peptide ligands (APLs) which differ from known immunogenic peptides by one amino acid involved in TCR contact (575) may alter the affinity of the TCR-peptide-MHC interaction. When naive TCR transgenic T-cells were stimulated with specific peptide or an APL of ~300-fold lower affinity for the TCR, the wild type peptide induced development of a Th1 response at the dose assayed (556). The lower affinity APL at the same dose favoured development of Th2 responses but could induce Th1 responses, suggesting that lower affinity TCR-peptide-MHC interactions promote Th2 cell development whilst higher affinity interactions promote development of Th1 cells. The pattern of TCRζ chain phosphorylation and ZAP-70 recruitment to the signalling complex was different when

activation was induced using wild-type peptide compared with APL (575). Distinct patterns of Ca^{2+} mobilisation within the cell were induced; wild-type peptide induced a strong, sustained calcium mobilisation, whilst the APL induced a smaller, more transient change. Interactions of differing affinities may induce qualitatively different signalling pathways which may signal for differentiation along different pathways. Further investigation of the different signalling pathways identified NFAT signalling, specifically the ratio between NFATc and NFATp (two forms of NFAT), as being important in determining the phenotype of an activated T-cell (576). The lower affinity interaction and transient calcium flux induced by APL favoured nuclear translocation of NFATc and the increased ratio promoted Th2 development.

Duration of signalling may also be important. Naive T-cells require prolonged antigenic stimulation (at least 20 hours) under optimal conditions (optimal antigen dose, co-stimulation through CD28, antigen presentation by 'professional' APCs) (577). The long time required for activation and development of effector functions may be due to the need to synthesise components of the signalling pathways and/or for chromatin remodelling of genes involved in T-cell differentiation. The effect of duration of signalling on differentiation of naive $CD4^+$ T-cells was analysed showing that a short burst of signalling (approximately 24 hours) in the presence of IL-12 was sufficient for differentiation of Th1 cells without any Th2 cell differentiation (578). Th2 cell differentiation was only seen after prolonged antigenic stimulation and absolutely required the presence of IL-4 during stimulation. Low levels of IL-4 can suppress Th1 cell development overriding the effects of IL-12 on developing cells. In the absence of added cytokines, 24 hours of stimulation induced proliferation in naive T-cells but significant development of effector phenotypes was only seen after 72 hours (Th1) or 96 hours (Th2), suggesting that duration of signalling through the TCR strongly influences differentiation of naive T-cells.

1.6.6 The serial triggering model

Whilst naive T-cells require prolonged antigenic stimulation for correct activation and differentiation into effector T-cells, the interaction between a TCR and peptide-MHC complex lasts only seconds (579, 580) due to its intrinsic low affinity (μM) and fast dissociation rate (off-rate). The TCRs of a T-cell undergoing activation must therefore interact with large numbers of peptide-MHC complexes. A single peptide-MHC

complex can activate a T-cell (450); these findings appear to contradict each other. The *serial triggering model* (581, 582) was proposed to explain how sustained signalling is achieved when the TCR-peptide-MHC interaction persists for only a few seconds. It suggests that a few peptide-MHC complexes on the APC surface serially engage many TCRs; the continued engagement of TCRs sustains signalling for as long as is required to activate the T-cell and direct its differentiation. The low affinity, fast dissociation rate and short half-life of TCR-peptide-MHC interactions facilitates serial triggering by limiting the duration of engagement, allowing one peptide-MHC complex to trigger many TCRs (581). The *kinetic proofreading model* (583) suggests that a basic 'triggered' TCR-CD3 complex, where ITAMs on CD3/TCRζ are phosphorylated and ZAP-70 is recruited must be formed before the TCR-peptide-MHC interaction dissociates for further signalling events to occur. If the duration of this interaction is too short, triggering will be incomplete leading to partial or no activation of the T-cell. If the interaction persists beyond the time required for triggering, failure to dissociate and allow engagement with other TCRs interferes with serial triggering, preventing sustained signalling and/or resulting in a qualitatively different signal. Comparison of the capacity of APLs to trigger signalling with wild-type peptide in a TCR transgenic system specific for an epitope of vesicular stomatitis virus (VSV) found that an alteration in peptide sequence changed the half-life of the TCR-peptide-MHC interaction (584). Different APLs had different effects; a decrease in affinity caused a decrease in half-life by increasing the dissociation rate and preventing full T-cell activation, whilst an increase in affinity either increased half-life leading to decreased T-cell activation or increased the rate of association between TCR and peptide-MHC, making T-cell activation more efficient. This suggests that there is an optimal range of half-life for the TCR-peptide-MHC interaction where T-cell activation is most efficient. Alternatively, this may form the basis for differential signalling leading to differential development; incomplete signalling, where ZAP-70 is not recruited to the signalling complex, may lead to development of Th2 cells (575).

1.6.7 The role of TCR structure in determining the affinity of the interaction with peptide-MHC

The affinity of binding between TCR and cognate peptide-MHC determines at least in part the fate of a T-cell when it is stimulated by antigen. The affinity of this interaction can be altered by changing residues within the peptide antigen, presumably due to loss

or gain of contacts with either TCR or MHC molecule which enhances or diminishes the stability of the interaction. As discussed in section 1.6.5, change in peptide structure through use of APLs can directly alter developmental fate of a naive T-cell upon antigen stimulation. It is possible that a change in TCR structure may influence the binding affinity and kinetics of the interaction with peptide-MHC and thus T-cell fate. Crystal structures of the interaction between TCR and peptide-MHC complex show that areas of TCR contact with the peptide-MHC complex (the antigen-binding site) are in the variable region, most specifically the CDRs (373, 376, 377). Comparison of crystal structures of TCR alone with the structure when complexed with peptide-MHC suggest that conformational change within the TCR occurs primarily at the antigen-binding site, with the CDR3s forming loops capable of undergoing significant conformational change to accommodate binding (585).

Moss and Bell (586) analysed CDR3 amino acid sequences of human αβ TCRs from peripheral blood, defining the CDR3α as being the amino acids between and not including the conserved alanine (A) residue in the Y-(L/F)-C-A motif found in most TCR Vα regions, and the phenylalanine (F) in the F-G-X-G-T motif found in most TCR Jα regions. The IMGT database now defines the CDR3α as containing the conserved A residue (378). The CDR3β was defined as being the amino acids between and not including the second conserved serine (S) residue in the Y-(L/F)-C-A-S-S motif found in most TCR Vβ regions, and the same phenylalanine residue as that used for the CDR3α. The IMGT database now defines the CDR3β as containing the conserved A and two S residues or their counterparts (378). Analysis of CDR3 lengths using a consensus definition of the CDR3 so that α and β lengths were comparable (by counting from the second serine residue in the CDR3β chain) suggested that in an unpolarised T-cell population, CDR3 lengths are normally distributed, CDR3α loops having a mean length of 9.7 (approximately 12 by IMGT definitions), and CDR3β loops having a mean length of 10.3 (approximately 12 by IMGT definitions). No significant difference in mean length was seen between adult and foetal blood T-cells, or between $CD4^+$ and $CD8^+$ T-cells. The amino acid composition of the CDR3 loops was also analysed; CDR3α loops contained a higher proportion of polar or charged residues at positions likely to contact the peptide (positions 2 and 3 from the conserved alanine described above). A less obvious distribution of amino acids was observed in the CDR3β loop; polar and charged residues were present throughout the loop with no preference for position and a higher proportion of glycine was seen.

Mutagenesis studies investigated the importance of the CDRs in antigen recognition and binding. Using APLs where the TCR contact residues were modified to hold opposite charge or polarity changed the gene segment usage of the TCRs that responded specifically, and in particular, changes were induced in the CDR3 regions of these TCRs to maintain peptide contact i.e. the residue thought to contact the peptide in the CDR3 of the responding TCR now carried the opposing charge (587). Alanine-scanning studies (where residues in the TCR thought to be crucial for antigen-binding are mutated to alanine) in murine and human TCRs have identified that most residues in the CDR1, CDR2 and CDR3 loops contact the peptide or the MHC molecule; the general consensus is that most of the peptide specificity is present in the CDR3 loops (588, 589). TCRs with higher affinity for their cognate ligands than their wild-type counterparts have been developed by mutation of CDR3 residues indicating that peptide specificity of TCR is seated in this region of the protein as alteration in this region changes TCR affinity for its ligand, but also suggesting that the low affinity of naturally-occurring TCRs is a function of their thymic selection rather than a physical limitation intrinsic to their framework (590, 591, 592).

1.6.8 Clonotypic expansion of T-cells in response to antigen stimulation and functional maturation of the T-cell response

A T-cell-mediated immune response to antigen is characterised by the clonotypic expansion of antigen-specific T-cells, where T-cells bearing antigen-specific receptors preferentially proliferate in response to antigen and dominate the T-cell population at the site of infection and nearby draining lymph nodes. Such antigen-specific expansions have been documented in $CD8^+$ T-cell responses to herpes simplex virus in mice (593), and in human $CD4^+$ T-cell responses to myelin basic protein in multiple sclerosis (594). In humans, limited expansions of particular TCR Vβ regions in BALF of both atopic and non-atopic asthmatic subjects has been observed (595, 149, 596).

Expansions of antigen-specific T-cells have been tracked in both $CD4^+$ (597) and $CD8^+$ (598) primary and recall immune responses in terms of TCR amino acid sequence particularly at the antigen-binding site. Activated $CD8^+$ T-cells isolated from peripheral blood of mice immunised through injection of HLA-Cw3-transfected cells were analysed by single-cell PCR (598). As this response shows a preference for TCRs containing a TCR Vβ10-Jβ1.2 chain, primers specific for this combination were used to

amplify the TCRβ chain of all such activated T-cells. Analysis of the CDR3 loops from these TCRs showed significant conservation of CDR3 amino acid sequence; in all but one sequence, a uniform length of 6 amino acids (as defined in 586) was seen and all but one sequence preserved a germline-encoded negatively-charged glutamate residue. There was also a high incidence of a glycine residue within the non-germline-encoded region suggesting that these residues were potentially important for enhancing contact with the peptide and for TCR specificity and those T-cells bearing receptors with these characteristics were therefore selected for expansion. Analysis of T-cells involved in recall responses showed that the TCR repertoire raised against this antigen remained very similar, suggesting that the responding repertoire is largely selected and defined during the primary response to antigen.

Another study followed the expansion of antigen-specific $CD4^+$ T-cells after primary and secondary immunisation of mice with pigeon cytochrome c (PCC) (597). Activated $CD4^+$ T-cells were isolated from draining lymph nodes on different days after immunisation and cDNA products were analysed by PCR. Antigen-specific T-cells increased in frequency as the response progressed, peaking at approximately day 7 of the primary response (250-fold increase compared with day 0) and day 3 (i.e. an accelerated response) after secondary immunisation. PCR analysis of the CDR3α and β loops after immunisation identified eight features that were partially conserved in the responding T-cells. One of these features (a glutamate residue in the CDR3α loop) was conserved amongst most TCR Vα11 chains, regardless of whether TCRs were PCC-specific or not; the remaining seven features only became apparent as the response proceeded. T-cells bearing receptors with such CDR3 features (conserved CDR3 lengths, conserved J region usage, particular conserved residues) became more dominant as the response progressed. In resting cells, such features were present in less than 30% of all Vα11 Vβ3 TCRs; by day 7, over 80% of isolated T-cells carried receptors containing six or more of these features and the TCR repertoire for this response was considered to be restricted. Analysis of TCR sequence after secondary immunisation showed that by day 3 of the recall response, 96% of all responding T-cells carried TCRs with six or more of these features, suggesting that the memory response was even more restricted than the primary response. This study suggested that as an immune response progresses, selective expansion of T-cells on the basis of their TCR structure occurs, favouring expansion of those TCRs particularly well-suited to respond to the antigen from the original pool of antigen-specific TCRs i.e. antigen-

driven selection of the T-cell repertoire. This leads to functional maturation of the T-cell response by favouring those TCRs with CDR3 loops containing particularly high capacity to bind and recognise antigen, giving a faster, more specific and higher affinity response upon subsequent challenge.

T-cell immune responses involve selection of particular T-cells for expansion based on the affinity of their TCR for antigen and this selection is based on the capacity of the TCR structure to bind antigen with higher affinity than other available TCRs. TCR structure itself may therefore play a role in determining T-cell phenotype upon antigen stimulation as small differences in the structure that increase antigen specificity or affinity can lead to their preferential expansion. At the time of activation, other factors present e.g. cytokines could lead to the preferential selection of T-cells bearing receptors favouring development of one T helper phenotype over another from the available pool of antigen-responsive T-cells. As Th2 development is associated with the transmission of a weaker signal through the TCR than Th1 development, expansion of TCRs that naturally transmit a weaker signal in response to antigen may be selected for when external conditions favour the development of a Th2 response and vice versa. In other words, the structure of the TCR itself could be an important factor in determining the fate of a naive $CD4^+$ T-cell upon its activation under certain circumstances.

1.6.9 Can TCR structure influence the fate of a naive T helper cell upon stimulation with antigen?

A number of studies have provided evidence that TCR structure may play a role in determining differentiation of a naive T helper cell into a Th1 or Th2 effector cell. A single point mutation in the CDR2 of a chicken conalbumin-specific TCR, mutating leucine to serine, altered the phenotype of cells from Th1 to Th2 (599). The mutated residue contacted a particular residue of the relevant peptide; mutation of this peptide from arginine to glycine restored the Th1 response in the cells carrying the mutated TCR. As TCR structure itself, particularly the CDR loops, determines peptide-MHC specificity and therefore affinity of the interaction with peptide-MHC, structure at the antigen-binding site may influence the fate of the cell upon its activation and a difference, even at one residue of the antigen-binding site, could have a dramatic effect on T-cell fate. Another study compared the response in Th1 and Th2 clones raised against a peptide epitope involved in EAE induction in mice, proteolipoprotein 139-151

($PLP_{139-151}$) (600). Whilst not all Th1 clones expressed TCRs composed of the same gene segments, each clone absolutely required the presence of a tryptophan residue at position 144 of the peptide. If this residue was mutated to alanine, Th1 clones failed to mount a response. In contrast, Th2 clones raised against the same peptide epitope could respond to the peptide altered at position 144 but showed a requirement for the residues at positions 141 (leucine) and 142 (glycine) as they failed to respond when challenged with peptides mutated at these positions, suggesting that TCRs favoured by the Th1 clones mediated their response through recognition of a different peptide residue than TCRs favoured by the Th2 clones. It is likely that the TCR structures favoured by each type of clone will be those best able to recognise the relevant residue.

A further study based in our laboratory investigated TCR usage in Th1- or Th2-polarised T-cell lines and clones raised against the same peptide-MHC complex (PLP_{56-70} bound to MHC class II $I\text{-}A^{g7}$) (601). Lines and clones were Th1 if they produced IFN-γ in the absence of IL-4, -5 or -10, and Th2 if they produced IL-4 and -5, but not IFN-γ. TCRα and β chains used in the long-term differentiated clones were analysed by PCR and gene segment selection and CDR3 features were compared. Selection of TCRβ chains showed no obvious differences between Th1 and Th2 clones in terms of CDR3 length. The main difference seen between Th1 and Th2 clones in terms of TCRα chains was in length and composition of the CDR3 loop – Th1 clones predominantly expressed TCRs with a CDR3α length of 10 amino acids, whilst CDR3α loops from Th2 clones were longer at 13 amino acids. A similar TCR sequence analysis was carried out on short-term Th1- or Th2-polarised T-cell lines that had been re-stimulated with peptide-MHC three times. Selection of dominant clonotypes was seen in these lines. The Th1 and Th2 lines selected different TCRs for expansion from the original bulk population from which they were both derived. The Th1 line favoured expansion of a TCR bearing a CDR3α loop of 12 amino acids, whilst the Th2 line favoured a TCR bearing a 14 amino acid CDR3α. The mean CDR3α lengths of all TCRs present in each line were significantly different with the Th2 line in general expressing TCRs with longer CDR3α loops. The Th1-dominant TCR was present in a small proportion of Th2 line cells, but the Th2-dominant TCR was not found in the Th1 line, suggesting that whilst cells may favour elongated CDR3α loops when developing along the Th2 pathway, they can also use TCRs with shorter loops. In contrast, the use of an elongated CDR3α does not seem to occur in Th1-developing cells, marking a difference between Th1 and Th2 cells in terms of TCR usage. Molecular modelling of TCRs isolated from

two clones, A10(2) (a Th1 clone) and D3(3) (a Th2 clone), which differed in CDR3α length by three amino acids suggested that the elongated loop in the Th2 TCR which was composed of amino acids with bulkier side-chains protruded into the TCR-peptide-MHC binding interface and provided steric hindrance. This would most likely lead to a lower affinity interaction with peptide-MHC, which is linked with the development of Th2 cells. This study suggested that the conditions under which a T-cell is activated can promote selection of particular TCRs that best fit the developmental fate being followed. Under Th2-polarising conditions, the expansion of T-cells bearing receptors with a lower affinity for the peptide-MHC complex may be favoured. The derivation of the T-cell clones A10(2) and D3(3) is shown in Figure 1.2.

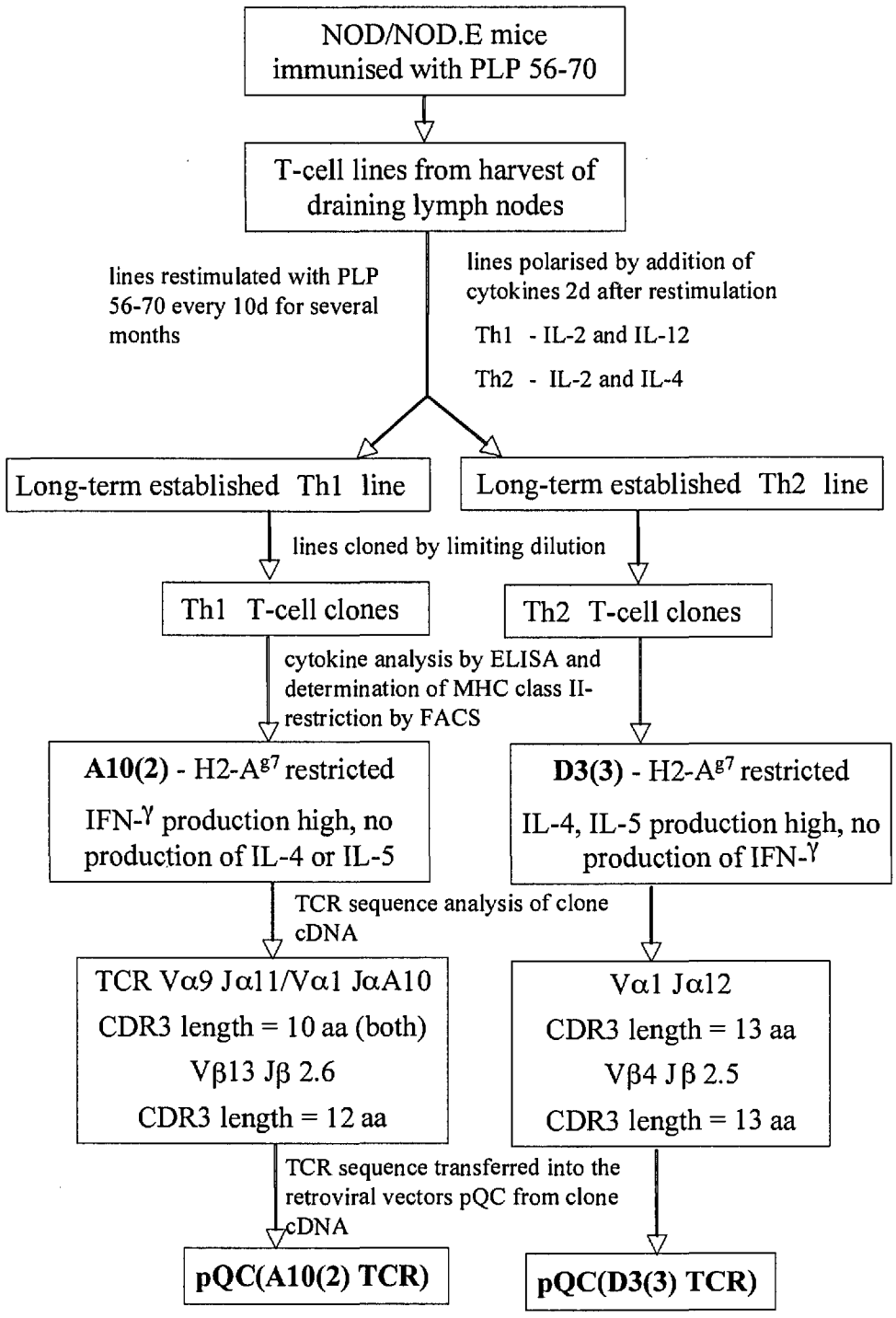


Figure 1.2 Characterisation of the TCRs expressed by PLP 56-70-specific T-cell clones A10(2) and D3(3) (see reference 601). The above scheme shows a summary of previous work carried out in the Boyton laboratory that led to the identification of TCRs from two independent T-cell clones derived from long-term T-cell lines raised against PLP_{56-70} and restricted to the same MHC class II molecule, H2-A^{g7}. The lines were polarised in vitro towards a Th1 (A10(2)) or Th2 (D3(3)) phenotype, and transferred into the pQC series of retroviral vectors.

1.7 Aims of this thesis

Previous work from our laboratory suggested that TCR structure may be important in determining T-cell phenotype upon activation through interaction with its cognate peptide-MHC complex, with elongated CDR3s being favoured by developing Th2 cells. This led to the hypothesis that in the human Th2-mediated disease allergic asthma, TCRs will expand in response to allergen challenge that carry elongated CDR3 loops. In order to test this hypothesis, Chapter 3 shows the analysis of TCR CDR3 usage in human T-cell lines derived from HLA-DR1$^+$ cat-allergic asthmatic subjects and generated against the important T-cell epitope of Fel d 1, peptide 4. Expanded T-cell populations expressing particular TCRs were identified in these lines that carried elongated CDR3α and β loops. Attempts to transduce the TCR-negative line BW7 (602) with TCR genes identified from this work and from the initial study (601) in order to further study the impact of these elongated CDR3 loops on T-cell function were not successful and I did not take this work forward.

A humanised TCR/MHC class II transgenic mouse model of allergic asthma has been developed in our laboratory by postdoctoral research associates funded by Asthma UK. It expresses a TCR identified through clonotypic analysis of HLA-DR1-restricted peptide 4-specific T-cell lines derived from HLA-DR1$^+$ cat allergic subjects, as well as transgenically expressed HLA-DR1, on a murine MHC class II knockout background. This model was developed in order to test the hypothesis that a humanised TCR/MHC class II transgenic model of allergic asthma would be an improved mouse model of allergic asthma, and the early experimental characterisation of this model that I carried out with Dr. Catherine Reynolds and Dr. Xiaoming Cheng is shown in Chapter 4. In addition, basic characterisation of the TCR transgenic mice in terms of expression of costimulatory molecules in the spleen and thymus in comparison to non-TCR transgenic mice was carried out to test the hypothesis that expression of a transgenic TCR alters the expression of other T-cell signalling associated molecules in both the thymus and the periphery. Differences in the expression of some costimulatory molecules, namely CD44, CD62L, ICOS and OX40, were seen in the thymus but not the spleen, and the possible implications of these findings are discussed.

2. Materials and Methods

All stock solutions and buffers are shown in appendix 1.

2.1 Molecular biology techniques

2.1.1 Human TCR CDR3 analysis

2.1.1.1 RNA isolation from human T-cell lines

HLA-DR1-restricted, peptide 4-specific human T cell lines at successive restimulations with peptide 4 (KALPVVLENARILKCNV) (these lines were generated from HLA-$DR1^+$ cat allergic individuals in Professor Mark Larché's laboratory, National Heart and Lung Institute, Imperial College, London) were supplied either frozen at -80°C in RNAlater (Ambion, 7020) or fresh on the day of restimulation. RNA from frozen cells was extracted using RNAzol B (Biogenesis, CS-105B) via the single-step guanidinium disruption/acid phenol extraction method. The product was solubilised in 20 µl RNase-free dH_2O (Sigma, W4502) with 0.5 µl (20U) RNase OUT ribonuclease inhibitor (Invitrogen, 10777-019) added. RNA from fresh cells was extracted on the same day by guanidine thiocyanate lysis followed by binding to a silica-based matrix and DNase treatment using the Absolutely RNA Nanoprep Kit (Stratagene, 400573) and eluted into 20 µl Elution Buffer (from the kit). RNA was stored at -20°C.

2.1.1.2 cDNA preparation from human T-cell RNA

First-strand cDNA synthesis was carried out using Cloned AMV Reverse Transcriptase with oligo$(dT)_{20}$ primers (Invitrogen, 12328-032). cDNA was synthesised from 5 µg of RNA. RNA was first mixed with 1 µl of 50 µM oligo$(dT)_{20}$ primers and 2 µl 10 mM dNTP mix and made up to 12 µl with RNase-free dH_2O. This mix was denatured at 65°C for 5 minutes before being placed on ice. cDNA was then synthesised in a final reaction volume of 20 µl comprising the 12 µl reaction mix described previously in 1x reaction buffer (50 mM Tris-acetate (pH 8.4), 75 mM potassium acetate, 8 mM magnesium acetate, 4 µg/ml BSA) and 5 mM dithiothreitol (DTT) with 40 U RNase OUT RNase inhibitor and 15 U cloned AMV reverse transcriptase added. The reaction was incubated at 25°C for 10 minutes, 50°C for 50 minutes and stopped by heating to

85°C for 5 minutes. The cDNA product was precipitated three times using a final concentration of 2M ammonium acetate (Sigma, A7262) in at least three volumes of 100% ethanol. The pellet was resuspended in 20 µl RNase-free dH_2O after the first two precipitations and in 11 µl RNase-free dH_2O after the third. This cDNA was polyG-tailed using recombinant terminal transferase (Roche, 3 333 566) in a reaction volume of 20 µl, comprising 11 µl cDNA, 1x enzyme buffer (200 mM potassium cacodylate, 25 mM Tris-HCl, 0.25 mg/ml BSA (bovine serum albumin), pH6.6), 0.75 mM cobalt chloride, 5 mM dGTP (Bioline, BIO-39037) and 400U terminal transferase. The reaction was incubated at 37°C for 15 minutes and stopped by heating to 75°C for 10 minutes. Enzyme was removed by addition of acid-equilibrated phenol:chloroform (5:1) (Sigma, P1944) and tailed cDNA was extracted in the aqueous phase. A final ammonium acetate/ethanol precipitation was carried out and the cDNA pellet was resuspended in 200 µl dH_2O. cDNA was stored at -20°C.

2.1.1.3 Polymerase chain reaction (PCR)

PCRs (see appendix 2 for primer sequences and reaction conditions) were carried out using the BIOTAQ PCR kit (Bioline, BIO-21071). Reactions occurred in a volume of 25 µl comprising 1x NH_4-based buffer (16 mM $(NH_4)_2SO_4$, 67 mM Tris-HCl, 0.01% Tween-20, pH 8.8), 1.5 mM $MgCl_2$, 200 µM dATP, dCTP, dGTP and dTTP (Bioline, BIO-39025), 50-100 ng template DNA, 0.5 µM forward and reverse primers (Sigma-Genosys) and 0.6U Taq polymerase. Each completed reaction was run in a separate lane on a 1% agarose TAE gel (appendix 1) with 3-10 µl (depending on gel size) of 10 mg/ml ethidium bromide (Sigma, E1510) added, alongside Promega 1 kb DNA ladder (G5711), and visualised under UV light. Loading buffer (appendix 1) was added to a 1x concentration to allow visualisation of how far the gel had run.

2.1.2 Cloning of TCR α and β chains into MFG and pTcass expression vectors

To transduce the murine thymoma line BW7 (602) with genes coding for TCRs identified from the CDR3 analysis of the human T-cell lines from cat allergic subjects and the TCRs identified from murine Th1 and Th2 clones A10(2) and D3(3) (from 601), I designed and carried out strategies to clone these genes into relevant expression vectors. In the first instance, a retroviral transduction system was used, requiring the transfer of TCR genes into a vector designed for use in such a system. Retroviral

transduction systems, such as the Phoenix system used here (603), comprise packaging lines which have been stably transduced with all the genes required for production of retroviral particles except for the packaging signal, ψ. This is supplied as a component of a retroviral expression vector which also includes the gene which is to be expressed in the target cell line. The retroviral expression vector chosen for use here was MFG (604, 605), shown in Figure 2.1, which was created using Moloney murine leukaemia virus (MoMuLV) long terminal repeat sequences to generate both full length viral RNA molecules (allowing packaging into functional viral particles) and a shorter subgenomic viral RNA molecule (analogous to the envelope gene in unmodified MoMuLV viral genome). It is this latter feature that allows the expression of inserted sequences in target cells. The vector also contains sequences in the viral gag region that have been shown to improve packaging and thus increase virus titre, as well as the splice donor and acceptor sites needed to generate the env mRNA and allow for the expression of the inserted genes. Whilst MFG lacks a selectable marker (such as an antibiotic resistance gene) found in many other retroviral expression vectors, an advantage of it is that unlike most other retroviral expression vectors, it also lacks a specific deletion in the 5'- long terminal repeat region of the genome. This deletion is deliberately incorporated into the sequence if it is present as a safety factor – virus harvested from packaging cells transfected with such a vector are replication-incompetent and are incapable of producing infectious virus in the target cells, as the packaging signal can no longer be expressed. It was found to be necessary here to use a serial system of two packaging lines (as will be discussed further in Chapter 3 of this thesis) and the lack of this deletion in MFG meant that it could be used in such a system. I was unsuccessful in transducing cells using a retroviral expression system so I also used a system based on electroporation, the Amaxa Nucleofector system (discussed in more detail in Chapter 3) to transduce the target cell line with TCR genes. This required transfer of the genes into a different expression vector, one which could initiate gene expression in cells of the T-cell lineage such as BW7. The pTcass vectors (346) were designed for use in the production of TCR transgenic mice, using T-cell-specific promoter and enhancer sequences to ensure that the transgene is only expressed in the T-cells of the mouse. These constructs have also been used in an electroporation system to successfully transduce the BW7 line with TCR genes (606) and so the human and murine TCRs of interest were moved into these vectors for use with the Amaxa system.

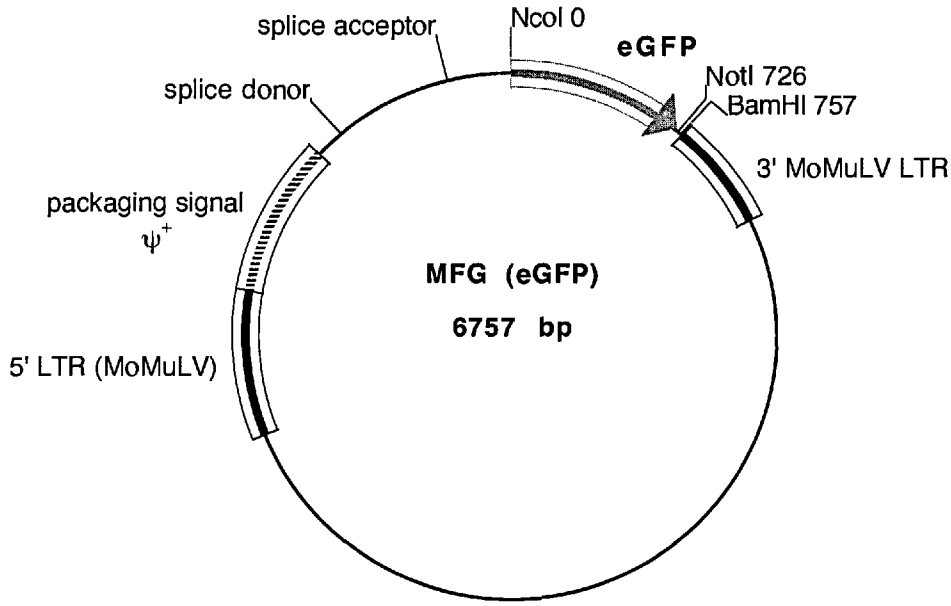


Figure 2.1 MFG(eGFP) (604, 605) This vector diagram shows the retroviral components of the vector MFG, derived from the Moloney murine leukaemia virus (MoMuLV) genome, and the target gene eGFP. The gene of interest (here, eGFP) is inserted between NcoI and BamHI restriction sites – the NcoI site contains an ATG motif that coincides with the start codon of the viral env gene. There is no selectable marker present in the vector.

The strategies devised to move the TCR genes into these vectors are described in detail in Chapter 3 of this thesis.

2.1.2.1 RNA isolation from murine T-cells

RNA was extracted from a single cell suspension of freshly-isolated mouse splenocytes using Trizol reagent (Invitrogen, 15596-018) via the single-step guanidinium disruption/acid phenol extraction method as for RNAzolB above. The product was solubilised in 20 µl RNase-free dH_2O with 0.5 µl (20U) RNase OUT ribonuclease inhibitor added.

2.1.2.2 cDNA preparation from murine T-cell RNA

RNA was first treated with RQ1 RNase-free DNase (Promega, M6101) to remove any contaminating genomic DNA. The reaction was carried out in a final volume of 20 µl comprising RNA (5 µg), RQ1 RNase-free DNase (1 U per 1 µg RNA) and 1x reaction buffer (40 mM Tris-HCl (pH 8.0), 10 mM magnesium sulphate and 1 mM calcium chloride) and was incubated at 37°C for 30 minutes. Enzyme was removed by addition of acid-equilibrated phenol:chloroform (5:1). The aqueous phase was extracted and all traces of phenol were removed through treatment with chloroform:isoamyl alcohol (24:1). The aqueous phase was again extracted and washed in at least 2.5 volumes of 100% ethanol. The final RNA pellet was resuspended in 20 µl RNase-free dH_2O with 20 U RNase OUT. First-strand cDNA synthesis was carried out using Superscript III Reverse Transcriptase with random hexamer primers (Invitrogen, 18080-093). RNA (2 µl) was first mixed with 1 µl of 50 ng/µl random hexamer primers and 1 µl 10 mM dNTP mix, made up to 13 µl with RNase-free dH_2O. This was denatured at 65°C for 5 minutes before being placed on ice for at least 1 minute before proceeding. cDNA was then synthesised in a final reaction volume of 20 µl comprising the 13µl mix described previously in 1x reaction buffer (50 mM Tris-HCl (pH 8.3), 75 mM potassium chloride, 0.75 mM magnesium chloride) and 5 mM DTT with 40 U RNase OUT RNase inhibitor and 200 U Superscript III reverse transcriptase added. The reaction was incubated at 25°C for 5 minutes, 50°C for 60 minutes and stopped by heating to 70°C for 15 minutes. cDNA was stored at -20°C.

2.1.2.3 PCR using high-fidelity DNA polymerase

PCRs to amplify DNA sequences to be used in cloning steps (see appendices 3 and 4 for primer sequences and reaction conditions) were carried out using the high-fidelity DNA Taq polymerase BIO-X-ACT SHORT (Bioline, BIO-21065). For the steps involving site-directed mutagenesis of one or more base pairs (or the addition of a base pair into the sequence), primers were designed accordingly. For the strategies designed to transfer TCR genes into the MFG vector, 22 primers were used in total of which I designed 15 and 7 of which were designed by other researchers in the Boyton laboratory (as indicated in Appendix 3). I redesigned one primer as the initial primer did not produce a PCR product – an extra restriction site added for ease of cloning was removed from the primer sequence (see Appendix 3). For the strategies designed to transfer TCR genes into the pTcass vectors, 26 primers were used in total of which I designed 23 and 3 of which were designed by other researchers in the Boyton laboratory (as indicated in Appendix 4). No primers were redesigned for these strategies.

Reactions occurred in a volume of 25 µl comprising 1x Optibuffer, $MgCl_2$ (see appendices 3 and 4 for concentration used for each reaction), 200 µM dATP, dCTP, dGTP and dTTP mix, 50-100 ng template DNA, 0.5 µM forward and reverse primers and 2U BIO-X-ACT SHORT. Each completed reaction was run in a separate lane on a 1% agarose TAE gel (or 2% gel for PCR products less than 100 bp in size) containing ethidium bromide alongside either Promega 1 kb DNA ladder (as before) or Invitrogen I kb DNA ladder (15615) and visualised under UV light. Loading buffer was added as described previously. All other PCR reactions (i.e. to check orientation of final inserts in MFG) were carried out using BIOTAQ polymerase as described above in 2.1.1.3 (primers and reaction conditions are shown in Appendices 3 and 4).

2.1.3 General DNA cloning techniques

2.1.3.1 Preparation of competent cells

Two strains of competent cells were used – XL-GOLD and K12 ER2925 (New England Biolabs, E4109S). K12 ER2925 was used for any step involving restriction digest with ClaI (Promega, R6551); for all other transformations, XL-GOLD cells were used. To prepare competent cells, cells from a previous stock of XL-GOLD or glycerol stock of

ER2925 were streaked onto an Luria-Bertani (LB) agar plate containing 50 μg/ml tetracycline (Sigma, T3258) (appendix 1) (XL-GOLD) or 25 μg/ml chloramphenicol (Sigma, C0378) (appendix 1) (ER2925) and grown overnight at 37°C. A single colony was expanded overnight at 37°C with shaking in 5 ml LB broth containing the same antibiotic at the same concentration. This culture was used to inoculate 200 ml autoclaved LB broth containing 3 ml 1M $MgCl_2$ (Sigma, M8266) and grown at 37°C with shaking until the OD_{600} was 0.6. The culture was then placed on ice for 10 minutes. Solutions A (60 ml) and B (12 ml) (appendix 1) were prepared previously and cooled on ice. The culture was centrifuged in pre-chilled centrifuge tubes at 1500 x *g* for 10 minutes at 4°C; pellets were resuspended in 30 ml solution A and chilled on ice for 20 minutes. The tubes were then centrifuged at 1500 x *g* for 10 minutes at 4°C and pellets were resuspended in 6 ml ice cold solution B. 250 μl aliquots were transferred to sterile eppendorfs on dry ice and tubes were stored at -80°C.

2.1.3.2 Restriction digests

Restriction digests for all cloning steps in the MFG and pTcass cloning strategies were carried out in 40 μl volume containing 1x restriction enzyme buffer (appendix 5), 2U restriction enzyme and 1-4 μg of plasmid DNA. The reaction was incubated at the specified temperature (appendix 5) for 1 hour followed by inactivation by heating to 65°C for 15 minutes. If a single restriction enzyme digest had been carried out, the vector was dephosphorylated using Calf Intestinal Alkaline Phosphatase (Promega, M1821) to prevent re-ligation without an insert. Two aliquots of 0.01U alkaline phosphatase per pmol DNA ends were required, where 1 μg of 1,000 bp DNA = 3.03 pmol ends. Each reaction was incubated for 1 hour at 37°C with the second aliquot of enzyme being added after 30 minutes. Completed digests were run down a 1% agarose TAE gel alongside a DNA ladder, correct bands (vector and insert) were excised from the gel and purified as described previously. 1 μl of the purified eluate was run down a 1% agarose TAE gel with Hyperladder I (Bioline, BIO-33025) to quantify the amount of DNA purified.

Restriction digests were also used to check for the presence of an insert in the human TCR CDR3 analysis or to check for the presence of a correctly-oriented and correctly-sized insert at each step in the MFG and pTcass cloning strategies. Reactions were carried out in a final reaction volume of 20 μl containing 1x restriction enzyme buffer

(appendix 5), 1U restriction enzyme and 1 μg of plasmid DNA. Reactions were incubated at the specified temperature (appendix 5) for 1 hour before being run down a 1% agarose TAE gel alongside a DNA ladder and analysed for correct insertion, size and/or orientation.

2.1.3.3 Oligonucleotide preparation

Oligonucleotides (single strands, Sigma-Genosys), reconstituted at 500 μg/ml in sterile dH_2O, were diluted to a concentration of 50 ng/μl in a volume of 20 μl, heated to 70°C for 5 minutes and allowed to anneal by slowly cooling to room temperature (annealed linkers were placed in a beaker of water at 65°C and left to cool). Annealed oligonucleotides were incubated in a volume of 50 μl with 20U polynucleotide kinase (Promega, M4101), 1x reaction buffer (70 mM Tris-HCl (pH 7.6), 10 mM $MgSO_4$, 5 mM DTT) and 1 mM ATP (Sigma, A6559) at 37°C for 1 hour before incubation for 1 hour at -20°C in 200 μl isopropanol. The final pellet was resuspended in 20 μl dH_2O and the annealed, phosphorylated linker was ligated into the vector.

2.1.3.4 Nuclease treatment

To destroy the NcoI restriction enzyme site in MFG, vector DNA (1-4 μg) was digested with restriction enzyme NcoI (appendix 6), treated with 0.5-4U S1 nuclease (Promega, M5761) in 1x reaction buffer (50 mM sodium acetate (pH 4.5), 280 mM sodium chloride, 4.5 mM $ZnSO_4$) and incubated at 37°C for 30 minutes. The reaction was stopped by heating to 70°C for 5 minutes and the digested vector was re-ligated without insert. Destruction of the restriction site had occurred if there was no cutting upon digestion of the re-ligated plasmid with NcoI. The re-ligated plasmid was also cut with NotI (appendix 6) to ensure that the nuclease digestion had not destroyed that site.

2.1.3.5 Cloning ligations

Ligations were carried out at varying vector:insert ratios. To determine the amount of insert DNA required for the correct ratio, the following formula was used:

$$\text{ng insert} = \frac{\text{ng vector x kb size of insert}}{\text{kb size of vector}} \times \text{molar ratio} \frac{\text{insert}}{\text{vector}}$$

Ratios of 1:1, 1:3, 1:6 and 1:12 were used with approximately 100 ng vector used per reaction. Controls were carried out at a 1:0 vector:insert ratio either with or without ligase to determine the efficiency of enzyme restriction and frequency of vector re-ligation. All ligations were carried out in a volume of 10 µl containing insert and vector DNA, 1x ligase buffer (described previously) and 2.5U T4 DNA ligase (Invitrogen, 15224-041) and incubated at 16°C overnight.

2.1.3.6 TA cloning ligations

DNA bands of the correct size for each reaction were excised from the gel and purified using a silica matrix protocol (QBiogene, 1101-200) to preserve the A overhangs incorporated by Taq polymerase. Products were cloned into pCR®2.1 (TA cloning kit, Invitrogen, R2000-01), supplied pre-linearised. 10-20 ng of PCR product were ligated into 25 ng of pCR®2.1 using 3U T4 DNA ligase (Invitrogen 15224-041) in 1x reaction buffer (50 mM Tris-HCl (pH 7.6), 10 mM $MgCl_2$, 1 mM ATP, 1 mM DTT and 5% (w/v) PEG-8000) in a reaction volume of 10µl and incubated at 16°C overnight.

2.1.3.7 *E.coli* transformation

XL-GOLD competent cells were used to transform TA cloning ligations and other cloning ligations. 2 µl of ligation mixture was added to 50 µl cells and incubated on ice for 30 minutes. Heat shock was carried out at 42°C for 30 seconds followed by addition of 250 µl of LB broth (Sigma, L3022) at room temperature. Cells were incubated with shaking for 1 hour at 37°C then spread onto LB agar (Sigma, L2897) plates containing 50 µg/ml ampicillin (Sigma, A9518) (appendix 1), previously spread with 40 µl of a 40 mg/ml solution of X-Gal (5-bromo-4-chloro-3-indolyl b-D-galactopyranoside) (Bioline, BIO-37035) and 8 µl of a 100 mM solution of IPTG (isopropyl beta-D-1-thiogalactopyranoside) (Sigma, I6758) to allow for blue/white screening of colonies (only TA cloning transformations).

Any plasmid involved in a cloning step requiring digestion with the enzyme ClaI was transformed into the dam^- (Dam methylase deficient) strain K12 ER2925 to allow ClaI digestion to occur correctly. Transformation occurred as for XL-GOLD (without X-gal or IPTG).

2.1.3.8 Plasmid DNA preparation

Successfully transformed colonies (white or mostly white colonies) were expanded in liquid culture (8 ml LB broth containing 50 μg/ml ampicillin) overnight at 37°C with shaking. Bacteria were pelleted by centrifugation at 1500 x *g* for 4 minutes followed by extraction and purification of plasmid DNA by alkaline lysis (Sigma, NA0160). Plasmids were screened for insertion of the PCR product by restriction digest as shown in Appendices 2 and 6. Diagnostic digests were carried out in a 20 μl volume containing 2 μg plasmid DNA, 1U restriction enzyme and 2 μl 10x restriction enzyme buffer. Reactions were incubated at the optimum temperature specified for 1 hour. Digests were run on a 1% agarose TAE gel with DNA ladder.

For the final MFG and pTcass constructs, once correct insertion and sequence had been ascertained, a larger-scale plasmid preparation was carried out using 500 ml bacterial culture. 5ml cultures were inoculated into 500 ml LB broth containing 50 μg/ml ampicillin and grown overnight at 37°C with shaking. Bacteria were pelleted by centrifugation at 1500 x *g* for 30 minutes at 4°C and plasmid DNA was extracted and purified by alkaline lysis (Invitrogen, K2100-07). Plasmids were screened by restriction digest as before.

2.1.3.9 Sequence analysis

For the human TCR clonotypic analysis and for the MFG and pTcass cloning strategies where the step involved a PCR amplification step and transformation into pCR®2.1, all plasmids yielding a correctly-sized fragment after digestion with EcoRI were sequenced at the Natural History Museum DNA Sequencing Facility (London, UK) using the M13 forward sequencing primer (appendix 2) and in the case of the MFG and pTcass sequences, with the M13 reverse primer also (appendices 3 and 4). For the final constructs of the MFG and pTcass cloning strategies, all plasmids yielding a correctly-sized fragment after diagnostic restriction enzyme digest and in the case of the MFG constructs, shown to be correctly oriented by PCR, were also sequenced at the Natural History Museum DNA Sequencing Facility using sequencing primers described in Appendices 3 and 4. Intermediate cloning steps that did not involve PCR were not sequenced but were confirmed using diagnostic restriction digests and/or PCRs where appropriate and as stated in Chapter 3. Sequence data was manipulated using

GeneJockeyII software, raw sequence data being read by EditView software (Perkin Elmer). Sequences were aligned against the International Immunogenetics (IMGT) information system database (http://imgt.cines.fr) and classified according to their definitions.

2.2 Genotyping of P4 TCR/DR1/ABO transgenic mice

2.2.1 Genomic DNA extraction from tail tips

Genomic DNA for use in genotyping of transgenic mice and for the amplification of J-region-intronic sequences in the pTcass cloning strategies was extracted from tail tips after digestion with proteinase K (Sigma, P2308). Tail tips were incubated overnight at 56°C in a final volume of 400 µl of tail digestion buffer (appendix 1) with 10 µl of 20 mg/ml proteinase K added and mixed by vortexing before incubation. Genomic DNA was isolated by high concentration salt extraction by adding 200 µl 6M saturated sodium chloride (Sigma, S7653) solution and mixing by shaking for 30 seconds to precipitate all protein in the sample. Samples were centrifuged at 16100 x *g* using a microcentrifuge to pellet the protein and the supernatant was extracted and treated with an equal volume of isopropanol to precipitate the DNA. Samples were centrifuged at 16100 x *g* and the DNA pellet was washed with 70% ethanol to remove any excess salt. The final pellet was left to air dry and resuspended in 50 µl sterile dH_2O (Sigma, W4502). DNA samples were diluted by 1 in 50 using sterile dH_2O before use in PCR.

2.2.2 Genotyping by PCR

Genotyping PCRs (see appendix 6 for primers and reaction conditions) were carried out as described above in 2.1.1.3.

2.2.3 Collection, preparation and staining of tailbleed samples for phenotyping by flow cytometry

Tailbleed samples were collected in 50µl heparin (Leo Laboratories) at 0.5U/µl, diluted in sterile PBS (pH 7.4, Invitrogen, 10010-015), with 6-8 drops of blood being collected from the tail vein of each mouse. The tail vein was nicked using a fresh sterile scalpel for each mouse which had previously been kept for at least 10 minutes in a heat-

controlled box at 37°C to enlarge the vein. Blood samples were mixed thoroughly with the heparin to prevent clotting. Red blood cells were lysed by the addition of 1 ml dH_2O and repeated passage through a 23G hypodermic needle for no more than 30 seconds before being added to 11 ml complete RPMI-1640 medium (appendix 1). After centrifugation at 300 x *g* the cell pellet was washed twice in 10 ml FACS buffer (appendix 1). Cells were then stained using 1µl anti-CD45R-FITC and 0.5µl anti-I-A/I-E-PE antibodies (all antibodies are shown in appendix 6), made up to a total volume of 20µl with FACS buffer. Control samples were stained with either 0.5µl anti-CD3e-FITC, 0.5µl anti-CD4-PE, both, or left unstained. Antibodies were selected on the advice of Prof. Danny Altmann and matched the antibodies used in his laboratory for phenotyping of DR1/ABO mice by this method. Samples were incubated at 4°C in the dark for 30 minutes and then washed twice in ample FACS buffer before being resuspended in a small volume of FACSFlow (BD Biosciences). Samples were run on a FACSCalibur (BD Biosciences) flow cytometer and data was analysed using CellQuest Pro software (BD Biosciences).

2.2.4 Genotyping by Southern analysis

2.2.4.1 Southern (DNA) blotting

10µg of genomic DNA was digested overnight with restriction enzyme at the specified temperature (appendix 6) in a reaction volume of 50µl comprising DNA, 5µl restriction enzyme, 1x restriction enzyme buffer, 0.1 mg/ml BSA (Promega, R396), 0.1 mg/ml RNase A (Sigma, R4875) and 1 mM spermidine (Sigma, S2501). Digests were run overnight on a 1% agarose TAE gel (300 ml) without ethidium bromide at 45V. The gel was then cut to size to remove unnecessary gel and incubated in depurination solution (appendix 1), so that the gel was completely covered, at room temperature for 10 minutes with shaking. The gel was washed briefly in dH_2O before incubation in denaturation solution (appendix 1) at room temperature with shaking for 40 minutes. Again, the gel was washed briefly in dH_2O and incubated in neutralisation buffer (appendix 1) at room temperature with shaking for at least 40 minutes. The DNA from the gel was then blotted overnight onto Hybond-N^+ nylon membrane (GE Healthcare, RPN203B) by upward neutral transfer using 20x SSC (appendix 1). After blotting, DNA was fixed to the membrane by UV cross-linking and air dried before being stored at 4°C until use.

2.2.4.2 Probe production

A probe of approximately 800 bp was produced by PCR amplification (appendix 6) using template containing the gene of interest. PCR products were run down a 1% agarose TAE gel, cut out and purified as described previously. 16µl of PCR product was boiled for 10 minutes before immediately being placed on ice to prevent reannealing. 4µl of DIG-High Prime (from Roche kit, 11 585 614 910) containing the optimal concentrations of random primers, nucleotides, DIG-dUTP, Klenow enzyme and buffer components at a 5x concentration was added to the DNA and the reaction was incubated for 20 hours at 37°C. The DIG-labelled DNA was purified from the reaction mix using a silica-based spin column (Bioline) and eluted into 20µl elution buffer (supplied with the kit). The extent of labelling was determined by use of a dilution series of the labelled probe compared against a dilution series of control DIG-labelled DNA (Roche, 11 585 738 910) of known labelling intensity. Probe and control DNA was diluted in DNA dilution buffer (appendix 1). Each dilution of probe and control DNA was spotted (1 µl) onto Hybond-N^+ nylon membrane, air dried and fixed by UV cross-linking. To determine the concentration of DIG-labelled DNA in the probe, the dot blot was first washed for 2 minutes in maleic acid buffer (appendix 1) at room temperature before detection of DIG-labelled DNA was carried out as described below.

2.2.4.3 Hybridisation of DIG-labelled probe to the DNA blot

The DNA blot was pre-hybridised for at least 30 minutes at 42°C in 10 ml DIG EasyHyb solution (Roche, 11 796 895 001) with rolling to ensure the blot did not dry. The pre-hybridisation solution was then replaced with 8 ml fresh DIG EasyHyb solution containing 17-25 ng/ml DIG-labelled probe and incubated overnight at 42°C with rolling. Excess unbound probe was then removed by stringency washing. The blot was removed from the hybridization solution and washed twice in 2x SSC, 0.1% SDS for 5 minutes at room temperature with shaking and then washed twice in 0.5x SSC, 0.1% SDS for 15 minutes at 65°C with shaking. The blot was then washed for 5 minutes in maleic acid washing buffer (appendix 1) before detection of bound probe DNA.

2.2.4.4 Detection of probe binding to membrane

The DNA blot was incubated for at least 30 minutes at room temperature with shaking in ample 1x blocking solution (Roche, 11 585 614 910, diluted to 1x concentration with maleic acid buffer) to allow complete coverage of the membrane. Antibody solution was prepared by the addition of anti-digoxigenin-alkaline phosphatase conjugate (Roche, 11 585 614 910) to 1x blocking solution to give a 1:10000 dilution of antibody. The antibody was centrifuged at 9300 x *g* in a microcentrifuge for 5 minutes immediately prior to its use. As small as volume as possible (25 ml for a DNA blot, 10ml for a dot blot) was used to allow complete coverage of the membrane whilst conserving antibody. The blocking solution was removed and replaced with the freshly-prepared antibody solution and the blot was incubated at room temperature with shaking for 30 minutes, after which the blot was washed twice in ample maleic acid washing buffer at room temperature with shaking for 15-20 minutes. The blot was then equilibrated to the required pH (pH 9.4) to allow correct function of the alkaline phosphatase in the chemiluminescent reaction with CSPD (disodium 3-chloro-3-(methoxyspiro {1,2-dioxetane-3,2'-(5'-chloro) tricyclo [3.3.1.1] decan}-4-yl) phenyl phosphate) by incubating for 2-5 minutes in DIG-detection buffer (appendix 1) at room temperature with shaking. The blot was removed from the detection buffer and placed on a development folder and 1 ml of CSPD ready-to-use (Roche, 11 585 614 910) (or 0.3 ml for a dot blot) was added dropwise to completely cover the blot with substrate. The blot was then immediately covered by the second sheet of the development folder and all air bubbles between the folder and the membrane were removed before incubation at room temperature for 5 minutes. Excess liquid was squeezed out from the folder and the edges sealed before exposure of the blot to photographic film (Kodak BioMax Light Film, Light-1, Sigma, Z378516) for 2 hours (25 minutes for a dot blot). The film was then developed and analysed. Further exposures could be taken if required up to 48 hours after addition of the CSPD substrate.

2.3 Tissue culture and transduction techniques

2.3.1 Culture of adherent cell lines EcoPhoenix, PT67 and NIH3T3

Cell lines were cultured from frozen stocks stored in liquid nitrogen. Vials were thawed quickly at 37°C and the cells were added to 25 ml of pre-warmed complete Dulbecco's

Modified Eagle's Medium (DMEM) medium (Appendix 1). Cells were spun at 300 x *g* for 3 minutes and supernatant decanted thoroughly. Cells were then resuspended in complete DMEM medium and cultured in either 25 cm^2 (8 ml) or 80 cm^2 (30 ml) culture flasks with filter caps (Nunclon, 136196/178905) in a humidified incubator at 37°C with 5% CO_2.

EcoPhoenix (Orbigen, RVK-10001), PT67 (BD Biosciences Clontech, 631510) and NIH3T3 (Sigma, 93061524) adherent cell line cultures were split by up to 1 in 5 when at 70-80% confluency by addition of 1 ml (25 cm^2) or 3 ml (80 cm^2) 1x trypsin-EDTA (Invitrogen, 15400-054, diluted in PBS, pH 7.4, Invitrogen, 10010-056) to cells that had been washed twice with PBS and incubation for 1 minute at 37°C. Cells were dislodged by gentle agitation. An equivalent volume of medium was added to quench trypsinisation, cells were spun at 300 x *g* for 3 minutes and resuspended in 1 ml medium. The correct volume of cells for the split was added to a new flask containing 8 ml or 30 ml of fresh medium as appropriate.

2.3.2 Reselection of PT67 cells

PT67 cells were reselected using hypoxanthine, aminopterin and thymidine (HAT) medium. Cells undergoing reselection were grown for 5 days in complete DMEM with 100 nM aminopterin (Sigma, A3411) added. The cells were then grown for 5 days in complete DMEM-HAT medium (appendix 1). Finally, cells were grown for 1 week in complete DMEM-HT medium (appendix 1) before being returned to normal culture conditions. Cells were split as described above as required.

2.3.3 Culture of non-adherent cell lines BW7 and CTLL-2

Cell lines were cultured from frozen stocks stored in liquid nitrogen. Vials were thawed quickly at 37°C and the cells were added to 25 ml of pre-warmed complete RPMI-1640 medium. Cells were spun at 300 x *g* for 3 minutes and supernatant decanted thoroughly. Cells were then resuspended in 40-50 ml complete RPMI-1640 in 80 cm^2 culture flasks with filter caps and cultured in a humidified incubator at 37°C with 5% CO_2. CTLL-2 cells required the addition of 20 U/ml recombinant IL-2 (R&D Systems, 402-ML-100) to the culture medium for survival. BW7 (569) and CTLL-2 cells were split every 2-3 days before becoming overgrown by spinning at 300 x *g* for 3 minutes and resuspending

the pellet in 1 ml medium and transferring the appropriate volume of cells to a new flask containing fresh medium.

2.3.4 Retroviral transduction

2.3.4.1 Retroviral transfection of packaging cell line EcoPhoenix

EcoPhoenix cells were plated in 25 cm^2 tissue culture flasks at the required density 24 hours prior to transfection. On the day of transfection cells were incubated at 37°C, 5% CO_2 in 3 ml of fresh medium with 25 μM chloroquine (Sigma, C6628, appendix 1) added if required for at least 30 minutes before transfection. A transfection cocktail (0.6ml/flask) was prepared containing 10 μg retroviral expression vector DNA containing a gene of interest, 125 mM $CaCl_2$ (Sigma, C3881, appendix 1) and 1x HEPES-buffered saline (HBS) (appendix 1) (or in later transfections, using the reagents provided in a calcium phosphate transfection kit from Invitrogen, K2780-01). HBS was added to the DNA/$CaCl_2$ with bubbling and was either added dropwise immediately to the cells or incubated at room temperature for 30 minutes before dropwise addition to the cells (Invitrogen kit). Cells were incubated at 37°C/5% CO_2 for 8 hours. After this time the medium was replaced with 5 ml fresh (trial and original protocols) or 2.5 ml (modified protocol). For the trial and original protocols the medium was again replaced with 3 ml fresh medium 12 hours later for supernatant collection 48 hours after initial transfection. For the modified protocol supernatant was harvested 36 hours after initial transfection and 2.5 ml fresh medium was added to the cells for a second collection of supernatant 24 hours later. Supernatant was collected and filtered to remove any cells (0.45 μm syringe filter - Nalgene, 190-2545) before being used to infect target cells. Supernatant was diluted as required in fresh medium and polybrene (hexadimethrine bromide, Sigma, 52495, appendix 1) was added to a final concentration of 4 μg/ml before infection.

2.3.4.2 Infection of secondary packaging line PT67 with retroviral supernatant

PT67 cells were plated at a density of 100,000 cells per 25 cm^2 flask 18 hours before infection. Retroviral supernatant, prepared as described previously, was then used to replace the medium on the cells. Cells were incubated at 37°C and 5% CO_2 for 3 hours before an extra 2 ml of fresh medium was added. Medium was changed after 24 hours

to remove retroviral supernatant. 48 hours after initial infection, medium was replaced with 3 ml fresh for retroviral supernatant collection. Supernatant was collected at 72 hours after infection (for the final modified protocol supernatant was replaced with 3 ml fresh medium for a second collection of supernatant at 96 hours after infection). Supernatant was filtered (0.45 μm syringe filter) and diluted if required before being used to infect target cells. Polybrene was added to a final concentration of 4 μg/ml before infection.

2.3.4.3 Infection of adherent target cell line NIH3T3 with retroviral supernatant

NIH3T3 cells were plated at a density of 50,000 cells per well of a 6-well tissue culture plate (Nunclon, 140675) 24 hours before infection. Retroviral supernatant, prepared as described previously, was then used to replace the medium on the cells. Cells were incubated at 37°C and 5% CO_2 for 3 hours before an extra 2 ml of fresh medium was added. Medium was changed after 24 hours to remove retroviral supernatant. Cells were harvested at different time points after infection (usually some or all of 24, 48, 72 and 96 hours) and analysed for eGFP expression by flow cytometry (no antibody staining required). Data analysis was carried out using CellQuest software (BD Biosciences).

2.3.4.4 Infection of non-adherent target cell line BW7 with retroviral supernatant

BW7 cells (1 x 10^5) were added to 2 ml retroviral supernatant, prepared as described previously, and centrifuged at 1000 x *g* for 90 minutes at 32°C for the trial and original protocols. For the final modified protocol BW7 cells (1 x 10^5) were added to 2 ml retroviral supernatant, prepared as described previously, and centrifuged at 680 x *g* for 30 minutes at room temperature. Cells were then resuspended in the same medium in wells of a 12-well tissue culture plate (Nunclon, 150628). Cells were incubated at 37°C/5% CO_2 for at least 3 hours after which 1 ml (BW7) of fresh medium was added. Medium was changed after 24 hours to remove retroviral supernatant. Cells were harvested at different time points after infection (usually some or all of 24, 48, 72 and 96 hours) and analysed for eGFP expression or TCR/TCRβ chain expression (see Appendix 7 for antibodies used and section 2.2.3 for protocol) by flow cytometry. Antibodies for the analysis of TCR expression were selected predominantly on the basis of availability, as in most cases, there is only one commercially available antibody for each TCRβ chain (and frequently no antibody available for a particular TCRα chain).

Where isotype controls were used, they were purchased from the same company as supplied the original antibody to match them as far as possible to each other in terms of concentration and intensity. Data analysis was carried out using CellQuest software.

2.3.4.5 Principles of flow cytometry

Flow cytometry involves the analysis of cells in terms of their size and granularity and when bound to fluorophore-labelled antibodies, analysis of cell surface molecule expression (and in some cases intracellular molecule expression) using light from a laser. Flow cytometry involves single cell analysis, as each individual cell is directed through the laser beam separately and is hence analysed individually. Light scattering properties (forward and side scatter) identify cells in terms of size and granularity, whilst cells can be incubated with fluorophore (eg. FITC/PE)-labelled antibodies before analysis. A number of fluorophores can be monitored simultaneously depending on the flow cytometer. Excitation of the fluorophore by the laser leads to emission of light which is intercepted by detectors set to receive light at ranges of wavelengths corresponding to the emission spectra of the fluorophores (one detector for each fluorophore). If the cell has bound such an antibody due to its expression of the molecule being assayed, the laser will excite the fluorophore, light will be emitted and detected and the cell will appear as positive. Detectors amplify the signal (linearly or logarithmically) and convert it into electronic data which is then collected and analysed on a computer.

Compensation of signals is required as the emission spectra from many fluorophores overlap (spectral overlap) and hence there is overlapping of the signals detected. This can lead to the appearance of a higher level of expression of a molecule than is actually there. Compensation reduces this overlap by removing the part of the signal that is due to fluorescence from other fluorophores by manipulating voltage levels of the various detectors. Gating allows the definition of a population of cells on the basis of their light scattering characteristics so as to isolate a particular population of cells within a mixed culture e.g. lymphocytes in a sample of PBMCs, or separation of live cells from dead cells. Gating is also used in analysis of the data to differentiate between cells that do or do not express a specific molecule and can be used to calculate the proportion of cells that express a number of molecules simultaneously.

2.3.5 Transfection of non-adherent target cell line BW7 with TCR expression vectors using the Amaxa Nucleofector™ electroporation system

3 x 10^6 BW7 cells were used in each transfection. Prior to transfection, Nucleofector™ solution V (component of Cell Line Nucleofector™ Kit V, Amaxa, VCA-1003) was warmed to room temperature and a 12-well culture plate was prepared containing 1 ml/well of complete RPMI-1640 without added penicillin/streptomycin for each transfection to be carried out and pre-warmed to 37°C. Cells were centrifuged at 300 x *g* for 5 minutes and all supernatant was carefully removed. Cells were then resuspended in 100 µl Nucleofector™ solution V (suggested for this cell line by the Amaxa Cell Line Database (www.amaxa.com)). Plasmid DNA (1 µg of the control plasmid pmaxGFP (component of Amaxa, VCA-1003) or up to 5 µg each of TCRα and TCRβ expression vectors containing the TCR chains of interest) was added to the cells and mixed. Cells were then transferred carefully into an Amaxa-certified cuvette (component of Amaxa, VCA-1003), ensuring that the suspension covered the bottom of the cuvette and that there were no air bubbles, and closed using the provided cap. The required programme (T-016 or T-001 as suggested for this cell line on the Amaxa Cell Line Database) was entered into the Amaxa Nucleofector-I™ (Amaxa, AAD-1001) and the cuvette was inserted into the cuvette holder. The button marked "X" on the Nucleofector™ was pressed to start the programme. Once the programme had finished, the cuvette was removed and the cells were immediately transferred into the previously prepared tissue culture plates using one of the provided Pasteur pipettes (component of Amaxa, VCA-1003). Cells were then incubated at 37°C and 5% CO_2 and analysed for expression of either GFP or TCRβ chain (see Appendix 7 for antibodies used and section 2.2.3 for staining protocol) by flow cytometry at different time points - 24 hours, 48 hours, 72 hours, 96 hours and 9 days after transfection. Data analysis was carried out using CellQuest software.

2.3.6 Analysis of cell death by flow cytometry using propidium iodide

Cells (either previously stained with fluorescently-conjugated antibody or unstained) were washed in 2 ml FACS buffer (appendix 1), centrifuged at 300 x *g* for 5 minutes, supernatant was decanted thoroughly and cells were resuspended in 100 µl FACS buffer (appendix 1). Cells were stained with 5 µl propidium iodide solution (PI, from Immunotech kit, PN IM3546), reconstituted at a concentration of 250 µg/ml in 1x

binding buffer (supplied at 10x concentration with the kit and diluted in dH_2O) and incubated on ice in the dark for 10 minutes. After this time, 400 µl of 1x binding buffer was added to the cells. Samples were run on a FACSCalibur (BD Biosciences) flow cytometer and data was analysed using CellQuest Pro software (BD Biosciences).

2.3.7 Measurement of IL-2 production in transduced BW7 cells using the CTLL-2 assay

5 x 10^4 BW7 cells (both transduced and untransduced) in HL-1 medium (appendix 1) were incubated with 25 or 50 µg/ml specific peptide (PLP_{56-70}) diluted in PBS and 5 x 10^5 irradiated (30 Gy) NOD.E splenocytes (also in HL-1 medium) in triplicate in a 96-well tissue culture plate (Nunclon, 163320) for 48 hours at 37°C and 5% CO_2. Negative (medium alone) and positive (5µg/ml concanavalin A (ConA), Sigma, L7647) controls were also included in the assay for both transduced and untransduced BW7. After 48 hours, 100 µl of supernatant from each well was transferred to a new plate and frozen at -20°C to lyse any remaining cells. After thawing of the supernatants, 100 µl of HL-1 medium containing 3 x 10^3 cells from the IL-2 dependent CTLL-2 cell line that had been starved of IL-2 for 24 hours prior to their use were added to each well. The cells were then incubated for 36 hours at 37°C and 5% CO_2. Negative (HL-1 medium alone) and positive (HL-1 medium containing 20U/ml recombinant IL-2) controls were also included in the assay, After 24 hours of culture, 5 µCi of [^{3}H]-thymidine (MP-2405905) was added to each well. After 36 hours, plates were stored at -20°C until processed. Plates were thawed completely before processing and were harvested (MACH III M Harvester 96) before liquid scintillation counting (Wallac 1450 microbeta TRILUX).

2.4 Induction of allergic asthma in a murine model using Fel d 1

These experiments were carried out with Dr. Catherine Reynolds and Dr. Xiaoming Cheng, postdoctoral research associates in the Lung Immunology Group, National Heart and Lung Institute, Imperial College, London.

2.4.1 Sensitisation with Fel d 1

This was carried out with Dr. Catherine Reynolds. To induce allergic inflammation in the lung, a suspension of recombinant Fel d 1 (made by Rebecca Beavil, MRC and

Asthma UK Centre in Allergic Mechanisms of Asthma Protein Production Facility) in alum (Alu-Gel-S suspension, Serva Electrophoresis, 12261) was prepared under sterile conditions by the addition of recombinant Fel d 1 solution to alum to a final concentration of 50 μg/ml Fel d 1. An equivalent volume of PBS was added to alum for treatment of control mice. The suspensions were then rolled for at least 1 hour to allow the Fel d 1 antigen to be adsorbed onto the alum before injection. Mice were injected intraperitoneally with 200 μl of Fel d 1/alum (treated groups) or PBS/alum (controls). Sensitisation occurred on days 0 and 11 of the protocol.

2.4.2 Challenge with cat dander extract

This was carried out with Dr. Catherine Reynolds. Mice were challenged with cat dander extract (obtained from Laboratorios Leti, SA Madrid, Spain) on days 21, 22 and 23 of the protocol by intranasal administration under general anaesthetic (isoflurane and oxygen) of 25 μl of cat dander extract at 10 mg/ml concentration (diluted in sterile PBS) for the experiment in P4 TCR/DR1/ABO line 4 mice and at 20 mg/ml concentration for the experiment in P4 TCR/DR1/ABO line 16 mice. Control mice received a corresponding intranasal administration of 25 μl sterile PBS.

2.4.3 Measurement of lung function - Penh

This was carried out with Dr. Catherine Reynolds. The Whole Body Plethysmography System (EMMS) was used to measure Penh in unanaesthetised, unrestrained mice. Mice were placed into plethysmograph chambers (PLY 310, EMMS) connected to a nebuliser aerosol delivery system (AEX 142, EMMS) and a bias flow unit (AEX 142, EMMS) to regulate levels of CO_2, heat and humidity in the chambers. Measurements were collected using EDacq software (EMMS) via transducers (TPF 100, EMMS) connected to the chambers. Baseline measurements of air flow in the chambers containing the mice were taken for 5 minutes using nebulised sterile PBS (200 μl) before challenge with methacholine (acetyl-β-methylcholine chloride, Sigma, A2251). Measurement of methacholine-induced airway hyperreactivity was carried out by nebulising 200 μl of solutions containing increasing concentrations of methacholine (3/10/30/100 mg/ml in sterile PBS) into the system and measuring airflow parameters for 5 minutes for each concentration.

2.4.4 Measurement of lung function - resistance and compliance

This was performed by Dr. Kate Choy. Resistance and Compliance Plethysmographs (EMMS) were used by Dr. Choy to measure pulmonary resistance (R_L) and dynamic compliance (Cdyn) in response to methacholine challenge in anaesthetized, tracheostomised, mechanically ventilated mice. Mice were anaesthetized by subcutaneous injection of 100 µl of a 1:0.55:0.42 mix of PBS, medetomidine hydrochloride (Domitor®, Pfizer) and ketamine (Ketaset®, Fort Dodge Animal Health Ltd.); an additional 150 µl was administered by intramuscular injection once the mice were immobilised. Once fully anaesthetized, an intratracheal cannula (EMMS) was inserted. Mice were placed into plethysmograph chambers connected to a nebuliser aerosol delivery system and the cannula was connected to a ventilator and a transducer to measure air flow parameters using EDacq software. Baseline measurements were taken using 50 µl nebulised sterile PBS and measuring for 5 minutes. Response to nebulised methacholine (50 µl) at increasing concentrations (3/10/30/100 mg/ml in sterile PBS) was then measured for 5 minutes after each nebulisation.

2.4.5 Collection of BAL fluid and cytospin preparation

This was carried out with Dr. Catherine Reynolds. Three 0.4 ml aliquots of PBS (1.2 ml total volume) were instilled into the lungs of anaesthetised mice through a cannulated trachea using a 1 ml syringe and collected. Samples were then centrifuged at 250 x *g* for 8 minutes. Supernatant was collected without disturbing the cell pellet for analysis of cytokine production by ELISA and stored at -20°C. Cells were resuspended in 100 µl PBS and counted on a haemocytometer. 5 x 10^4 cells were spun onto a polysine microscope slide (VWR, 631-0107) at 400 rpm using a Cytospin 4 (Thermo Shandon), air dried and fixed in methanol for 5 minutes. Slides were then stored at room temperature until stained for analysis.

2.4.6 Collection of serum for measurement of total serum [IgE]

This was carried out with Dr. Catherine Reynolds. Blood was collected from anaesthetised mice after BAL fluid collection by cardiac puncture. Blood was incubated overnight at room temperature to allow clotting to occur. Samples were centrifuged at

full speed in a microcentifuge for 10 minutes after which the supernatant (serum) was collected for measurement of total IgE production. Serum samples were stored at -20°C.

2.4.7 Lung inflation for histological analysis

This was carried out with Dr. Catherine Reynolds. After collection of BAL fluid and blood, the lungs and heart were excised from the mouse. The left lobe of the lung was clamped and all but one of the right lobes were tied off to prevent them being inflated. The remaining lobe of the lung was inflated using a 1:1 mixture of sterile PBS and O.C.T. compound (VWR, 361603E) and placed in a mould filled with O.C.T. compound, in the same orientation for each mouse. The tissue was held in place with a cork disk before being snap frozen in ultra-cold cyclopentane on dry ice. The frozen tissue was then stored at -80°C.

2.4.8 Disaggregation of cells from lung tissue and cytospin preparation

The left lobe of the excised lung was used for disaggregation. The lung was chopped into small pieces using a mechanised tissue mincer and stored on ice in 2 ml RPMI-1640 until processed. 25 µl aliquots of stock solutions of collagenase D (Roche, 11 088 858 001) and DNase I (Roche, 11 284 932 001) (Appendix 1) were added to 3 ml RPMI-1640 for each sample and added to the tissue. The tissue was incubated at 37°C with gentle agitation for 1 hour and strained through a 70 µm cell strainer (BD Falcon, 352350) with cells being washed through gently with extra RPMI-1640. Cells were centrifuged at 300 x *g* for 5 minutes and washed twice more in RPMI-1640. The final pellet was resuspended in 1 ml RPMI-1640 and cells were counted on a haemocytometer. 5 x 10^4 cells were spun onto a polysine microscope slide at 400 rpm using a Cytospin 4, air dried and fixed in methanol for 5 minutes. Slides were then stored at room temperature until stained for analysis.

2.4.9 Staining of cytospins for differential cell count analysis

Cytospin slides were stained for analysis using modified Wright-Giemsa stain (Sigma, WG16). Slides were immersed in Wright-Giemsa stain to cover the cells for 1 minute without agitation before the slides were immersed in deionised water without agitation for 6 minutes to allow blueing to occur. The slides were then briefly dipped into running

deionised water 2-3 times to rinse them and left to air dry. Once the slides were thoroughly dried, a coverslip was applied using DPX mountant (BDH, 360294H) and slides were left to dry flat overnight before analysis.

2.4.10 Differential cell counting

300 cells per cytospin were analysed and identified on the basis of cell morphology as shown in Appendix 8. The proportions of neutrophils, eosinophils, macrophages and lymphocytes were then calculated, first as percentages of the total cell count, before this was used in conjunction with the total cell count to calculate the total number of each cell type in each sample. Slides were randomized and coded before counting was carried out by three blinded investigators (myself, Dr. Catherine Reynolds and either Dr. Xiaoming Cheng or Eleanor Raynsford).

2.4.11 Lung tissue homogenisation

At the time of harvesting, one lobe of the lung was placed in a cryovial and snap frozen in liquid nitrogen for subsequent processing. Samples were weighed and 1 ml 1x Hanks' Buffered Saline Solution (HBSS) (without calcium or magnesium) (Invitrogen, 14175-137) containing 1x complete mini protease inhibitor cocktail with EDTA (Roche, 11 836 153 001) per 100 mg tissue was added and machine homogenised. Homogenised samples were centrifuged at full speed in an ultracentrifuge for 10 minutes. Supernatant was collected for measurement of cytokine production by ELISA and stored at -20°C.

2.4.12 Measurement of total [IgE] in serum by ELISA

Immunosorbent plates (Nunc-Immuno Maxisorp 96-well plate, Nunc, 456537) were coated with 100µl anti-IgE capture antibody (appendix 9) diluted to a concentration of 2 µg/ml in PBS (appendix 1), sealed and incubated overnight at 4°C. Antibody was removed and plates were washed three times with 400 µl/well wash buffer (appendix 1). After the last wash, excess buffer was removed by tapping the plates on paper towels. 200 µl blocking/diluent buffer (appendix 1) was then added to each well, plates were covered and incubated at room temperature for at least 1 hour. Plates were then washed three times as before. Samples were diluted 1 in 2 and 1 in 10 in blocking/diluent buffer

before addition to the plate. A standard curve was prepared in duplicate by diluting an IgE standard (appendix 9) in a series of seven 1 in 2 dilutions from a starting concentration of 500 ng/ml. 50µl of sample or standard was added to each well, with an additional two wells containing 100 µl blocking/diluent buffer only as a measure of background. Plates were covered and incubated at room temperature for 1 hour before being washed three times as before. 100µl biotinylated detection antibody (anti-IgE, appendix 9) at a concentration of 2 µg/ml was added to each well, plates were covered and incubated at room temperature for 1 hour. Plates were washed six times as before. Streptavidin-horseradish peroxidase conjugate (R&D Systems, DY998) was diluted in blocking/dilution buffer as directed on the vial and 100µl was added to each well before plates were covered and incubated at room temperature for 30 minutes, after which plates were washed six times as before. Substrate solution - a 1:1 mix of Color Reagent A (stabilised hydrogen peroxide) and Color Reagent B (stabilised tetramethylbenzidine) (Substrate Reagent Pack, R&D Systems, DY999) was prepared immediately prior to use and 100 µl was added to each well. Plates were then incubated in the dark at room temperature for approximately 30 minutes to allow colour to develop. The reaction was stopped by the addition of 50 µl stop solution (appendix 1). Plates were read on a Sunrise plate-reader (Tecan) with a measurement absorbance of 405 nm and a reference absorbance of 570 nm using Magellan (Tecan) software. Readings were corrected by subtracting the background measurement, a standard curve was plotted and total [IgE] in each sample was calculated from the equation of the standard curve.

2.4.13 Measurement of cytokine concentrations in BAL fluid and lung homogenate by ELISA

Immunosorbent plates were coated with 100µl anti-cytokine capture antibody diluted to the specified working concentration in PBS (appendix 9), sealed and incubated overnight at room temperature. Antibody was removed and plates were washed three times with 400 µl/well wash buffer. After the last wash, excess buffer was removed by tapping the plates on paper towels. 300 µl blocking buffer (appendix 1) was then added to each well, the plates were covered and incubated at room temperature for at least 1 hour. Plates were then washed three times as before. Samples were diluted 1 in 2 in diluent buffer (appendix 1) before addition to the plate. A standard curve was prepared in duplicate by diluting cytokine standards (appendix 9) in a series of eight 1 in 2 dilutions from a starting concentration of 4000 pg/ml. 50µl of sample or standard was

added to each well with an additional two wells containing 100 µl diluent buffer only as a measure of background. Plates were covered and incubated at room temperature for 2 hours before being washed three times as before. 100µl biotinylated anti-cytokine detection antibody at the specified working concentration (appendix 9) was added to each well, plates were covered and incubated at room temperature for 2 hours. Plates were washed three times as before. Streptavidin-horseradish peroxidase conjugate was diluted in diluent buffer as directed and 100µl was added to each well before plates were covered and incubated at room temperature for 20 minutes, after which plates were washed three times as before. Substrate solution - a 1:1 mix of Color Reagent A and Color Reagent B was prepared immediately prior to use and 100 µl was added to each well. Plates were then incubated in the dark at room temperature for approximately 20 minutes to allow colour to develop. The reaction was stopped by the addition of 50 µl stop solution (appendix 1). Plates were read on a Sunrise plate-reader with a measurement absorbance of 540 nm and a reference absorbance of 570 nm using Magellan software. Readings were corrected by substracting the background measurement, a standard curve was plotted and cytokine concentration in each sample was calculated from the equation of the standard curve.

2.4.14 Preparation of lung sections and staining with haematoxylin and eosin for histological analysis

Frozen lung sections were cut to a thickness of 5 µm using a cryostat (Bright Instruments, OTF model) and mounted on polysine microscope slides by Dr. Catherine Reynolds. Slides were left to air dry completely before staining - no fixative was required. Slides were immersed in mercury-free Harris' haematoxylin (VWR, 351945S) for 15 seconds before blueing in running tap water. Slides were then immersed in 1% eosin solution (appendix 1) for 5 seconds and rinsed briefly in running tap water. Slides were dehydrated by immersion with gentle agitation in 70% industrial methylated spirit (IMS) (15 seconds), 90% IMS (15 seconds), 100% IMS (30 seconds) and 100% IMS (30 seconds). Slides were then given 3 x 5 minute changes of Histoclear (National Diagnostics, HS-200) before the slides were drained and a coverslip was applied using DPX mountant. Slides were air dried lying flat overnight before analysis.

2.4.15 Inflammation scoring system (for haematoxylin and eosin stained slides)

The system used for scoring lung sections for inflammation was based on the system outlined in reference 607. Each airway and blood vessel in a section was scored separately for the degree of inflammatory infiltrate surrounding it and assigned a score between 0 and 3. Scores were assigned according to the following criteria: 0 - no inflammatory cells surrounding the airway or vessel, 1 - a few inflammatory cells cuffing an airway or vessel, 2 - a thin layer (1-5 cells thick) of inflammatory cells surrounding the airway or vessel, 3 - a thick layer (more than 5 cells thick) of inflammatory cells surrounding the airway or vessel. Two scores were then calculated for airway or vessel inflammation - an absolute score, where the modal value for airways and for vessels gave the score for each section and an average score, where the scores for all airways or vessels were summed and divided by the total number of airways or vessels. These scores were then averaged to give a final score for each group being assessed. Slides were randomized and coded before scoring was carried out by 2 blinded investigators (myself and Dr. Catherine Reynolds).

2.4.16 Preparation of lung sections and staining with periodic acid-Schiff's reagent (PAS reagent) for histological analysis

Frozen lung sections were cut to a thickness of 5 μm using a cryostat (Bright Instruments, OTF model) and mounted on polysine microscope slides by Dr. Catherine Reynolds. Slides were balanced to 0°C and fixed in ice-cold acetone for 15 minutes before being air-dried. Slides were oxidised in ice-cold 1% periodic acid (appendix 1) and rinsed in deionised water. Slides were then immersed in Schiff's reagent (Fisher Scientific, J/7300/PB08) in a fume cupboard for 10 minutes and rinsed in deionised water. Slides were then rinsed in running tap water for approximately 5 minutes. Nuclei were counterstained by immersion of the slides in mercury-free Harris' haematoxylin for 15 seconds before blueing in running tap water. Slides were dehydrated by immersion with gentle agitation in 70% industrial methylated spirit (IMS) (15 seconds), 90% IMS (15 seconds), 100% IMS (30 seconds) and 100% IMS (30 seconds). Slides were then given 3 x 5 minute changes of Histoclear before the slides were drained and a coverslip was applied using DPX mountant. Slides were air dried lying flat overnight before analysis.

2.4.17 Scoring of mucus-producing cells (for PAS reagent stained slides)

The system used for scoring lung sections for mucus-producing goblet cells was based on the system outlined in reference 608. Each airway in a section was scored separately for the extent of PAS-stained goblet cells in the airway and assigned a score between 0 and 4. Scores were assigned according to the following criteria: 0 - <5% goblet cells in the airway, 1 - 5-25% goblet cells in the airway, 2 - 25-50% goblet cells in the airway, 3 - 50-75% goblet cells in the airway, 4 - >75% goblet cells in the airway. Two scores were then calculated - an absolute score where the modal value gave the score for each section and an average score where the scores for all airways were summed and divided by the total number of airways. These scores were then averaged to give a final score for each group being assessed. Slides were randomized and coded before scoring was carried out by 2 blinded investigators (myself and Dr. Catherine Reynolds).

2.5 Analysis of costimulatory molecule expression in P4 TCR/DR1/ABO transgenic mice

2.5.1 Isolation of splenocytes for flow cytometric analysis or RNA isolation

Mice were sacrificed by cervical dislocation and the spleen was removed by dissection, placed in 15 ml complete RPMI-1640 medium and kept on ice. Each spleen was then transferred into a Petri dish along with the medium it was stored in and the medium was used to flush the splenocytes from the spleen using a 5 ml syringe equipped with a 23G hypodermic needle. The medium containing the splenocytes was collected and centrifuged at 300 x *g* for 5 minutes. Supernatant was discarded and cells were haemolysed in dH_2O. Haemolysed cells were collected in 11 ml fresh complete RPMI-1640 and stored on ice until needed.

2.5.2 Isolation of thymocytes for flow cytometric analysis

Mice were sacrificed by cervical dislocation and the thymus was removed by dissection, placed in 10 ml complete RPMI-1640 medium and stored on ice. Each thymus was then mashed through a 70 μm cell strainer using the plunger of a 5 ml syringe, and cells were washed through with fresh complete RPMI-1640 medium and collected in a fresh centrifuge tube and stored on ice until needed.

2.5.3 Staining of cells with fluorescently-conjugated antibodies for flow cytometric analysis

Splenocytes and thymocytes kept on ice in complete RPMI-1640 medium were centrifuged for 5 minutes at 300 x *g* and supernatant was discarded. Cells were washed twice in 10 ml FACS buffer (appendix 1) and resuspended in FACS buffer (400 µl - splenocytes, 800 µl - thymocytes). Antibody mixes (20 µl per sample comprising antibodies required and made up to volume with FACS buffer) were prepared during the washing steps and kept on ice in the dark before use - splenocytes were stained with two antibodies, either anti-CD4 or anti-CD8 and one of the following antibodies: anti-CD3, anti-CD25, anti-CD44, anti-CD54, anti-CD62L, anti-CD69, anti-OX40, anti-OX40L or anti-ICOS. Thymocytes were stained with three antibodies - anti-CD4, anti-CD8 and one of the following antibodies: anti-CD3, anti-CD25, anti-CD44, anti-CD54, anti-CD62L, anti-CD69, anti-OX40, anti-OX40L or anti-ICOS. All antibodies used, including the source and clone used as well as the required working concentration of each, are shown in Appendix 10. Single stain controls for each antibody were also prepared to allow for correct gating and compensation of the flow cytometer. Antibody mixes were transferred into wells of a 96-well plate and 20 µl of splenocyte or thymocyte suspensions were added as required and mixed. Plates were wrapped in aluminium foil and incubated at 4°C for 30 minutes to allow staining to occur. After staining, plates were centrifuged at 250 x *g* for 3 minutes, supernatant was flicked off and cells were washed twice in 200 µl of FACS buffer. Cells were then resuspended in 100 µl FACS buffer and transferred into tubes for analysis on the flow cytometer. Samples were run on a FACScalibur flow cytometer, with 50,000 events counted for each sample, and analysed using CellQuest Pro software.

2.6 Statistical analysis

For both analysis of allergic disease induction in the P4 TCR/DR1/ABO mice and analysis of costimulatory molecule expression in P4 TCR/DR1/ABO mice the same statistical analysis was carried out using Prism software. First, all samples were tested for normal distribution using the Kolmogorov-Smirnov goodness-of-fit test unless sample number was too small. If both samples being compared for a particular test were normally distributed according to this test, an F test to compare variances of the samples

was carried out. Where variances were the same or similar by this test a two-tailed unpaired Student's t test was used to calculate statistical significance; if the variances were different, Welch's correction to the Student's unpaired two-tailed t test was used (and is stated where appropriate). Two-tailed tests were used for statistical significance as a means of identifying whether the mean values of the two samples being compared were significantly different from each other regardless of the direction in which the change occurred. Where sample size was too small to test for normality, the nonparametric two-tailed Mann-Whitney U test, which does not assume that data is distributed normally, was used to test for statistical significance. Where the Mann-Whitney U test could not be applied (if group numbers were too small or sample sizes too different), a two-tailed unpaired Student's t test was used as above. P values of less than 0.05 were considered significant.

It should be borne in mind when carrying out multiple tests on a set of data that the greater the number of tests carried out when comparing one group to another (e.g. Fel d 1-sensitised against non-sensitised or TCR transgenic against non-TCR transgenic as here), the more likely it is that an apparent difference between the two groups will appear by chance. Using a p value of less than 0.05 as significant indicates that in every 20 tests carried out, one will appear to give a difference by chance. One means of addressing this problem would be to use Bonferroni's correction, which uses a level of statistical significance that is 1/n (where n is the number of tests being carried out on the data) i.e. here, 0.05 x 1/n. This provides a more stringent means of testing for statistical significance (a result is statistically significant when the probability of a difference between two populations being due to chance alone is less than a particular value set by the researcher assuming that the original hypothesis is correct). However, due to the small group numbers used here, this correction was not applied to the data shown in this thesis.

3. TCR CDR3 analysis of cat allergic asthmatic patients and a transduction system to express TCRs of interest in the TCR-negative murine thymoma line BW7

3.1 TCR CDR3 analysis in cat allergic asthmatic individuals

3.1.1 Overview

Three T-cell lines generated in the laboratory of Professor Mark Larché, Imperial College, London, from peripheral blood of HLA-DR1$^+$ cat-allergic patients were grown *in vitro* against the major allergen in cat dander, Fel d 1 and a peptide derived from Fel d 1 known as peptide 4. Peptide 4 is an important epitope of Fel d 1 in cat-allergic individuals expressing the MHC class II molecule HLA-DR1 (221). Analysis of TCR usage in these lines was carried out to identify if there is a peptide-specific expansion of T-cells with particular TCR Vα/Vβ, Jα/Jβ and CDR3α/β regions to test the hypothesis that in the human Th2-mediated disease allergic asthma, TCRs carrying elongated CDR3 loops expand in response to allergen challenge.

Of the three T-cell lines CIR014 had been re-stimulated twice, initially with whole Fel d 1 protein and then with peptide 4. Lines B1 and CIR010 had each been re-stimulated four times, initially with whole Fel d 1 protein and subsequently with peptide 4.

RNA was extracted from cells from each line at these time points and converted to cDNA for analysis of TCR usage. TCR usage was studied using a strategy designed by Henwood et al. (609), which is outlined in Figure 3.1. The cDNA products of each line are modified by addition of a poly(dG) tail and used in an anchor PCR. PCR products corresponding to rearranged TCR V-J regions for both α and β TCR chains, as shown in Figure 3.2, were cloned and sequenced. TCR sequences were analysed in terms of V and J region usage (according to IMGT definitions) and also the length and sequence of the CDR3 for both TCR α and β chains. The CDR3 was defined (according to the IMGT database definition) as being those amino acids forming the junction between the V and J regions, between but not including the conserved cysteine residue at the end of the V region and the conserved FGXG motif at the beginning of the J region (610).

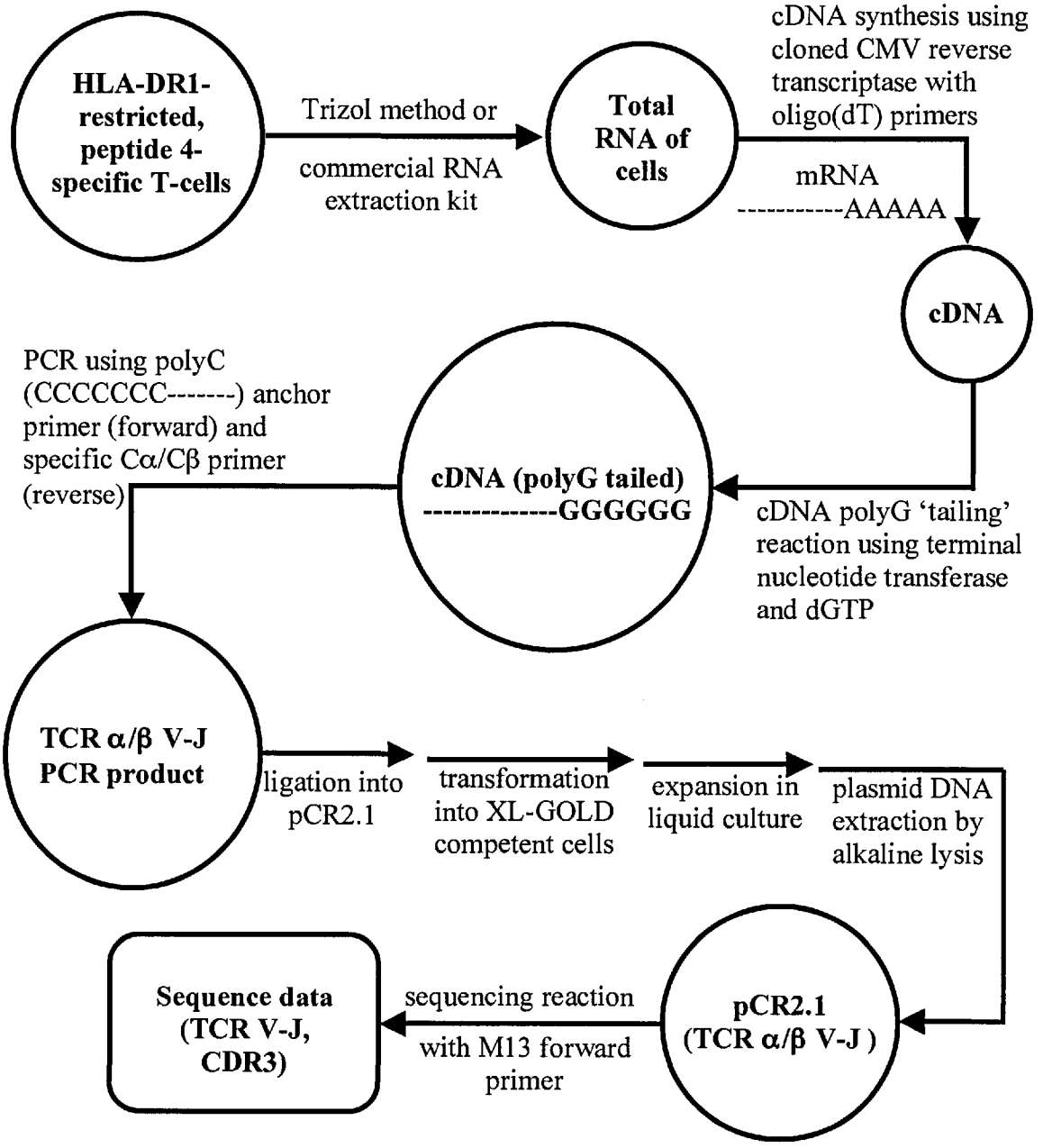


Figure 3.1 Outline of the strategy used to investigate TCR usage in HLA-DR-1 restricted T-cell lines against peptide 4. RNA was extracted from HLA-DR-1-restricted, peptide 4-specific T cells and first strand cDNA synthesis was carried out. Addition of poly(dG) tails to the cDNA products occurred using terminal nucleotide transferase and dGTP. Such 'tailing' allowed PCR amplification of TCR V-J regions expressed by the cells through use of a poly(dC) anchor forward primer and a specific TCR α or β constant region reverse primer. PCR products between 300 and 700 base pairs in size were ligated into pCR2.1 (shown in Appendix 11) and transformed into XL-GOLD competent cells. Successfully transformed colonies were expanded in liquid culture, and plasmid DNA was extracted from the cultures by alkaline lysis ('miniprep'). EcoRI digests were carried out on each sample, and plasmids containing inserts of the correct size were sequenced with the M13 forward primer. Resulting sequence data were aligned against the IMGT database. All PCR primer sequences and reaction conditions, and restriction enzyme digest conditions are shown in Appendix 2.

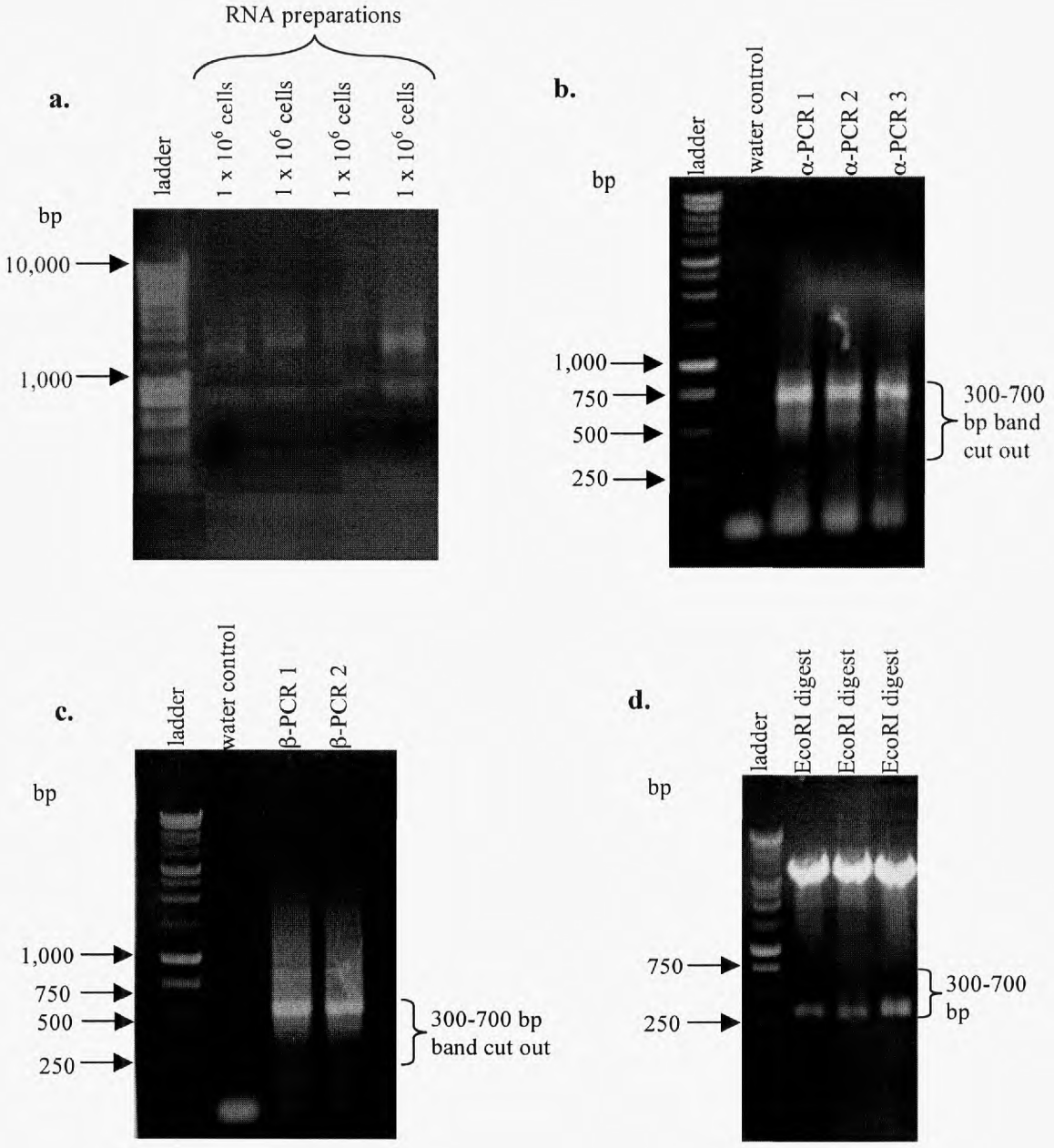


Figure 3.2 Agarose gel pictures at different stages of the human TCR analysis. (a) A typical RNA preparation from the HLA-DR-1-restricted, peptide-4 specific cell lines. RNA from each preparation of 1 x 10^6 cells (1 μl) was run on an agarose gel and showed a characteristic pattern of RNA: two distinct bands with an indistinct smear between them, which comprises mRNA; the larger band is 18S rRNA, the smaller band is composed of small RNA species. (b) and (c) Typical products obtained from the α (b) and β (c) human TCR PCRs carried out on tailed cDNA derived from the isolated RNA. Products of interest were between 300 and 700 bp and appeared as a 'smear' of DNA around a more defined central band – this band was excised and purified for TA cloning. (d) Typical EcoRI digest of the final plasmid pCR2.1 containing the TCR V-J inserts. Plasmids with an insert of the correct size (300-700 bp) were sequenced. The proportion of plasmids containing an insert of the correct size that were subsequently sequenced ranged from 54% (for the TCR CDR3β analysis of line CIR010) to 84% (for the TCR CDR3β analysis of line B1).

3.1.2 TCRα chain and CDR3 usage in human peptide 4-specific, DR1-restricted T-cell lines

Analysis of TCRα chain V region and J region usage as well as the CDR3 sequence and length was carried out in the lines CIR014, B1 and CIR010. Tables of the results of this analysis are shown in Table 3.1 (CIR014 TCRα usage), Table 3.2 (B1 TCRα usage) and Table 3.3 (CIR010 TCRα usage). In all cases, a population of cells and in the case of line B1 two populations of cells expressing a particular TCR were seen to have expanded. In line CIR014, the population of expanded cells (which represented 33% of all cDNA clones analysed from this line that corresponded to a TCRα chain, 30 in total) expressed a TCRα chain comprising TRAV 26-2 TRAJ 48. There were two populations of expanded cells in line B1 - the TCRα chains expressed by these populations were TRAV 13-1 TRAJ 52 and TRAV 21 TRAJ 28. Both represented about 40% of all cDNA clones corresponding to a TCRα chain that were analysed for this line (23 in total). In line CIR010, the expanded TCRα represented 70% of all cDNA clones corresponding to a TCRα chain analysed in the line (of which there were 43) and comprised TRAV 8-4 TRAJ 32. The expanded TCRα chains in each line were different and there appeared to be no common or similar V or J region usage from this analysis. It was also noted that in lines B1 and CIR010 which had been restimulated three times with peptide 4 there was more restriction of the TCRα repertoire, with only five different TCRα chains in total being identified in line B1 and eight in line CIR010. In the line which had only been restimulated once with peptide 4, CIR014, there was less restriction in the repertoire with 18 different V-J combinations being identified. This might be expected as the lines which had been restimulated a greater number of times would be more peptide-specific.

The PCR used in this TCR CDR3 analysis used a C region-specific reverse primer to bind to all TCR sequences in the cDNA sample and a polyC anchor forward primer to bind to the poly(dG) tail previously added to the cDNA. As the cDNA samples used comprised a heterogeneous mixture of mRNA products, the proportion of these products corresponding to TCR chains was likely to be low and there was also likely to be more than one TCR chain within each sample. Therefore, even if a clonal expansion of one chain had occurred, the overall frequency of this chain would be very low. The apparent clonal expansions seen could therefore be an artefact caused by the preferential

TRAV	CDR3 α	TRAJ	CDR3 length	% of total sequences	
2	A V F H G S S N T G K L I	37	13	3.3	
8-4	A V S D R Y S G G G A D G L T	45	15	6.7	
8-6	A V R S T A G S Y Q L T	28	12	3.3	
9-2	A A E R N T D K L I	34	10	3.3	
12-3	A M S A G T G R R A L T	5	12	3.3	
13-1	A A S E S G G G A D G L T	45	13	3.3	
	A A S K D N D M R	43	9	3.3	
20	A V H A G N N R K L I	38	11	3.3	
	A V Q A V P A S G T Y K Y I	40	14	3.3	
	A V Q S P N A G G T S Y G K L T	52	16	3.3	
23/DV 6	A A G P N S G Y A L N	41	11	3.3	
24	A F R A N Q A G T A L I	15	12	3.3	
26-2	I L R E S Y N D Y K L S	20	12	3.3	
	I L R D P T S G T Y K Y I	40	13	3.3	
	I L L F G N E K L T	**48**	**10**	**3.3**	
	I L R F G N E K L T		**10**	**6.7**	
	I L I F G N E K L T		**10**	**3.3**	
	I L R D N F G N E K L T		**12**	**6.7**	
	I L R D V S N F G N E K L T		**14**	**3.3**	
	I L R G G N E K L T		**10**	**6.7**	**Total:**
	I L R D D Y E K L T		**10**	**3.3**	**33.3**
27	A G A I N N A G N M L T		12	3.3	
38-2/ DV8	A Y R S A G S G G G A D G L T	39	15	6.7	
	A L R G G G G A D G L T	45	12	6.7	
			Mean length	**12.1 ± 0.4**	

Table 3.1 TCRα sequences obtained from TCR CDR3 analysis of HLA-DR1-restricted, peptide 4-specific T-cell line CIR014 at its 1st restimulation with peptide 4 TRAV and TRAJ selection is shown for each receptor identified, along with the amino acid sequence at the CDR3 junction and the length of the CDR3. Also shown is the percentage of total TCR sequences obtained for this line that each TCR comprised. The major expansion identified is shown in bold type. Mean length is shown as mean ± standard error of the mean. 66% of the total plasmid sequences obtained for this line corresponded to a correctly-rearranged TCRα chain.

TRAV	CDR3 α	TRAJ	CDR3 length	% of total sequences
1-1	A V R D K G Q K L L	16	10	13.0
13-1	**A A T V P W A G G T S Y G K L T**	**52**	**16**	**39.1**
21	**A V S G G A G S Y Q L T**	**28**	**12**	**39.1**
	A V R P R L M	31	7	4.3
26-1	I V R V E D T G K L I	37	11	4.3
			Mean length	**13.0 ± 0.6**

Table 3.2 TCRα sequences obtained from TCR CDR3 analysis of HLA-DR1-restricted, peptide 4-specific T-cell line B1 at its 3rd restimulation with peptide 4
TRAV and TRAJ selection is shown for each receptor identified, along with the amino acid sequence at the CDR3 junction and the length of the CDR3. Also shown is the percentage of total TCR sequences obtained for this line that each TCR comprised. The two equally dominant expansions are shown in bold type. Mean length is shown as mean ± standard error of the mean. 33% of the total plasmid sequences obtained for this line corresponded to a correctly-rearranged TCRα chain. In the analysis of this line, it was notable that 26% of the total plasmid sequences represented TCR sequences containing a frameshift in the CDR3, and they are not included in this analysis.

TRAV	CDR3 α	TRAJ	CDR3 length	% of total sequences
8.3	A V G A R G D S N Y Q L I	33	13	11.6
	A V G A I G N E K L T	48	11	9.3
8-4	**A V W S G A T N K L I**	**32**	**11**	**67.4**
8-6	A V S D Q S G G Y Q K V T	13	13	2.3
12-2	A V I T G R R A L T	5	10	2.3
14/DV4	A I V G R G S T L G R L Y	18	13	2.3
20	A V Q E A G F Q K L V	8	11	2.3
21	A V K D P A G G G T S G S R L T	58	16	2.3
			Mean length	**11.4 ± 0.2**

Table 3.3 TCRα sequences obtained from TCR CDR3 analysis of an HLA-DR1-restricted, peptide 4-specific T-cell line, CIR010, at the 3rd restimulation with peptide 4 TRAV and TRAJ selection is shown for each receptor identified, along with the amino acid sequence at the CDR3 junction and the length of the CDR3. Also shown is the percentage of total TCR sequences obtained for this line that each TCR comprised. The expanded population identified is shown in bold type. Mean length is shown as mean ± standard error of the mean. 79% of the total plasmid sequences obtained for this line corresponded to a correctly-rearranged TCRα chain.

amplification of one particular TCR chain over the others which is unrelated to its actual frequency within the sample and gives the false impression that it is a clonally expanded TCR chain. For each line analysed here, this PCR was carried out multiple times and in all cases the frequency of the identified chains remained approximately constant for each reaction, suggesting that the expansions seen were not artefacts but were accurate representations of the TCR chain frequencies within the samples. Single cell RT-PCR or cloning the original T-cell line by limiting dilution and analysing each clone separately could be used to confirm this, where each T-cell in the original sample would be analysed in a separate reaction. This would identify the TCR chain expressed by each individual T-cell and the frequency of T-cells expressing a particular chain would determine whether it was clonally expanded.

Analysis of CDR3α sequences and length in each line was also carried out. For the expanded TCRα chains in lines B1 (TRAV 13-1 TRAJ 52 and TRAV 21 TRAJ 28) and CIR010 (TRAV 8-4 TRAJ 32), each example of the combination that was analysed expressed the same CDR3 amino acid sequence. For line B1, the two CDR3s were the 16 amino acid AATVPWAGGTSYGKLT (TRAV 13-1 TRAJ 52) and the 12 amino acid AVSGGAGSYQLT (TRAV 21 TRAJ 28). For line CIR010, the expanded CDR3 was 11 amino acids long and comprised the sequence AVWSGATNKLI. In the case of the line at a lesser restimulation, line CIR014, however, this was not true. For the expanded TCRα VJ region TRAJ 26-2 TRAJ 48 there were seven different CDR3 loops, as shown in Table 3.1. Most of the loops were 10 amino acids long but CDR3 loops of 12 and 14 amino acids were also identified and no particular sequence dominated the response. There was a high degree of similarity in amino acid usage at the beginning and end of the sequences and there were most differences (including insertion of the extra amino acids for the longer CDR3s) in the centre of the sequence. The amino acids which are the same in each case (the first two and last four) are likely to be those encoded in the germline sequence of the V and J regions, whilst the differing amino acids are more likely to be coded for by non-germline DNA that is inserted through the action of TdT during recombination events in the developing T-cell (402, 403). In comparison to the mean length of the human CDR3α loop as defined by Moss and Bell (586) which when interpreted using the IMGT definition (610) is approximately 12, one of the TCRα chains from line B1, TRAV 13-1 TRAJ 52, expresses a CDR3α loop which is notably long in comparison as it is 16 amino acids long. The CDR3α loops expressed by the expanded TCRα chains in line CIR010 and

CIR014 as well as the other chain in line B1 express CDR3α loops which are more comparable in length to the mean value defined by Moss and Bell (586).

The mean length of all CDR3 loops identified from the analysis in line CIR014 was 12.1 ± 0.4 (range - 9 to 16) which is similar to the mean length of 12 for human TCR CDR3α loops (586). In line B1 the mean length was 13.0 ± 0.6 (range 7 to 16) which is slightly increased in comparison to the mean length of 12 (586), due to the expansion of a T-cell population expressing a 16 amino acid CDR3α. In line CIR010 the mean length of CDR3α loops was 11.4 ± 0.2 (range 10 to 16), perhaps a slight decrease in comparison to the mean published length of 12 amino acids due to the expansion of a T-cell population expressing an 11 amino acid CDR3α loop. The mean lengths of expanded CDR3α loops in these lines are similar and close to the mean length of CDR3α loops in unstimulated human T-cells; in line B1, expansion of T-cells bearing a receptor with a CDR3α loop that is 4 amino acids longer than this mean value gave the line a mean length which was slightly longer.

In summary, expansions of T-cells bearing specific TCRα chains was seen in each line analysed, occurring to a greater extent in the two lines which had been restimulated more often with peptide 4. One line, B1, showed expansion of two populations of T-cells bearing different receptors, one of which also expressed a CDR3α loop of 16 amino acids which is notably longer than the published mean length of CDR3α loops of unstimulated human T-cells (12 amino acids, 586).

3.1.3 TCRβ chain and CDR3 usage in human peptide 4-specific, DR1-restricted T-cell lines

As for the TCRα chains, TCRβ chain composition in terms of V and J region usage as well as CDR3 amino acid sequence and length was analysed in the lines CIR014 (shown in Table 3.4), B1 (shown in Table 3.5) and CIR010 (shown in Table 3.6). Expansions of T-cells bearing specific receptors were seen in each line, as for the TCRα chain analysis. The extent of the expansion seen in line CIR014 was small with the expanded TCRβ chain, TRBV 20-1 TRBJ 2-2, only comprising 14.3% of all TCR sequences obtained for this line (42 clones in total). This was in contrast to the expansions seen in lines B1 and CIR010 which were represented by a much larger

TRBV	CDR3 β	TRBJ	CDR3 length	% of total sequences
2	A S R G G G E P Q H	1-5	10	2.4
	A S R G G R K Q Y	2-3	9	7.1
3-1	A S S G G T G P Y E Q Y	2-7	12	2.4
4-2	A S S F Q G G G Q P Q H	1-5	12	4.8
5-1	A S S W G D R V A M N T E A F	1-1	15	4.8
	A S S L L S G V E T Q Y	2-5	12	2.4
	A S S F G E T Q Y		9	4.8
	A S S Y R T S S S Y E Q Y	2-7	13	2.4
	A S S R L P G Q G A Y E Q Y		14	2.4
5-5	A S S L R V A M T Y E Q Y	2-7	13	2.4
7-8	A S S P T G G E Q Y	2-7	10	2.4
12-3	A S S P G P Y Y G Y T	1-2	11	2.4
	A S S L T S R N Q P Q H	1-5	12	2.4
	A S S T R S V R E T Q Y	2-5	12	2.4
13	A S S R G T R N T E A F	1-1	12	2.4
19	A S R N R R D R G M R G A F	1-1	14	2.4
	A S S P D R A S L Q P Q H	1-5	13	2.4
	A S S I L R Q S Y N E Q F	2-1	13	4.8
	A S S K P S G P S T D T Q Y	2-3	14	2.4
20-1	S A R K R T T N E K L F	1-4	12	2.4
	S A R D L A R S T Q P Q H	1-5	13	2.4
	S A L S G I Y N E Q L	2-1	11	2.4
	S A R S A G R S G E L F	**2-2**	**12**	**14.3**
	S A R Q G A R G E T Q Y	2-5	12	4.8
28	A S S L R S G G F N Y G Y T	1-2	14	2.4
29-1	S V S R T G F F T E A F	1-1	12	4.8
30	A W A I G A A N E G F	2-1	11	4.8
	A W S V H R A A T Q Y	2-5	11	2.4
			Mean length	**11.9 ± 0.2**

Table 3.4 TCRβ sequences obtained from TCR CDR3 analysis of HLA-DR1-restricted, peptide 4-specific T-cell line CIR014 at its 1st restimulation with peptide 4 TRBV and TRBJ selection is shown for each receptor identified, along with the amino acid sequence at the CDR3 junction and the length of the CDR3. Also shown is the percentage of total TCR sequences obtained for this line that each TCR comprised. The modest expansion identified is shown in bold type. Mean length is shown as mean ± standard error of the mean. 71% of the total plasmid sequences obtained for this line corresponded to a correctly-rearranged TCRβ chain.

TRBV	CDR3 β	TRBJ	CDR3 length	% of total sequences
4-1	A S S Q V Q N E Q F	2-1	10	4.1
	A S S Q G V N G N I Q Y	2-4	12	2.0
6-5	**A S S T R D R W S G G L T**	**2-6**	**13**	**36.7**
7-8	A S S L G P P L A V Y N E Q F	2-1	15	2.0
11-1	**A S S Q N P N E Q F**	**2-1**	**10**	**40.8**
20-1	S A R G F G H D E Y N E Q F	2-1	14	2.0
27	A S S L L G S T G E L F	2-2	12	12.2
			Mean length	**11.6 ± 0.2**

Table 3.5 TCRβ CDR3 sequences obtained from an HLA-DR1-restricted, peptide 4-specific T-cell line, B1, at its 3rd restimulation with peptide 4 TRBV and TRBJ selection is shown for each receptor identified, along with the amino acid sequence at the CDR3 junction and the length of the CDR3. Also shown is the percentage of total TCR sequences obtained for this line that each TCR comprised. The expanded populations are identified in bold type. Mean length is shown as mean ± standard error of the mean. 76% of the total plasmid sequences obtained for this line corresponded to a correctly-rearranged TCRβ chain.

TRBV	CDR3 β	TRBJ	CDR3 length	% of total sequences
3-1	A S S Q G G G P Y E Q Y	2-7	12	2.8
5-1	A S S F L T A T N E K L F	1-4	13	2.8
	A S S L A T G G V D T Q Y	2-3	13	2.8
	A S S L E W T R N Q E T Q Y	2-5	14	2.8
6-1	**A S S E A G W G A S G T E A F**	**1-1**	**15**	**36.1**
6-2	A S G G V A E T Q Y	2-5	10	5.6
7-2	A S S L D R Q I G Q P Q H	1-5	13	13.9
	A S S L D S S A G N T G E L F	2-2	15	2.8
9	A S S V A G T G Q E T Q Y	2-5	13	2.8
	A S S V A P S G G H L E Q Y	2-7	14	2.8
11-1	A S S Q N P N E Q F	2-1	10	2.8
20-1	S A R D P D G Y G Y T	1-2	11	19.4
	S A A A G T S G A Y P L T Q Y	2-5	15	2.8
			Mean length	**13.2 ± 0.3**

Table 3.6 TCRβ sequences obtained from TCR CDR3 analysis of the HLA-DR1-restricted, peptide 4-specific T-cell line, CIR010, at its 3rd restimulation with peptide 4 TRBV and TRBJ selection is shown for each receptor identified, along with the amino acid sequence at the CDR3 junction and the length of the CDR3. Also shown is the percentage of total TCR sequences obtained for this line that each TCR comprised. The dominant expansion identified is shown in bold type. Mean length is shown as mean ± standard error of the mean. 60% of the total plasmid sequences obtained for this line corresponded to a correctly-rearranged TCRβ chain.

proportion of the analysed TCR sequences. This would perhaps be expected as these lines have been restimulated more often with peptide 4 and are therefore more peptide-specific and the peptide-specific T-cells would have expanded to a greater degree. In line B1, as for the TCRα chain analysis in this line, the expansion of two populations of T-cells expressing different receptors was seen; one expressed the receptor TRBV 6-5 TRBJ 2-6 and the other expressed the receptor TRBV 11-1 TRBJ 2-1. These receptors comprised 36.7% (TRBV 6-5 TRBJ 2-6) and 40.8% (TRBV 11-1 TRBJ 2-1) of all TCR sequences analysed (49 in total). This compares with the extent to which the two TCRα chains from line B1 were expanded in the line and it is likely that each of the expanded TCRα chains pairs with one of the TCRβ chains from this analysis. It is not possible to tell which chain would pair with which from this analysis - this would requiring cloning of the line and analysis of TCR usage within the clones. In line CIR010 there was more than one population of T-cells which expanded in response to peptide 4 stimulation and none of these matched the expansion seen in the TCRα analysis from this line in terms of extent. The largest expansion, represented by 36.1% of all TCR sequences analysed from this line (49 in total), was TRBV 6-1 TRBJ 1-1 and the two smaller expansions were TRBV 11-1 TRBJ 1-2 (19.4%) and TRBV 7-2 TRBJ 1-5 (13.9%). It is most likely that the dominant TCRα chain from this line, TRAV 8-4 TRAJ 32, pairs with the most frequent TCRβ chain, TRBV 6-1 TRBJ 1-1, although there is also the possibility that it could be pairing with one of the other expanded chains instead of or alongside the most frequent chain. Again, as for the TCRα chains, there was no similarity in V and J region usage between the three lines in the expanded TCRβ chains.

CDR3β analysis of the expanded TCRβ chains in each line indicated that for the expanded TCR chain (or chains) expressed, the same CDR3β amino acid sequence was also expressed. In line CIR014, the CDR3β loop expressed by the expanded TCR, TRBV 20-1 TRBJ 2-2, was 12 amino acids in length, SARSAGRSGELF. This was in contrast to the expanded TCRα chain in this line in which the expanded VJ combination expressed a number of different CDR3α sequences. In line B1, the two expanded TCRβ chains expressed the CDR3s ASSTRDRWSGGLT (13 amino acids, TRBV 6-5 TRBJ 2-6) and ASSQNPNEQF (10 amino acids, TRBV 11-1 TRBJ 2-1). In line CIR010 the TCRβ chain which had expanded to the greatest degree, TRBV 6-1 TRBJ 1-1, expressed the 15 amino acid CDR3β ASSEAGWGASGTEAF. The mean length of the CDR3β loop in human unstimulated T-cells as defined by Moss and Bell (586) is

approximately 12 when interpreted using the IMGT definition (610). In comparison to this length, only the expanded TCRβ chain in line CIR010 is noticeably longer at 15 amino acids. The lengths of the expanded receptors in line CIR014, 12 amino acids, and in line B1, 13 and 10 amino acids, are comparable with the mean defined length in unstimulated T-cells.

In line CIR014 the mean length of all CDR3β loops expressed in the cDNA clones analysed was 11.9 ± 0.2 (range - 9 to 15) which is similar to the mean length of 12 for human TCR CDR3β loops (586) and is very similar to the mean length of CDR3α loops from the same line. The mean length of CDR3β loops in line B1 was 11.6 ± 0.2 (range 10 to 15); this is similar when compared with the published mean length of 12 (586) and is shorter than the corresponding mean length for the CDR3α loops from this line which is not surprising as the expanded CDR3 loops in the TCRβ analysis had lengths of 10 and 13, compared with 12 and 16. In line CIR010 the mean length of CDR3β loops was 13.2 ± 0.3 (range 10 to 15). This is the longest mean length seen in any of the lines for either CDR3α or CDR3β and is probably due to the expansion of a T-cell population bearing a receptor with a 15 amino acid CDR3β. With the exception of line CIR010 where the mean CDR3β length appears to be longer, the mean CDR3β lengths in these lines are comparable to the published CDR3β length in unstimulated human T-cells (586).

To summarise, in each line analysed there was at least one expansion of T-cells bearing specific receptors and these expansions occurred with more frequency in lines B1 and CIR010 which had been restimulated more often with peptide 4 than line CIR014. Line B1 expanded two populations of T-cells bearing different receptors, as was also seen for this line in the TCRα analysis. Line CIR010 expanded a population of T-cells expressing a TCRβ chain with a CDR3β loop of 15 amino acids which is noticeably longer than the published mean length of CDR3β loops in unstimulated human T-cells (12 amino acids, 586). The lengths of the expanded CDR3β loops from the other lines were similar to this mean length and the mean lengths of CDR3β loops analysed in each line were also comparable to this value; only in line CIR010 did the mean length appear to be increased.

3.1.4 Summary

The expansions seen in each line of both TCRα and TCRβ chains are shown as pie charts in Figure 3.3 (line CIR014), Figure 3.4 (line B1) and Figure 3.5 (line CIR010). The pie charts highlight how the size of the expansion in response to peptide 4 stimulation tends to increase with increasing numbers of restimulation, being smaller in line CIR014 (restimulated once with peptide 4) and larger in lines B1 and CIR010 (each restimulated three time with peptide 4).

For each T-cell line analysed individual expansions were seen of certain TCRα and TCRβ V-J combinations and CDR3s and these are summarised in Table 3.7.

Between the lines there was no obvious correlation in terms of V or J region selection or CDR3 amino acid sequence. In lines B1 (CDR3α) and CIR010 (CDR3β), one of the expanded chains was long in comparison to the published mean length for the CDR3 loops in unstimulated human T-cells, 12 amino acids (586), whilst all other expanded CDR3 loop lengths were similar to this length. The mean lengths of all CDR3α or CDR3β loops analysed in each line were also broadly comparable to this mean length with the exception of CDR3α length in line B1 and CDR3β length in CIR010, where the mean lengths were both at least 1 amino acid longer than the published mean length, suggesting that expressed TCRs carried longer CDR3 loops lengths in these instances. There was no obvious sequence homology between the dominant CDR3 loops in each line at the amino acid level.

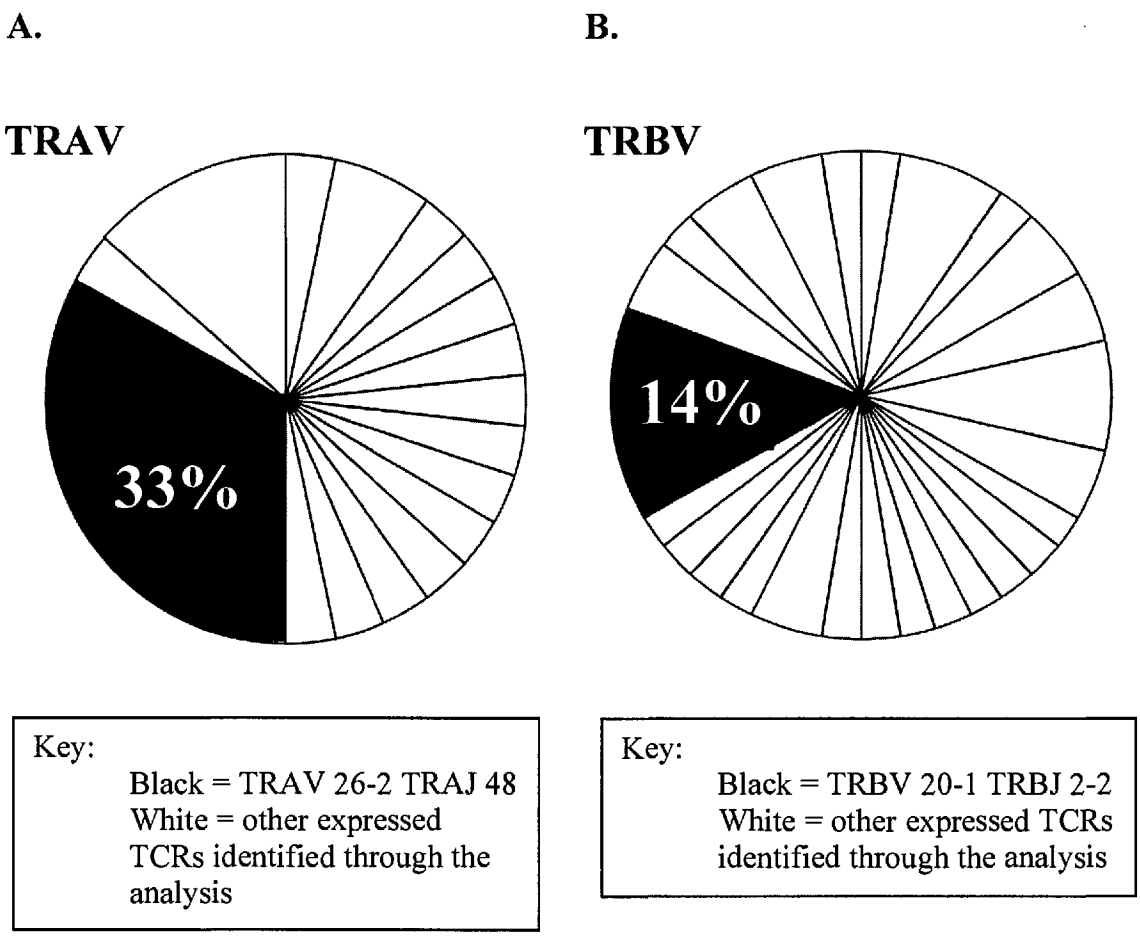


Figure 3.3 Expansion of T-cells with specific TCRα (A) and TCRβ (B) CDR3 regions in an HLA-DR1-restricted T-cell line, CIR014, after one restimulation with peptide 4 Each segment of each pie chart corresponds to a particular V region-J region combination identified through TCR analysis of the mRNA products from the line. The dominant expansion (i.e. the V-J combination found at the highest frequency) is shown in black with its extent shown as a percentage of all chains analysed for the line. For the α chain the dominant expansion was TRAV 26-2 TRAJ 48, comprising 33% of all TCRα chain PCR products sequenced. For the β chain the dominant expansion was TRBV 20-1 TRBJ 2-2, and comprising 14% of all TCRβ chain PCR products sequenced.

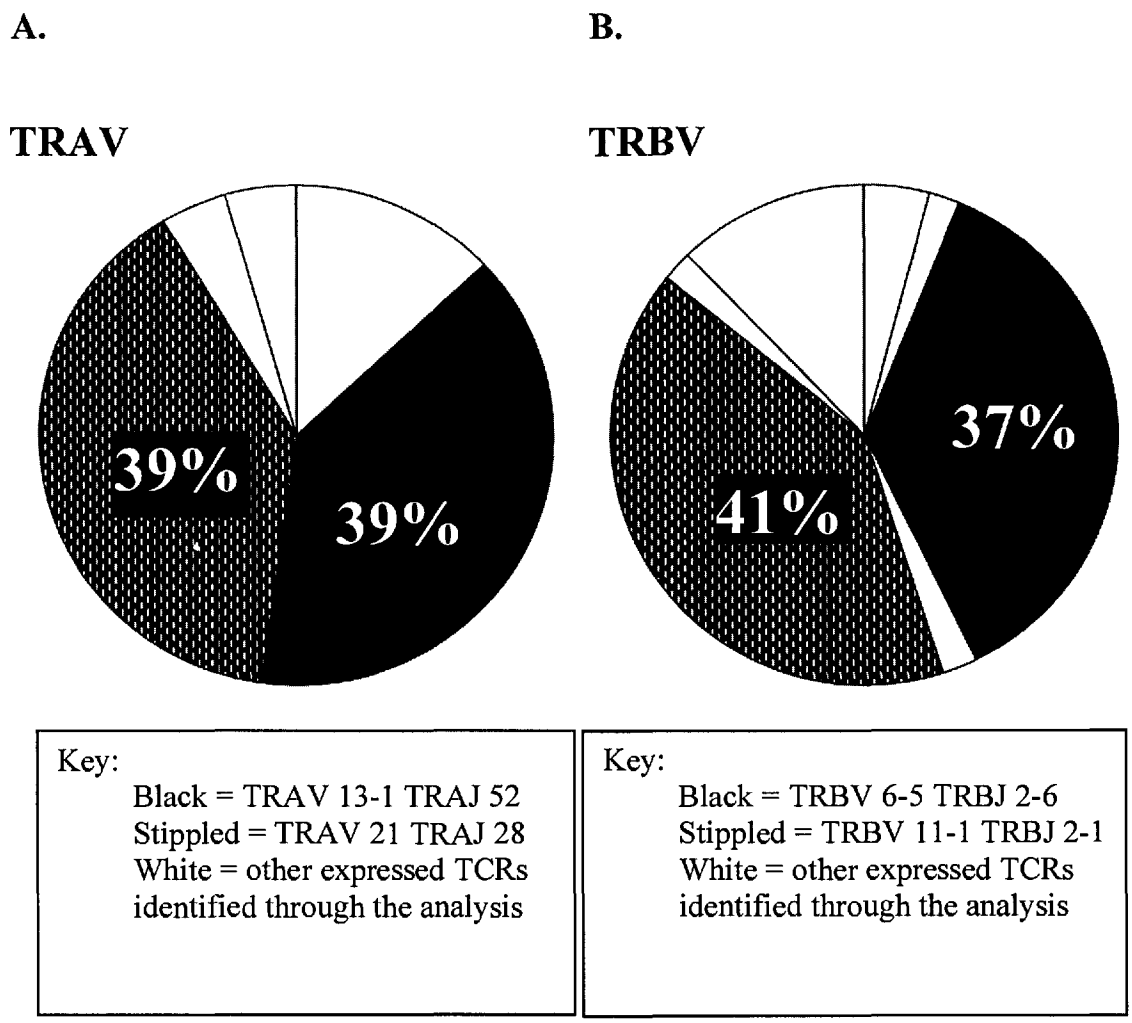


Figure 3.4 Expansion of T-cells with specific TCRα (A) and TCRβ (B) CDR3 regions in an HLA-DR1-restricted T-cell line, B1, at its 3rd restimulation with peptide 4 Each segment of the pie chart corresponds to a particular V region-J region combination identified through TCR CDR3 analysis of the mRNA products from the line. The dominant expansions (i.e. the V-J combinations found at the highest frequency) are shown in black or stippled with the percentage of all chains analysed for the line; there were two equally dominant expansions in both α and β chains in this line – the α chain expansions were TRAV 13-2 TRAJ 52 and TRAV 21 TRAJ 28, comprising 39% each of all TCRα chain PCR products sequenced. For the β chain the dominant expansions were TRBV 6-5 TRBJ 2-6 (37% of all TCRβ chain PCR products sequenced), and TRBV 11-1 TRBJ 2-1 (41% of all TCRβ chain PCR products sequenced).

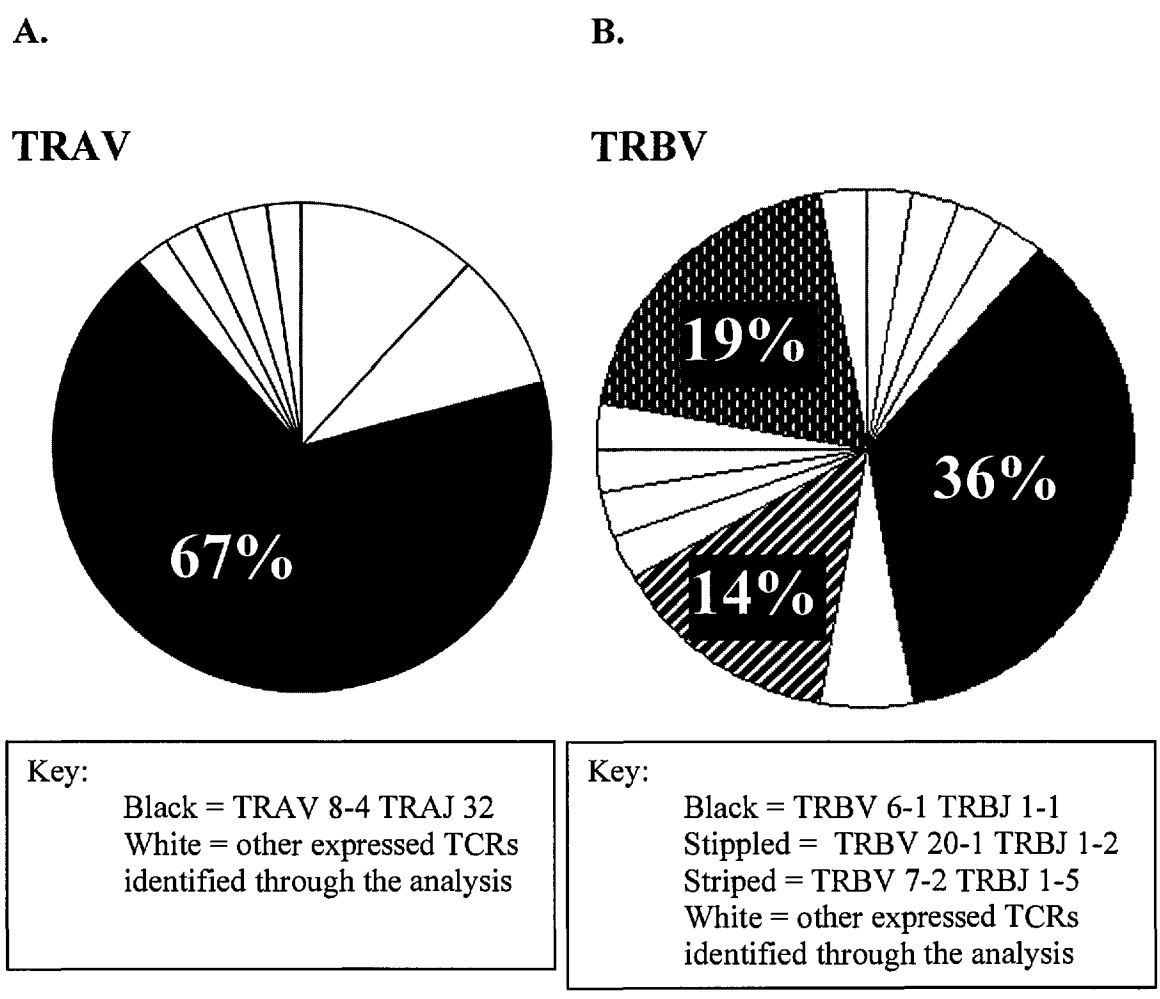


Figure 3.5 Expansion of TCRα (A) and TCRβ (B) chains in the HLA-DR1-restricted T-cell line CIR010 at its 3rd restimulation with peptide 4 Each segment of the pie charts corresponds to a particular V region-J region combination identified through TCR analysis of the mRNA products from the line. Expansions (i.e. V-J combinations found at the highest frequencies) are shown in black only for the TCRα analysis, and in black, stippled and striped for the TCRβ analysis. The extent of each expansion is shown as a percentage of all chains analysed for the line. For the α chain the dominant expansion was TRAV 8-4 TRAJ 32, comprising 67% of all TCRα chain PCR products sequenced. For the β chain the largest expansion was TRBV 6-1 TRBJ 1-1, comprising 36% of all TCRβ chain PCR products sequenced, but there were two lesser expansions.

Line/re-stimulation with peptide 4	TRAV/ TRBV	CDR3α	TRAJ/ TRBJ	CDR3 length
CIR014, 1st	TRAV 26-2	I L L F G N E K L T	TRAJ 48	10
		I L R F G N E K L T		10
		I L I F G N E K L T		10
		I L R D N F G N E K L T		12
		I L R D V S N F G N E K L T		14
		I L R G G N E K L T		10
		I L R D D Y E K L T		10
	TRBV 20-1	S A R S A G R S G E L F	TRBJ 2-1	12
B1, 3rd	TRAV 13-1	A A T V P W A G G T S Y G K L T	TRAJ 52	16
	TRAV 21	A V S G G A G S Y Q L T	TRAJ 28	12
	TRBV 6-5	A S S T R D R W S G G L T	TRBJ 2-6	13
	TRBV 11-1	A S S Q N P N E Q F	TRBJ 2-1	10
CIR010, 3rd	TRAV 8-4	A V W S G A T N K L I	TRAJ 32	11
	TRBV 6-1	A S S E A G W G A S G T E A F	TRBJ 1-1	15

Table 3.7 α and β expansions of the three lines CIR014, B1 and CIR010 with their related CDR3 amino acid sequences For lines CIR014 and CIR010, there is only one expansion seen for both α and β chains; for line B1, there are two α and two β chains, suggesting that there are two dominant T-cell populations in this line capable of responding to the HLA-DR-1/peptide 4 complex.

3.2 Preparation of TCR expression constructs for the transduction of the cell line BW7

One of the aims of the TCR CDR3 analysis of the T-cell lines derived from HLA-DR1$^+$ cat allergic asthmatic subjects was to identify peptide 4-specific dominant TCRs that could be used to address the question as to what extent TCR structure/sequence, particularly at the CDR3 loops, can impact upon T-cell phenotype. Previous work in the Boyton laboratory (601) has showed that T-cell clones raised against the same antigen, PLP_{56-70} complexed with the murine MHC class II molecule I-A^{g7}, and polarised through the addition of exogenous cytokines to develop into a Th1 or Th2 phenotype expressed different TCRs, most notably differing in terms of the length and amino acid sequence of the CDR3α loops. Short-term Th1 and Th2 polarised T-cell lines raised against the same antigen were then analysed for expression of both TCRs. The Th1 line did not express the TCR with an elongated CDR3α loop from the Th2 clone. In contrast, the TCR from the Th1 clone was expressed in the Th2-polarised line, although the Th2 TCR was more predominant. This work suggested that TCR structure, specifically the structure of the CDR3 loops, can impact on effector T-cell phenotype. Molecular modelling of the two TCRs suggested that the longer CDR3α loop of the Th2 TCR, which contained a higher proportion of amino acids with large, bulky sidechains that protrude into the TCR-peptide-MHC interface would hinder this interaction, thus predicting that a reduced affinity/avidity interaction is associated with the development of a Th2 response.

Cytokine polarisation may, therefore, favour T-cells expressing TCRs with structural characteristics that promote development into effector cells with a particular phenotype. To further explore this relationship between TCR sequence/structure and the prevailing cytokine milieu at the time of initial peptide-MHC encounter and the subsequent activation of particular antigen-specific T-cells, it was considered useful to develop a system whereby TCRs of interest could be expressed in a TCR-negative immortalised cell line of T-cell lineage, known as BW7 (602). TCRs intended for expression using this system include those identified here in human allergic asthma; those TCRs identified in the TCR CDR3 analysis that expanded in response to repeated activation by antigen *in vitro*, and those TCRs associated with specific T-cell phenotypes (Th1 and Th2) identified in the previous study using polarised T-cell clones raised against PLP_{56-70}/I-A^{g7} (601).

The cell line BW7 was chosen for use in this system for several reasons. It is a transformed murine thymoma line, modified to lack expression of TCR (602), but still retaining the signalling systems and other machinery that are required for T-cell function. The transduction of this line with constructs allowing the expression of a particular TCR has a number of advantages over using T-cell clones. The line is transformed, so it is more robust than a T-cell clone, and does not require re-stimulation or addition of exogenous cytokines to survive and proliferate, and as it grows quickly regardless of the presence of TCR or not, it can be rapidly expanded to yield a large number of cells for use in experiments. As BW7 is a transformed line, it is not as physiologically relevant as using a T-cell clone, but the line retains enough of its T-cell nature that results obtained using TCR-transduced BW7 lines will have relevance.

Such transduced lines would be useful reagents to investigate the extent to which TCR structure itself can influence T-cell function upon stimulation with its cognate peptide-MHC complex. TCR-transduced BW7 lines provide large numbers of cells expressing the same TCR allowing the impact of TCR structure on downstream events to be studied. Avenues of investigation could include basic studies on T-cell phenotype, TCR-peptide-MHC interaction kinetics, or the effect of TCR structure on the downstream signalling pathways following TCR engagement.

A retroviral transduction system was selected to transduce BW7 cells with the TCRs of interest. The retroviral transduction of a gene of interest leads, in many cases, to the stable expression of the transduced gene in the target cell line (611). Genes encoding the human TCR from line CIR010 and the two murine TCRs expanded from T-cell lines polarised towards either a Th1 or Th2-type phenotype in response to $PLP_{56\text{-}70}/I\text{-}A^{g7}$ (as described in reference 568 and shown in Figure 1.2) were cloned into the retroviral expression vector MFG (604) for use in the Phoenix retroviral transduction system (603).

I was not able to transduce BW7 cells using the retroviral transduction system outlined above, and so tried using an alternative system, using pTαcass and pTβcass TCR expression constructs (346) containing genes for the same TCRs and nucleofection using Amaxa technology (www.amaxa.com/technology). This system is based on electroporation as a means of transferring construct DNA into the target cells, but has the disadvantage that it does not lead to stable expression of the gene or genes of

interest in the target cell. I was unable to transduce BW7 cells using the nucleofection system and was not able to take this line of investigation any further.

3.2.1 Preparation of TCR expression constructs for use in a retroviral transduction system

A retroviral transduction system allows the stable expression of a gene of interest in a cell type where it is not endogenously found. Retroviral transduction systems utilise packaging cell lines which have been previously stably transduced with the genes necessary for production of retroviral particles except for one, the packaging signal ψ. This is supplied to the packaging cells as part of a retroviral expression vector which can also contain a gene of interest to be expressed in the target cell line. The retroviral vector MFG (604) (shown in Figure 2.1 with the target gene eGFP inserted and described in more detail in Section 2.1.2) was selected for use in the TCR transduction system due to its lack of a mutation in the long terminal repeat sequence of the viral genome encoded in the plasmid. Such a mutation is often included in retroviral vectors and renders the virus produced from use of these constructs replication-incompetent after one round of viral production, and is used as a safety factor to prevent any chance of there being further virus production in the target cell line. It also prevents these vectors from being used in a serial infection system where more than one viral packaging cell line is used before infection of the target line, and this was found to be required for successful transduction of the BW7 line. MFG was therefore used in preference to the other retroviral vectors available in the laboratory, the pQC (Clontech, 631516) series of vectors (Figure 3.6, with the target gene eGFP inserted), in spite of the advantage they have of containing antibiotic resistance genes allowing for selection of successfully transfected cells, as these vectors contain such a self-inactivating mutation.

The genes for the two murine PLP_{56-70}-specific TCRs had previously been cloned into the pQC vectors by Dr. Alexander Annenkov, a postdoctoral scientist in the laboratory, and these vectors were the source of the genes that were transferred into MFG. For the peptide 4-specific human TCR from the line CIR010, the same cDNA as that used for the TCR CDR3 analysis was used as the source of the TCR chains.

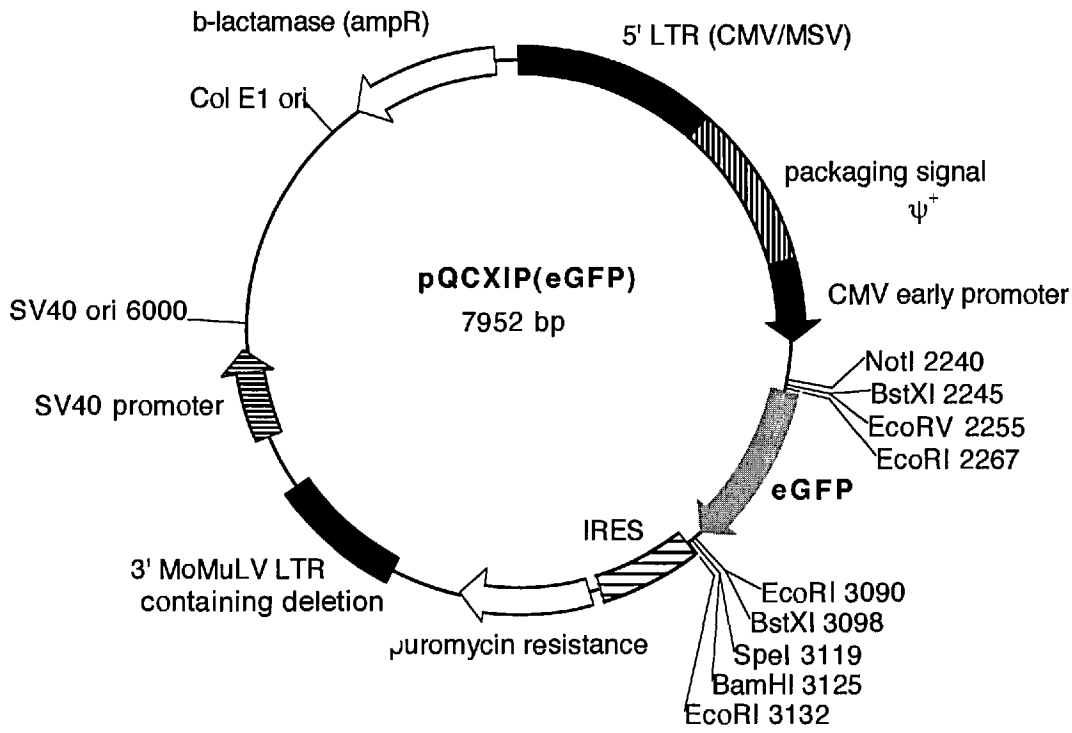


Figure 3.6 pQCXIP(eGFP) (Clontech, 631516) The vector diagram shows the retroviral components of the vector pQC and the target gene eGFP. It also shows the positioning of two genes that confer antibiotic resistance to any cell transformed or transduced with this plasmid, ampicillin and puromycin resistance (other variants of this plasmid carry neomycin or hygromycin resistance genes in place of puromycin resistance). Ampicillin resistance allows the plasmid to be cloned and amplified in bacteria, whilst puromycin resistance gives a means of selecting successfully infected target cells at the end of the transduction process. The deletion in the 3'-LTR renders the vector self-inactivating after one round of transfection/transcription, as it destroys the MoMuLV promoter required for transcription of the packaging signal.

3.2.1.1 Transfer of genes encoding TCR α and β chains from the PLP_{56-70}-specific murine T-cell clones A10(2) and D3(3) into the retroviral expression vector MFG

3.2.1.1.1 Vector modifications

MFG was originally supplied with restriction sites for NcoI and NotI allowing the target gene to be cloned into the vector (see Figure 2.1). As part of the NcoI restriction site (CCATGG), there is an ATG motif that is intended to be used as the start codon for expression of the target gene. However, in order to clone genes into the vector using this site, there is a requirement for the second codon of the gene to begin with G, which was not the case for a number of the TCR genes being transferred here. To overcome this obstacle, the vector MFG was modified to destroy the NcoI restriction site through nuclease digestion of NcoI-cut plasmid, and to henceforth use NotI as the sole site for inserting genes into the vector. The strategy followed to achieve this is shown in steps (a)-(d) of Figure 3.7. Briefly, a linker containing an additional NotI site was inserted into MFG(eGFP) using NcoI. The eGFP gene was then removed using NotI. The vector was then cut with NcoI and treated with S1 nuclease to degrade the sticky ends formed by the digest, before the now blunt-ended vector was re-ligated. This led to the formation of a vector where the NcoI site had been destroyed whilst the NotI site remained intact for use in the insertion of target genes. The steps of the strategy are shown as gel images in Figure 3.8.

For insertion of the TCR chains into MFG, there was now a requirement for the genes to be flanked on either side with a NotI site, which was not the case for the A10(2) and D3(3) TCR chains in pQC. A strategy was designed to transfer the TCR chains into MFG through pBluescriptII (vector diagram is shown in Appendix 12) which had also been modified, through insertion of a linker, to carry two NotI sites in its multiple cloning site, as shown in steps (e)-(f) of Figure 3.7 (gel images of this step are shown in Figure 3.8). These sites were placed in such a way as to allow the TCR chains from pQC to be transferred into pBluescriptII so that they were flanked by NotI sites, which would then allow their transfer into MFG.

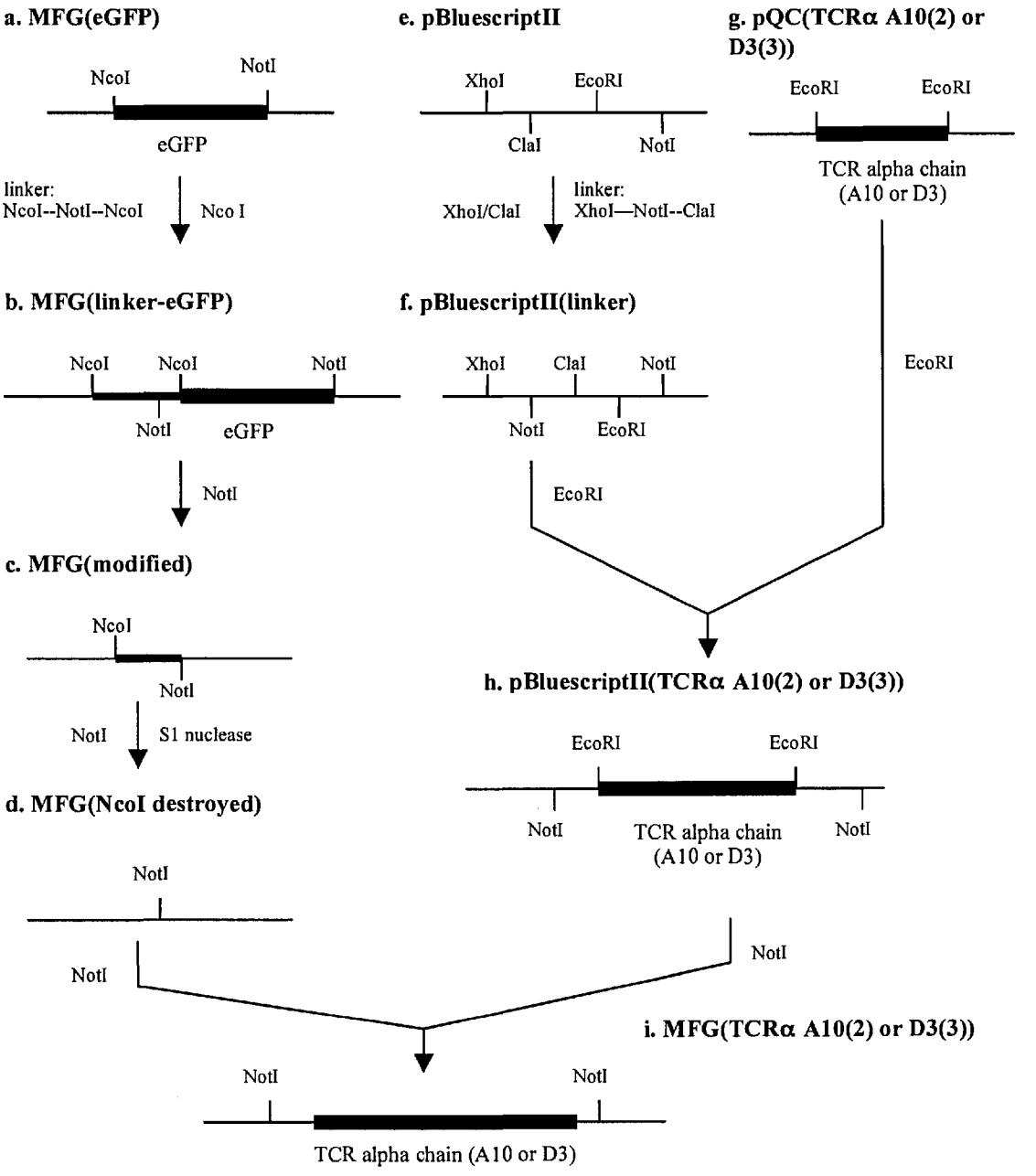


Figure 3.7 The cloning strategy designed to move TCRα chains for clones A10(2) (chains 5-D4 and 7-D3) and D3(3) from the vector pQC into MFG. TCRα chains of A10(2) and D3(3) had been previously inserted into pQC (g). MFG was available as MFG(eGFP) (a) and required modification before the TCR chains could be inserted. A linker was inserted containing a NotI site (b) allowing the removal of eGFP from the vector using NotI (c). The NcoI site was then destroyed (to remove the start codon in the restriction site) by digestion of the NcoI-cut vector with S1 nuclease (d), producing a vector into which the TCR chain genes could be inserted using NotI. The TCR chains were subcloned into pBluescriptII (e), previously modified by insertion of a linker containing an additional NotI site (f), using EcoRI (h). They were then transferred into MFG using NotI (i). A PCR was carried out on each inserted chain to ascertain its orientation, as described in the text. Vectors with correctly oriented genes were sequenced. All PCR primers, reaction conditions, oligonucleotide linkers and sequencing primers are shown in Appendix 3. All restriction enzymes and digests are shown in Appendix 5.

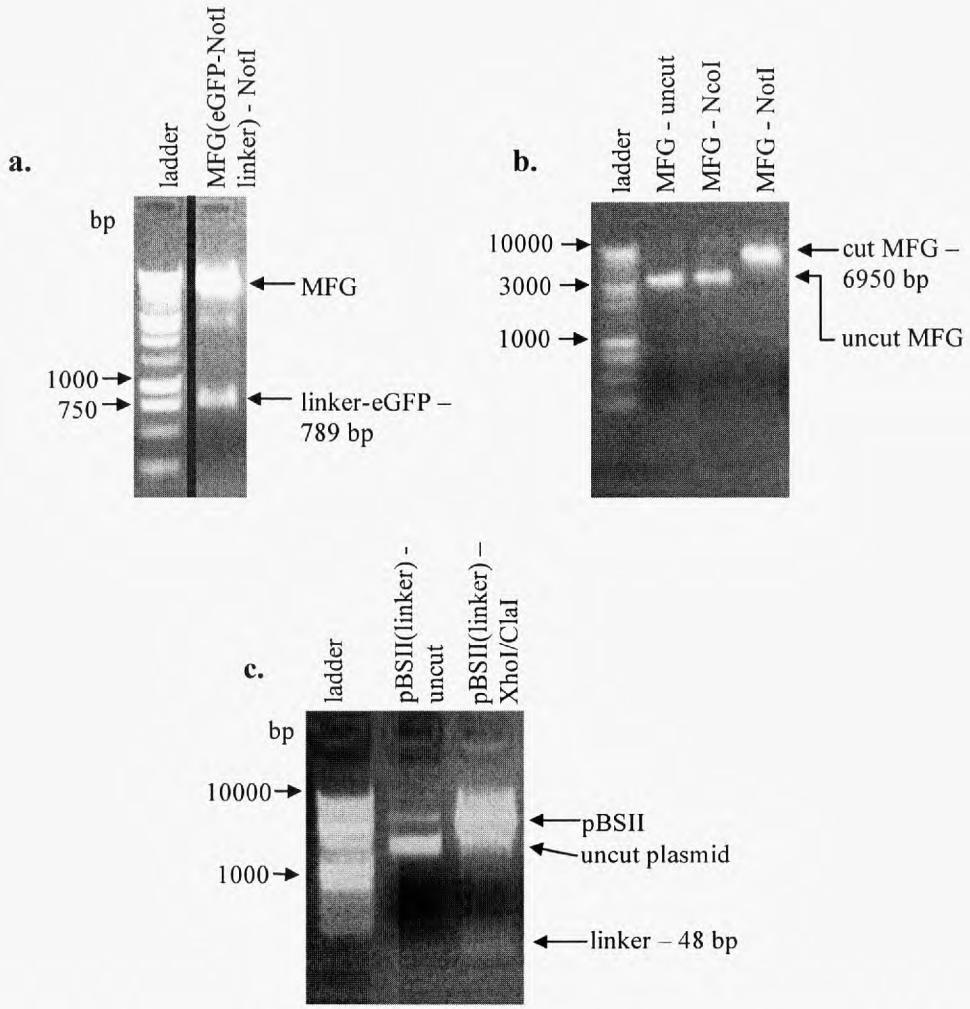


Figure 3.8 Gel images showing stages of the cloning strategy followed to modify the vectors MFG and pBluescriptII to allow cloning of the TCR chains from murine T cell clones A10(2) and D3(3) and the dominant TCR from the human T cell line CIR010 into MFG from pQC The images above show the steps involved in the modification of the cloning vector pBluescriptII and the retroviral vector MFG to allow the TCR chains from the murine T cell clones A10(2) and D3(3) and the dominant TCR from the human T cell line 010 to be cloned into MFG using NotI (as outlined in the strategy for the TCR α chains from A10(2) and D3(3) shown in Figure 3.8). (a) shows a NotI digest of MFG(eGFP) (a in Figure 3.8) after insertion of a 50 bp oligonucleotide linker containing an additional NotI site into the plasmid, upstream of the gene sequence (b in Figure 3.8). This allowed the eGFP insert (789 bp) to be excised from MFG using NotI, c in Figure 3.8. (b) shows restriction digests of S1 nuclease-treated MFG (d in Figure 3.8). The S1 nuclease removed overhanging single-stranded ends of DNA caused by digestion with NcoI, destroying the site. The plasmid was then rejoined by blunt-end ligation. Uncut plasmid was run as a comparison, alongside a NcoI digest (which did not cut, as the band appears to be the same size as the uncut plasmid) and a NotI digest (which did cut, as the band is of a different size (6950 bp) to the uncut plasmid, which has an apparent smaller band size due to uncut plasmid being supercoiled and therefore migrating atypically on a gel). This indicated that the NcoI site had been successfully destroyed without destruction of the NotI site just downstream. (c) shows a XhoI/ClaI digest of pBluescriptII after insertion of an oligonucleotide linker (48 bp) containing a NotI site (f in Figure 3.8). The gel was only run a very short distance to allow visualisation of the 48 bp linker, and 1 μl of uncut plasmid was run alongside as a comparison.

3.2.1.1.2 Transfer of TCRα chains from T-cell clones A10(2) and D3(3) into the vector MFG

The genes for each TCRα chain were transferred into MFG in the same way, shown in steps (g)-(i) of Figure 3.7. Each gene was transferred into the modified pBluescriptII vector using EcoRI, and subsequently transferred into the modified MFG vector using NotI. As only one restriction enzyme was used to clone the chains into MFG, a PCR was carried out on each inserted chain to ascertain its orientation in MFG, using MFG-specific forward and reverse primers situated on either side of the NotI insertion sites, and a TCR-specific V region forward primer. Vectors with correctly oriented genes (giving a band of 962 bp (A10 5-D4), 957 bp (A10 7-D3) or 965 bp (D3) with the TCR-specific forward and MFG-specific reverse primers) were sequenced to check for any mutations incorporated during the cloning process, after which the constructs were ready for use in the retroviral expression system. Gel images of the predicted PCR products for both correctly and incorrectly aligned TCRα chains are shown in Figure 3.9.

Gel images for the production of MFG (A10(2)α 5-D4) are shown in Figure 3.10, and a diagram of the final construct is shown in Figure 3.11. Sequence data for the TCR chain is shown in Appendix 13. For the construct MFG (A10(2)α 7-D3), gel images of its production are shown in Figure 3.12, with a vector diagram being shown in Figure 3.13, and sequence data for the TCR chain in Appendix 14. Gel images of MFG (D3(3)α) production are shown in Figure 3.14. A vector diagram of the final construct is shown in Figure 3.15, and sequence data for the TCR chain is shown in Appendix 15.

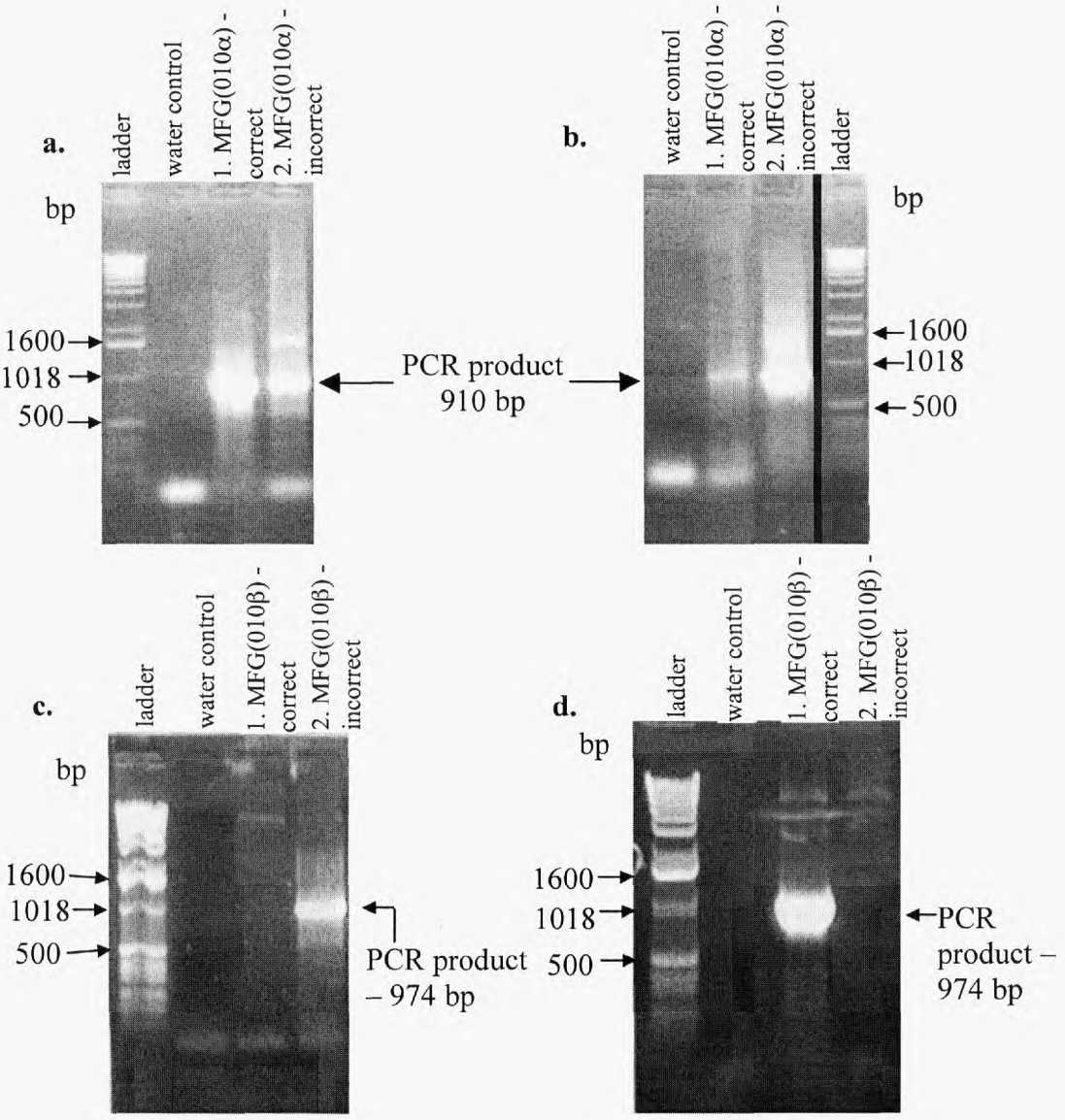


Figure 3.9 Orientation of TCR chains in MFG using PCR The images above show representative examples of the PCRs used to orient the TCR chains in MFG once they had been inserted. The gels above were obtained from orientation PCRs on MFG(CIR010αmCα) and MFG(CIR010βmCβ), using the PCR primers as described in the text. Constructs with a TCR insert were assayed using both sets of primers. Those clones giving a product of 910 bp (TCR α) or 974 bp (TCR β) with the V region-specific primer and the MFG reverse primer were oriented correctly and sequenced. (a) and (b) above show the two PCRs for the α construct, (a) shows the PCR using the V region-specific primer and the MFG reverse primer (i.e. correct orientation) (NB 1 and 2 indicate two clones that are the same in both reactions), and (b) shows the PCR using the V region-specific primer and the MFG forward primer (i.e. incorrect orientation). (c) and (d) show the same PCRs for the β construct – (c) shows correct orientation and (d) shows incorrect orientation. NB. As the PCRs were carried out on plasmid DNA, non-specific bands of the same size as the expected band may be seen. In such cases, whilst it was likely that the higher intensity band indicated the orientation of the insert, sequencing these clones was used as further confirmation of the correct orientation having been achieved. Primers used to orient each TCR chain are shown in Appendix 3. Forward primers were those used to originally clone the TCR chains into pQC vectors by Dr. Alexander Annenkov.

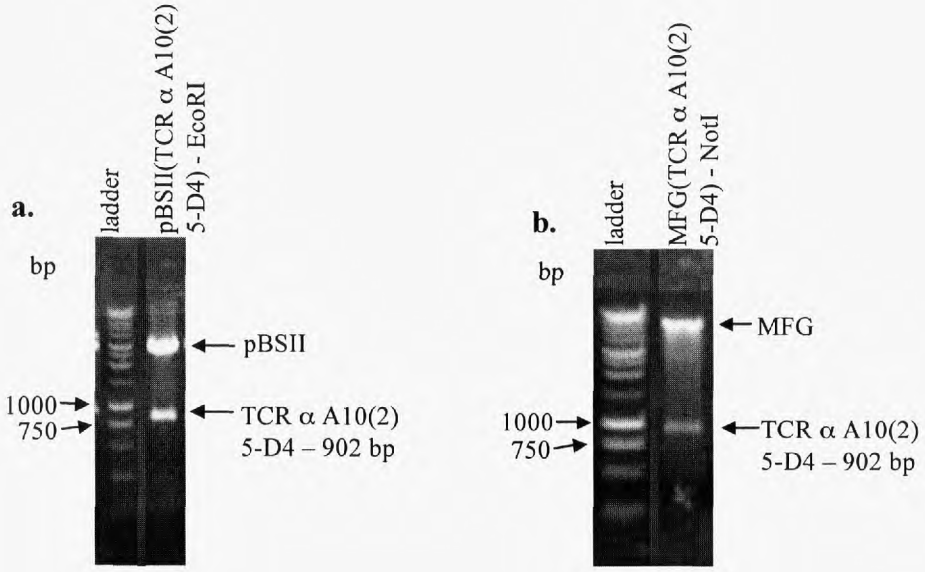


Figure 3.10 Gel images of the stages involved in moving the TCRα chain 5-D4 of murine clone A10(2) into MFG The TCR chain (902 bp) was supplied already cloned into vector pQC, another retroviral vector. The TCR chain was moved from the pQC vector into cloning vector pBluescriptII using EcoRI (a above, h in figure 3.7). pBluescriptII had previously been modified by insertion of an oligonucleotide linker to contain an extra NotI site, in addition to one already present (see Figure 3.7). The linker was inserted such that the NotI sites flanked the EcoRI insertion site, allowing the TCR chain to be moved from pBluescriptII into MFG using NotI. A clone of pBluescriptII showing insertion of a correctly sized insert upon EcoRI digestion was subsequently digested with NotI and inserted into MFG (b above, i in Figure 3.7). Correct insertion was ascertained by NotI digest, and orientation of the TCR chain in MFG was determined by PCR (see Figure 3.9). Correctly oriented clones were sequenced.

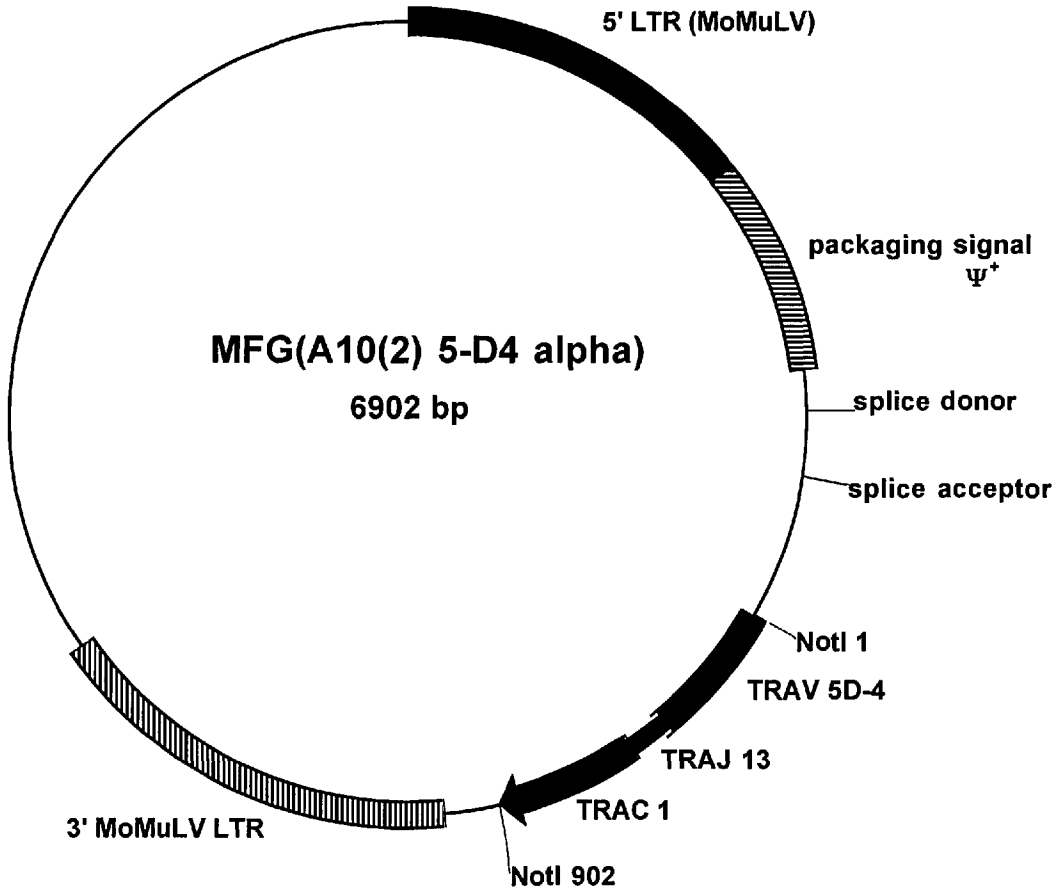


Figure 3.11 Final construct map of TCRα chain 5-D4 from the murine Th1 T-cell clone A10(2) in the retroviral expression vector MFG The diagram shows the composition of the vector in terms of the genes required for its function in a retroviral packaging gene transduction system and the position of the inserted TCR gene along with the restriction sites used in cloning the sequence into MFG.

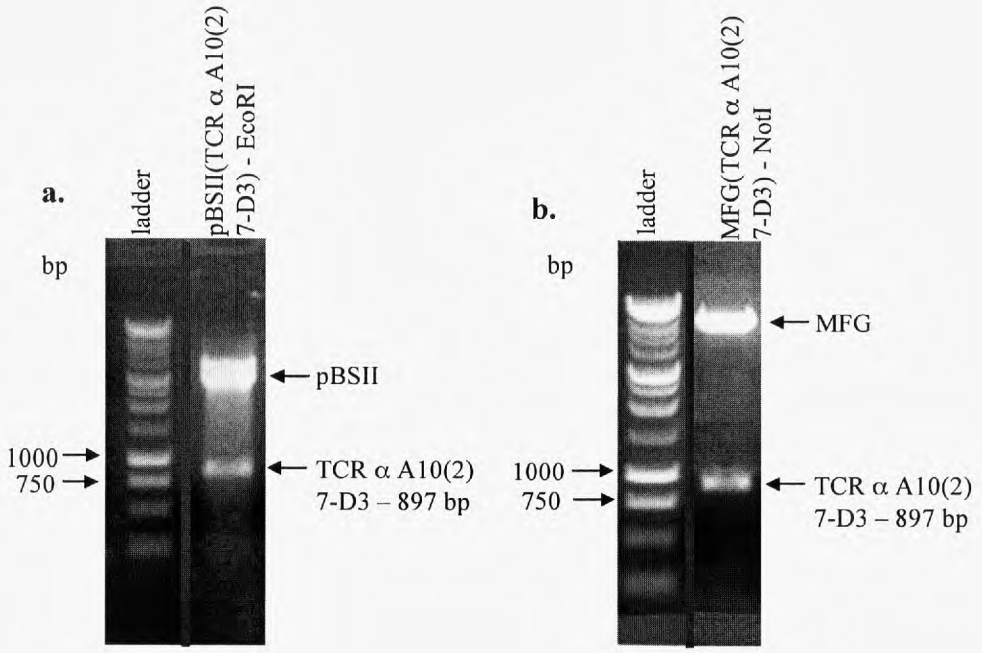


Figure 3.12 Gel images of the stages involved in moving the TCR α chain 7-D3 of murine clone A10(2) into MFG The 897 bp TCR chain had previously been cloned into vector pQC by Dr Alexander Annenkov. The TCR chain was transferred into modified pBluescriptII using EcoRI (a above, h in figure 3.7). pBluescriptII had previously been modified, as shown in Figure 3.7, to contain an extra NotI site in addition to the one already present, such that the NotI sites flanked the EcoRI insertion site, thus allowing the TCR chain to be moved into MFG using NotI. A clone of pBluescriptII that showed insertion of a correctly sized insert upon diagnostic EcoRI digestion was digested with NotI and the TCR chain was inserted into MFG (b above, i in Figure 3.7). A diagnostic Not I digest identified correct insertion of the TCR chain before its orientation MFG was determined by PCR (see Figure 3.9). Correctly oriented clones were sequenced.

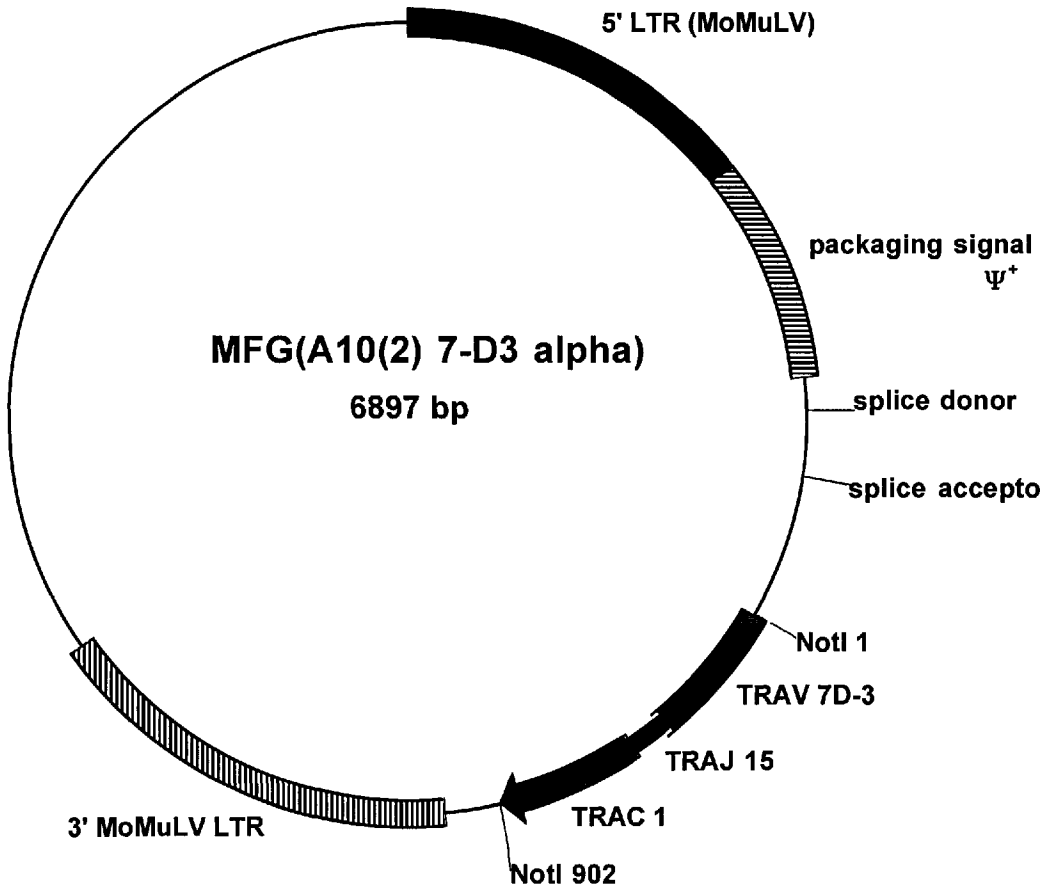


Figure 3.13 Final construct map of TCRα chain 7-D3 from the murine Th1 T-cell clone A10(2) in the retroviral vector MFG The composition of the vector in terms of the genes required for correct functioning in a retroviral packaging system is shown in addition to the position of the inserted TCR chain gene and the restriction sites used in cloning the sequence into MFG.

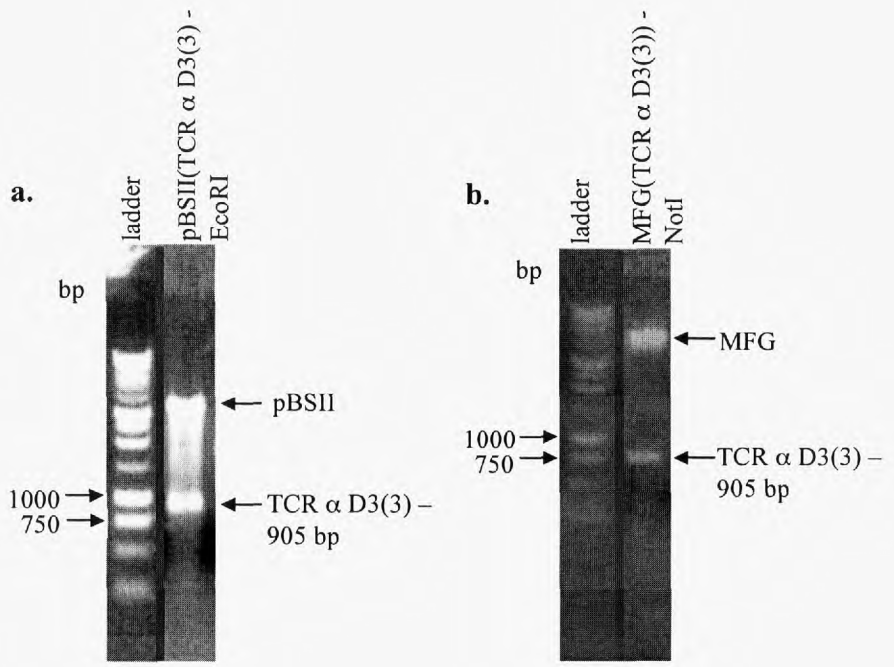


Figure 3.14 Gel images of the stages involved in moving the TCR α chain of murine clone D3(3) into MFG The TCR chain (905 bp) was supplied already cloned into vector pQC. The TCR chain was moved from pQC into modified pBluescriptII using EcoRI (a above, h in figure 3.7). pBluescriptII had been modified to contain an extra NotI site in addition to the one already present (as shown in Figure 3.7). The two NotI sites flanked the EcoRI insertion site, and allowed the TCR chain to be moved from pBluescriptII into MFG using NotI. A clone of pBluescriptII containing a correctly sized insert upon EcoRI digestion was then digested with NotI and inserted into MFG (b above, i in Figure 3.7). Correct insertion of the TCR chain was ascertained by NotI digest and its orientation in MFG was then determined by PCR (as shown in Figure 3.9). Correctly oriented clones were sequenced.

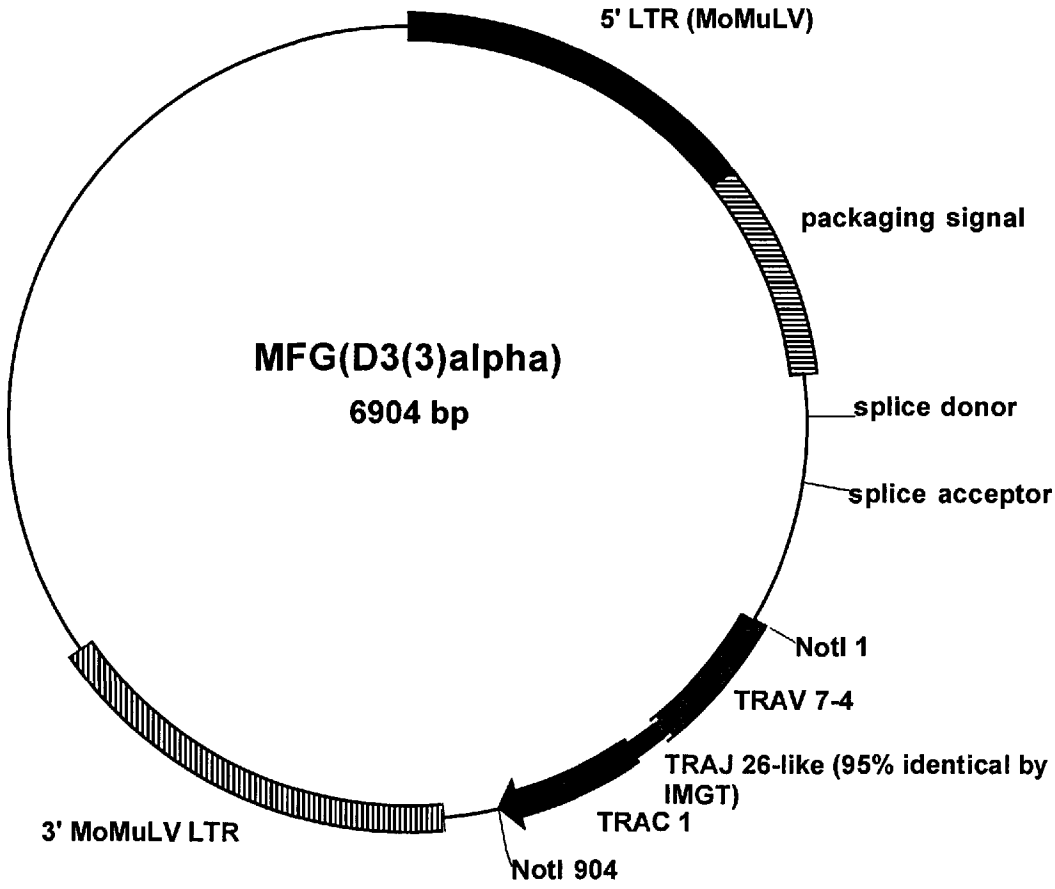


Figure 3.15 Final construct map of the TCRα chain from the murine Th2 T-cell clone D3(3) in the retroviral vector MFG The diagram shows the vector composition in terms of genes required for function in a retroviral packaging system, as well as the position of the inserted TCR gene sequence and the restriction sites used in cloning it into MFG.

3.2.1.1.3 Transfer of TCRβ chains from T-cell clones A10(2) and D3(3) into the vector MFG

Each TCRβ chain was transferred into the modified MFG vector via modified pBluescriptII, according to the strategy outlined in Figure 3.16. However, upon sequencing of the final constructs, the same mutation was discovered in the TCR C region of both constructs, a deletion of one base pair at the 3' end of the sequence. When the TCR chains were previously cloned into the pQC vector, the same mutated C region was used to construct both TCRβ chains. As such, new strategies were developed to correct the mutation in both constructs by PCR site-directed mutagenesis. These strategies made use of unique restriction sites in the sequence of the TCRβ genes, ClaI for the A10(2) TCRβ chain and BstXI for the D3(3) TCRβ chain, allowing the corrected PCR product to replace the mutated version of the gene, producing a final gene product with the missing base pair inserted.

The strategy to correct the mutated version of the A10(2) TCRβ gene is shown in Figure 3.17. Briefly, a PCR using high-fidelity DNA polymerase was carried out on the gene in pBluescriptII, using a reverse primer containing the missing base pair and an additional EcoRI site for ease of cloning, and a forward primer just upstream of the unique ClaI restriction site in the TCR V-J region. This product was ligated into the TA cloning vector pCR2.1 and transferred into unmodified pBluescriptII. The mutated version of the TCR chain was then replaced with the corrected version through use of ClaI, and the complete corrected TCR chain was moved into MFG. Gel images of this strategy are shown in Figure 3.18, and the full corrected sequence of this TCR chain with the inserted base highlighted is shown in Figure 3.19. Figure 3.20 shows the final construct as a vector diagram.

The strategy to correct the mutated version of the D3(3) TCRβ gene is shown in Figure 3.21. The same basic PCR mutagenesis strategy as used for the A10(2) TCRβ chain was followed to correct the D3(3) TCRβ chain, making use of a unique BstXI restriction site to replace the mutated version with the corrected version, before the complete corrected TCR chain was moved into MFG. Figure 3.22 shows gel images of the steps in this strategy, and the full corrected sequence with the inserted base highlighted is shown in Figure 3.23. The final construct is shown as a vector diagram in Figure 3.24.

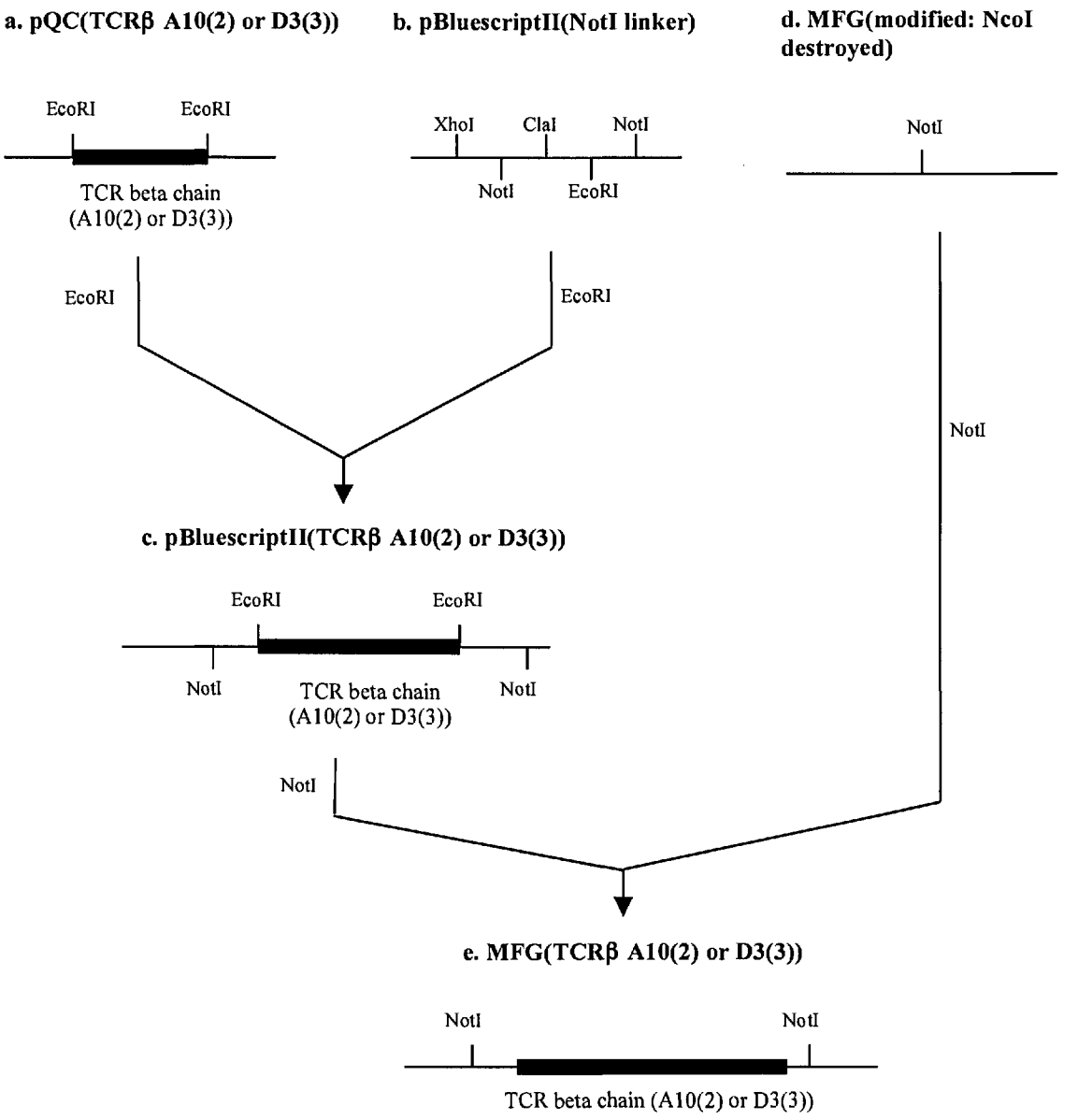


Figure 3.16 A schematic diagram showing the cloning strategy designed to move TCR β chains for clones A10(2) and D3(3) from the vector pQC into MFG. The TCR chains for A10(2) and D3(3) had previously been inserted into pQC by Dr. Alexander Annenkov in our laboratory (a). pBluescriptII (b) had previously been modified by insertion of a linker containing an additional NotI site as shown in Figure 3.8. The TCRβ chains were transferred into the modified pBluescriptII using EcoRI (c). MFG (d) had previously been modified to destroy the NcoI site in its multiple cloning site (as shown in Figure 3.8). TCRβ chains were transferred to MFG from pBluescriptII using NotI (e). A PCR was carried out on each inserted chain to ascertain its orientation, as described in the text. Vectors with correctly oriented genes were sequenced. All PCR primers, reaction conditions, oligonucleotide linkers and sequencing primers are shown in Appendix 3. All restriction enzymes and digests are shown in Appendix 5.

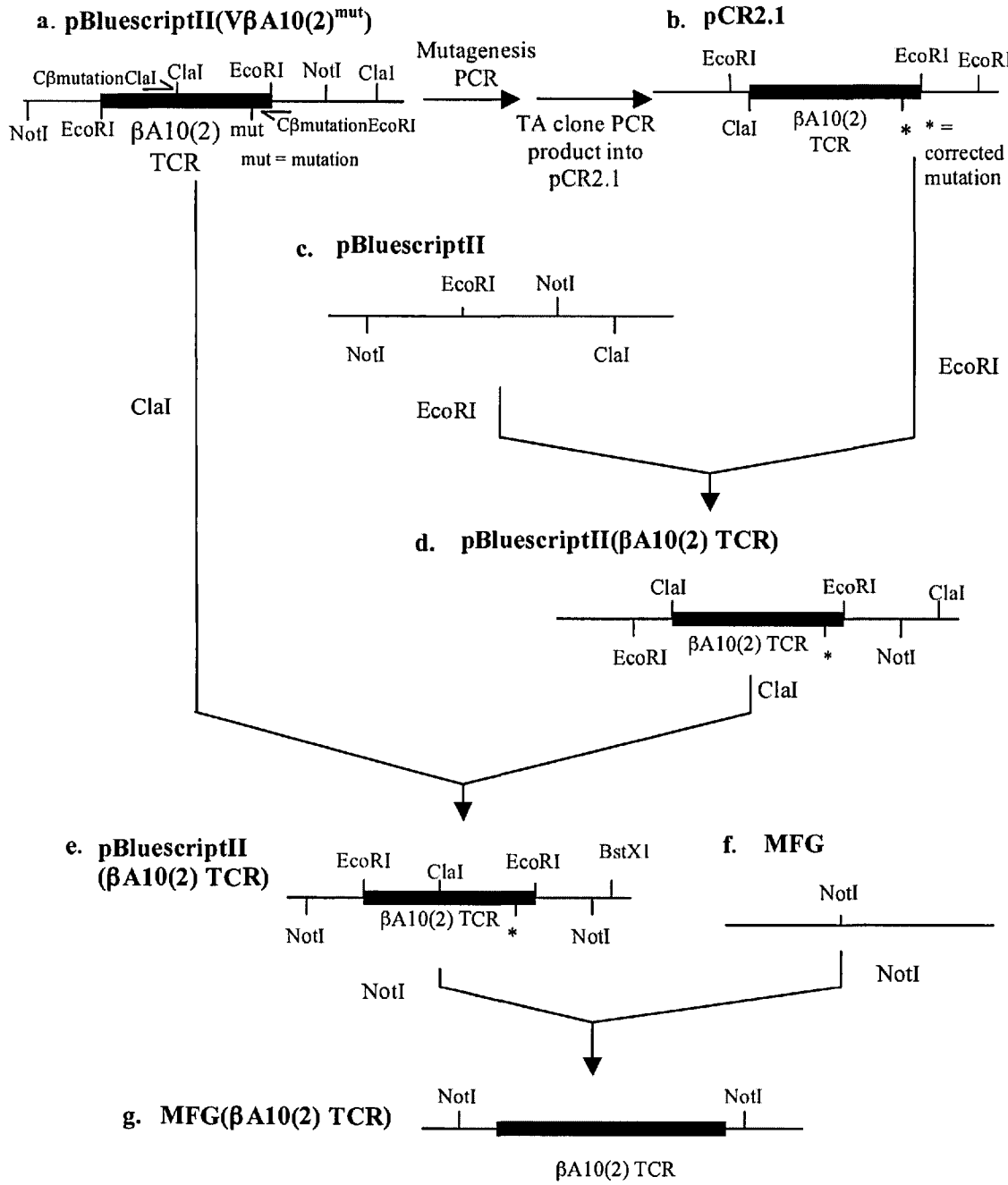


Figure 3.17 Cloning strategy designed to mutate the Cβ region of TCR chain βA10(2) The incorrect β chain was already inserted into pBluescriptII from the strategy in Figure 3.16 (a). A PCR using a primer incorporating the missing base pair and a primer just upstream of a unique restriction site, ClaI, within the TCR sequence was used to insert the missing base pair. The PCR product was ligated into pCR2.1 (b). The insert was sequenced to check for successful mutagenesis and a correct clone was moved into linker-modified pBluescriptII (c) using EcoRI (d). Using ClaI, the corrected fragment was used to replace the incorrect fragment of the chain inserted into pBluescriptII (e). Inserts were checked for their correct orientation by diagnostic digest with EcoRI. A correctly oriented clone was moved into MFG (f) using NotI (g). Clones were oriented and sequenced as described previously. All PCR primers, reaction conditions, and sequencing primers are shown in Appendix 3. All restriction enzymes used and digest conditions are shown in Appendix 5.

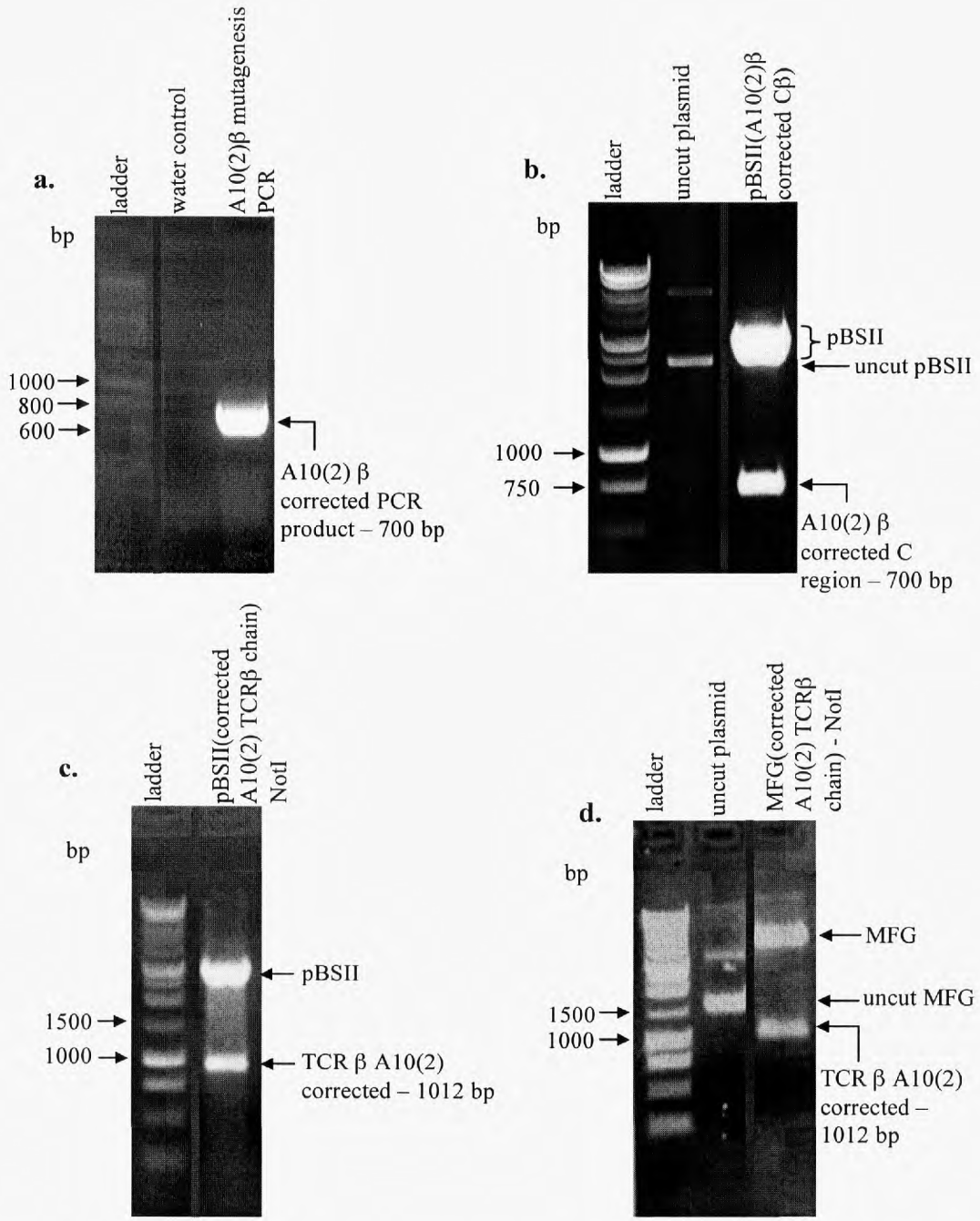


Figure 3.18 Gel images of the stages involved in moving the TCR β chain from the murine T cell clone A10(2) into MFG including correcting a mutation in the Cβ region The images above show the steps involved in the strategy as outlined in Figure 3.17. (a) shows the PCR product for the Cβ region in which the mutation has been corrected (700 bp), using a primer incorporating the missing base pair. Template DNA was the TCR chain in the cloning vector pBluescriptII, a in Figure 3.17. The PCR product was ligated into pCR2.1 by TA cloning, and moved into pBluescriptII subsequently, as shown in (b) above, d in Figure 3.17. This was then combined with the original TCR chain in pBluescriptII to replace the mutated sequence by restriction digest, as shown in (c) above, and e in Figure 3.17. The corrected TCRβ chain (1012 bp) was then moved into MFG using NotI as shown in (d) above, corresponding to g in Figure 3.17, (e) above. Orientation of the insert was determined by PCR, as shown in Figure 3.17, and clones with a correctly oriented TCR chain were sequenced.

1
ATG GGC ACC AGG CTT CTT GGC TGG GCA GTG TTC TGT CTC CTT GAC ACA GTA CTG TCT GAA GCT
M G T R L L G W A V F C L L D T V L S E A

64
GGA GTC ACC CAG TCT CCC AGA TAT GCA GTC CTA CAG GAA GGG CAA GCT GTT TCC TTT TGG TGT
G V T Q S P R Y A V L Q E G Q A V S F W C

127
GAC CCT ATT TCT GGA CAT GAT ACC CTT TAC TGG TAT CAG CAG CCC AGA GAC CAG GGG CCC CAG
D P I S G H D T L Y W Y Q Q P R D Q G P Q

190
CTT CTA GTT TAC TTT CGG GAT GAG GCT GTT ATA GAT AAT TCA CAG TTG CCC TCG GAT CGA TTT
L L V Y F R D E A V I D N S Q L P S D R F

253
TCT GCT GTG AGG CCT AAA GGA ACT AAC TCC ACT CTC AAG ATC CAG TCT GCA AAG CAG GGC GAC
S A V R P K G T N S T L K I Q S A K Q G D

316
ACA GCC ACC TAT CTC TGT GCC AGC AGC CCC CTC GAC TGG GGG GAT GAA CAG TAC TTC GGT CCC
T A T Y L C A S S P L D W G D E Q Y F G P

379
GGC ACC AGG CTC ACG GTT TTA GAG GAT CTG AGA AAT GTG ACT CCA CCC AAG GTC TCC TTG TTT
G T R L T V L E D L R N V T P P K V S L F

442
GAG CCA TCA AAA GCC GAG CTG GCA AAC AAA CAA AAG GCT ACC CTC GTG TGC TTG GCC AGG GGC
E P S K A E L A N K Q K A T L V C L A R G

505
TTC TTC CCT GAC CAC GTG GAG CTG AGC TGG TGG GTG AAT GGC AAG GAG GTC CAC AGT GGG GTC
F F P D H V E L S W W V N G K E V H S G V

568
AGC ACG GAC CCT CAG GCC TAC AAG GAG AGC AAT TAT AGC TAC TGC CTG AGC AGC CGC CTG AGG
S T D P Q A Y K E S N Y S Y C L S S R L R

631
GTC TCT GCT ACC TTC TGG CAC AAT CCT CGA AAC CAC TTC CGC TGC CAA GTG CAG TTC CAT GGG
V S A T F W H N P R N H F R C Q V Q F H G

694
CTT TCA GAG GAG GAC AAG TGG CCA GAG GGC TCA CCC AAA CCT GTC ACA CAG AAC ATC AGT GCA
L S E E D K W P E G S P K P V T Q N I S A

757
GAG GCC TGG GGC CGA GCA GAC TGT GGA ATC ACT TCA GCA TCC TAT CAT CAG GGG GTT CTG TCT
E A W G R A D C G I T S A S Y H Q G V L S

820
GCA ACC ATC CTC TAT GAG ATC CTA CTG GGG AAG GCC ACC CTA TAT GCT GTG CTG GTC AGT GGC
A T I L Y E I L L G K A T L Y A V L V S G

883 921
CTG GTG CTG ATG GCC ATG GTC AAG AAA AAA AAT TCC TGA
L V L M A M V K K K N S **STOP**

Figure 3.19 Amino acid sequence of the TCR β chain (TRBV 14 TRBJ 2-7 TRBC 1) from the murine T cell clone A10(2) cloned into retroviral vector MFG TRBV 14 is highlighted in green, TRBJ 2-7 in purple and TRBC 1 in turquoise. The CDR3 is highlighted in blue with the coding DNA sequence underlined. The letter underlined in red indicates the base pair that was inserted by site-directed mutagenesis in order to convert the incorrect sequence to the original DNA sequence, thus allowing for correct read-through of the amino acid sequence and correct positioning of the stop codon.

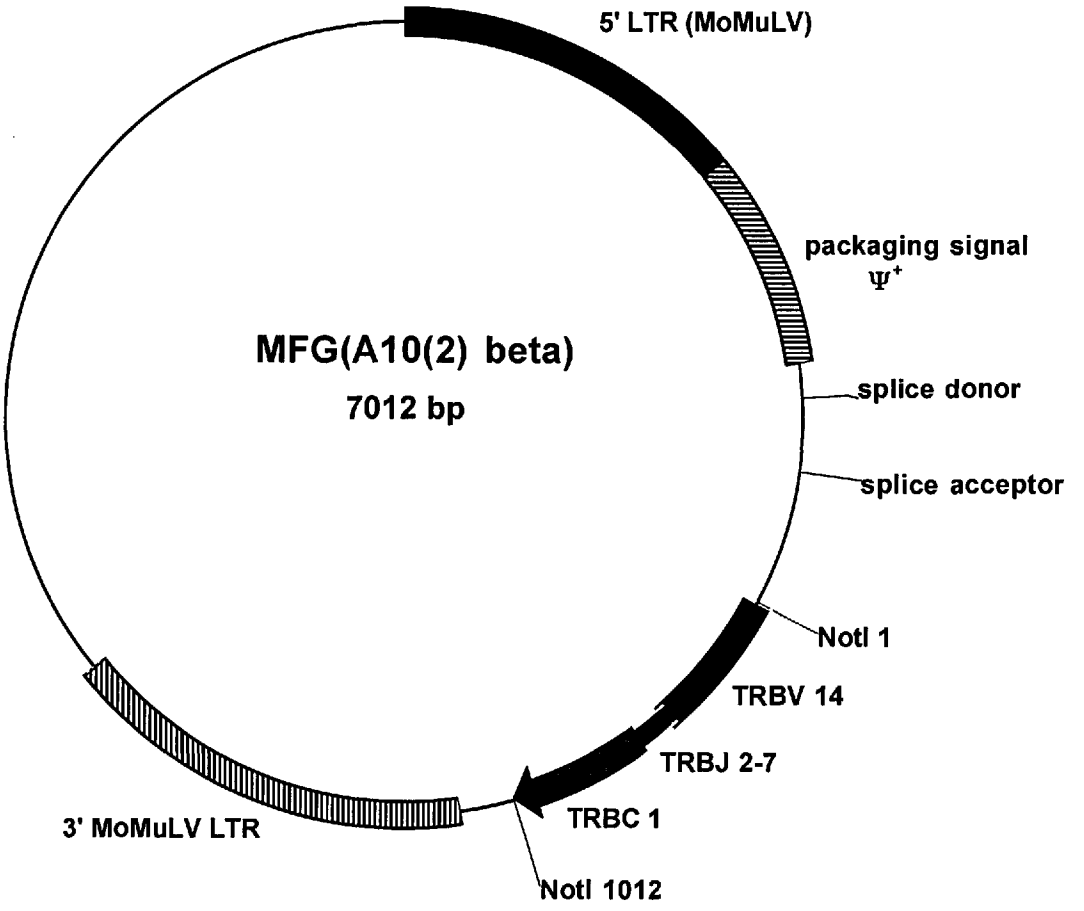


Figure 3.20 Final construct map of the TCR β chain from the murine Th1 T-cell clone A10(2) in the retroviral vector MFG The position of the genes required for correct function in a retroviral packaging system as well as the position of the inserted TCR gene and the restriction sites used in cloning the sequence into MFG are shown.

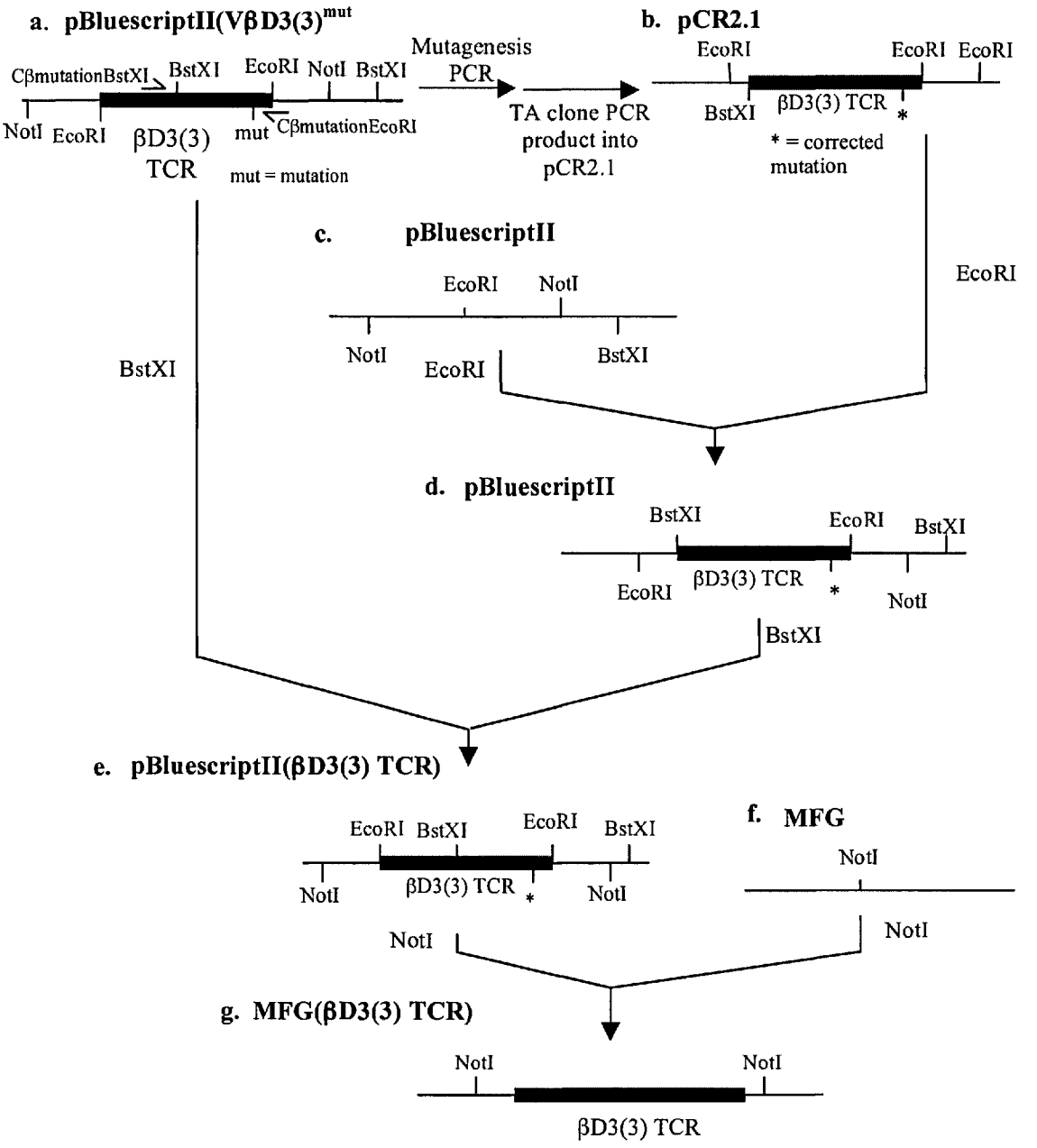


Figure 3.21 Cloning strategy designed to mutate the Cβ region of TCR chain βD3(3) The incorrect β chain (a) had already been inserted into pBluescriptII from the strategy in Figure 3.16. A mutagenesis PCR using a primer incorporating the missing base pair (the same primer as that used in the strategy to correct the mutation in the A10(2) TCRβ chain with a primer just upstream of a unique restriction site, BstXI, within the TCR sequence, was used to correct the mutation. The resulting PCR product was cloned into pCR2.1 (b). The insert was sequenced to check for successful correction of the mutation before a correct clone was moved into linker-modified pBluescriptII using EcoRI (c to d). The incorrect fragment was then replaced in pBluescriptII by the corrected fragment using BstXI in order to produce a correct TCR gene sequence (e). Diagnostic digest of clones using EcoRI determined the correct orientation of the insert and a correctly oriented clone was moved into MFG (f) using NotI (g). Clones were oriented and sequenced as described previously. All PCR primers, reaction conditions, and sequencing primers are shown in Appendix 3. All restriction enzymes used and digest conditions are shown in Appendix 5.

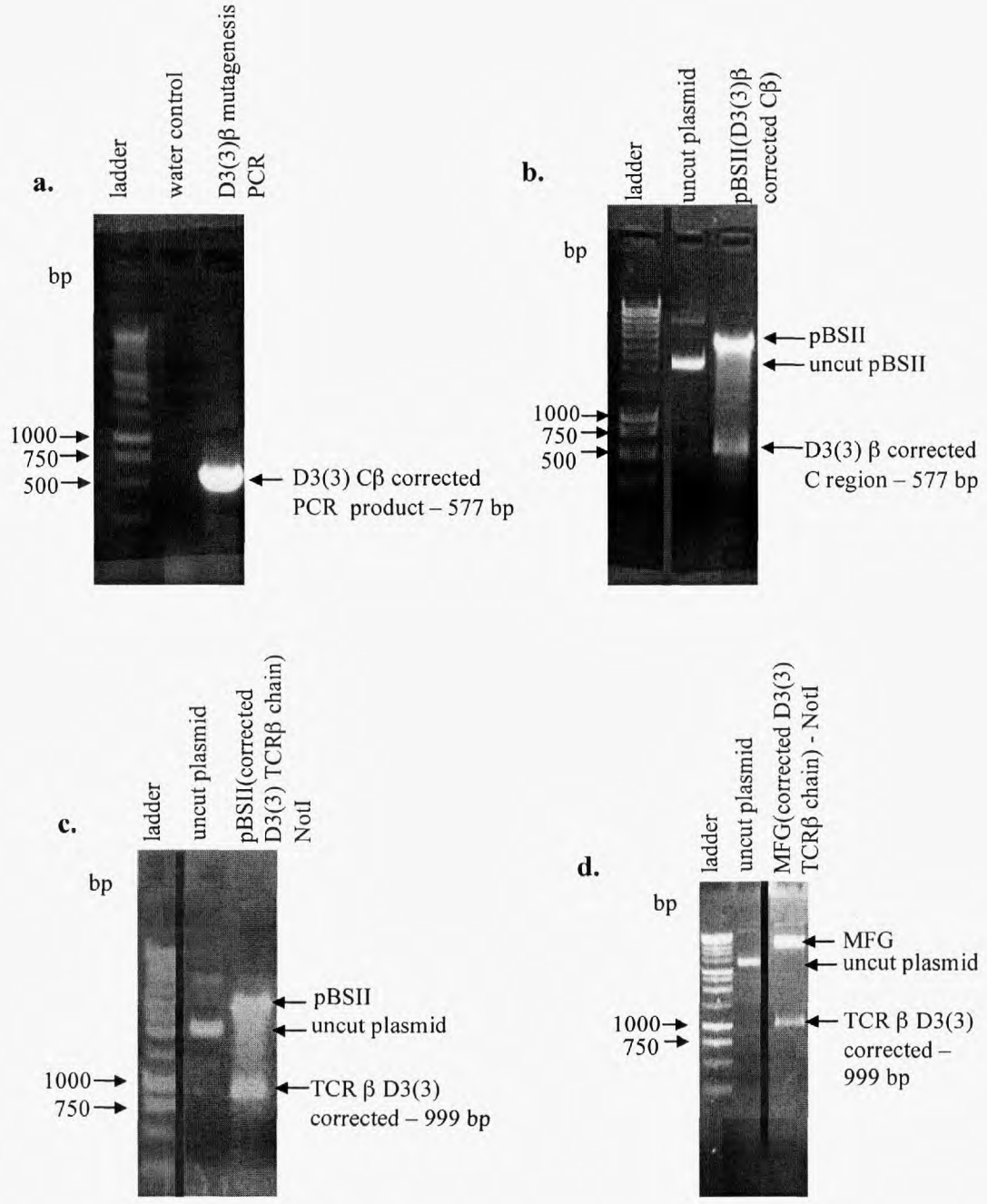


Figure 3.22 Gel images of the stages involved in moving the TCR β chain from the murine T cell clone D3(3) into MFG including correcting a mutation in the Cβ region The images above show the steps involved in the strategy as outlined in Figure 3.21. The PCR product for the Cβ region in which the mutation has been corrected (577 bp) using a primer incorporating the missing base pair is shown in (a). Template DNA used was the TCR chain in the cloning vector pBluescriptII, a in Figure 3.22. The PCR product was ligated into pCR2.1, sequenced, and moved into pBluescriptII as shown in (b), d in Figure 3.21. The corrected fragment was then combined with the original TCR chain in pBluescriptII using BstXI to replace the mutated sequence, and diagnostic digest with NotI was carried out to confirm correct insertion, as shown in (c), and e in Figure 3.22. The corrected TCRβ chain (999 bp) was moved into MFG using NotI as shown in (d), corresponding to g in Figure 3.21. Orientation of the insert was determined by PCR, as shown in Figure 3.9. Clones with a correctly oriented TCR chain were sequenced.

1
ATG GGC TCC ATT TTC CTC AGT TGC CTG GCC GTT TGT CTC CTG GTG GCA GGT CCA GTC GAC CCG
M G S I F L S C L A V C L L V A G P V D P

64
AAA ATT ATC CAG AAA CCA AAA TAT CTG GTG GCA GTC ACA GGG AGC GAA AAA ATC CTG ATA TGC
K I I Q K P K Y L V A V T G S E K I L I C

127
GAA CAG TAT CTA GGC CAC AAT GCT ATG TAT TGG TAT AGA CAA AGT GCT AAG AAG CCT CTA GAG
E Q Y L G H N A M Y W Y R Q S A K K P L E

190
TTC ATG TTT TCC TAC AGC TAT CAA AAA CTT ATG GAC AAT CAG ACT GCC TCA AGT CGC TTC CAA
F M F S Y S Y Q K L M D N Q T A S S R F Q

253
CCT CAA AGT TCA AAG AAA AAC CAT TTA GAC CTT CAG ATC ACA GCT CTA AAG CCT GAT GAC TCG
P Q S S K K N H L D L Q I T A L K P D D S

316
GCC ACA TAC TTC TGT GCC AGC AGC CAA GCC GGG ACT GGA GAA GAC ACC CAG TAC TTT GGG CCA
A T Y F C A S S Q A G T G E D T Q Y F G P

379
GGC ACT CGG CTC CTC GTG TTA GAG GAT CTG AGA AAT GTG ACT CCA CCC AAG GTC TCC TTG TTT
G T R L L V L E D L R N V T P P K V S L F

442
GAG CCA TCA AAA GCC GAG CTG GCA AAC AAA CAA AAG GCT ACC CTC GTG TGC TTG GCC AGG GGC
E P S K A E L A N K Q K A T L V C L A R G

505
TTC TTC CCT GAC CAC GTG GAG CTG AGC TGG TGG GTG AAT GGC AAG GAG GTC CAC AGT GGG GTC
F F P D H V E L S W W V N G K E V H S G V

568
AGC ACG GAC CCT CAG GCC TAC AAG GAG AGC AAT TAT AGC TAC TGC CTG AGC AGC CGC CTG AGG
S T D P Q A Y K E S N Y S Y C L S S R L R

631
GTC TCT GCT ACC TTC TGG CAC AAT CCT CGA AAC CAC TTC CGC TGC CAA GTG CAG TTC CAT GGG
V S A T F W H N P R N H F R C Q V Q F H G

694
CTT TCA GAG GAG GAC AAG TGG CCA GAG GGC TCA CCC AAA CCT GTC ACA CAG AAC ATC AGT GCA
L S E E D K W P E G S P K P V T Q N I S A

757
GAG GCC TGG GGC CGA GCA GAC TGT GGA ATC ACT TCA GCA TCC TAT CAT CAG GGG GTT CTG TCT
E A W G R A D C G I T S A S Y H Q G V L S

820
GCA ACC ATC CTC TAT GAG ATC CTA CTG GGG AAG GCC ACC CTA TAT GCT GTG CTG GTC AGT GGC
A T I L Y E I L L G K A T L Y A V L V S G

883 921
CTG GTG CTG ATG GCC ATG GTC AAG AAA AAA AAT TCC TGA
L V L M A M V K K K N S **STOP**

Figure 3.23 Amino acid sequence of the TCR β chain (TRBV 2 TRBJ 2-5 TRBC 1) from the murine T cell clone D3(3) cloned into retroviral vector MFG TRBV 2 is highlighted in green, TRBJ 2-5 in purple and TRBC 1 in turquoise. The CDR3 is highlighted in blue with the coding sequence underlined. The letter underlined in red indicates the base pair inserted by site-directed mutagenesis to convert the incorrect sequence to the original DNA sequence, allowing for correct read-through of the amino acid sequence and correct positioning of the stop codon.

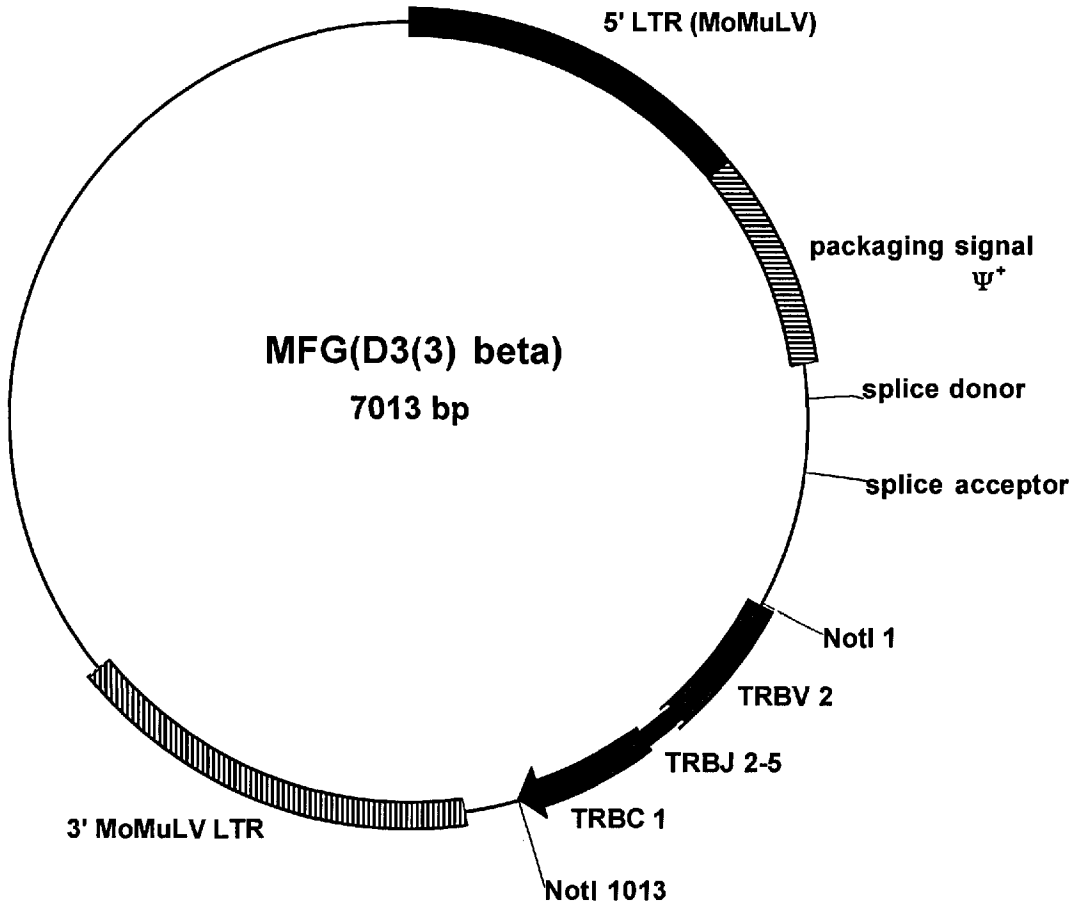


Figure 3.24 Final construct map of the TCR β chain from the murine Th2 T-cell clone D3(3) in the retroviral vector MFG The diagram shows the position of the genes required for correct function of the vector in a retroviral packaging gene transduction system and also the position of the inserted TCR gene and the restriction sites used in cloning the sequence into MFG.

3.2.1.2 Transfer of genes encoding dominant TCR α and β chains from the peptide 4-specific human T-cell line CIR010 into retroviral expression vector MFG

3.2.1.2.1 Transfer of the dominant TCRα chain from human T-cell line CIR010 into MFG

A strategy was designed to transfer the gene encoding the dominant TCRα chain from the line CIR010 into MFG, which is shown in Figure 3.25. Briefly, a PCR was carried out using high-fidelity DNA polymerase to amplify the full TCRα chain from cDNA obtained from the line at its 3rd re-stimulation with peptide 4. The primers used incorporated NotI sites into the PCR product at either end, allowing the TCR chain to be moved directly into MFG from the TA cloning vector into which the PCR product was originally ligated. The final construct was then sequenced. Gel images of the process are shown in Figure 3.26, and the final construct is shown as a vector diagram in Figure 3.27. The full sequence data for this TCR chain is shown in Appendix 18.

3.2.1.2.2 Combination of the dominant recombined TCRα V-J segment from the human T-cell line CIR010 with a murine TCRα C region and transfer into MFG

It was realised that in order to allow the expression of a human TCR in the murine line BW7, it would be necessary to combine the human V-J region with a mouse C region; it has been shown previously that there is a defect in signalling through the TCR in the periphery of human TCRβ transgenic mice when the full human VJC structure is used (612). Peripheral T-cell function in human TCR transgenic mice generated using the pTcass constructs (346), however, which contain an endogenous murine C region in the vector to which the inserted rearranged VJ region is spliced, is as expected (283). In order to achieve this, a new strategy was designed based on PCR, shown in Figure 3.28. Briefly, two PCRs were carried out, the first to amplify the human TCRα V-J region from cDNA isolated from the line CIR010 at its fourth re-stimulation with peptide 4. The second PCR was carried out on murine T-cell cDNA to amplify the mouse Cα region TRAC. The primers for these PCRs incorporated a base change from C→A in the sequences of both products, to introduce a PstI site into the sequence at the J region-C region junction without changing the underlying amino acid sequence of the

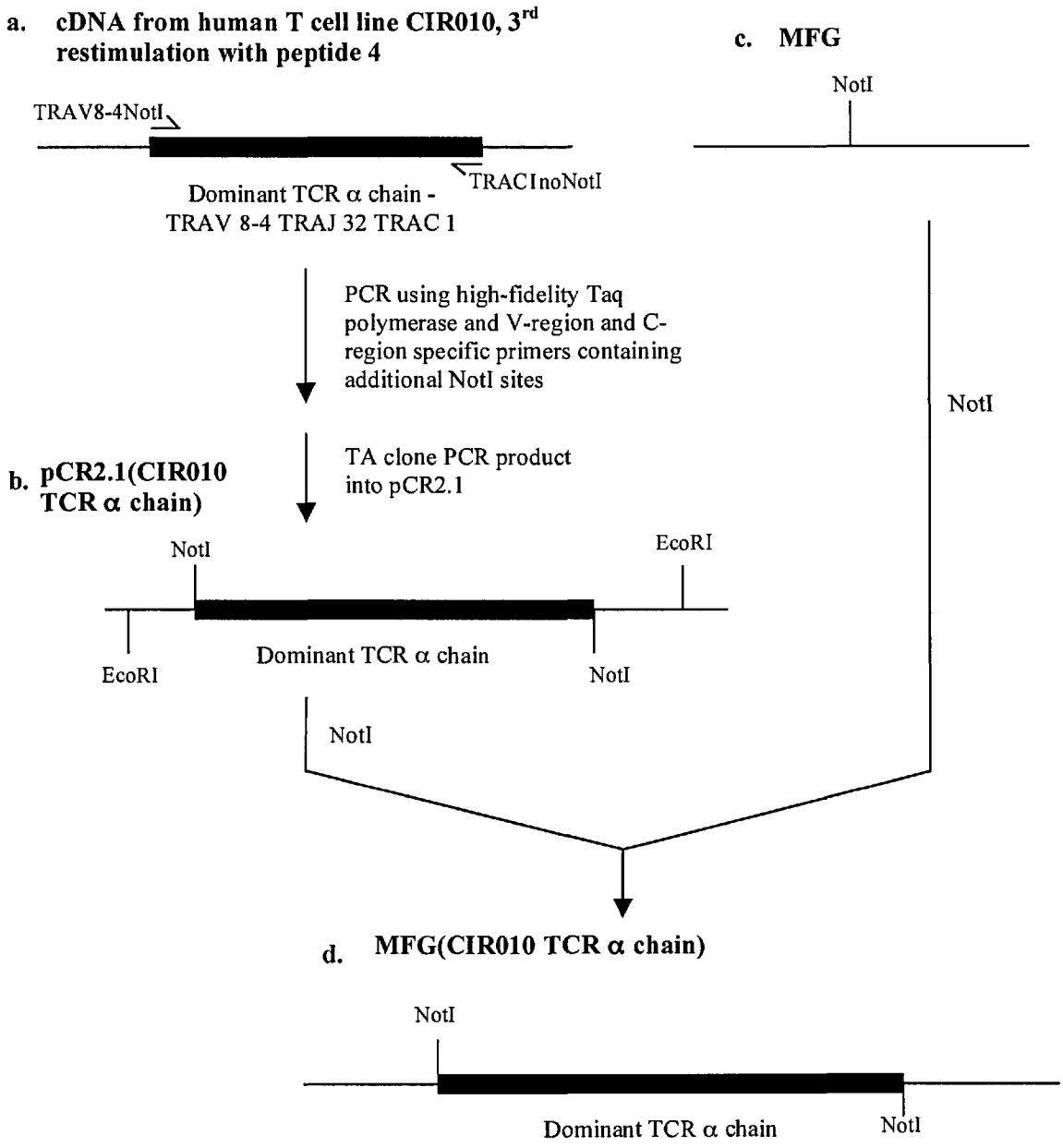


Figure 3.25 Cloning strategy designed to transfer the dominant TCRα chain from the human T cell line CIR010 into the retroviral vector MFG The α chain for the dominant TCR from line CIR010 was amplified from cDNA extracted from the line at its 3rd restimulation with peptide 4 of Fel d 1 (a) using PCR and the product was ligated into pCR2.1 (b). The insert was then sequenced to check that no mutations had been incorporated by the PCR before the TCRα chain was moved into MFG (previously modified to destroy its endogenous NcoI site as shown in Figure 3.7) (c) using NotI (d). Clones were checked for correct orientation of the insert by PCR, as described previously and shown in Figure 3.9. Correctly-oriented clones were sequenced. All PCR primers, reaction conditions, and sequencing primers are shown in Appendix 3. All restriction enzymes used and digest conditions are shown in Appendix 5.

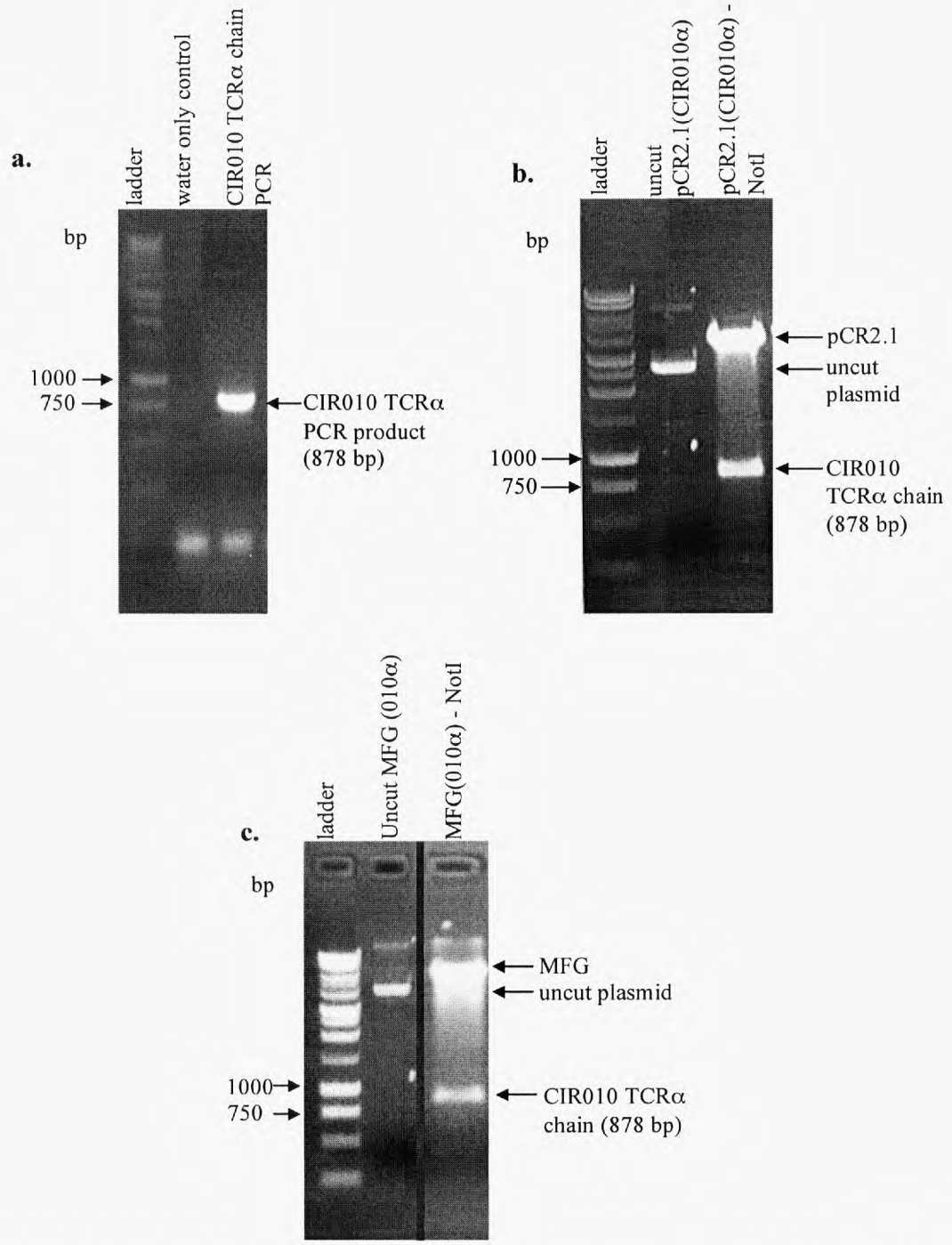


Figure 3.26 Gel images of the stages involved in moving the dominant TCR α chain of human T cell line CIR010 into the retroviral vector MFG The images above show the steps involved in the strategy as outlined in Figure 3.25. (a) shows the PCR product (of 878 bp) obtained from cDNA from the human T cell line CIR010 (a in Figure 3.25). The band was excised from the gel, purified and ligated into the TA cloning vector pCR2.1. (b) shows a NotI digest of the PCR product ligated into pCR2.1 (b in Figure 3.25). Uncut plasmid (1μl) was run as a comparison. Clones containing a correctly-sized insert were used to move the TCR chain into MFG. The final product, MFG(CIR010α TRAV 8-4 TRAJ 32 TRAC 1) (d in Figure 3.25) is shown in (c), as a NotI digest. Uncut plasmid (1μl) was run as a comparison. Clones with a correctly-sized insert were checked for correct orientation of the sequence by PCR (see figure 3.9), and correctly oriented clones were sequenced.

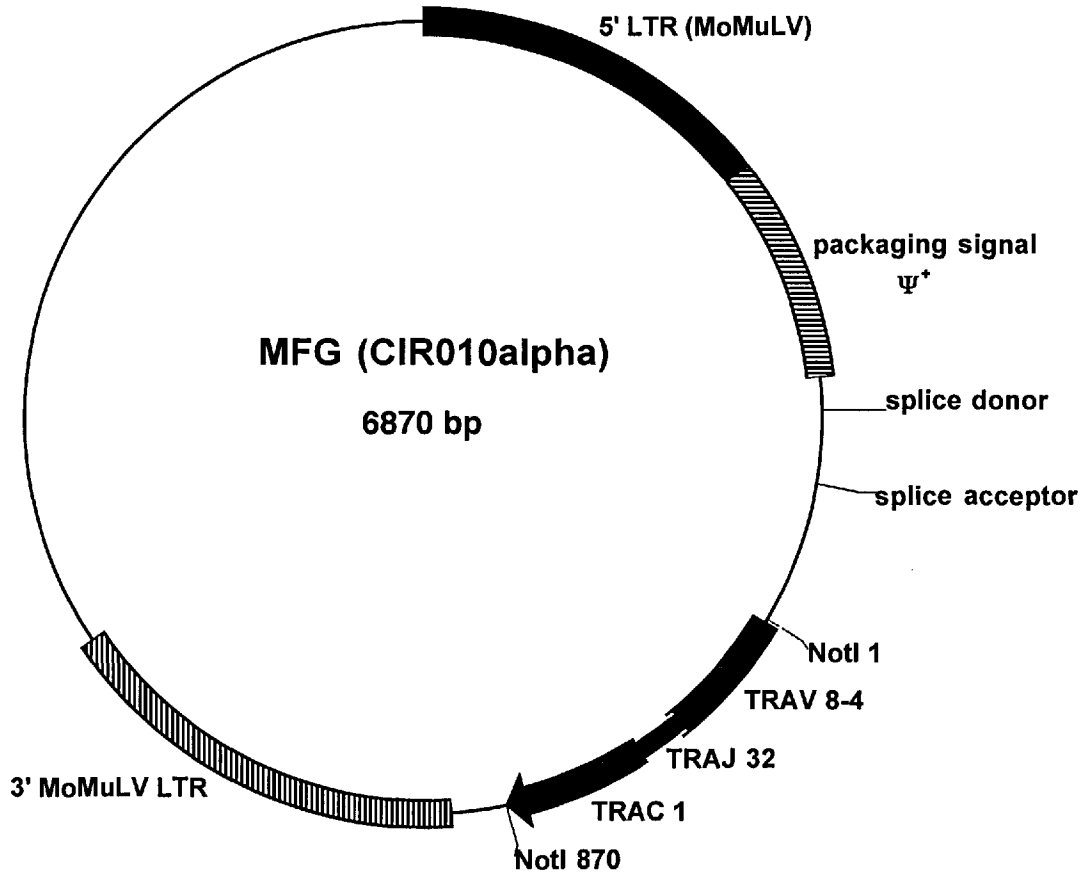


Figure 3.27 Final construct map of the dominant TCR α chain from the human T cell line CIR010 in the retroviral vector MFG The diagram shows the composition of the vector; the position of the genes required for its function in a retroviral packaging as well as the position of the inserted TCR gene and restriction sites used in cloning the sequence into MFG are shown.

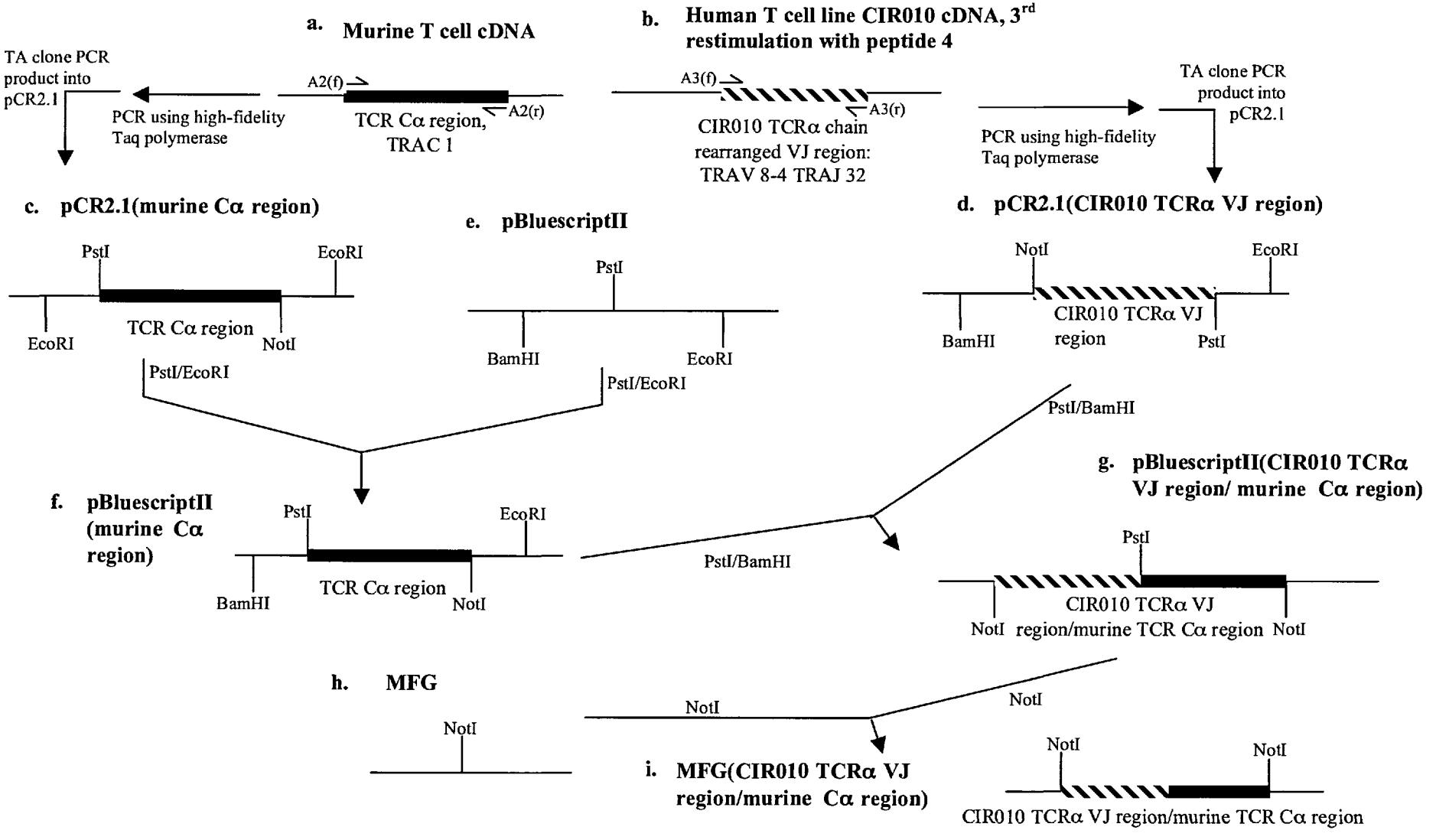

a. Murine T cell cDNA
TA clone PCR product into pCR2.1
PCR using high-fidelity Taq polymerase
A2(f)
A2(r)
TCR Cα region, TRAC 1
b. Human T cell line CIR010 cDNA, 3rd restimulation with peptide 4
A3(f)
A3(r)
CIR010 TCRα chain rearranged VJ region: TRAV 8-4 TRAJ 32
PCR using high-fidelity Taq polymerase
TA clone PCR product into pCR2.1
c. pCR2.1(murine Cα region)
PstI
EcoRI
EcoRI
TCR Cα region
NotI
PstI/EcoRI
e. pBluescriptII
PstI
BamHI
EcoRI
PstI/EcoRI
d. pCR2.1(CIR010 TCRα VJ region)
NotI
EcoRI
BamHI
CIR010 TCRα VJ region
PstI
PstI/BamHI
f. pBluescriptII (murine Cα region)
PstI
EcoRI
BamHI
TCR Cα region
NotI
PstI/BamHI
g. pBluescriptII(CIR010 TCRα VJ region/ murine Cα region)
PstI
CIR010 TCRα VJ
NotI region/murine TCR Cα region NotI
h. MFG
NotI
NotI
NotI
i. MFG(CIR010 TCRα VJ region/murine Cα region)
NotI
NotI
CIR010 TCRα VJ region/murine TCR Cα region

Figure 3.28 Cloning strategy designed to combine the VJ region from the dominant TCRα chain from the human T cell line CIR010 with a murine TCR Cα region in the retroviral vector MFG A murine TCR Cα region was amplified from murine T cell cDNA (a) using high-fidelity PCR. The forward primer incorporated a base change to the sequence to introduce a unique restriction site, PstI, into the nucleic acid sequence (without altering the amino acid sequence) to allow later combination with the human VJ sequence using this enzyme. The reverse primer incorporated a NotI site to allow ease of cloning into MFG at a later stage of the strategy. The PCR product was TA cloned into vector pCR2.1 using T4 ligase (c). The VJ regions of the α chain for the dominant TCR from line CIR010 was amplified from cDNA extracted from the line at its 3rd restimulation with peptide 4 of Fel d 1 (b) using high-fidelity PCR. The forward primer incorporated a NotI site to allow ease of cloning into MFG at a later step, and the reverse primer incorporated a base change into the TCR sequence to incorporate a PstI site, allowing direct overlap between the human variable region and murine constant region at this point without change to the overall amino acid sequence. The PCR product was TA cloned into vector pCR2.1 using T4 ligase (d). Clones containing an insert for both PCRs were then sequenced to check that no unintended mutations had been incorporated during the reaction. The murine C region from a correct clone was then moved into pBluescriptII (e) using PstI and EcoRI, and correct insertion was determined by restriction digest (f). The human VJα sequence from pCR2.1 was then inserted into a correct clone using PstI and BamHI, and correct insertion was checked by restriction digest (g). A correctly combined and oriented sequence was moved into MFG (previously modified to destroy its endogenous NcoI site) (h) using NotI, and checked for insertion by restriction digest (i). Clones were checked for correct orientation of the insert by PCR as described previously. Correctly-oriented clones were sequenced, after which the constructs were ready for use in the retroviral expression system. All PCR primers, reaction conditions and sequencing primers are shown in Appendix 3. All restriction enzymes used and digest conditions are shown in Appendix 5.

expressed protein. This allowed the combination of the two products in pBluescriptII to produce a gene consisting of the CIR010 dominant V-J region combined to a mouse Cα region in such a way as to produce a full-length TCRα chain gene, which could then be transferred into MFG. Gel images of this process are shown in Figure 3.29, with the final construct being shown as a vector diagram in Figure 3.30. The full-length sequence of the human V-J region-mouse C region TCRα chain, including the incorporated base change, is shown in Appendix 19.

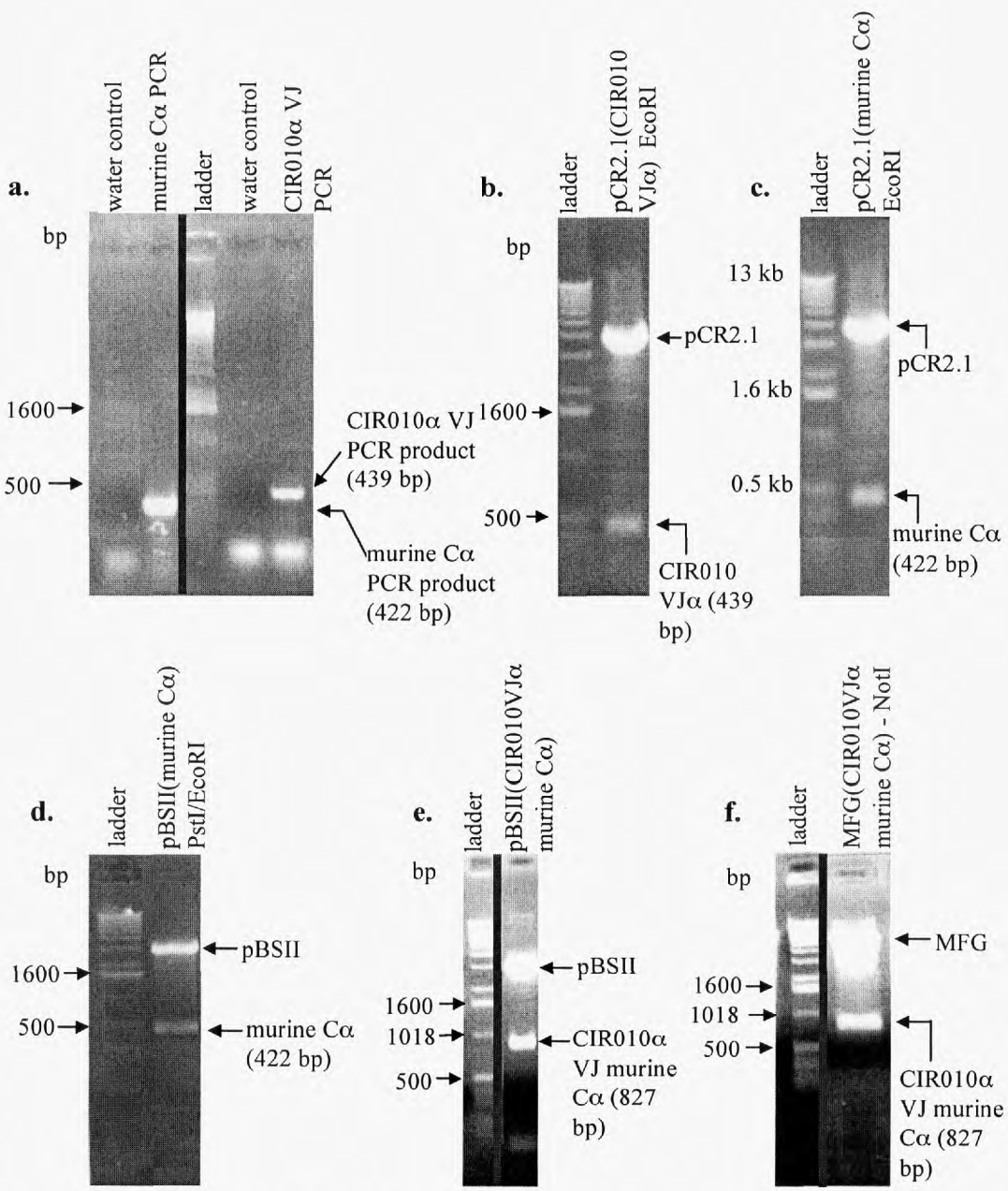


Figure 3.29 Gel images of the stages involved in moving the variable region (VJ) of the dominant TCRα chain of human T cell line CIR010 combined with a murine constant region (C) into MFG The images above show the steps involved in the strategy as outlined in Figure 3.28. (a) shows the PCR products for the murine Cα region (left-hand side of ladder, 422 bp) and the human VJα region (right hand side of ladder, 439 bp). The murine Cα region was obtained from mouse T cell cDNA, and the human VJα region was obtained from cDNA from the human T cell line CIR010 (a and b in Figure 3.28). EcoRI digests of the PCR products ligated into pCR2.1 are shown in (b) - pCR2.1(CIR010 VJα), d in Figure 3.29, and (c) - pCR2.1(murine Cα), c in Figure 3.29. (d) shows a PstI/EcoRI digest of pBluescriptII(murine Cα) (f in Figure 3.28) showing a correctly-sized insert corresponding to the murine Cα region. (e) shows a PstI/BamHI digest of pBluescriptII (CIR010 VJα murine Cα) (g in Figure 3.28), with an insert corresponding to the correctly combined TCR chain. The final product, MFG(CIR010α TRAV 8-4 TRAJ 32 TRAC 1) (i in Figure 3.28) is shown in (f), as a NotI digest. Clones with a correctly-sized insert were checked for correct orientation of the sequence by PCR (see figure 3.9). Correctly oriented clones were sequenced.

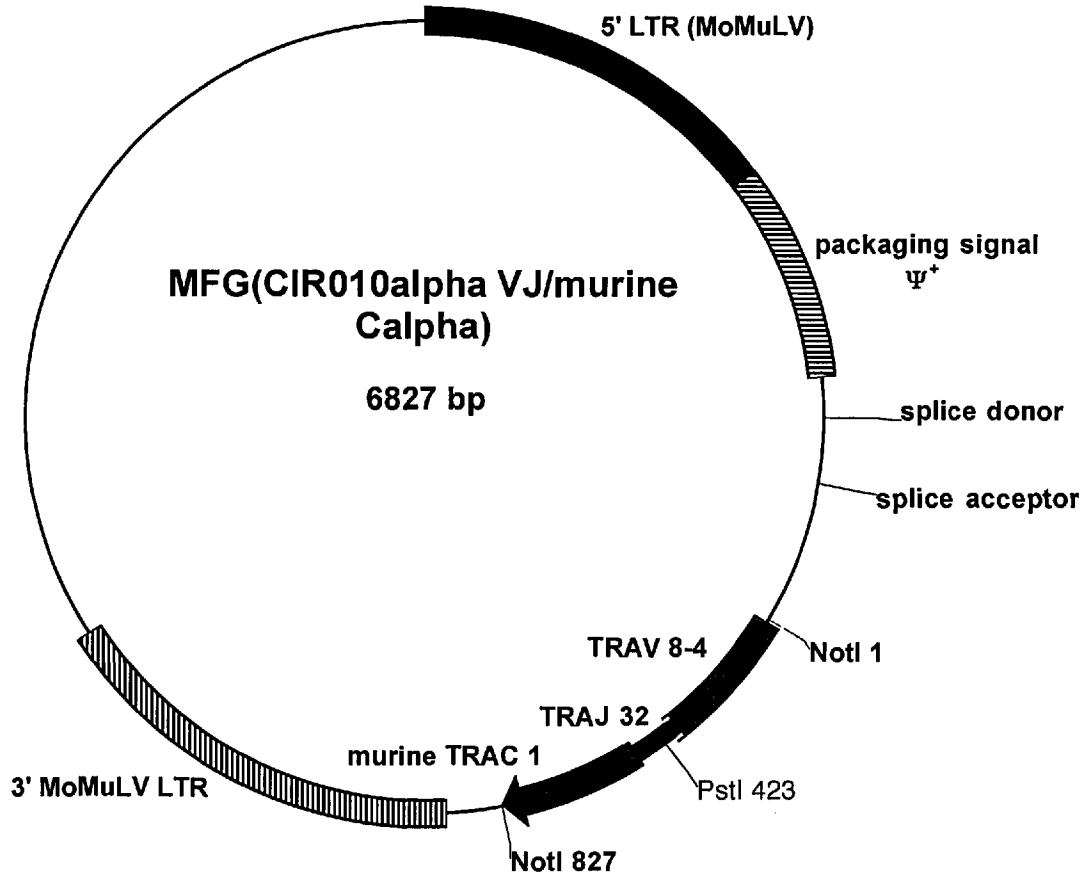


Figure 3.30 Final construct map of the dominant TCR α chain (combined with a murine Cα region) from the human T cell line CIR010 in the retroviral vector MFG The diagram shows the composition of the vector in terms of the genes required for its function in a retroviral packaging gene transduction system as well as the position of the inserted TCR gene, and restriction sites used in the cloning of the sequence into MFG.

3.2.1.2.3 Combination of the dominant recombined TCRβ V-J segment from the human T-cell line CIR010 with a murine TCRβ C region and transfer into MFG

A similar strategy was designed to allow the combination of the dominant TCRβ V-J region from the human T-cell line CIR010 with a murine Cβ region. The strategy is shown in Figure 3.31. Briefly, two PCRs were carried out, the first to amplify the human TCRβ V-J region from cDNA isolated from the line CIR010 at its fourth re-stimulation with peptide 4. The second PCR was carried out on murine T-cell cDNA to amplify the mouse Cβ region TRBC 1. In addition, a short linker corresponding to the J region-C region junction was inserted into pBluescriptII to allow correct joining of the V-J region to the C region. The linker was required as there was no part of the sequence that could be easily mutated in both products to form a restriction site to allow combination of the two PCR products. Instead, an endogenous HindIII site in the human V-J region was used to combine it to the linker in pBluescriptII. The forward primer for the murine Cβ region incorporated a base change from T→C, to introduce a PpuMI site into the sequence at the 5'-end of the C region without changing the amino acid sequence of the expressed protein. This allowed the combination of the C region with the linker (designed to include this base change from the underlying sequence) in pBluescriptII. The two PCR products were thus combined through the linker to produce a full length TCRβ gene consisting of the CIR010 dominant V-Jβ region combined to a murine Cβ region, which was then transferred into MFG. Gel images of this process are shown in Figure 3.32. The final construct is shown as a vector diagram in Figure 3.33, and the full-length sequence of the human V-J region-mouse C region TCRβ chain, including the base change incorporated into the sequence, is shown in Appendix 20.

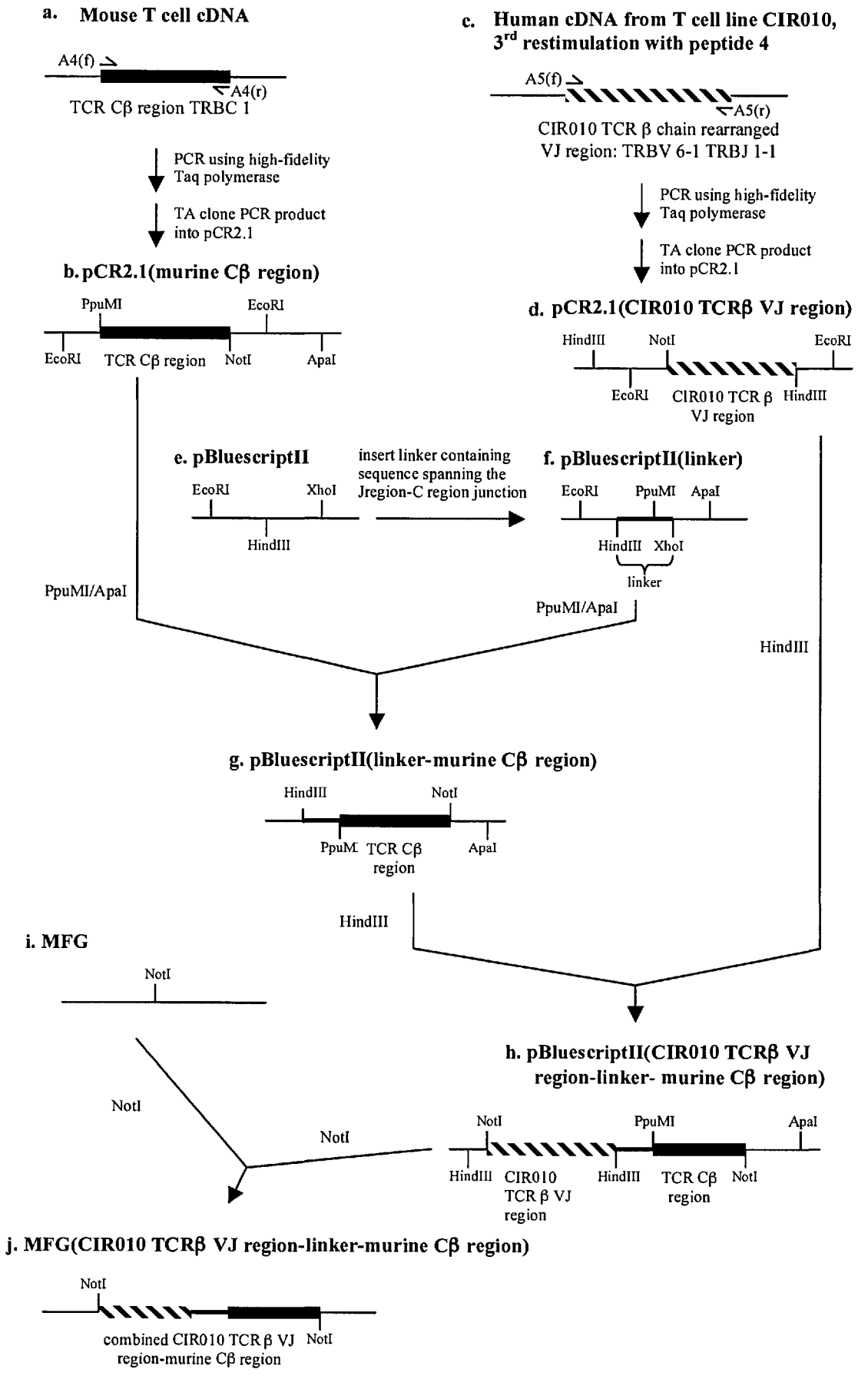

a. Mouse T cell cDNA
A4(f)
A4(r)
TCR Cβ region TRBC 1
PCR using high-fidelity Taq polymerase
TA clone PCR product into pCR2.1
b. pCR2.1(murine Cβ region)
PpuMI
EcoRI
EcoRI
TCR Cβ region
NotI
ApaI
c. Human cDNA from T cell line CIR010, 3rd restimulation with peptide 4
A5(f)
A5(r)
CIR010 TCR β chain rearranged VJ region: TRBV 6-1 TRBJ 1-1
PCR using high-fidelity Taq polymerase
TA clone PCR product into pCR2.1
d. pCR2.1(CIR010 TCRβ VJ region)
HindIII
NotI
EcoRI
EcoRI
CIR010 TCR β VJ region
HindIII
e. pBluescriptII
EcoRI
XhoI
HindIII
insert linker containing sequence spanning the Jregion-C region junction
f. pBluescriptII(linker)
EcoRI
PpuMI
ApaI
HindIII
XhoI
linker
PpuMI/ApaI
PpuMI/ApaI
HindIII
g. pBluescriptII(linker-murine Cβ region)
HindIII
NotI
PpuM
TCR Cβ region
ApaI
HindIII
i. MFG
NotI
NotI
NotI
h. pBluescriptII(CIR010 TCRβ VJ region-linker- murine Cβ region)
NotI
PpuMI
ApaI
HindIII
CIR010 TCR β VJ region
HindIII
TCR Cβ region
NotI
j. MFG(CIR010 TCRβ VJ region-linker-murine Cβ region)
NotI
combined CIR010 TCR β VJ region-murine Cβ region
NotI

Figure 3.31 Cloning strategy designed to combine the VJ region from the dominant TCRβ chain from the human T cell line CIR010 with a murine TCR Cβ region in the retroviral vector MFG High-fidelity PCR was used to amplify a murine TCR Cβ region from murine T cell cDNA (a). The forward primer incorporated a base change to introduce a unique restriction site, PpuMI, into the nucleic acid sequence (without altering the underlying amino acid sequence) to allow later combination with the human VJ sequence using this enzyme. The reverse primer incorporated a NotI site to allow easier cloning into MFG at a later stage of the strategy. The PCR product was then TA cloned into vector pCR2.1 using T4 ligase (b). The VJ regions of the β chain for the dominant TCR from line CIR010 was amplified from cDNA extracted from the line at its 3rd restimulation with peptide 4 of Fel d 1 (c) using high-fidelity PCR. The forward primer incorporated a NotI site to allow easier cloning into MFG at a later step, and the reverse primer included an endogenous HindIII site in the TCR sequence, allowing combination with the mouse C region. The resulting PCR product was TA cloned into vector pCR2.1 using T4 ligase (d). Inserts from both PCRs were sequenced to check that no unintended mutations had been incorporated. Simultaneously, a linker was inserted into the subcloning vector pBluescriptII (e) corresponding to the sequence at the junction between the J and C regions to allow the joining of the murine C region with the human VJ region. The linker contained a base change from the original C region sequence to incorporate a PpuMI site and contained the HindIII site from the human VJ region, as well as a XhoI site to allow insertion into pBluescriptII using XhoI and HindIII (f). Correct insertion was determined by restriction digest. The murine C region was then moved into pBluescriptII(linker) using PpuMI and ApaI, and correct insertion was determined by restriction digest (g). The human VJβ sequence was inserted into pBluescriptII(linker-murine Cβ) using HindIII (h), and checked for correct insertion and orientation by restriction digest. A correctly combined sequence was moved into modified MFG (its endogenous NcoI site destroyed) (i) using NotI, and checked by restriction digest (j). Inserts were checked for correct orientation by PCR as described previously. Correctly-oriented clones were sequenced, after which the constructs were ready for use in the retroviral expression system. All PCR primers, reaction conditions, oligonucleotide linkers and sequencing primers are shown in Appendix 3. All restriction enzymes used and digest conditions are shown in Appendix 5.

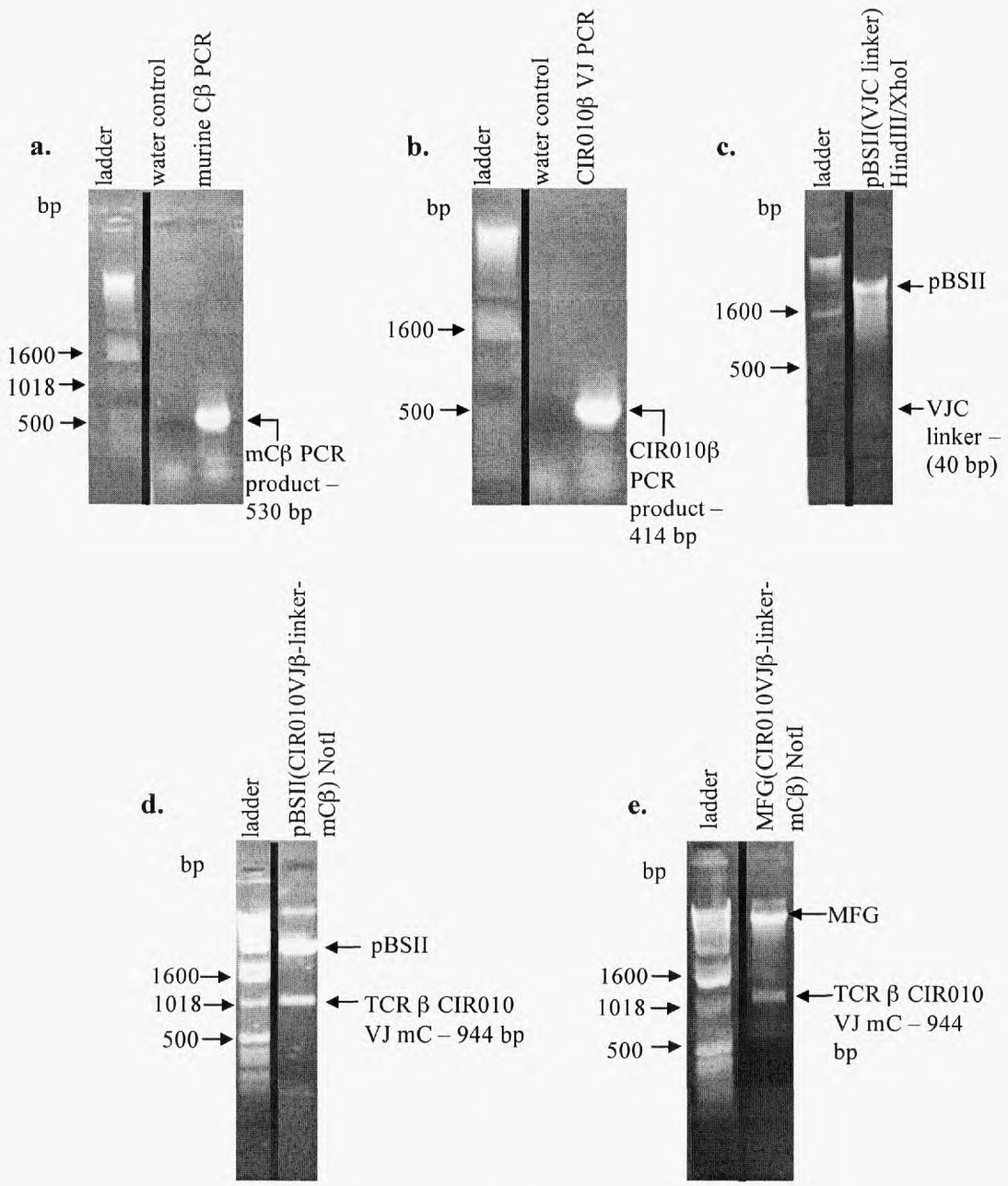


Figure 3.32 Gel images of the stages involved in moving the variable region (VJ) of the dominant TCR β chain of the human T cell line CIR010 combined with a murine constant region (C) into MFG The images above show the steps involved in the strategy as outlined in Figure 3.31. (a) shows the PCR product for the murine Cβ region, (b) shows the PCR product for the human VJβ region and (c) shows a HindIII/XhoI digest of a 40 bp VJC-linking oligonucleotide inserted into pBluescriptII (f in Figure 3.31). The murine Cβ region was obtained from mouse T cell cDNA, and the human VJβ region was obtained from cDNA from the human T cell line CIR010 (a and b in Figure 3.31). PCR products were ligated into pCR2.1, and then combined in pBluescriptII(VJC-linker) via two restriction digests to form pBluescript (CIR010VJβ-linker-mCβ), shown as a NotI digest in (d) above and corresponding to h in Figure 3.31. This insert was transferred into MFG using NotI, as shown in (e) above, corresponding to j in Figure 3.31. Orientation of the insert was determined by PCR, as shown in Figure 3.9, and clones with the TCR chain correctly oriented in MFG were sequenced.

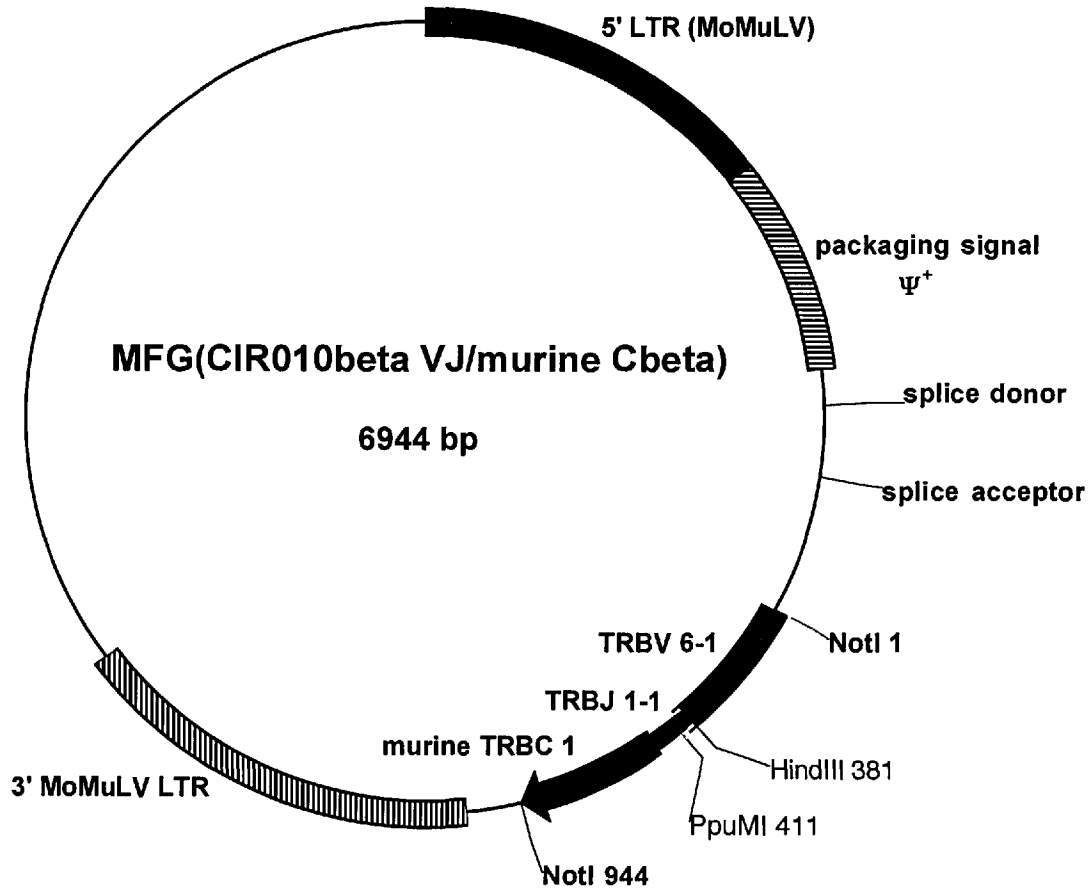


Figure 3.33 Final construct map of the dominant TCR β chain (combined with a murine Cβ region) from the human T cell line CIR010 in the retroviral vector MFG The diagram shows the position of the genes required for its function in a retroviral packaging gene transduction system and of the inserted TCR gene, along with the restriction sites used in the cloning of the sequence into MFG.

3.2.2 Preparation of TCR expression constructs for use in the Amaxa transduction system

3.2.2.1 Overview of the Amaxa Nucleofector system and TCR expression vectors

The Amaxa Nucleofector system (www.amaxa.com) is a proprietary technology: a non-viral method of transducing cell lines with a target gene that is based on electroporation. An expression vector containing a gene of interest is transfected into a target cell line using one of the many programmes provided by the Nucleofector device. Any type of expression vector can be used in this system. It can be used as a means of transfecting retroviral packaging lines with a retroviral vector, but can also be used as a means of transducing a target cell line directly, if the correct expression vector is used.

As the Amaxa system involves transduction of the target line directly, it was necessary to transfer the TCR genes from the murine PLP_{56-70}-specific T-cell clones A10(2) and D3(3) and the dominant TCR genes from the peptide 4-specific human T-cell line CIR010 into vectors designed specifically to allow the expression of TCRs in a T-cell-restricted manner. The TCR expression cassette vectors, pTαcass and pTβcass, designed by Mathis and Benoist (346) for use in the production of TCR-transgenic mice, have been previously used to express the Ob1A12 TCR in T-cell hybridomas based on the BW7 line (602) using electroporation. As such, it was decided to transfer the TCRs of interest into the pTαcass and pTβcass vectors for use in the Amaxa system to transduce the BW7 line with these TCR genes.

The pTαcass and pTβcass vectors have been specifically designed and constructed to direct the expression of TCR exclusively in cells of the T-cell lineage. They are large vectors (approximately 20 kb in size) as they contain extensive segments of the TCRα and β promoter regions as well as the intronic sequence between the rearranged V-J region and the C region, in order to ensure that all necessary promoter and enhancer elements required for successful TCR expression in cells of the T-cell lineage are included. The murine C region is included within the vector, hence only the rearranged V-J region of the TCR is inserted into the vector to make the final construct. The V-J region can be obtained from T-cell genomic DNA or cDNA; however, if the sequence is obtained from cDNA, it is necessary to include approximately 50 bp of intronic sequence immediately downstream of the J region to allow for correct splicing of the

gene. Rearranged TCRα chains are inserted into the pTαcass vector at a specific point using XmaI and SacII; in the pTβcass vector, rearranged TCRβ chains are inserted using XhoI and SacII.

The rearranged V-J segments for the two murine PLP_{56-70}-specific TCRs were obtained from the relevant MFG constructs and the intronic sequence was obtained from murine genomic DNA. The rearranged V-J segments for the peptide 4-specific human TCR from line CIR010 were obtained from the same cDNA as that used for the TCR CDR3 analysis. The required intronic sequence was obtained from the IMGT database and synthesised as an oligonucleotide linker.

3.2.2.2 Transfer of genes encoding TCR α and β chains from the PLP_{56-70}-specific murine T-cell clone A10(2) into the pTcass TCR expression vectors

3.2.2.2.1 Transfer of TCRα chain 5-D4 from the T-cell clone A10(2) into the vector pTαcass

A strategy to allow the rearranged TCRα 5-D4 V-J segment (TRAV 5-D4 TRAJ 13) from the murine T-cell clone A10(2) to be transferred into the TCR expression vector pTαcass is shown in Figure 3.34. As the source of the rearranged V-J segment was the complete TCRα chain from the MFG construct, MFG(TCR A10(2)α 5-D4), it was necessary to combine this with intronic sequence immediately downstream of the J region. To achieve this, PCR primers were designed to make use of an endogenous BstXI site in the J region to join the two products. The first product was the rearranged V-J segment as far as the BstXI site, amplified from the MFG construct, and the second product was the J region-intron segment, comprising the J region from its BstXI site to a point approximately 55 base pairs into the downstream intron. The products were combined in the subcloning vector pUC19 (shown in Appendix 21) before being transferred into pTαcass using XmaI and SacII. Gel images of the process are shown in Figure 3.35, and the final construct is shown in Figure 3.36. The full sequence of the insert in pTαcass is shown in Appendix 22.

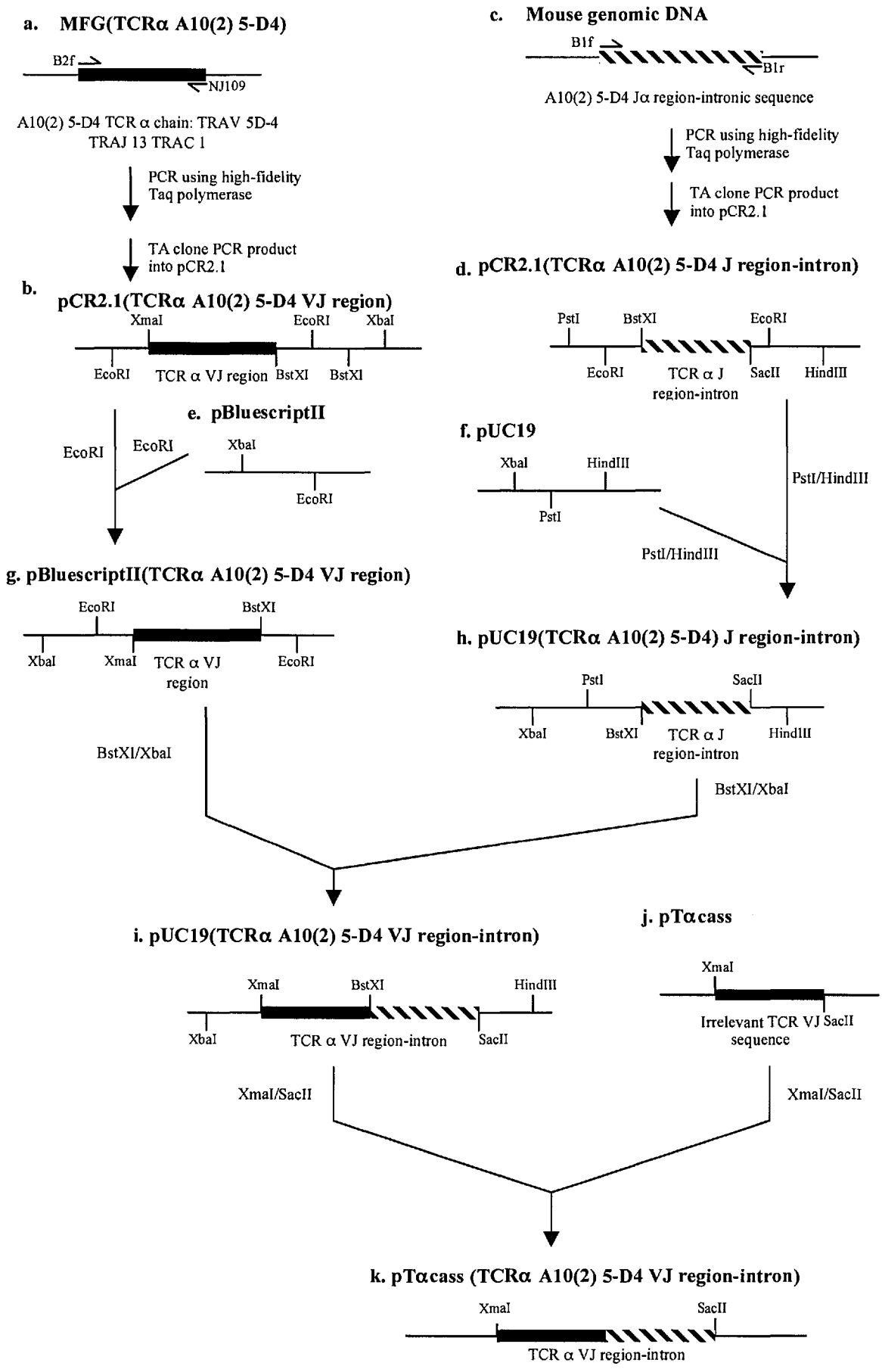

a. MFG(TCRα A10(2) 5-D4)
B2f
NJ109
A10(2) 5-D4 TCR α chain: TRAV 5D-4
TRAJ 13 TRAC 1
PCR using high-fidelity
Taq polymerase
TA clone PCR product
into pCR2.1
b.
pCR2.1(TCRα A10(2) 5-D4 VJ region)
XmaI
EcoRI
XbaI
EcoRI
TCR α VJ region
BstXI
BstXI
c. Mouse genomic DNA
B1f
B1r
A10(2) 5-D4 Jα region-intronic sequence
PCR using high-fidelity
Taq polymerase
TA clone PCR product
into pCR2.1
d. pCR2.1(TCRα A10(2) 5-D4 J region-intron)
PstI
BstXI
EcoRI
EcoRI
TCR α J
region-intron
SacII
HindIII
e. pBluescriptII
EcoRI
EcoRI
XbaI
EcoRI
f. pUC19
XbaI
HindIII
PstI
PstI/HindIII
PstI/HindIII
g. pBluescriptII(TCRα A10(2) 5-D4 VJ region)
EcoRI
BstXI
XbaI
XmaI
TCR α VJ
region
EcoRI
BstXI/XbaI
h. pUC19(TCRα A10(2) 5-D4) J region-intron)
PstI
SacII
XbaI
BstXI
TCR α J
region-intron
HindIII
BstXI/XbaI
i. pUC19(TCRα A10(2) 5-D4 VJ region-intron)
XmaI
BstXI
HindIII
XbaI
TCR α VJ region-intron
SacII
XmaI/SacII
j. pTαcass
XmaI
Irrelevant TCR VJ SacII
sequence
XmaI/SacII
k. pTαcass (TCRα A10(2) 5-D4 VJ region-intron)
XmaI
SacII
TCR α VJ region-intron

Figure 3.34 Cloning strategy designed to move the TCRα chain (VJ region plus intronic sequence) from the mouse Th1-type T cell clone A10(2) 5-D4 into the TCR expression vector pTαcass As pTαcass contains as part of its structure a murine TCR Cα region, only the VJ region of the A10(2) 5-D4 TCR α chain was moved into the vector. This was combined with a short length of intronic sequence downstream of the J region to allow for correct splicing of the sequence to the endogenous C region, as the VJ region was amplified from a fully rearranged sequence and not from genomic DNA. The VJ region was amplified from MFG(TCR α A10(2) 5-D4) which contained the full version of the TCR chain gene (a) using high-fidelity PCR. The forward primer incorporated an XmaI site at its 3' end to allow for eventual cloning of the TCR sequence into pTαcass. The reverse primer incorporated an endogenous BstXI site in the J region to allow the VJ region and the J-intron region to be combined in a later cloning step. The PCR product was inserted into pCR2.1 (b). The J region-intron was amplified from mouse genomic DNA (c), the forward primer incorporating the BstXI site from the J region and the reverse primer incorporating a SacII site at its 5' end to allow for cloning of the combined product into pTαcass. The PCR product was inserted into pCR2.1 (d). Clones containing an insert of the correct size upon EcoRI digestion were sequenced to check that no unintended mutations had been incorporated during the reactions. As the vector pCR2.1 contains two BstXI sites in its MCS, this prevented the use of BstXI as a means of combining the two segments directly from this plasmid, and so it was necessary to move the VJ region into pBluescriptII (e) using EcoRI. Correct insertion and orientation of the sequence was determined by restriction digest (g). Simultaneously, the J region-intron segment was moved into the subcloning vector, pUC19 (f), using PstI and HindIII, and correct insertion was determined by restriction digest (h). The VJ region from pBluescriptII was then moved into pUC19 containing the J region-intron segment using BstXI and XbaI, and correct combination was determined by restriction digest (i). The combined sequence was moved into pTαcass (supplied already containing an irrelevant TCR α chain as a circular plasmid) (j) using XmaI and SacII, and correct insertion was determined by restriction digest (k). Correct clones were sequenced, after which the constructs were ready for use in the Amaxa transfection system. All PCR primers, reaction conditions and sequencing primers are shown in Appendix 4. All restriction enzymes used and digest conditions are shown in Appendix 5.

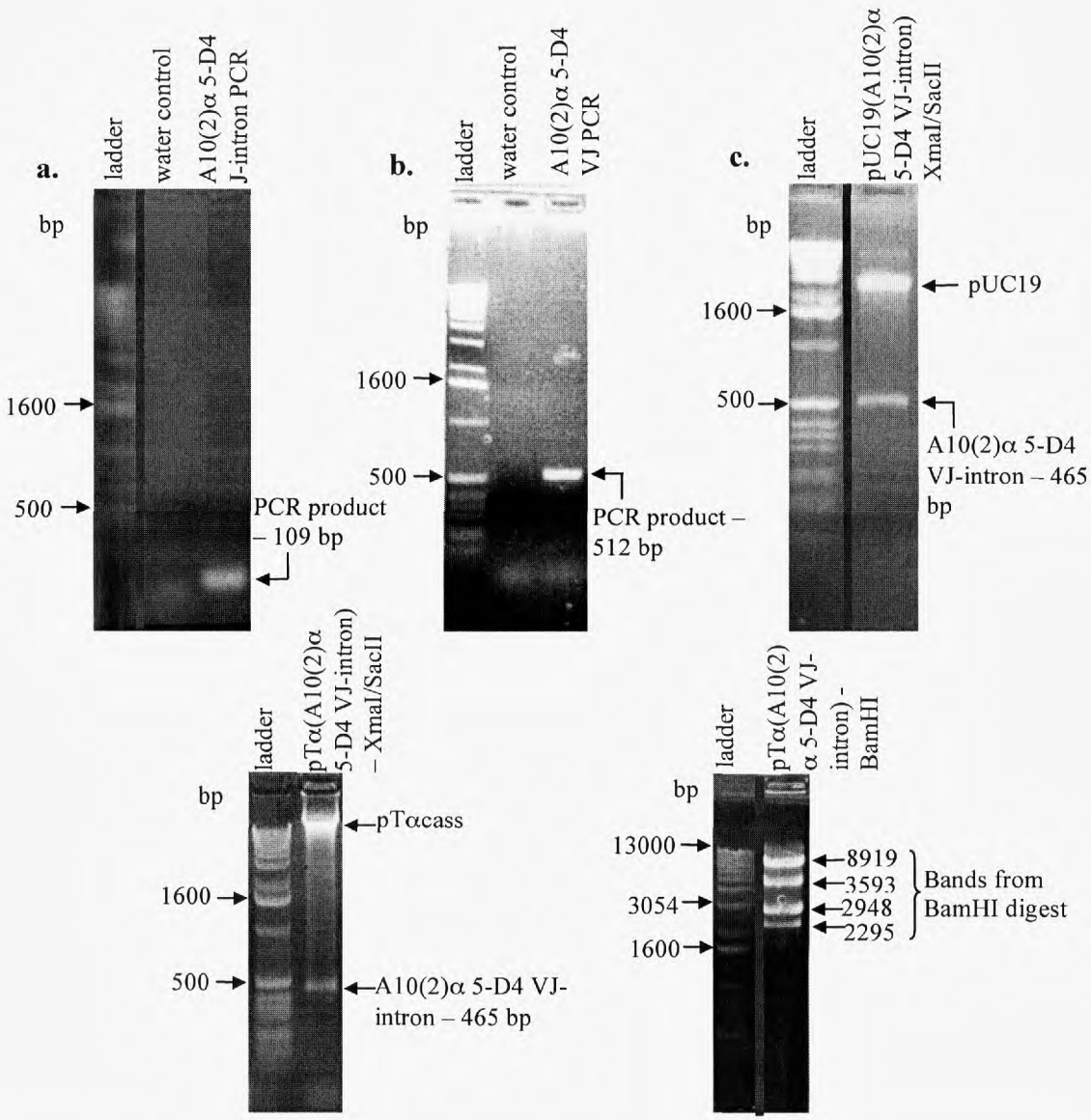


Figure 3.35 Gel images of the stages involved in moving the rearranged VJ region from the TCR α chain from murine T cell clone A10(2) 5-D4 combined with intronic sequence immediately downstream of the J region terminus into the TCR expression vector pTαcass The images above show the steps involved in the strategy as outlined in Figure 3.34. (a) and (b) show the PCR products corresponding to the J region-intron of the TCRα chain (a) obtained from murine NOD.E T cell genomic DNA (c in Figure 3.34) and the rearranged VJ region (b) obtained from MFG(A10(2) 5-D4) (a in Figure 3.34). PCR products were ligated into pCR2.1 and sequenced to check that no unintended mutations had occurred. (c) shows a SacII/XmaI digest of the combined VJ-intron sequence inserted into pUC19 (h in Figure 3.34). The correctly combined TCRα VJ-intron segment was moved into pTαcass. The final product of the strategy, pTαcass(A10(2)α TRAV 5D-4 TRAJ 13 intron) (k in Figure 3.34) is shown in (d) as a SacII/XmaI digest to show correct insertion of the insert and (e) as a BamHI digest, to check that the integrity of the plasmid remained intact. Band sizes shown are those expected for the plasmid; there is an extra band compared to other pTαcass constructs as there is a BamHI site in the inserted sequence. Clones with a correctly-sized insert were sequenced.

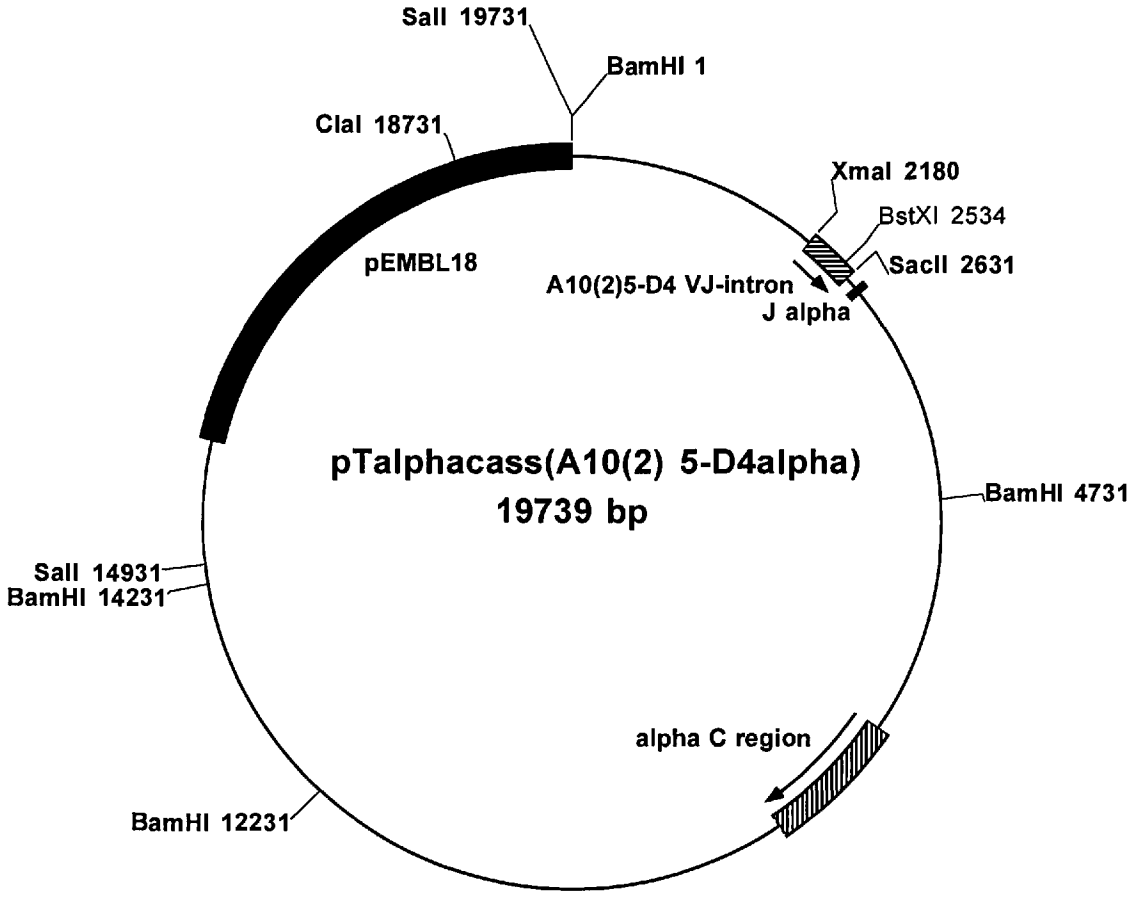


Figure 3.36 Final construct map showing the insertion of the TCRα chain 5-D4 from the Th1 murine T-cell clone A10(2) into the TCR expression vector pTαcass Only the rearranged VJ region (TRAV 5-D4 TRAJ 13) from the sequence was inserted as the vector contains a murine Cα region already, designed to be spliced to the VJ region during mRNA processing to produce a full-length TCR chain gene. As the VJ region was amplified from cDNA, it was necessary to include the beginning of the intronic sequence immediately downstream of the J region, to allow correct splicing to occur. Restriction sites that were used to create the VJ-intron sequence and to clone the sequence into pTαcass are shown, along with the position of the bacterial sequence required for the propagation of the construct in bacterial culture.

3.2.2.2.2 Transfer of TCRα chain 7-D3 from the T-cell clone A10(2) into the vector pTαcass

Figure 3.37 shows the strategy used to transfer the rearranged TCRα 7-D3 V-J segment (TRAV 7-D3 TRAJ 15) from the murine T-cell clone A10(2) into the TCR expression vector pTαcass. As for the 5-D4 TCRα chain, the rearranged V-J segment, amplified from the complete TCRα chain in the MFG construct, MFG(TCR A10(2)α 7-D3), was combined with intronic sequence immediately downstream of the J region. An endogenous SacI site in the J region was used to join the two sequences, and PCR primers were designed to allow this. The first PCR product was the rearranged V-J segment as far as the SacI site, amplified from the MFG construct. The second product was the J region-intron segment, consisting of the J region from its SacI site to a point approximately 50 base pairs into the downstream intron. The products were combined in pBluescriptII before being transferred into pTαcass using XmaI and SacII. Gel images of the steps of the strategy are shown in Figure 3.38, with a vector diagram of the final construct being shown in Figure 3.39. The full sequence of the insert in pTαcass is shown in Appendix 23.

3.2.2.2.3 Transfer of the TCRβ chain from the T-cell clone A10(2) into the vector pTβcass

A similar strategy was used to transfer the rearranged TCRβ V-J segment (TRBV 14 TRAJ 2-7) from the murine T-cell clone A10(2) into the TCR expression vector pTβcass, which is shown in Figure 3.40. Primers were designed to incorporate an XmaI site into the J region by changing one base pair from C→G without changing the underlying amino acid sequence, which could then be used to join the two segments of the sequence. The first PCR product was the rearranged V-J segment as far as the introduced XmaI site, which was amplified from the MFG construct. The second product was the J region-intron segment, starting in the J region at the introduced XmaI site and extending to a point 56 base pairs into the downstream intron. The products were combined in pBluescriptII before transfer into pTβcass using XhoI and SacII. Figure 3.41 shows gel images of the steps involved, and the final construct is shown in Figure 3.42. The full sequence of the insert in pTβcass including the base pair change to incorporate the XmaI site is shown in Appendix 24.

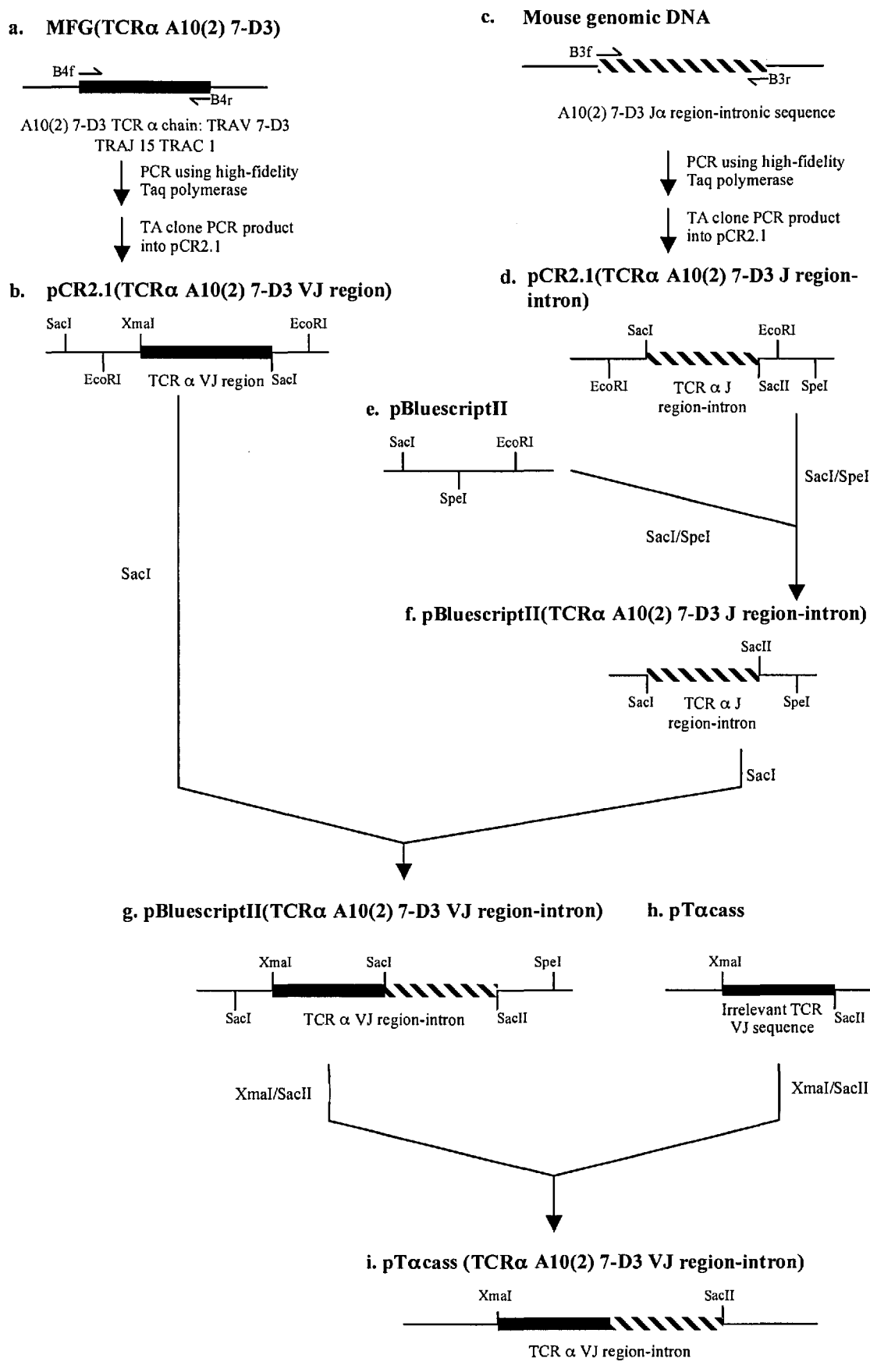

a. MFG(TCRα A10(2) 7-D3)
B4f
B4r
A10(2) 7-D3 TCR α chain: TRAV 7-D3
TRAJ 15 TRAC 1
PCR using high-fidelity
Taq polymerase
TA clone PCR product
into pCR2.1
b. pCR2.1(TCRα A10(2) 7-D3 VJ region)
SacI
XmaI
EcoRI
EcoRI
TCR α VJ region
SacI
c. Mouse genomic DNA
B3f
B3r
A10(2) 7-D3 Jα region-intronic sequence
PCR using high-fidelity
Taq polymerase
TA clone PCR product
into pCR2.1
d. pCR2.1(TCRα A10(2) 7-D3 J region-intron)
SacI
EcoRI
EcoRI
TCR α J
region-intron
SacII
SpeI
e. pBluescriptII
SacI
EcoRI
SpeI
SacI/SpeI
SacI/SpeI
SacI
f. pBluescriptII(TCRα A10(2) 7-D3 J region-intron)
SacII
SacI
TCR α J
region-intron
SpeI
SacI
g. pBluescriptII(TCRα A10(2) 7-D3 VJ region-intron)
h. pTαcass
XmaI
SacI
SpeI
SacI
TCR α VJ region-intron
SacII
XmaI
Irrelevant TCR
VJ sequence
SacII
XmaI/SacII
XmaI/SacII
i. pTαcass (TCRα A10(2) 7-D3 VJ region-intron)
XmaI
SacII
TCR α VJ region-intron

Figure 3.37 Cloning strategy designed to move the TCRα chain (VJ region plus intronic sequence) from the mouse Th1-type T cell clone A10(2) 7-D3 into the TCR expression vector pTαcass pTαcass contains a murine TCR Cα region within its structure, and thus only the VJ region of the A10(2) 7-D3 TCR α chain was moved into the vector, combined with a short stretch of intronic sequence immediately downstream of the J region to allow correct splicing of the VJ sequence to the endogenous C region, as the VJ region was amplified from a fully rearranged TCR sequence and not from genomic DNA. High-fidelity PCR was used to amplify the VJ region from MFG(TCR α A10(2) 7-D3) containing the full version of the TCR chain gene (a). The forward primer incorporated an XmaI site at its 3' end to allow for cloning of the TCR sequence into pTαcass. The reverse primer incorporated an endogenous SacI site in the J region to allow the VJ region to be combined with the J-intron region in a later cloning step. This PCR product was ligated into pCR2.1 (b). The J region-intron was amplified from mouse genomic DNA (c), with the forward primer incorporating the SacI site from the J region and the reverse primer including a SacII site at its 5' end to allow cloning of the combined product into pTαcass. The PCR product was ligated into pCR2.1 (d). Clones containing an insert of the correct size upon EcoRI digestion were sequenced to check that no unintended mutations had been incorporated. The J region-intron segment was moved into pBluescriptII (e) using SacI and SpeI. Correct insertion was determined by restriction digest (f). The VJ region segment was moved into this construct using SacI and correct insertion and orientation was determined by restriction digest (g). A correctly combined sequence was moved into pTαcass (supplied already containing an irrelevant TCR α chain as a circular plasmid) (h) using XmaI and SacII, and its correct insertion was determined by restriction digest (i). Correct clones were sequenced, after which the constructs were ready for use in the Amaxa transfection system. All PCR primers, reaction conditions, and sequencing primers are shown in Appendix 4. All restriction enzymes used and digest conditions are shown in Appendix 5.

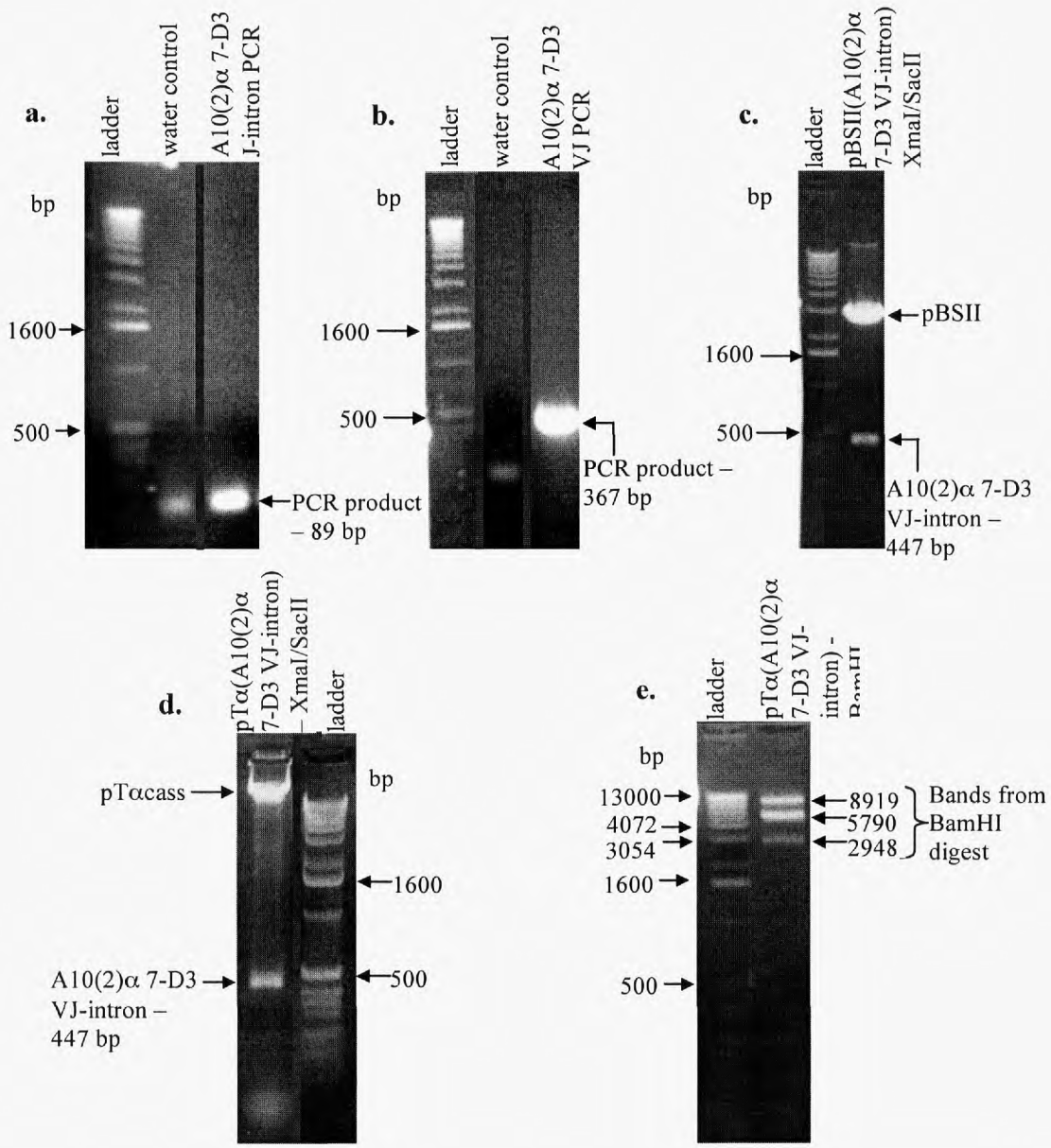


Figure 3.38 Gel images of the stages involved in moving the rearranged VJ region from the TCR α chain of murine T cell clone A10(2) 7-D3 combined with intronic sequence immediately downstream of the J region terminus into the TCR expression vector pTαcass The images show the steps involved in the strategy outlined in Figure 3.37. The PCR product in (a) is the J region-intron of the TCRα chain obtained from murine NOD.E T-cell genomic DNA (c in Figure 3.37) and the product in (b) is the rearranged V-J region obtained from MFG(A10(2) 7-D3) (a in Figure 3.37). Both products were ligated into pCR2.1 and sequenced to check that no mutations had been introduced during the PCRs. (c) shows a SacII/XmaI digest of the combined VJ-intron sequence inserted into pBluescriptII (g in Figure 3.37). This was then moved into pTαcass. The final product, pTαcass(TRAV 7D-3 TRAJ 15 intron) (i in Figure 3.37) is shown in (d) as a SacII/XmaI digest to show insertion of the sequence into the vector and in (e) as a BamHI digest, to demonstrate the maintenance of plasmid integrity. Band sizes shown are those expected. Clones with a correctly-sized insert were sequenced.

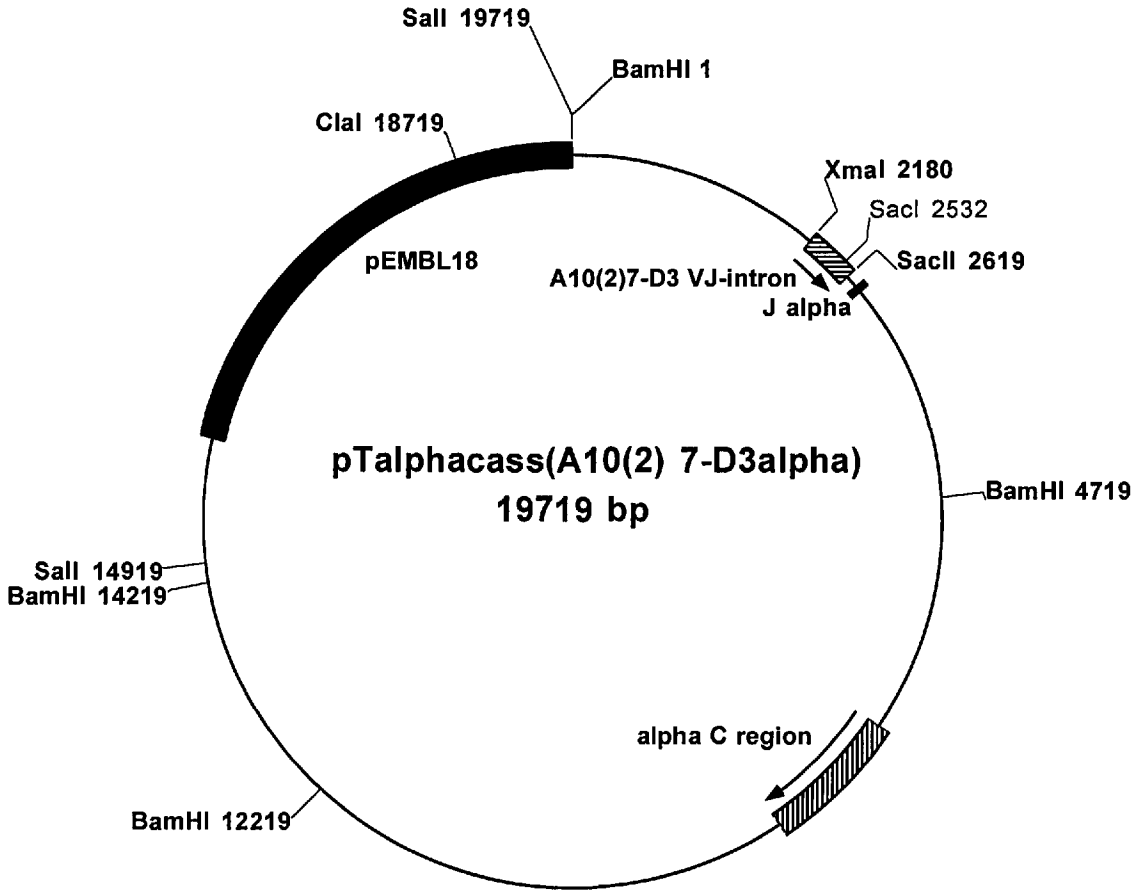


Figure 3.39 Final construct map showing the insertion of the TCRα chain 7-D3 from the Th1 murine T-cell clone A10(2) into the TCR expression vector pTαcass Only the rearranged VJ region (TRAV 7-D3 TRAJ 15) from the sequence was inserted into the vector, as there is an endogenous a murine Cα region already present, which is designed to be spliced to the VJ region during mRNA processing to produce a full-length TCR chain gene. As the VJ region inserted here was amplified from cDNA, it was necessary to include the first ~50bp of the intronic sequence downstream of the J region, to allow correct splicing to occur. Restriction sites that were used to create the VJ-intron sequence and to clone the sequence into pTαcass are shown, along with the position of the bacterial sequence required for the propagation of the construct in bacterial culture.

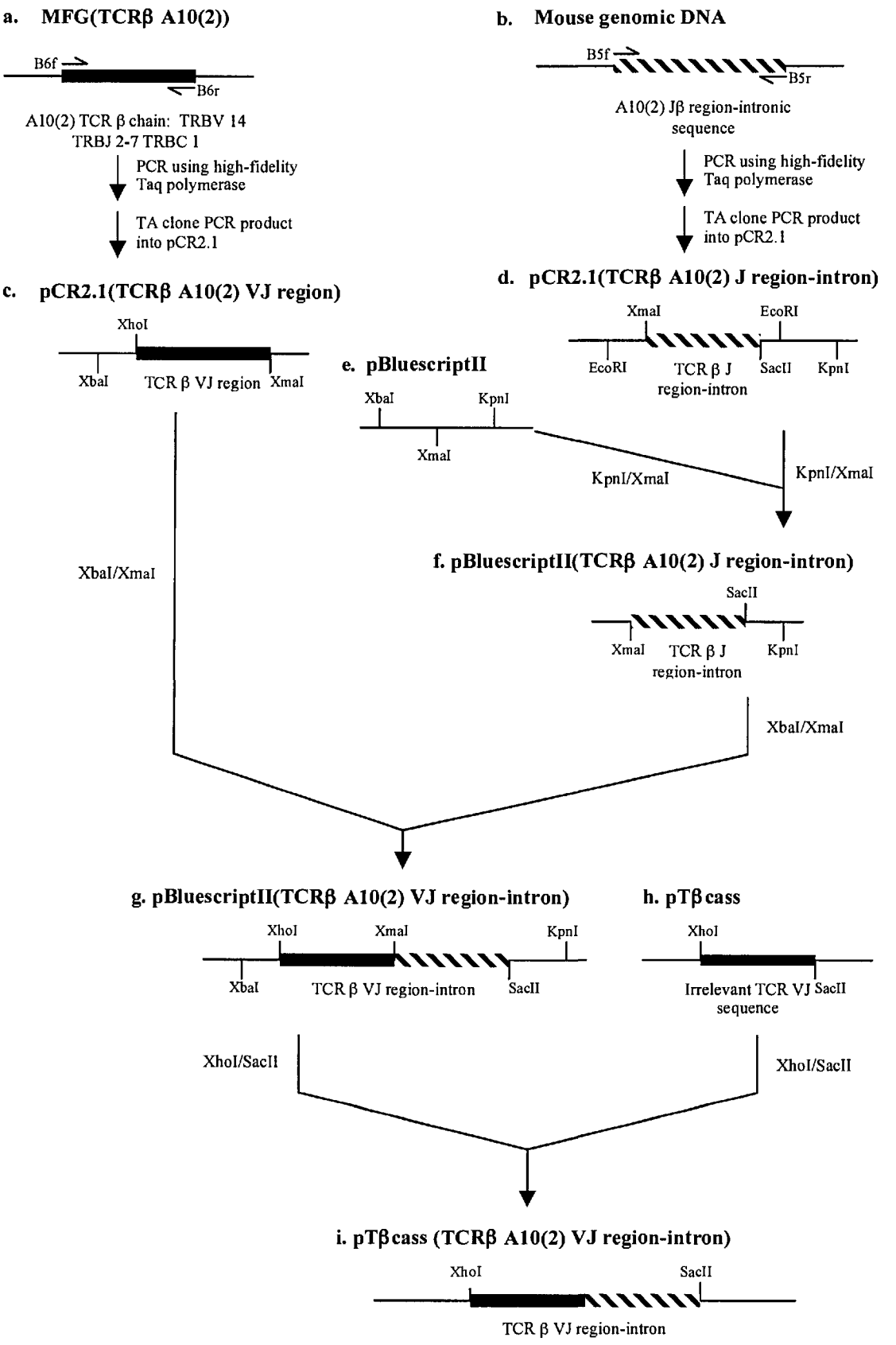

a. MFG(TCRβ A10(2))
B6f
B6r
A10(2) TCR β chain: TRBV 14
TRBJ 2-7 TRBC 1
PCR using high-fidelity
Taq polymerase
TA clone PCR product
into pCR2.1
b. Mouse genomic DNA
B5f
B5r
A10(2) Jβ region-intronic
sequence
PCR using high-fidelity
Taq polymerase
TA clone PCR product
into pCR2.1
c. pCR2.1(TCRβ A10(2) VJ region)
XhoI
XbaI
TCR β VJ region
XmaI
d. pCR2.1(TCRβ A10(2) J region-intron)
XmaI
EcoRI
EcoRI
TCR β J
region-intron
SacII
KpnI
e. pBluescriptII
XbaI
KpnI
XmaI
KpnI/XmaI
KpnI/XmaI
XbaI/XmaI
f. pBluescriptII(TCRβ A10(2) J region-intron)
SacII
XmaI
TCR β J
region-intron
KpnI
XbaI/XmaI
g. pBluescriptII(TCRβ A10(2) VJ region-intron)
XhoI
XmaI
KpnI
XbaI
TCR β VJ region-intron
SacII
XhoI/SacII
h. pTβcass
XhoI
Irrelevant TCR VJ SacII
sequence
XhoI/SacII
i. pTβcass (TCRβ A10(2) VJ region-intron)
XhoI
SacII
TCR β VJ region-intron

Figure 3.40 Cloning strategy designed to move the TCRβ chain (VJ region plus intronic sequence) from the mouse Th1-type T cell clone A10(2) into the TCR expression vector pTβcass pTβcass contains as part of its structure a murine TCR Cβ region, hence only the VJ region of the A10(2) TCR β chain was moved into the vector along with some intronic sequence (to allow for correct splicing of the sequence to the endogenous C region, as the VJ region was amplified from a fully rearranged sequence and not from genomic DNA). The VJ region was amplified from the MFG(TCR β A10(2)) construct which contained the full version of the TCR chain gene (a) using high-fidelity PCR. The forward primer included an XhoI site at its 3' end to allow for cloning of the TCR sequence into pTβcass. The reverse primer included a base change to incorporate an XmaI site into the J region, without changing the amino acid sequence, to allow the VJ region and the J-intron region to be combined. The PCR product was ligated into pCR2.1 (b). The J region-intron was amplified from mouse genomic DNA (c), the forward primer including a base change to incorporate the necessary XmaI site into the J region and the reverse primer including a SacII site at its 5' end to allow for cloning into pTβcass. The PCR product was ligated into pCR2.1 (d). Clones containing an insert of the correct size upon digestion with EcoRI were sequenced to check that no unintended mutations had been incorporated. The J region-intron segment was moved into pBluescriptII (e) using KpnI and XmaI., and correct insertion was determined by restriction digest (f). The VJ region segment was moved into this construct using XbaI and XmaI. Correct insertion was determined by restriction digest (g). A correctly combined sequence was moved into pTβcass (supplied containing an irrelevant TCR β chain as a circular plasmid) (h) using XhoI and SacII, and correct insertion was determined by restriction digest (i). Correct clones were sequenced, after which the constructs were ready for use in the Amaxa transfection system. All PCR primers, reaction conditions, and sequencing primers are shown in Appendix 4. All restriction enzymes used and digest conditions are shown in Appendix 5.

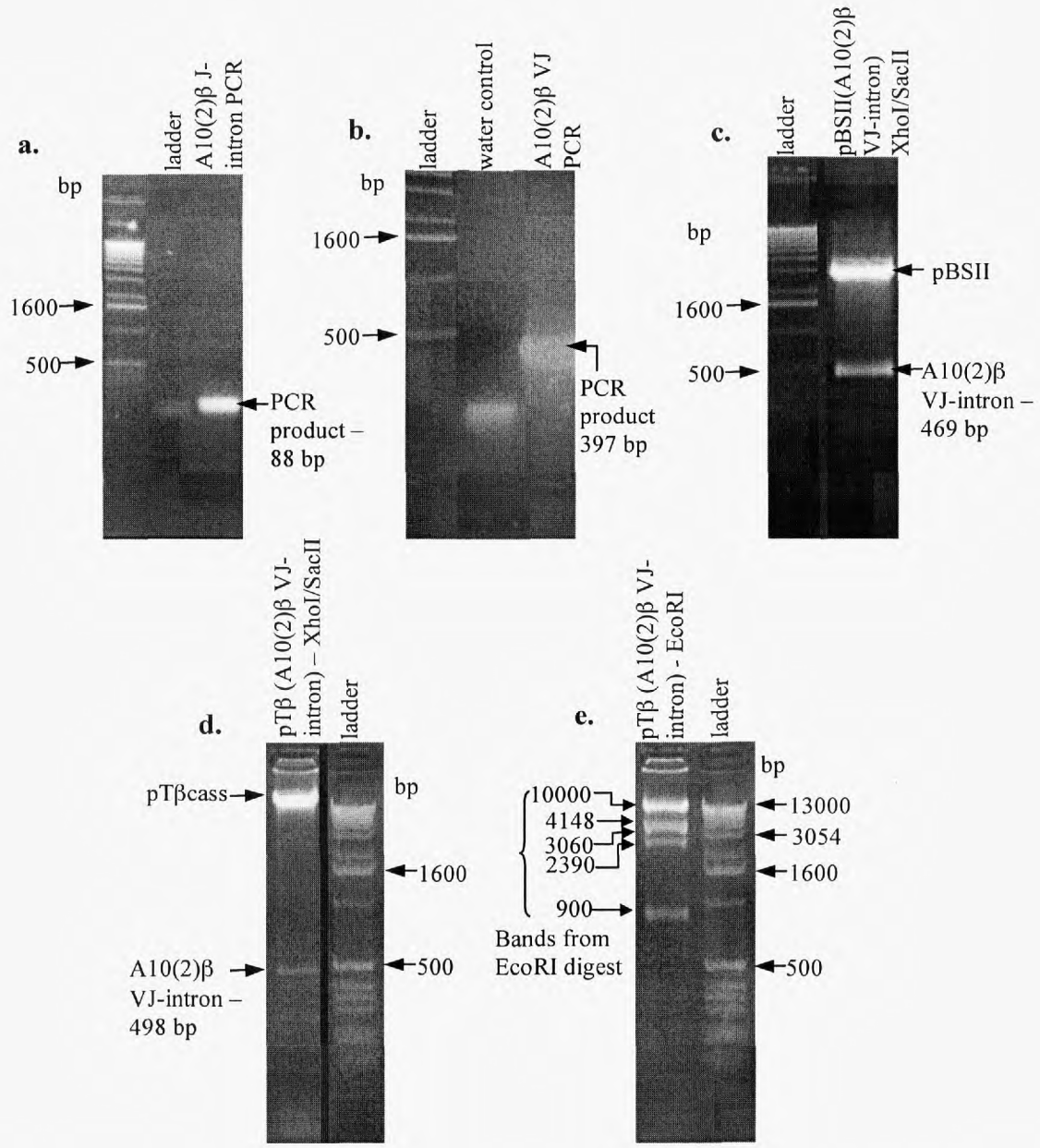


Figure 3.41 Gel images of the stages involved in moving the rearranged VJ region from the TCR β chain of murine T cell clone A10(2) combined with intronic sequence immediately downstream of the J region terminus into the TCR expression vector pTβcass The images show the steps involved in the strategy as outlined in Figure 3.40. PCR products corresponding to the J region-intron of the TCRβ chain (a) obtained from murine NOD.E T-cell genomic DNA (b in Figure 3.40) and to the rearranged V-J region (b) obtained from MFG(A10(2)β) (a in Figure 3.40) are shown. The bands were ligated into pCR2.1 and sequenced to check for any unintended mutations. (c) shows a SacII/XhoI digest of the combined VJ-intron sequence (469 bp) inserted into pBluescriptII (g in Figure 3.40). The correctly combined TCRβ VJ-intron segment was then moved into pTβcass, and the final product of the strategy, pTβcass(TRBV 14 TRBJ 2-7 intron) (i in Figure 3.40) is shown in (d) as a SacII/XhoI digest to show correct insertion and in (e) as an EcoRI digest, to show that the integrity of the plasmid remained intact. Band sizes shown are those expected. Clones with a correctly-sized insert were sequenced.

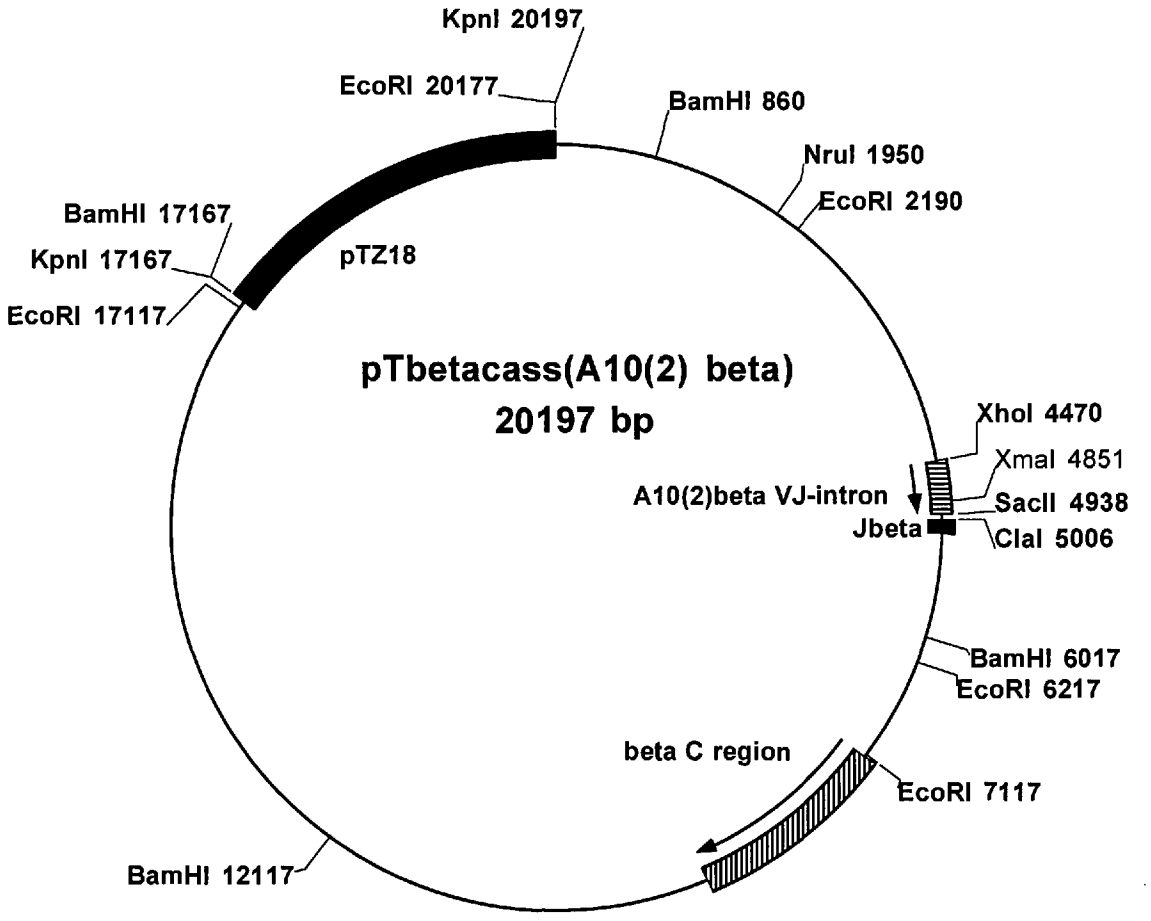


Figure 3.42 Final construct map showing the insertion of the TCR β chain from the Th1 T-cell clone A10(2) into the TCR expression vector pTβcass Only the rearranged VJ region (TRBV 14, TRBJ 2-7) from the sequence was inserted into the vector as it already contains a murine Cβ region which is designed to be spliced to the VJ region during mRNA processing to produce a full-length TCR chain gene. As the VJ region was amplified from cDNA, it was necessary to include ~50 bp of the intronic sequence immediately downstream of the J region, to allow for correct splicing. Restriction sites that were used to create the VJ-intron sequence and to clone the sequence into pTβcass are shown, along with the position of the bacterial sequence required for the propagation of the construct in bacterial culture.

3.2.2.3 Transfer of genes encoding TCR α and β chains from the PLP_{56-70}-specific murine T-cell clone D3(3) into the pTcass TCR expression vectors

3.2.2.3.1 Transfer of the TCRα chain from T-cell clone D3(3) into vector pTαcass

Figure 3.43 shows the strategy used to transfer the rearranged TCRα V-J segment (TRAV 7-D4 TRAJ 26-like (95% identity with IMGT database sequence)) from murine T-cell clone D3(3) into pTαcass. As for the A10(2) constructs, it was necessary to combine the rearranged TCRα V-J segment with intronic sequence immediately downstream of the J region. Primers were designed to incorporate a KpnI site into the J region by changing one base pair from C→T without changing the underlying amino acid sequence. The incorporated site was then used to join the two segments. The first PCR product was amplified from the MFG construct, consisting of the rearranged V-J segment as far as the introduced KpnI site. The second product was the J region-intron segment amplified from murine T-cell genomic DNA, consisting of the J region from the introduced KpnI site to a point 50 base pairs into the downstream intron. Products were combined in pBluescriptII and transferred into pTαcass using XmaI and SacII. Figure 3.44 shows gel images of the process, and Figure 3.45 shows the final construct. The full sequence of the insert in pTαcass is shown in Appendix 25.

3.2.2.3.2 Transfer of the TCRβ chain from T-cell clone D3(3) into vector pTβcass

The strategy used to transfer the rearranged TCRβ V-J segment (TRBV 2 TRAJ 2-5) from the murine T-cell clone D3(3) into the TCR expression vector pTβcass is shown in Figure 3.46. As for the D3(3) TCRα construct, the rearranged TCRβ V-J segment was combined with intronic sequence immediately downstream of the J region. To achieve this, primers were designed to make use of an endogenous BstXI site in the J region to join the two sequences. The first PCR product was the rearranged V-J segment as far as the BstXI site, amplified from the MFG construct, and the second product was the J region-intron segment, comprising the J region from its BstXI site to a point approximately 85 base pairs into the downstream intron. These products were joined in pUC19 before being transferred into pTβcass using XhoI and SacII. Gel images of the process are shown in Figure 3.47, and the final construct is shown in Figure 3.48. The full sequence of the insert in pTβcass is shown in Appendix 26.

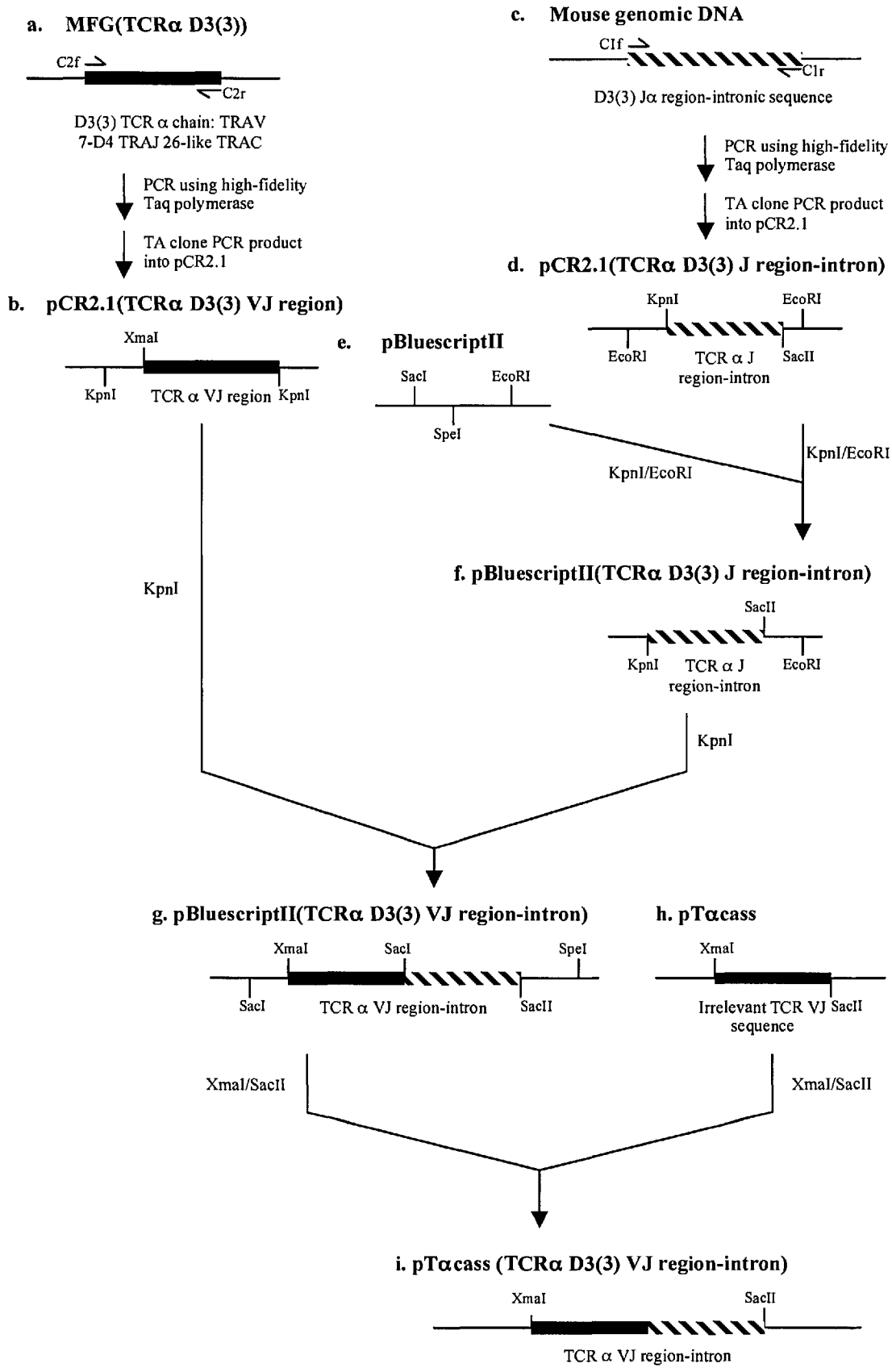

a. MFG(TCRα D3(3))
C2f
C2r
D3(3) TCR α chain: TRAV 7-D4 TRAJ 26-like TRAC
PCR using high-fidelity Taq polymerase
TA clone PCR product into pCR2.1
b. pCR2.1(TCRα D3(3) VJ region)
XmaI
KpnI
TCR α VJ region
KpnI
c. Mouse genomic DNA
CIf
CIr
D3(3) Jα region-intronic sequence
PCR using high-fidelity Taq polymerase
TA clone PCR product into pCR2.1
d. pCR2.1(TCRα D3(3) J region-intron)
KpnI
EcoRI
EcoRI
TCR α J region-intron
SacII
e. pBluescriptII
SacI
EcoRI
SpeI
KpnI/EcoRI
KpnI/EcoRI
f. pBluescriptII(TCRα D3(3) J region-intron)
SacII
KpnI
TCR α J region-intron
EcoRI
KpnI
KpnI
g. pBluescriptII(TCRα D3(3) VJ region-intron)
XmaI
SacI
SpeI
SacI
TCR α VJ region-intron
SacII
XmaI/SacII
h. pTαcass
XmaI
Irrelevant TCR VJ SacII sequence
XmaI/SacII
i. pTαcass (TCRα D3(3) VJ region-intron)
XmaI
SacII
TCR α VJ region-intron

Figure 3.43 Cloning strategy designed to move the TCRα chain (VJ region plus intronic sequence) from the mouse Th2 T cell clone D3(3) into the TCR expression vector pTαcass As pTαcass contains as part of its structure a murine TCR Cα region, only the VJ region of the D3(3) TCR α chain was moved into the vector along with some intronic sequence downstream of the J region to allow correct splicing of the sequence to the endogenous C region, as the VJ region was amplified from a fully rearranged sequence and not from genomic DNA. The VJ region was amplified from MFG(TCRα D3(3)) which contains the full version of the TCR chain gene (a) using high-fidelity PCR. The forward primer incorporated an XmaI site at its 3' end to allow for cloning of the TCR sequence into pTαcass. The reverse primer included a base change to incorporate a KpnI site into the J region, without changing the underlying amino acid sequence, to allow the VJ region and the J-intron region to be combined in a later cloning step. The PCR product was ligated into pCR2.1 (b). The J region-intron was amplified from mouse genomic DNA (c), the forward primer including a base change to incorporate the necessary KpnI site into the J region and the reverse primer including a SacII site at its 5' end to allow for cloning of the combined product into pTαcass. The PCR product was ligated into pCR2.1 (d). Clones containing an insert of the correct size upon digestion with EcoRI were sequenced to check that no unintended mutations had been introduced. The J region-intron segment was moved into pBluescriptII (e) using KpnI and EcoRI. Correct insertion of the sequence was determined by restriction digest (f). The VJ region segment was then moved into this construct using KpnI and correct insertion and orientation was determined by restriction digest (g). A correctly combined sequence was moved into pTαcass (supplied containing an irrelevant TCRα chain as a circular plasmid) (h) using XmaI and SacII, and correct insertion was determined by restriction digest (i). Correct clones were sequenced, after which the constructs were ready for use in the Amaxa transfection system. All PCR primers, reaction conditions, and sequencing primers are shown in Appendix 4. All restriction enzymes used and digest conditions are shown in Appendix 5.

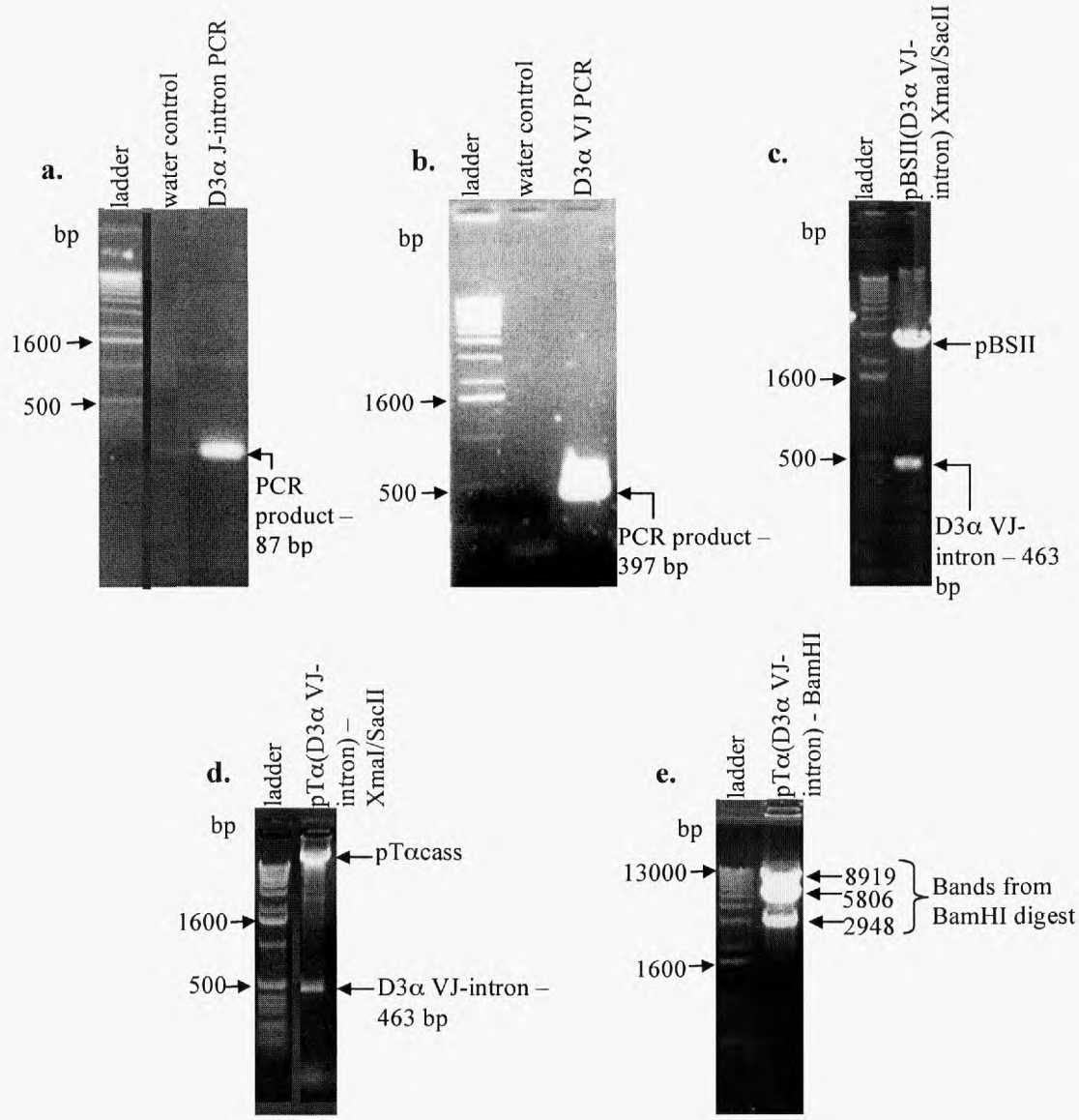


Figure 3.44 Gel images of the stages involved in moving the rearranged VJ region from the TCRα chain of murine T cell clone D3(3) combined with intronic sequence immediately downstream of the J region terminus into the TCR expression vector pTαcass The images above show the steps involved in the strategy as outlined in Figure 3.43. The PCR product of the J region-intron of the TCRα chain obtained from murine NOD.E T cell genomic DNA (c in Figure 3.43) is shown in (a) and that of the rearranged VJ region obtained from MFG(D3(3)α) (a in Figure 3.43) is shown in (b). PCR products were ligated into pCR2.1 and sequenced to check that no unintended mutations had occurred. (c) shows a SacII/XmaI digest of the combined VJ-intron sequence inserted into pBluescriptII (g in Figure 3.43). The correctly combined TCRα VJ-intron segment was moved into pTαcass. The final product of the strategy, pTαcass(TRAV 7D-4 TRAJ ? intron) (i in Figure 3.43) is shown in (d) as a SacII/XmaI digest to show correct insertion and in (e) as a BamHI digest, to check that the plasmid retained its integrity. Band sizes shown are those expected. Clones with a correctly-sized insert were sequenced.

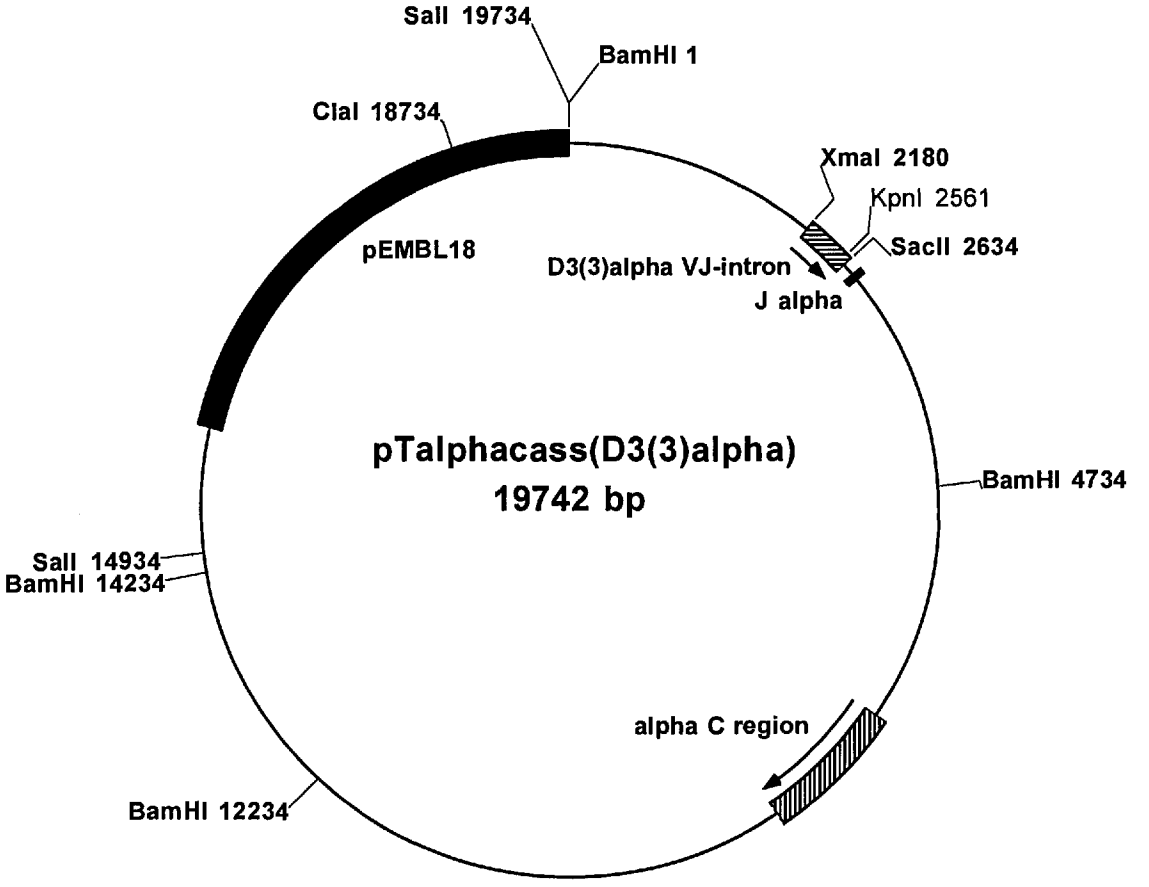


Figure 3.45 Final construct map showing the insertion of the TCRα chain from the Th2 T cell clone D3(3) into the TCR expression vector pTαcass Only the rearranged VJ region (TRAV 7-D4 TRAJ 26-like) from the sequence was inserted as there is an endogenous murine Cα region already in the vector, designed to be spliced to the VJ region during mRNA processing to produce a full-length TCR chain gene. As the VJ region was amplified from cDNA, it was necessary to include intronic sequence (~50 bp) immediately downstream of the J region to allow correct splicing. Restriction sites that were used to create the VJ-intron sequence and to clone the sequence into pTαcass are shown, along with the position of the bacterial sequence needed for amplification of the construct in bacterial culture.

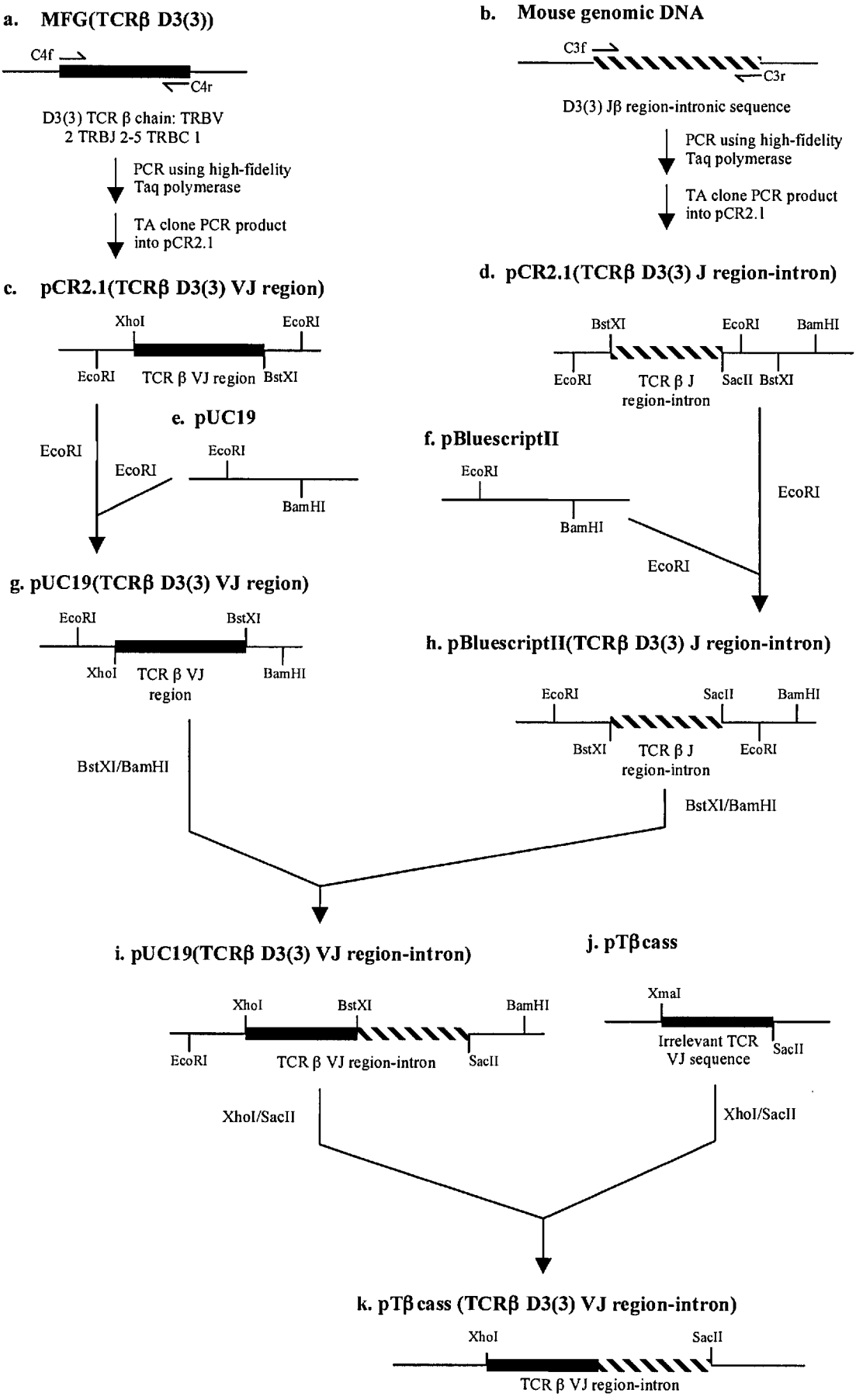

a. MFG(TCRβ D3(3))
C4f
C4r
D3(3) TCR β chain: TRBV 2 TRBJ 2-5 TRBC 1
PCR using high-fidelity Taq polymerase
TA clone PCR product into pCR2.1
b. Mouse genomic DNA
C3f
C3r
D3(3) Jβ region-intronic sequence
PCR using high-fidelity Taq polymerase
TA clone PCR product into pCR2.1
c. pCR2.1(TCRβ D3(3) VJ region)
XhoI
EcoRI
EcoRI
TCR β VJ region
BstXI
d. pCR2.1(TCRβ D3(3) J region-intron)
BstXI
EcoRI
BamHI
EcoRI
TCR β J region-intron
SacII
BstXI
e. pUC19
EcoRI
EcoRI
EcoRI
BamHI
f. pBluescriptII
EcoRI
BamHI
EcoRI
EcoRI
g. pUC19(TCRβ D3(3) VJ region)
EcoRI
BstXI
XhoI
TCR β VJ region
BamHI
h. pBluescriptII(TCRβ D3(3) J region-intron)
EcoRI
SacII
BamHI
BstXI
TCR β J region-intron
EcoRI
BstXI/BamHI
BstXI/BamHI
i. pUC19(TCRβ D3(3) VJ region-intron)
j. pTβcass
XhoI
BstXI
BamHI
EcoRI
TCR β VJ region-intron
SacII
XmaI
Irrelevant TCR VJ sequence
SacII
XhoI/SacII
XhoI/SacII
k. pTβcass (TCRβ D3(3) VJ region-intron)
XhoI
SacII
TCR β VJ region-intron

Figure 3.46 Cloning strategy designed to move the TCRβ chain (VJ region plus intronic sequence) from the mouse Th2 T-cell clone D3(3) into the TCR expression vector pTβcass pTβcass contains as part of its structure a murine TCR Cβ region, hence only the rearranged VJ region of the D3(3) TCRβ chain was moved into the vector along with ~50bp intronic sequence immediately downstream of the J region. This allows correct splicing of the sequence to the endogenous C region as the VJ region in this case was amplified from a fully rearranged sequence and not from genomic DNA. The VJ region was amplified from MFG(TCRβ D3(3)) which contains the full version of the TCR chain gene (a) using high-fidelity PCR. The forward primer incorporated an XhoI site at its 3' end to allow for cloning of the TCR sequence into pTβcass. The reverse primer incorporated an endogenous BstXI site in the J region to allow the VJ region and the J-intron region to be combined in a later step. The PCR product was ligated into pCR2.1 (b). The J region-intron was amplified from mouse genomic DNA (c), the forward primer incorporating the BstXI site from the J region and the reverse primer including a SacII site at its 5' end to allow cloning of the combined product into pTβcass. The PCR product was ligated into pCR2.1 (d). Clones containing an insert of the correct size upon EcoRI digestion were sequenced to check that no unintended mutations had occurred. As the vector pCR2.1 contains two BstXI sites in its MCS, this prevented the use of BstXI as a means of combining the two segments from this plasmid, and so it was necessary to move the J-intron region from a correct clone into pBluescriptII (f) using EcoRI. Correct insertion and orientation of the sequence was determined by restriction digest (h). Simultaneously, the VJ region was moved into another cloning vector, pUC19 (e), using EcoRI and correct insertion and orientation was determined by restriction digest (g). The J region-intron segment from pBluescriptII was then moved into pUC19 (containing the VJ region) using BstXI and BamHI, and correct combination was determined by restriction digest (i). A correctly combined sequence was moved into pTβcass (supplied as a circular plasmid containing an irrelevant TCRβ chain) (j) using XhoI and SacII, and correct insertion was determined by restriction digest (k). Correct clones were sequenced, after which the constructs were ready for use in the Amaxa transfection system. All PCR primers, reaction conditions, and sequencing primers are shown in Appendix 4. All restriction enzymes used and digest conditions are shown in Appendix 5.

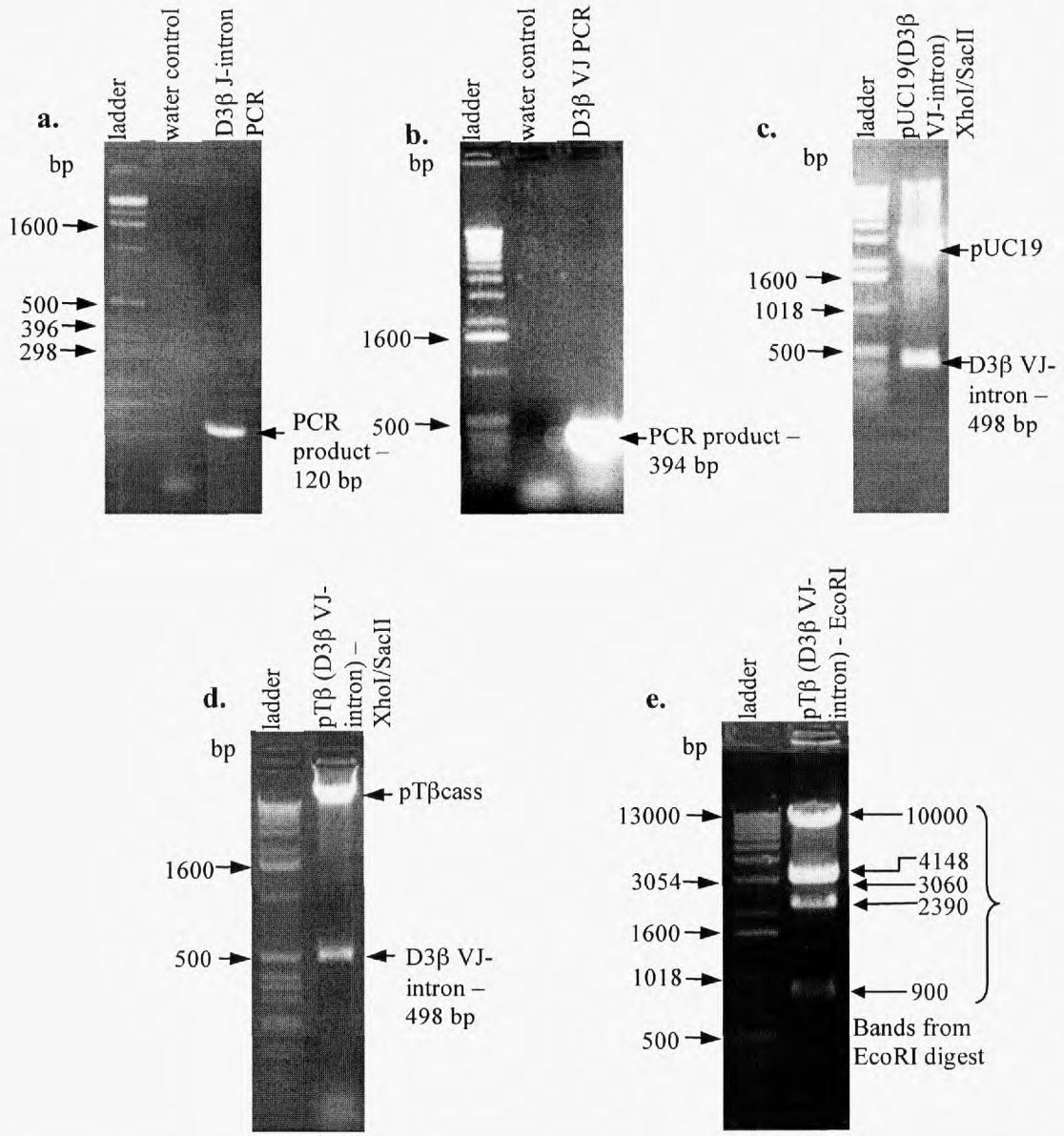


Figure 3.47 Gel images of the stages involved in moving the rearranged VJ region from the TCRβ chain of murine T cell clone D3(3) combined with intronic sequence immediately downstream of the J region terminus into the TCR expression vector pTβcass The images above show the steps involved in the strategy as outlined in Figure 3.46. (a) and (b) show the PCR products corresponding to the J region-intron of the TCRβ chain (a), obtained from murine NOD.E T-cell genomic DNA (b in Figure 3.46), and the rearranged V-J region (b), obtained from MFG(D3(3)β) (a in Figure 3.46). The products were ligated into pCR2.1 and sequenced to check that no unintended mutations had occurred. (c) shows a SacII/XhoI digest of the combined VJ-intron sequence inserted into pUC19 (i in Figure 3.46). The correctly combined TCRβ VJ-intron segment was moved into pTβcass. The final product of the strategy, pTβcass(D3β TRBV 2 TRBJ 2-5 intron) (k in Figure 3.46) is shown in (d) as a SacII/XhoI digest to show correct insertion of the insert and in (e) as an EcoRI digest, to show that the integrity of the plasmid remained intact. Band sizes shown are those expected. Clones with a correctly-sized insert were sequenced.

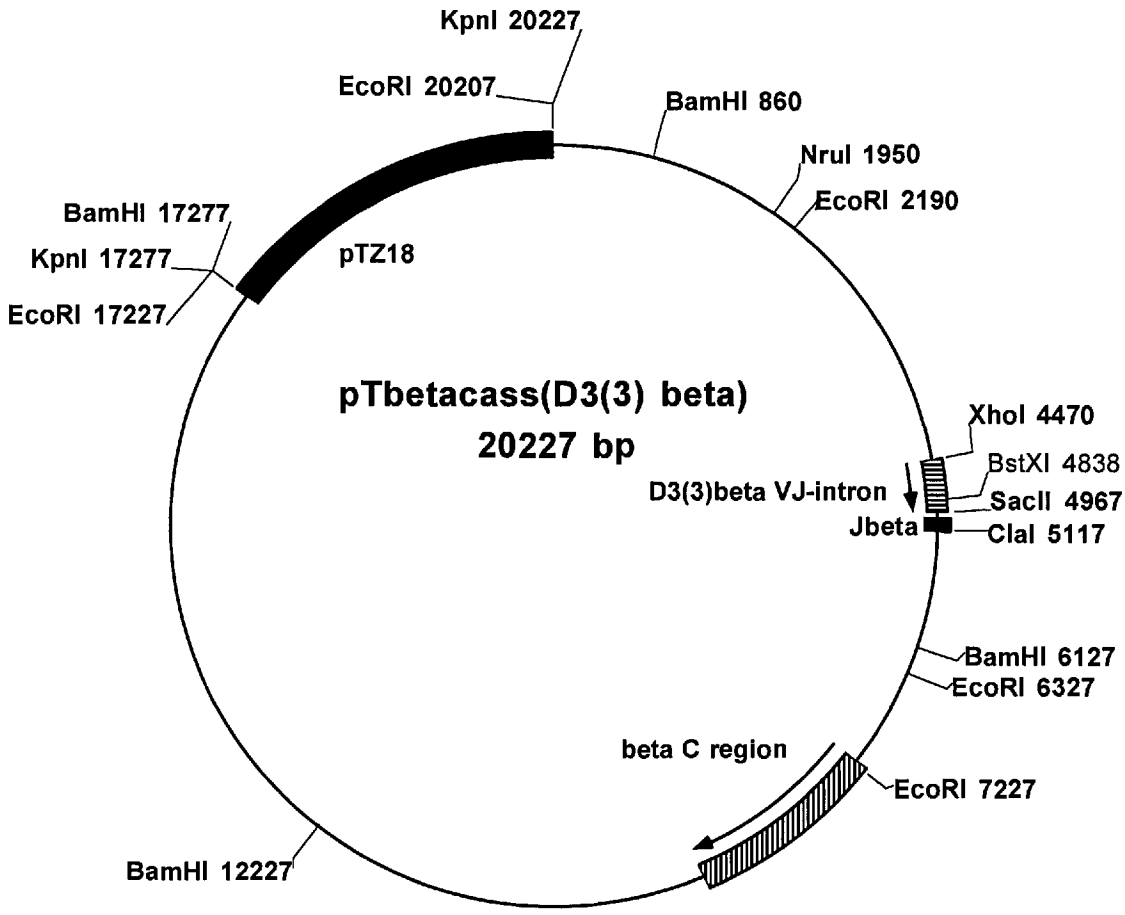


Figure 3.48 Final construct map showing the insertion of the TCRβ chain from the Th2 T-cell clone D3(3) into the TCR expression vector pTβcass Only the rearranged VJ region (TRBV 2 TRBJ 2-5) of the sequence was inserted as the vector already contains a murine Cβ region, designed to be spliced to the VJ region during mRNA processing to produce a full-length TCR chain gene. As the VJ region was amplified from cDNA, it was necessary to include the beginning of the intronic sequence immediately downstream of the J region to allow correct splicing to occur. Restriction sites that were used to create the VJ-intron sequence and to clone the sequence into pTβcass are shown, along with the position of the bacterial sequence required for the propagation of the construct in bacterial culture.

3.2.2.4 Transfer of genes encoding dominant TCR α and β chains from the human peptide 4-specific T-cell line CIR010 into pTcass TCR expression vectors

3.2.2.4.1 Transfer of the TCRα chain from T-cell line CIR010 into vector pTαcass

The strategy to transfer the dominant rearranged TCRα V-J segment (TRAV 8-4 TRAJ 32) from the human T-cell line CIR010 into the TCR expression vector pTαcass is shown in Figure 3.49. As the rearranged TCRα V-J segment was amplified from T-cell line cDNA and hence from a rearranged TCRα chain, it was necessary to combine this segment with intronic sequence immediately downstream of the J region. To achieve this, primers were designed to amplify the rearranged V-J region from the cDNA, and to incorporate a HindIII site into the J region by changing one base pair from C→T without changing the underlying amino acid sequence. In addition, a linker corresponding to the J region downstream of the incorporated HindIII site (also present in the linker) and the first 50 base pairs of the intron immediately following the J region was inserted into pBluescriptII. The HindIII site was then used to join the rearranged V-J segment to the linker, before transfer into pTαcass using XmaI and SacII. Figure 3.50 shows gel images of the process, with the final construct shown in Figure 3.51. The sequence of the insert in pTαcass is shown in Appendix 27.

3.2.2.4.2 Transfer of the TCRβ chain from T-cell line CIR010 into vector pTβcass

Figure 3.52 shows the strategy used to transfer the dominant rearranged TCRβ V-J segment (TRBV 6-1 TRBJ 1-1) from the human T-cell line CIR010 into the TCR expression vector pTβcass. As for the TCRα construct, the rearranged V-J segment, amplified from T-cell line cDNA, was combined with intronic sequence immediately downstream of the J region. Primers were designed to amplify the rearranged V-J region from the cDNA as far as an endogenous HindIII site in the J region for use in joining the V-J region to the J-intron segment. This segment, corresponding to the J region downstream of the endogenous HindIII site and the first 50 base pairs of the intron immediately following, was inserted as a linker into pBluescriptII. The two segments were combined using HindIII, before transfer into pTβcass using XhoI and SacII. Gel images of the process are shown in Figure 3.53, and the final construct is shown in Figure 3.54. The full sequence of the insert in pTβcass is shown in Appendix 28.

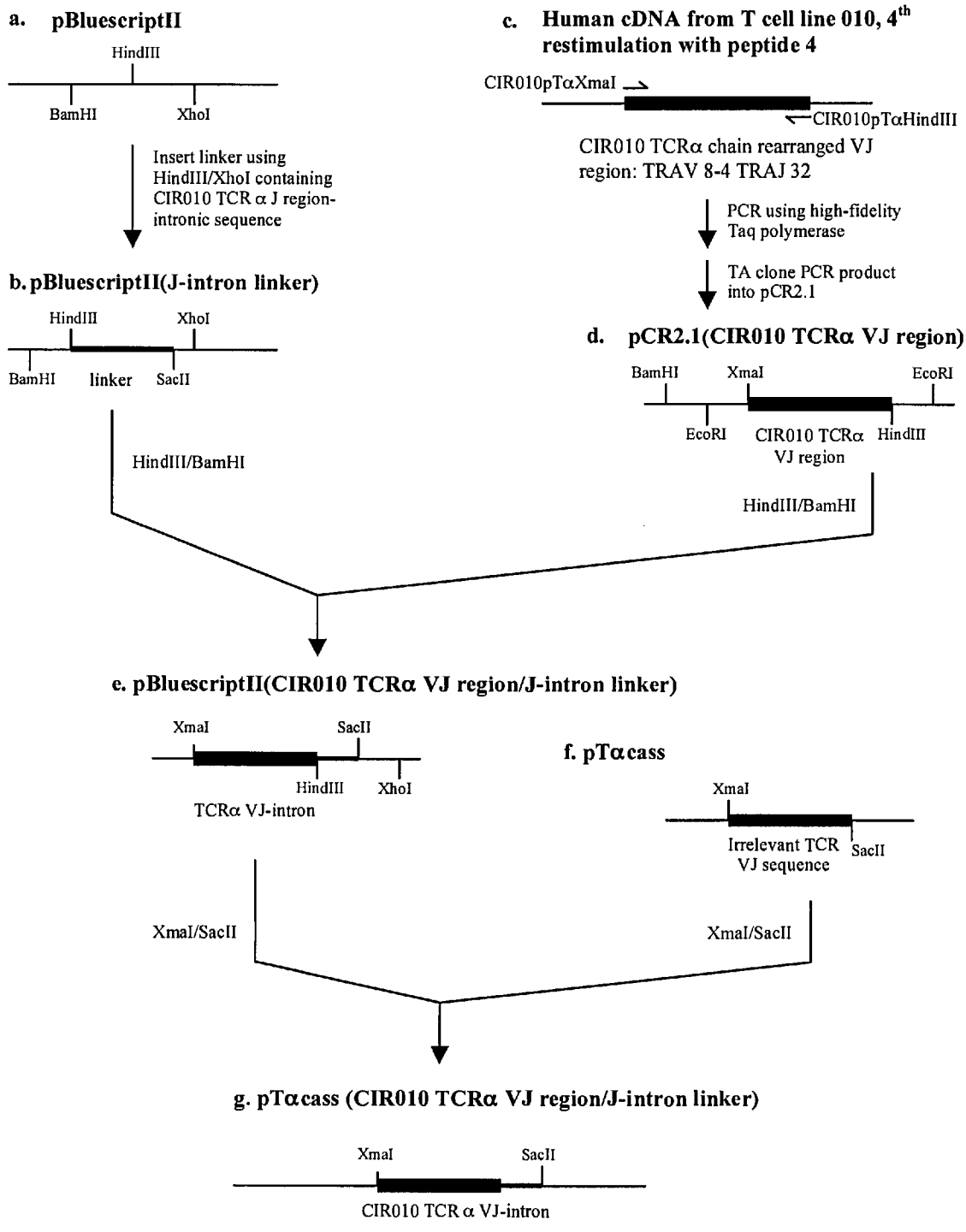

a. pBluescriptII
HindIII
BamHI
XhoI
Insert linker using HindIII/XhoI containing CIR010 TCR α J region-intronic sequence
b. pBluescriptII(J-intron linker)
HindIII
XhoI
BamHI
linker
SacII
HindIII/BamHI
c. Human cDNA from T cell line 010, 4th restimulation with peptide 4
CIR010pTαXmaI
CIR010pTαHindIII
CIR010 TCRα chain rearranged VJ region: TRAV 8-4 TRAJ 32
PCR using high-fidelity Taq polymerase
TA clone PCR product into pCR2.1
d. pCR2.1(CIR010 TCRα VJ region)
BamHI
XmaI
EcoRI
EcoRI
CIR010 TCRα VJ region
HindIII
HindIII/BamHI
e. pBluescriptII(CIR010 TCRα VJ region/J-intron linker)
XmaI
SacII
HindIII
XhoI
TCRα VJ-intron
f. pTαcass
XmaI
Irrelevant TCR VJ sequence
SacII
XmaI/SacII
XmaI/SacII
g. pTαcass (CIR010 TCRα VJ region/J-intron linker)
XmaI
SacII
CIR010 TCR α VJ-intron

Figure 3.49 Cloning strategy designed to move the dominant TCRα chain (VJ region plus intronic sequence) from the human T cell line CIR010 into the TCR expression vector pTαcass As pTαcass contains as part of its structure a murine TCR Cα region, only the VJ region of the CIR010 TCRα chain was moved into pTαcass, along with some intronic sequence immediately downstream of the J region as the VJ region was amplified from cDNA and not genomic DNA, to allow correct splicing of the sequence to the endogenous C region. A linker was inserted into pBluescriptII (a) using HindIII and XhoI. The linker corresponded to the 5'-end of the Jα region and 50 bp of intronic sequence immediately downstream and also included a base change to incorporate a HindIII site in the sequence. This would allow the subsequent combination of the J-intron sequence with the VJ sequence (but without changing the overall amino acid sequence). A SacII site was added to the end of the intronic sequence to allow for cloning into pTαcass. The linker also contained a XhoI site to allow insertion of the vector into pBluescriptII. Insertion was determined by restriction digest (b). The VJ region was amplified from cDNA from the human T cell line CIR010 at its 3rd restimulation with peptide 4 (c) using high-fidelity PCR. The forward primer incorporated an XmaI site to allow for cloning of the TCR sequence into pTαcass. The reverse primer included a base change to incorporate a HindIII site to allow the VJ region and the J-intron region to be combined in a later cloning step. The PCR product was ligated into pCR2.1 (d). Clones containing an insert of the correct size upon digestion with EcoRI were sequenced to check that no unintended mutations had been incorporated during the reaction. The VJ region was moved into pBluescriptII(linker) using HindIII and BamHI, and correct insertion was determined by restriction digest (e). A correctly combined sequence was moved into pTαcass (supplied already containing an irrelevant TCR α chain as a circular plasmid) (f) using XmaI and SacII, and correct insertion was determined by restriction digest (g). Correct clones were sequenced, after which the constructs were ready for use in the Amaxa transfection system. All PCR primers, reaction conditions, oligonucleotide linkers and sequencing primers are shown in Appendix 4. All restriction enzymes used and digest conditions are shown in Appendix 5.

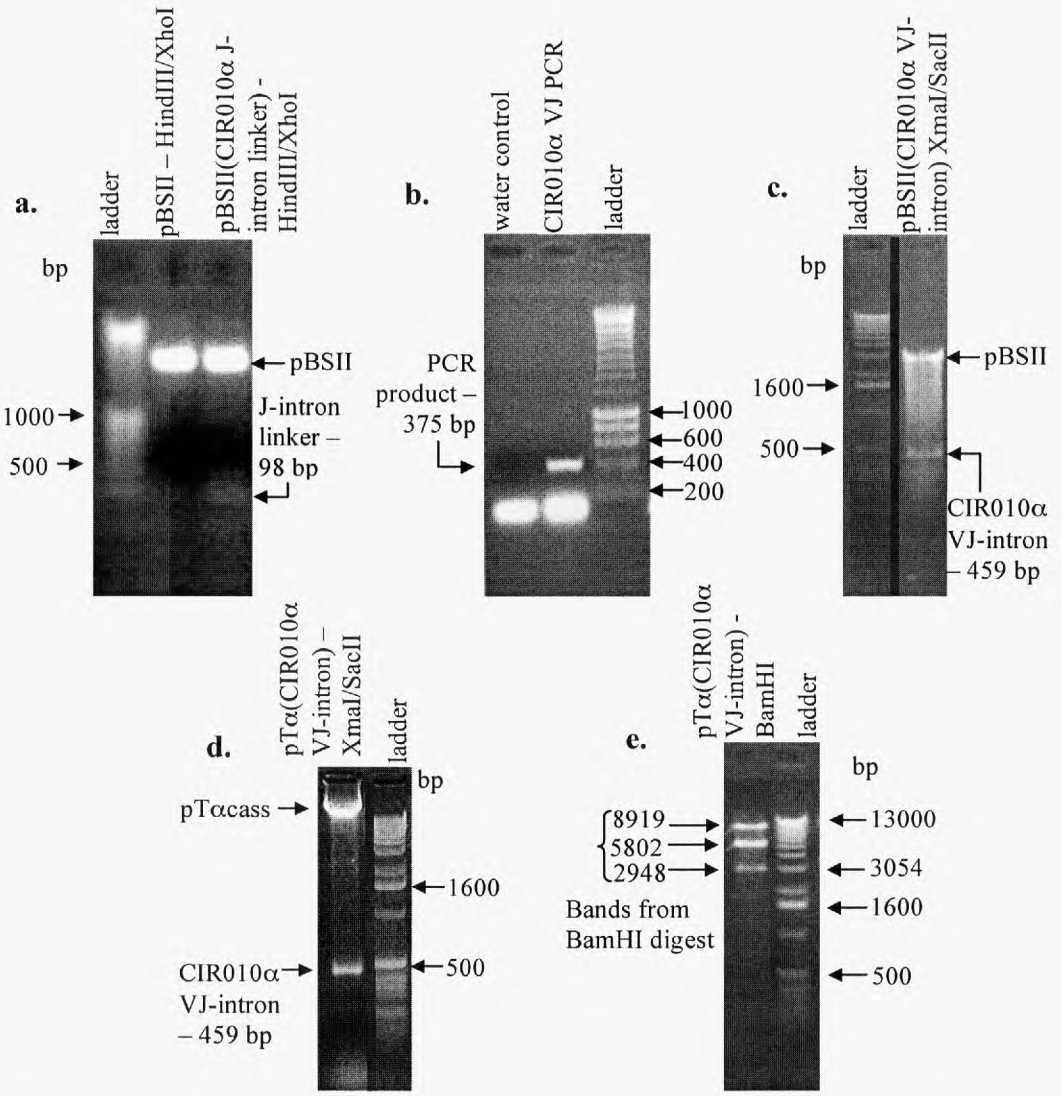


Figure 3.50 Gel images of the stages involved in moving the rearranged VJ region from the dominant TCRα chain from human T cell line CIR010 combined with intronic sequence immediately downstream of the J region terminus into the TCR expression vector pTαcass The images above show the steps involved in the strategy as outlined in Figure 3.49. (a) shows the insertion of an oligonucleotide linker comprising the 3'-end of the J region from the dominant TCRα chain in line CIR010 and the first 50bp of the intronic sequence immediately following it into pBluescriptII (b in Figure 3.50). Correct insertion was determined by restriction digest with the enzymes (HindIII and XhoI) originally used to insert the linker. A HindIII/XhoI digest of pBluescriptII with no linker inserted is shown as a comparison. (b) shows the PCR product obtained from cDNA from the human T cell line CIR010 (c in Figure 3.49). The product was ligated into pCR2.1 and sequenced to check that no unintended mutations had occurred. (c) shows a SacII/XmaI digest of the combined VJ-intron sequence inserted into pBluescriptII (e in Figure 3.49). The correctly combined TCRα VJ-intron segment was moved into pTαcass. The final product of the strategy, pTαcass(TRAV 8-4 TRAJ 32 intron) (g in Figure 3.49) is shown in (d) as a SacII/XmaI digest to show correct insertion of the insert and in (e) as a BamHI digest, to show that the integrity of the plasmid remained intact. Band sizes shown are those expected. Clones with a correctly-sized insert were sequenced.

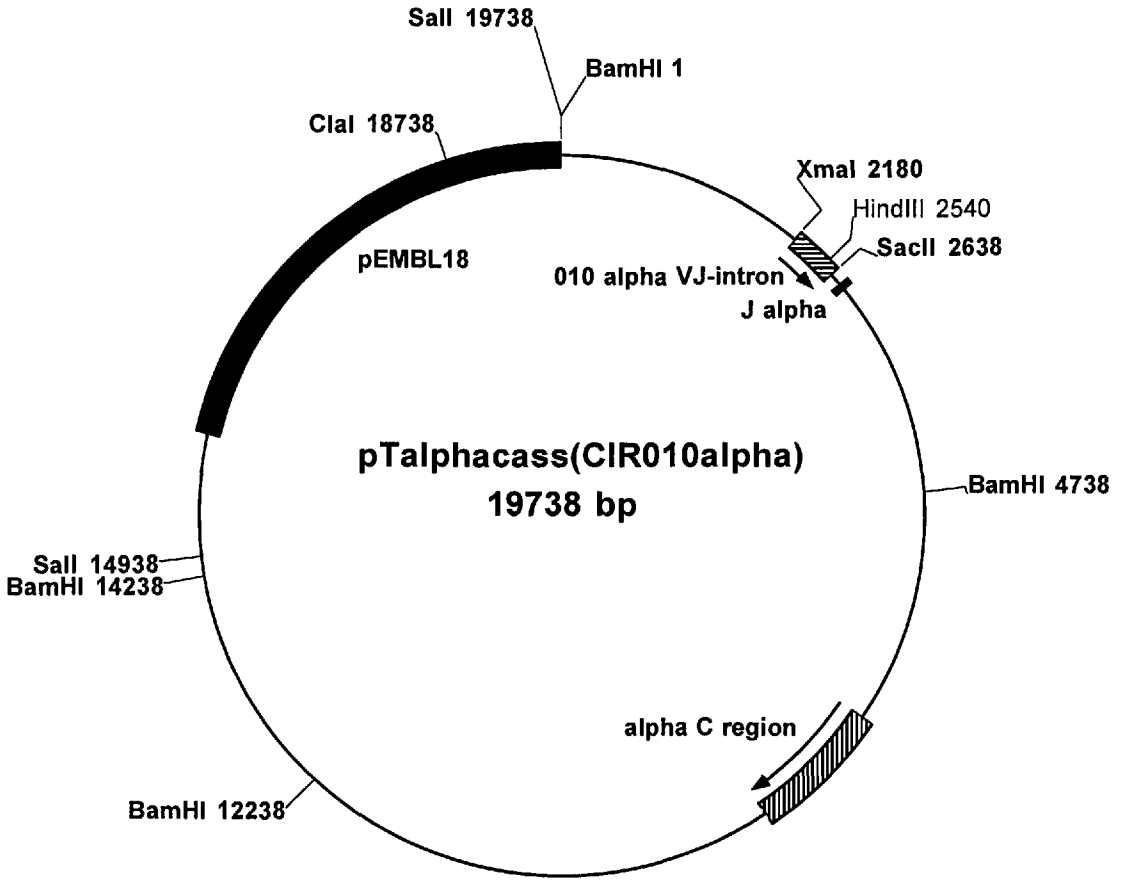


Figure 3.51 Final construct map showing the insertion of the dominant TCRα chain from the human T cell line CIR010 into the TCR expression vector pTαcass Only the rearranged VJ region (TRAV 8-4 TRAJ 32) from the human sequence was inserted as the vector contains a murine Cα region already, which is designed to be spliced to the VJ region during mRNA processing to produce a full-length TCR chain gene. As the human VJ region was amplified from cDNA, it was necessary to include ~50bp of the intronic sequence immediately downstream of the J region, to allow correct splicing to occur. Restriction sites that were used to create the VJ-intron sequence and to clone the sequence into pTαcass are shown, along with the position of the bacterial sequence required for construct amplification in bacterial culture.

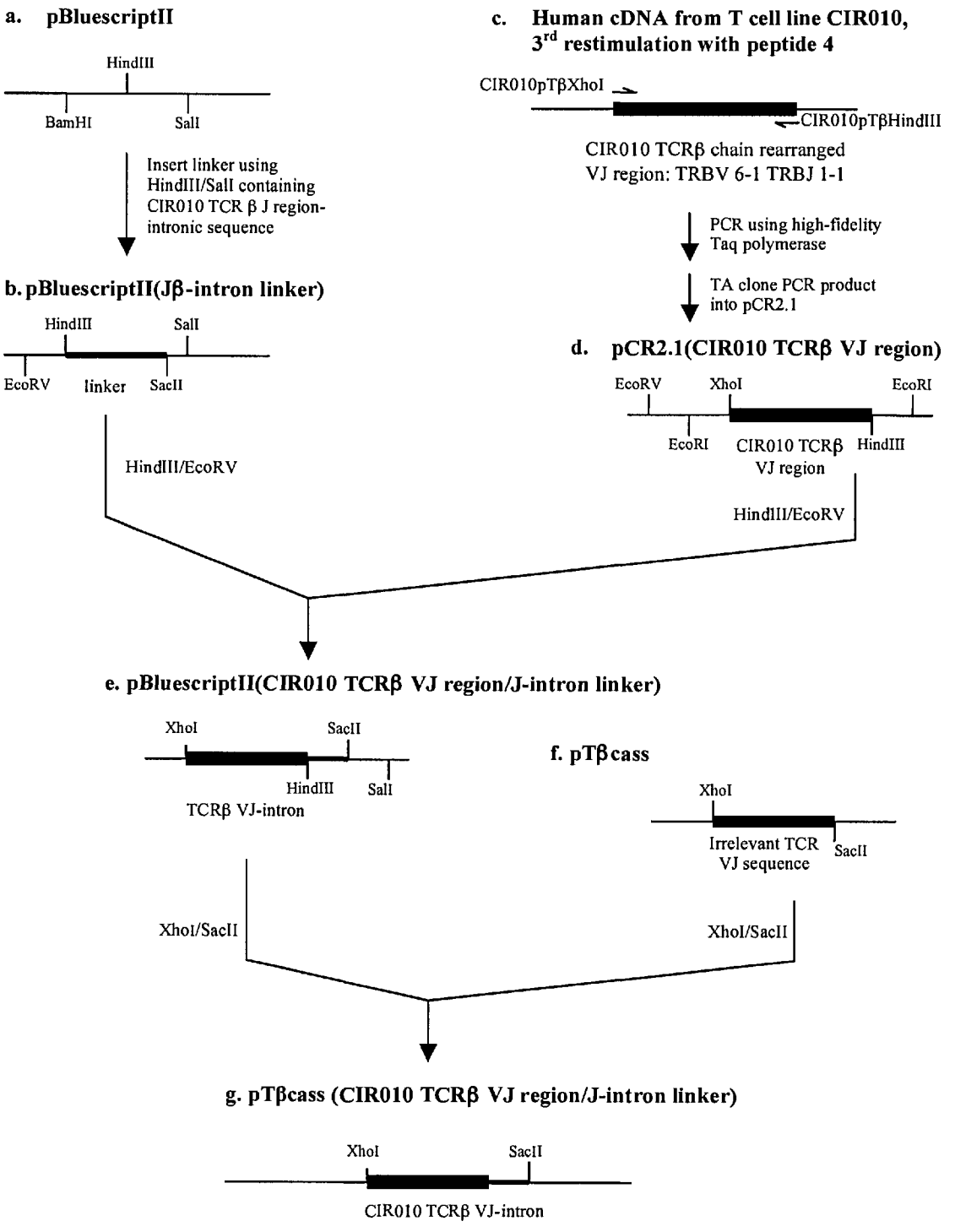

a. pBluescriptII
HindIII
BamHI
SalI
Insert linker using HindIII/SalI containing CIR010 TCR β J region-intronic sequence
b. pBluescriptII(Jβ-intron linker)
HindIII
SalI
EcoRV
linker
SacII
HindIII/EcoRV
c. Human cDNA from T cell line CIR010, 3rd restimulation with peptide 4
CIR010pTβXhoI
CIR010pTβHindIII
CIR010 TCRβ chain rearranged
VJ region: TRBV 6-1 TRBJ 1-1
PCR using high-fidelity Taq polymerase
TA clone PCR product into pCR2.1
d. pCR2.1(CIR010 TCRβ VJ region)
EcoRV
XhoI
EcoRI
EcoRI
CIR010 TCRβ VJ region
HindIII
HindIII/EcoRV
e. pBluescriptII(CIR010 TCRβ VJ region/J-intron linker)
XhoI
SacII
HindIII
SalI
TCRβ VJ-intron
f. pTβcass
XhoI
Irrelevant TCR VJ sequence
SacII
XhoI/SacII
XhoI/SacII
g. pTβcass (CIR010 TCRβ VJ region/J-intron linker)
XhoI
SacII
CIR010 TCRβ VJ-intron

Figure 3.52 Cloning strategy designed to move the dominant TCRβ chain (VJ region plus intronic sequence) from the human T cell line CIR010 into the TCR expression vector pTβcass pTβcass contains as part of its structure a murine TCR Cβ region, so only the VJ region of the CIR010 TCRβ chain was moved into the vector along with ~50bp intronic sequence immediately downstream of the J region to allow for correct splicing of the sequence to the endogenous C region, as the VJ region was amplified from cDNA and not genomic DNA. A linker was inserted into pBluescriptII (a) using HindIII and SalI. The linker corresponded to the 5'-end of the Jβ region and 50 bp of intronic sequence immediately downstream of it and incorporated an endogenous HindIII site in the J region of the sequence, to allow subsequent combination of the J-intron sequence with the VJ sequence. A SacII site was added to the end of the intronic sequence to allow cloning into pTβcass. The linker also contained a SalI site to allow insertion of the vector into pBluescriptII. Insertion was determined by restriction digest (b). The VJ region was amplified from cDNA from the human T cell line CIR010 at its 3rd restimulation with peptide 4 (c) using high-fidelity PCR. The forward primer incorporated a XhoI site to allow for cloning of the TCR sequence into pTβcass. The reverse primer incorporated the HindIII site in the J region to allow the VJ region and the J-intron region to be combined in a later step. The PCR product was ligated into pCR2.1 (d). Clones containing an insert of the correct size upon digestion with EcoRI were sequenced to check that no unintended mutations had been incorporated during the reaction. The VJ region was moved into pBluescriptII(linker) using HindIII and EcoRV, and correct insertion was determined by restriction digest (e). A correctly combined sequence was moved into pTβcass (supplied as a circular plasmid containing an irrelevant TCRβ chain) (f) using XhoI and SacII, and correct insertion was determined by restriction digest (g). Correct clones were sequenced, after which the constructs were ready for use in the Amaxa transfection system. All PCR primers, reaction conditions, oligonucleotide linkers and sequencing primers are shown in Appendix 4. All restriction enzymes used and digest conditions are shown in Appendix 5.

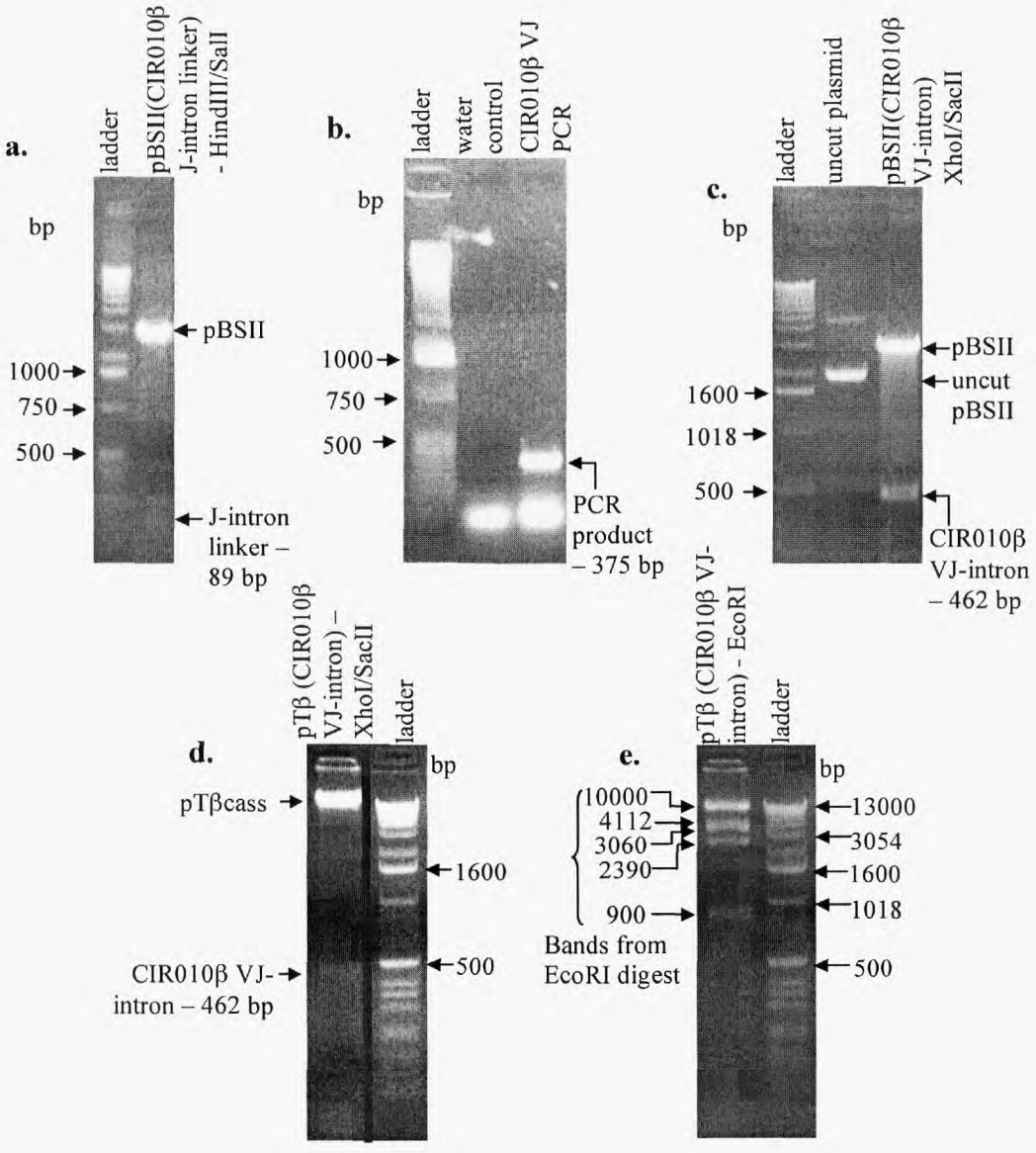


Figure 3.53 Gel images of the stages involved in moving the rearranged VJ region from the dominant TCRβ chain from human T cell line CIR010 combined with intronic sequence immediately downstream of the J region terminus into the TCR expression vector pTβcass The images above show the steps involved in the strategy as outlined in Figure 3.52. (a) shows insertion of an oligonucleotide linker comprising the 3'-end of the J region from the dominant TCRβ chain in line CIR010 and the first 60bp of the intronic sequence immediately following it in the genomic DNA into pBluescriptII (b in Figure 3.52). Correct insertion was determined by restriction digest with the enzymes (HindIII and SalI) originally used for linker insertion. (b) shows the PCR product obtained from cDNA from the human T cell line CIR010 (c in Figure 3.52). The product was ligated into pCR2.1 and sequenced to check that no unintended mutations had occurred. (c) shows a XhoI/SacII digest of the combined VJ-intron sequence inserted into pBluescriptII (e in Figure 3.52). The correctly combined TCRβ VJ-intron segment was moved into pTβcass. The final product of the strategy, pTβcass(TRBV 6-1 TRβJ 1-1 intron) (g in Figure 3.52) is shown in (d) as a XhoI/SacII digest to show correct insertion of the insert and in (e) as an EcoRI digest, to show that the integrity of the plasmid remained intact. Band sizes shown are those expected. Clones with a correctly-sized insert were sequenced.

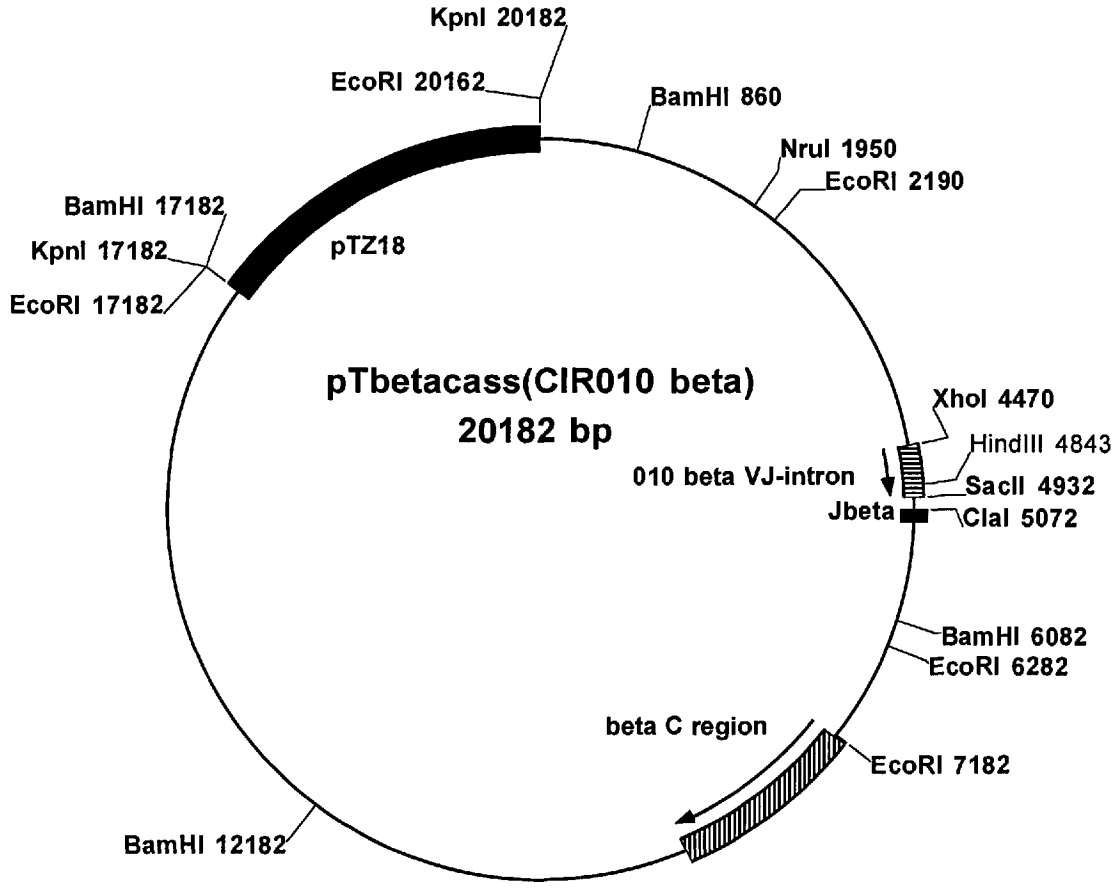


Figure 3.54 Final construct map showing the insertion of the dominant TCRβ chain from the human T cell line CIR010 into the TCR expression vector pTβcass Only the rearranged VJ region (TRBV 6-1 TRBJ 1-1) from the human sequence was inserted as the vector contains a murine Cβ region already, designed to be spliced to the VJ region during mRNA processing to produce a full-length TCR chain gene. As the human VJ region was amplified from cDNA, it was necessary to include the beginning of the intronic sequence immediately downstream of the J region, to allow correct splicing to occur. Restriction sites that were used to create the VJ-intron sequence and to clone the sequence into pTβcass are shown, along with the position of the bacterial sequence required for the propagation of the construct in bacterial culture.

3.2.3 Summary

To summarise, seven constructs were produced for use in the retroviral transduction system:

- MFG (TCR A10(2) α 5-D4)
- MFG (TCR A10(2) α 7-D3)
- MFG (TCR A10(2) β)
- MFG (TCR D3(3) α)
- MFG (TCR D3(3) β)
- MFG (TCR CIR010 α murine Cα)
- MFG (TCR CIR010 β murine Cβ)

Seven constructs were produced for use in the Amaxa transduction system:

- pTαcass (TCR A10(2) α 5-D4)
- pTαcass (TCR A10(2) α 7-D3)
- pTβcass (TCR A10(2) β)
- pTαcass (TCR D3(3) α)
- pTβcass (TCR D3(3) β)
- pTαcass (TCR CIR010 α)
- pTβcass (TCR CIR010 β)

3.3 Transduction of the TCR-negative murine thymoma line BW7 with TCR

3.3.1 Retroviral transduction of BW7 with TCR

3.3.1.1 Overview of the retroviral transduction system

A retroviral transduction system allows stable expression of a gene of interest in a cell type where it is not endogenously found. The system used here (shown as a diagram in Figure 3.55) was first described by Pear et al. (613). It employs a packaging cell line known as EcoPhoenix. The Phoenix line contains two stably integrated retroviral constructs – one that encodes and expresses the gag-pol structural genes but contains a mutated env gene that cannot produce envelope protein, and a second construct that contains a mutated gag-pol region and thus only expresses the env gene. Both constructs are engineered to lack a packaging signal that controls construction of functional viral particles from their individual components, thus preventing the production of functional retrovirus without the addition of this packaging signal. The signal is supplied via transfection with a third plasmid, also containing an extra gene of interest. Upon transfection, the cells produce retrovirus containing the gene of interest; subsequent infection of a target cell line leads to stable expression of the gene in the target cells as the DNA from the construct is integrated into the host cell chromosomes by the action of the retrovirus. The constructs that are part of the packaging cell line are not transmitted hence the retrovirus produced is replication-deficient.

The infectivity of the retrovirus produced by a particular packaging line is dependent upon the envelope protein that it expresses. The four main types of packaging line – ecotropic, amphotropic, dualtropic and pantropic - increase in the number of species and cell types that they can infect from ecotropic to pantropic. Table 3.8 shows the different types of packaging line and the envelope proteins that they express, as well as the receptors on their target cells that they interact with. This determines the target species they can infect.

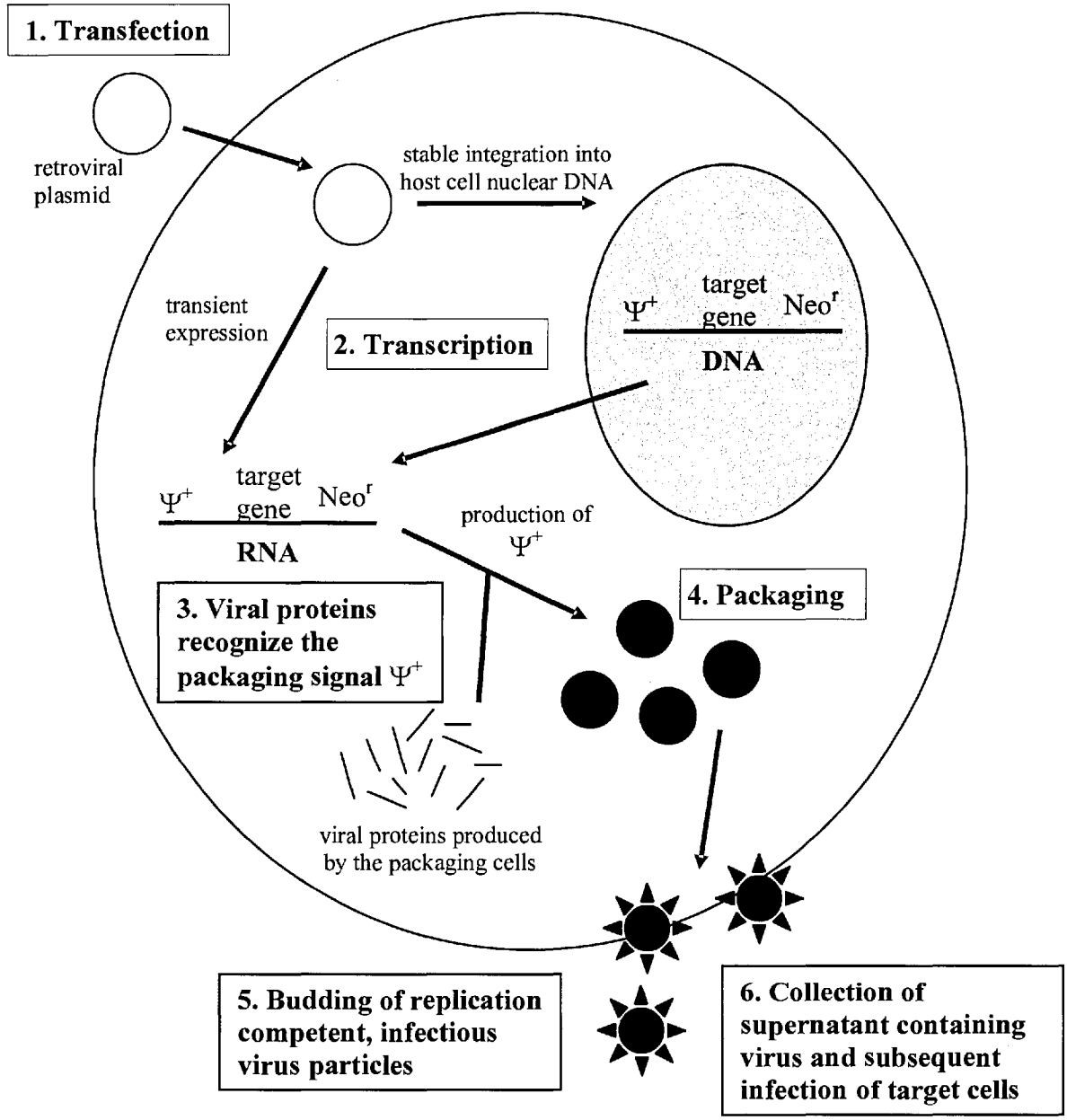


Figure 3.55 Outline of the basis of the Phoenix retroviral transduction system (reference 613) This system allows expression of a gene in a cell type where it would not normally be found. The retroviral vector contains both the gene of interest (or target gene) and also a packaging signal, Ψ^+, that is crucial for the correct packaging of virus into infectious particles. This vector is then transfected into a packaging cell line using one of a number of methods, such as calcium phosphate transfection, electroporation of the use of cationic lipids ('lipofection'). Packaging cell lines have been engineered to contain stably transfected genes for the structural gag, pol and env genes of a particular retrovirus (the Phoenix system makes use of the Moloney murine leukaemia virus or MoMuLV), but they lack the packaging signal Ψ^+. This signal is provided by transcription and translation of the retroviral vector, and is recognized by the viral proteins produced in the cell, upon which the proteins are packaged into viral particles which include the target gene. These particles bud off from the cell membrane into the cell growth media, which can then be harvested and used for the infection of target cells.

Target cells	Envelopes			
	Ecotropic (gap70)	**Amphotropic (4070A)**	**Dualtropic (10A1)**	**Pantropic (VSV-G)**
Rodent (rat, mouse)	+	+	+	+
Human	-	+	+	+
Other mammalian cell types	-	+	+	+
Avian	-	-	-	+
Fish	-	-	-	+
Insect	-	-	-	+

Table 3.8 Packaging cell line types Packaging cell lines are defined by the viral envelope protein that they express, as this determines the range of cell types that the virus they produce can infect. Ecotropic virus has the most limited range of infectivity, as the env protein that it expresses, gap70, is a rodent-specific protein, only capable of infecting rat or mouse cells through the rodent receptor protein mCAT-1 found on the target cell membrane. Amphotropic and dualtropic viruses have a wider range of infectivities, encompassing most mammalian cell types, including rodent cells. They express different envelope proteins – the amphotropic env protein, 4070A, binds to the mammalian receptor protein RAM1 (Pit2), whilst the dualtropic env protein, 10A1, is capable of not only binding to RAM1 but also another mammalian target, GALV (Pit1). This increases its range of potential target cell types over the amphotropic virus, as it may be able to infect cell types on which RAM1 is expressed at a very low level through its second target receptor. Pantropic virus is capable of infecting not only mammalian but also some avian, fish and insect cell lines, giving it by far the widest range of infectivities. This is achieved through its env protein, VSV-G, which does not target a specific protein receptor, but rather lipid components of the plasma membrane such as phosphatidylserine or phosphatidylinositol, which are components of cell membranes of most cell types. VSV-G is toxic to the packaging line that expresses it, and as such it is not stably transfected into the line as in the other packaging lines but is instead co-transfected with the retroviral vector encoding the packaging signal and the target gene.

Examples of previous use of the Phoenix system include investigation of the effects on NK-T cell lineage of overexpression of a transcriptional regulator, Id3 (inhibitor of DNA binding protein 3), in haematopoietic progenitor cells (614). It has also been used to investigate the role of a T cell adaptor protein, SKAP55 (Src kinase associated phosphoprotein of 55 kDa) in adhesion and immune complex formation between T cells and antigen-presenting cells (615), as well as the effect of transduction of myelin basic protein-specific autoreactive T cells with a Th1 cytokine antagonist, the p40 subunit of IL-12, in the EAE model in mice (616).

3.3.1.2 Retroviral vectors

Vectors are available containing the necessary retroviral components and the capacity to incorporate a gene of interest. The vector selected for use in this system was MFG (Figure 2.1), and the production of constructs containing the TCR genes of interest inserted into MFG has been previously described in Section 3.2.1. MFG was chosen for use as it lacks a self-inactivating mutation that is often present in other retroviral vectors and which allows it to be used in a system requiring the use of packaging lines in series, allowing the second packaging line to produce infectious retroviral particles.

3.3.1.3 Optimisation of the system using eGFP

The intrinsically fluorescent protein eGFP was used when designing this system as it could be easily analysed by flow cytometry. The success of individual steps of the protocol could also be monitored on a fluorescent microscope. An initial protocol was designed to discover the best conditions for transduction of BW7. A second target line, NIH3T3, the 'gold standard' cells for optimising retroviral transduction systems, was used as a marker of transduction efficiency. Initial parameters tested included original plating density of the EcoPhoenix cells before transfection and the retroviral vector used (MFG or pQC). Efficiency of infection was compared between BW7 and NIH3T3 cells when infected directly with supernatant harvested from EcoPhoenix cells, or when infected with supernatant harvested from the dualtropic line PT67 that had been infected with EcoPhoenix supernatant. The initial protocol followed is shown in Table 3.9.

	EcoPhoenix	PT67	Target cells (BW7 and 3T3)
Day			
0	Plate cells at required density		
1	Transfect cells with 10μg retroviral vector, using calcium phosphate in the presence of 25 μM chloroquine		
2		Plate cells at required density	(3T3 only) Plate cells at required density
3	Collect retroviral supernatant and infect target cells	Infection with retroviral supernatant (EcoPhoenix)	Infect with retroviral supernatant (EcoPhoenix)
4			Grow cells as normal until analysis by FACS at 48h post-infection
5			(3T3 only) Plate cells (previously uninfected) at required density
6		Collect retroviral supernatant and infect target cells	Infection with retroviral supernatant (PT67)
7			Grow cells as usual until FACS analysis
8			Analyse cells for gene expression by FACS

Table 3.9 A simple representation of the retroviral system being tested On day 0, EcoPhoenix cells were plated in 25 cm^2 tissue culture flasks at densities of 0.5, 1 and 1.5 x 10^6 24 hours prior to transfection on day 1. Cells were incubated with 25 μM chloroquine for 30 minutes before transfection if required, and transfection mixes containing 10 μg of the relevant retroviral vector were prepared. This mix was added to the cells, which were then incubated at 37°C and 5% CO_2, and the mix was removed after 8 hours (to prevent damage to the cells from the toxic chloroquine). Supernatant was harvested from the cells 48 hours after transfection and used to infect one of three target lines – NIH3T3, BW7, the ultimate target line, and a second packaging line, PT67. NIH3T3 and PT67 cells were plated at a density of 1 x 10^5 cells 18 hours before infection. In each case, infection occurred in the presence of 4 μg/ml polybrene – PT67 cells were infected using undiluted supernatant, whilst NIH3T3 and BW7 cells were infected with supernatant diluted to 1 in 10. BW7 cells were infected by 'spinoculation'; cells were centrifuged in the presence of polybrene and retroviral supernatant for 90 minutes at 2000 rpm at 32°C. All cells were then incubated at 37°C and 5% CO_2. Target cells were then grown normally until they were analysed by FACS. Retroviral supernatant from the PT67 line was harvested after 72 hours and used to infect NIH3T3 cells (plated 18 hours previously) and BW7 cells as before. Cells were harvested 48 hours after the second infections and analysed by FACS.

Figure 3.56 shows the results obtained using the protocol outlined in Table 3.9 and the retroviral vector pQC(eGFP). Cells were analysed for eGFP expression by flow cytometry 48 hours after infection. It was apparent that EcoPhoenix supernatant derived using pQC(eGFP) was unable to infect BW7 cells under any of the conditions tested, despite infecting the NIH3T3 cells to a maximum of 21.7% when using the highest original density of EcoPhoenix cells. This in itself was not optimal as transduction levels of over 70% should be achieved in NIH3T3 cells. In addition, as expected when using packaging lines in series with this vector, no transduction of the target line is seen, hence pQC is not a useful vector for use in this system. As EcoPhoenix supernatant appears to be unable to infect BW7 cells directly, a serial system of packaging lines would be required, precluding the use of pQC in the system.

Figure 3.57 shows the results obtained using the protocol in Table 3.9 using only the highest original density of EcoPhoenix cells (1.5×10^6) and comparing the efficiency of infection using MFG(eGFP) with that of pQC(eGFP). The results here were more encouraging; whilst EcoPhoenix supernatant was unable to infect BW7 cells directly using MFG as the transfected vector, the serial system involving both EcoPhoenix and PT67 led to 23.9% infection of the target line BW7 with eGFP. The corresponding level of NIH3T3 cell infection was 57.9%, a level close to what is considered to be optimal. It appears that the system involving transfection of EcoPhoenix cells with the retroviral vector MFG, using EcoPhoenix supernatant to infect a second packaging line, PT67, and using the resulting supernatant from this line to infect BW7, results in successful transduction of the target line. Whilst 23.9% is considerably lower than the 'optimal' level of transduction of approximately 70%, it is significant and should allow for successful transduction of BW7 cells with TCR genes.

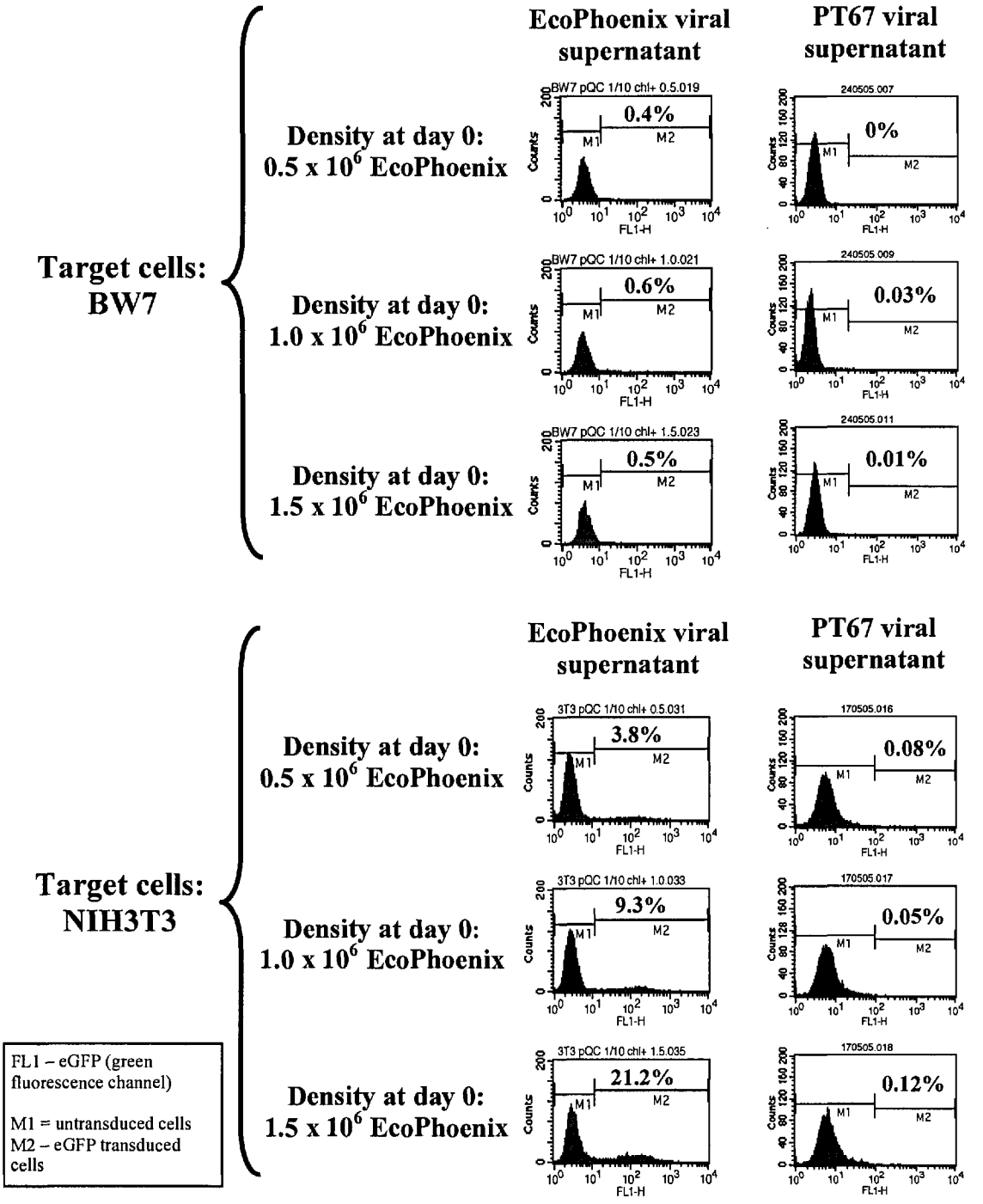


Figure 3.56 Transduction of the target lines BW7 and NIH3T3 with eGFP using pQC(eGFP) and retroviral supernatant harvested from the EcoPhoenix packaging cell line or the PT67 packaging cell line Transductions occurred according to the protocol outlined in Table 3.9. The PT67 packaging line was transduced with the eGFP gene through infection with EcoPhoenix supernatant as this was determined to be the best way to achieve transduction in this line. EcoPhoenix supernatant alone could not transduce the BW7 line with eGFP, despite successfully transducing the NIH3T3 line with eGFP at the highest original plating density. Using the serial transduction system with PT67 was unsuccessful in transducing either line with eGFP using this vector.

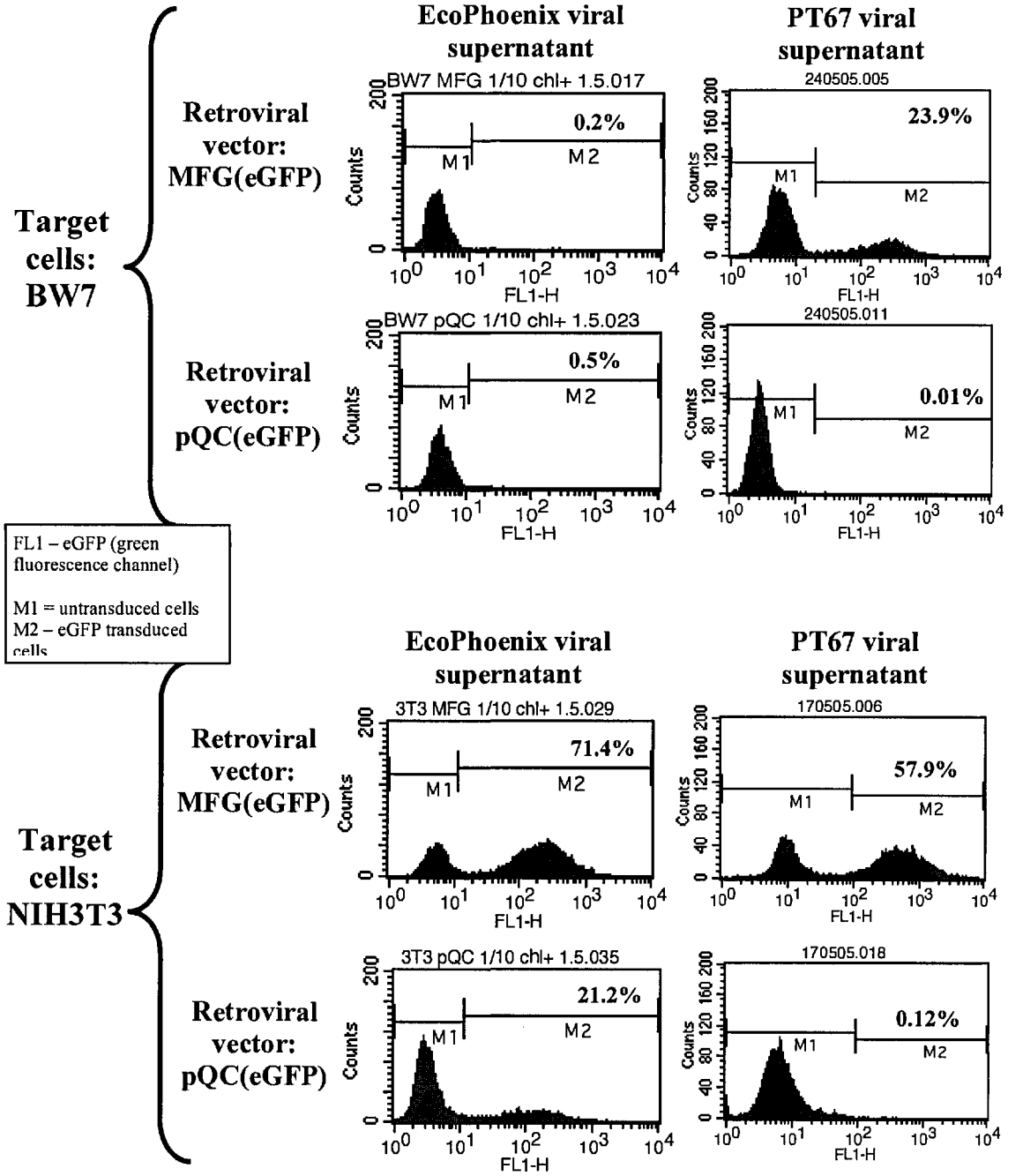


Figure 3.57 Transduction of the target lines BW7 and NIH3T3 with either pQC(eGFP) or MFG(eGFP) using retroviral supernatant harvested from the EcoPhoenix packaging cell line or the PT67 packaging cell line Transductions occurred according to the protocol outlined in Table 3.9. The original density of EcoPhoenix cells was 1.5 x 10^6. The PT67 packaging line was transduced with eGFP through infection with EcoPhoenix supernatant as before. EcoPhoenix supernatant alone could not transduce the BW7 line with eGFP using either vector, despite both vectors successfully transducing the NIH3T3 line with eGFP at the highest original plating density. Using the serial transduction system with PT67 was successful in transducing both target lines with eGFP only when using the vector MFG.

An additional experiment, shown in Figure 3.58, investigated the persistence of the target gene expression over the first 96 hours following infection. Retroviral transduction can give rise to stable integration of the target gene into the host cell chromosomes, but if this does not occur, transduction is transient as the plasmid is eventually lost from the cells or not transferred during cell division so that transduced cells become an increasingly smaller population within the culture. NIH3T3 cells were transduced with eGFP using the conditions previously found to give the highest level of transduction of this line, and cells were analysed by flow cytometry at 24 hour intervals starting 24 hours after infection until 96 hours after infection. At 24 hours after transduction, 79.00% of NIH3T3 cells were expressing the eGFP gene, and this level of transduction persisted for the course of the experiment, with approximately 80% of cells showing expression of eGFP throughout. This suggests that the transduction of target cells using this system is stable, as no decrease in target gene expression was seen in the days after the infection. A transiently transduced line would be expected to show a gradual decrease in target gene expression during the same time frame.

A modified protocol was designed for use in transducing BW7 with TCR genes, as shown in Table 3.10. This protocol incorporated the conditions that gave the highest level of BW7 transduction with eGFP, including using the serial system with both EcoPhoenix and PT67 packaging lines, using the highest original plating density of EcoPhoenix and using the MFG retroviral vector.

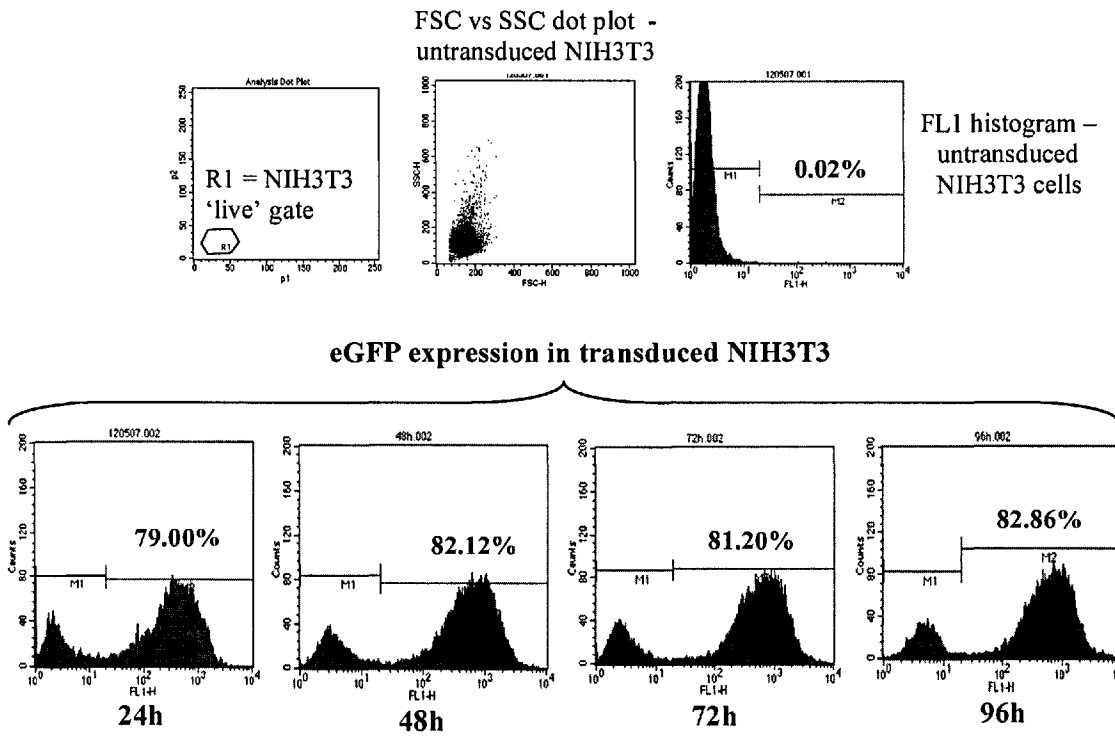


Figure 3.58 eGFP expression in NIH3T3 cells transduced according to the optimised retroviral transduction system outlined in Table 3.9 The top panels show the forward scatter-side scatter properties of NIH3T3 cells, and the gate that corresponds to live NIH3T3 cells. The top right-hand panel shows fluorescence in the FL1 (green) channel of untransduced NIH3T3 cells, showing that NIH3T3 cells have no intrinsic fluorescence in this channel, as demonstrated by the lack of cells in the M2 region (corresponding to eGFP-transduced cells in the lower panels). The lower panels show the level of eGFP expression in transduced NIH3T3 cells. Expression was analysed by flow cytometry 24, 48, 72 and 96 hours after the final infection with supernatant from PT67 cells. The initial level of eGFP expression in NIH3T3 cells at 24 hours was 79%, indicating that the system being used was capable of achieving high levels of transduction in these cells. Over the four time points, expression of eGFP in this line remained steady at approximately 80% (the percentage of cells from gate R1 in M2), suggesting that transduction of the cells was stable.

	EcoPhoenix	PT67	Target cell – BW7
Day			
0	Plate cells at density of 1.5×10^6		
1	Transfect cells with 10μg MFG, using calcium phosphate, in the presence of 25 μM chloroquine for 8 hours		
2		Plate cells at density of 1×10^5	
3	Collect retroviral supernatant and infect target cells	Infection with retroviral supernatant – undiluted – in the presence of 4μg/ml polybrene	
4/5			
6		Collect retroviral supernatant and infect target cells	Infection with retroviral supernatant – 1 in 10 dilution - in the presence of 4μg/ml polybrene
7			Analyse cells for gene expression by FACS
8			Analyse cells for gene expression by FACS
9			Analyse cells for gene expression by FACS
10			Analyse cells for gene expression by FACS

Table 3.10 The protocol used to transduce the target line BW7 with the D3(3) TCR EcoPhoenix cells were plated on day 0 at a density of 1.5×10^6 24 hours prior to transfection on day 1. Cells were incubated with 25 μM chloroquine for 30 minutes before transfection, whilst transfection mixes containing 10 μg of the relevant retroviral vector (MFG with TCR chain gene inserted) were prepared. This mix was added to the cells, which were then incubated at 37°C and 5% CO_2, and the mix was removed after 8 hours (to prevent damage to the cells from the toxic chloroquine). Supernatant was harvested from the cells 48 hours after transfection and used to infect the second packaging line, PT67, which had been plated at a density of 1×10^5 cells 18 hours before infection. Infection occurred using undiluted supernatant in the presence of 4 μg/ml polybrene. Retroviral supernatant from the PT67 line was harvested after 72 hours and used to infect BW7 cells by 'spinoculation', in the presence of 4 μg/ml polybrene, as described previously. Cells were harvested at 24, 48, 72 and 96 hours after the second infection and analysed for TCR gene expression by FACS. Transfection with eGFP was carried out as a positive control.

3.3.1.4 Retroviral transduction of the line BW7 with genes encoding the TCR from the PLP_{56-70}-specific murine T-cell clone D3(3)

The protocol outlined in Table 3.10 was used to transduce BW7 cells with the retroviral constructs MFG (TCR D3(3)α) and MFG (TCR D3(3)β) (5 μg of each). The cells were analysed after infection with PT67 retroviral supernatant by flow cytometry. Figure 3.59 shows the analysis at 48 hours after infection. The cells were stained with two antibodies – the first an antibody specific for the D3(3) TCRβ chain V region, FITC-conjugated anti-Vβ4-antibody (Vβ4 corresponds to the IMGT TRBV 2). The second antibody was a general PE-conjugated anti-TCR Cβ region antibody, which should be capable of recognising any expressed αβ TCR. As shown in Figure 3.59, a slight shift in fluorescence intensity is seen when staining TCR-transduced BW7 cells with the anti-Vβ4 antibody as compared with untransduced cells stained with the same antibody. This may suggest that a small number of BW7 cells have been successfully transduced with the D3(3) TCR. Staining with the anti-TCR Cβ antibody gives a much less clear answer – as the lower left-hand panel of Figure 3.59 shows, even in untransduced BW7 cells, there is a high level of staining with this antibody. As the cell line does not express TCR endogenously, this staining is likely to be non-specific binding to the cells. In the TCR-transduced lines, the peak of staining with this antibody appears to shift backwards when compared to the untransduced cells, which is unexpected, as TCR expression would be expected to increase antibody staining. Due to the high level of non-specific staining seen with this antibody, however, it is unlikely that any specific staining would be obvious, particularly if the level of transduction is low, as suggested by the anti-Vβ4 staining. As a difference between the transduced and untransduced cells can be seen using the antibody that is specific to the D3(3) TCR, this antibody was used in further analysis of D3(3) TCR-transduced lines.

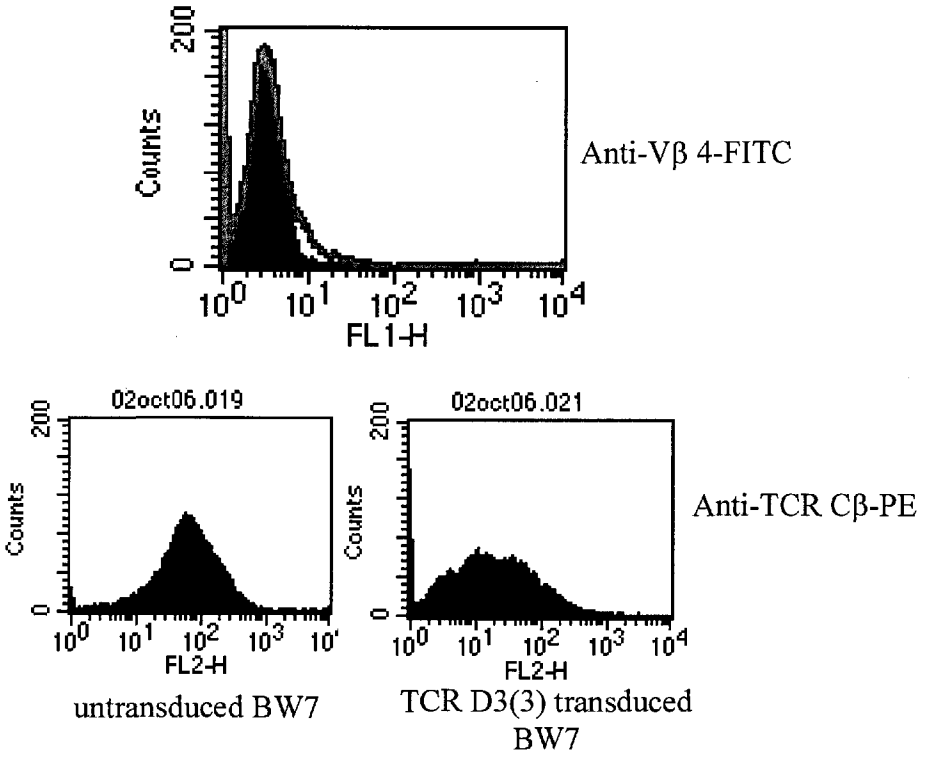


Figure 3.59 Expression of TCR D3(3) on transduced BW7 Using an anti-Vβ 4 FITC-conjugated antibody, which is specific for the D3(3) TCR, and a general anti-TCR Cβ PE-conjugated antibody, the expression of TCR on BW7 cells transduced with MFG plasmid encoding the D3(3) TCR α and β chain genes was analysed by flow cytometry. The top histogram shows anti-Vβ 4 staining on untransduced BW7 (filled histogram) overlaid with anti-Vβ 4 staining on TCR D3(3) transduced BW7 (open histogram). A very slight shift in fluorescence can be seen. The bottom panels show anti-TCR Cβ staining on untransduced BW7 (right-hand panel) and TCR D3(3) transduced BW7 (left-hand panel). The high fluorescence intensity of staining shown in the untransduced, TCR-negative BW7 cells suggests a high level of non-specific staining – a shift in the pattern of staining is seen in the transduced cells, but rather than increasing staining intensity, as would be expected if cells were successfully transduced, the staining appears to have decreased in intensity. Antibodies used in staining are shown in Appendix 7.

As the level of transduction suggested by the anti-Vβ4 staining is very low, the transduced line was cloned by limiting dilution, and individual clones were analysed by staining with the same anti-Vβ4 antibody after 14 days of growth. Figure 3.60 shows the analysis for two representative clones, A6(4) and A5(4). When analysing the culture as a whole (as shown in the FL-1 histograms marked 'No gate'), it appeared that in both clones there were two populations of cells, one staining with the antibody and one not i.e. there was a transduced population of BW7 cells expressing the D3(3) TCR. However, when looking at a forward scatter vs. side-scatter dot plot of BW7 cells (as seen in the top right-hand panel), there are two clear populations of cells in the culture, labelled R1 and R2. R1 is the region thought to correspond to live cells in the culture, whilst R2 is thought to contain predominantly dead or dying cells. When these regions were applied as gates to the two clones, shown in the lower panels of Figure 3.60, it was seen that the 'Vβ4-positive' population was only found in R2, and not the live region R1. As such, the increase in fluorescence was more likely to come from the natural autofluorescence seen in dead or dying cells.

It is possible that successful transduction of the cells with a target gene could alter the forward scatter-side scatter characteristics of the cells such that they might appear in the region associated with dead or dying cells. D3(3) transduced BW7 cells were stained with propidium iodide (PI), a stain that is taken up by dead cells, causing them to fluoresce in the FL-2 (red) channel. The two populations R1 and R2 were then analysed individually, as shown in Figure 3.61a. In both populations, there was a certain proportion of PI-positive cells, 46.7% in R1 and 89.7% in R2. The staining seen in population R1, the 'live' gate, could be due to a slight overlap between the populations. The much higher proportion of PI-positive cells in R2 confirms that this population consists primarily of dead and dying cells. However, as not all cells in R2 stained with PI (again, this could possibly be due to overlap with R1 or due to the presence of live cells in R2), there was a possibility that the non-staining and therefore alive cells could be the TCR-transduced cells. Figure 3.61b shows the same culture of cells stained with both PI and the FITC-conjugated anti-Vβ4 antibody, again analysed as separate populations. PI staining was only seen in population R2, whilst little anti-Vβ4 staining was seen in either population; however, there appeared to be a slight increase in this staining seen in population R2, suggesting that the TCR-transduced cells might be found in this region.

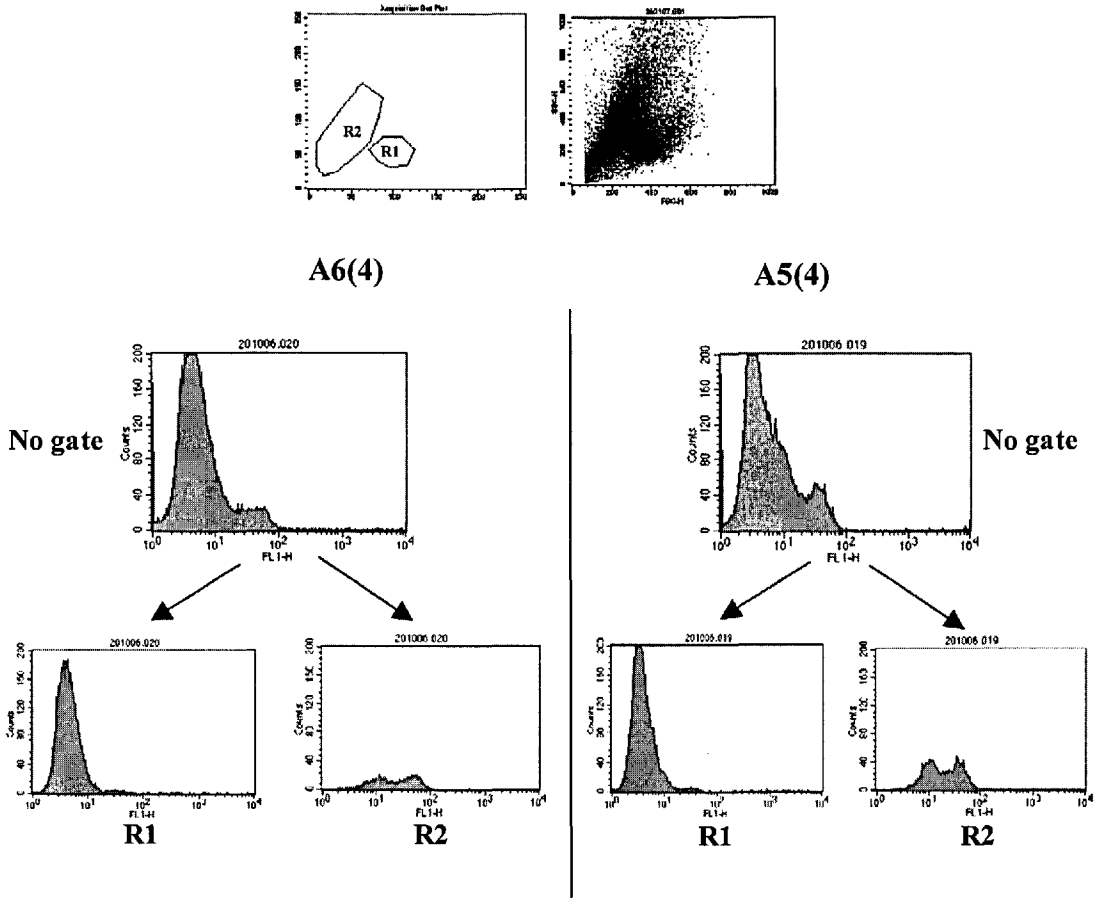


Figure 3.60 Analysis of TCR D3(3) expression in clones derived from the D3(3) transduced BW7 line Analysis was carried out using a D3(3) TCR specific anti-Vβ4 antibody conjugated to FITC (FL-1 channel). The top panel shows a representative forward scatter vs side scatter dot plot for these cells (right-hand side) and a diagram defining the populations R1 and R2 (left-hand side). Two clones, A6(4) (left-hand panels) and A5(4) (right-hand panels), derived from limiting dilution of the original transduced line are shown in the lower panels. Data was initially obtained on samples with no gate applied i.e. every cell shown in the dot plot in the top panel was counted and analysed as shown in the histograms labelled 'no gate'. In each case, there appears to be a population of cells staining positively for the antibody. When the cells in each region, R1 and R2, are analysed separately however (lower panels), it can be seen that the 'positive' population is found in region R2, the region found to contain dead and dying cells, and so this staining is likely to be an artefact. Antibodies and chemicals used in staining are shown in Appendix 7.

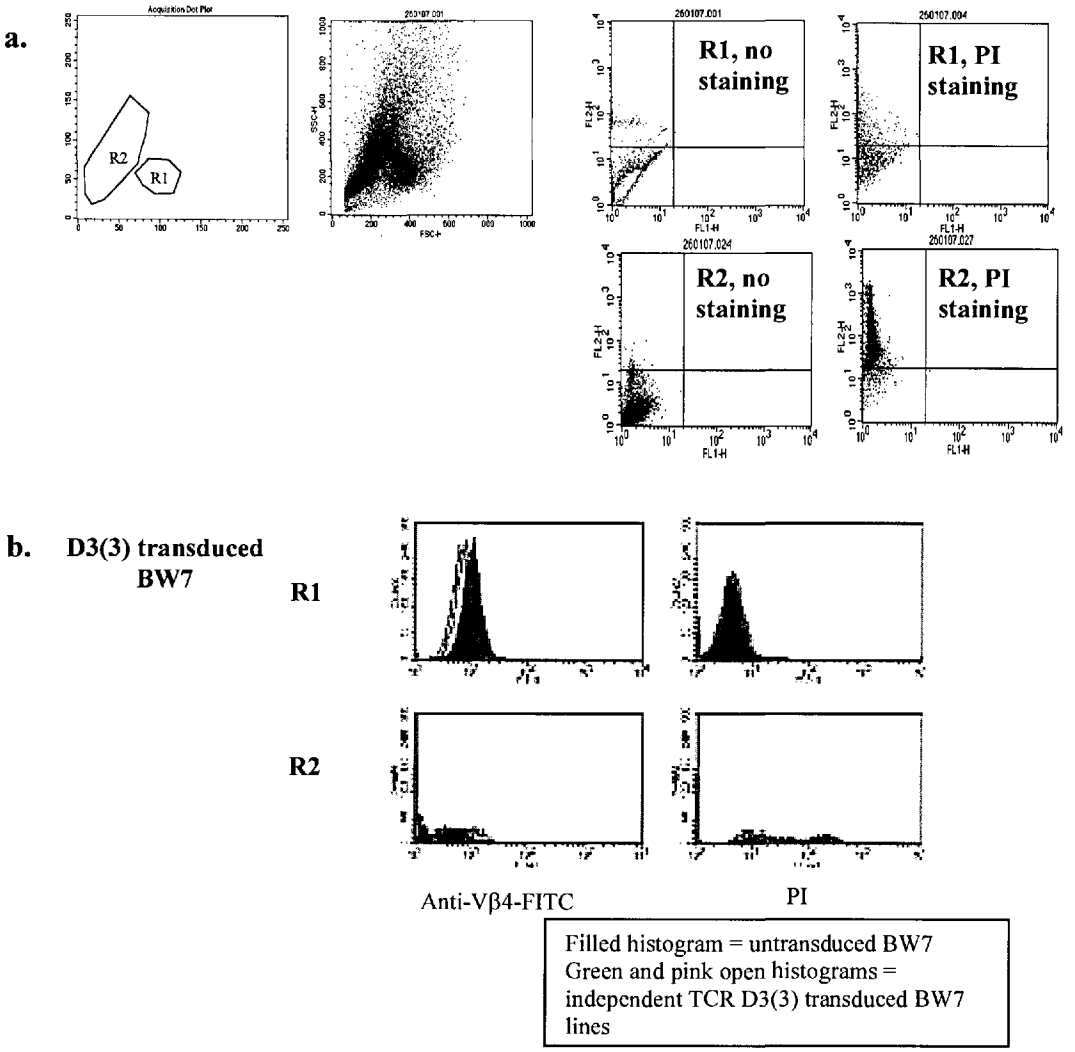


Figure 3.61 Characterisation of the disparate BW7 populations defined on the basis of their light scattering properties. As can be seen in the left-hand panel of a, BW7 cells in a typical forward-scatter vs side-scatter plot divide into two distinct populations (labelled R1 and R2). When staining untransduced BW7 cells with the cell death marker propidium iodide, which is detected in the red fluorescence channel FL-2, and gating on and compensating for each population separately, as shown in the right-hand panels of a, there is a higher proportion of PI staining in R2 than R1 (89.7% of cells are in the upper left quadrant in the R2 plot compared with only 46.7% in the corresponding quadrant in the R1 plot).This suggests that the region R2 corresponds to dead or dying cells, whose light-scattering properties have changed accordingly. Staining both populations in TCR transduced BW7 for specific Vβ region or PI is shown in b. D3(3) transduced BW7 (open histograms, each histogram corresponds to an independent transduction) are compared with untransduced BW7 (filled histograms). In region R1, containing live cells, there is little PI staining in any line, and there is no increase in anti-Vβ staining, suggesting transduction has failed. In region R1, containing the majority of dead cells, whilst there is, as expected, an extensive amount of PI staining, there is also a potential increase in staining with the anti-Vβ4 antibody in the transfected lines. All antibodies and chemicals used in staining are shown in Appendix 7.

In order to finally confirm if retrovirally transduced BW7 cells did change their forward scatter-side scatter characteristics such that they then appeared in the R2 population of dead and dying cells, eGFP transduced cells were stained with PI and analysed as described above, and as shown in Figure 3.62. The populations R1 and R2 were analysed separately. The lower panels of the figure show FL1 (corresponding to eGFP fluorescence) and FL2 (corresponding to PI fluorescence) dot plots of the two populations (R1 on the left, R2 on the right). PI-positive cells are those in the upper two quadrants of the dot plots, eGFP-positive cells are those in the right-hand quadrants. Although the level of eGFP expression in these lines was low (only 3%), this was a high enough level to show that eGFP-positive cells were only seen in population R1, in the lower right-hand quadrant of the plot. No corresponding eGFP-positive population was seen in the lower right-hand quadrant of the dot plot for population R2. This therefore suggests that the process of retroviral transduction does not in itself alter the light-scattering properties of the cells, and transduced cells reside in the region corresponding to live cells. The apparent increase in fluorescence intensity seen in R2 in TCR-transduced lines is therefore likely to be due a non-specific staining artefact, although it cannot be ruled out that transduction with a construct leading to the expression of a surface TCR might change the properties of the transduced cells in a different way to intracellular eGFP expression.

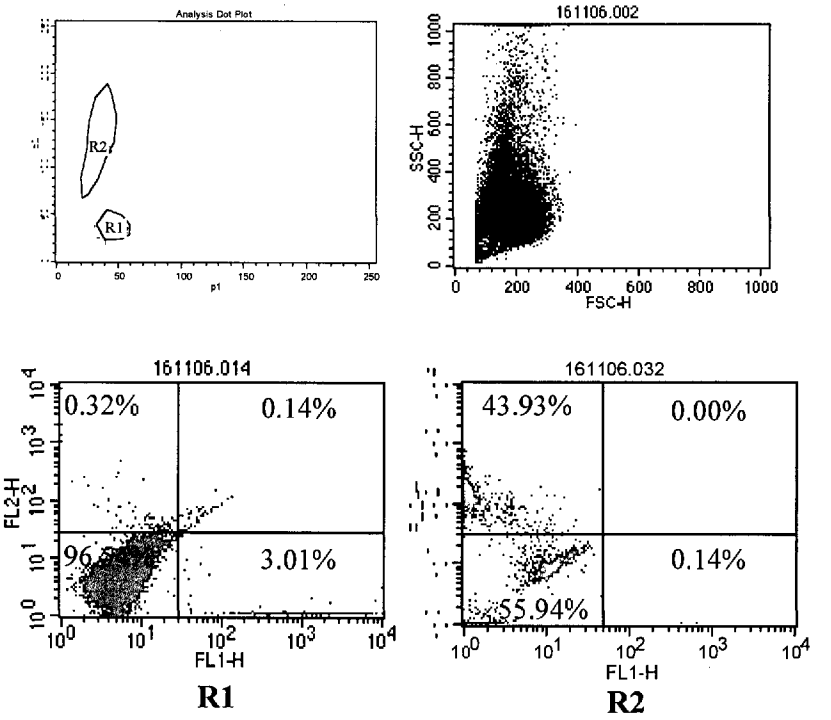


Figure 3.62 eGFP expression in disparate populations of transduced BW7 cells
The top left-hand panel shows the definition of the two populations, R1 and R2, according to their light-scattering properties; a representative dot plot is shown in the top righthand panel. The lower panels show FL1 vs FL2 dot plots obtained from an eGFP-transduced BW7 line, gating on and compensating for R1 (green, right) or R2 (pink, left). The lower right quadrant of each plot shows the live, eGFP-transduced cells. In R2, 3.01% of BW7 cells are positive for eGFP; in R3, this figure is negligible, suggesting that transduced BW7 are found in the same population as live untransduced cells, and their physical properties (size and granularity) are not affected by the process of transduction itself.

3.3.1.5 Use of a modified retroviral transduction protocol to transduce the line BW7 with genes encoding the TCRs from the PLP_{56-70}-specific murine T-cell clones A10(2) and D3(3)

As the previous protocol appeared to be unable to successfully transduce BW7 cells with TCR genes, a new protocol was designed with the help of Dr. Hongyan Wang, Imperial College, London, based on the protocol she had determined to be optimal for the transduction of cell lines using the Phoenix retroviral packaging system, and then adapted to accommodate the use of the second packaging line, PT67, after initial transfection of the EcoPhoenix line with the MFG retroviral constructs. The protocol is shown in Table 3.11, and involves infecting the target line BW7 on four successive days with retroviral supernatant from the PT67 line. In order to achieve this, two rounds of transfection of EcoPhoenix (newly re-selected cells provided by Professor Julian Dyson were used to ensure optimum levels of transfection and retrovirus production) occurred two days apart using a total of 20 μg of vector for each transfection. Supernatant was collected on two occasions, at 36 and 60 hours after initial transfection, and used to infect PT67 cells (also newly re-selected). Supernatant harvested from the first transfection of EcoPhoenix cells was used to infect one culture of PT67 cells, and supernatant from the second transfection was used to infect a second culture of PT67 cells. Supernatant was then collected from PT67 cells at 48 and 72 hours after infection and used to infect BW7 cells. In contrast to the previous protocol, all infections were carried out using undiluted supernatant. In addition, the 'spinoculation' used for the infection of BW7 cells was modified to be less harsh – the previous procedure led to a high level of cell death, and a reduced yield of cells for flow cytometric analysis. The new procedure involved spinning cells at a lower speed for less time, yielding a higher level of cell survival after infection.

The new protocol was initially tested using eGFP transduction in both BW7 and NIH3T3 cells. The results are shown in Figure 3.63 for both cell types (NIH3T3 in the upper panels, BW7 in the lower panels). Use of the new system yielded 65.5% transduction of NIH3T3 cells at 24 hours after the final infection, compared with 19.5% transduction of BW7 cells (subsequent transductions using eGFP showed expression in up to 44.5% of BW7 cells). These levels are higher than those seen initially using the first optimised protocol, and so this protocol appeared to be more efficient in transducing the line BW7.

	EcoPhoenix	PT67	Target cell – BW7
Day			
0	Plate cells at density of 1 x 10^6		
1	Transfect cells with 10μg retroviral vector, using calcium phosphate, in the presence of 25 μM chloroquine for 8 hours	Plate cells at density of 1 x 10^5	
2	Plate cells at density of 1 x 10^6 Collect retroviral supernatant and infect target cells	Infection with retroviral supernatant – undiluted – in the presence of 4μg/ml polybrene	
3	Transfect cells with 10μg retroviral vector, using calcium phosphate, in the presence of 25 μM chloroquine for 8 hours Collect retroviral supernatant and infect target cells	Infection as on day 2 Plate cells at density of 1 x 10^5	
4	Collect retroviral supernatant and infect target cells	Infection as on day 2	
5	Collect retroviral supernatant and infect target cells	Infection as on day 2 Collect retroviral supernatant and infect target cells	Infection with retroviral supernatant – undiluted - in the presence of 4μg/ml polybrene
6		Collect retroviral supernatant and infect target cells	Infection as on day 5
7		Collect retroviral supernatant and infect target cells	Infection as on day 5
8		Collect retroviral supernatant and infect target cells	Infection as on day 5
9-12			Analyse cells for gene expression by FACS

Table 3.11 The modified protocol used to transduce the target line BW7 with the D3(3) and A10(2) TCRS Newly re-selected EcoPhoenix cells were plated on day 0 and day 2 (shown in blue) at a density of 1 x 10^6 cells 24 hours prior to transfection on day 1 or day 3. Cells were incubated with 25 μM chloroquine for 45 minutes before transfection, whilst transfection mixes containing 20 μg of the relevant retroviral vector were prepared and left to stand at room temperature for at least 30 minutes. This mix was added to the cells, which were then incubated at 37°C and 5% CO_2, and the mix was removed after 8 hours. Supernatant was harvested from the cells 36 hours after transfection (on days 2 and 4) and used to infect the second packaging line, PT67, which had been plated at a density of 1 x 10^5 cells 18 hours before infection (on days 1 and 3). A second collection of EcoPhoenix supernatant occurred 60 hours after transfection and used to infect the same culture of PT67 as the first supernatant. Undiluted supernatant was used for infection in the presence of 4 μg/ml polybrene. Supernatant from the PT67 cultures was harvested 72 and 96 hours after initial infection and used to infect BW7 cells – cells were centrifuged at 1800 rpm for 30 minutes at room temperature in the presence of 4 μg/ml polybrene. Cells were harvested 24, 48, 72 and 96 hours after the final infection and analysed for TCR gene expression by FACS. Transfection with eGFP was carried out as a positive control.

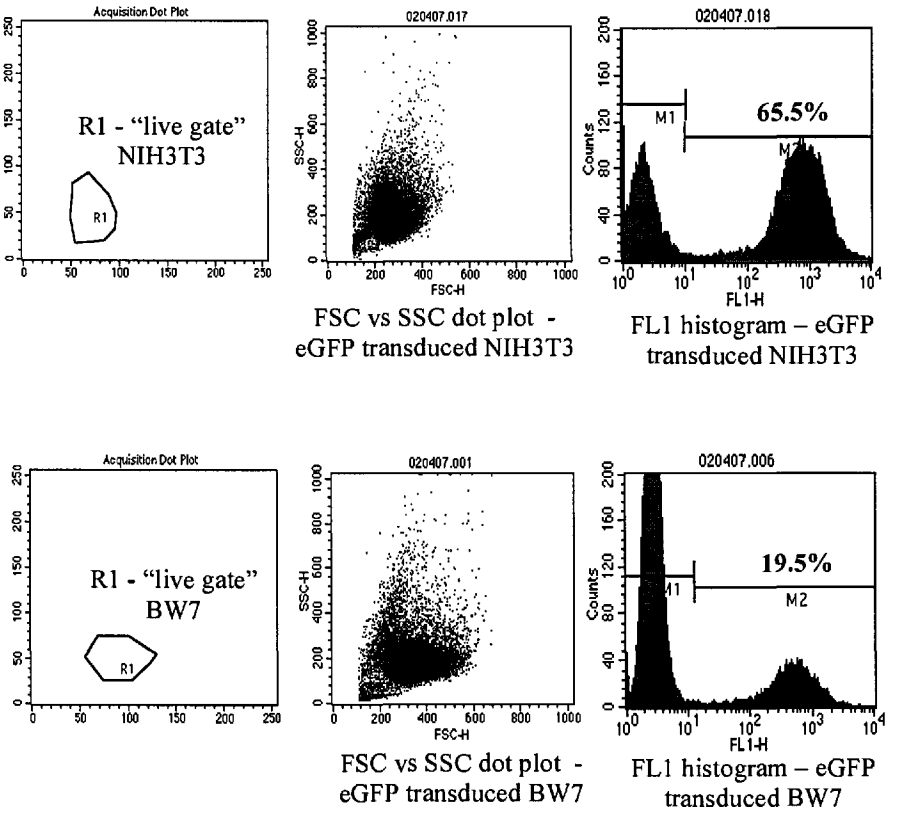
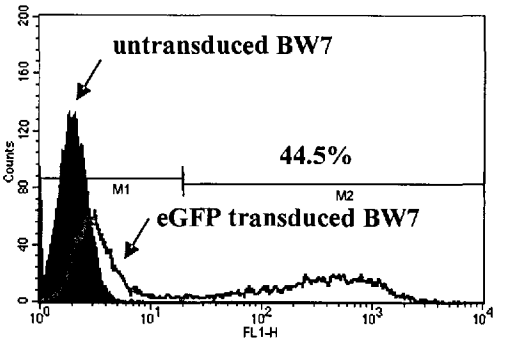


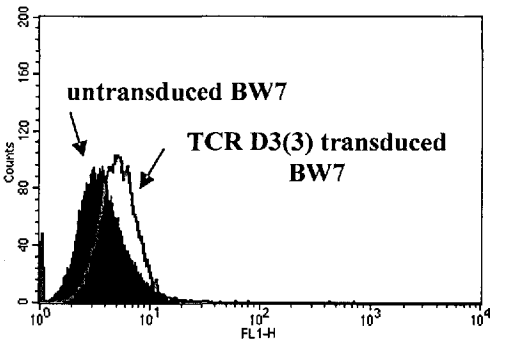
Figure 3.63 eGFP expression in NIH3T3 and BW7 cells transduced according to the modified retroviral transduction system outlined in Table 3.11 The top panels show the level of eGFP expression (65.5%) in transduced NIH3T3 cells (right-hand panel) when infected by supernatant from PT67 cells, 24 hours after the final infection. Forward scatter-side scatter properties of NIH3T3 cells, and the gate that corresponds to live NIH3T3 cells are shown in the left-hand panels. The lower panels show the level of eGFP expression in transduced BW7 cells, as a comparison with the level of transduction obtained in the 'gold standard' line NIH3T3. Expression of eGFP 24 hours after the final infection with supernatant from PT67 cells was at 19.5% in these cells. Whilst being only approximately one-third of the level achieved in NIH3T3 cells, this is nonetheless a reasonable level of transduction.

This protocol was then used to transduce the BW7 cells with the TCR from the clone D3(3) (in this case, 10 μg of α construct and 10 μg of β construct were used making a total of 20 μg retroviral construct per transfection). Flow cytometric analysis of the cells 24 hours after the final infection is shown in Figure 3.64. TCR transduced cells were stained with FITC-conjugated anti-Vβ4 antibody as before (upper left-hand panel). Transduction with eGFP is shown as a comparison (upper right-hand panel). As can be seen for the TCR-transduced cells, there is a small shift in the fluorescence intensity of the anti-Vβ4 staining in the transduced cells compared with the untransduced cells. The shift is not large, but is greater than that seen when using the original protocol, suggesting that this system may have allowed successful transduction of the line BW7 with the D3(3) TCR. The lower panel in Figure 3.64 shows the same transduced line, again stained with anti-Vβ4 antibody, 15 days after the final infection with retroviral supernatant. A similar shift in fluorescence intensity is seen, suggesting that transduction is stable.

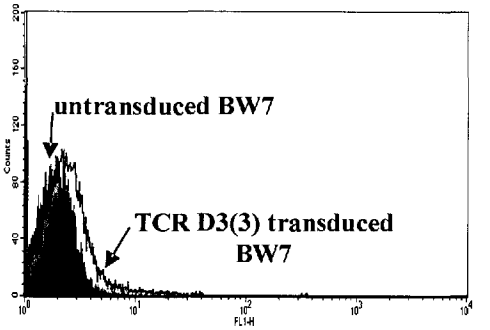
The same protocol was then used to transduce the BW7 cells with the two possible TCRs from the clone A10(2) (either the TCRα 5-D4 or TCRα 7-D3 chain with the common TCRβ chain). Figure 3.65 shows the flow cytometric analysis of the cells 24 hours after the final infection. TCR transduced cells were stained with FITC-conjugated anti-Vβ13 antibody (Vβ13 corresponds to the IMGT-defined TRBV 14) as shown in the left-hand panels of the figure, with TCRα 5-D4 TCRβ being shown in the upper panel and TCRα 7-D3 TCRβ being shown in the lower panel. Transduction with eGFP is shown as a comparison (upper right-hand panel). However, in this case, no positive shift is seen for either TCR-transduced line; instead, as was seen with the anti-TCR Cβ antibody used previously on the D3(3) TCR-transduced lines, the peak of staining shifts backwards, meaning it is impossible to tell from the staining whether transduction has been successful. The anti-Vβ 13 antibody, like the anti-TCR Cβ antibody, appears to stain BW7 cells non-specifically to a significant degree.



eGFP transduced BW7 – FL1 histogram – no staining -24h



TCR D3(3) transduced BW7 – FL1 histogram – anti-Vβ4-FITC staining – 24h



TCR D3(3) transduced BW7 – FL1 histogram – anti-Vβ4-FITC staining – 15 d

Figure 3.64 Expression of the TCR D3(3) in transduced BW7 cells BW7 cells were transduced with the α and β chains for the D3(3) TCR according to the protocol outlined in Table 3.11. Transduction with eGFP was carried out as a positive control. The filled histograms represent untransduced BW7 cells, either unstained (left-hand panel) or stained with anti-Vβ 4-FITC (right-hand panels), the open histograms represent the transduced cells. Expression of eGFP is shown in the left-hand plot as an FL1 histogram 24 hours after the final infection, showing that 44.5% of BW7 cells were expressing eGFP at this time point, and that the system had worked in this instance. The right hand panels show TCR D3(3)-transduced BW7 cells stained with anti-Vβ 4-FITC as an FL1 histogram. The upper panel shows expression levels 24 hours after the final infection. The shift seen is not easily quantifiable as a measure of TCR expression, but it indicates that the transduced cells may be expressing TCR to some degree. The lower right-hand panel shows expression levels 15 days after the final infection, showing that a shift in staining is still appreciable in this line, and suggests that the line may be stably transduced with TCR. All antibodies used for staining are shown in Appendix 7.

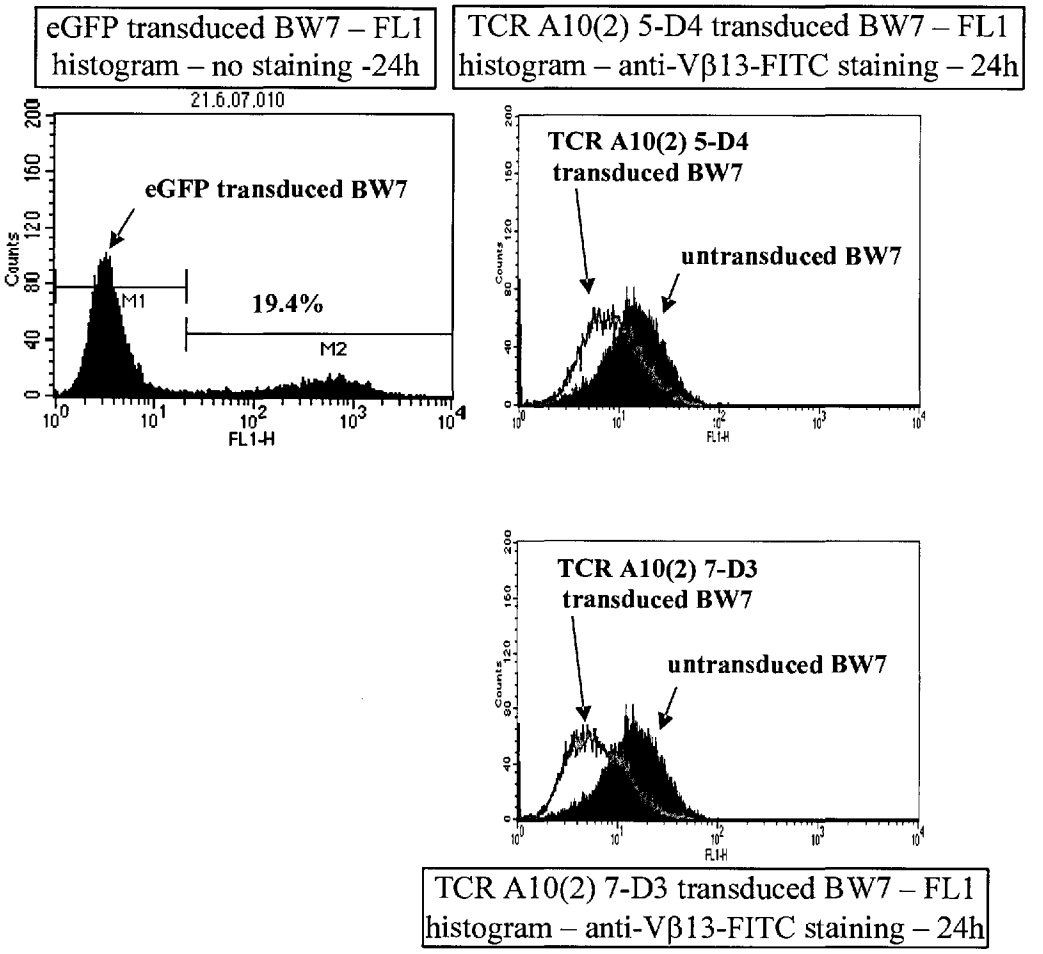


Figure 3.65 Expression of the TCRs A10(2) 5-D4 and A10(2) 7-D3 in transduced BW7 cells BW7 cells were transduced with the α and β chains for the A10(2) TCRs according to the protocol outlined in Table 3.11. Transduction with eGFP was carried out as a positive control. The filled histograms represent untransduced BW7 cells, either unstained (left-hand panel) or stained with anti-Vβ 13-FITC (right-hand panels), the open histograms represent the transduced cells, stained as described for the untransduced cells. Expression of eGFP is shown in the left-hand plot as an FL1 histogram 24 hours after the final infection, showing that 19.4% of BW7 cells were expressing eGFP at this time point, and that the system had worked in this instance. The right hand panels show TCR A10(2)-transduced BW7 cells stained with anti-Vβ 13-FITC as an FL1 histogram. The upper panel shows expression levels 24 hours after the final infection in the cells transduced with TCR A10(2) 5-D4. The lower right-hand panel shows expression levels 24 hours after the final infection in the cells transduced with TCR A10(2) 7-D3. It is impossible to tell from these plots whether transduction of the cells with TCR has been successful as the fluorescence has shifted downwards. Untransduced BW7 cells do not express any TCR, and so the staining seen here is non-specific in nature – the fact that the staining has changed suggests something has happened in the transduced cells but gives no evidence of this being TCR expression. All antibodies used for staining are shown in Appendix 7.

Figure 3.66 investigates the extent to which the staining seen in the TCR-transduced BW7 lines is non-specific. Transduced and untransduced BW7 were stained with both the specific anti-Vβ antibody and the corresponding FITC-conjugated isotype control (rat IgG2b for the anti-Vβ4 antibody and mouse IgG1 for the anti-Vβ13 antibody). Specific antibody staining was then overlaid with the isotype control staining and compared. In both the D3(3) TCR-transduced line and the A10(2) TCR-transduced lines, the staining with isotype overlapped with the specific antibody staining. The only difference seen was that whilst with untransduced BW7, the isotype for the anti-Vβ4 antibody seemed to stain more strongly than the specific antibody, the staining overlapped fully in the D3(3) TCR-transfected cells i.e. there was a shift in anti-Vβ4 staining between untransduced and TCR-transduced cells, whilst the isotype staining remained the same. However, the shift in specific antibody staining did not increase the intensity of the fluorescence beyond that seen with the corresponding isotype. It is therefore possible that there is no transduction with TCR in this line.

An alternative approach to detect successful transduction of BW7 cells with the TCRs from T-cell clones D3(3) and A10(2) 7-D3 involved carrying out PCRs probing for the presence of the TCR genes in both genomic DNA (for detection of insertion into the cell genome) and cDNA (for detection of mRNA expression of the TCR genes within the cell). The primers used to determine if there had been successful transduction of the TCR genes were those that were originally used in the cloning of these sequences into the pQC vectors by Dr. Alexander Annenkov, and they amplified from the beginning of the V region to just into the C region and are shown, along with PCR conditions, in Appendix 3. Genomic DNA and cDNA from untransduced BW7 cells was also assayed to serve as a negative control. As shown in Figure 3.67, PCR analysis showed that the TCRα chains from both D3(3) and A10(2) 7-D3 were both present in the cDNA products (and in the case of A10(2) 7-D3 also integrated into the host cell genomic DNA). Analysis of TCRβ chain expression in these cells was inconclusive. This result suggests that BW7 cells may have been in some cases positively transduced with the genes encoding at least the TCRα chains. This suggests that the transduction system itself is capable of transferring the constructs into the target cells, and the lack of apparent expression at the cell surface may either be due to a failure in expression at the cell surface or that the high apparent levels of non-specific antibody staining in these cells prevents specific detection of the TCRs using flow cytometry.

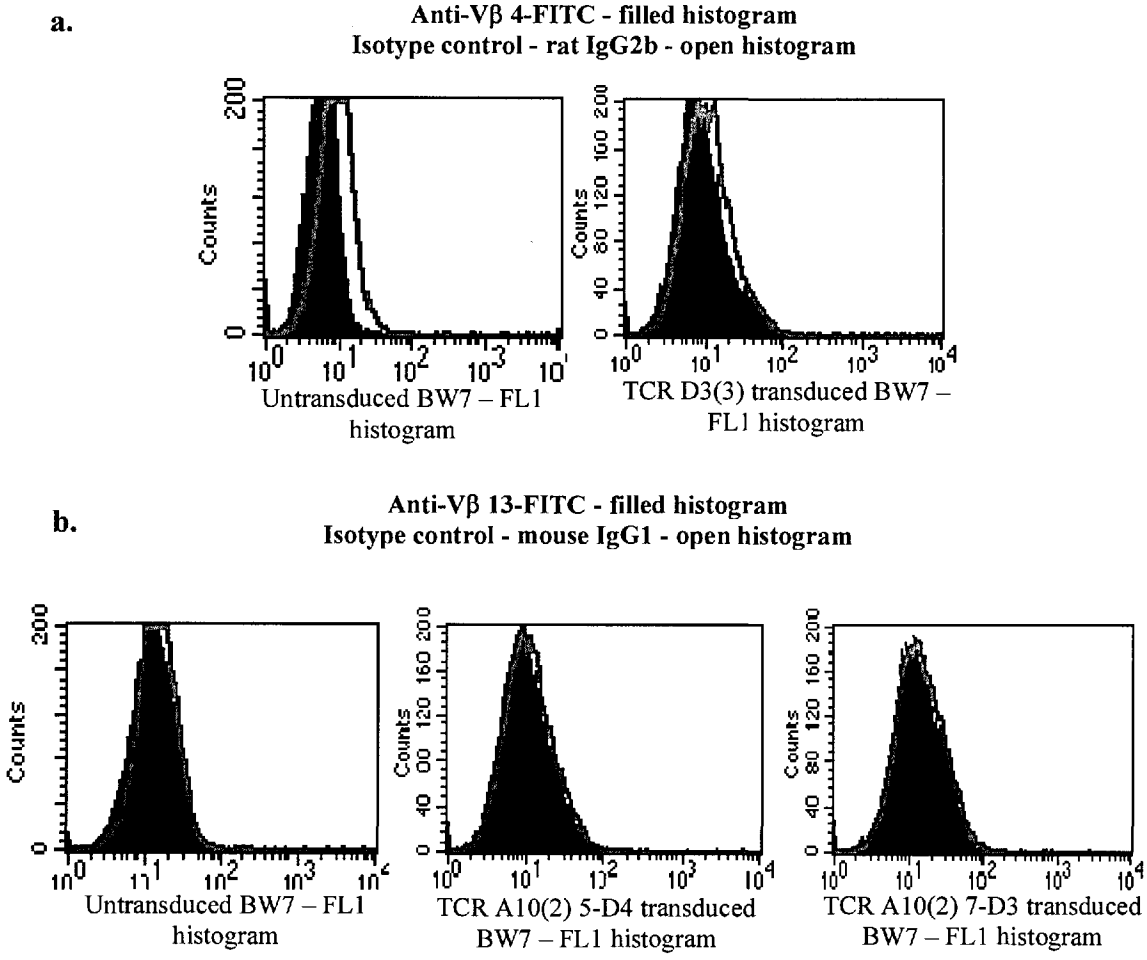


Figure 3.66 Comparison of specific anti-Vβ antibody staining with isotype controls in TCR-transduced and untransduced BW7 To investigate the extent of non-specific staining that occurs on BW7 cells, cells were stained either with the specific Vβ antibody (FITC-conjugated) or the corresponding FITC-conjugated isotype. (a) Staining of untransduced BW7 with the TCR D3(3) specific anti-Vβ 4-antibody or the rat IgG2b isotype (left-hand panel) shows that a higher level of staining occurs with the isotype as shown by the small shift upwards in fluorescence intensity. Staining of the transduced line with these antibodies (right-hand panel) shows almost total overlap between the antibody and its isotype, suggesting that all staining seen is non-specific and not due to TCR expression. (b) Staining of untransduced BW7 with the TCR A10(2) specific anti-Vβ 13-antibody or the mouse IgG1 isotype (left-hand panel) shows a very similar pattern of staining for both, suggesting that any staining is non-specific in nature. Staining of the transduced line with these antibodies shows total overlap between the antibody and its isotype, suggesting that all staining seen is non-specific and not due to TCR expression. All antibodies used for staining are shown in Appendix 7.

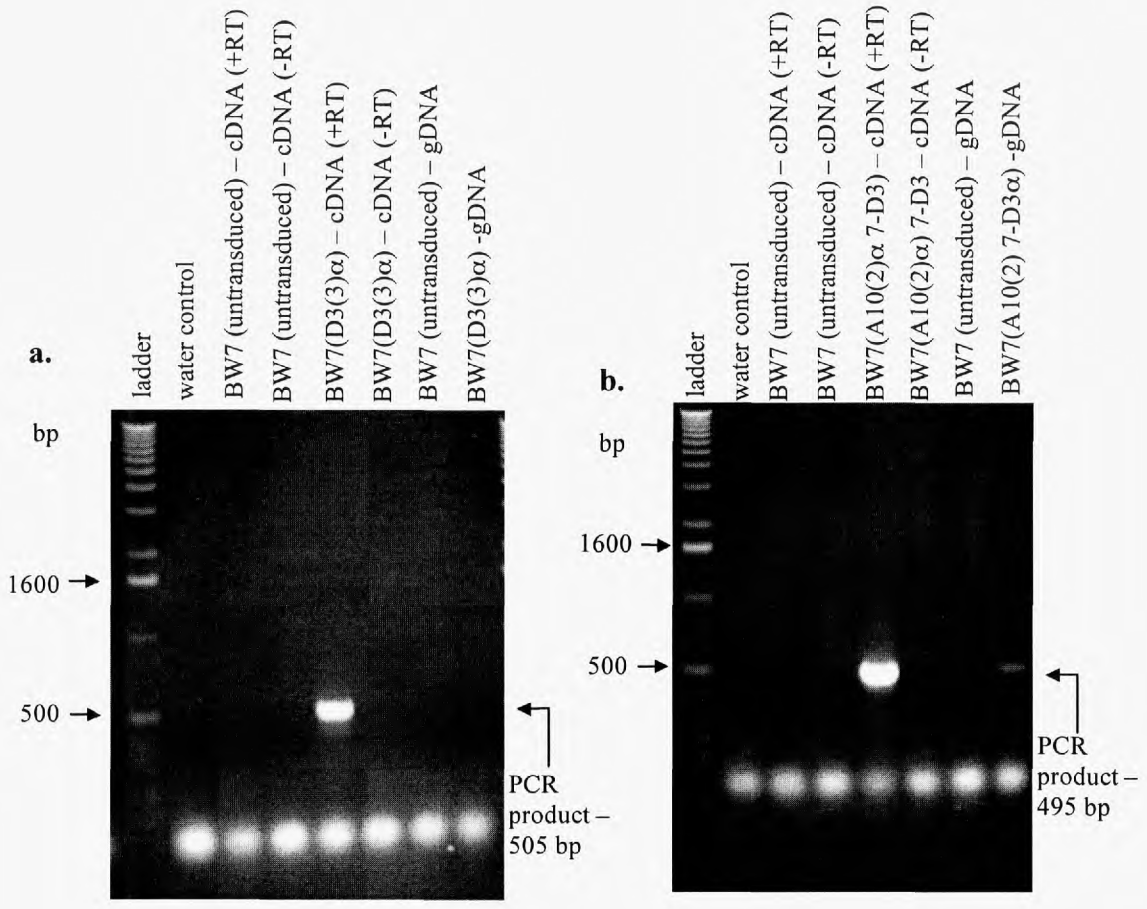


Figure 3.67 Agarose gel images of the PCR products obtained when analysing D3(3) and A10(2) 7-D3 TCR-transduced BW7 cells for the presence of specific TCRα chain PCRs assaying for the specific VJ region using a forward primer specific for the V region (the same forward primer was used for both D3(3) and A10(2) 7-D3 as they use V regions with sequence that is identical at the 5' end) and a reverse primer specific for the murine region TRAC (the same reverse primer was used for both D3(3) and A10(2) 7-D3 as there is only one murine C region) were carried out on both genomic DNA and cDNA isolated from the transduced BW7 lines. Genomic DNA and cDNA from untransduced BW7 cells was used as a negative control. Band sizes for the PCR product were expected to be the same in both genomic DNA and cDNA as the genes in MFG were fully rearranged. Expected band size for D3(3), shown in (a), was 505 bp, and for A10(2) 7-D3, shown in (b), was 495 bp. Primers and reaction conditions are shown in Appendix 3. (+RT – cDNA produced in the presence of reverse transcriptase, -RT – control cDNA reaction lacking reverse transcriptase), gDNA – genomic DNA)

3.3.1.6 Measurement of TCR expression using the IL-2 dependent cell line CTLL-2

The BW7 lines transduced with TCRs from the murine T-cell clones A10(2) and D3(3) were analysed for evidence of TCR expression through use of the IL-2-dependent cell line CTLL-2. The lines were stimulated with PLP_{56-70}, presented by NOD.E APCs; any cells expressing the peptide-specific TCR will respond to this stimulation by proliferating and by producing the cytokine IL-2. As BW7 is a transformed line, and unlike a T-cell line can grow indefinitely in the absence of any peptide stimulation, use of the CTLL-2 line gives a better estimation of TCR expression than a proliferation assay of the BW7 cells themselves. Supernatant from the stimulated lines was harvested from the cells 48 hours after peptide stimulation and added to CTLL-2 cultures to investigate the ability of the supernatant to promote survival and proliferation in the IL-2 dependent line. Any line that had responded to peptide would be expected to have produced significant quantities of IL-2 and hence would induce a higher level of proliferation in the CTLL-2 cells. The results of the assays are shown in Figure 3.68. Untransduced BW7 were also assayed as a comparison, and induced higher levels of proliferation in the CTLL-2 cells than any of the transduced lines. BW7 cells appear to produce a small amount of IL-2 under baseline conditions, as the counts achieved in the untransduced line were much lower than would have been expected for a peptide-specific response. Of the TCR-transduced lines, none induced a higher level of proliferation in the CTLL-2 cells when stimulated with peptide than when left unstimulated. The results of the assay therefore suggest that none of the TCR-transduced lines are expressing TCR as shown by their inability to respond to the peptide for which the TCR is specific.

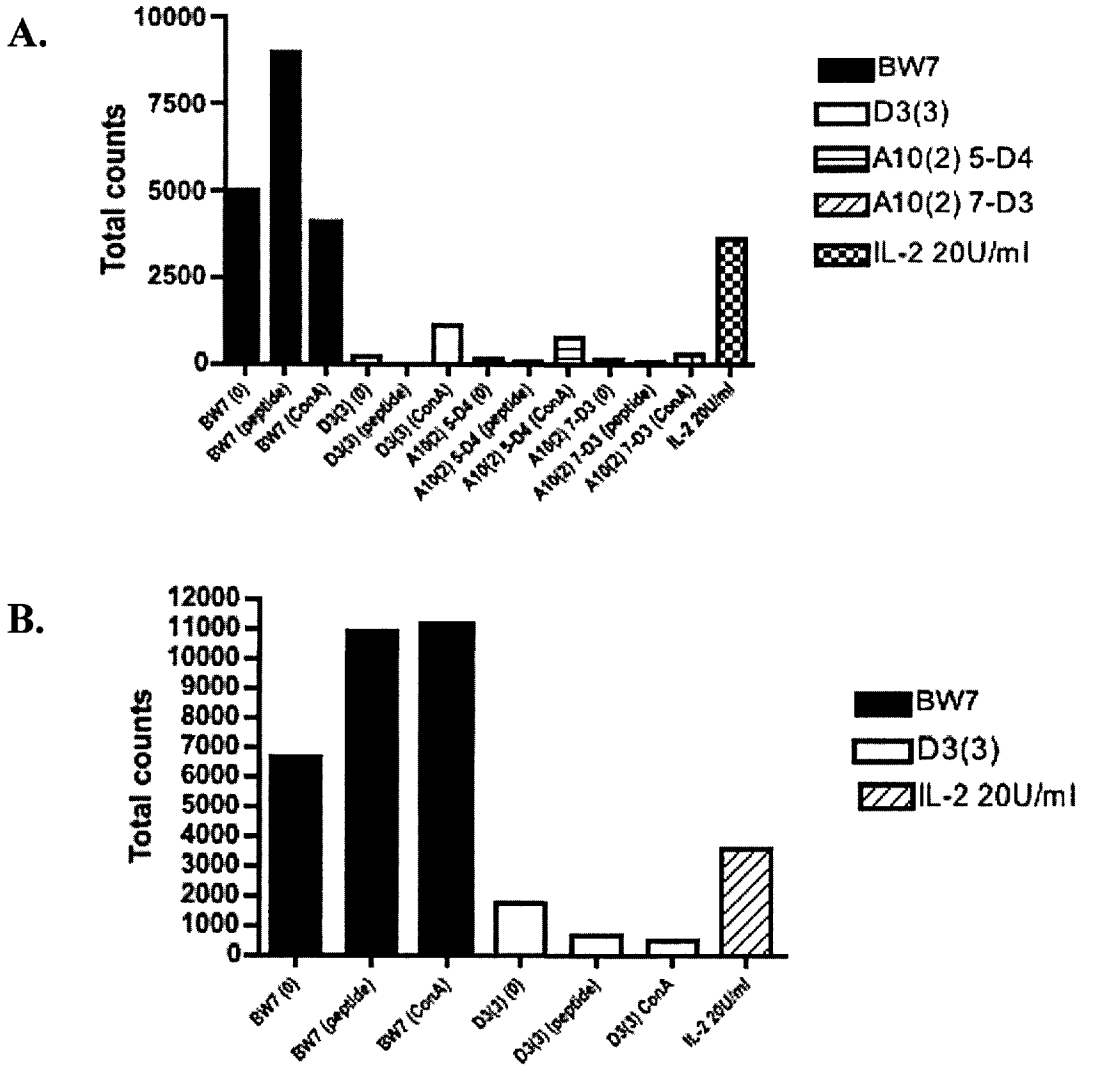


Figure 3.68 Proliferation of the IL-2 dependent CTLL-2 line in supernatant derived from retrovirally-transduced BW7 lines expressing TCRs from the PLP_{56-70}-specific murine T-cell clones A10(2) and D3(3) that had been stimulated with PLP_{56-70} peptide Assays were carried out independently on two separate occasions. In A, three transfected lines (the lines shown in Figures 3.64 and 3.65) were assayed for TCR expression through their ability to respond to stimulation with specific peptide, measured as stimulation-induced production of IL-2 through the IL-2 dependent line CTLL-2. Untransduced cells were also assayed. A positive control for T-cell activation, stimulation with ConA (5μg/ml), and a positive control for CTLL-2 proliferation, stimulation with 20 U/ml IL-2, were included. Responses of the cells were measured at baseline or at a peptide concentration of 25 μg/ml. In B, only the D3(3) TCR-transfected line (the line shown in Figures 3.64) was assayed, as described in A, except that a peptide concentration of 50 μg/ml was used. Responses in all three 'TCR-transduced' lines were significantly lower than for the untransfected line at baseline, as well as when stimulated with peptide or ConA in all assays.

3.3.2 Transduction of BW7 with TCR genes using the Amaxa Nucleofector system

3.3.2.1 Principles of the Amaxa Nucleofector system

The Amaxa Nucleofector system is an electroporation-based non-viral method of transducing cell lines with a target gene. An expression vector containing a gene of interest is transfected into a target cell line using one of the many programmes provided by the Nucleofector device. The target cells are also resuspended prior to transfection in one of a number of Nucleofector solutions provided by Amaxa which to promote transfection. The electrical programme used and the solution in which the cells are resuspended is dependent upon the cell type being transfected, but the company does not release information about the components of the Nucleofector solutions or details about the different programmes that can be used. An extensive database (www.amaxa.com/cell-database) provided by Amaxa contains information on the optimal conditions for transfecting particular cell types.

Transfection using the Amaxa Nucleofector system is usually transient, as the plasmid constructs transfected into the cells do not integrate into the host cell chromosomes as happens in retroviral transduction. However, as the target gene can be transduced directly into the target cell line of choice, it is possible to achieve a far higher level of initial expression with this system than is achieved with retroviral transduction systems. Stable transfection can be achieved with this system, if a linearised construct is used, but the extent of transfection in this case is significantly lower than when circularised constructs are used.

Here, I describe my attempts to transduce the BW7 line using the Amaxa system and the specialised TCR expression vectors, pTαcass and pTβcass, containing TCRs of interest, the production of which were outlined in Section 3.2.2.

3.3.2.2 Use of the Amaxa system to transfect BW7 with GFP

A control vector containing the GFP gene is supplied with all Amaxa Nucleofector kits, pmaxGFP (shown in Appendix 29). Transfection of BW7 cells was attempted using this vector, which has been specifically designed for use with the Amaxa system. As suggested by the Amaxa cell line database for the line BW7, transfection was attempted using Nucleofector Solution V, and the programmes T-001 and T-016. Results obtained for these conditions are shown in Figure 3.69. Transfected cells were analysed for GFP expression by flow cytometry at 24 hour intervals for 3 days after transfection, and then at 3 day intervals until 6 days post-transfection (for the programme T-001) or 9 days post-transfection (for the programme T-016). Untransfected cells were also analysed as a comparison. Both programmes induced GFP gene expression in BW7 cells, programme T-001 to a maximum level of 36.07%, whilst programme T-016 induced GFP expression to a maximum level of 88.12%. However, this programme induced a much higher level of cell death than T-001, so that cells undergoing protocol T-001 looked healthier than those transfected using T-016. Expression of GFP fell off steadily in cells transfected by both protocols, so that by day 6, levels of GFP expression in the cells transfected using T-001 had fallen to less than 1%. High levels of GFP expression (nearly 30%) were seen in the line transfected by T-016 at this time point, but by 9 days after transfection, GFP expression in this line had also fallen to less than 1%. Transfection of BW7 cells using this system appears to be transient in nature, but using programme T-016, significant target gene expression is seen up to 6 days after transfection.

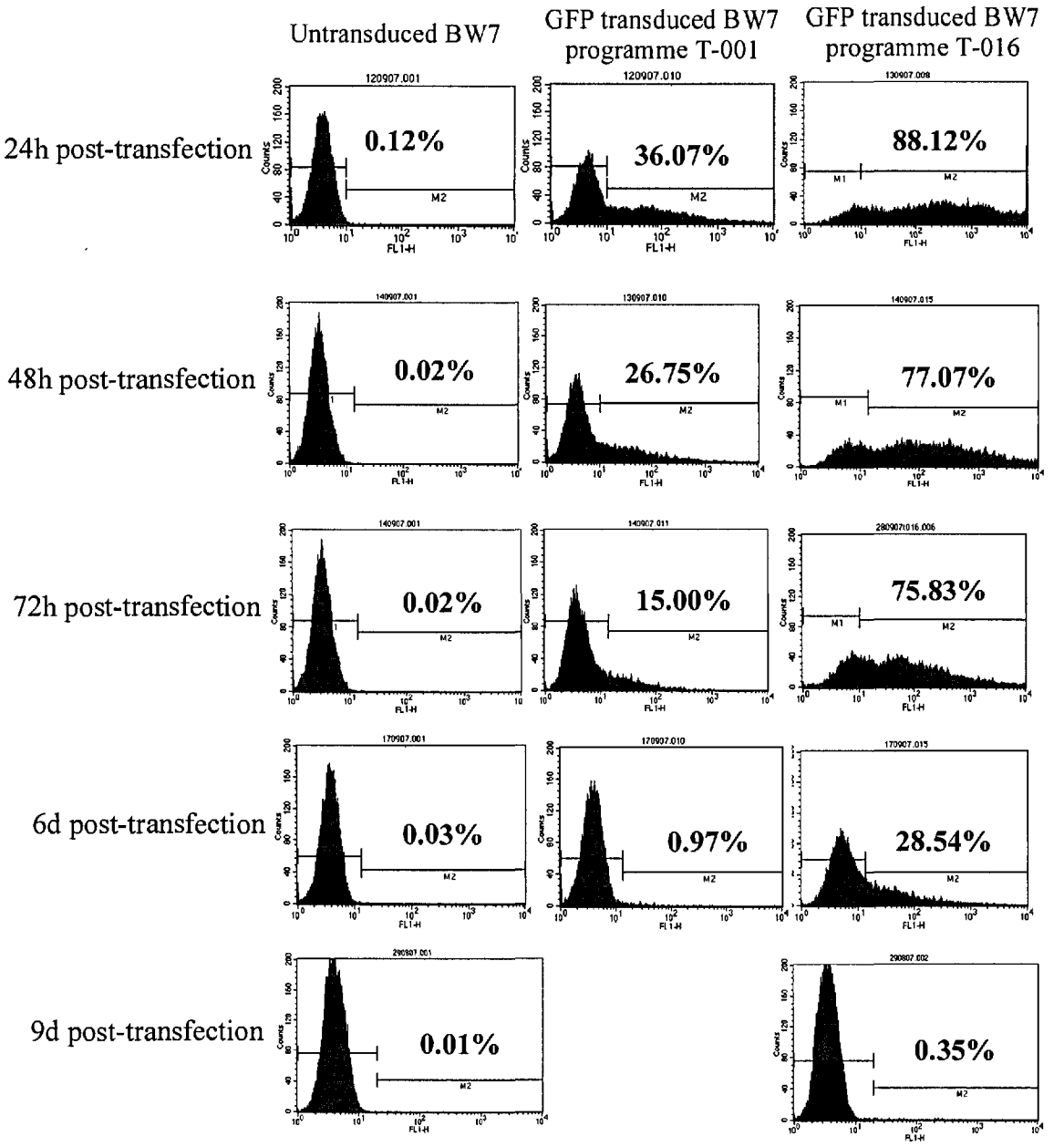


Figure 3.69 GFP expression in BW7 cells transduced with the vector pmaxGFP using the Amaxa Nucleofector system Amaxa programmes T-001 and T-016 were used to transduce BW7 cells according to the manufacturers protocol with 1 μg pmaxGFP control vector, and analysed by flow cytometry every 24 hours for the first three days, and then every three days until GFP expression was comparable to untransduced BW7 cells. The highest level of expression occurred in cells transduced using programme T-016, with over 88% of cells expressing GFP (measured as an increase in fluorescence in the FL-1 (green) channel compared with untransduced cells), compared with maximal expression of over 35% in the cells transduced using programme T-001. GFP expression decreased with time, with no expression detectable in the cells transduced using programme T-001 by 6 days after initial transfection, and no expression in the cells transduced using programme T-016 by 9 days after initial transfection, indicating that transduction using the Amaxa system is transient in nature, and expression of the transduced gene is rapidly lost from the cells.

3.3.2.3 Use of the Amaxa system to transfect BW7 with the TCR from the PLP_{56-70}-specific murine T-cell clone D3(3)

Programmes T-001 and T-016 were used to transfect BW7 cells with the D3(3) TCR using the pTαcass (TCR D3(3) α) and pTβcass (TCR D3(3) β) constructs. Cells were analysed by flow cytometry for TCR expression by staining with the D3(3)-specific FITC-conjugated anti-Vβ4 antibody at 24 and 72 hours after transfection, as shown in Figure 3.70. At 24 hours after transfection, there was no TCR expression apparent from the analysis, as anti-Vβ4 staining was the same in both transfected and sham-transfected (i.e. subjected to the same Nucleofector protocol but without the addition of plasmid DNA) BW7. Staining at 72 hours after transfection showed the same lack of TCR expression, suggesting that the system had failed under these conditions to transfect the BW7 cells with genes encoding the D3(3) TCR.

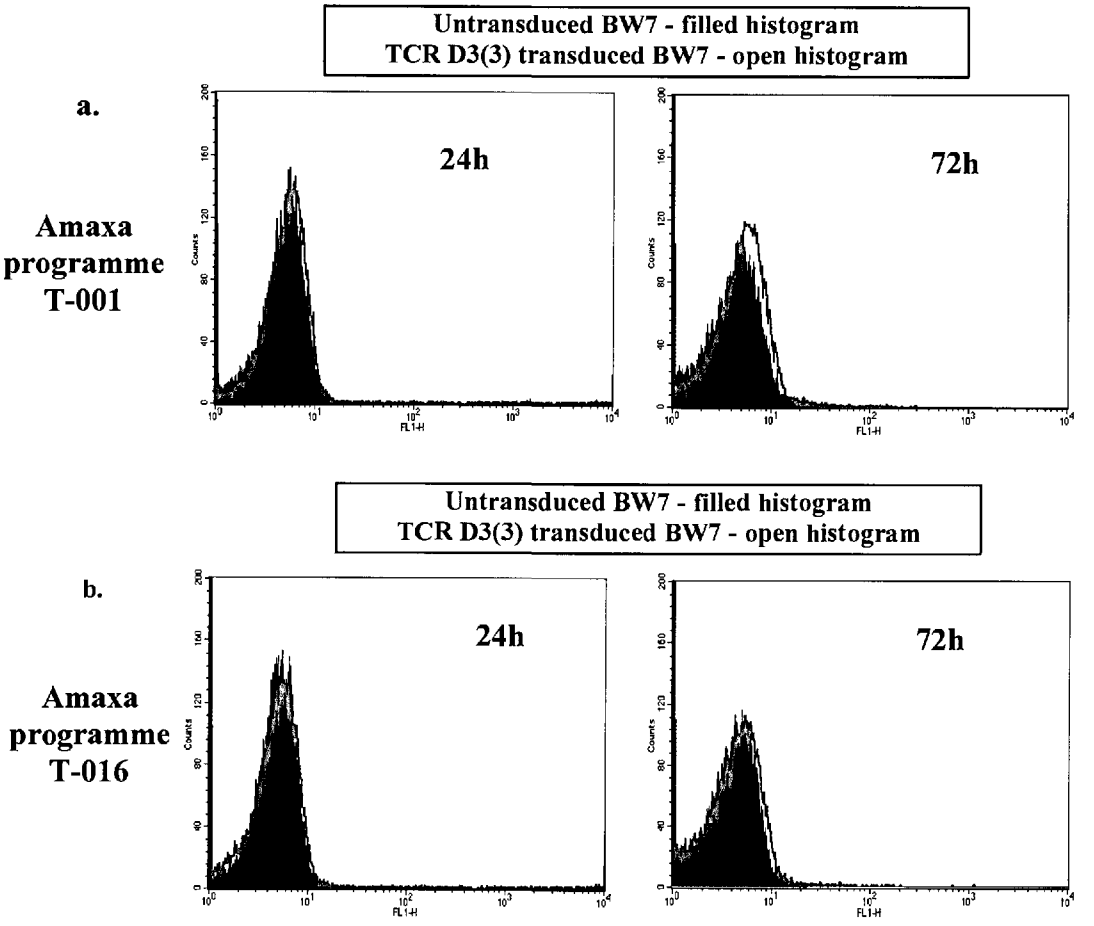


Figure 3.70 Specific anti-Vβ 4-FITC staining to assess TCR D3(3) expression in BW7 transduced using the Amaxa Nucleofector BW7 cells were transduced using one of the two programmes recommended by the manufacturer for use in transduction of this cell line, T-001 or T-016. TCR expression induced through using the programme T-001 is shown in a. TCR expression induced through using the programme T-016 is shown in b. Expression was assessed at 24 and 72 hours after transduction. Untransduced BW7 cells were stained as a negative comparison. At both 24 and 72 hours, staining of both TCR-transduced and untransduced BW7 cells from both programmes was the same, suggesting that transduction had been unsuccessful. All antibodies used for staining are shown in Appendix 7.

3.3.3 Summary

Two different systems of transduction were used to try to transduce the TCR-negative murine thymoma line BW7 with TCRs from the PLP_{56-70}-specific murine T-cell clones A10(2) and D3(3). For retroviral transduction of the lines, a system was used that allowed good transduction of the target line BW7 with the gene eGFP. This involved the transfection of a series of packaging lines, EcoPhoenix and PT67, with the retroviral vector MFG containing the target gene. BW7 cells were transduced with the genes encoding the TCRs from clones A10(2) and D3(3), after which TCR expression was assessed by flow cytometry, staining for the specific Vβ region of each TCR. The flow cytometry results for the D3(3) TCR, suggested that successful transduction had occurred at a low level. However, when the TCR-transduced lines were further assayed for their ability to induce proliferation in the IL-2-dependent cell line CTLL-2 upon stimulation with the peptide PLP_{56-70}, none of the transduced lines were able to induce proliferation in the CTLL-2 cells when stimulated with peptide. I was not successful in the transduction of TCR using the retroviral system.

The Amaxa Nucleofector system was then used to transduce the BW7 line with the TCRs from the clone D3(3). The system was initially tested for its ability to transduce BW7 using the control vector pmaxGFP, and it showed the capacity to transduce BW7 to a high extent. Constructs encoding the D3(3) TCRα and TCRβ chains (pTαcass (TCR D3(3) α) and pTβcass (TCR D3(3) β)) were transfected into BW7 cells using this system and TCR expression was assessed by flow cytometry, staining for the specific Vβ region of the TCR. No difference in staining was seen between TCR-transduced and sham-transduced BW7. I was once again unable to successfully transduce the BW7 line with TCR using the Amaxa Nucleofector system.

3.4 Discussion

TCR CDR3 analysis of HLA-DR1-restricted T-cell lines grown in response to an important epitope (peptide 4) of Fel d 1 identified the presence of expanded populations of T-cells bearing a particular TCR. The greater the number of times a line had been stimulated with peptide, the more restricted the repertoire of expressed TCRs became, and the more dominant the expanded TCR was within the population. Expanded TCRs sometimes had elongated CDR3 α or β loops, in support of the hypothesis being tested, that in the human Th2-mediated disease allergic asthma, TCRs carrying elongated CDR3 loops expand in response to allergen challenge. During a T-cell-mediated immune response, it has been observed that there is a rapid expansion of pathogen-specific T-cells expressing a particular receptor (593, 594) which is somehow selected for as being particularly well-suited to driving the response in an appropriate direction. Clonal expansions of cells bearing particular receptors has been observed in a range of immune responses mediated by both $CD4^+$ T-helper type cells, and $CD8^+$ cytotoxic T-cells. For example, expansions of cytotoxic T-cells bearing the same (or highly similar) TCRs have been documented in responses to infection with human immunodeficiency virus (HIV) (617), acute infectious mononucleosis caused by Epstein-Barr virus (EBV) infection (618) and influenza virus infection (619). Analysis of TCR usage in $CD4^+$ T-cells in a number of these systems, namely HIV (620) and EBV (618), suggested that whilst expansions in $CD4^+$ T-cells could be identified (in the case of HIV infection), expansions were smaller and more polyclonal than those seen in $CD8^+$ T-cells. However, a different study instead found a greater degree of clonality in $CD4^+$ T-cells than $CD8^+$ T-cells in HIV-infected patients (621). EBV infection did not appear to be associated with the development of any $CD4^+$ T-cell clonal expansion (618), although it was suggested that the system used for analysis may have been unable to detect any such expansions.

In diseases more strongly associated with aberrant T-helper cell immune responses such as autoimmune diseases, a similar pattern of clonal expansion is seen as that in virally-induced responses, with expansions of antigen-specific $CD8^+$ T-cells tending to be more oligoclonal or monoclonal than expansions of antigen-specific $CD4^+$ T-cells, which in general are more variable and polyclonal in nature. For example, in aplastic anaemia (622), an association between disease severity and prevalence of a particular $CD8^+$ T-cell clonotype expressing a specific TCR was demonstrated (623). Whilst this study

observed only small, polyclonal expansions in $CD4^+$ T-cells, another study described marked clonal expansions in $CD4^+$ T-cells in aplastic anaemia (624). These cells had a Th1 phenotype (i.e. produced IFN-γ) and were strongly implicated in causing disease. A similar pattern of expansion has been seen in T-cells isolated from lesions in the brain tissue of multiple sclerosis patients, with both $CD4^+$ and $CD8^+$ T-cells showing clonal expansion, but which was more marked and limited in $CD8^+$ T-cells (625). However, analysis of TCR usage in the mouse model of multiple sclerosis, EAE, showed a clear clonotypic expansion of $CD4^+$ T-cells specific for the antigen used to induce disease, MBP (594). A highly clonotypic response to a particular epitope of glutamic acid decarboxylase (GAD65), $GAD65_{530\text{-}543}$, which is implicated in the development of spontaneous diabetes in NOD mice was identified (626). The TCRβ chain involved in this response is consistently present in the pancreatic islets of pre-diabetic NOD mice, but is not seen in other strains of mice or in other inflamed organs in NOD mice. The V, D and J regions of this TCR are identical in each case, with the TCR differing only at the CDR3, and here only slightly - all receptors share a specific DWG motif preceded in most cases by a polar glutamine or arginine residue.

Whilst clonal expansions of specific TCRs in both viral infections and autoimmune disease have been extensively described, the situation in atopic disease is less well characterised. Analysis of T-cell responses in atopic dermatitis caused by house dust mite extract demonstrated the presence of clonotypic expansions in both peripheral blood lymphocytes cultured *in vitro* with HDM extract and also in T-cells extracted from atopic dermatitis lesions in the skin and analysed immediately *ex vivo* (627). However, only in rare cases was expansion of cells expressing the same TCR seen in both peripheral blood and skin lesion T-cells, but where this phenomenon did occur, it was associated with increased disease severity. It was also noted that the T-cell response in both compartments was of a highly oligoclonal nature. In addition, clonotypic expansion of T-cells bearing a TCR containing Vβ11 (TRBV 25) was observed after stimulation of PBMCs *in vitro* with crude peanut extract in peanut-allergic subjects (628). PBMCs from non-allergic siblings did not show this expansion in response to *in vitro* stimulation with peanut extract, suggesting that the expansion was allergen-specific. A study of TCR usage in house dust mite allergy associated clonal expansions of T-cells expressing TCRs composed of Vβ18.1 (TRBV 18-1) or Vα2.3 (TRAV 12-1) with disease (629). Allergies to cat and birch pollen have also been linked to particular Vβ subsets (630). Birch pollen allergy was associated with expansions of $V\beta16.1^+$

(TRBV 14) and Vβ20.1$^+$ (TRBV 30) T-cells during the pollen season, whilst cat allergy was associated with the expansion of Vβ17.1$^+$ (TRBV 19) T-cells. The findings described here, of expansions of Fel d 1-specific T-cells bearing a particular receptor in response to *in vitro* stimulation with peptide 4, are in agreement with previous findings of allergen-specific T-cell responses in allergic disease. Repeated stimulation with peptide 4 appeared to further focus the response in favour of particular dominant TCR chains (either TCRα or TCRβ) with identical CDR3 loops. There are a number of reservations concerning the propensity for *in vitro* culture and re-stimulation to bias a T-cell response. Such restimulation polarises the line and encourages the expansion of antigen-specific T-cells that are not present in such large numbers *in vivo*, even in a target organ (for example, 1-2% of T-cells isolated from HDM-sensitive atopic dermatitis skin lesions were clonotypically expanded in response to antigen (627), and this has also been observed in other systems (631, 632)). In the case of HDM-sensitive atopic dermatitis, TCRs expanded from a pool of PBMCs through *in vitro* culture were not in many instances found in the skin lesions, and it may therefore be possible to expand T-cells that would not reach the target organ *in vivo*, despite their potential antigen responsiveness. As such, analysis of TCR usage in T-cells isolated directly from the target organ, in this case the lung, of allergic asthmatic subjects, either from BAL fluid, induced sputum or lung biopsy samples would support the data presented here if T-cells expressing such TCRs were also found to be present in the lungs of these subjects. Such a finding would demonstrate the pathological importance of T-cells bearing specific TCRs in allergic asthma pathogenesis.

Dominant TCRs that are clonally expanded in response to antigen challenge often have a number of structural features, especially in the antigen-binding site (made up of CDRs 1, 2 and 3), that mediate the interaction with cognate peptide-MHC, optimising it to give an appropriate response (597). Some of these features are encoded in the germline V and J sequences, hence selection for particular V and J regions with these features will be promoted, as has been observed both here and elsewhere. Other features may be incorporated during N region addition of nucleotides by terminal deoxynucleotidyl transferase at the V-J region junction making up the CDR3 (402, 403). Those receptors with the requisite amino acid types or numbers incorporated in this region will be further promoted by the developing response. This is possibly demonstrated in the TCRα chain selection seen in line CIR014, where the main expansion in terms of V and J region usage (TRAV 26-2 TRAJ 48) did not show the same clonality in terms of

CDR3α selection. Seven different CDR3α loops were identified, which differed mostly in terms of the non-germline N region, where insertions and the use of diverse residues could be seen. Analysis of this line through a number of restimulations with peptide 4 would allow tracking of the response to determine whether one of these early selected CDR3 loops comes to dominate the response, or whether all seven (or a proportion of them) contain a required structural motif that allows the correct response to be elicited. In addition, in line B1, it was observed that two TCRα and two TCRβ chains were expanded to the same extent. There was no obvious correlation between the chains in terms of germline segment usage or CDR3 length/composition, and it was not possible to tell which TCRα and which TCRβ chains paired with each other from this analysis. Further analysis of the line through cloning by limiting dilution would allow the TCR pairs to be identified. It is possible that the two TCRs formed in this response either contain different motifs that mediate the same level of response or, at the three-dimensional level, the structure at the antigen-binding site may be similar, despite the different components used to construct it, but modelling studies and/or structural studies would be required to confirm this. Alternatively, the two expanded TCRs could mediate different responses through their interaction with the same peptide-MHC, though this may be less likely due to their existence in the same cytokine conditions. The ability to study the responses induced by each TCR separately and to compare them, perhaps through their expression in a system such as the BW7 expression system that was attempted here, could clarify the roles of these TCRs.

An interesting aspect of the TCR CDR3 analysis described here was that, despite the analysis of T-cell lines derived from cat allergic asthmatic subjects who were HLA-DR1$^+$ and therefore likely to be able to respond to the same peptide epitope of Fel d 1, peptide 4, the expanded TCR (or TCRs) identified in each case were different. TCRs that are expanded by only one or a few individuals in response to the same stimulus is known as private TCRs, whilst a TCR or TCR chain that is widely expressed amongst all or most individuals in a population (e.g. all people with a certain HLA haplotype) in response to a particular antigen is known as a public TCR. Public TCR responses have been described in genetically identical strains of mice, for example, in influenza infection in response to an epitope of viral nucleoprotein (633), in the response to GAD65 in the development of autoimmune diabetes in NOD mice (626) and in the development of EAE in response to MBP in B10.PL mice (634), amongst others. Private TCR responses were also elicited in response to antigen challenge in each of the

examples described above (633, 626, 634), but always to a lesser extent than the public response, suggesting that a public response may be the most appropriate or 'best fit' response to the antigen in question (alternatively, the genetically identical background of the mice in each case may enhance the frequency of appearance of the public TCR, but this does not necessarily preclude the public response from being the 'best fit' response). Other studies have suggested an alternative explanation, that public responses may be induced by peptide antigens of a particular shape – for example, those peptides that form relatively flat surfaces when bound to MHC molecule may provide few features for recognition by TCR, resulting in only a small number of TCRs being capable of mounting a response to the antigen (635, 636). Other studies have suggested that a peptide that protrudes from the MHC binding cleft, and forms a bulged conformation may also constrain the repertoire of TCRs that are able to form the correct interface with the peptide-MHC, and again lead to the formation of a public response (637). Those antigens presumed to induce private responses in this hypothesis are therefore thought to have a shape intermediate between the two extremes and are hence capable of being recognised by a number of TCRs with different V(D)J and CDR3 compositions. Another theory suggests that the conformational change induced upon binding of TCR to its cognate peptide-MHC antigen can drive development of a public T-cell response through limiting antigen specificity to those TCRs with a structure capable of inducing the required change in conformation (585). In addition, it has been suggested that public responses may arise as a result of their being more likely to occur due to the increased number of ways in which the same amino acid sequence can be generated from different underlying nucleotide sequences due to the degeneracy of the genetic code (638, 639). Not only can multiple recombination events produce the same nucleotide sequence, but also differing nucleotide sequences can produce the same amino acid sequence; the greater the number of ways of generating the same amino acid sequence at the CDR3 loop, the higher the probability of its forming a public response to an antigen for which it is specific. The lack of any overlap in TCR usage between lines in the expansions seen in the peptide 4-specific HLA-DR1-restricted T-cell lines indicates that this particular response may be primarily governed by private TCR responses. However, the finding in another study of TCR usage in cat-sensitive allergic asthma that a particular TCR Vβ chain was associated with allergic responses to cat allergen (630) may suggest that public responses to allergen may be possible, depending on the epitope and MHC class II haplotype involved in the response. Further extensive study of TCR usage in allergic asthma, with particular reference to HLA haplotypes,

would be required to determine if there are public responses involved in allergic asthma pathogenesis, or if the disease is mediated wholly by private, individual responses. Such a finding would have implications for the development of therapies to treat allergic asthma – if a public response could be demonstrated, it might be possible to develop an antibody treatment targeted against the public TCR which would have broad applicability. A similar approach could be possible even with private TCRs, but each patient would require treatment with a different anti-TCR antibody therapeutic.

The interaction between TCR and peptide-MHC complex may govern the strength and efficiency of TCR triggering and signalling, and in such a way determine the phenotype of the response i.e. development of a naive $CD4^+$ T-cell into a Th1 or Th2 effector cell upon activation, so that it is appropriate to the nature of the pathogen or the environment of the cell. It has therefore been suggested that the prevailing conditions surrounding the activation of a T-cell may determine the structure of the TCR that is preferentially expanded, by selecting those receptors for which the kinetics of binding peptide-MHC are optimal for developing the appropriate response. For example, TCRs expanded in Th2-promoting conditions may be preferentially selected for the presence of elongated CDR3α loops with a high proportion of bulky side chains within their structure compared with the lengths of CDR3α loops expanded in the corresponding Th1-promoting conditions (601). The three-dimensional structure of such an elongated loop has been predicted by computer modelling to impede the interaction between TCR and peptide-MHC, resulting in an interaction that is lower in affinity and with a reduced half-life. The development of Th2 cells from naive precursors has been linked to predicted weaker signalling through the TCR, and a lower affinity interaction with peptide-MHC. The expansion of TCRs with structural features in the antigen-binding site that lead to this outcome, such as elongated CDR3 loops, could therefore be favoured under Th2-promoting conditions. The identification of some TCRs with elongated CDR3 loops (compared to the mean length of CDR3 regions in human T-cells as defined by Moss and Bell (586) which under IMGT definitions are approximately 12 amino acids for both TCRα and TCRβ chains) in the TCR CDR3 analysis described here supports this hypothesis.

In addition, the lack of any common TCR gene usage between the three lines analysed demonstrates how diverse the T-cell response to a single antigen can be; the lines were derived from three cat-sensitive allergic asthmatic patients who were all HLA-$DR1^+$,

and yet the TCR (or TCRs) expanded in response to peptide 4 stimulation in each case was different, but presumably capable of eliciting the same response (i.e. allergic disease). This suggests that if the structure of the TCR is selected for on the basis of its ability to elicit the most appropriate response, there is not necessarily only one defined structure that is capable of effecting this response, and the dominant structure(s) selected for in each individual will also be determined by the available repertoire established in the thymus during T-cell development and thymic selection events.

This chapter also outlined attempts to develop a system in which the impact of TCR structure on T-cell function and differentiation could be studied. As discussed previously, it may be that the structure of expanded TCRs in a T-cell response may play a role in promoting the development of a particular response i.e. Th1 or Th2. At the point of identification, however, the T-cells bearing the receptors of interest are already committed to a mature phenotype, and thus the impact of the TCR structure on its differentiation is difficult to assess. The use of expression systems that allow the transduction of such TCRs should allow analysis of the extent to which TCR structure itself can influence downstream events in T-cell activation. The ability to compare the responses induced by stimulation of the I-A^{g7}/PLP_{56-70}-specific 'Th1' and 'Th2' TCRs (601) with cognate peptide-MHC in a system where the only difference between the transduced lines is the TCR they express may identify the capacity of a particular TCR to influence cell function. For example, cytokine production, proliferation and signalling events downstream of the TCR-CD3 complex could be compared, as well as the measurement of kinetic parameters such as affinity for peptide-MHC complex and the interaction half-life using tetramer analysis (640) or surface plasmon resonance (641). Any differences between the two lines could only be due to the structure of the TCR itself, and in this way the effect of structure on function could be determined. In addition, T-cell signalling induced by the expanded TCR from the HLA-DR1/peptide 4-specific line could be analysed. These responses could be compared against the PLP-specific responses in the first instance to give a general idea of how TCR signalling compares in the two systems. In addition, it might also be informative to compare the responses induced by the asthma-related TCRs with responses induced by a TCR carrying the same peptide-MHC specificity but isolated from either a non-allergic subject or from a line that has been polarised towards a Th1-phenotype by the addition of exogenous cytokines.

The attempts by me to create such a system that are shown in this chapter proved unsuccessful. A number of factors may have contributed to the failure to achieve successful transduction of BW7 with TCRs of interest. For example, the original packaging line, EcoPhoenix, is an ecotropic cell line, which means that its range of infectivity is limited to rodent cell lines (603, 613). BW7 is a line of murine origin and thus would be expected to be susceptible to infection with virus produced from this line. However, attempts at directly infecting BW7 with retrovirus derived from EcoPhoenix were unsuccessful. It is therefore possible that BW7 cells lack significant expression of the ecotropic receptor (mCAT-1) (642) at the cell surface. This difficulty was apparently overcome by the use of a serial system using a second packaging line, the dualtropic line PT67 (attempts to transfect PT67 directly with retroviral vector were also unsuccessful). Dualtropic lines have a greater range of infectivity, and are potentially able to infect all mammalian cell types (643), and this was shown by the ability of virus derived from PT67 cells to infect BW7 with eGFP. However, the use of a serial system decreased the overall efficiency of the system (as seen when comparing the level of infection of NIH3T3 cells with EcoPhoenix-derived virus directly and with virus from PT67 which had been infected itself with EcoPhoenix-derived virus. Use of a serial system decreased efficiency of infection by at least one-fifth). In addition, optimisation with eGFP involved transduction with one vector. Transduction with TCR genes involved the use of two vectors, and for a cell to be successfully transduced, it had to be infected with copies of both vector. In the BW7 line, approximately 20% of cells were successfully transduced with eGFP; if approximately the same rate of transduction was achieved for both TCRα and TCRβ vectors (i.e. 1 in 5 cells would be transduced with the TCRα vector, and 1 in 5 cells would be transduced with the TCRβ vector), this could mean that less than 5% (1/5 x 1/5 = 1/25, or 4%) of BW7 cells would be transduced with both simultaneously. Transduction using a non-retroviral system, the Amaxa Nucleofector, was also attempted, and also ultimately proved unsuccessful, despite the ability to transduce BW7 cells with eGFP. Possible reasons for this could be that the TCR expression vectors used, the pTcass vectors, are over 20 kb in size (346). The control GFP vector used for optimising the system is 6 kb, and so for the same concentration of DNA (for which there is a maximum that can be used per transfection), the number of copies of pTcass available would be more than three times lower than the same concentration of control vector. This would presumably impact on the efficiency of transfection and may explain why this system was also unsuccessful.

An alternative explanation for the failure to express TCR in the BW7 line may not be due to problems with the transduction systems used, but instead it may be due to problems with expression of the genes from the constructs. As the methods used to assess correct transduction (flow cytometry and IL-2 production through use of the CTLL-2 line) require the expression of TCR at the cell surface, they do not assess the possibility that the cells may be transduced with the constructs, but the genes may not be expressing correctly. The presence of the MFG constructs within the BW7 cells was assayed on one occasion, where it was shown that the TCRα genes for both clones D3(3) and A10(2) were present, suggesting that transduction of the line retrovirally was possible to some degree. However, as no corresponding TCRβ chain gene could be identified, the expression of the genes could not be assessed, as expression of TCR at the cell surface requires both chains to be present. The MFG constructs containing the TCR genes were modified from the MFG(eGFP) construct through the addition of a short oligonucleotide linker to allow destruction of the unwanted NcoI site – it is possible that the extra base pairs incorporated through this linker have altered the relationship between the gene sequence and promoter and/or enhancer regions within the construct, and therefore expression of the gene could have been diminished compared to eGFP which was situated at exactly the correct position in the construct (604) for expression. In the case of the Amaxa system, the pTcass constructs have been previously used in an electroporation system (but not the Amaxa system) to transduce the BW7 line (606). However, in this study, the TCR chain genes were amplified from genomic DNA, whereas here, the genes were amplified from cDNA. Although the addition of intronic sequence from downstream of the J region should have allowed correct expression of these genes, it is possible that there was a problem in expression in these constructs.

There are a number of ways in which the systems used here could be modified to achieve successful transduction. Although the PT67 packaging line could not be used as the sole packaging cell line due to its resistance to transfection with retroviral vector using calcium phosphate, virus produced from this line was able to successfully infect BW7, at least with eGFP. One possibility therefore would be to use a different packaging cell line, either a dualtropic line like PT67 or possibly an amphotropic line, such as AmphoPhoenix (between ecotropic and dualtropic lines in its range of infectivity of mammalian cell types) as the packaging line. The susceptibility of these cells to calcium phosphate transfection and the best conditions for transfection and

infection would have to be determined through optimisation experiments. Alternatively, a different means of transfecting PT67 could be attempted, such as lipofection (use of lipofectamine instead of calcium phosphate as a means of facilitating DNA entry into cells), or electroporation with the Amaxa Nucleofector. Another approach could be to use different expression vectors - either the use of vectors with a selectable antibiotic resistance marker, or the use of a vector which is able to incorporate both genes on the same plasmid, so that successful transduction with one plasmid leads to transduction of both genes simultaneously. The advantage of using selectable markers is that transduction with each chain could be carried out separately, and selection of those cells containing the first plasmid before transduction with the second could greatly enhance the efficiency of TCR transduction. In addition, use of a different vector would potentially also solve the problem if the lack of apparent transduction was due to a failure of expression from the constructs used here. None of the above modifications are trivial; for example, use of a different packaging line would require optimisation of the system to determine the conditions giving the highest level of transduction. The same would be true of using a different method of transfection, not least as the use of the Nucleofector system to transfect an adherent cell line such as PT67 is more technically difficult than transfection of a non-adherent line such as BW7. Also, the use of different vectors would involve cloning of the TCR genes into new vectors, and optimisation of the systems using them. A retroviral vector containing more than one gene of interest requires an IRES, or internal ribosomal entry site, between the two to ensure the transcription and translation of both genes. Use of such vectors can be problematic, and whilst potentially the most useful of vectors for the transduction of cells with TCR, are also more difficult to use successfully. However, the potential value of such a system if it can be developed is such that trying one or more of these modifications, though time-consuming, would be worthwhile. Because I was not able to transduce the BW7 cell line with TCR using these systems, I was unfortunately not able to take this line of work forward and was not able to study the impact of TCR structure on function *in vitro*.

4. Induction of allergic disease and analysis of T-cell costimulatory molecule expression in P4 TCR/DR1/ABO transgenic mouse lines 4 and 16

4.1 Characterisation of P4 TCR/DR1/ABO transgenic mice

4.1.1 Overview

P4 TCR transgenic mice were generated previously in our laboratory. Dr. Carol Pridgeon (National Heart and Lung Institute, Imperial College, London) generated and characterised the HLA-DR1-restricted human T-cell lines against peptide 4, derived from cat allergic individuals with allergic asthma. Dr. Daniel Douek (National Institutes of Health/VRC, United States of America) carried out a detailed clonotypic analysis of the human T-cell lines and identified the dominant TCRs expressed. Dr. Alexander Annenkov (Lung Immunology Group, Imperial College, London) cloned the rearranged V-J regions from a dominant TCR (α and β chains) (shown in Appendix 30) into the pTαcass and pTβcass vectors (346, supplied by Diane Mathis and Christophe Benoist). Dr. Catherine Reynolds (Lung Immunology Group, Imperial College, London) prepared the constructs for injection. Ms. Zoe Webster (Research Technician, Central Biomedical Services, Hammersmith Hospital, Imperial College, London) injected the constructs into C57BL/6 x CBA oocytes. Dr. Catherine Reynolds screened the founders by TCR-specific PCR and identified two P4 TCR transgenic founder mice. Dr. Catherine Reynolds and Dr. Xiaoming Cheng carried out the initial characterisation of the P4 TCR transgenic mouse lines and crossed them with a DR1/ABO transgenic mouse line, to produce P4 TCR/DR1/ABO transgenic mouse lines 4 and 16. Dr. Catherine Reynolds and Dr. Xiaoming Cheng developed the protocols to induce allergic inflammation in the lung in this transgenic model. All the experiments described using this model were carried out with Dr. Catherine Reynolds and Dr. Xiaoming Cheng.

4.1.2 PCR genotyping identifies P4 TCR/DR1/ABO transgenic mice

Five PCRs are used to genotype the P4 TCR/DR1/ABO transgenic mice, the products of which are shown in Figure 4.1 for both a P4 TCR positive (P4 TCR/DR1/ABO) and a P4 TCR negative (DR1/ABO) mouse from each line. All PCR primers and reaction conditions are shown in Appendix 6. Primers for the PCR to identify the P4 TCR (α and

β chains) were designed by Dr. Catherine Reynolds, primers identifying the HLA-DR1 α and β chains and the murine MHC class II H2-A knockout status were designed by Danny Altmann. PCRs amplifying the transgenic TCRα and TCRβ chains, if present, are shown in a and b of Figure 4.1. PCRs amplifying the α and β chains of the human MHC class II molecule HLA-DR1 are shown in c and d of Figure 4.1. As the DR1/ABO transgenic line is bred to express transgenic human HLA-DR1 homozygously, all mice are expected to give a positive result for these genes. The PCR assaying for murine MHC class II H2-A knockout status amplifies a product of the neomycin resistance cassette insert that was used to disrupt their expression, shown in e of Figure 4.1. The DR1/ABO transgenic line is also bred for homozygosity of the knockout insertion and as such, all mice are expected to give a positive result. This PCR is unable to differentiate between mice which are heterozygous or homozygous for the knockout insertion, as both will give a positive result with this PCR, hence mice were also phenotyped for expression of murine MHC class II H2-A by flow cytometry, as described in section 4.1.3. A P4 TCR/DR1/ABO transgenic mouse was therefore defined as a mouse with positive products for all five of the PCRs. Mice negative for the TCR transgenes but positive for the HLA-DR1 and murine MHC class II knockout PCRs were defined as DR1/ABO transgenic mice.

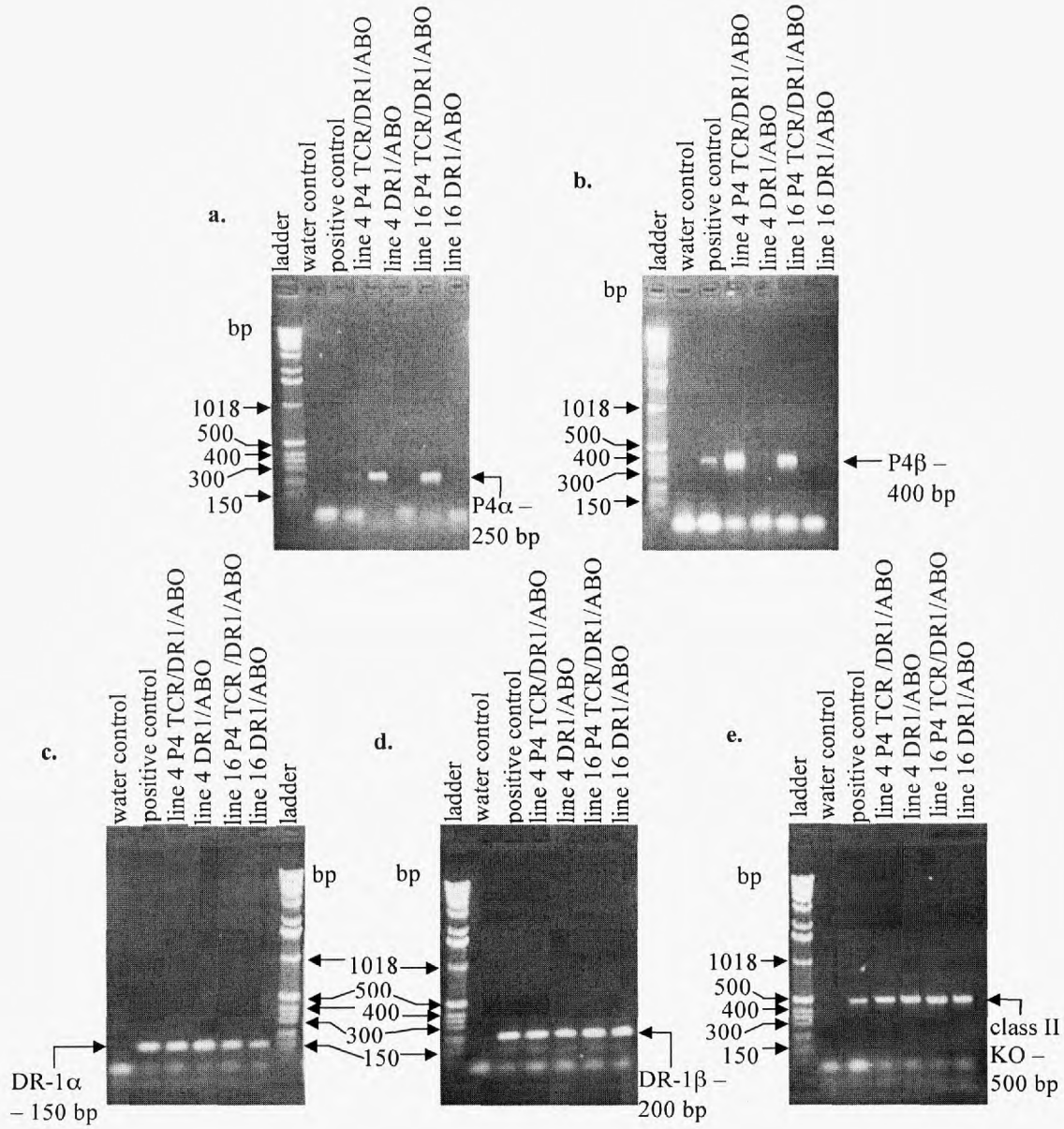


Figure 4.1 Genotyping PCRs to identify P4 TCR/DR1/ABO mice in lines 4 and 16 (a) – (e) show representative gels of the five PCRs required to identify a P4 TCR positive mouse. Each gel shows a TCR positive transgenic (P4 TCR/DR1/ABO above) mouse and a TCR negative transgenic (DR1/ABO above) mouse from each line for comparison. (a) shows the typical product of 250 bp for the P4 TCRα gene; a band is only seen in the mice which are TCR positive. (b) shows the typical product of 400 bp for the P4 TCRβ gene; a band is only seen in the mice which are TCR positive. The positive control for both P4 α and β PCRs above was human genomic DNA from which the P4 TCR was originally identified. (c) shows the typical product of 150 bp for the human MHC class II HLA-DR1 α gene and (d) shows the typical product of 200 bp for the human MHC class II HLA-DR1 β gene; a band is seen for all mice. (e) shows the typical product of 500 bp seen in murine class MHC II H2-A knockout mice – a band is seen for all mice. The positive control for the HLA-DR1 α and β and the class II knockout PCRs was murine genomic DNA from the HLA-DR1/mouse class II knockout line.

4.1.3 FACS phenotyping of P4 TCR/DR1/ABO transgenic mouse lines confirms murine MHC class II knockout status

The status of the transgenic lines in terms of murine MHC class II molecule expression was determined by flow cytometry, as shown in Figure 4.2. A generic anti-mouse MHC class II antibody (anti I-A/I-E) was used in conjunction with an anti-CD45R antibody to stain B-cells, which under normal conditions express MHC class II, to identify whether a mouse was homozygous or heterozygous for the knockout insertion, as the genotyping PCR used to probe for presence of the knockout insertion cannot differentiate between them. All antibodies and their working concentrations are shown in Appendix 6. B-cells from a mouse homozygous for the knockout insertion do not stain with the anti-I-A/I-E antibody. B-cells from a heterozygous mouse do stain with the anti-I-A/I-E antibody, but the levels of MHC class II expression would be lower than for a wild-type mouse, which would manifest as decreased brightness of staining. Typical FL1 vs FL2 plots for a homozygous knockout mouse from line 4 (A) or 16 (B), and typical plots for homozygous knockout, heterozygous knockout and wild-type mice from the DR1/ABO line (C) are shown for comparison in Figure 4.2. The TCR transgenic founder/HLA-DR1 murine MHC class II knockout cross generated offspring that were heterozygous (this would be expected as the TCR transgenic founders expressed murine MHC class II molecules normally whereas the DR1/ABO line has been bred for homozygosity of the knockout insertion). All subsequent breeding was carried out so as to create offspring homozygous for the knockout insertion at the earliest possible opportunity. In mice that are homozygous for the knockout insertion, the only MHC class II molecule available for presenting peptides and binding to T-cells is the human molecule HLA-DR1. As this is the molecule to which the transgenic TCR is restricted, knocking out expression of endogenous MHC class II molecules prevents other MHC class II-TCR interactions from occurring. However, these mice still retain the capacity to rearrange and express endogenous TCRα chains on T-cells, and all such TCRs will be restricted to HLA-DR1.

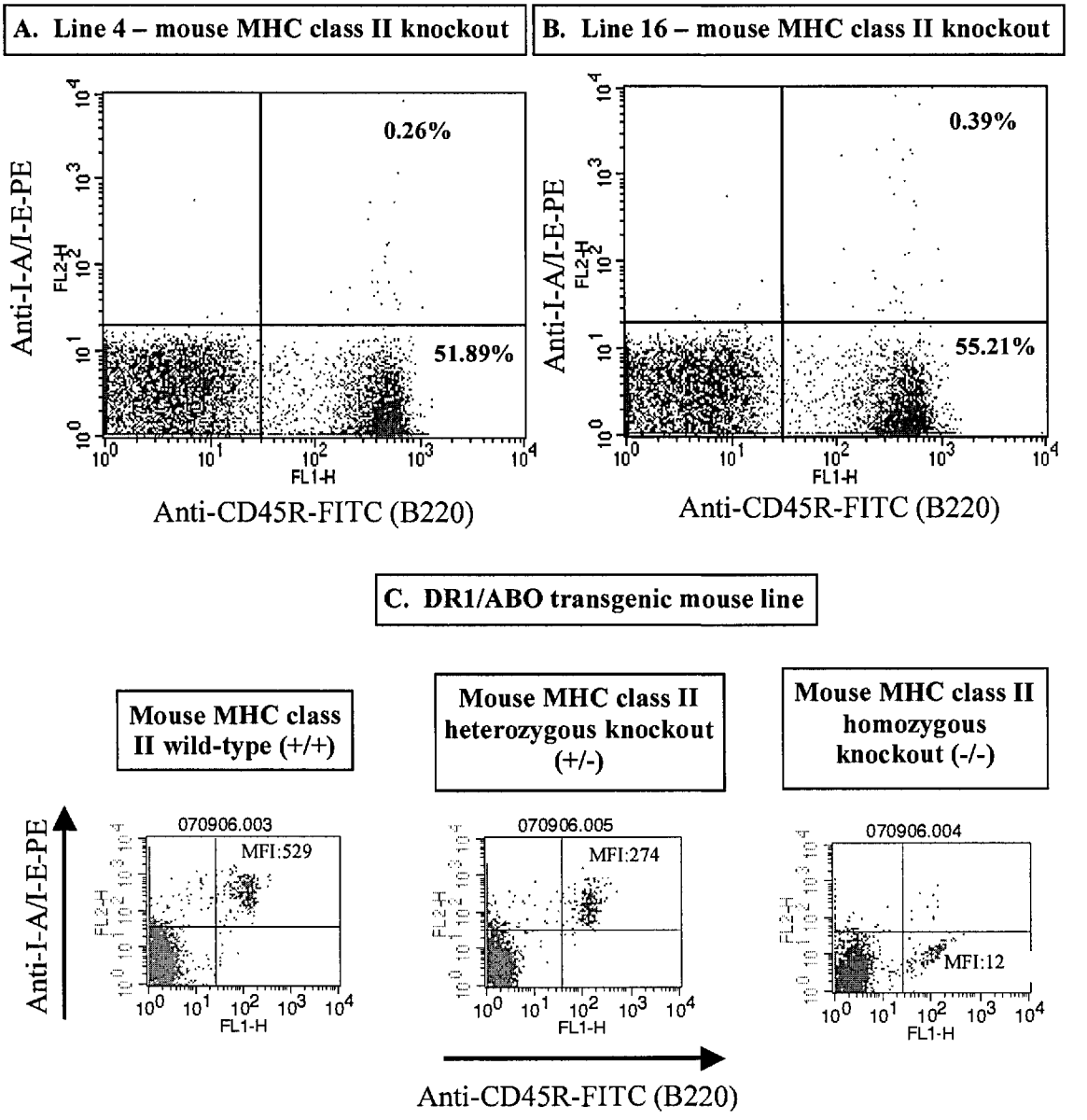


Figure 4.2 Phenotyping FACS to show mouse MHC class II H2-A knockout status of P4 TCR/DR1/ABO transgenic mice in lines 4 and 16 To ascertain the mouse MHC class II knockout status of the P4 TCR/DR1/ABO transgenic mice, freshly isolated PBMCs from tailbleed samples were stained with anti-CD45R-FITC (a B-cell marker) and anti-I-A/I-E-PE (a general mouse MHC class II-reactive antibody). Representative FACS plot for a line 4 (A) and a line 16 (B) transgenic mouse are shown in the upper panels indicating that B cells from these mice show no staining with the anti-I-A/I-E-antibody. The plots in the lower panel (C) show the expected plots from a wild type MHC class II mouse, an heterozygous MHC class II knockout mouse, and a homozygous MHC class II knockout mouse. The mean fluorescence intensity of the $CD45R^+$ cells is shown: it is highest in the wild type mice, which have the highest expression of murine MHC class II, intermediate in the heterozygous MHC class II knockout mice, which have intermediate levels of expression, and lowest in the homozygous knockout mice which do not express murine MHC class II.

4.1.4 Southern analysis confirms the presence of TCR transgenes in the genomic DNA of P4 TCR/DR1/ABO transgenic mice

Southern analysis of the lines was carried out, probing for the transgenic TCRα and TCRβ chains in genomic DNA from transgenic mice, shown for line 4 in Figure 4.3. A similar result was also seen for line 16 (data not shown). Southern analysis is a more robust genotyping method than PCR, as the probe used in detecting the DNA sequence is several hundred base pairs long in comparison to the 20-25 base pairs that is the usual length of a PCR primer. Southern hybridisation is therefore less prone to errors through binding of the probe to non-specific sequences than PCR, making it a more accurate method of ascertaining whether a particular gene sequence is present or absent in a DNA sample. In addition, the pattern and/or intensity of the bands obtained in a Southern hybridisation can give information on the copy number of an inserted transgene. The more intense a band is, the higher the number of copies that have been inserted into the genomic DNA of the recipient animal.

From the known sequence data for the pTαcass and pTβcass vectors and the TCRα and TCRβ chains, it was predicted that digesting genomic DNA with EcoRV and probing for the TCRα chain would yield a band of 3.2 kb in TCR transgene-positive animals. Digesting with the enzyme HindIII and probing for the TCRα chain would yield a positive band of 4.5 kb. It was also predicted that digesting genomic DNA with BamHI and probing for the TCRβ chain would yield a band of 5.6 kb in TCR transgene-positive animals. Probes were derived from PCR products of about 600 bp amplifying a portion of the TCR chain gene sequences (restriction enzymes, primers and PCR conditions are shown in Appendix 6) which were then DIG-labelled before hybridisation. This strategy was designed with the help of Dr. Catherine Reynolds.

For the P4 TCR Southern hybridisations, bands were seen using the probes for the TCRα and TCRβ chains when genomic DNA from TCR-positive P4 TCR/DR1/ABO transgenic mice (as determined by PCR genotyping) was digested with the appropriate restriction enzyme, as shown in Figure 4.3. Bands were not seen in equivalently-digested genomic DNA from TCR-negative (by PCR) DR1/ABO transgenic mice. However, staining the gel with ethidium bromide caused a very high background upon development of the blot and made it impossible to interpret them, hence the gels for these hybridisations were not stained – unfortunately, this prevented the use of a DNA

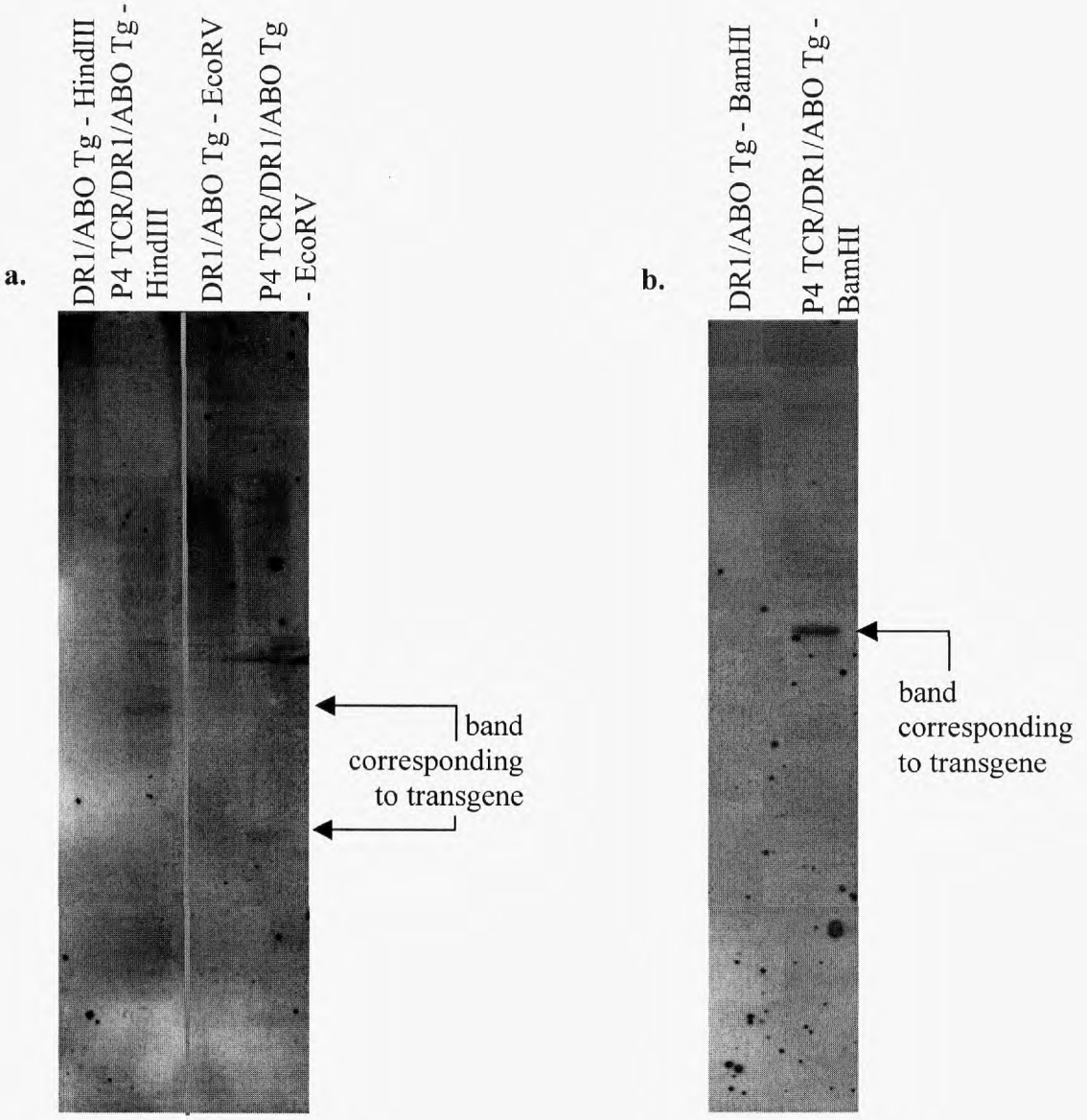


Figure 4.3 Southern analysis of the P4 TCR/DR1/ABO transgenic line 4 (a) shows a representative Southern blot, probing for the P4 TCRα chain in a line 4 P4 TCR/DR1/ABO transgenic mouse (by PCR analysis) (P4 TCR/DR1/ABO Tg above) and a TCR-negative (by PCR) DR1/ABO transgenic mouse (DR1/ABO Tg above) from the same line. (b) shows a representative Southern blot, probing for the P4 TCRβ chain in a P4 TCR/DR1/ABO line 4 transgenic mouse (by PCR analysis) and a TCR-negative (by PCR) DR1/ABO transgenic mouse from the same line. As no band of the same size as that seen in the TCR transgenic mice is seen in the littermate mice, these bands appear to be transgene-specific and thus confirm the transgenic status of the mice.

ladder with bands of known size as a marker for determination of band sizes. As such, the presence of bands in the DNA of TCR-positive (by PCR) mice and the absence of any bands in the DNA of TCR-negative (by PCR) mice suggests that these bands correspond to the probe binding to transgenic TCR-specific DNA, and confirm the findings from the genotyping PCRs.

4.1.5 mRNA products of the TCR transgenes in P4 TCR/DR1/ABO transgenic mice are correctly spliced

To investigate if the transgene was being processed correctly at the transcriptional level, a PCR strategy was designed by Dr. Catherine Reynolds and Dr. Xiaoming Cheng making use of an intron contained within TCRα and TCRβ chains between the leader peptide of the TCR chain and the rearranged V-J regions. The sequence inserted into the pTαcass and pTβcass vectors was derived from T-cell genomic DNA, hence this intron is present within the TCR chain transgenes and thus the primary mRNA transcript. For the transcripts to be correctly translated, this intronic sequence must be spliced out of the mRNA during processing of the primary transcript. As the intron is of a sufficient size in both chains (132 bp in the TCRα chain, 153 bp in the TCRβ chain), it is possible to visualise whether the intron has been removed by PCR. PCRs were carried out using primers positioned on either side of the intronic sequence on genomic DNA and also cDNA isolated from splenocytes (as the promoter in the pTcass constructs is T-cell lineage-specific, only cDNA products from cells of this lineage will transcribe the transgenes). All PCR primers and reaction conditions are shown in Appendix 6. In genomic DNA, where the intron is not removed from the sequence, a product size corresponding to the unspliced message should be seen (478 bp for the TCRα chain, 425 bp for the TCRβ chain). In T-cell cDNA, if correct processing has occurred, the product size should correspond to the unspliced product size minus the intron (346 bp for the TCRα chain, 272 bp for the TCRβ chain). Figure 4.4 shows PCR products from genomic DNA and T-cell cDNA from P4 TCR/DR1/ABO transgenic mice from lines 4 and 16 and also from a DR1/ABO transgenic mouse. The TCRα chain PCR is shown in a, and the TCRβ chain PCR in b. For P4 TCR/DR1/ABO transgenic mice from both lines 4 and 16, a larger band corresponding to the unspliced sequence was amplified from the genomic DNA in both PCRs. A smaller band, corresponding to the correctly-spliced mRNA, was amplified from the spleen cDNA for both PCRs, indicating that

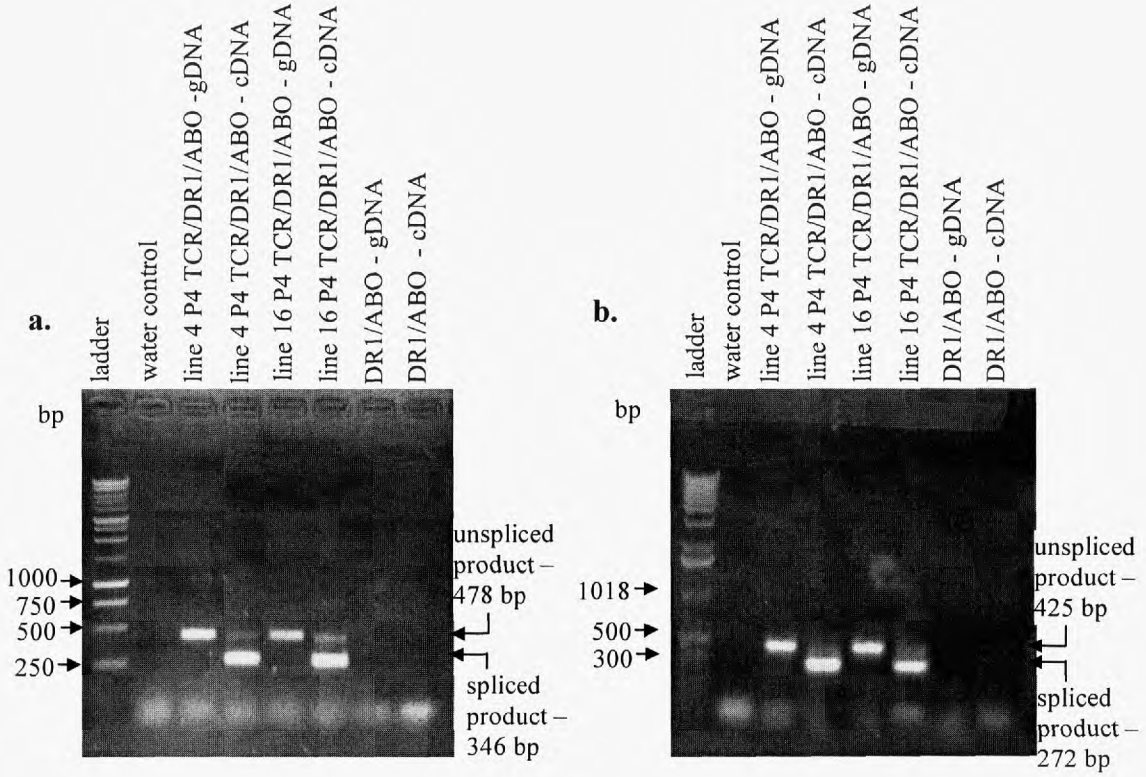


Figure 4.4 PCRs to identify correct splicing of the TCR mRNA gene products to remove intronic sequence in P4 TCR/DR1/ABO transgenic mice in lines 4 and 16 (a) and (b) show representative gels of the PCRs that identify correct splicing of the P4 TCR α (a) and β (b) mRNA products in P4 TCR/DR1/ABO transgenic mice. A difference in size between the bands obtained from the genomic DNA and the cDNA from TCR-positive mice indicates correct splicing of the transgenes to remove the intron is occurring. No band is seen for the PCRs carried out in the TCR-negative DR1/ABO transgenic mouse as it does not carry the TCR transgenes. Each gel shows the PCR products obtained from genomic DNA (gDNA) and cDNA in a line 4 P4 TCR/DR1/ABO transgenic mouse, a line 16 P4 TCR/DR1/ABO transgenic mouse and a DR1/ABO transgenic mouse.

correct processing of the primary mRNA transcript occurs in both lines. A less intense band was seen corresponding to the unspliced product in the cDNA lanes – this band represented transcripts that had not yet been processed. No bands were seen in any PCR using the DNA or cDNA from DR1/ABO transgenic mice, as they lack the TCR transgenes.

4.2 Induction of allergic inflammation in the lung of P4 TCR/DR1/ABO transgenic mice using Fel d 1

4.2.1 Overview

A murine model of allergic inflammation in the lung using Fel d 1 in transgenic DR1/ABO mice on a mouse MHC class II knockout background was previously developed by our laboratory in collaboration with Altmann, Larché and Lloyd (submitted for publication in the Journal of Experimental Medicine). As the TCR for which P4 TCR mice are transgenic recognises peptide 4 of Fel d 1 bound to HLA-DR1, the TCR transgenic mice were crossed with the DR1/ABO mice on a mouse MHC class II knockout background. This model was developed to test the hypothesis that a humanised TCR/MHC class II transgenic model of allergic asthma would be an improved model of disease. The protocols for inducing allergic inflammation in this model were developed by Dr. Catherine Reynolds and Dr. Xiaoming Cheng in our laboratory.

This protocol, outlined in Figure 4.5, involves two sensitisations 11 days apart comprising an intraperitoneal injection of recombinant Fel d 1 protein in alum, followed by intranasal challenges with whole cat dander extract on three consecutive days starting ten days after the second sensitisation. The Penh response to increasing doses of methacholine was measured by whole-body plethysmography 24 hours after the last challenge. Resistance and compliance measurements, also in response to increasing doses of methacholine, were made 24 hours later before tissues were harvested for further analysis.

Other mouse models of asthma, such as the ovalbumin model, have shown induction of allergic disease characterised by increased bronchial hyperreactivity, increased production of IgE, airway eosinophilia and lung inflammation (287). In addition to measuring lung function, blood was taken from the mice for measurement of total IgE in the serum, BAL fluid was collected for differential cell counting and for cytokine measurement, one lobe of the lung was inflated and frozen for histological analysis and lung tissue was collected and either disaggregated for differential cell counting or homogenised for the cytokine measurement. All work described here about the TCR transgenic model of allergic inflammation was carried out with Dr. Catherine Reynolds.

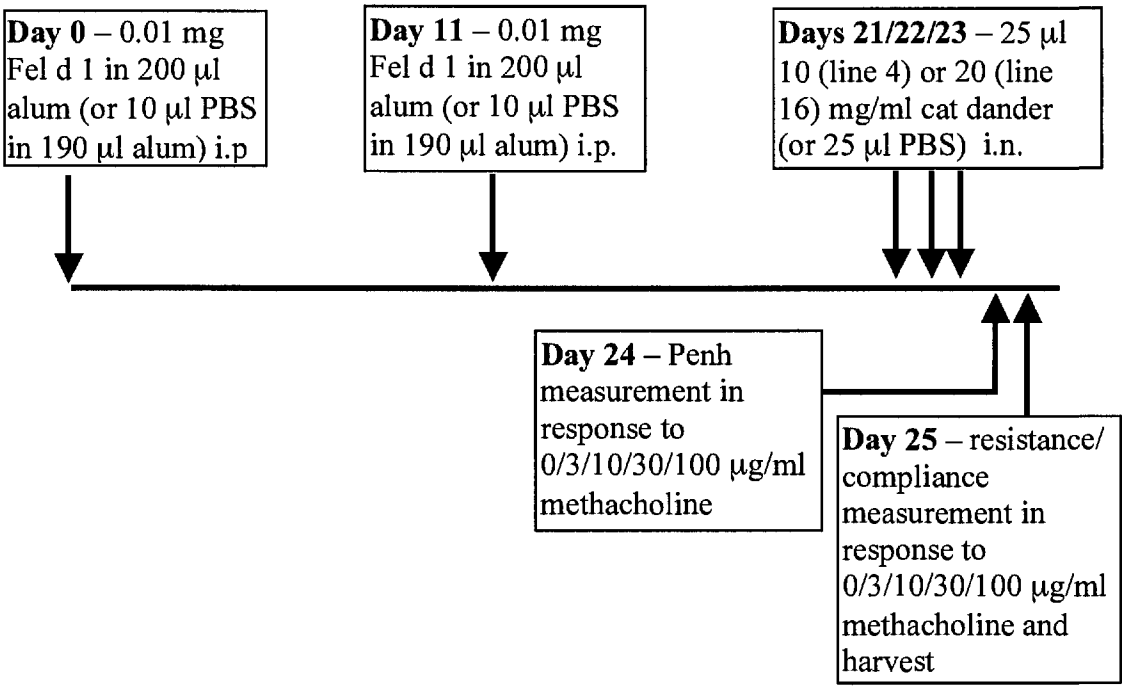


Figure 4.5 The disease induction protocol used to induce allergic lung inflammation in the P4 TCR/DR1/ABO transgenic lines 4 and 16 Mice were sensitised twice intraperitoneally with recombinant Fel d 1 in alum, or, in the case of control mice, with an equivalent volume of PBS in alum. Mice were then challenged with intranasally administered cat dander extract, at a concentration of either 10 (250 µg per challenge) or 20 mg/ml (500 µg per challenge). Penh in response to methacholine provocation was measured by whole body plethysmography 24 hours after the last intranasal challenge. Resistance/compliance measurements were recorded in response to methacholine provocation 24 hours after Penh measurement, after which BAL fluid, blood and lung tissue was harvested, for analysis of cytokine production, serum IgE and for differential cell counting. One lobe of the lung was inflated and frozen for histological analysis.

Both lines were analysed for disease induction following this protocol. Two doses of whole cat dander extract were used for intranasal challenge (as shown in Figure 4.5). The sensitisation dose of Fel d 1 was constant for all experiments. Numbers of mice per group for the two experiments carried out are shown in Table 4.1. In line 4, a lower dose of whole cat dander extract (25 µl at 10 mg/ml) was used for challenge; in line 16, a higher dose (25 µl at 20 mg/ml) was used for challenge. Four groups were used in the experiments – a P4 TCR/DR1/ABO transgenic Fel d 1-sensitised group, a DR1/ABO transgenic Fel d 1-sensitised group, and P4 TCR/DR1/ABO transgenic and DR1/ABO transgenic PBS-treated control groups. In the line 4 experiment, it was notable that of the P4 TCR/DR1/ABO transgenic mice sensitised with Fel d 1, approximately half of the mice died before the end of the experiment (3 out of 7). This did not happen in the experiment using line 16 mice. It is possible that more severe disease had been induced in the mice that died in the line 4 experiments; unfortunately, it was not possible to examine any of the mice that died to see if this was the case.

4.2.2 Disease induction with Fel d 1 induces increased airway hyperreactivity and bronchoconstriction in response to methacholine challenge

Lung function was assayed by three parameters: measurement of Penh by unrestrained whole-body plethysmography, and measurement of pulmonary resistance and dynamic compliance in anaesthetised tracheotomised mice by whole-body plethysmography. Penh measurement was carried out with the help of Dr. Catherine Reynolds; measurement of resistance and compliance was performed by Dr. Kate Choy and Dr. Catherine Reynolds.

4.2.2.1 Lung function data from the line 4 experiment

Lung function measurements for the line 4 experiment are shown for both P4 TCR/DR1/ABO transgenic and DR1/ABO transgenic mice in Figure 4.6. Penh measurements for the P4 TCR/DR1/ABO transgenic mice showed that in general, Fel d 1-sensitised mice responded to a greater degree to methacholine provocation than PBS-treated controls, although this did not reach statistical significance at any dose assayed (Student's unpaired t test, two-tailed). This suggests that there may have been a greater degree of airway hyperreactivity in the Fel d 1-sensitised P4 TCR/DR1/ABO transgenic mice than in the PBS-treated controls. This was in contrast to the DR1/ABO transgenic

		Group numbers			
line	i.n. challenge dose	TCR/DR1 Tg Fel d 1	TCR/DR1 Tg PBS	DR1 only Tg Fel d 1	DR1 only Tg PBS
4	250 μg	4/7*	2	2	2
16	500 μg	7	2	5	2

Table 4.1 Group numbers used in the Fel d 1 disease induction experiments Two disease induction experiments were carried out. In the experiments in line 4, for the P4 TCR/DR1/ABO transgenic mice sensitised with Fel d 1 (denoted by *), the first number indicates the number of mice surviving until day 25 for lung function measurements and harvest, whilst the second number shows the number of mice originally entered into the experiment. All mice survived the protocol in the line 16 experiment. (TCR/DR1 Tg = P4 TCR/DR1/ABO transgenic mice, DR1 only Tg = DR1/ABO transgenic mice)

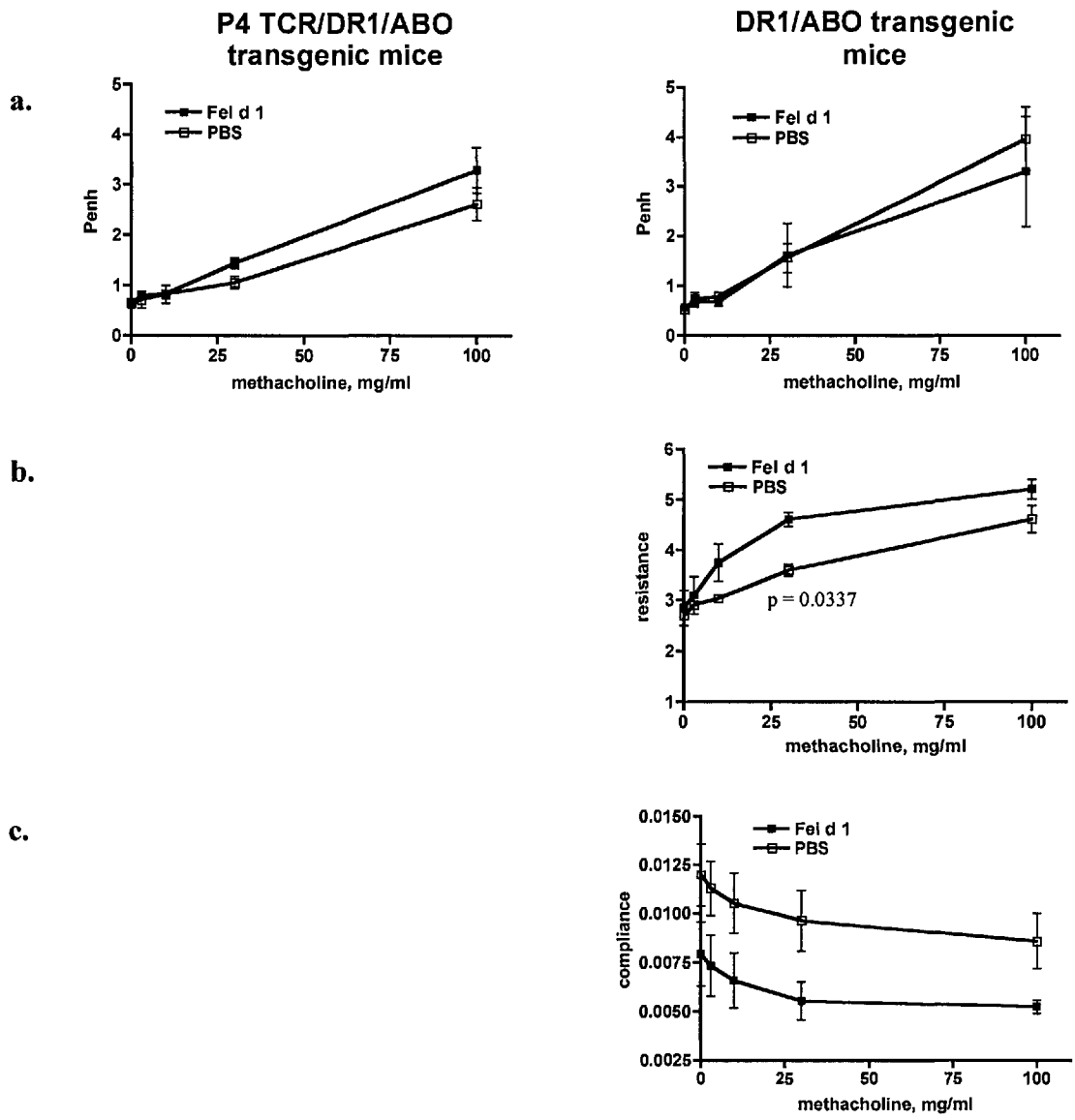


Figure 4.6 Lung function parameter measurements in response to methacholine provocation in the line 4 Fel d 1 disease induction experiment P4 TCR/DR1/ABO transgenic mice and DR1/ABO transgenic mice are shown separately – P4 TCR/DR1/ABO transgenic mice are shown on the left-hand side, DR1/ABO transgenic mice on the right. (a) shows Penh data, with Fel d 1- and PBS-treated groups compared for P4 TCR/DR1/ABO transgenic mice and DR1/ABO transgenic mice. (b) shows resistance data and (c) shows compliance data. Group size for P4 TCR/DR1/ABO transgenic mice sensitised with Fel d 1 was n = 4. Group size for DR1/ABO transgenic mice treated with Fel d 1 was n = 2. Group size for both TCR transgenic and littermate PBS-treated mice was n = 2. Data are shown as mean ± SEM. Where significance values are shown, the statistical test used was Student's t test (two-tailed).

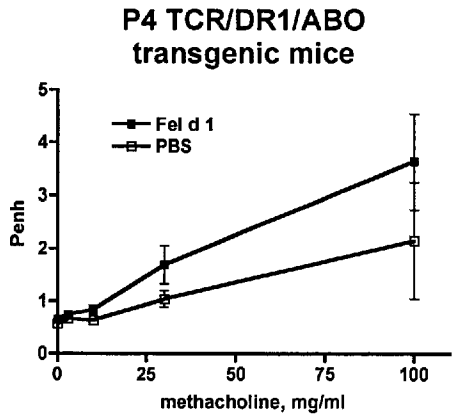
mice which, although responding to methacholine to a similar extent overall as the P4 TCR/DR1/ABO transgenic mice, did not noticeably differ between Fel d 1-sensitised and PBS-treated groups. Resistance and compliance measurements for the P4 TCR/DR1/ABO transgenic mice were uninterpretable due to technical difficulties. Measurement of resistance in the DR1/ABO transgenic mice followed the expected pattern, with Fel d 1-sensitised mice responding to a greater extent in response to methacholine than the PBS-treated mice, and this was significant at the 30 mg/ml methacholine dose ($p = 0.0337$, Student's unpaired t test, two-tailed). The compliance measurements for DR1/ABO transgenic mice showed that the Fel d 1-sensitised mice responded to methacholine to a greater extent than the PBS-treated controls, but this was not significant at any dose. These results follow the expected pattern as dynamic compliance would be expected to decrease as airway resistance increased.

4.2.2.2 Lung function data from the line 16 experiment

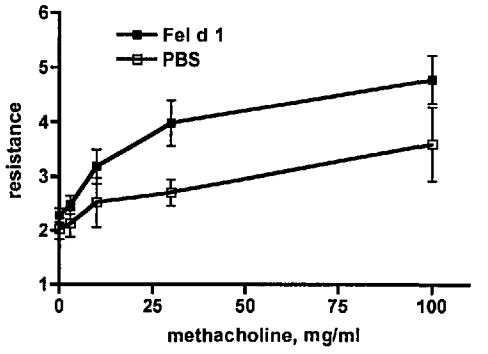
Lung function measurements for the line 16 experiment are shown for P4 TCR/DR1/ABO transgenic mice in Figure 4.7. Penh measurements for the P4 TCR/DR1/ABO transgenic mice showed that Fel d 1-sensitised mice appeared to respond to a greater extent to methacholine provocation than PBS-treated controls, which could be seen particularly at the 30 mg/ml dose although this was not statistically significant (using Student's unpaired two-tailed t test). For the P4 TCR/DR1/ABO transgenic mice, there was a greater increase in resistance in response to methacholine in the Fel d 1-sensitised mice than in the PBS-treated mice; this was in correlation with the Penh data. The difference between the groups at the 30 mg/ml methacholine dose was the most marked, but was not statistically significant (Student's unpaired two-tailed t test). Dynamic compliance in these mice decreased to a greater extent in response to methacholine provocation in the Fel d 1-sensitised mice, but to a lesser extent than that seen in the Penh and resistance measurements; this correlated with the Penh and resistance data overall.

The data obtained for the P4 TCR/DR1/ABO transgenic mice is consistent with the induction of airway hyperreactivity in the Fel d 1-sensitised mice, as an increase in AHR in response to methacholine provocation was consistently seen for all three parameters.

a.



b.



c.

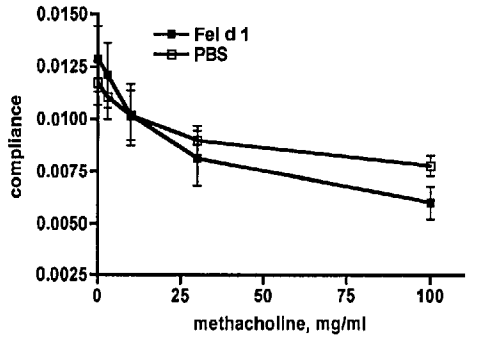


Figure 4.7 Lung function parameter measurements in response to methacholine provocation in the line 16 Fel d 1 disease induction experiment Data for P4 TCR/DR1/ABO transgenic mice are shown. (a) shows Penh data, with Fel d 1- and PBS-treated groups compared for P4 TCR/DR1/ABO transgenic mice. (b) shows resistance data and (c) shows compliance data. Group size for P4 TCR/DR1/ABO transgenic mice sensitised with Fel d 1 was n = 7. Group size for P4 TCR/DR1/ABO transgenic mice treated with PBS was n = 2. Data are shown as mean ± SEM.

4.2.3 Differential cell counts in BAL fluid and disaggregated lung tissue of Fel d 1-treated mice showed substantial eosinophilic influx into the lungs

Cytospins were prepared from cells isolated from BAL fluid and disaggregated lung tissue and stained with Wright-Giemsa stain. Cells were counted (300 per slide) on the basis of differential cell morphology and staining pattern (as shown in Appendix 8). Neutrophils, eosinophils, macrophages and lymphocytes were counted, and total numbers of each cell type in the original samples was calculated based on total cell counts, as shown in Figure 4.8.

4.2.3.1 Differential cell counts in BAL fluid from line 4 and line 16 experiments

Fel d 1-sensitised groups in both P4 TCR/DR1/ABO transgenic mice and DR1/ABO transgenic mice showed a large increase in cells recovered from BAL fluid compared with PBS-treated control groups (in each group, the mean cell count increased from less than 50,000 to at least 100,000. This result reached significance for the line 16 P4 TCR/DR1/ABO transgenic group ($p = 0.0150$, Student's unpaired t test with Welch's correction, two-tailed)). Total number of cells recovered from BAL fluid in the line 16 experiment (which used the higher dose challenge) was higher than in the line 4 experiment for the Fel d 1-sensitised P4 TCR/DR1/ABO transgenic groups (645,427 ± 181018 compared with 132,000 ± 104467). Total cells recovered from BAL fluid in the Fel d 1-sensitised DR1/ABO transgenic groups were comparable to the P4 TCR/DR1/ABO transgenic Fel d 1-sensitised groups in each experiment (78,000 ± 22800 for line 4 and 652,400 ± 220278 for line 16). This increase in total cells between the Fel d 1- and PBS-treated groups was predominantly caused by an increase in eosinophils in BAL fluid in both experiments which would be expected as an allergic phenotype had been induced by Fel d 1 sensitisation and cat dander challenge. The increase in eosinophils reached significance for the DR1/ABO transgenic group in the line 4 experiment ($p = 0.0108$, Student's unpaired two-tailed t test), and for the P4 TCR/DR1/ABO transgenic ($p = 0.0158$, Student's unpaired two-tailed t test with Welch's correction) mice in the line 16 experiment.

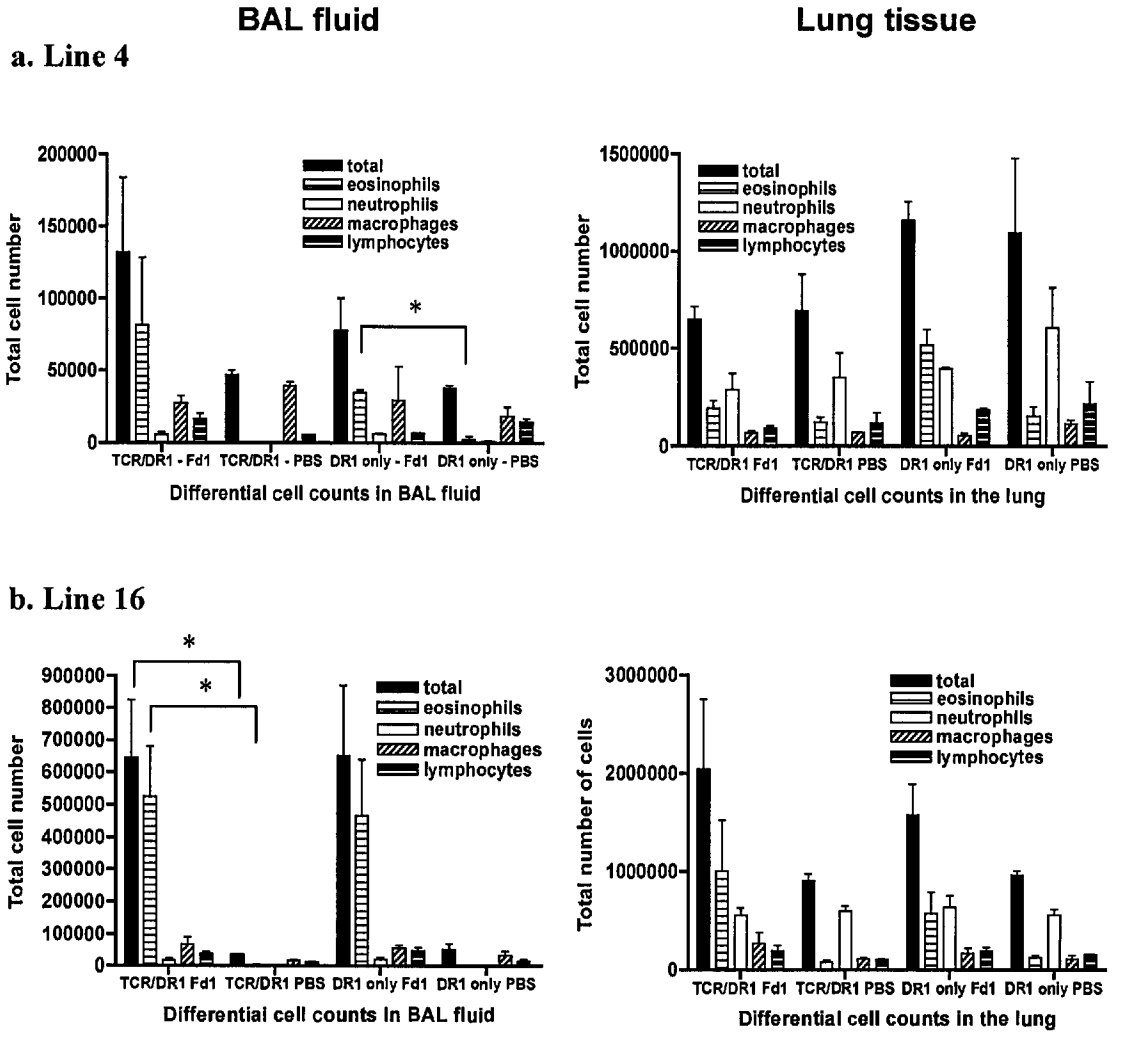


Figure 4.8 Differential cell counts in BAL fluid and lung tissue in the Fel d 1 disease induction experiments in TCR P4/DR1/ABO lines 4 and 16 Cells were harvested from BAL fluid (left-hand side) and from disaggregated lung tissue (right-hand side) and total cells were counted. Cytospin slides for each sample were prepared and cells were differentially counted (300 cells per slide) on the basis of cell morphology. Total cells are shown for each group alongside the numbers of cells comprising each subset. Slides were counted by three independent, blinded investigators and counts for each slide were averaged. Data is shown as mean values ± SEM. (a) shows cell counts obtained from the line 4 experiment. (b) shows cell counts obtained from the line 16 experiment. Group size for line 4 P4 TCR/DR1/ABO transgenic mice sensitised with Fel d 1 was n = 4. Group size for DR1/ABO transgenic mice treated with Fel d 1 in the line 4 experiment was n = 2. Group size for both P4 TCR/DR1/ABO transgenic and DR1/ABO transgenic PBS-treated mice in the line 4 experiment was n = 2. Group size for line 16 P4 TCR/DR1/ABO transgenic mice sensitised with Fel d 1 was n = 7. Group size for DR1/ABO transgenic mice treated with Fel d 1 in the line 16 experiment was n = 5. Group size for both P4 TCR/DR1/ABO transgenic and DR1/ABO transgenic PBS-treated mice in the line 16 experiment was n = 2. (TCR/DR1 = P4 TCR/DR1/ABO transgenic mice, DR1 only = DR1/ABO transgenic mice, Fd1 = Fel d 1 sensitised, PBS = PBS control.) * = $p \leq 0.05$ (Student's unpaired two-tailed t test)

4.2.3.2 Differential cell counts in disaggregated lung tissue from line 4 and line 16 experiments

Total cell numbers recovered from disaggregated lung tissue was similar for both Fel d 1-sensitised and PBS-treated groups in the line 4 experiment for the P4 TCR/DR1/ABO transgenic mice and also the DR1/ABO transgenic mice.

Despite there being no overall increase in total cell count from the disaggregated lung tissue between Fel d 1- and PBS-treated mice in either experiment, the proportions of cell types making up the total number differed between the two treatment groups in all cases. The main difference between Fel d 1-sensitised and PBS-treated mice was an increase in lung eosinophils in the Fel d 1-sensitised mice. This increase was seen in both line 4 and line 16, in both P4 TCR/DR1/ABO transgenic and DR1/ABO transgenic mice, but did not reach statistical significance in any case (Student's unpaired two-tailed t test).

4.2.4 Fel d 1 treatment induced an increase in serum total IgE

Serum was isolated from blood obtained by cardiac puncture and assayed for IgE content by ELISA. The capture and detection antibodies and standard used are shown in Appendix 9. In both lines 4 and 16, IgE production was only seen at high levels in the Fel d 1-sensitised/cat dander challenged groups, as shown in Figure 4.9. The difference in IgE production reached significance in the line 16 experiment when comparing the Fel d 1- and PBS-treated P4 TCR/DR1/ABO transgenic groups ($p = 0.0304$, Student's unpaired two-tailed t test with Welch's correction). The lack of IgE production in the PBS-treated mice compared against the production of high levels of IgE in the Fel d 1-sensitised mice is relevant in a biological context, indicating that there is induction of IgE production in response to sensitisation and challenge with cat allergen in these mice which is a characteristic feature of allergic disease induction. Where P4 TCR/DR1/ABO transgenic mice were compared with DR1/ABO transgenic mice, there was a tendency for IgE production to be higher in the P4 TCR/DR1/ABO transgenic mice.

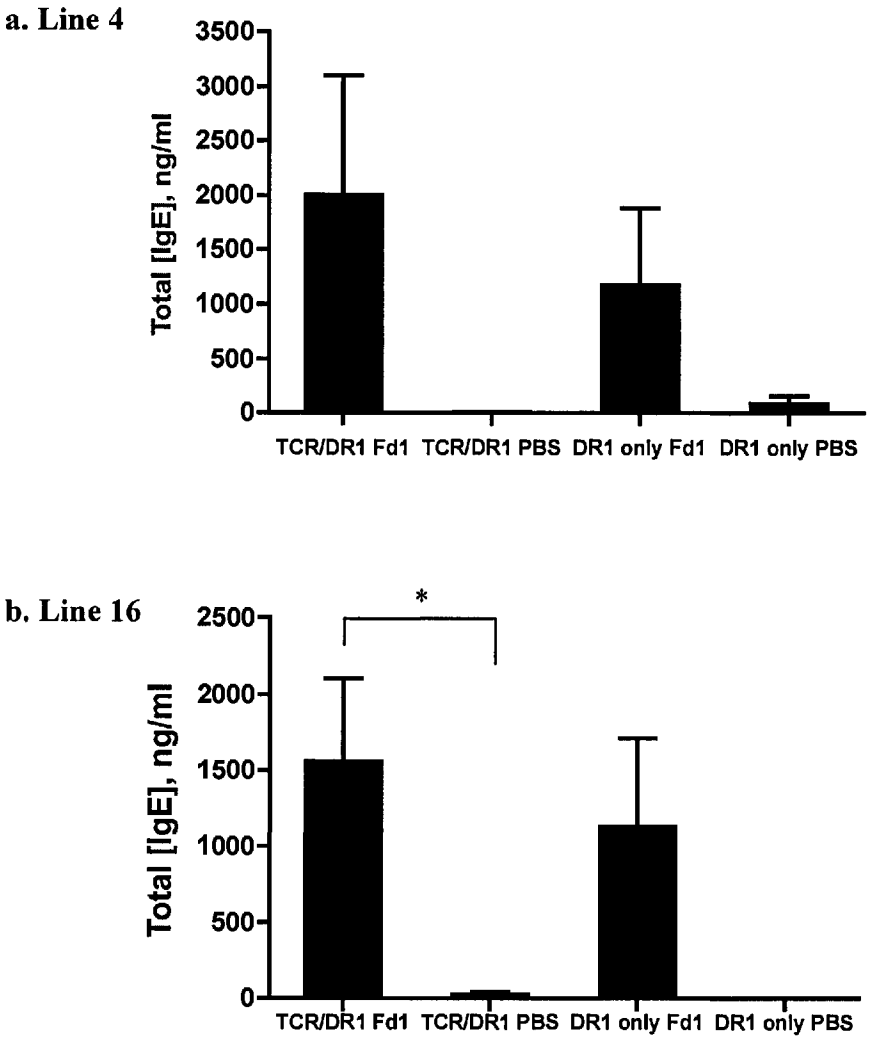


Figure 4.9 Total serum IgE production in the Fel d 1 disease induction experiments in TCR P4/DR1/ABO lines 4 and 16 Total [IgE] was measured in the serum of mice undergoing the Fel d 1 disease induction protocol by ELISA, against a general IgE standard. Data is shown as mean values for each group ± SEM. (a) shows total serum [IgE] obtained from the line 4 experiment. (b) shows shows total serum [IgE] obtained from the line 16 experiment. Group size for line 4 P4 TCR/DR1/ABO transgenic mice sensitised with Fel d 1 was n = 4. Group size for DR1/ABO transgenic mice treated with Fel d 1 in the line 4 experiment was n = 2. Group size for both P4 TCR/DR1/ABO transgenic and DR1/ABO transgenic PBS-treated mice in the line 4 experiment was n = 2. Group size for line 16 P4 TCR/DR1/ABO transgenic mice sensitised with Fel d 1 was n = 7. Group size for DR1/ABO transgenic mice treated with Fel d 1 in the line 4 experiment was n = 5. Group size for both P4 TCR/DR1/ABO transgenic and DR1/ABO transgenic PBS-treated mice in the line 16 experiment was n = 2. (TCR/DR1 = P4 TCR/DR1/ABO transgenic mice, DR1 only = DR1/ABO transgenic mice, Fd1 = Fel d 1 sensitised, PBS = PBS controls.) * = $p \leq 0.05$ (Student's unpaired two-tailed t test)

4.2.5 Levels of the Th2-type cytokines IL-4, IL-5 and IL-13 were increased in BAL fluid in response to treatment with Fel d 1 when using the lower dose challenge protocol

Cytokines were analysed by ELISA of BAL fluid against recombinant standards of known concentration. All capture and detection antibodies and recombinant standards used are shown in Appendix 9.

In the line 4 experiment, higher levels of the Th2-associated cytokines IL-4, IL-5 and IL-13 were seen in the BAL fluid of the Fel d 1-sensitised groups than the PBS-treated groups for the P4 TCR/DR1/ABO transgenic mice only, as shown in Figure 4.10. This did not reach significance for any of the cytokines assayed, probably due to small group sizes (using the Student's unpaired two-tailed t test). No difference was seen between Fel d 1- and PBS-treated groups in the DR1/ABO transgenic mice. There was very little IFN-γ in the BAL fluid in any group.

In the line 16 experiment, there was no statistically significant difference (Student's unpaired two-tailed t test) in the amount of IL-4, IL-5 and IL-13 seen in BAL fluid in PBS-treated groups compared with Fel d 1-sensitised groups in both P4 TCR/DR1/ABO transgenic mice and DR1/ABO transgenic mice, as shown in Figure 4.11. No IFN-γ was detected under any of the experimental conditions.

4.2.6 The amount of IL-4, IL-5 and IL-13 in lung tissue homogenate supernatant following disease induction

Cytokines were analysed by ELISA in the supernatant of homogenised lung tissue against recombinant standards of known concentration. All capture and detection antibodies and recombinant standards used are shown in Appendix 9.

Levels of IL-4, IL-5, IL-13 and IFN-γ detected in the supernatant of lung homogenate from the two disease induction experiments are shown in Figure 4.12. There was an increase in IL-4, IL-5 and IL-13 production in the Fel d 1-sensitised line 16 P4 TCR/DR1/ABO transgenic mice. This approached significance for IL-13 ($p = 0.0565$, Student's unpaired two-tailed t test).

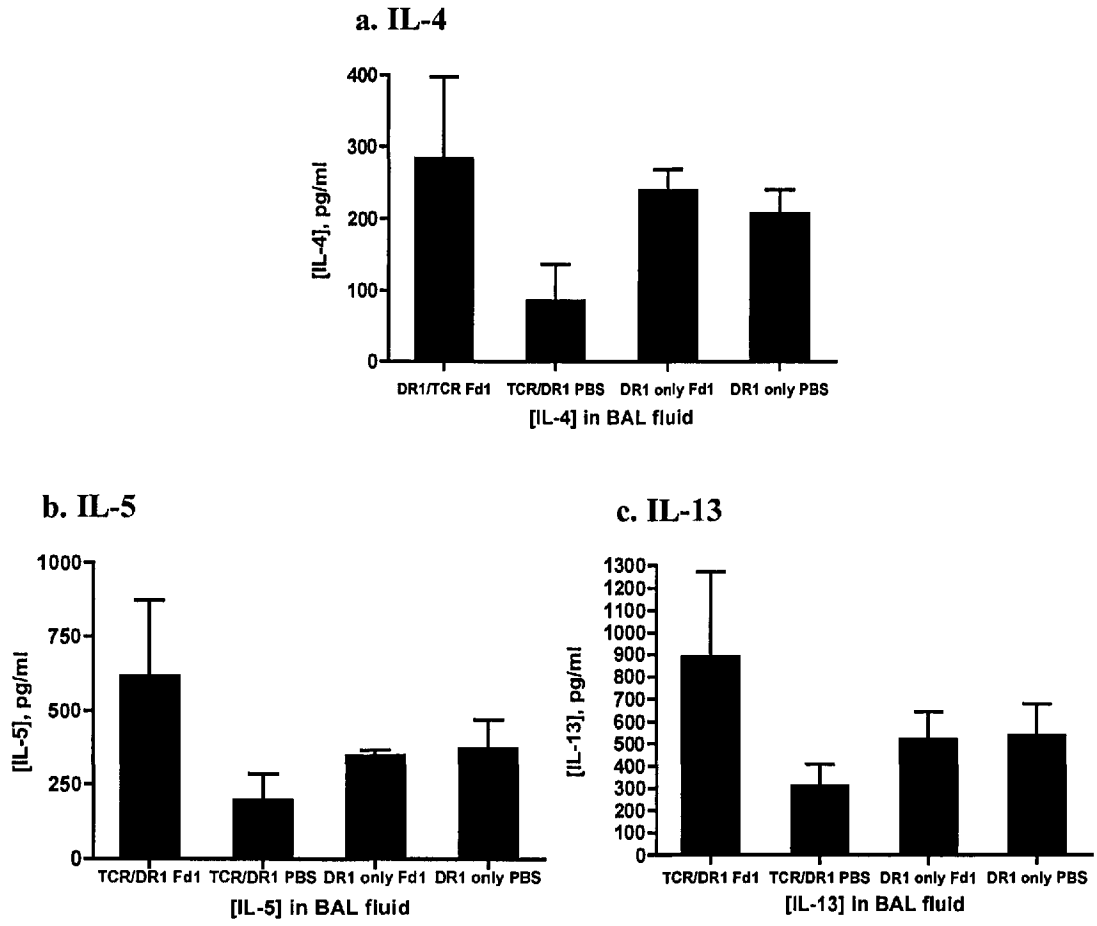
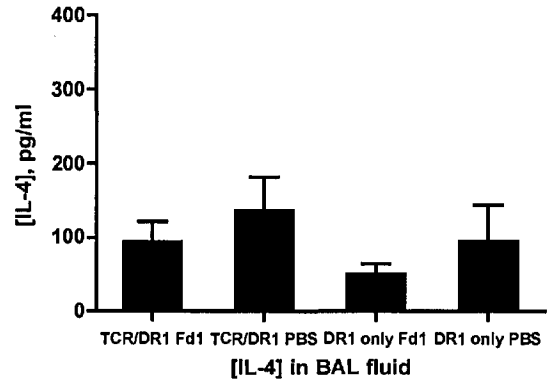
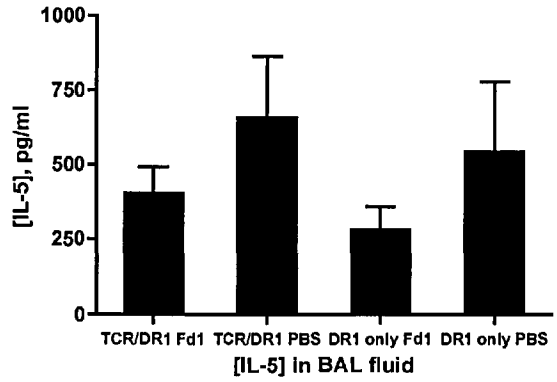


Figure 4.10 Th2-associated cytokines in the BAL fluid of line 4 P4 TCR/DR1/ABO transgenic mice and DR1/ABO transgenic mice after Fel d 1 sensitisation/cat dander challenge Cytokines were measured in BAL fluid samples from each mouse by ELISA, against recombinant standards. Data is shown as mean values ± SEM. (a) shows the concentration of IL-4 measured in the BAL fluid. (b) shows the concentration of IL-5 measured in the BAL fluid. (c) shows the concentration of IL-13 measured in the BAL fluid. Group size for P4 TCR/DR1/ABO transgenic mice sensitised with Fel d 1 was n = 4. Group size for DR1/ABO transgenic mice treated with Fel d 1 was n = 2. Group size for both P4 TCR/DR1/ABO transgenic and DR1/ABO transgenic PBS-treated mice was n = 2. (TCR/DR1 = P4 TCR/DR1/ABO transgenic mice, DR1 only = DR1/ABO transgenic mice, Fd1 = Fel d 1 sensitised, PBS = PBS controls)

a. IL-4



b. IL-5



c. IL-13

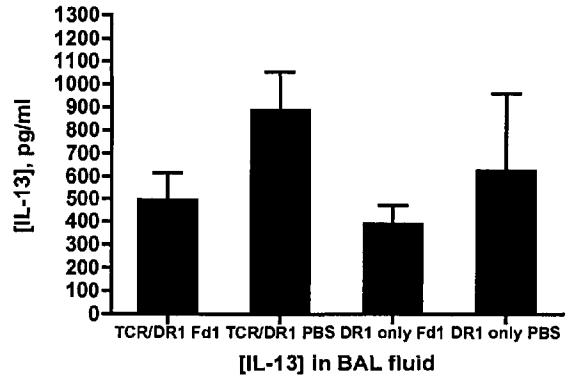


Figure 4.11 Production of Th2-associated cytokines in the BAL fluid of line 16 P4 TCR/DR1/ABO transgenic mice and DR1/ABO transgenic mice after Fel d 1 sensitisation/cat dander challenge Cytokines were measured in the supernatant of BAL fluid samples from each mouse by ELISA, against recombinant standards. Data is shown as mean ± SEM. (a) shows the concentration of IL-4 measured in the BAL fluid. (b) shows the concentration of IL-5 measured in the BAL fluid. (c) shows the concentration of IL-13 measured in the BAL fluid. Group size for P4 TCR/DR1/ABO transgenic mice sensitised with Fel d 1 was n = 7. Group size for DR1/ABO transgenic mice treated with Fel d 1 was n = 5. Group size for both P4 TCR/DR1/ABO transgenic and DR1/ABO transgenic PBS-treated mice was n = 2. (TCR/DR1 = P4 TCR transgenic mice, DR1 only = DR1/ABO transgenic mice, Fd1 = Fel d 1 sensitised, PBS = PBS controls).

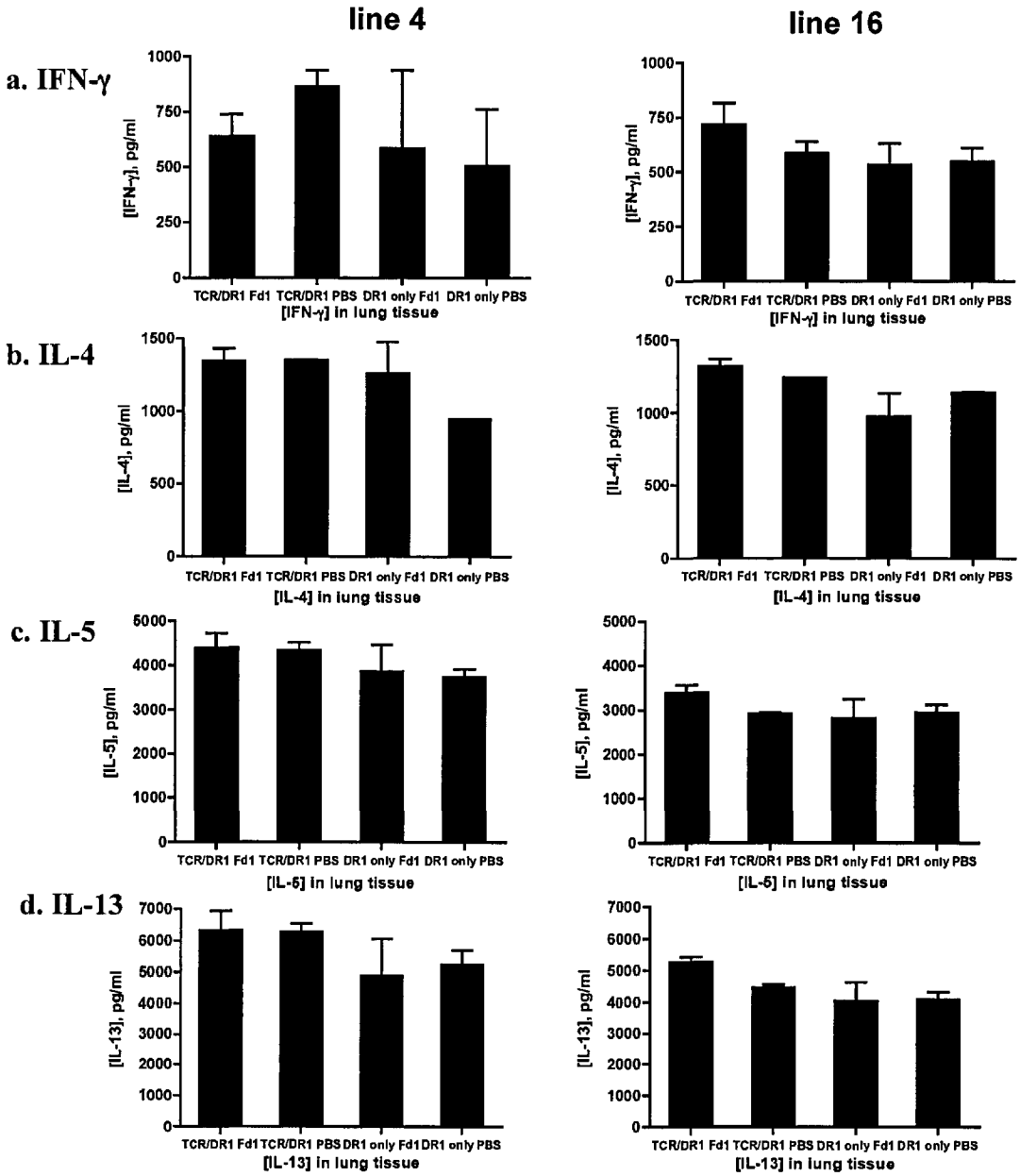


Figure 4.12 Th1- and Th2-associated cytokines in the lung tissue of line 4 and line 16 P4 TCR/DR1/ABO transgenic and DR1/ABO transgenic mice after Fel d 1 sensitisation/cat dander challenge Cytokines were measured in the supernatant of lung homogenate samples resuspended at 100 mg/ml tissue by ELISA against recombinant standards. Data are shown as mean ± SEM. Results from line 4 mice are shown on the left, results from line 16 are shown on the right. The concentrations of (a) IFN-γ, (b) IL-4, (c) IL-5 and (d) IL-13 are shown. Group size for line 4 P4 TCR/DR1/ABO transgenic mice sensitised with Fel d 1 was n = 4. Group size for DR1/ABO transgenic mice treated with Fel d 1 in the line 4 experiment was n = 2. Group size for both P4 TCR/DR1/ABO transgenic and DR1/ABO transgenic PBS-treated mice in the line 4 experiment was n = 2. Group size for line 16 P4 TCR/DR1/ABO transgenic mice sensitised with Fel d 1 was n = 7. Group size for DR1/ABO transgenic mice treated with Fel d 1 in the line 16 experiment was n = 5. Group size for both P4 TCR/DR1/ABO transgenic and DR1/ABO transgenic PBS-treated mice in the line 16 experiment was n = 2. (TCR/DR1 = P4 TCR/DR1/ABO transgenic mice, DR1 only = DR1/ABO transgenic mice, Fd1 = Fel d 1 sensitised, PBS = PBS controls).

4.2.7 Histological analysis of frozen lung sections shows inflammation in the lungs of Fel d 1-treated mice

Frozen lung inflations were sectioned by Dr. Catherine Reynolds and stained with haematoxylin and eosin for analysis of inflammation. Scoring of the sections was carried out as described in Chapter 2, and as defined in ref. 607 by two independent, blinded investigators, and both absolute (modal value) and average (mean value) scores for both bronchioles and blood vessels were calculated for each group. Figure 4.13 shows the absolute and average scores obtained for the two experiments for bronchioles and blood vessels. Figure 4.14 shows stained sections for control and Fel d 1-sensitised mice in the line 16 experiment as a general illustration of the inflammation induced by Fel d 1 sensitisation and cat dander challenge. For both line 4 and line 16, both absolute and average scores suggest that there is more inflammation in Fel d 1-sensitised mice than in PBS-treated controls. When using the average score, some inflammation was seen in the control groups as well as the sensitised groups. The scoring system assesses each individual bronchiole and blood vessel separately, so each contributes to the average score. It is possible for occasional mild inflammation to occur in an otherwise healthy animal which could therefore potentially skew the average score towards indicating the presence of lung inflammation where there is actually none. As such, use of the absolute scores (i.e. the most frequent score) to represent the overall level of inflammation in the lung may give a more accurate picture of what is happening by excluding these values. This is borne out by the results obtained here; when using the absolute score, inflammation is only seen in the Fel d 1-sensitised mice and not in the PBS-treated controls. The absolute score is more differentiating between the Fel d 1- and PBS-treated groups than the average score and is a better measure of inflammation in this model.

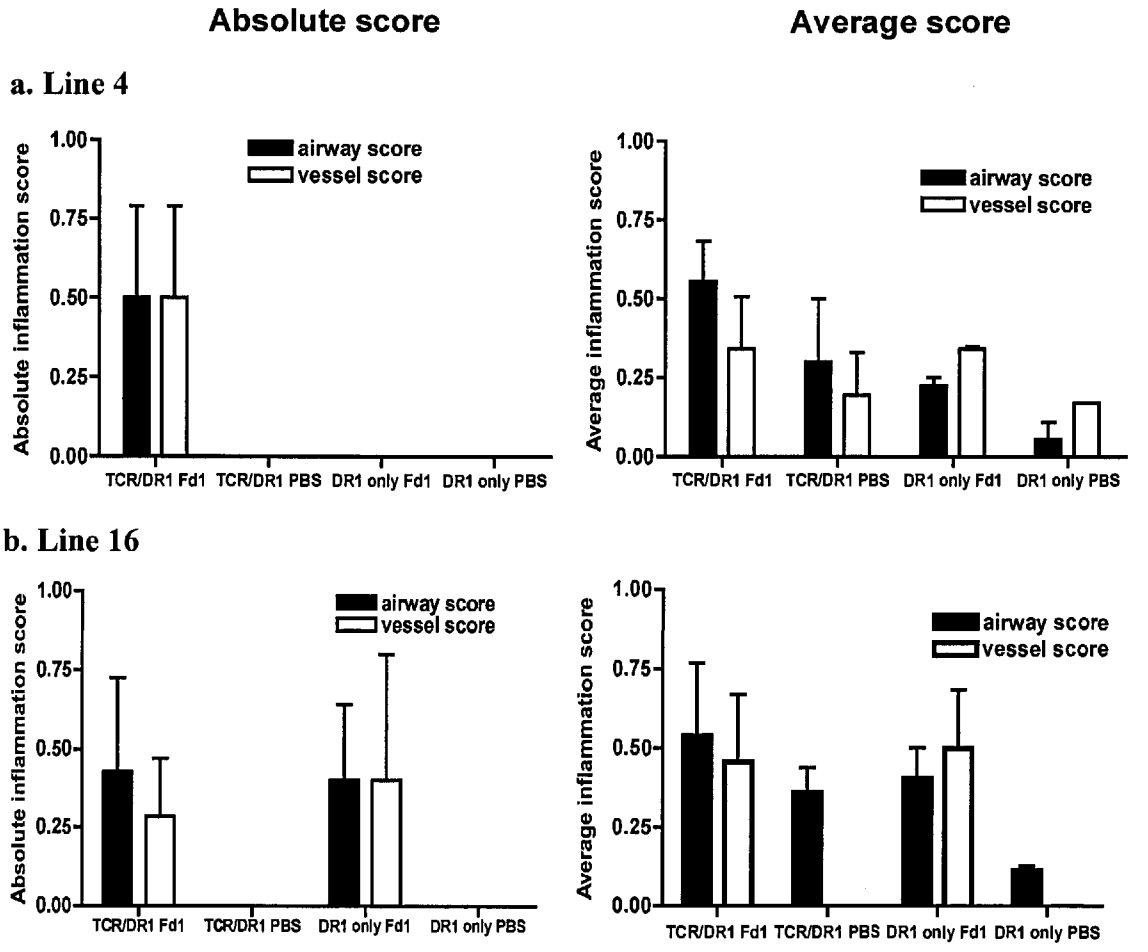


Figure 4.13 Inflammation scores obtained from H&E-stained sections of inflated lung from line 4 and line 16 P4 TCR/DR1/ABO transgenic and DR1/ABO transgenic mice (a) shows the scores obtained from the line 4 experiment. (b) shows the scores obtained from the line 16 experiment. The absolute score is shown on the left, whilst the average score is shown on the right. All sections were scored by at least two independent blinded investigators. Representative scores from one of the investigators are shown above for each experiment – scores obtained from the other investigator scoring each experiment were in agreement with the scores shown above. Data are shown as mean ± SEM. Group size for line 4 P4 TCR/DR1/ABO transgenic mice sensitised with Fel d 1 was n = 4. Group size for DR1/ABO transgenic mice treated with Fel d 1 in the line 4 experiment was n = 2. Group size for both P4 TCR/DR1/ABO transgenic and DR1/ABO transgenic PBS-treated mice in the line 4 experiment was n = 2. Group size for line 16 P4 TCR/DR1/ABO transgenic mice sensitised with Fel d 1 was n = 7. Group size for DR1/ABO transgenic mice treated with Fel d 1 in the line 16 experiment was n = 5. Group size for both P4 TCR/DR1/ABO transgenic and DR1/ABO transgenic PBS-treated mice in the line 16 experiment was n = 2. (TCR/DR1 = P4 TCR/DR1/ABO transgenic mice, DR1 only = DR1/ABO transgenic mice, Fd1 = Fel d 1 sensitised, PBS = PBS controls)

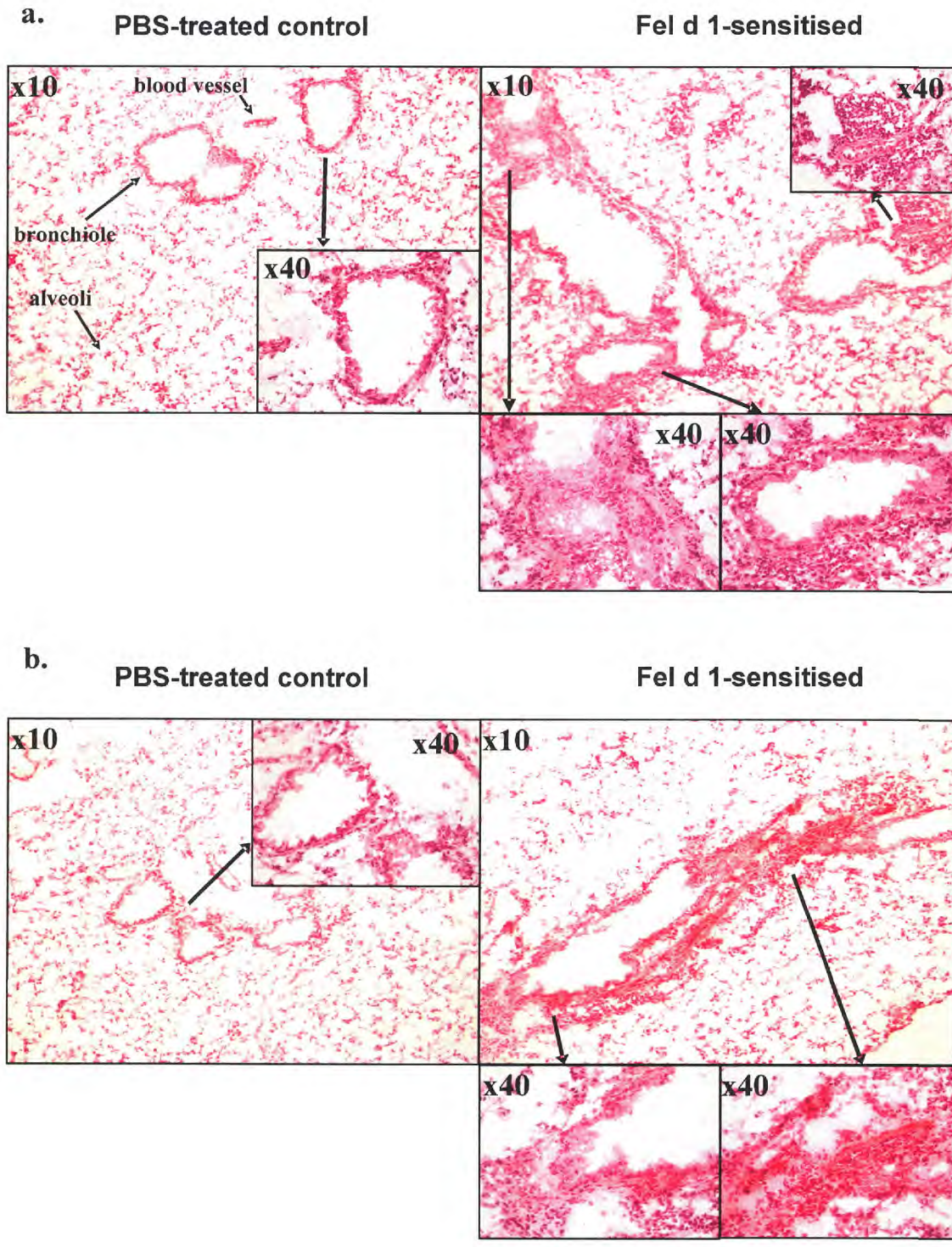


Figure 4.14 Haematoxylin and eosin stained sections used for scoring lung inflammation in line 16 P4 TCR/DR1/ABO mice The scores shown in Figure 4.13 were derived from scoring of slides such as these. (a) shows stained lung sections from P4 TCR/DR1/ABO transgenic mice in the line 16 experiment; a section from a PBS-treated control is shown on the left, and a section from a Fel d 1-sensitised mouse on the right. Each section is shown at x10 magnification, with additional images of bronchioles and blood vessels shown at x40 magnification. (b) shows stained lung sections from DR1/ABO transgenic mice in the line 16 experiment, set out as described for (a). Typical structures of alveoli, bronchioles and blood vessels are marked.

4.2.8 Histological analysis of frozen lung sections shows goblet cell hyperplasia and mucus production in the lungs of Fel d 1-treated mice

Frozen lung inflations were sectioned by Dr. Catherine Reynolds and stained using Periodic acid-Schiff's (PAS) reagent for analysis of mucus production and goblet cell hyperplasia. Scoring of the sections was carried out as described in Chapter 2 and as defined in ref. 608; both absolute (modal value) and average (mean value) scores for all bronchioles were calculated for each group. The scores were too low to merit reporting here but did show positive results in the Fel d 1-sensitised groups compared with PBS controls in both experiments. Figure 4.15 shows stained sections for control and Fel d 1-sensitised mice in the line 16 experiment as a general illustration of mucus production and goblet cell hyperplasia induced by Fel d 1 sensitisation and cat dander challenge.

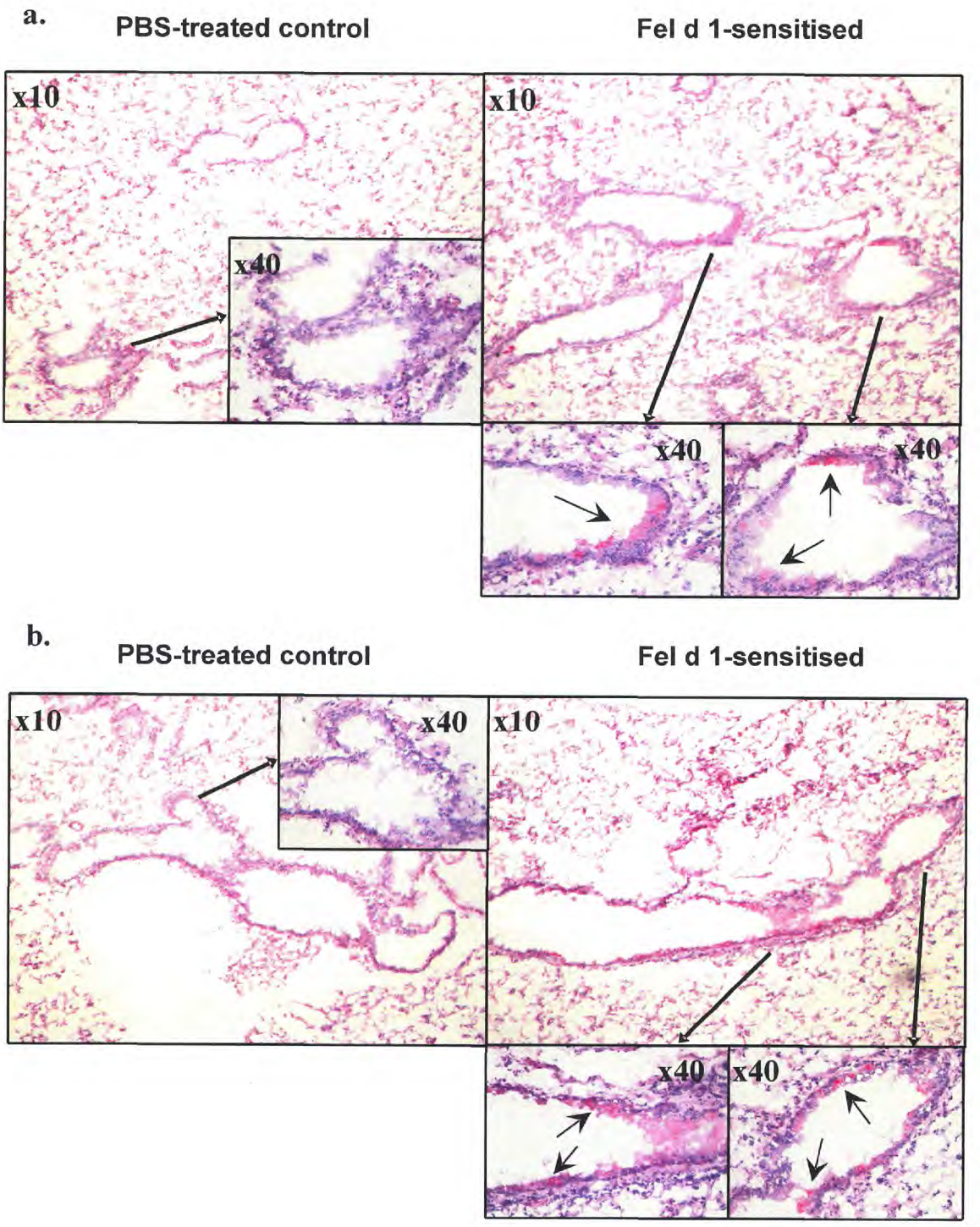


Figure 4.15 PAS stained (and haematoxylin counter-stained) sections used for scoring goblet cell hyperplasia and mucus production in line 16 P4 TCR/DR1/ABO mice (a) shows stained lung sections from P4 TCR/DR1/ABO transgenic mice in the line 16 experiment; a section from a PBS-treated control is shown on the left, and a section from a Fel d 1-sensitised mouse on the right. Each section is shown at x10 magnification, with additional images of bronchioles shown at x 40 magnification. (b) shows stained lung sections from DR1/ABO transgenic mice in the line 16 experiment, set out as described for (a). PAS has a characteristic pink colour, and stains mucus and mucus-producing cells; examples of positive staining are indicated by the arrows.

4.2.9 Summary of findings

Allergic lung inflammation occurred in the Fel d 1-sensitised groups in both line 4 and line 16 P4 TCR/DR1/ABO transgenic and DR1/ABO transgenic mice.

Disease was assessed through a number of factors – lung function parameters, cell numbers and types in BAL fluid and lung tissue, total IgE levels in serum, Th2-associated cytokine levels in BAL fluid and homogenised lung tissue and histological assessment of frozen lung sections for the presence of inflammatory infiltrates and goblet cell hypertrophy.

Lung function results in general suggested that sensitisation with Fel d 1 led to an increase in AHR in response to methacholine provocation, as measured by changes in Penh, airway resistance and dynamic compliance. Fel d 1 sensitisation was associated with eosinophilic influx into the BAL fluid and lung tissue, causing an overall increase in cell number in the BAL fluid and the lung tissue. Fel d 1 sensitisation was also associated with high levels of IgE in the serum. IL-4, IL-5 and IL-13 were increased in the BAL fluid by Fel d 1 sensitisation in the line 4 P4 TCR/DR1/ABO transgenic mice. Analysis of lung inflammation by histological examination indicated that there was an inflammatory infiltrate in response to Fel d 1 sensitisation in both lines 4 and 16 in the P4 TCR/DR1/ABO transgenic and DR1/ABO transgenic mice. Mucus production and goblet cell hypertrophy occurred in Fel d 1-sensitised groups.

These findings suggest that this sensitisation and challenge protocol using cat allergen is biologically successful in inducing allergic lung disease in the P4 TCR/DR1/ABO transgenic mice and DR1/ABO transgenic mice. However, the small group sizes prevented many of the findings from reaching statistical significance. These early preliminary findings indicate that the P4 TCR/DR1/ABO transgenic mice may be a more refined model than the DR1/ABO transgenic mice. Further experiments with modified protocols and increased group numbers ($\geq$ 10 per group) will need to be undertaken to clarify this point.

4.3 Analysis of T-cell costimulatory molecule expression in P4 TCR/DR1/ABO transgenic mouse lines 4 and 16

4.3.1 Overview

T-cell development in the thymus of an αβ TCR transgenic mouse is abnormal due to the expression at an early stage (the DN stage) of a rearranged αβ TCR (425). This is most often seen as an increased number of DN cells in the thymus due to the inability of the αβ TCR to efficiently signal for the cell to pass the β-selection checkpoint (424), for which the pre-TCR (comprising the pre-TCRα chain and a rearranged TCRβ chain) is required (423). In addition, the expression of a transgenic αβ TCR leads to restriction of the T-cell TCR repertoire - the presence of an already rearranged TCRβ chain prevents the rearrangement and production of endogenous TCRβ chains and to a lesser extent, the same is true of an already rearranged TCRα chain with regard to the rearrangement and production of endogenous TCRα chains (644). This can potentially act to restrict the responses of T-cells in the periphery (645) although this has not always been shown to be the case (646). It is therefore possible that these abnormalities may lead to differences in expression of costimulatory molecules associated with the TCR signalling events that occur in T-cells, both in the thymus and the periphery, hence the expression of some of these molecules was analysed in the thymus and spleen of P4 TCR/DR1/ABO transgenic mice and compared with their expression in DR1/ABO transgenic control mice.

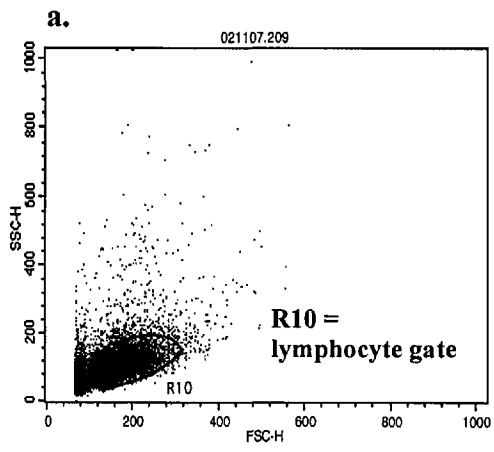
The expression and function of a number of costimulatory molecules has been analysed in the thymus of non-transgenic mice and they have been found to play important roles in T-cell development. For example, CD44 is implicated in the correct homing of T-cell precursors to the thymus and its expression is seen at high levels at the DN stage of thymocyte development where, along with CD25, its expression or lack of defines a further four populations within the DN subset (416). As the expression of a rearranged αβ TCR at this stage of development causes a block in development here, it might be expected that expression levels or patterns of CD44 expression may differ between TCR transgenic and non-TCR transgenic mice. CD3 is required in both the thymus and the periphery for correct assembly of the TCR complex and in the thymus is also required for the expression at the cell surface of the pre-TCR (384); its level of expression changes throughout T-cell development. The expression of a transgenic TCR in T-cells

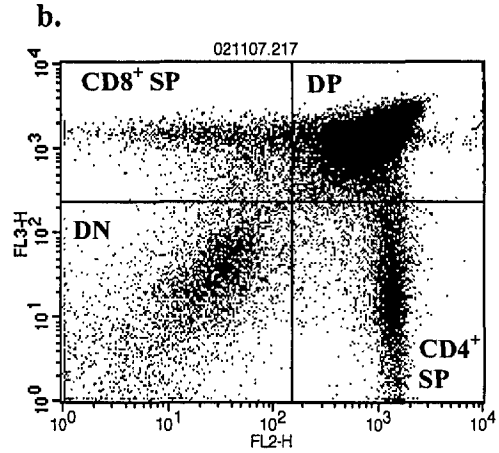
undergoing thymic development might therefore be expected to affect the levels of CD3 expression; CD3 expression would be required whenever TCR expression was occurring and its expression would in some way be related to the levels of expression of the transgenic TCR on the thymocyte surface. It might therefore be expected that expression of a transgenic TCR would increase CD3 expression throughout thymocyte development. Other molecules such as CD69 and CD62L are more strongly associated with later stages of thymocyte development (although CD62L is also thought to be expressed on those common lymphoid progenitors (CLPs) that will ultimately develop into T-cells (647) and thus CD62L expression may also be associated with very early thymocyte development); they are expressed at different stages of the maturation process in SP thymocytes. CD69 is thought to be associated with ongoing positive selection (648) and so is expressed in DP and immature SP thymocytes – its expression diminishes as a SP thymocyte matures and this decrease correlates with an increase in CD62L expression, an indication that the thymocyte is reaching maturity and will soon emigrate from the thymus (649). The impact of transgenic TCR expression on the later stages of thymocyte development is less well characterised but if there is an effect on either selection or maturation and egress from the thymus, it might be expected that there would be an effect discernible on the levels of expression of these molecules. The adhesion molecule CD54, through its interaction with its ligand, the integrin LFA-1, has been suggested to play an important role in T-cell development in the thymus as blocking of this interaction prevents the development of DP cells (650). Levels of CD54 expression on thymocytes change as they develop, being highly expressed on the DN subset and at a low level on DP cells; in SP cells differential expression is seen with CD54 being expressed to a much higher level on CD8 SP than CD4 SP, a phenomenon also seen in the periphery (650). In addition, expression of secondary costimulatory molecules such as ICOS and OX40, which are associated in peripheral T-cells with T-cell activation and the promotion of survival and development of memory T-cells respectively (651, 652), have been seen in the thymus (653, 649). Both molecules are expressed in the thymic medulla, which is predominantly populated by cells of the SP subsets and cells undergoing thymic selection, and to a lesser extent in the cortex. Although the function of these molecules in the thymus is unknown, it is likely that it will relate to their function in the periphery and it is therefore possible that expression of a transgenic TCR may affect their expression levels.

In order to investigate the hypothesis that expression of a transgenic TCR alters the expression of other T-cell signalling-associated molecules on cells of the T-cell lineage in both the thymus and the periphery, expression of such molecules was analysed on unstimulated, freshly isolated thymocytes and splenocytes. The expression of CD3, CD25, CD44, CD54, CD62L, CD69, OX40 (and its ligand OX40L) and ICOS was analysed immediately *ex vivo* in the thymus and the periphery in P4 TCR/DR1/ABO transgenic lines 4 and 16 and in DR1/ABO transgenic controls by flow cytometry and analysed against the expression of the T-cell co-receptors CD4 and CD8. All antibodies used are shown in Appendix 10.

4.3.2 A block in thymocyte development is seen at the double negative (DN) stage in P4 TCR/DR1/ABO transgenic mice

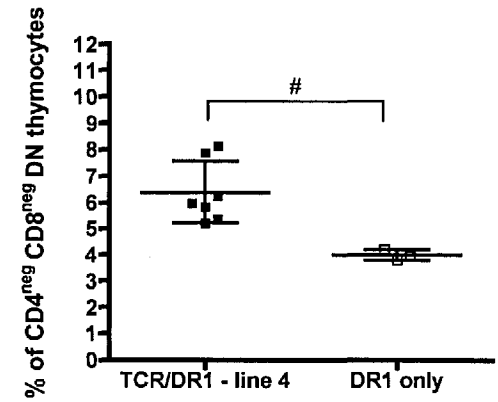
Development of T-cell precursors in the thymus can be tracked by expression of the T-cell coreceptors CD4 and CD8. During the earliest phase of development neither coreceptor is expressed and cells are characterised as belonging to the double negative (DN) subset. As the cells develop further they express both coreceptors concurrently and are characterised as belonging to the double positive (DP) subset. The last stage of development before thymic emigration is characterised by the loss of expression of one of the coreceptors and these cells belong to the CD4 (CD4 SP) or CD8 (CD8 SP) single positive subsets, depending upon which coreceptor they continue to express. When isolated thymocytes falling within a live lymphocyte gate, as shown in a in Figure 4.16, are analysed in terms of CD4 and CD8 expression a characteristic dot plot is obtained, shown in b in Figure 4.16. Four clear populations are seen, corresponding to the DN, DP, CD4 SP and CD8 SP subsets. The proportions of each subset in P4 TCR/DR1/ABO transgenic mice from lines 4 and 16 as well as in DR1/ABO transgenic controls were calculated and are shown for line 4 in Figure 4.16c and in Figure 4.16d for line 16. The proportions of cells that were present in the DP, CD4 SP and CD8 SP subsets are shown in tables on the left-hand side along with the numbers of mice in each group. In each case, the proportions were similar in both P4 TCR/DR1/ABO transgenic mice and DR1/ABO transgenic control mice for each of these subsets and comparable to the proportions seen in wild-type mice of the same strains i.e. C57BL/6 and CBA (416), with possibly a slightly lower proportion of CD8 SP seen in both P4 TCR/DR1/ABO transgenic mice and DR1/ABO transgenic control mice; the published proportion is 4-4.5% whilst the mean proportion seen in the mice in these experiments was less than





c.

	DP (%)	$CD4^+$ SP (%)	$CD8^+$ SP (%)	n
TCR/DR1 Tg - line 4	80.60 ± 3.28	10.09 ± 2.11	2.95 ± 0.52	7
DR1 only Tg	82.60 ± 0.55	11.08 ± 0.90	2.35 ± 0.52	3



d.

	DP (%)	$CD4^+$ SP (%)	$CD8^+$ SP (%)	n
TCR/DR1 Tg - line 16	78.63 ± 2.88	10.12 ± 1.68	2.86 ± 1.10	4
DR1 only Tg	79.42 ± 2.40	12.79 ± 2.09	1.95 ± 0.95	2

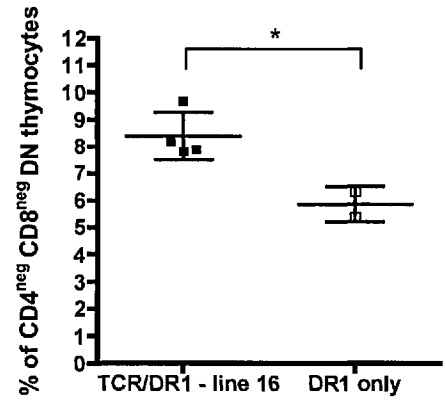
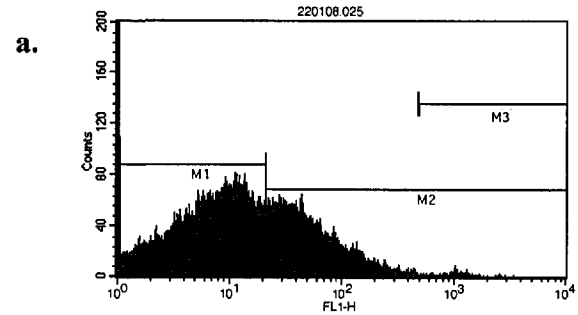


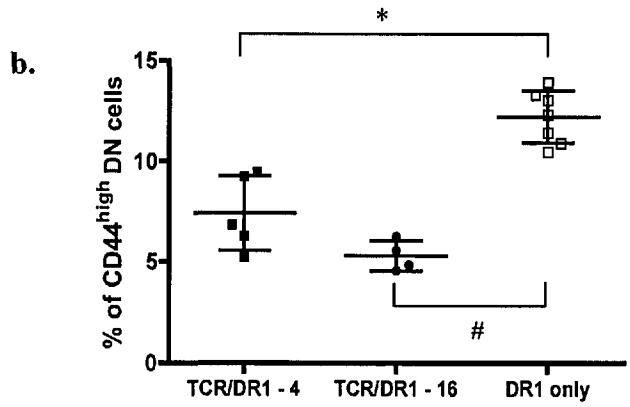
Figure 4.16 Analysis of CD4 vs. CD8 staining on thymocytes from P4 TCR/ DR1/ABO transgenic mice Thymocytes were analysed on the basis of their staining for CD4 and CD8 expression. The gate used to identify live thymocytes, R10, is shown in (a) on a forward scatter-side scatter plot. The division of thymocytes into four subsets according to their staining for CD4 and CD8 is shown in (b). Thymocytes were defined as double negative (DN) $CD4^-CD8^-$, double positive (DP) $CD4^+CD8^+$ or single positive for either CD8 (CD8 SP), $CD4^-CD8^+$ or CD4 expression (CD4 SP), $CD4^+CD8^-$. The extent of each population as a proportion of total thymocytes is shown in (c) for line 4 and in (d) for line 16. In each case, P4 TCR/DR1/ABO transgenic mice were compared against DR1/ABO transgenic control mice. Where no difference was seen between P4 TCR/DR1/ABO transgenic mice and DR1/ABO transgenic control mice, data is displayed in a table as mean ± s.d. For DN cells, data is displayed as a scatter graph with the mean and error bars representing the standard deviation shown. # = $p < 0.05$ (Mann-Whitney U test, two-tailed), * = $p < 0.05$ (unpaired Student's t test, two-tailed)

3%. A significant difference was seen between the proportion of DN cells in the P4 TCR/DR1/ABO transgenic mice and the DR1/ABO transgenic control mice for both lines 4 ($p = 0.0167$, Mann-Whitney U test, two-tailed) and 16 ($p = 0.025$, Student's unpaired two-tailed t test) (shown in the graphs on the right-hand side in Figures 4.16c and d), with the proportion being higher by 2.38% (difference between the means) for line 4 P4 TCR/DR1/ABO transgenic mice and by 2.53% (difference between the means) for line 16 P4 TCR/DR1/ABO transgenic mice. An increase in DN cells in the P4 TCR/DR1/ABO transgenic mice is indicative of a block in development at this stage due to the expression of a pre-rearranged functional TCR interfering with normal TCRβ chain rearrangement, and has been shown previously (425). It is an indication that the TCR transgenes in the P4 TCR/DR1/ABO mice are being expressed in the transgene-positive mice.

4.3.3 Expression of CD44 on DN thymocytes is decreased in P4 TCR/DR1/ABO transgenic mice

CD44 is expressed in the thymus, particularly in the DN and CD4 and CD8 SP subsets; very low expression is generally seen in the DP subset (414). Thymocytes, defined as outlined in Figure 4.16 in terms of CD4/CD8 subsets, were analysed for CD44 expression within these subsets. Figure 4.17a shows the gates used to analyse the cells in terms of CD44 expression. Three gates were used to allow differentiation - M1 and M2 differentiated between $CD44^-$ and all $CD44^+$ cells (regardless of whether expression was low or high) whilst M3 indicated cells where expression of CD44 was especially high ($CD44^{high}$), as there was a separate peak corresponding to these cells. The proportion of $CD44^{high}$ i.e. gate M3 DN cells in both line 4 ($p = 0.0003$, Student's unpaired two-tailed t test) and line 16 ($p = 0.0061$, Mann-Whitney U test, two-tailed) P4 TCR/DR1/ABO transgenic mice was significantly lower than for the DR1/ABO transgenic control mice, as shown in Figure 4.17b. The proportion of $CD44^{high}$ in DR1/ABO transgenic control mice was 4.79% higher (difference between the means) than line 4 P4 TCR/DR1/ABO transgenic mice and 6.90% higher (difference between the means) than line 16 P4 TCR/DR1/ABO transgenic mice. The table in Figure 4.17b shows the number of mice in the experiment and the proportion of $CD44^{high}$ cells in the remaining subsets where no difference was seen between P4 TCR/DR1/ABO transgenic mice and DR1/ABO transgenic control mice. A decrease in the mean fluorescence intensity (MFI) of the $CD44^{high}$ and $CD44^+$ (i.e. M2) populations in the DN subset in P4





	Double positive (%)	CD4 single positive (%)	CD8 single positive (%)	N
TCR/DR1 Tg - line 4	0.13±0.03	3.96±1.76	4.60±1.31	5
TCR/DR1 Tg - line 16	0.08±0.02	2.97±1.48	2.22±0.82	4
DR1 only Tg	0.15±0.06	4.69±0.92	3.78±0.92	7

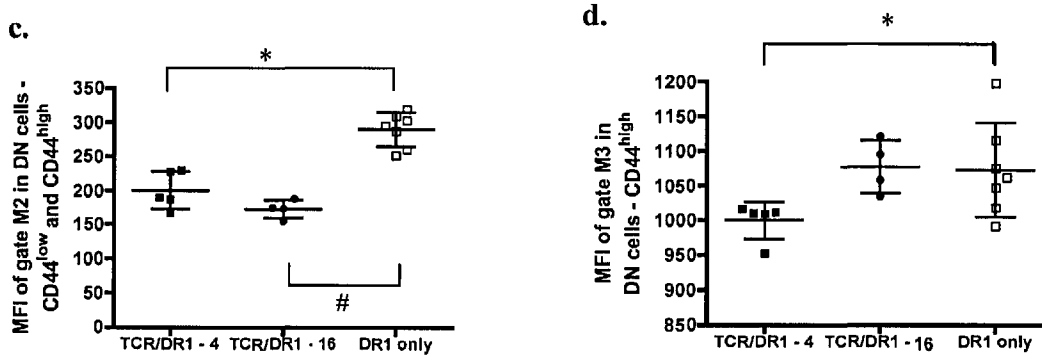


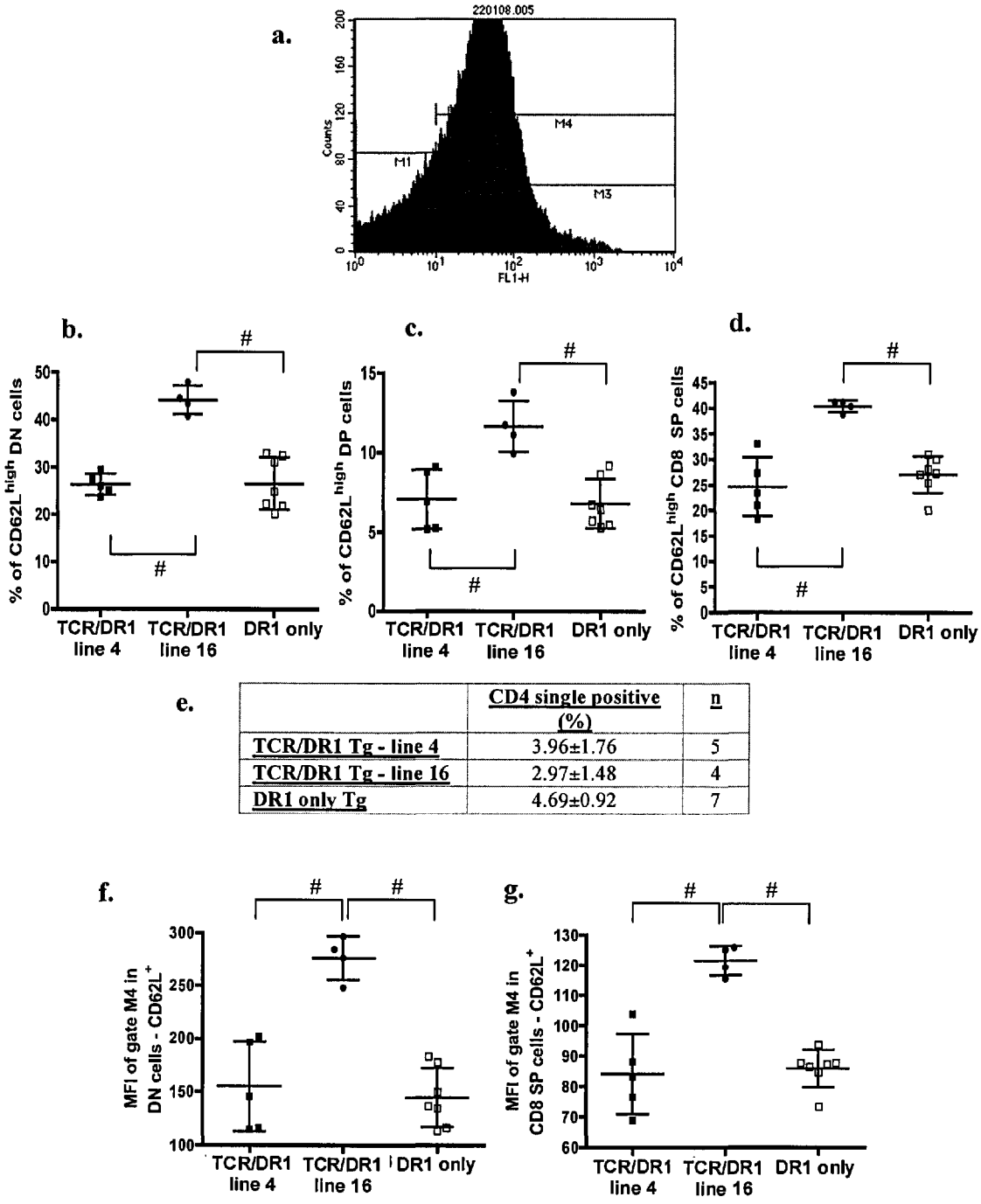
Figure 4.17 CD44 expression on thymocyte subsets in P4 TCR/DR1/ABO transgenic mice Thymocyte subsets were defined as in Figure 4.16 on the basis of CD4 and CD8 expression. Subsets were also analysed for CD44 expression (FL-1 channel). (a) shows an anti-CD44 single-stained sample indicating the gates used to distinguish populations on the basis of CD44 expression. M1 defines the $CD44^-$ population, M2 defines the total $CD44^+$ population and M3 defines the $CD44^{high}$ population. P4 TCR/DR1/ABO transgenic mice were compared against DR1/ABO transgenic control mice. In (b), where no differences were seen between groups in CD44 expression, data is displayed in a table as mean ± s.d. For DN cells, data is displayed as a scatter graph with the mean and error bars representing the standard deviation shown. In (c) and (d), a comparison of mean fluorescence intensity (MFI) in the M2 (c) and M3 (d) gates for DN cells is shown with data displayed as in b. # = $p < 0.05$ (Mann-Whitney U test, two-tailed), * = $p < 0.05$ (unpaired two-tailed Student's t test).

TCR/DR1/ABO transgenic mice was also seen as shown in Figures 4.17c and d. For the $CD44^{high}$ population (shown in d), the downward shift in MFI was only significant in the line 4 P4 TCR/DR1/ABO transgenic mice (mean 999.7 compared with mean 1072.0, $p = 0.0335$, Student's unpaired two-tailed t test with Welch's correction) - there was no difference between the MFI obtained for the line 16 P4 TCR/DR1/ABO transgenic mice (mean 1077.0) and the DR1/ABO transgenic control mice. However, in the case of all $CD44^{+}$ cells whether high- or low- expressing, shown in Figure 4.17c, the downward shift in MFI in P4 TCR/DR1/ABO transgenic mice from both lines was significant when compared to DR1/ABO transgenic control mice. The difference between the mean MFI values in line 4 P4 TCR/DR1/ABO transgenic mice was -89.9 ($p = 0.0001$, Student's unpaired two-tailed t test) and in line 16 P4 TCR/DR1/ABO transgenic mice was -117.0 ($p = 0.0061$, Mann-Whitney U test, two-tailed) compared with DR1/ABO transgenic control mice. In summary, the numbers of DN cells expressing CD44 to a high extent was lower in P4 TCR/DR1/ABO transgenic mice in both lines 4 and 16 in comparison to the DR1/ABO transgenic control mice.

4.3.4 Expression of CD62L on thymocyte subsets is generally increased in P4 TCR/DR1/ABO transgenic mice from line 16

CLPs, the precursor cells of early T- and B-lineage progenitors, can be differentiated on the basis of CD62L expression, with $CD62L^+$ cells developing along the T lineage pathway and migrating to the thymus and $CD62L^-$ cells developing along the B lineage pathway and migrating to the bone marrow (647). As such, recent migrant cells into the thymus (in the DN subset) express CD62L which is gradually down-regulated as the cells develop in the thymus. Expression is then up-regulated at the SP stage of development as cells mature to become ready to emigrate from the thymus (654).

Thymocytes, as defined in Figure 4.16 in terms of CD4 and CD8 expression, were analysed for CD62L expression within each subset. The gates used for analysis are shown in Figure 4.18a. Four gates were used - M1, M2 and M3 differentiated between dead/$CD62L^-$ cells (M1), $CD62L^{low}$ (M2) and $CD62L^{high}$ (M3) cells whilst M4 represented all $CD62L^+$ cells. The proportion of $CD62L^{high}$ (M3) DN cells was significantly higher by 17.56% (difference between the means) in P4 TCR/DR1/ABO transgenic mice from line 16 ($p = 0.0061$, Mann-Whitney U test, two-tailed) than the DR1/ABO transgenic control mice, as shown in Figure 4.18b. This increase in expression was not seen in DN cells from the P4 TCR/DR1/ABO transgenic mice from line 4, which had a level of $CD62L^{high}$ expression (26.34% ± 2.23) that was similar to the DR1/ABO transgenic control mice (26.53% ± 5.52) and was significantly lower than that seen in line 16 P4 TCR/DR1/ABO transgenic mice ($p = 0.0159$, Mann-Whitney U test, two-tailed, difference between means of 17.75%). The same phenomenon of an increase in $CD62L^{high}$ cells in the line 16 P4 TCR/DR1/ABO transgenic mice but not in the line 4 P4 TCR/DR1/ABO transgenic mice as compared to DR1/ABO transgenic control mice was seen in the DP subset and the CD8 SP subset. For the DP cells, as shown in Figure 4.18c, the proportion of $CD62L^{high}$ cells was 4.88% higher (difference between the means) in the line 16 P4 TCR/DR1/ABO transgenic mice than in DR1/ABO transgenic control mice ($p = 0.0061$, Mann-Whitney U test, two-tailed) and 4.61% higher (difference between the means) than in line 4 P4 TCR/DR1/ABO transgenic mice ($p = 0.0159$, Mann-Whitney U test, two-tailed). For the CD8 SP subset, as shown in Figure 4.18d, high-level expression of CD62L was 13.31% higher in the line 16 P4 TCR/DR1/ABO transgenic mice (difference between the means) than in the DR1/ABO transgenic control mice ($p < 0.0061$, Mann-Whitney



e.

	CD4 single positive (%)	n
TCR/DR1 Tg - line 4	3.96±1.76	5
TCR/DR1 Tg - line 16	2.97±1.48	4
DR1 only Tg	4.69±0.92	7

Figure 4.18 CD62L expression on thymocyte subsets in P4 TCR/DR1/ABO transgenic mice Thymocyte subsets were defined as shown in Figure 4.16 on the basis of CD4 and CD8 expression. Subsets were analysed for CD62L expression (FL-1 channel). (a) shows an anti-CD62L single-stained sample, indicating the gates used to distinguish different populations on the basis of CD62L expression, where M1 defines dead or $CD62L^-$ cells, M2 defines $CD62L^{low}$ cells, M3 defines $CD62L^{high}$ cells and M4 defines all $CD62L^+$ cells. P4 TCR/DR1/ABO transgenic mice were compared against DR1/ABO transgenic control mice. In (b)-(d), data is displayed as a scatter graph with error bars representing the mean ± s.d. for DN (b), DP (c) and CD8 SP (d) subsets. In (e), where no differences were seen between groups, the data is displayed in a table as mean ± s.d. MFI of the cells in the $CD44^+$ (M4) gate for DN (f) and CD8 SP (g) subsets is shown, with the data displayed as scatter graphs with error bars representing the mean ± s.d. # = $p < 0.05$ (Mann-Whitney U test, two-tailed)

U test, two-tailed) and 15.71% higher than in the line 4 P4 TCR/DR1/ABO transgenic mice (difference between the means, p = 0.0159, Mann-Whitney U test, two-tailed). Expression of $CD62L^{high}$ in CD4 SP cells did not differ between any of the groups as shown in the table in Figure 4.18e.

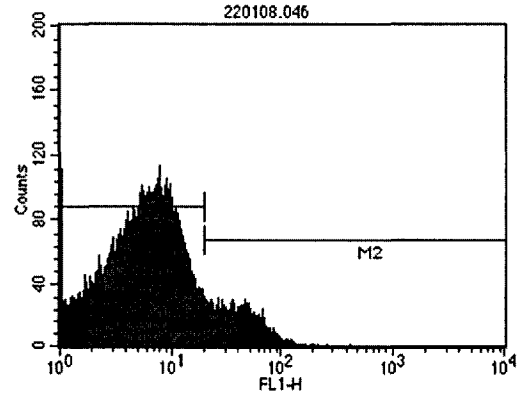
The same pattern with respect to the line 16 P4 TCR/DR1/ABO transgenic mice compared with the line 4 P4 TCR/DR1/ABO transgenic mice and DR1/ABO transgenic control mice was also seen in the MFI of the $CD62L^{+}$ cells (i.e. those in gate M4) in the DN (Figure 4.18f) and CD8 SP (Figure 4.18g) subsets. The MFI in gate M4 for the thymocytes from line 16 P4 TCR/DR1/ABO transgenic mice was significantly higher than for the thymocytes from line 4 P4 TCR/DR1/ABO transgenic mice (p = 0.0159 (Mann-Whitney U test, two-tailed) for DN, difference between means, 121.2 and p = 0.0159 (Mann-Whitney U test, two-tailed) for CD8 SP, difference between means, 37.05) and DR1/ABO transgenic control mice (p = 0.0061 (Mann-Whitney U test, two-tailed) for DN, difference between means, 131.6 and p = 0.0061 (Mann-Whitney U test, two-tailed) for CD8 SP, difference between means, 36.56). These results support the findings from analysis of the proportion of $CD62L^{high}$ cells in the thymocyte subsets as MFI is higher in the line 16 P4 TCR/DR1/ABO transgenic mice than the line 4 P4 TCR/DR1/ABO transgenic mice and DR1/ABO transgenic control mice, which corresponds to there being a higher proportion of $CD62L^{high}$ cells present in gate M4.

In summary, CD62L expression is higher in DN, DP and CD8 SP subsets in line 16 P4 TCR/DR1/ABO transgenic mice in comparison to both DR1/ABO transgenic control mice and also P4 TCR/DR1/ABO transgenic mice from line 4.

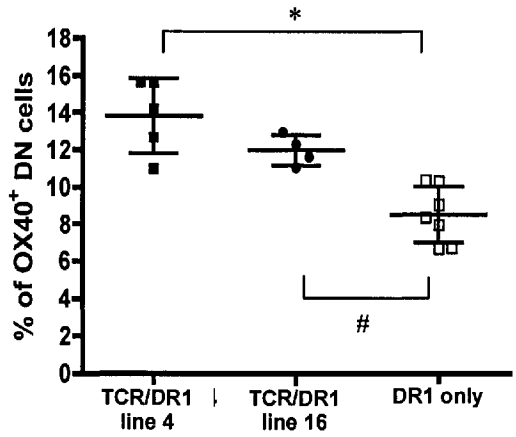
4.3.5 There is a small increase in expression of OX40 on cells of the DN thymocyte subset in line 4 and line 16 TCR transgenic mice

OX40 is expressed in the thymus, particularly in the CD4 and CD8 SP subsets (low levels of expression are also seen in the DP and DN subsets). It is more highly expressed on the CD4 SP than the CD8 SP subset (649). Thymocyte CD4/CD8 subsets were defined as outlined in Figure 4.16 and analysed for OX40 expression within these subsets. Figure 4.19a shows the gates used to analyse the cells for OX40 expression. Two gates, M1 and M2, were used to differentiate between $OX40^{+}$ (M2) and $OX40^{-}$ (M1) cells. OX40 expression on DN thymocytes was slightly but significantly higher on

a.



b.



c.

	Double positive (%)	CD4 single positive (%)	CD8 single positive (%)	n
TCR/DR1 Tg - line 4	13.25±3.60	74.82±3.88	44.54±7.44	5
TCR/DR1 Tg - line 16	15.49±3.37	69.63±8.04	43.20±2.44	4
DR1 only Tg	13.20±1.63	72.87±3.39	37.30±5.17	7

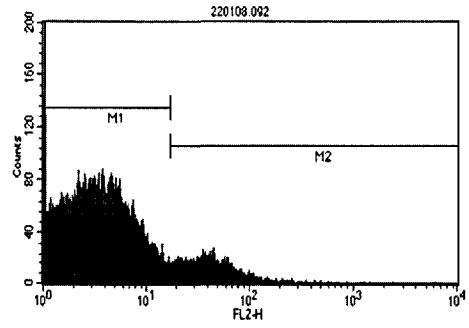
Figure 4.19 OX40 expression on thymocyte subsets in P4 TCR/DR1/ABO transgenic mice Thymocyte subsets were defined as shown in Figure 4.16 on the basis of CD4 and CD8 expression. Subsets were additionally analysed for OX40 expression (FL-1 channel). (a) shows a single-stained anti-OX40 sample, indicating the gates used to distinguish $OX40^+$ (M2) and $OX40^-$ (M1) staining. P4 TCR/DR1/ABO transgenic mice were compared against DR1/ABO transgenic control mice. In (b), data is displayed as a scatter graph with error bars representing the mean ± s.d. for DN cells. In (c), where no differences were seen between groups in terms of OX40 expression, the data is displayed in a table as mean ± s.d. * = $p < 0.05$ (Student's unpaired two-tailed t test), # = $p < 0.05$ (Mann-Whitney U test, two-tailed).

line 4 ($p = 0.0004$, Student's unpaired two-tailed t test) and line 16 ($p = 0.0061$, Mann-Whitney U test, two-tailed) P4 TCR/DR1/ABO transgenic mice than on DR1/ABO transgenic control mice, as shown in Figure 4.19b, with the difference between line 4 P4 TCR/DR1/ABO transgenic mice and DR1/ABO transgenic control mice being 4.32% (difference between means) and between line 16 P4 TCR/DR1/ABO transgenic mice and DR1/ABO transgenic control mice being 3.47% (difference between means). OX40 expression in the DP, CD8 SP and CD4 SP subsets did not differ between P4 TCR/DR1/ABO transgenic mice and DR1/ABO transgenic control mice in either line 4 or line 16, as shown in the table in Figure 4.19c. Expression of OX40 was highest in the CD4 SP subset (70-75% of all cells were $OX40^+$), lower but still substantial in the CD8 SP subset (40-45%) and lowest in the DP subset (approximately 14%). This correlates with levels and extent of expression reported in the literature (616). In summary, in the DN subset only, there was a small increase in the expression of OX40 in the P4 TCR/DR1/ABO transgenic mice compared with the DR1/ABO transgenic control mice in lines 4 and 16.

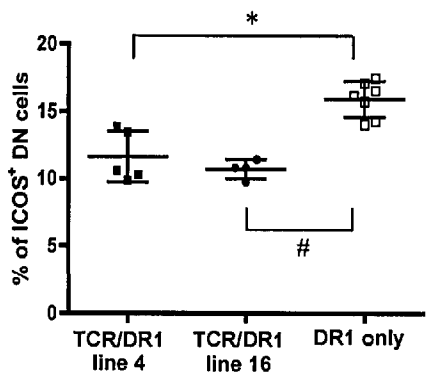
4.3.6 Expression of ICOS in P4 TCR/DR1/ABO transgenic mice is significantly decreased on the DN, CD4 SP and CD8 SP thymocyte subsets in comparison to DR1/ABO transgenic control mice

ICOS is a member of the CD28 family, sharing 20% sequence homology with CD28 and in terms of function it is very similar to CD28 in promoting T-cell proliferation, survival and differentiation with a similar degree of potency (618). It is more strongly associated with $CD4^+$ than $CD8^+$ T-cells (653). ICOS is also expressed in the thymus (620) where it is predominantly associated with the thymic medulla, and thus is likely to be expressed primarily within the SP subsets. Some expression is also seen in the cortical areas of the thymus, so it is likely that cells in the DN and/or DP subsets may also express ICOS to some extent (653). ICOS expression was analysed in thymocyte subsets, as defined in Figure 4.16. The gates used for analysis of ICOS expression are shown in Figure 4.20a - two gates, M1 and M2, differentiated between $ICOS^+$ (M2) and $ICOS^-$ (M1) cells. ICOS expression was significantly lower in line 4 ($11.62\% \pm 1.88$, $p = 0.0009$, Student's unpaired two-tailed t test) and line 16 ($10.71\% \pm 0.71$, $p = 0.0061$, Mann-Whitney U test, two-tailed) P4 TCR/DR1/ABO transgenic mice compared with DR1/ABO transgenic control mice ($15.91\% \pm 1.32$) in the DN subset, as shown in Figure 4.20b. ICOS expression in these mice was notably higher in the medullary SP

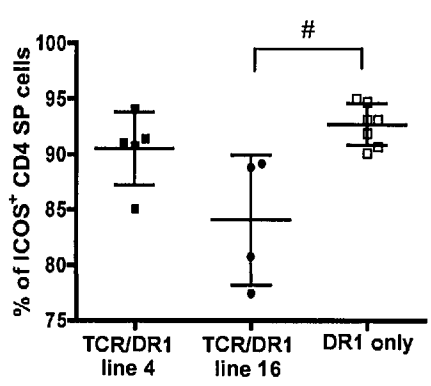
a.



b.



c.



d.

	Double positive (%)	CD8 single positive (%)	n
TCR/DR1 Tg - line 4	5.62±2.27	28.15±11.23	5
TCR/DR1 Tg - line 16	4.68±0.83	24.02±3.85	4
DR1 only Tg	6.01±1.77	30.62±3.31	7

Figure 4.20 ICOS expression on thymocyte subsets in P4 TCR/DR1/ABO transgenic mice Thymocyte subsets were defined as shown in Figure 4.16 on the basis of CD4 and CD8 expression. Cells were additionally analysed for ICOS expression (FL-2 channel). (a) shows an anti-ICOS single-stained sample, indicating the gates used to distinguish $ICOS^+$ (M2) and $ICOS^-$ (M1) staining. P4 TCR/DR1/ABO transgenic mice were compared against DR1/ABO transgenic control mice. In (b)-(c), the data is displayed as a scatter graph with the mean indicated and error bars representing the standard deviation shown for DN cells (b) and CD4 SP (c) cells. In (d), as no differences were seen between groups, the data is displayed in a table as mean ± s.d. * = $p < 0.05$ (Student's unpaired two-tailed t test), # = $p < 0.05$ (Mann-Whitney U test, two-tailed).

SP subsets as expected from previous findings in the literature, shown in Figure 4.20c for CD4 SP and Figure 4.20d for CD8 SP. ICOS expression was highest in the CD4 SP subset, where more than 80% of CD4 SP cells were $ICOS^+$. In line 16 P4 TCR/DR1/ABO transgenic mice, ICOS expression was significantly lower in the CD4 SP subset (84.04% ± 5.88, $p = 0.0061$, Mann-Whitney U test, two-tailed) than in DR1/ABO transgenic control mice (92.67% ± 1.86), a difference of 8.63% (difference between means). This was not seen in line 4 P4 TCR/DR1/ABO transgenic mice (90.49% ± 3.28). No difference in ICOS expression was seen in either the DP or CD8 SP subsets of thymocytes between P4 TCR/DR1/ABO transgenic mice from either line 4 or 16 and DR1/ABO transgenic control mice, as shown in the table in Figure 4.20d. ICOS expression in the CD8 SP subset was lower than in the CD4 SP, with approximately 30% of cells being $ICOS^+$. ICOS expression was lowest overall in the DP subset; only 5-6% of DP cells were $ICOS^+$. In summary, the expression of ICOS in the DN and CD4 SP subsets of line 16 P4 TCR/DR1/ABO transgenic mice was lower than in DR1/ABO transgenic control mice; a similar phenomenon was not seen in the line 4 P4 TCR transgenic mice, where levels of ICOS expression were similar to those of the controls.

4.3.7 Expression of T-cell costimulatory molecules CD69, CD3, CD54 and CD25 on thymocytes in P4 TCR/DR1/ABO transgenic mice is similar to the expression seen in DR1/ABO transgenic controls

CD69, CD3, CD54 and CD25 all participate in the events surrounding T-cell activation upon signalling through the TCR in the periphery. Each of these molecules is also expressed during T-cell development in the thymus and levels of expression differ between the subsets depending on the molecule and its purported function. Thymocytes from P4 TCR/DR1/ABO transgenic mice from both lines 4 and 16 as well as DR1/ABO transgenic control mice were analysed for the expression of CD4, CD8 and the relevant signalling molecule. Figure 4.21 shows the definition of the thymocyte subsets used (a and b) and the gating of cells into negative and positive populations for the molecules CD69 (c), CD3 (d), CD54 (e) and CD25 (f). The extent of each subset that was defined as positively expressing the molecule being investigated is shown for both line 4 and line 16 P4 TCR/DR1/ABO transgenic mice and compared with the DR1/ABO transgenic control mice in Table 4.2 as mean ± s.d. values. No statistically significant differences (Student's unpaired two-tailed t test) were seen between the expression of any of these molecules on any thymocyte subset in P4 TCR/DR1/ABO transgenic mice and DR1/ABO transgenic control mice.

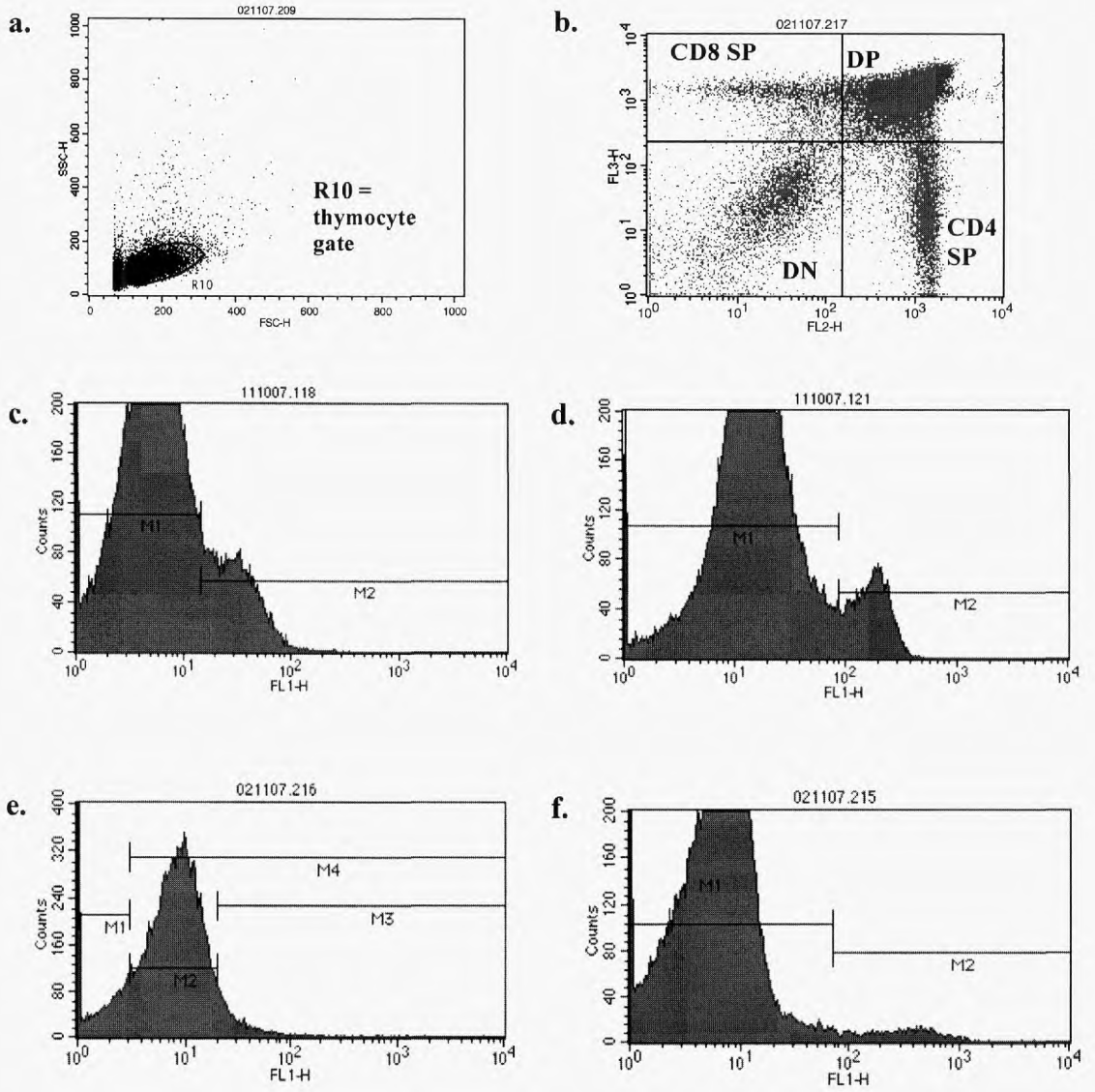


Figure 4.21 Gating used for analysis of expression of T-cell co-stimulatory molecules on thymocytes from P4 TCR/DR1/ABO transgenic mice by flow cytometry (a) shows the gate used to define live thymocytes. The expression of each costimulatory molecule (FL-1 channel, x-axis) was analysed for each thymocyte subset, defined by their expression of CD4 and CD8, shown in (b) above. Staining was either positive or negative, shown by the gates on the histograms above in (c), (d) and (f), where M1 indicates negative staining and M2 indicates positive staining. For the staining shown in (e), the M1 gate defines dead cells, M2 defines negative/low staining, and gate M3 defines positive/high staining. FL-1 stains used: (c) CD69, (d) CD3, (e) CD54 and (f) CD25.

	$CD4^-$ $CD8^-$ double negative (%)	$CD4^+$ $CD8^+$ double positive (%)	$CD4^+$ $CD8^-$ single positive (%)	$CD4^-$ $CD8^+$ single positive (%)
CD69				
TCR/DR1 Tg line 4	14.73 ± 3.90	5.43 ± 1.28	54.24 ± 8.61	26.35 ± 5.47
DR1 only Tg	13.25 ± 0.85	5.48 ± 1.90	58.37 ± 3.10	30.31 ± 9.41
TCR/DR1 Tg line 16	7.22 ± 5.29	9.78 ± 1.55	61.49 ± 7.41	23.24 ± 2.06
DR1 only Tg	6.79 ± 2.48	9.56 ± 0.72	65.05 ± 0.19	30.82 ± 4.65
CD3				
TCR/DR1 Tg line 4	30.57 ± 2.99	12.55 ± 1.38	94.57 ± 0.90	56.68 ± 4.01
DR1 only Tg	22.50 ± 2.30	8.32 ± 0.38	94.83 ± 0.57	54.53 ± 1.05
TCR/DR1 Tg line 16	9.96 ±1.70	7.58 ± 1.32	87.27 ± 3.06	55.71 ± 13.29
DR1 only Tg	9.96 ± 8.24	5.75 ± 1.58	91.51 ± 1.94	62.89 ± 0.47
CD54				
TCR/DR1 Tg line 4	21.46 ± 8.09	2.83 ± 1.70	5.50 ± 2.78	20.33 ± 12.68
DR1 only Tg	16.12 ± 4.08	1.84 ± 0.40	3.81 ± 0.42	13.93 ± 2.95
TCR/DR1 Tg line 16	16.53 ± 4.60	8.28 ± 2.67	9.66 ± 3.45	14.93 ± 3.47
DR1 only Tg	16.31 ± 12.52	8.32 ± 4.21	10.89 ± 0.57	15.45 ± 0.47
CD25				
TCR/DR1 Tg line 4	32.14 ± 3.41	0.35 ± 0.05	1.94 ± 0.54	1.16 ± 0.74
DR1 only Tg	34.33 ± 4.91	0.29 ± 0.03	1.59 ± 0.28	1.23 ± 0.73
TCR/DR1 Tg line 16	26.10 ± 8.50	0.42 ± 0.21	1.78 ± 0.26	4.45 ± 0.88
DR1 only Tg	28.57 ± 21.39	0.35 ± 0.04	1.15 ± 0.06	3.24 ± 1.27

Table 4.2 Expression of T-cell costimulatory molecules on thymocytes from P4 TCR/DR1/ABO transgenic mice Values shown are the percentages (± standard deviation) of each thymocyte subset (as defined in Figure 4.22) that express the molecule being analysed (the gates used to define positive and negative expression are shown in Figure 4.22). Numbers of mice in each group: P4 TCR/DR1/ABO line 4 transgenic mice (TCR/DR1 Tg line 4 above) - n = 7, P4 TCR/DR1/ABO line 16 transgenic mice (TCR/DR1 Tg line 16 above) – n = 4, DR1/ABO transgenic control mice (DR1 only Tg above) – line 4 experiment - n = 3, line 16 experiment - n = 2.

CD69 is rapidly induced upon T-cell activation in the periphery with expression at the surface being detectable 2-3 hours after activation (655). Expression reaches a peak at approximately 24 hours after activation and it is down-regulated within 48 hours. It is not appreciably expressed on naïve or resting cells. It is expressed on approximately 10% of total thymocytes (648); in these experiments, levels of CD69 expression were calculated to be approximately 15%. CD69 expression in the thymus is thought to be associated with positive selection events (648) and thus expression is strongest in the DP and SP subsets. Exact proportions of subsets expressing CD69 differ in the literature between studies - one report (648) showed very low levels of CD69 expression on DP and SP subsets of less than 5%, whilst analysis of CD69 expression in an *in vitro* culture of thymocytes suggested approximately 12% of DN thymocytes and approximately 78% of CD4 SP thymocytes expressed CD69 (656). The values expressed here (shown in Table 4.2) are more in line with the latter levels of expression in terms of extent and pattern. The levels of CD69 expression in the SP subsets appeared to be lower in the P4 TCR/DR1/ABO transgenic mice in both lines 4 and 16 when compared to the DR1/ABO transgenic control mice in each case - as CD69 is associated with positive selection events, the apparent lower levels of expression in the P4 TCR/DR1/ABO mice may indicate a difference in positive selection that is associated with the expression of a transgenic TCR.

CD3 is implicated in events during thymic development; progression from the DN to DP stage of development upon correct rearrangement of a TCRβ chain within the cell requires CD3 expression (384). In TCR transgenic mice where a rearranged TCRαβ molecule is expressed throughout thymic development, CD3 expression may therefore occur differently. CD3 expression is generally extremely low on cells in the DP subset (429) but is up-regulated to a high level as the cells mature into the SP subsets. CD3 expression on the SP subsets ranges from low to high (657); it is expressed at high levels on mature thymocytes with a higher degree of expression on CD4 SP cells than CD8 SP cells. As such, CD3 expression in the CD4/CD8 subsets of the thymus was compared between the P4 TCR/DR1/ABO transgenic mice and the DR1/ABO transgenic control mice. The levels of CD3 expression in P4 TCR/DR1/ABO transgenic mice and the DR1/ABO transgenic control mice, shown in Table 4.2, correlate well with this described pattern. Expression of CD3 is seen in the DN subset, ranging from 10 to 30%, which is then decreased in the DP subset. A small proportion of DP cells in these mice express high levels of CD3, probably corresponding to those cells

undergoing maturation into SP cells. In the SP subsets, CD3 expression is much higher (more than 90% in CD4 SP cells and over 50% in CD8 SP cells) as would be expected from published reports. Whilst the differences when comparing P4 TCR/DR1/ABO transgenic mice to DR1/ABO transgenic control mice in lines 4 and 16 did not reach statistical significance, there was an apparent difference which could be biologically important - in the line 4 experiment, CD3 expression in the DN subset did appear to be higher in the P4 TCR/DR1/ABO transgenic mice than the DR1/ABO transgenic control mice. This may be related to the expression of the transgenic rearranged TCR molecule at the cell surface at this stage.

CD54 is an intracellular adhesion molecule that binds to integrins such as LFA-1 on the surface of endothelial cells, enhancing and facilitating the traffic of T-cells to sites of inflammation (658). It is up-regulated on activated T-cells in the periphery and is expressed at a low basal level on resting T-cells. CD54 expression has also been seen on thymocytes with levels changing throughout development (650). CD54 is expressed highly on the DN subset and at a low level on DP cells; in SP cells, differential expression is seen with CD54 being expressed to a much higher level on CD8 SP than CD4 SP, a phenomenon also seen in the periphery. The values obtained for the mice in the experiments described here correlate with these previous findings; the values shown in Table 4.2 for CD54 expression show the proportion of the subsets expressing high levels of the molecule. CD54 expression was highest in the DN and CD8 SP subsets (approximately 15-20% of cells expressed CD54 at a high level), at an intermediate level in CD4 SP (approximately 5-10% of cells expressed a high level of CD54), and lowest in the DP subset (approximately 2-8% of cells expressed a high level of CD54). CD54 expression in the DN and CD8 SP subsets appeared to be higher in the P4 TCR/DR1/ABO transgenic mice than the corresponding DR1/ABO transgenic controls in the line 4 experiment but the large standard deviations from the mean of the results from the DR1/ABO transgenic controls prevented this from reaching significance. Repeating the experiment with larger group numbers might confirm this finding.

The expression of CD25, the IL-2Rα chain, is up-regulated early after activation of T-cells in the periphery (659, 660). It is also used as a marker in conjunction with Foxp3 for regulatory T-cells, or Tregs (196). Expression of CD25 is well-documented in the DN subset of thymocytes where, along with CD44, its expression defines four sub-stages in the subset development, from migration into the thymus through to the

development into DP cells (416). CD25 expression is then up-regulated in a small population of CD4 SP cells, thought to be the precursors of Tregs (661). The values obtained for the mice in the experiments described here, shown in Table 4.2, correlate with previous findings; CD25 expression was highest in the DN subset as expected (approximately 30% of cells expressed CD25), whilst in the DP and SP subsets, expression of CD25 was at a much lower level (negligible in DP cells, and approximately 1-4% in the CD4 and CD8 SP subsets). There was no difference in CD25 expression in any subset in P4 TCR/DR1/ABO transgenic mice from either line 4 or line 16 when compared to the corresponding DR1/ABO transgenic control mice.

In summary, no statistically significant differences in the levels of expression of CD69, CD3, CD54 or CD25 were seen in line 4 or line 16 P4 TCR/DR1/ABO transgenic mice compared with DR1/ABO transgenic control mice. However, some differences that may have biological importance were seen. CD69 expression appeared to be lower in the SP subsets of P4 TCR/DR1/ABO transgenic mice in both lines 4 and 16 than in DR1/ABO transgenic control mice. CD3 expression in the DN subset of the line 4 P4 TCR/DR1/ABO transgenic mice was higher than in the corresponding DR1/ABO transgenic control mice, whilst CD54 expression in the DN and CD8 SP subsets appeared to be higher; changes in CD3 or CD54 expression were not seen in the line 16 experiment. No difference in CD25 expression between P4 TCR/DR1/ABO transgenic mice and DR1/ABO transgenic control mice was detected.

4.3.8 Expression of the T-cell costimulatory molecules CD69, CD3, CD54, CD25, CD44 and CD62L on freshly-isolated splenocytes in P4 TCR/DR1/ABO transgenic mice is similar to the expression seen in DR1/ABO transgenic control mice

Splenocytes were isolated from the same mice as those used for analysis of costimulatory molecule expression in thymocytes and analysed for expression of the same molecules in conjunction with either CD4 or CD8, in order to investigate if the findings from the analysis of thymocytes were replicated in the spleen and hence the periphery. The gates used to define populations of splenocytes are shown in Figure 4.22. The live splenocyte (or lymphocyte) gate determined on the basis of light-scattering properties is shown in Figure 4.22a (as R3). Definition of populations on the basis of CD4 or CD8 expression and the expression of the costimulatory molecule being analysed are shown as FL-1 vs. FL-2 dot plots in Figure 4.22 b-g. Populations that were analysed are labelled accordingly. Table 4.3 shows the percentage of total splenocytes that were $CD4^+$ or $CD8^+$ only, and those that expressed CD4 or CD8 and were also positive for expression of the relevant costimulatory molecule.

CD69 expression on P4 TCR/DR1/ABO transgenic thymocytes was broadly similar to the expression seen in DR1/ABO transgenic control thymocytes. In the spleen, very little CD69 expression was seen on either $CD4^+$ or $CD8^+$ T-cells, with $CD4^+CD69^+$ and $CD8^+CD69^+$ populations each accounting for less than 1.5% of total splenocytes. This is perhaps not surprising as the cells in this case were freshly isolated from the spleen and had not been activated *in vitro* before analysis and CD69 is a marker of activated T-cells. In addition, they were isolated from healthy animals kept in clean conditions, so that no ongoing immune responses would be expected. There was no discernible difference in expression between P4 TCR/DR1/ABO transgenic mice and the DR1/ABO transgenic control mice in the line 4 experiment.

There was no difference in the levels of CD3 expression seen in the thymocyte subsets of P4 TCR/DR1/ABO transgenic mice compared to DR1/ABO transgenic control mice, except for a possible increase in CD3 expression in the DN subset in the line 4 P4 TCR/DR1/ABO transgenic mice. In the spleen, no difference in CD3 expression on either $CD4^+$ or $CD8^+$ T-cells between P4 TCR/DR1/ABO transgenic mice and DR1/ABO transgenic control mice was seen for the line 4 mice, as shown in Table 4.3.

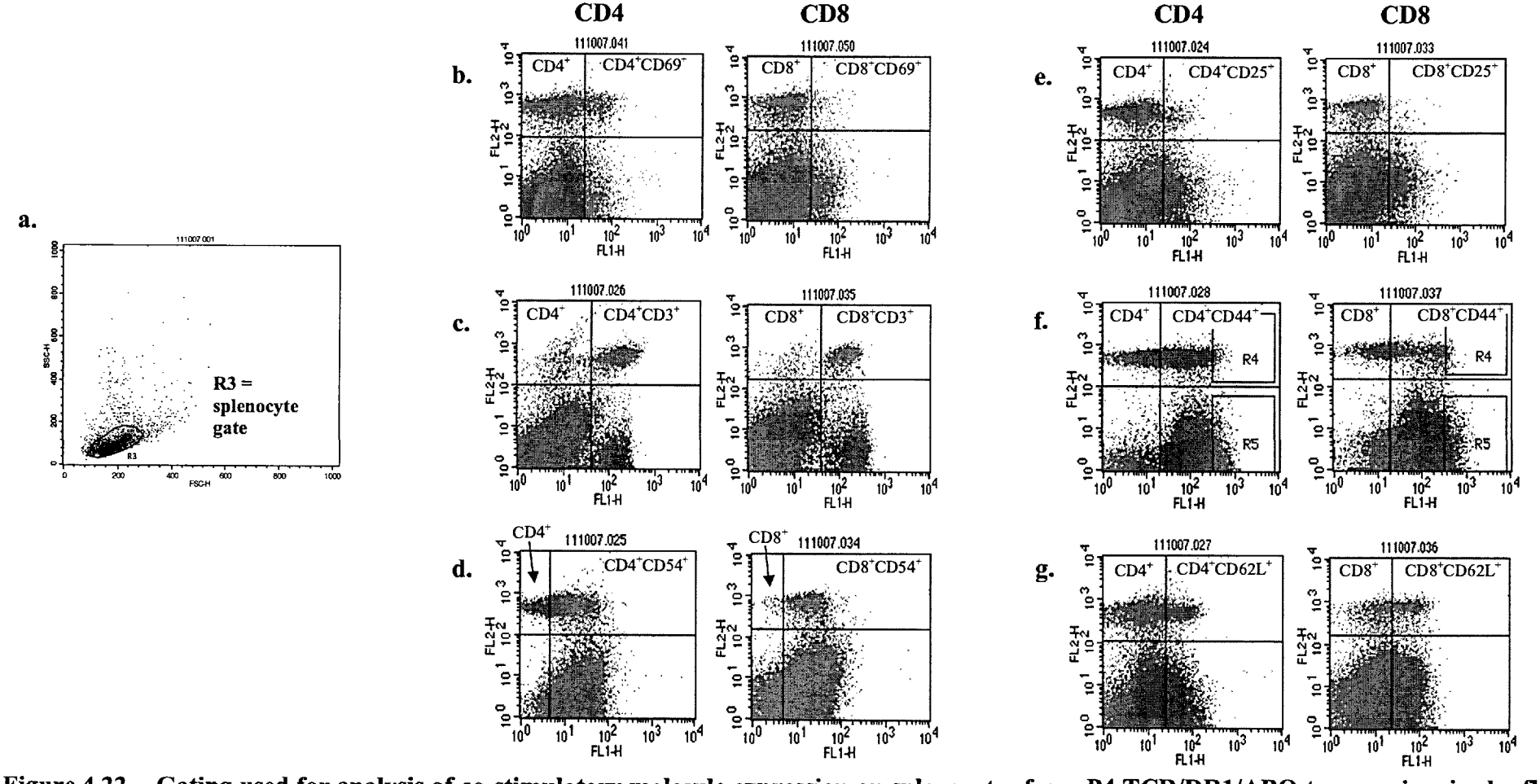


Figure 4.22 Gating used for analysis of co-stimulatory molecule expression on splenocytes from P4 TCR/DR1/ABO transgenic mice by flow cytometry Each costimulatory molecule (in the FL-1 channel, x-axis) was analysed against CD4 (left-hand plot in (b)-(g) above) or CD8 expression (right-hand plot in (b)-(g) above) in the FL-2 channel (y-axis). Staining was positive or negative as shown by the quadrant gates above. (a) shows a forward- vs side-scatter plot identifying the live splenocyte gate. FL-1 stains used: (b) CD69, (c) CD3, (d) CD54, (e) CD25, (f) CD44 and (g) CD62L.

	TCR/DR1 Tg - line 4	DR1 only Tg - line 4	TCR/DR1 Tg - line 16
	n = 7	n = 3	n = 4
CD69			
$CD4^+$ $CD69^+$	1.40 ± 0.44	1.24 ± 0.09	1.19 ± 0.48
$CD4^+$ only	15.65 ± 4.32	15.89 ± 1.64	10.47 ± 0.99
$CD8^+$ $CD69^+$	0.47 ± 0.12	0.44 ± 0.05	0.32 ± 0.07
$CD8^+$ only	6.71 ± 1.12	6.66 ± 0.59	3.98 ± 0.93
CD3			
$CD4^+$ $CD3^+$	12.12 ± 4.38	11.66 ± 3.33	7.12 ± 1.04
$CD4^+$ only	1.62 ± 0.46	1.65 ± 0.19	1.26 ± 0.35
$CD8^+$ $CD3^+$	3.23 ± 0.45	3.38 ± 0.46	3.76 ± 0.90
$CD8^+$ only	0.92 ± 0.19	0.92 ± 0.16	0.47 ± 0.14
CD54			
$CD4^+$ $CD54^+$	13.60 ± 2.01	14.97 ± 1.29	12.13 ± 1.95
$CD4^+$ only	5.80 ± 2.64	7.25 ± 1.07	1.91 ± 0.40
$CD8^+$ $CD54^+$	4.52 ± 0.86	4.55 ± 0.77	4.93 ± 1.07
$CD8^+$ only	0.26 ± 0.12	0.43 ± 0.14	0.16 ± 0.06
CD25			
$CD4^+$ $CD25^+$	0.99 ± 0.20	0.90 ± 0.11	0.65 ± 0.06
$CD4^+$ only	16.94 ± 4.01	17.98 ± 2.20	10.74 ± 0.90
$CD8^+$ $CD25^+$	0.45 ± 0.12	0.32 ± 0.13	0.17 ± 0.03
$CD8^+$ only	3.81 ± 0.87	3.75 ± 0.96	4.15 ± 1.31
CD44			
$CD4^+$ $CD44^{high}$	14.18 ± 2.23	13.72 ± 1.35	8.20 ± 3.06
$CD4^+$ $CD44^{low}$	9.85 ± 3.49	9.51 ± 1.31	7.33 ± 3.02
$CD8^+$ $CD44^{high}$	5.54 ± 2.45	4.60 ± 0.95	4.76 ± 1.65
$CD8^+$ $CD44^{low}$	2.96 ± 0.93	3.31 ± 0.64	2.48 ± 0.77
CD62L			
$CD4^+$ $CD62L^{high}$	7.85 ± 2.85	8.25 ± 1.90	3.16 ± 0.48
$CD4^+$ $CD62L^{low}$	15.64 ± 3.74	13.70 ± 0.39	10.04 ± 2.16
$CD8^+$ $CD62L^{high}$	2.41 ± 0.62	3.04 ± 1.26	1.27 ± 0.25
$CD8^+$ $CD62L^{low}$	1.75 ± 0.31	1.42 ± 0.82	2.43 ± 0.96

Table 4.3 Expression of T-cell costimulatory molecules on splenocytes from P4 TCR/DR1/ABO transgenic mice Values shown are percentages (± standard deviation) of total cells analysed in the R3 splenocyte gate as shown in Figure 4.23. Only $CD4^+$ or $CD8^+$ cells are shown. No DR1/ABO transgenic control mouse data is available for the line 16 experiment.

Approximately 12% of total splenocytes were $CD4^+CD3^+$ and approximately 4% of total splenocytes were $CD8^+CD3^+$. Also, in agreement with published reports, the majority of $CD4^+$ (approximately 88%) and $CD8^+$ (approximately 80-90%) cells also expressed CD3.

No statistically significant difference in the level of CD54 expression was seen in the thymus of P4 TCR/DR1/ABO transgenic mice compared to DR1/ABO transgenic control mice; however, in the line 4 experiment, there was an apparent higher level of CD54 expression in the DN and CD8 SP subsets in P4 TCR/DR1/ABO transgenic mice. There was also no discernible difference in CD54 expression between P4 TCR/DR1/ABO transgenic mice from line 4 and DR1/ABO transgenic control mice in the spleen, as shown in Table 4.3. Approximately 15% of total splenocytes were $CD4^+CD54^+$ whilst approximately 5% of total splenocytes were $CD8^+CD54^+$. The majority of $CD4^+$ cells were also $CD54^+$ (ranging from 70 to 90%) as were the majority of $CD8^+$ cells (approximately 90 to 95%). As can be seen in Figure 4.22d, staining with anti-CD54 antibody did not give rise to a discrete $CD54^+$ population but rather a range of expression from low to high. Those $CD4^+$ or $CD8^+$ cells that did not express CD54 in this analysis may express very low levels and therefore appear in the $CD54^-$ gate. In summary, no difference in CD54 expression was seen on the $CD4^+$ or $CD8^+$ cells in the spleen of P4 TCR/DR1/ABO transgenic mice compared with the corresponding DR1/ABO transgenic control mice in the line 4 experiment.

CD25 expression on P4 TCR/DR1/ABO transgenic thymocytes was similar to the level of expression seen in DR1/ABO transgenic control thymocytes. In the spleen, very little CD25 expression was seen on either $CD4^+$ or $CD8^+$ T-cells, as shown in Table 4.3. $CD4^+CD25^+$ and $CD8^+CD25^+$ populations each accounted for less than 1% of total splenocytes. As the cells in this case were freshly isolated from the spleen and therefore not activated and had not been activated *in vitro* before analysis, it was not expected that they would express high levels of CD25. There was no discernible difference in CD25 expression between P4 TCR/DR1/ABO transgenic mice in line 4 and the corresponding DR1/ABO transgenic control mice.

CD44 is a cell adhesion molecule that is thought to be involved in the migration and homing of T-cells. There are a number of CD44 isotypes and it can also be differentially glycosylated; it is thought that CD44 may regulate tissue-specific homing of T-cells in

addition to its interaction with a number of different ligands, including hyaluronic acid and other components of the extracellular matrix such as collagen and fibronectin (662). CD44 is expressed at variable levels on peripheral T-cells depending upon the degree of differentiation of the cell. Memory T-cells are associated with the expression of high levels of CD44 but most peripheral T-cells express CD44 to some degree. CD44 expression is also up-regulated on T-cells shortly after their activation (663). A decrease in CD44 expression on the DN subset of thymocytes was seen when comparing P4 TCR/DR1/ABO transgenic mice with DR1/ABO transgenic control mice in both lines 4 and 16, possibly as a consequence of the block in thymocyte development that is often seen in TCR transgenic mice in the DN subset. When analysing the extent of CD44 expression on splenocytes these differences were not seen, as shown in Table 4.3. Using the gating shown in Figure 4.22f, approximately 14% of total splenocytes in line 4 P4 TCR/DR1/ABO transgenic mice and DR1/ABO transgenic control mice were defined as $CD4^+CD44^{high}$ (59% of total $CD4^+$ cells) and approximately 10% of total splenocytes were defined as $CD4^+CD44^{low}$ in these same mice. Approximately 5% of total splenocytes from these mice were defined as $CD8^+CD44^{high}$ (55-65% of total $CD8^+$ cells) and approximately 3% of total splenocytes were defined as $CD8^+CD44^{low}$.

CD62L is a homing receptor for T-cells, facilitating interactions between T-cells and high endothelial venules (HEVs) and hence entry into the lymph nodes (664). As such, it is more highly expressed on non-activated cells such as naïve and some memory T-cells and is rapidly shed from the surface of the cell through proteolytic cleavage upon T-cell activation (665). Expression of CD62L in thymocytes from P4 TCR/DR1/ABO transgenic line 16 mice was higher in the DN, DP and CD8 SP subsets when compared to DR1/ABO littermates and P4 TCR/DR1/ABO transgenic mice from line 4. No difference in expression between DR1/ABO transgenic control mice and P4 TCR/DR1/ABO transgenic mice from line 4 was seen. In the line 4 experiment, no difference in CD62L expression on $CD4^+$ or $CD8^+$ cells between P4 TCR/DR1/ABO transgenic mice and DR1/ABO transgenic control mice was seen, as shown in Table 4.3. CD62L expression on $CD4^+$ and $CD8^+$ cells was defined as being either high or low as shown in Figure 4.23g. 30-40% of $CD4^+$ splenocytes were thus defined as also being $CD62L^{high}$ in P4 TCR/DR1/ABO transgenic mice from both line 4 and line 16 as well as the DR1/ABO transgenic control mice from the line 4 experiment.

4.3.9 Expression of the T-cell costimulatory molecules OX40 and its ligand OX40L and ICOS on freshly-isolated splenocytes in P4 TCR/DR1/ABO transgenic mice is similar to the expression seen in DR1/ABO transgenic control mice

As described previously, splenocytes were isolated from the same mice as those used for analysis of costimulatory molecule expression in thymocytes and analysed for expression of those molecules in conjunction with either CD4 or CD8. The gates used to define populations of splenocytes are shown in Figure 4.23. The live lymphocyte gate was determined on the basis of light-scattering properties (forward and side) and is shown in Figure 4.23a (R3). Populations, defined on the basis of CD4 or CD8 expression and the expression of the costimulatory molecule being analysed, are shown as FL-1 vs. FL-2 dot plots in Figure 4.23 b-d. Table 4.4 shows the percentage of total splenocytes that were $CD4^+$ or $CD8^+$ only and those that expressed CD4 or CD8 and were also positive for expression of the relevant costimulatory molecule. In the case of OX40L, which is not appreciably expressed on T-cells, $OX40L^+$ cells are also shown.

OX40, through interaction with its ligand OX40L, is a costimulatory molecule that is expressed only after activation of a T-cell and expression peaks 2-3 days after initial activation (666). It is associated more strongly with CD4 T-cell responses than CD8 T-cell responses. OX40L is only expressed on antigen-presenting cells that have previously been activated themselves (652). OX40 promotes survival of T-cells through production of anti-apoptotic factors and promotes the development of memory T-cells (667). Expression of OX40 in thymocytes from P4 TCR/DR1/ABO transgenic line 4 and line 16 mice was slightly higher in the DN subsets when compared to DR1/ABO transgenic control mice. In the spleen, very little OX40 expression was seen on either $CD4^+$ or $CD8^+$ T-cells as shown in Table 4.4, with $CD4^+OX40^+$ and $CD8^+OX40^+$ populations each accounting for less than 1% of total splenocytes. As the cells in this case were freshly isolated from the spleen and therefore not activated and had not been activated *in vitro* before analysis, it was not expected that they would express appreciable levels of OX40. There was no discernible difference in OX40 expression between P4 TCR/DR1/ABO transgenic mice and the DR1/ABO transgenic control mice in line 4. OX40L is not highly expressed upon T-cells under any circumstances and hence $CD4^+$ and $CD8^+$ cells from the spleen did not express OX40L to a detectable extent.

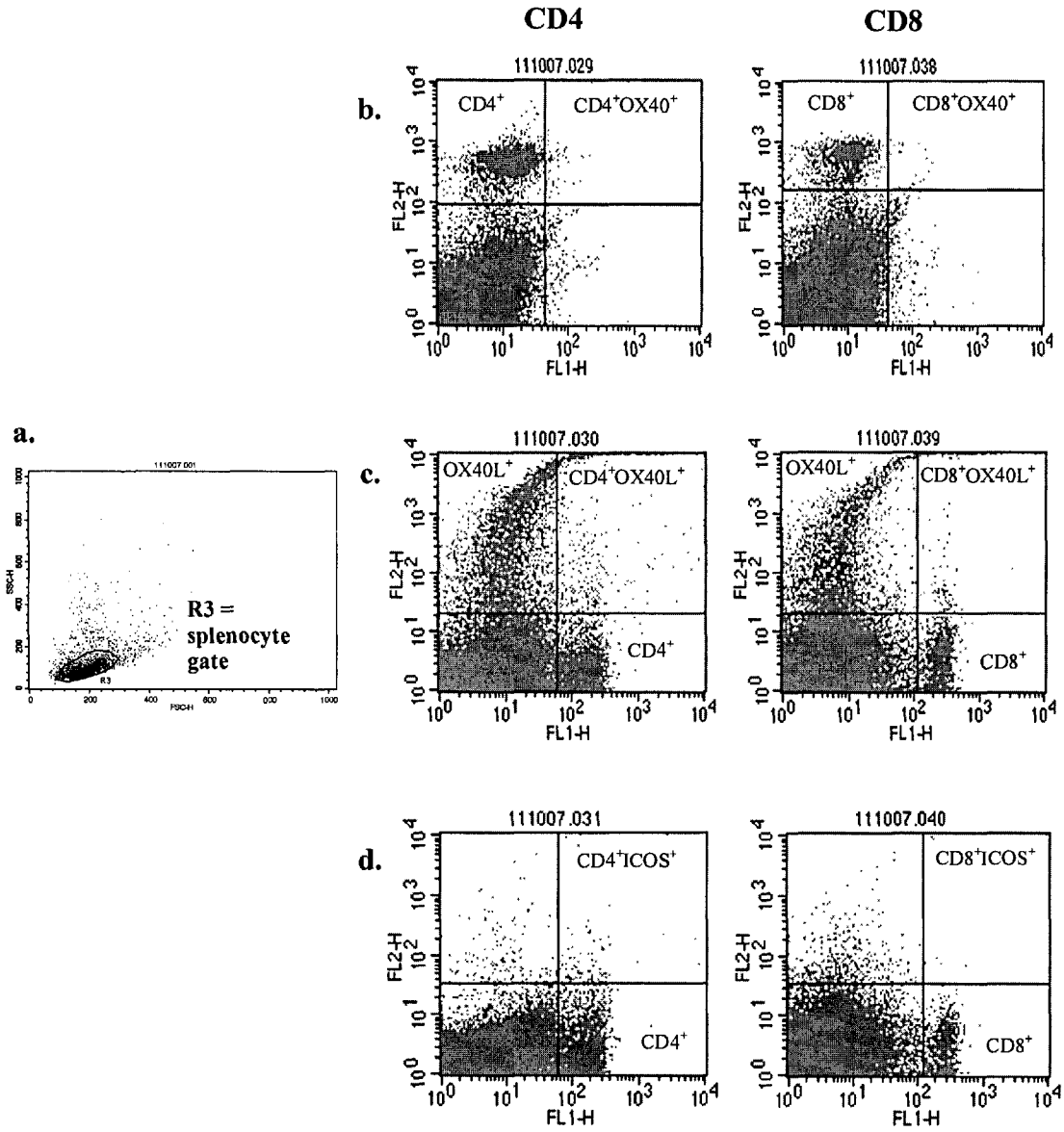


Figure 4.23 Gating used for analysis of expression of late activation-associated T-cell co-stimulatory molecules on splenocytes from P4 TCR/DR1/ABO transgenic mice by flow cytometry Each costimulatory molecule (FL-1 channel, x-axis for (b), FL-2 channel, y-axis for (c) and (d)) was analysed against CD4 (left-hand plot in (b)-(d) above) or CD8 expression (right-hand plot in (b)-(d) above) in the FL-2 channel (y-axis) for (b), or the FL-1 channel (x-axis) for (c) and (d). Staining was either positive or negative, as shown by the quadrant gates above. (a) shows a forward scatter vs side-scatter plot identifying the live splenocyte gate. FL-1 stains used: (b) OX40, (c) OX40L and (d) ICOS.

	TCR/DR1 Tg - line 4 (%)	DR1 only Tg - line 4 (%)	TCR/DR1 Tg - line 16 (%)
	n = 7	n = 3	n = 4
OX40			
$CD4^+$ $OX40^+$	1.16 ± 0.41	0.97 ± 0.28	0.13 ± 0.03
$CD4^+$ only	16.93 ± 3.76	18.37 ± 2.35	11.76 ± 1.28
$CD8^+$ $OX40^+$	0.14 ± 0.07	0.09 ± 0.04	0.05 ± 0.02
$CD8^+$ only	4.67 ± 1.04	5.51 ± 0.50	4.66 ± 1.79
OX40L			
$CD4^+$ $OX40L^+$	0.12 ± 0.04	0.12 ± 0.03	1.59 ± 0.81
$CD4^+$ only	6.70 ± 2.72	8.95 ± 2.03	6.54 ± 1.22
$CD4^-$ $OX40L^+$	0.87 ± 0.31	0.82 ± 0.12	8.42 ± 1.49
$CD8^+$ $OX40L^+$	0.01 ± 0.01	0.01 ± 0.01	0.49 ± 0.23
$CD8^+$ only	1.91 ± 0.68	1.87 ± 0.94	1.68 ± 0.83
$CD8^-$ $OX40L^+$	0.88 ± 0.58	0.56 ± 0.11	6.36 ± 1.43
ICOS			
$CD4^+$ $ICOS^+$	0.19 ± 0.11	0.26 ± 0.08	0.23 ± 0.06
$CD4^+$ only	6.75 ± 2.43	7.53 ± 2.12	5.36 ± 0.74
$CD8^+$ $ICOS^+$	0.01 ± 0.00	0.01 ± 0.01	0.02 ± 0.01
$CD8^+$ only	2.46 ± 0.49	2.45 ± 0.72	1.57 ± 0.49

Table 4.4 Expression of the late activation-associated T-cell costimulatory molecules OX40, ICOS and OX40L on splenocytes from P4 TCR/DR1/ABO transgenic mice Values shown are percentages (± standard deviation) of total cells analysed in the R3 splenocyte gate as shown in Figure 4.24. Only $CD4^+$ or $CD8^+$ cells are shown, except for the analysis of OX40L, where $CD4^-$ $CD8^-$ $OX40L^+$ cells are also shown. No data for DR1/ABO transgenic control mice in the line 16 experiment was available.

ICOS, like OX40, is an inducible costimulatory molecule that is only expressed on T-cells some time after they have been activated. Expression of ICOS in thymocytes from P4 TCR/DR1/ABO transgenic line 4 and line 16 mice was lower in the DN subsets than in DR1/ABO transgenic control mice, and in the line 16 P4 TCR/DR1/ABO transgenic mice ICOS expression was also lower in the CD4 and CD8 SP subsets than when compared to DR1/ABO transgenic control mice. Very little ICOS expression was seen in the spleen of line 4 or line 16 P4 TCR/DR1/ABO transgenic mice or the DR1/ABO transgenic control mice from the line 4 experiment on either $CD4^+$ or $CD8^+$ T-cells. $CD4^+ICOS^+$ and $CD8^+ICOS^+$ populations both accounted for less than 1% of total splenocytes. As the cells in this case were freshly isolated from spleen and hence were not activated, they were not expected to express appreciable levels of ICOS. There was no discernible difference in ICOS expression between P4 TCR/DR1/ABO transgenic mice and the DR1/ABO transgenic control mice in line 4.

4.3.10 Summary of findings

Expression of the costimulatory molecules CD69, CD3, CD54, CD25, CD44, CD62L, OX40, OX40L and ICOS was analysed on the surface of freshly isolated splenocytes and thymocytes of P4 TCR/DR1/ABO transgenic mice from line 4 and line 16 and compared with the expression on DR1/ABO transgenic control mice. No differences were seen between P4 TCR/DR1/ABO transgenic mice from line 4 and DR1/ABO transgenic control mice in the expression of any of the studied molecules on freshly isolated splenocytes. In addition, no statistically significant differences were seen in the expression of CD69, CD3, CD54 or CD25 on freshly isolated thymocytes between P4 TCR/DR1/ABO transgenic mice from either line and DR1/ABO transgenic control mice. However, some differences were noted between P4 TCR/DR1/ABO transgenic mice and DR1/ABO transgenic control mice. A block in thymocyte development at the DN stage was apparent in both line 4 and line 16 P4 TCR/DR1/ABO transgenic mice, shown as an increase in the proportion of $CD4^-CD8^-$ cells in the thymus when compared with DR1/ABO transgenic control mice. In addition, CD44 expression in P4 TCR/DR1/ABO transgenic mice from line 4 and line 16 was decreased in the DN subset when compared to DR1/ABO transgenic control mice. An increase in high expression of CD62L in the DN, DP and CD8 SP subsets was seen in line 16 P4 TCR/DR1/ABO transgenic mice when compared to both DR1/ABO transgenic control mice and line 4 P4 TCR/DR1/ABO transgenic mice. In addition, a small but significant increase in

OX40 expression was seen on DN thymocytes from line 4 and line 16 P4 TCR/DR1/ABO transgenic mice when compared to DR1/ABO transgenic control mice. Finally, down-regulation of ICOS expression was seen in DN thymocytes from both line 4 and line 16 P4 TCR/DR1/ABO transgenic mice when compared to DR1/ABO transgenic control mice. ICOS expression was also down-regulated in CD4 SP thymocytes from line 16 P4 TCR/DR1/ABO transgenic mice in comparison to both line 4 P4 TCR/DR1/ABO transgenic mice and DR1/ABO transgenic control mice. The main differences identified through this analysis are shown in Table 4.5.

Molecule	Difference seen in the thymus
CD4/CD8	Increase in the number of DN (i.e. $CD4^-$ $CD8^-$) thymocytes in P4 TCR/DR1/ABO transgenic mice compared with DR1/ABO transgenic controls
CD44	Decreased level of expression on cells of the DN subset in P4 TCR/DR1/ABO transgenic mice compared with DR1/ABO transgenic controls
CD62L	Increased levels of expression on cells of the DN, DP and CD8 SP subsets of P4 TCR/DR1/ABO transgenic mice compared with DR1/ABO transgenic controls **(line 16 only)**
OX40	Small increase in expression on DN cells of TCR/DR1/ABO transgenic mice compared with DR1/ABO transgenic controls
ICOS	Decreased expression on cells of the DN and CD4 SP subsets in TCR/DR1/ABO transgenic mice compared with DR1/ABO transgenic controls **(line 16 only)**

Table 4.5 The differences identified in levels of expression of costimulatory molecules at the cell surface of thymocyte subsets between P4 TCR/DR1/ABO transgenic mice from lines 4 and 16 and DR1/ABO transgenic control mice by flow cytometry.

4.4 Discussion

This chapter describes some very preliminary experiments on the characterisation of a humanised TCR/MHC class II transgenic mouse, the P4 TCR/DR1/ABO mouse, developed for use as a model of allergic asthma in the Boyton laboratory by three post-doctoral scientists (Dr. Alexander Annenkov, Dr. Catherine Reynolds and Dr. Xiaoming Cheng) with funding from Asthma UK. Sensitisation (by intraperitoneal injection of Fel d 1) and challenge (by intranasal administration of whole cat dander extract) was used to investigate whether an allergic airway disease phenotype was seen in these mice (287). Fel d 1-sensitised mice responded to methacholine challenge to a greater extent than did unsensitised mice (both Penh and resistance/compliance parameters). The use of larger groups (n=10) and repeat experiments to refine the protocols should improve the disease phenotype of the model. Cell counts in the BAL fluid and lung tissue of mice that had been sensitised with Fel d 1 were increased compared to controls, and in line 16 this result was statistically significant. Such an influx of cells into the lung is consistent with the development of an immune response in the lungs of these mice. In all cases, this influx of cells was predominantly eosinophilic. A similar result was seen when analysing cell counts recovered from the lung tissue in terms of eosinophilic influx - the proportion of cells recovered that were eosinophils was greatly increased in sensitised mice. Allergic asthmatic disease in humans is associated with an influx of eosinophils into the lung and is thus a feature of the disease that is replicated faithfully in this mouse model. Another common feature of allergic asthma in humans is the increase in incidence of IgE in the serum and this was also seen in the Fel d 1-sensitised mice. Analysis of Th2-type cytokine production in the experiment using line 4 mice (lower dose of cat dander extract for challenge) showed increased IL-4, IL-5 and IL-13 in the BAL fluid with Fel d 1 sensitisation. IL-4, IL-5 and IL-13 cytokine production in the lung tissue increased in line 16 P4 TCR/DR1/ABO transgenic mice between sensitised and unsensitised groups. Histological analysis of frozen lung sections suggested that there was mild lung inflammation (both peribronchiolar and perivascular) and mucus production in Fel d 1-sensitised mice. Both of these are features of the human disease and their induction in this system further lends to the faithfulness of the TCR/MHC class II transgenic mouse model of allergic asthma to human disease.

Use of a mouse expressing human genes as the basis for the development of a model of allergic asthma may make the model more relevant to the human disease than the other models currently in use. This has been shown to be the case in mouse models of multiple sclerosis (EAE) where use of humanised TCR transgenic mice produced a model that replicated the disease in humans more faithfully than using non-humanised mice (283). Most mouse models of allergic asthma in use today make use of ovalbumin as an allergen, often in the Balb/c strain of mice (286). Whilst a phenotype correlating with allergic asthma (lung function defects, increased levels of IgE, lung inflammation and mucus hypersecretion) is seen in these mice, there are disadvantages to this approach. Humans do not develop allergic asthma in response to ovalbumin and hence this model utilises an irrelevant antigen and the use of mice which do not naturally become sensitised to allergen through inhalational exposure and are of a strain that have a tendency to mount Th2-biased immune responses means that a highly artificial system of sensitisation is employed, involving systemic injection of high doses of allergen. It is also difficult to develop a chronic phenotype in such mice as they quickly become tolerised to the allergen; however, a chronic phenotype, particularly involving remodelling of the lung, is far more relevant to human disease. Other models have attempted to address these issues and have had more success – use of a more relevant allergen, Der p 1 from house dust mite, has shown more promising results in terms of development of a chronic disease phenotype (315); however, systemic sensitisation is often (though not always) required in this model. There are TCR transgenic mouse models of both OVA- (DO11.10, 326, 328) and HDM-induced (330) allergic asthma which appear to be somewhat more receptive to induction of disease through inhalation, making them more relevant to the human disease.

Induction of a disease-like phenotype was achieved in the P4 TCR/DR1/ABO mice. It will now be possible to develop this model of allergic airway disease to study prolonged (chronic) exposure to allergen through inhalation, thus providing a model that is highly similar in terms of both disease induction and disease pathogenesis to the human disease. In addition, the presence of a human TCR implicated in disease pathogenesis in allergic asthma may allow additional study of the precise role of dominant TCR-expressing T-cells in allergic asthmatic disease. The mechanisms underlying the tolerance to allergen that is induced by peptide immunotherapy in humans can also be investigated through the development of a model of peptide-induced tolerance in this mouse line. The transgenic T-cells are likely to act as pathogenic effector cells in this

allergic disease model and the effect of peptide immunisation on the development of disease in these mice could give valuable insights into the underlying mechanisms involved in tolerance induction in human allergic asthma. In addition, these mice may also be useful in the study of other aspects of allergic disease pathogenesis. For example, the role of pulmonary infections such as respiratory syncytial virus (RSV) or influenza virus, especially the role such infections may have on the T-cells involved in causing asthma pathogenesis, could be investigated using this model. In particular, the impact of the timing of viral infection on the development and severity of allergic asthma pathogenesis has been shown to be important (668, 26). Viral infection prior to allergen exposure is thought to exacerbate the allergic syndrome which develops, somewhat counter-intuitively, as such infections promote a Th1-type response and the production of significant quantities of IFN-γ. It was therefore supposed that such infections would protect against the development of asthma by antagonising the development of Th2-type responses in the lung but findings from other mouse studies have contradicted this view (668, 26). The development of a humanised TCR transgenic mouse model of allergic asthma may allow a more detailed investigation of the effect of such infections on the allergen-specific TCR transgenic T-cells. Another aspect of allergic asthma that is difficult to study in humans is lung remodelling, both the underlying mechanisms of remodelling and its function. Mouse models have been developed that show features of remodelling such as airway smooth muscle hyperplasia, basement membrane thickening and epithelial cell changes (293, 315) and have begun to identify factors that are important in the development of lung remodelling such as TGF-β (669, 670) and VEGF (671). The development of a humanised TCR transgenic mouse model of allergic asthma that shows features of remodelling would also allow, among other lines of study, the investigation of the role of allergen-specific T-cells in inducing remodelling.

It has been observed in other TCR transgenic mice that T-cell development is often abnormal, particularly in the thymus where expression of a rearranged TCRα chain at the DN stage of development impedes normal progression through the β-selection checkpoint (425). This causes a block in development at this point due to the TCRα chain having a higher affinity for newly rearranged (or transgenic) TCRβ chains than the pre-TCRα chain and it is the signals transmitted through the pre-TCRα-TCRβ complex that allow progression through the checkpoint. This manifests as an increase in DN cell number in TCR transgenic mice when compared to non-TCR transgenic mice

and this phenomenon was observed in both line 4 and line 16 P4 TCR/DR1/ABO transgenic mice, suggesting that transgenic TCR expression is occurring in these mice. T-cell numbers and function in the peripheral circulation of TCR transgenic mice is comparable to that seen in non-transgenic mice but the repertoire of expressed TCRs is usually more restricted and dominated by the transgenic TCR.

To investigate whether the expression of a transgenic TCR affected the expression of membrane-bound costimulatory molecules involved in T-cell signalling and function, expression of these molecules was analysed immediately *ex vivo* by flow cytometry in the P4 TCR/DR1/ABO transgenic mice in both the thymus and the spleen (i.e. peripheral T-cells) and compared to the expression seen in non-TCR transgenic DR1/ABO mice. Differences in the expression of a number of these analysed molecules were seen in the thymi of P4 TCR/DR1/ABO transgenic mice when compared to the non-TCR transgenic DR1/ABO transgenic control mice. CD44 expression in the DN subset of thymocytes was shown to be lower in the P4 TCR/DR1/ABO transgenic mice than in the DR1/ABO transgenic control mice in both lines 4 and 16. Together with CD25, CD44 expression defines a further four subsets in the DN population, DN1-DN4 (DN1 - $CD44^+CD25^-$, DN2 - $CD44^+CD25^+$, DN3 - $CD44^-CD25^+$ and DN4 - $CD44^-CD25^-$) (416). A decrease in CD44 expression in DN cells from P4 TCR/DR1/ABO transgenic thymi indicates either a decrease in the number of CD44-expressing cells or an increase in the number of $CD44^-$ cells. As it has been shown that transgenic TCR expression in the thymus at the DN stage prevents progression through the β-selection checkpoint (424), this results in a build-up of thymocytes at the DN3 ($CD44^-CD25^+$) stage as the checkpoint occurs at the DN3 to DN4 transition. This would be shown not only as an overall increase in DN cell number (which is also seen in these mice) but more particularly an increase in the number of DN3 cells and this would manifest as a decrease in the proportion of DN cells expressing CD44 which is also seen in these mice. A corresponding increase in the levels of expression of CD25 might also be expected in these mice - however, this was not seen in these experiments.

Analysis of CD62L expression in the thymus showed differences in expression levels between TCR transgenic and non-TCR transgenic mice in line 16 mice only, more specifically an increase in expression in the DN (by 15%), DP (by 5%) and CD8 SP (by 15%) subsets. In addition, a concomitant increase in MFI of the $CD62L^+$ cells in these mice was seen. None of these differences were seen in the CD4 SP subset. CD62L

identifies those cells of the common lymphoid progenitor lineage that are destined to migrate to the thymus and develop along the T-cell lineage (647). An increase in CD62L expression in the DN subset which has been shown to gradually down-regulate as the cell progresses through the thymus, may indicate a higher proportion of the earliest T-cell progenitors in the thymus in this line of mice. This might suggest that a higher number of common lymphoid progenitors in these mice have been directed to the T-cell lineage or that there may be an early block (at the DN1 stage) in thymocyte development in these mice. No other data from this experiment suggests this however, and the analysis of CD44 expression in the DN subset would appear to contradict it. In addition, CD62L expression is up-regulated on mature SP thymocytes prior to their emigration from the thymus and it is thus used as a marker for the most mature thymocytes in the SP populations (655). Interestingly, in the line 16 P4 TCR/DR1/ABO transgenic mice expression of CD62L was higher in the CD8 SP subset than in DR1/ABO transgenic control mice and line 4 P4 TCR/DR1/ABO mice - the difference in expression seen in these lines may represent a difference in emigration rates of $CD8^+$ mature thymocytes with mature CD8 SP thymocytes not emigrating as efficiently as CD4 SP in the line 16 mice. This is perhaps not borne out by analysis of T-cell numbers in the periphery where numbers of $CD4^+$ and $CD8^+$ T-cells and the ratio of CD4/CD8 T-cells was similar in both P4 TCR/DR1/ABO transgenic mice and their DR1/ABO transgenic control mice, but there are likely to be other mechanisms of controlling T-cell numbers and maintaining their homeostasis in the periphery.

In the analysis of differences in costimulatory molecule expression in the thymi of P4 TCR/DR1/ABO transgenic mice compared with their DR1/ABO transgenic control mice, it became apparent that in some cases only line 16 P4 TCR/DR1/ABO transgenic mice showed a difference in expression when compared with DR1/ABO transgenic control mice, whilst line 4 P4 TCR/DR1/ABO transgenic mice showed similar responses to the non-TCR transgenic DR1/ABO controls. As line 4 and line 16 mice were generated from different founders and were not interbred, they may differ in terms of TCR transgene expression e.g. copy number or position of insertion into the genome. Such differences may lead to a difference in expression levels of the transgenes and thus differences in the response of the two lines to varying stimuli. Increased copy number may translate into increased surface expression whilst different locations of transgene insertion may cause differences in expression levels due to differing influences on expression from nearby endogenous promoter or repressor regions within the genome.

Insertion near a strong global enhancer or promoter region could increase expression levels; conversely, insertion near a strong global repressor region could decrease expression. It might be possible to develop a Southern hybridisation strategy that could determine the number of insertion sites for each line - this was not possible with the Southern hybridisation protocol described here as the restriction enzyme used to digest the genomic DNA cut on either side of the transgene within the pTcass construct sequence - and which might also give some information as to the number of transgene copies inserted.

Other molecules that were assessed including CD3, CD25, CD54 and CD69, showed no statistically significant differences in expression in thymocytes between P4 TCR/DR1/ABO transgenic mice and DR1/ABO transgenic control mice in either line. Levels of expression of these molecules correlated in terms of expression patterns and approximate extent of expression with levels reported in the literature. It was predicted that CD3 expression would be altered in the TCR transgenic mice due to the presence of a transgenic TCR which would alter the levels of TCR expression in each subset and would be reflected in the alteration of CD3 expression. An increase in CD3 expression in the DN subset was seen in the P4 TCR/DR1/ABO mice from line 4 when compared with DR1/ABO transgenic control mice which was not statistically significant. Nonetheless this difference could be of genuine relevance, caused by the expression of the transgenic rearranged TCR molecule at the cell surface at this stage where TCR expression is not normally seen. CD69, an early activation marker on peripheral T-cells, is associated with positive selection events in the thymus (648) and hence is expressed most strongly on DP and SP thymocytes. The effect of a transgenic TCR in the thymus at this stage of development has not been well characterised; a change in the levels of CD69 might indicate that there is an effect. Although not a statistically significant finding, CD69 expression in the SP subsets appeared to be lower in the P4 TCR/DR1/ABO transgenic mice in both lines 4 and 16 when compared to the DR1/ABO transgenic control mice in each case – this might suggest that there is a difference in positive selection that is associated with the expression of a transgenic TCR.

Other costimulatory molecules such as ICOS and OX40 are expressed later in activation, reaching a peak of expression 2-3 days after activation. The roles of these secondary costimulatory molecules in the thymus are not well characterised although

expression of both OX40 (649) and ICOS (653) in the thymus has been reported. They are predominantly expressed in the thymic medulla which suggests that they are associated with SP thymocytes. In the periphery, ICOS is more associated with $CD4^+$ T-cells than $CD8^+$ T-cells and it is related to CD28, exerting a similar function as CD28 but later in the activation process (651) where it is thought to promote survival of activated cells through inhibition of apoptosis. Although the function of ICOS in the thymus is currently unknown, its function might be related to its peripheral function, perhaps through promotion of survival of thymocytes undergoing thymic selection or which have been positively selected and this function may be affected by the presence of a transgenic TCR. Thymocytes in the line 16 P4 TCR/DR1/ABO transgenic mice showed down-regulated levels of ICOS in the CD4 single positive subset (a phenomenon not observed in the line 4 P4 TCR/DR1/ABO transgenic mice); as yet the significance of this is unclear as the role of ICOS in the thymus has not been determined in any detail, but this difference between TCR transgenic and non-TCR transgenic mice suggests that it warrants further investigation. If, as suggested above, the function of ICOS is to prolong survival of thymocytes undergoing selection, giving them more opportunity to produce a positively-selectable TCR, the down-regulation of ICOS expression in the line 16 P4 TCR/DR1/ABO transgenic mice may reflect this role - as TCR transgenic thymocytes already express a rearranged $\alpha\beta$ TCR, there may be less opportunity for endogenous TCRα rearrangement to occur and therefore less requirement for ICOS expression to prolong the life of these thymocytes, hence its lower expression.

As with ICOS, the role of OX40 (and its ligand OX40L) in the thymus is not well-characterised. OX40 is expressed in the CD4 and CD8 SP subsets of the thymus and expression is higher on the CD4 SP than the CD8 SP subset, although lower levels of expression in the DP and DN subsets have also been reported (649). This is similar to the distribution of ICOS in the thymus and as both molecules play a role in the periphery in promoting T-cell survival (667) this may also be their thymic function. The analysis of OX40 expression in the thymus undertaken here showed a small increase in OX40 expression in the DN cells of P4 TCR/DR1/ABO transgenic thymi. However, OX40 expression was not related to the expression of other DN cell markers such as CD44 or CD25, hence it was not possible to tell whether this increase was common to all DN cells or a particular subset or subsets, and thus it is difficult to suggest the role of OX40 in the thymus in these mice. Possibly, OX40 is involved in promoting survival of

thymocytes at the β-selection checkpoint, perhaps through prolonging the lifespan of thymocytes undergoing TCRβ chain rearrangement and giving them more opportunity to correctly rearrange the gene; the increase in OX40 expression in TCR transgenic DN thymocytes may be due to the failure of thymocytes expressing a transgenic TCR to progress through the checkpoint. However, further study of the expression of OX40 in conjunction with other molecules such as CD3, CD44 or CD25 would be required to confirm this theory.

The immediately *ex vivo* analysis of the expression of these molecules in splenocytes did not show any differences between the P4 TCR/DR1/ABO transgenic mice and the DR1/ABO transgenic control mice and thus the differences seen in the thymus were not replicated in the periphery. It is possible that differences would be seen if the splenocytes were activated *in vitro,* either specifically with peptide 4/DR1 or non-specifically with anti-CD3/anti-CD28, before analysis, particularly in the case of molecules such as ICOS which are associated with activated T-cells. The expression of these molecules could be assessed at different time points after activation to investigate if there are any differences in the splenocyte responses and if analysis of activated thymocytes was also carried out, whether the same or other differences are apparent in the thymocytes under these circumstances.

5. Summary

In this thesis, analysis of TCR CDR3 usage in human T-cell lines derived from HLA-DR1$^+$, cat-allergic asthmatic subjects and generated against the important T-cell epitope of Fel d 1 (the major cat allergen), peptide 4, identified populations of T-cells expressing particular TCRs which expanded in response to peptide stimulation. Some expanded TCRs carried CDR3α and β loops which were elongated when compared to the mean length of these loops in unstimulated human T-cells, as defined by Moss and Bell (586). Previous work from our laboratory (601) had suggested that the length of TCR CDR3 loops may influence T-cell phenotype upon activation through interaction with cognate peptide-MHC complex, with elongated CDR3s being favoured by developing Th2 cells. Attempts were made to transduce the murine lymphoma TCR-negative line BW7 with TCRs both from this previous study (601) and those identified in the human TCR CDR3 analysis here but these attempts were not successful and I did not take this line of investigation forward.

Early characterisation of a humanised TCR/MHC class II transgenic mouse model of allergic asthma, the P4 TCR/DR1/ABO model, originally developed by postdoctoral research associates in our laboratory, is described. The P4 TCR expressed by these mice was identified through clonotypic analysis of multiple HLA-DR1-restricted peptide 4-specific T-cell lines derived from HLA-DR1$^+$ cat allergic subjects. It is expressed with HLA-DR1 on a murine MHC class II knockout background. Characterisation of this TCR transgenic mouse in terms of the expression of costimulatory molecules in the spleen and thymus is described. Differences in the expression of some costimulatory molecules, namely CD44, CD62L, ICOS and OX40, were seen in the thymus but not spleen.

Many factors have been shown to affect the fate of a naive T-cell upon its activation by encounter with antigen, such as the prevailing cytokine environment (i.e. IL-12 favours Th1 (511) whilst IL-4 favours Th2 (232)) or the type of cell presenting the antigen (e.g. DC1 or DC2 (547)). Other factors that influence the development of an activated naive T-cell are related to the direct interaction between the TCR and peptide-MHC complex, such as the dose of antigen available (very high or very low favours Th2 whilst intermediate doses favour Th1 (572, 573)) and the affinity/avidity of the TCR itself for peptide-MHC, which may influence the strength and duration of binding. The strength

of the interaction and the length of time for which it persists directly affect the T-cell's fate – it is thought that a shorter, less optimal binding may promote Th2 development through its failure to initiate the full TCR signalling complement whilst interactions that persist for long enough to initiate full signalling appear to promote Th1 differentiation (575, 576). The affinity and avidity of the TCR-peptide-MHC interaction is likely to be at least in part a function of TCR structure. CDR loops 1, 2 and 3 in the variable (V(D)J) regions of the TCRα and β chains have been shown by crystallographic studies to contact the peptide-MHC and thus constitute the antigen-binding site (379, 380). The structure of the TCR at this region is therefore likely to be the most crucial in terms of affecting the affinity/avidity of the interaction. Mutagenesis studies suggest that these loops are responsible for antigen specificity and that the CDR3 loop (formed during gene rearrangement events at the V(D)J junction (404)) in particular confers specificity for peptide onto the TCR (589, 592). Clonal expansions of T-cells bearing receptors with not only identical V(D)J usage but also identical CDR3 loop amino acid sequence (or sequence motifs) suggest the importance of features in the CDR3 loops in conferring this specificity (597). In our laboratory, analysis of CDR3 loop structure in TCRs isolated from T-cell clones raised against the same antigen but polarised towards Th1 or Th2 differentiation by the addition of exogenous cytokines suggested that Th2-polarising conditions favoured the expansion of TCRs containing elongated CDR3 loops with bulkier amino acid sidechains when compared with those favoured by Th1-polarising conditions (601). Molecular modelling studies of the CDR3 loops from the Th1 and Th2 clones suggested that the elongated loop and the bulky sidechains protruded into the interface with the cognate antigen peptide-MHC complex and prevented tight binding, thus promoting a less optimal interaction that has been linked to the development of a Th2 response, suggesting that the structure of the TCR expressed by a T-cell may influence the ability of the T-cell to mount a particular immune response in response to challenge with antigen.

The clonal expansion of T-cells bearing a particular TCR in response to an antigenic challenge have been well documented in instances of CTL responses to viral infection (618, 621) and in T helper cell responses implicated in autoimmune diseases such as multiple sclerosis (625, 626) or rheumatoid arthritis (631) but have not been extensively investigated in Th2-mediated responses such as those implicated in the development of allergic disease. As such, TCR CDR3 sequence analysis was carried out (as shown in Chapter 3 of this thesis) on T-cell lines derived from allergic asthmatic subjects who

were sensitive to the major allergen of cat dander, Fel d 1, and carried the MHC class II molecule HLA-DR1. Such subjects mount T-cell responses to a particular epitope of Fel d 1 known as peptide 4 (221) and lines were grown and restimulated *in vitro* in response to this peptide presented by HLA-DR1$^+$ APCs and analysed at different restimulation timepoints. TCR sequence analysis of these lines identified the expansion of T-cells bearing the same or similar receptors within each line, with the expansions becoming more oligoclonal in nature as the number of restimulations the line had been subjected to increased. In addition, in two out of three lines one of the expanded CDR3 loops was elongated in comparison to the defined mean lengths of CDR3 loops in unstimulated human T-cells (586) on either the TCR α or β chain. My attempts to express the TCRs identified from the human T-cell lines and the Th1 and Th2 clone TCRs (601) in the immortalised T-cell lineage cell line, BW7, were unsuccessful. The transduction of such a line would have allowed the study of the impact of TCR structure on T-cell phenotype.

Allergic asthma is a human disease that is widely accepted to be caused by the actions of allergen-specific Th2 cells in the lung (215-218) leading to airway hyperreactivity, eosinophilic lung inflammation (238), the production of allergen-specific IgE (60), mucus hypersecretion in the airways (241) and chronic remodelling changes in the lung. There are difficulties, as with any human disease, in conducting *in vivo* studies in humans due to both practical and ethical constraints and so investigations into disease mechanisms in a human system are limited to *in vitro* cell cultures and histological analysis. As such, the development of animal models of the disease in order to study the mechanisms involved in allergic airway disease is crucially important. The most common model in use is the ovalbumin model in Balb/c mice (286, 287) or its variant in the DO11.10 OVA-specific TCR transgenic mouse (325, 326) in spite of problems with the model, namely that it uses an irrelevant antigen and the method of disease induction used, systemic sensitisation followed by challenge in the lung, is the only method that has been found that consistently induces allergic lung disease in this model but bears little relation to the disease induction pathways in humans. In addition, it is difficult to induce a chronic disease phenotype through the airways in this model (292). As such, there is little relation between this model and the human disease although there have been modifications made to the protocol that are reported to improve the accuracy of this model. A significant body of work has also been carried out in a model that makes use of house dust mite allergen (312). Use of this allergen has allowed the development

of a protocol for the induction of chronic disease which shows some features of remodelling (315). There are TCR transgenic models for both OVA and HDM which both show some promise in improving the accuracy of the disease model to the human condition (325, 330). However, in both cases the transgenic TCR was derived from the murine systems that were originally used. There are no published humanised TCR transgenic models for allergic asthma despite their superiority as models of other human diseases, for example in multiple sclerosis/EAE. The P4 TCR/DR1/ABO transgenic mouse lines described in Chapter 4 were developed in the Boyton laboratory by postdoctoral research associates funded by Asthma UK. Here, these mice were subjected to an allergic disease induction protocol, comprising an intraperitoneal sensitisation phase (with Fel d 1) and an intranasal challenge phase (with whole cat dander extract) and the induction of disease was measured by various parameters. The disease phenotype induced comprised induction of AHR, lung eosinophilia, increased total serum IgE, lung inflammation and mucus secretion. This is a potentially excellent model of allergic airway disease that has the advantage of being a humanised TCR/MHC class II transgenic model of allergic disease against a relevant allergen.

The presence of a rearranged αβ TCR in the thymus in TCR transgenic mice has been shown to cause abnormalities in T-cell development in the thymus as its expression at the thymocyte cell surface interferes with the progression of the thymocyte through the β-selection checkpoint (424). The effect of transgenic TCR expression on the expression of costimulatory molecules involved in T-cell function and signalling through the TCR was therefore investigated in the thymus and spleen of the P4 TCR/DR1/ABO mice, as shown in Chapter 4 of this thesis. Cells were analysed immediately *ex vivo* without any further intervention to give a biologically relevant picture of events in the thymus as they were occurring *in vivo* and then compared against splenocytes in the same unactivated state. It might be that further differences will be seen if the cells are analysed after *in vitro* activation (or *in vivo* activation in the mouse itself), particularly in the peripheral T-cells, as no differences were seen in any of the molecules analysed between P4 TCR/DR1/ABO transgenic mice and DR1/ABO transgenic control mice in the periphery, despite differences being seen in the thymus. In thymocytes, a block in development at the DN stage identified as an increase in the number of cells expressing neither CD4 nor CD8 was seen. This is a characteristic of TCR transgenic mice due to the premature expression of a rearranged TCRα chain at this stage of development preventing efficient passage through the β-selection

checkpoint (425). In addition, a decrease in CD44 expression was seen in the TCR transgenic mice, also at the DN stage, which may also be linked to the block in development seen in TCR transgenic thymocytes at this stage; as the block in development occurs at the DN3 stage ($CD44^-$ $CD25^+$), one might expect there to be an overall apparent decrease in CD44 expression in these mice, as there are increased numbers of cells in this subset present in the thymus. Other molecules showing differences included CD62L, the expression of which was increased in all subsets except the CD4 SP subset but this was seen only in TCR transgenic mice from line 16. The increase in CD62L expression in the DN subset (where it is thought to be particularly expressed on cells that have recently migrated into the thymus (647)) may indicate a block in development at a very early stage and the later increase in the CD8 SP may indicate a difference in the TCR transgenic mice in the rates of emigration of mature thymocytes from the thymus, with CD8 SP emigrating less efficiently than CD4 SP thymocytes. Both OX40 and ICOS expression showed differences between the TCR transgenic mice when compared against the non-TCR transgenic control mice. ICOS and OX40 are both expressed late after T-cell activation in the periphery (667, 651) and although both are expressed in the thymus (primarily in the medulla) their function there is currently unknown (653, 649). OX40 expression was shown to be slightly increased in the DN subset in TCR transgenic mice whilst ICOS expression decreased in the DN and CD4 SP subsets in TCR transgenic mice from line 16 mice only. In the periphery, both OX40 and ICOS promote the survival of activated T-cells through inhibition of apoptosis in these cells. OX40 also promotes the development of activated T-cells into memory cells (667). If these molecules have a similar anti-apoptotic role in the thymus then it would be expected that the presence of a transgenic TCR might have some impact on their function. As a difference in OX40 expression was seen in the DN subset, OX40 may be involved in promoting the survival of thymocytes at the β-selection checkpoint, increasing the time available for correct rearrangement of the TCRβ chain, and the increase in expression seen might be caused by the inefficiency with which thymocytes expressing a transgenic TCR can pass the checkpoint. Part of the function of ICOS in the thymus may be to prolong survival of thymocytes undergoing positive and negative selection, thus allowing such thymocytes a greater opportunity of correctly rearranging a TCRα chain to produce a fully-rearranged TCR that can be positively selected. The observed down-regulation of ICOS expression in the line 16 TCR transgenic mice may therefore be caused by the decreased requirement for endogenous TCRα rearrangement due to the presence of an already rearranged αβTCR

and the ensuing decreased requirement for ICOS to prolong the life of these thymocytes leads to its lower expression. Further study of the expression of these molecules in terms of each other and other processes such as TCR signalling will enable elucidation of the meaning of such findings.

There are a number of different approaches that could be used to further the research described in this thesis. For example, the P4 TCR/DR1/ABO transgenic mice can be used to develop an improved humanised model of allergic disease by attempting to develop a model in which disease can be induced through a more physiologically relevant protocol i.e. with both sensitisation and challenge occurring through the airways and which induces a chronic condition with features of remodelling. Such a model can then be used to investigate aspects of allergic airway disease, such as the impact of viral infection on allergic airway disease and the development of a model that will allow the investigation of the mechanisms underlying the development of peptide-induced tolerance as this has particularly important therapeutic applications. In addition, these mice could be used in the investigation of the impact of TLR signalling through various receptors and ligands on both the development and progression of allergic disease. The hygiene hypothesis suggests that as standards of cleanliness and hygiene have improved, children are being exposed to lower levels of foreign pathogens which results in the incorrect development of their immune system (5). The TLR system works as an 'early warning system', alerting the immune system to the presence of foreign antigens through recognition of particular pathogen-associated motifs followed by signalling to raise the alarm (672). This implicates TLR signalling in the correct development of a naive immune system and suggests that signals through different TLRs could differentially impact upon allergic airway disease, and this model would provide a means of investigating TLR signalling in allergic asthma. As the T-cell (Th2 cell) is so strongly implicated in the development of allergic asthma, the presence of a transgenically expressed allergen-specific TCR in these mice may allow the easier investigation of the role of the T-cell and the impact of other phenomena (e.g. viral infection, different TLR signals, tolerance induction) on the allergen-specific transgenic TCR-expressing T-cell response. The existence of HLA-DR1-peptide 4 tetramers allows the cells to be easily isolated for culture *in vitro* or identified in histological analysis to show their distribution in affected lung tissue. In addition, the development of a model which is similar to human disease in terms of disease induction, progression and pathogenesis will be very useful as a means of testing new asthma therapies, in

identifying new possible targets, elucidating the underlying mechanisms of disease pathogenesis and using all of the above to develop more effective strategies for disease treatment. As the model is humanised, the results of investigations, particularly in terms of testing new therapies, will be more relevant to the human disease.

In addition, the use of a humanised TCR transgenic model should facilitate the investigation of the role of pathogenic T-cells in allergic asthma in more general terms. The original view of allergic asthma is of a Th2-mediated disease where all aspects of disease pathogenesis can be linked back to Th2 T-cells, either as direct mediators of inflammation or through their effects on other aspects of the response, such as the cells implicated in the early asthmatic response (e.g. mast cells, basophils). It was therefore believed that a potential means of therapy would be to skew the responses in an asthmatic lung back towards the opposing Th1 phenotype, much as the reverse was believed to be a means of treating autoimmune disease. However, attempts to skew pulmonary immune responses towards a Th1 phenotype in allergic asthma often had little effect or exacerbated disease (175). The original idea of a Th1/Th2 dichotomy has not only been challenged by these findings but also by the emergence of another T helper cell subset, the Th17 subset (161, 162) and the likelihood that there are yet more subsets (such as the recently described Th9 subset (673)) to be discovered. In the specific case of allergic asthma, there is also controversy over the relative importance of invariant NKT cells over Th2 cells with some evidence in support of the idea that iNKT cells may be a more significant contributor to asthma pathogenesis (138-141). There are many cells of the innate immune system, such as mast cells and eosinophils, that are also believed to play a role in asthmatic disease and the importance of these cell types in development and persistence of disease is also debated, particularly in light of the recent finding that mast cells in airway smooth muscle cells may be required for the development of AHR, a hallmark of allergic asthma (79, 81). As such, it is crucial to be able to study the interplay between these differing cell types in order to eludicate mechanisms of disease development and to attempt to quantify the importance of each cell type in causing disease to allow identification of new targets for therapy. Peptide immunotherapy appears to show much promise in the treatment of allergic asthma (341, 342), suggesting the importance of controlling T-cell responses to control asthmatic disease. As such, a TCR transgenic mouse model of the disease should aid in investigating the exact role of pathogenic Th2-type cells and also the role that Tregs may play in the induction of tolerance, in order to identify new potential therapies. It is

also true that there is another form of asthma that is not believed to be related to atopy or allergy. This form of asthma is characterised by lung neutrophilia as opposed to eosinophilia and tends to present with a more severe phenotype (30). Neutrophils can be directed to areas of inflammation through the action of the cytokine IL-8 (674); IL-8 production can be induced through the action of Th17 cells in an inflammatory response (168, 169). It may be that it is not just Th2 cells that are capable of mediating asthmatic disease and production of a mouse model of this form of asthma will also potentially be useful for the development of novel therapies.

The P4 TCR transgenic mice can also be used to investigate aspects of T-cell signalling and T-cell activation. The analysis of T-cell costimulatory molecule expression described here can be extended further and investigated in situations of *in vivo* and *in vitro* activation. In addition, any differences in expression of costimulatory molecules can be linked to other events occurring in the T-cells and investigation into why there are differences in expression will lead to further elucidation of the complex mechanisms involved in signalling through the TCR and T-cell activation and differentiation.

The findings from the analysis of the human T-cell lines are relevant in the study of allergic asthma, in particular in the attempts to develop an effective therapy. The expansion of peptide-specific TCRs from human asthmatic subjects and the identification of the particular epitopes to which they respond may allow for the more rational design of peptide immunotherapy vaccines, allowing the use of peptides that have been identified as major epitopes of the allergen in question and matched to the MHC class II restriction of the patient. The use of a mixture of peptides derived from the whole allergen amino acid sequence has previously been shown to have some promise in the down-regulation of Th2-cell mediated immune responses caused by cat allergen; the ability to identify the immunoreactive epitopes and develop vaccines based on them may increase the efficacy of the therapy. The potential for use of peptide vaccines in the treatment of autoimmune diseases such as rheumatoid arthritis (675, 676) and myasthenia gravis (677) has been investigated in experimental models in mice, particularly in the use of altered peptide ligands based on the immunoreactive peptide epitope sequences. Altered peptide ligands have been shown to be able to skew T-cell-mediated responses from one phenotype to another and in some instances, such as those diseases mentioned previously, show tolerogenic potential and the reversal of symptoms in some diseases. The use of peptides in immunotherapy strategies decreases the risk of

the induction of systemic anaphylaxis that is a significant problem with the use of whole allergen in specific immunotherapy. The use of APLs may further decrease the risk of induction of immunoglobulin-mediated responses by changing the inherent structure of the epitope that could otherwise potentially still be recognised by specific antibody (678). In order to be able to design a vaccine based on the use of altered peptide ligands however, it is necessary to identify the sequences of the major epitopes of the allergen and the residues that are important in mediating T-cell and MHC class II molecule contact, so as to maintain these residues within the APL. Another approach to treating T-cell-mediated diseases is the use of specific antibody directed against the dominant TCR implicated in causing the pathogenic response. Such an approach has been shown in mice to have some efficacy in the treatment of allergic asthma (679); to develop this therapy for use in human patients it would be necessary to identify the dominant allergen-specific TCRs involved. The TCR CDR3 analysis described here was minimal but did not identify any common TCR selection in the lines from three patients; analysis of multiple lines from a large panel of patients should be carried out to confirm this. It may be that the T-cell response, even to the same peptide presented on the same MHC class II molecule, may be significantly heterogeneous. This would decrease the likelihood of a universally effective anti-TCR antibody therapy being developed but this approach could still have efficacy if the dominant TCR in each patient could be identified and antibodies raised against it. Such an approach could also be used with the development of peptide vaccines to target the epitopes most relevant to each patient on the basis of their T-cell responses.

To further investigate the role of TCR structure on the response induced upon activation of a T-cell and its subsequent differentiation, molecular modelling of the TCRs identified in the TCR CDR3 analysis of the human allergic asthmatic T-cell lines might identify features of the TCRs that lead to them being particularly well-suited to the induction of an allergic asthmatic response. Although there were no obvious differences identified from the analysis of the CDR3 amino acid sequences, the three-dimensional structure would be informative and it might be possible to identify a shared structural feature or features that could be used to predict the fate of a T-cell upon its activation on the basis of the receptor it expresses.

My attempts to express TCRs of interest in the murine thymoma line BW7 were unsuccessful but it should be possible to achieve this. Once such lines are in existence,

they can be used as a means of investigating the role of the TCR itself in determining the signalling pathways that are activated and the phenotype that is induced upon antigen-specific activation of the cells. As the only difference between the lines would be the TCR that they express, any differences between the lines would be due to the TCR itself and would hopefully allow dissection of the different events that occur in the development of a Th1 and a Th2 response. These cells would also be useful for binding studies to measure interaction kinetics between the TCR and peptide-MHC tetramers using flow cytometry and surface plasmon resonance to determine if there is a noticeable difference in the avidity of the interactions from the 'Th1' and 'Th2' TCRs.

Bibliography

1. **Anderson H. R., Gupta R., Strachan D.P. and Limb E.S.** (2007) 50 years of asthma: UK trends from 1955 to 2004. *Thorax* **62**:85-90

2. **Robertson, C.F., Heycock, E., Bishop, J., Nolan, T., Olinsky, A., and Phelan, P. D.** (1991) Prevalence of asthma in Melbourne school children: changes over 26 years. *Brit. Med. J.* **302**:1116-1118

3. **Pearce, N., Ait-Khaled, N., Beasley, R., Mallol, J., Keil, U., Mitchell, E., Robertson, C. and the ISAAC Phase Three Study Group** (2007) Worldwide trends in the prevalence of asthma symptoms: phase III of the International Study of Asthma and Allergies in Childhood (ISAAC). *Thorax* **62**:758-766

4. **Chinn, S., Jarvis, D., Burney, P., Luczynska, C., Ackermann-Liebrich, U., Antó, J. M., Cerveri, I., de Marco, R., Gislason, T., Heinrich, J., Janson, C., Künzli, N., Leynaert, B., Neukirch, F., Schouten, J., Sunyer, J., Svanes, C., Vermeire, P. and Wjst, M.** (2004) Increase in diagnosed asthma but not in symptoms in the European Community Respiratory Health Survey. *Thorax* **59**:646-651

5. **Strachan, D. P.** (1989) Hay fever, hygiene, and household size. *Brit. Med. J.* **299**:1259-1260

6. **Braun-Fahrländer, C. H., Gassner, M., Grize, L., Neu, U., Sennhauser, F. H., Varonier, H. S., Vuille, J. C., Wüthrich, B. and the SCARPOL team.** (1999) Prevalence of hay fever and allergic sensitisation in farmer's children and their peers living in the same rural community. *Clin. Exp. Allergy* **29**:28-34

7. **von Ehrenstein, O. S., von Mutius, E., Illi, S., Baumann, L., Böhm, O. and von Kries, R.** (2000) Reduced risk of hay fever and asthma among children of farmers. *Clin. Exp. Allergy* **30**:187-193

8. **Riedler, J., Braun-Fahrländer, C., Eder, W., Schreuer, M., Waser, M., Maisch, S., Carr, D., Schierl, R., Nowak, D., von Mutius, E. and the ALEX study team.** (2001) Exposure to farming in early life and development of asthma and allergy: a cross-sectional survey. *Lancet* **358**:1129-1133

9. **Gerhold, K., Bluemchen, K., Franke, A., Stock, P. and Hamelmann, E.** (2003) Exposure to endotoxin and allergen in early life and its effect on allergen sensitisation in mice. *J. Allergy Clin, Immunol.* **112**:389-398

10. **Banerjee, B., Kelly, K. J., Fink, J. N., Henderson Jr., J. D., Bansal, N. K. and Kurup, V. P.** (2004) Modulation of airway inflammation by immunostimulatory CpG oligodeoxynucleotides in a murine model of allergic aspergillosis. *Infect. Immun.* **72(10)**:6087-6094

11. **Lauener, R. P., Birchler, T., Adamski, J., Braun-Fahrländer, C., Bufe, A., Herz, U., von Mutius, E., Nowak, D., Riedler, J., Waser, M., Sennhauser, F. H. and the ALEX study group.** (2002) Expression of CD14 and Toll-like receptor 2 in farmers' and nonfarmers' children. *Lancet* **360(9331)**:465-466

12. **Eder, W., Klimecki, W., Yu, L., von Mutius, E., Riedler, J., Braun-Fahrländer, C., Nowak, D., Martinez, F. D. and the ALEX Study Team.** (2004) Toll-like receptor 2 as a major gene for asthma in children of European farmers. *J. Allergy Clin. Immunol.* **113(3)**:482-488

13. **Koppelman, G. H., Reijmerink, N. E., Stine, O. C., Howard, T. D., Whittaker, P. A., Meyers, D. A., Postma, D. S. and Bleecker, E. R.** (2001) Association of a promoter polymorphism of the CD14 gene and atopy. *Am. J. Resp. Crit, Care Med.* **163(4)**:965-969

14. **Koch, A., Knobloch, J., Dammhayn, C., Raidl, M., Ruppert, A., Hag, H., Rottlaender, D., Müller, K. and Erdmann, E.** (2007) Effect of bacterial endotoxin on expression of IFN-gamma and IL-5 in T-lymphocytes from asthmatics. *Clin. Immunol.* **125(2)**:194-204

15. **Debarry, J., Garn, H., Hanuszkiewicz, A., Dickgreber, N., Blümer, N., von Mutius, E., Bufe, A., Gatermann, S., Renz, H., Holst, O. and Heine, H.** (2007) Acinetobacter Iwoffii and Lactococcus lactis strains isolated from farm cowsheds possess strong allergy-protective properties. *J. Allergy Clin. Immunol.* **119**:1514-1521

16. **Mosmann, T. R., Cherwinski, H., Bond, M. W., Giedlin, M. A. and Coffman, R. L.** (1986) Two types of murine helper T cell clone. I. Definition according to profiles of lymphokine activities and secreted proteins. *J. Immunol.* **136(7)**:2348-2357

17. **Kay, A. B., Ying, S., Varney, V., Gaga, M., Durham, S. R., Moqbel, R., Wardlaw, A. J. and Hamid, Q.** (1991) Messenger RNA expression of the cytokine gene cluster, interleukin 3 (IL-3), IL-4, IL-5, and GM-CSF in allergen-induced late-phase cutaneous reactions in atopic subjects. *J. Exp. Med.* **173**:775-778

18. **Ying, S., Humbert, M., Barkans, J., Corrigan, C. J., Pfister, R., Menz, G., Larché, M., Robinson, D. S., Durham, S. R. and Kay, A. B.** (1997) Expression of IL-4 and IL-5 mRNA and protein product by CD4+ and CD8+ T cells, eosinophils, and mast cells in bronchial biopsies obtained from atopic and nonatopic (intrinsic) asthmatics. *J. Immunol.* **158(7)**:3539-3544

19. **Soltesz, G., Patterson, C. C. and Dahlquist, G. on behalf of EURODIAB Study Group.** (2007) Worldwide childhood type 1 diabetes incidence - what can we learn from epidemiology? *Pediatr. Diabetes* **8(s6)**: 6-14

20. **van den Biggelaar, A. H. J., van Ree, R., Rodrigues, L. C., Deelder, A. M., Kremsner, P. G. and Yazdanbakhsh, M.** (2000) Decreased atopy in children infected with Schistosoma haematobium: a role for parasite-induced interleukin-10. *Lancet* **356(9243)**:1723-1727

21. **Urban, Jr, J. F., Katona, I. M., Paul, W.E. and Finkelman, F. D.** (1991) Interleukin 4 is important in protective immunity to a gastrointestinal nematode infection in mice. *Proc. Natl. Acad. Sci. USA* **88(13)**:5513-5517

22. **La Flamme, A. C., Ruddenklau, K. and Bäckström, B. T.** (2003) Schistosomiasis decreases central nervous system inflammation and alters the progression of experimental autoimmune encephalomyelitis. *Infect. Immun.* **71(9)**:4996-5004

23. **Zaccone, P., Fehérvári, Z., Jones, F. M., Sidobre, S., Kronenberg, M., Dunne, D. W. and Cooke, A.** (2003) Schistosoma mansoni antigens modulate the activity of the innate immune response and prevent onset of type 1 diabetes. *Eur. J. Immunol.* **33(5)**:1439-1449

24. **Park, J.-H., Gold, D. G., Spiegelman, D. L., Burge, H. A. and Milton, D. K.** (2001) House dust endotoxin and wheeze in the first year of life. *Am. J. Respir. Crit. Care Med.* **163(2)**:322-328

25. **Eldridge, M. W. and Peden, D. B.** (2000) Allergen provocation augments endotoxin-induced nasal inflammation in subjects with atopic asthma. *J. Allergy Clin. Immunol.* **105**:475-481

26. **Dahl, M. E., Dabbagh, K., Liggitt, K., Kim, S. and Lewis, D. B.** (2004) Viral-induced T helper type 1 responses enhance allergic disease by effects on lung dendritic cells. *Nature Immunol.* **5(3)**:337-343

27. **Platts-Mills, T. A. E.** (2001) The role of immunoglobulin E in allergy and asthma. *Am. J. Respir. Crit. Care Med.***164(8pt2)**:S1-S5

28. **Wenzel, S. E., Schwartz, L. E., Langmack, E. L., Halliday, J. L., Trudeau, J. B., Gibbs, R. L. and Chu, H. W.** (1999) Evidence that severe asthma can be divided pathologically into two inflammatory subtypes with distincy physiologic and clinical characteristics. *Am. J. Respir. Crit. Care Med.* **166**:1001-1008

29. **Pearce, N., Pekkanen, J. and Beasley, R.** (1999) How much asthma is really attributable to atopy? *Thorax* **54**:268-272

30. **Douwes, J., Gibson, P., Pekkanen, J. and Pearce, N.** (2002) Non-eosinophilic asthma: importance and possible mechanisms. *Thorax* **57**:643-648

31. **Bousquet, J., Jeffery, P. K., Busse, W. W., Johnson, M. and Vignola, A. M.** (2000) Asthma - from bronchoconstriction to airways inflammation and remodelling. *Am. J. Respir. Crit. Care Med.* **161(5)**:1720-1745

32. **Sobande, P. O. and Kercsmar, C. M.** (2008) Inhaled corticosteroids in asthma management. *Respir. Care* **53(5)**:625-634

33. **Pavord, I. D., Brightling, C. E., Woltmann, G. and Wardlaw, A. J.** (1999) Non-eosinophilic corticosteroid unresponsive asthma. *Lancet* **353(9171)**:2213-2214

34. **Green, R. H., Brightling, C. E., Woltmann, G., Parker, D., Wardlaw, A. J. and Pavord, I. D.** (2002) Analysis of induced sputum in adults with asthma: identification of subgroup with isolated sputum neutrophilia and poor response to inhaled corticosteroids. *Thorax* **57**:875-879

35. **Akdis, M. and Akdis, C. E.** (2007) Mechanisms of allergen-specific immunotherapy. *J. Allergy Clin. Immunol.* **119(4)**:780-791

36. **Abramson, M. J., Puy, R. M. and Weiner, J. M.** (2003) Allergen immunotherapy for asthma. *Cochrane DB Syst. Rev.* **4**:CD001186

37. **Frew, A. J., Powell, R. J., Corrigan, C. J. and Durham, S. R. on behalf of the UK Immunotherapy Study Group.** (2006) Efficacy and safety of specific immunotherapy with SQ allergen extract in treatment-resistant seasonal allergic rhinoconjunctivitis. *J. Allergy Clin. Immunol.* **117(2)**:316-325

38. **Holt, P. G., Macaubas, C., Stumbles, P. A. and Sly, P. D.** (1999) The role of allergy in the development of asthma. *Nature* **402(suppl)**:B12-B17

39. **Bellini, A., Vittori, E., Marini, M., Ackerman, V. and Mattoli, S.** (1993) Intraepithelial dendritic cells and selective activation of Th2-like lymphocytes in patients with atopic asthma. *Chest* **103**:997-1005

40. **Schon-Hegrad, M. A., Oliver, J., McMenamin, P. G. and Holt, P. G.** (1991) Studies on the density, distribution and surface phenotype of intraepithelial class II major histocompatibility complex antigen (Ia)-bearing dendritic cells (DC) in the conducting airways. *J. Exp. Med.* **173**:1345-1356

41. **Holt, P. G., Schon-Hegrad, M. A., Phillips, M. J. and McMenamin, P. G.** (1989) Ia-positive dendritic cells form a tightly meshed network within the human airway epithelium. *Clin. Exp. Allergy* **19**:597-601

42. **Hammad, H. and Lambrecht, B. N.** (2008) Dendritic cells and epithelial cells: linking innate and adaptive immunity in asthma. *Nature Rev. Immunol.* **8**:193-204

43. **Vyas, J. M., Van der Veen, A. G. and Ploegh, H. L.** (2008) The known unknowns of antigen processing and presentation. *Nature Rev. Immunol.* **8(8)**:607-618

44. **Hoogsteden, H. C., Verhoeven, G. T., Lambrecht, B. N. and Prins, J.-B.** (1999) Airway inflammation in asthma and chronic obstructive pulmonary disease with special emphasis on the antigen-presenting cell: influence of treatment with fluticasone propionate. *Clin. Exp. Allergy* **29(s2)**:116-124

45. **Upham, J. W., Denburg, J. A. and O'Byrne, P. M.** (2002) Rapid response of circulating myeloid dendritic cells to inhaled allergen in asthmatic subjects. *Clin. Exp. Allergy* **32**:818-823

46. **Jahnsen, F. L., Moloney, E. D., Hogan, T., Upham, J. W., Burke, C. M. and Holt, P. G.** (2001) Rapid dendritic cell recruitment to the bronchial mucosa of patients with atopic asthma in response to local allergen challenge. *Thorax* **56**:823-826

47. **Xia, W., Pinto, C. E. and Kradin, R. L.** (1995) The antigen-presenting activities of Ia^+ dendritic cells shift dynamically from lung to lymph node after an airway challenge with soluble antigen. *J. Exp. Med.* **181**: 1275-1283

48. **Bratke, K., Lommatzsch, M., Julius, P., Kuepper, M., Kleine, H.-D., Luttmann, W. and Virchow, J. C.** (2007) Dendritic cell subsets in human bronchoalveolar lavage fluid after segmental allergen challenge. *Thorax* **62**:168-175

49. **Farkas, L., Kvale, E. O., Johansen, F.-E., Jahnsen, F. L. and Lund-Johansen, F.** (2004) Plasmacytoid dendritic cells activate allergen-specific Th2 memory cells: Modulation by CpG oligodeoxynucleotides. *J. Allergy Clin, Immunol.* **114**:436-443

50. **de Heer, H. J., Hammad, H., Soullié, T., Hijdra, D., Vos, N., Willart, M. A. M., Hoogsteden, H. C. and Lambrecht, B. N.** (2004) Essential role of lung plasmacytoid dendritic cells in preventing asthmatic reactions to harmless inhaled antigen. *J. Exp. Med.* **200**:89-98

51. **Eisenbarth, S. C., Piggott, D. A., Huleatt, J. W., Visintin, I., Herrick, C. A. and Bottomly, K.** (2002) Lipopolysaccharide-enhanced, Toll-like receptor 4-dependent T helper cell type 2 responses to inhaled antigen. *J. Exp. Med.* **196**:1645-1651

52. **Keane-Myers, A., Gause, W. C., Linsley, P. S., Chen, S.-J. and Wills-Karp, M.** (1997) B7-CD28/CTLA-4 costimulatory pathways are required for the development of T helper cell 2-mediated allergic airway responses to inhaled antigens. *J. Immunol.* **158**:2042-2049

53. **van Rijt, L. S., Vos, N., Willart, M., KleinJan, A., Coyle, A. J., Hoogsteden, H. C. and Lambrecht, B. N.** (2004) Essential role of dendritic cell CD80/CD86 costimulation in the induction, but not reactivation, of Th2 effector responses in a mouse model of asthma. *J. Allergy Clin. Immunol.* **114**:166-173

54. **Lambrecht, B. N., de Veerman, M., Coyle, A. J., Gutierrez-Ramos, J.-C., Thielemans, K. and Pauwels, R. A.** (2000) Myeloid dendritic cells induce Th2 responses to inhaled antigen, leading to eosinophilic airway inflammation. *J. Clin. Invest.* **106**:551-559

55. **King, C. L., Poindexter, R. W., Ragunathan, J., Fleisher, T. A., Ottesen, E. A. and Nutman, T. B.** (1991) Frequency analysis of IgE-secreting B lymphocytes in persons with normal or elevated serum IgE levels. *J. Immunol.* **146(5)**:1478-1483

56. **Rihet, P., Demeure, C. E., Bourgois, A., Prata, A. and Dessein, A. J.** (1991) Evidence for an association between human resistance to *Schistosoma mansoni* and high anti-larval IgE levels. *Eur. J. Immunol.* **21**:2679-2686

57. **Mahanty, S., Abrams, J. S., King, C. L., Limaye, A. P and Nutman, T. B.** (1992) Parallel regulation of IL-4 and IL-5 in human helminth infections. *J. Immunol.* **148(11)**:3567-3571

58. **Lebman, D. A. and Coffman, R. L.** (1988) Interleukin 4 causes isotype switching to IgE in T cell-stimulated clonal B cell cultures. *J. Exp. Med.* **168**:853-862

59. **Sunyer, J., Antó, J. M., Castellsagué, J., Soriano, J. B., Roca, J. and the Spanish Group of the European Study of Asthma.** (1996) Total serum IgE is associated with asthma independently of specific IgE levels. *Eur. Respir. J.* **9**:1880-1884

60. **Wilson, D. R., Merrett, T. G., Varga, E. M., Smurthwaite, L., Gould, H. J., Kemp, M., Hooper, J., Till, S. J. and Durham, S. R.** (2002) Increases in allergen-specific IgE in BAL after segmental allergen challenge in atopic asthmatics. *Am. J. Respir. Crit. Care Med.* **165**:22-26

61. **Sherrill, D. L., Stein, R., Halonen, M., Holberg, C. J., Wright, A. and Martinez, F. D.** (1999) Total serum IgE and its association with asthma symptoms and allergic sensitization among children. *J. Allergy Clin. Immunol.* **104**:28-36

62. **Rajakulasingam, K., Durham, S. R., O'Brien, F., Humbert, M., Barata, L. T., Reece, L., Kay, A.B and Grant, J. A.** (1997) Enhanced expression of high-affinity IgE receptor (FcεRI) α chain in human allergen-induced rhinitis with co-localization to mast cells, macrophages, eosinophils, and dendritic cells. *J. Allergy Clin. Immunol.* **100**:78-86

63. **Gagro, A. and Rabatić, S.** (1994) Allergen-induced CD23 on $CD4^+$ T lymphocytes and CD21 on B lymphocytes in patients with allergic asthma: evidence and regulation. *Eur. J. Immunol.* **24**:1109-1114

64. **Takhar, P., Corrigan, C. J., Smurthwaite, L., O'Connor, B. J., Durham, S. R., Lee T. H. and Gould, H. J.** (2007) Class switch recombination to IgE in the bronchial mucosa of atopic and nonatopic patients with asthma. *J. Allergy Clin. Immunol.* **119**:213-218

65. **Xu, L. and Rothman, P.** (1994) IFN-γ represses ε germline transcription and subsequently down-regulates switch recombination to ε. *Int. Immunol.* **6(4)**:515-521

66. **Punnonen, J., Aversa, G., Cocks, B. G., McKenzie, A. N. J., Menon, S., Zurawski, G., Malefyt, R. de W. and de Wries, J. E.** (1993) Interleukin 13 induces interleukin 4-independent IgG4 and IgE synthesis and CD23 expression by human B cells. *Proc. Natl. Acad. Sci. USA* **90**:3730-3734

67. **Toru, H., Ra, C., Nonoyama, S., Suzuki, K., Yata, J.-I. and Nakahata, T.** (1996) Induction of the high-affinity IgE receptor (FcεRI) on human mast cells by IL-4. *Int. Immunol.* **8(9)**: 1367-1373

68. **Kaur, D., Hollins, F., Woodman, L., Yang, W., Monk, P., May, R., Bradding, P. and Brightling, C. E.** (2006) Mast cells express IL-13Rα1: IL-13 promotes human lung mast cell proliferation and FcεRI expression. *Allergy* **61**:1047-1053

69. **MacGlashan, Jr., D., Lichtenstein, L. M., McKenzie-White, J., Chichester, K., Henry, A. J., Suttin, B. J. and Gould, H. J.** (1999) Upregulation of FcεRI on human basophils by IgE antibody is mediated by interaction of IgE with FcεRI. *J. Allergy Clin. Immunol.* **104**:492-498

70. **Lin, H., Boesel, K. M., Griffith, D. T., Prussin, C., Foster, B., Romero, F. A., Townley, R. and Casale, T. B.** (2004) Omalizumab rapidly decreases nasal allergic response and FcεRI on basophils. *J. Allergy Clin. Immunol.* **113**:297-302

71. **Prussin, C., Griffith, D. T., Boesel, K. M., Lin, H., Foster, B. and Casale, T. B.** (2003) Omalizumab treatment downregulates dendritic cell FcεRI expression. *J. Allergy Clin. Immunol.* **112**:1147-1154

72. **Maurer, D., Fiebiger, E., Reininger, B., Ebner, C., Petzelbauer, P., Shi, G.-P., Chapman, H. A. and Stingl, G.** (1998) Fcε Receptor I on dendritic cells delivers IgE-bound multivalent antigens into a cathepsin S-dependent pathway of MHC class II presentation. *J. Immunol.* **161**:2731-2739

73. **Reth, M.** (1989) Antigen receptor tail clue. *Nature* **338**:384-385

74. **Jouvin, M.-H. E., Adamczewski, M., Numerof, R., Letourneur, O., Vallé, A. and Kinet, J.-P.** (1994) Differential control of the tyrosine kinases Lyn and Syk by the two signaling chains of the high affinity immunoglobulin E receptor. *J. Biol. Chem.* **269(8)**:5918-5925

75. **Liu, Y., Graham, C., Parravicini, V., Brown, M. J., Rivera, J. and Shaw, S.** (2001) Protein kinase C θ is expressed in mast cells and is functionally involved in Fcε receptor 1 signaling. *J. Leukoc. Biol.* **69**:831-840

76. **Bradding, P., Walls, A. W. and Holgate, S. T.** (2006) The role of the mast cell in the pathophysiology of asthma. *J. Allergy Clin. Immunol.* **117**:1277-1284

77. **Ogawa, Y. and Calhoun, W. C.** (2006) The role of leukotrienes in airway inflammation. *J. Allergy Clin. Immunol.* **118**:789-798

78. **Sandig, H., Pease, J. E. and Sabroe, I.** (2007) Contrary prostaglandins: the opposing roles of PGD_2 and its metabolites in leukocyte function. *J. Leukoc. Biol.* **81**:372-382

79. **Brightling, C. E., Bradding, P., Symon, F. A., Holgate, S. T., Wardlaw, A. J. and Pavord, I. D.** (2002) Mast-cell infiltration of airway smooth muscle in asthma. *New Engl, J. Med.* **346**:1699-1705

80. **Siddiqui. S., Mistry, V., Doe, C., Roach, K., Morgan, A., Wardlaw, A., Pavord, I., Bradding, P. and Brightling, C.** (2008) Airway hyperresponsiveness is dissociated from airway wall structural remodeling. *J. Allergy Clin. Immunol.* **122(2)**:335-341

81. **Brightling, C. E., Symon, F. A., Holgate, S. T., Wardlaw, A. J., Pavord, I. D. and Bradding, P.** (2003) Interleukin-4 and -13 expression is co-localized to mast cells within the airway smooth muscle in asthma. *Clin. Exp. Allergy* **33**:1711-1716

82. **Walter, D. M., McIntire, J. J., Berry, G., McKenzie, A. N. J., Donaldson, D. D., DeKruyff, R. H. and Umetsu, D. T.** (2001) Critical role for IL-13 in the development of allergen-induced airway hyperreactivity. *J. Immunol.* **167**:4668-4675

83. **Woolley, K. L., Adelroth, E., Woolley, M. J., Ellis, R., Jordana, M. and O'Byrne, P. M.** (1994) Granulocyte-macrophage colony-stimulating factor, eosinophils and eosinophil cationic protein in subjects with and without mild, stable, atopic asthma. *Eur. Respir. J.* 7:1576-1584

84. **Sehmi, R., Wood, L. J., Watson, R., Foley, R., Hamid, Q., O'Byrne. P. M. and Denburg, J. A.** (1997) Allergen-induced increases in IL-5 receptor α-subunit expression on bone marrow-derived $CD34^+$ cells from asthmatic subjects. *J. Clin. Invest.* **100**:2466-2475

85. **Rankin, S. M., Conroy, D. M. and Williams, T. J.** (2000) Eotaxin and eosinophil recruitment: implications for human disease. *Mol. Med. Today* **6**:20-27

86. **Kitaura, M., Nakajima, T., Imai, T., Harada, S., Combadiere, C., Tiffany, H. L., Murphy, P. M. and Yoshie, O.** (1996) Molecular cloning of human eotaxin, an eosinophil-selective CC chemokine, and identification of a specific eosinophil eotaxin receptor, CC chemokine receptor 3. *J. Biol. Chem.* **271(13)**:7725-7730

87. **Collins, P. D., Marleau, S., Griffiths-Johnson, D. A., Jose, P. J. and Williams, T. J.** (1995) Cooperation between interleukin-5 and the chemokine eotaxin to induce eosinophil accumulation in vivo. *J. Exp. Med.* **182**:1169-1174

88. **Gounni, A. S., Hamid, Q., Rahman, S. M., Hoeck, J., Yang, J. and Shan, L.** (2004) IL-9-mediated induction of eotaxin1/CCL11 in human airway smooth muscle cells. *J. Immunol.* **173**:2771-2779

89. **Li, L., Xia, Y., Nguyen, A., Lai, Y. H., Feng, L., Mosmann, T. R. and Lo, D.** (1999) Effects of Th2 cytokines on chemokine expression in the lung: IL-13 potently induces eotaxin expression by airway epithelial cells. *J. Immunol.* **162**:2477-2487

90. **Hogan, S. P., Rosenberg, H. F., Moqbel, R., Phipps, S., Foster, P. S., Lacy, P.. Kay, A. B. and Rothenberg, M. E.** (2008) Eosinophils: biological properties and role in health and disease. *Clin, Exp. Allergy* **38**:709-750

91. **MacKenzie, J. R., Mattes, J., Dent, L. A. and Foster, P. S.** (2001) Eosinophils promote allergic disease of the lung by regulating $CD4^+$ Th2 lymphocyte function. *J. Immunol.* **167**:3146-3155

92. **van Rijt, L. S., Vos, N., Hijdra, D., de Vries, V. C., Hoogsteden, H. C and Lambrecht, B. N.** (2003) Airway eosinophils accumulate in the mediastinal lymph nodes but lack antigen-presenting potential for naïve T-cells. *J. Immunol.* **171**:3372-3378

93. **Minshall, E. M., Leung, D. Y. M., Martin, R. J., Song, Y. L., Cameron, L., Ernst, P. and Hamid, Q.** (1997) Eosinophil-associated TGF-β_1 mRNA expression and airways fibrosis in bronchial asthma. *Am. J. Respir. Cell Mol. Biol.* **17**:326-333

94. **Horiuchi, T. and Weller, P. F.** (1997) Expression of vascular endothelial growth factor by human eosinophils: upregulation by granulocyte macrophage colony-stimulating factor and interleukin-5. *Am. J. Respir. Cell Mol. Biol.* **17**:70-77

95. **Boxall, C., Holgate, S. T. and Davies, D. E.** (2006) The contribution of transforming growth factor-β and epidermal growth factor signalling to airway remodelling in chronic asthma. *Eur. Respir. J.* **27**:208-229

96. **Chetta, A., Zanini, A., Foresi, A., D'Ippolito, R., Tipa, A., Castagnaro, A., Baraldo, S., Neri, M., Saetta, M. and Olivieri, D.** (2005) Vascular endothelial growth factor up-regulation and bronchial wall remodelling in asthma. *Clin. Exp. Allergy* **35**:1437-1442

97. **Humbles, A. A., Lloyd, C. M., McMillan, S. J., Friend, D. S., Xanthou, G., McKenna, E. E., Ghiran, S., Gerard, N. P., Yu, C., Orkin, S. H. and Gerard, C.** (2004) A critical role for eosinophils in allergic airways remodeling. *Science* **305(5691)**:1776-1779

98. **Cho, J. Y., Miller, M., Baek, K. J., Han, J. W., Nayar, J., Lee, S. Y., McElwain, S., Friedman, S. and Broide, D. H.** (2004) Inhibition of airway remodeling in IL-5-deficient mice. *J. Clin. Invest.* **113(4)**:551-560

99. **Tanaka, H., Komai, M., Ishikazi, M., Kajiwara, D., Takatsu, K., Delespesse, G. and Nagai, H.** (2004) Role of interleukin-5 and eosinophils in allergen-induced airway remodeling in mice. *Am. J. Respir. Cell Mol. Biol.* **31(1)**:62-68

100. **Aalbers, R., Kauffman, H. F., Vrugt, B., Koeter, G. H. and de Monchy, J. G.** (1993) Allergen-induced recruitment of inflammatory cells in lavage 3 and 24 h after challenge in allergic asthmatic lungs. *Chest* **103**:1178-1184

101. **Leckie, M. J., ten Brinke, A., Khan, J., Diamant, Z., O'Connor, B. J., Walls, C. M., Mathur, A. K., Cowley, H. C., Chung, K. F., Djukanovic, R., Hansel, T. T., Holgate, S. T., Sterk, P. J. and Barnes, P.J.** (2000) Effects of an interleukin-5 blocking monoclonal antibody on eosinophils, airway hyper-responsiveness, and the late asthmatic response. *Lancet* **356**:2144-2148

102. **Menzies-Gow, A., Flood-Page, P., Sehmi, R., Burman, J., Hamid, Q., Robinson, D. S., Kay, A. B. and Denburg, J.** (2003) Anti-IL-5 (mepolizumab) therapy induces bone marrow eosinophil maturational arrest and decreases eosinophil progenitors in the bronchial mucosa of atopic asthmatics. *J. Allergy Clin. Immunol.* **111**: 714-719

103. **Falcone, F. H., Zillikens, D. and Gibbs, B. F.** (2006) The 21st century renaissance of the basophil? Current insights into its role in allergic responses and innate immunity. *Exp. Dermatol.* **15**:855-864

104. **Min, B., Prout, M., Hu-Li, J., Zhu, J., Jankovic, D., Morgan, E. S., Urban, Jr., J. F., Dvorak, A. M., Finkelman, F. D., LeGros, G. and Paul, W. E.** (2004) Basophils produce IL-4 and accumulate in tissues after infection with a Th2-inducing parasite. *J. Exp. Med.* **200(4)**:507-517

105. **Devouassoux, G., Foster, B., Scott, L. M., Metcalfe, D. D. and Prussin, C.** (1999) Frequency and characterisation of antigen-specific IL-4- and IL-13-producing basophils and T cells in peripheral blood of healthy and asthmatic subjects. *J. Allergy Clin. Immunol.* **104**;811-819

106. **Macfarlane, A. J., Kon, O. M., Smith, S. J., Zeibecoglou, K., Khan, L. N., Barata, L. T., McEuen, A. R., Buckley, M. G., Walls, A. F., Meng, Q., Humbert, M., Barnes, N. C., Robinson, D. S., Ying, S. and Kay, A. B.** (1999) Basophils, eosinophils, and mast cells in atopic and nonatopic asthma and in late-phase allergic reactions in the lung and skin. *J. Allergy Clin. Immunol.* **105(1 Pt 1)**:99-107

107. **Gauvreau, G. M., Lee, J. L., Watson, R. M., Irani, A.-M. A., Schwartz, L. B. and O'Byrne, P. M.** (2000) Increased numbers of both airway basophils and mast cells in sputum after allergen inhalation challenge of atopic asthmatics. *Am. J. Respir. Crit.* **161**:1473-1478

108. **Koshino, T., Arai, Y., Miyamoto, Y., Sano, Y., Itami, M., Teshima, S.-I., Hirai, K., Takaishi, T., Ito, K. and Morita, Y.** (1996) Airway basophil and mast cell density in patients with bronchial asthma: relationship to bronchial hyperresponsiveness. *J. Asthma* **33(2)**:89-95

109. **Kepley, C. L., McFeeley, P. J., Oliver, J, M. and Lipscomb, M. F.** (2001) Immunohistochemical detection of human basophils in postmortem cases of fatal asthma. *Am. J. Respir. Crit. Care Med.* **164**:1053-1058

110. **Hirai, H., Tanaka, K., Yoshie, O., Ogawa, K., Kenmotsu, K., Takamori, Y., Ichimasa, M., Sugamura, K., Nakamura, M., Takano, S. and Nagata, K.** (2001) Prostaglandin D2 selectively induces chemotaxis in T helper type 2 cells, eosinophils, and basophils via seven-transmembrane receptor CRTH2. *J. Exp. Med.* **193(2)**:255-261

111. **Uguccioni, M., Mackay, C. R., Ochensberger, B., Loetscher, P., Rhis, S., LaRosa, G. J., Rao, P., Ponath, P. D., Baggiolini, M. and Dahinden, C. A.** (1997) High expression of the chemokine receptor CCR3 in human blood basophils. *J. Clin. Invest.* **100(5)**:1137-1143

112. **Lantz, C. S., Boesiger, J., Song, C. H., Mach, N., Kobayashi, T., Mulligan, R. C., Nawa, Y., Dranoff, G. and Galli, S. J.** (1998) Role for interleukin-3 in mast cell and basophil development and in immunity to parasites. *Nature* **392**:90-93

113. **Brunner, T., Heusser, C. H. and Dahinden, C. A.** (1993) Human peripheral blood basophils primed by interleukin 3 (IL-3) produce IL-4 in response to immunoglobulin E receptor stimulation. *J. Exp. Med.* **177**:605-611

114. **Gibbs, B. F., Haas, H., Falcone, F. H., Albrecht, C., Vollrath, I. B., Noll, T., Wolff, H. H. and Amon, U.** (1996) Purified human peripheral blood basophils release interleukin-13 and preformed interleukin-4 following immunological activation. *Eur. J. Immunol.* **26**:2493-2498

115. **Oh, K., Shen, T., LeGros, G. and Min, B.** (2007) Induction of type 2 immunity in a mouse system reveals a novel immunoregulatory role of basophils. *Blood* **109**:2921-2927

116. **Yanagihara, Y., Kajiwara, K., Basaki, Y., Ikizawa, K., Ebisawa, M., Ra, C., Tachimoto, H. and Saito, H.** (1998) Cultured basophils but not cultured mast cells induce human IgE synthesis in B cells after immunologic stimulation. *Clin. Exp. Immunol.* **111**:136-143

117. **Wenzel, S. E., Szefler, S. J., Leung, D. Y. M., Sloan, S. I., Rex, M. D. and Martin, R. J.** (1997) Bronchoscopic evaluation of severe asthma - persistent inflammation associated with high dose glucocorticoids. *Am. J. Respir. Crit, Care* **156**:737-743

118. **Little, S. A., MacLeod, K. J., Chalmers, G. W., Love, J. G., McSharry, C. and Thomson, N. C.** (2002) Association of forced expiratory volume with disease duration and sputum neutrophils in chronic asthma. *Am. J. Med.* **112**:446-452

119. **Hauber, H.-P., Gotfried, M., Newman, K., Danda, R., Servi, R. J., Christodoulopoulos, P. and Hamid, Q.** (2003) Effect of HFA-flunisolide on peripheral lung inflammation in asthma. *J. Allergy Clin. Immunol.* **112**:58-63

120. **Cox, G.** (1995) Glucocorticoid treatments inhibits apoptosis in human neutrophils. *J. Immunol.* **154**:4719-4725

121. **Mattoli, S., Marini, M. and Fasoli, A.** (1992) Expression of the potent inflammatory cytokines, GM-CSF, IL6, and IL8, in bronchial epithelial cells of asthmatic patients. *Chest* **101**:27-29

122. **Baggiolini, M., Walz, A. and Kunkel, S. L.** (1989) Neutrophil-activating peptide-1/interleukin 8, a novel cytokine that activates neutrophils. *J. Clin. Invest.* **84**:1045-1049

123. **Fukakusa, M., Bergeron, C., Tulic, M. K., Fiset, P.-O., Al Dewachi, O., Laviolette, M., Hamid, Q. and Chakir, J.** (2005) Oral corticosteroids decrease eosinophil and CC chemokine expression but increase neutrophil, IL-8, and IFN-γ-inducible protein 10 expression in asthmatic airway mucosa. *J. Allergy Clin. Immunol.* **115**:280-286

124. **Foley, S. C. and Hamid, Q.** (2007) Images in allergy and immunology: neutrophils in asthma. *J. Allergy Clin. Immunol.* **119**:1282-1286

125. **Reader, J. R., Hyde, D. M., Schelegle, E. S., Aldrich, M. C., Stoddard, A. M., McLane, M. P., Levitt, R. C. and Tepper, J. S.** (2003) Interleukin-9 induces mucous cell metaplasia independent of inflammation. *Am. J. Respir. Cell Mol. Biol.* **28**:664-672

126. **Vermeer, P. D., Harson, R., Einwalter, L. A., Moninger, T. and Zabner, J.** (2003) Interleukin-9 induces goblet cell hyperplasia during repair of human airway epithelia. *Am. J. Respir. Cell Mol. Biol.* **28**:286-295

127. **Abdelilah, S. G., Latifa, K., Esra, N., Cameron, L., Bouchaib, L., Nicolaides, N. C., Levitt, R. C. and Hamid, Q.** (2001) Functional expression of IL-9 receptor by human neutrophils from asthmatic donors: role in IL-8 release. *J, Immunol.* **166**:2768-2774

128. **Chu, H. W., Trudeau, J. B., Balzar, S. and Wenzel, S. E.** (2000) Peripheral blood and airway tissue expression of transforming growth factor β by neutrophils in asthmatic subjects and normal control subjects. *J. Allergy Clin. Immunol.* **106**:1115-1123

129. **Cundall, M., Sun, Y., Miranda, C., Trudeau, J. B., Barnes, S. and Wenzel, S. E.** (2003) Neutrophil-derived matrix metalloproteinase-9 is increased in severe asthma and poorly inhibited by glucocorticoids. *J. Allergy Clin. Immunol.* **112**:1064-1071

130. **Spada, F. M., Koezuka, Y. and Porcelli, S. A.** (1998) CD1d-restricted recognition of synthetic glycolipid antigens by human natural killer T cells. *J. Exp. Med.* **188(8)**:1529-1534

131. **Exley, M., Garcia, J., Balk, S. P. and Porcelli, S.** (1997) Requirements for CD1d recognition by human invariant Vα24$^+$ CD4$^-$CD8$^-$ T cells. *J. Exp. Med.* **186(1)**:109-120

132. **Porcelli, S., Yockey, C. E., Brenner, M. B. and Balk, S. P.** (1993) Analysis of T cell antigen receptor (TCR) expression by human peripheral blood CD4$^-$8$^-$ α/β T cells demonstrates preferential use of several Vβ genes and an invariant TCR α chain. *J. Exp. Med.* **178**:1-16

133. **Canchis, P. W., Bhan, A. K., Landau, S. B., Yang, L., Balk, S. P. and Blumberg, R. S.** (1993) Tissue distribution of the non-polymorphic major histocompatibility complex class I-like molecule, CD1d. *Immunology* **80**:561-565

134. **Exley, M., Garcia, J., Wilson, S. B., Spada, F., Gerdes, D., Tahir, S. M. A., Patton, K. T., Blumberg, R. S., Porcelli, S., Chott, A. and Balk, S. P.** (2000) CD1d structure and regulation on human thymocytes, peripheral blood T cells, B cells and monocytes. *Immunology* **100(1)**:37-47

135. **Lee, P. T., Benlagha, K., Teyton, L. and Bendelac, A.** (2002) Distinct functional lineages of human Vα24 natural killer T cells. *J. Exp. Med.* **195(5)**:637-641

136. **Takahashi, T., Chiba, S., Nieda, M., Azuma, T., Ishihara, S., Shibata, Y., Juji, T. and Hirai, H.** (2002) Cutting edge: analysis of human Vα24$^+$CD8$^+$ NK T cells activated by α-galactosylceramide-pulsed monocyte-derived dendritic cells. *J. Immunol.* **168**:3140-3144

137. **Stein-Streilein, J.** (2003) Invariant NKT cells as initiators, licensors, and facilitators of the adaptive immune response. *J. Exp. Med.* **198(12)**:1779-1783

138. **Akbari, O., Stock, P., Meyer, E., Kronenberg, M., Sidobre, S., Nakayama, T., Taniguchi, M., Grusby, M. J., DeKruyff, R. H. and Umetsu, D. T.** (2003)

Essential role of NKT cells producing IL-4 and IL-13 in the development of allergen-induced airway hyperreactivity. *Nature Med.* **9(5)**:582-588

139. **Meyer, E. H., Goya, S., Akbari, O., Berry, G. J., Savage, P. B., Kronenberg, M., Nakayama, T., DeKruyff, R. H. and Umetsu, D. T.** (2006) Glycolipid activation of invariant T cell receptor^{+} NK T cells is sufficient to induce airway hyperreactivity independent of conventional CD4^{+} T cells. *Proc. Natl. Acad. Sci. USA* **103(8)**:2782-2787

140. **Akbari, O., Faul, J. L., Hoyte, E. G., Berry, G. J., Wahlström, J., Kronenberg, M., DeKruyff, R. H. and Umetsu, D. T.** (2006) CD4+ invariant T-cell-receptor+ Natural Killer T cells in bronchial asthma. *New Engl. J. Med.* **354**:1117-1129

141. **Pham-Thi, N., de Blic, J., Le Bourgeois, M., Dy, M., Scheinmann, P. and Leie-de-Moraes, M. C.** (2006) Enhanced frequency of immunoregulatory invariant natural killer T cells in the airways of children with asthma. *J. Allergy Clin. Immunol.* **117(1)**:217-218

142. **Hamzaoui, A., Rouhou, S. C., Graïri, H., Abid, H., Ammar, J., Chelbi, H. and Hamzaoui, K.** (2006) NKT cells in the induced sputum of asthmatics. *Mediators Inflamm.* **2006**:1-6

143. **Thomas, S. Y., Lilly, C. M. and Luster, A .D.** (2006) Invariant natural killer T cells in bronchial asthma – letter to the editor. *New Engl. J. Med.* **354**:2613-2615

144. **Vijayanand, P., Seumois, G., Pickard, C., Powell, R. M., Angco, G., Sammut, D., Gadola, S. D., Friedmann, P. S. and Djukanović, R.** (2007) Invariant natural killer T cells in asthma and chronic obstructive pulmonary disease. *New Engl. J. Med.* **356**:1410-1422

145. **Mutalithas, K., Croudace, J., Guillen, C., Siddiqui, S., Thickett, D., Wardlaw, A., Lammas, D. and Brightling, C.** (2007) Bronchoalveolar lavage invariant natural killer T cells are not increased in asthma. *J. Allergy Clin. Immunol.* **119(5)**:1274-1276

146. **Bratke, K., Julius, P. and Virchow, J. C.** (2007) Invariant natural killer T cells in asthma and chronic obstructive pulmonary disease – letter to the editor. *New Engl. J. Med.* **357**:194

147. **van Kaer, L.** (2002) Major histocompatibility complex class I-restricted antigen processing and presentation. *Tissue Antigens* **60**:1-9

148. **Finotto, S., Fabbri, L. M., Rado, V., Mapp, C. E. and Maestrelli, P.** (1991) Increase in numbers of CD8 positive lymphocytes and eosinophils in peripheral blood of subjects with late asthmatic reactions induced by toluene diisocyanate. *Br. J. Ind. Med.* **48**:116-121

149. **Yurovsky, V. V., Weersink, E. J. M., Meltzer, S. S., Moore, W. C., Postma, D. S., Bleecker, E. R. and White, B.** (1998) T-cell repertoire in the blood and lungs of atopic asthmatics before and after ragweed challenge. *Am. J. Respir. Cell Mol. Biol.* **18**:370-383

150. **Wahlström, J., Dahlén, B., Ihre, E., Wigzell, H., Grunewald, J. and Eklund, A.** (1998) Selective $CD8^+$ T cells accumulate in the lungs of patients with allergic asthma after allergen bronchoprovocation. *Clin. Exp. Immunol.* **112**:1-9

151. **Till, S., Li, B., Durham, S., Humbert, M., Assoufi, B., Huston, D., Dickason, R., Jeannin, P., Kay, A. B. and Corrigan, C.** (1995) Secretion of the eosinophil-active cytokines interleukin-5, granulocyte/macrophage colony-stimulating factor and interleukin-3 by bronchoalveolar lavage $CD4^+$ and $CD8^+$ T cell lines in atopic asthmatics, and atopic and non-atopic controls. *Eur. J. Immunol.* **25**:2727-2731

152. **Stanciu, L. A., Roberts, K., Papadopoulos, N. G., Cho, S.-H., Holgate, S. T., Coyle, A. J. and Johnston, S. L.** (2005) IL-4 increases type 2, but not type 1, cytokine production in $CD8^+$ T cells from mild atopic asthmatics. *Respir. Res.* **6**:67-73

153. **Bratke, K., Haupt, F., Kuepper, M., Bade, B., Faehndrich, S., Luttmann, W. and Virchow, Jr., J. C.** (2006) Decrease of cytotoxic T cells in allergic asthma correlates with total serum immunoglobulin E. *Allergy* **61**:1351-1357

154. **Coyle, A. J., Erard, F., Bertrand, C., Walti, S., Pircher, H. and LeGros, G.** (1995) Virus-specific $CD8^+$ cells can switch to interleukin 5 production and induce airway eosinophilia. *J. Exp. Med.* **181**:1229-1233

155. **Miyahara, N., Takeda, K., Kodama, T., Joetham, A., Taube, C., Park, J.-W., Miyahara, S., Balhorn, A., Dakhama, A. and Gelfand, E. W.** (2004) Contribution of antigen-primed $CD8^+$ T cells to the development of airway hyperresponsiveness and inflammation is associated with IL-13. *J. Immunol.* **172**:2549-2558

156. **Koya, T., Miyahara, N., Takeda, K., Matsubara, S., Matsuda, H., Swasey, C., Balhorn, A., Dakhama, A. and Gelfand, E. W.** (2007) $CD8^+$ T cell-mediated airway hyperresponsiveness and inflammation is dependent on $CD4^+IL\text{-}4^+$ T cells. *J. Immunol.* **179**:2787-2796

157. **McMenamin, C. and Holt, P. G.** (1993) The natural immune response to inhaled soluble protein antigens involves major histocompatibility complex (MHC) class I-restricted $CD8^+$ T cell-mediated but MHC class II-restricted $CD4^+$ T cell-dependent immune deviation resulting in selective suppression of immunoglobulin E production. *J. Exp. Med.* **178**:889-899

158. **Holmes, B. J., MacAry, P. A., Noble, A. and Kemeny, D. M.** (1997) Antigen-specific $CD8^+$ T cells inhibit IgE responses and interleukin-4 production by $CD4^+$ T cells. *Eur. J. Immunol.* **27**:2657-2665

159. **Wells, J. W., Cowled, C. J., Giorgini, A., Kemeny. D. M. and Noble, A.** (2007) Regulation of allergic airway inflammation by class I-restricted allergen presentation and CD8 T-cell infiltration. *J. Allergy Clin. Immunol.* **119**:226-234

160. **Salagianni, M., Loon, W. K., Thomas, M. J., Noble, A. and Kemeny, D. M.** (2007) An essential role for IL-18 in CD8 T cell-mediated suppression of IgE responses. *J. Immunol.* **178**:4771-4778

161. **Harrington, L. E., Hatton, R. D., Mangan, P. R., Turner, H., Murphy, T. L., Murphy, K. M. and Weaver, C. T.** (2005) Interleukin 17-producing $CD4^+$ effector T cells develop via a lineage distinct from the T helper type 1 and 2 lineages. *Nature Immunol.* **6(11)**;1123-1132

162. **Park, H., Li, Z., Yang, X. O., Chang, S. H., Nurieva, R., Wang, Y.-H., Wang, Y., Hood, L., Zhu, Z., Tian, Q. and Dong, C.** (2005) A distinct lineage of CD4 T cells regulates tissue inflammation by producing interleukin 17. *Nature Immunol.* **6(11)**:1133-1141

163. **Kolls, J. K. and Lindén, A.** (2004) Interleukin-17 family members and inflammation. *Immunity* **21**:467-476

164. **Molet, S., Hamid, Q., Davoine, F., Nutku, E., Taha, R., Pagé, N., Olivenstein, R., Elias, J. and Chakir, J.** (2001) IL-17 is increased in asthmatic airways and induces human bronchial fibroblasts to produce cytokines. *J. Allergy Clin. Immunol.* **108**:430-438

165. **Barczyk, A., Pierzcha, W. and Sozañska, E.** (2003) Interleukin-17 in sputum correlates with airway hyperresponsiveness to methacholine. *Respir. Med.* **97**:726-733

166. **Hashimoto, T., Akiyama, K., Kobayashi, N. and Mori, A.** (2005) Comparison of IL-17 production by helper T cells among atopic and nonatopic asthmatics and control subjects. *Int. Arch. Allergy Immunol.* **137(suppl 1)**:51-54

167. **Rahman, M. S., Yamasaki, A., Yang, J., Shan, L., Halayko, A. J. and Gounni, A. S.** (2006) IL-17A induces eotaxin-1/CC chemokine ligand 11 expression in human airway smooth muscle cells: role of MAPK (Erk1/2, JNK, and p38) pathways. *J. Immunol.* **177**:4064-4071

168. **Dragon, S., Rahman, M. S., Yang, J., Unruh, H., Halayko, A. and Gounni, A. S.** (2007) IL-17 enhances IL-1β-mediated CXCL-8 release from human airway smooth muscle cells. *Am. J. Physiol. Lung Cell Mol. Physiol.* **292**:1023-1029

169. **van den Berg, A., Kuiper, M., Snoek, M., Timens, W., Postma, D. S., Jansen, H. M. and Lutter, R.** (2005) Interleukin-17 induces hyperresponsive interleukin-8 and interleukin-6 production to tumor necrosis factor-α in structural lung cells. *Am. J. Respir. Cell Mol. Biol.* **33**:97-104

170. **Chakir, J., Shannon, J., Molet, S., Fukakusa, M., Elias, J., Laviolette, M., Boulet, L.-P. and Hamid, Q.** (2003) Airway remodelling-associated mediators in moderate to severe asthma: effect of steroids on TGF-β, IL-11, IL-17, and type I and type III collagen expression. *J. Allergy Clin. Immunol.* **111**:1293-1298

171. **Bullens, D. M. A., Truyen, E., Coteur, L., Dilissen, E., Hellings, P. W., Dupont, L. J. and Ceuppens, J. L.** (2006) IL-17 mRNA in sputum of asthmatic

patients: linking T cell driven inflammation and granulocytic influx? *Respir. Res.* 7:135-143

172. **Chen, Y., Thai, P., Zhao, Y.-H., Ho, Y.-S., DeSouza, M. M. and Wu, R.** (2003) Stimulation of airway mucin gene expression by interleukin (IL)-17 through IL-6 paracrine/autocrine loop. *J. Biol. Chem.* **278(19)**:17036-17043

173. **Romagnani, S.** (2006) Regulation of the T cell response. *Clin. Exp. Allergy* **36**:1357-1366

174. **Abbas, A. K., Murphy, K. M. and Sher, A.** (1996) Functional diversity of helper T lymphocytes. *Nature* **383**:787-793

175. **Boguniewicz, M., Martin, R. J., Martin, D., Gibson, U., Celniker, A., Williams, M. and Leung, D. Y.** (1995) The effects of nebulized recombinant interferon-γ in asthmatic airways. *J. Allergy Clin. Immunol.* **95(1 Pt 1)**:133-135

176. **Nurse, B., Haus, M., Puterman, A. S., Weinberg, E. G. and Potter, P.C.** (1997) Reduced interferon-γ but normal IL-4 and IL-5 release by peripheral blood mononuclear cells from Xhosa children with atopic asthma. *J. Allergy Clin. Immunol.* **100**:662-668

177. **Renzi, P. M., Turgeon, J. P., Marcotte, J. E., Drblik, S. P., Bérubé, D., Gagnon, M. F. and Spier, S.** (1999) Reduced interferon-γ production in infants with bronchiolitis and asthma. *Am. J. Respir. Crit. Care Med.* **159**:1417-1422

178. **Kim, J.-H., Kim, B.-S., Lee, S.-Y., Seo, J.-H., Shim, J.-Y., Hong, T.-J. and Hong, S.-J.** (2004) Different IL-5 and IFN-γ production from peripheral blood T-cell subsets in atopic and nonatopic asthmatic children. *J. Asthma* **41(8)**:869-876

179. **De Rose, V., Cappello, P., Sorbello, V., Ceccarini, B., Gani, F., Bosticardo, M., Fassio, S. and Novelli, F.** (2004) IFN-γ inhibits the proliferation of allergen-activated T lymphocytes from atopic, asthmatic patients by inducing Fas/FasL-mediated apoptosis. *J. Leukoc. Biol.* **76**:423-432

180. **Chen, X.-Q., Yang, J., Hu, S.-P., Nie, H.-X., Mao, G.-Y. and Chen, H.-B.** (2006) Increased expression of CD86 and reduced production of IL-12 and IL-10 by monocyte-derived dendritic cells from allergic asthmatics and their effects on Th1- and Th2-type balance. *Respiration* **73**:34-40

181. **Coyle, A. J., Tsuyuki, S., Bertrand, C., Huang, S., Aguet, M., Alkan, S. S. and Anderson, G. P.** (1996) Mice lacking the IFN-γ receptor have an impaired ability to resolve a lung eosinophilic inflammatory response associated with a prolonged capacity of T cells to exhibit a Th2 cytokine profile. *J. Immunol.* **156**:2680-2685

182. **Cohn, L., Homer, R. J., Niu, N. and Bottomly, K.** (1999) T helper 1 cells and interferon-γ regulate allergic airway inflammation and mucus production. *J. Exp. Med.* **190(9)**:1309-1317

183. **Huang, T.-J., MacAry, P. A., Eynott, P., Moussavi, A., Daniel, K. C. Askenase, P. W., Kemeny, D. M. and Chung, K. F.** (2001) Allergen-specific Th1 cells counteract efferent Th2 cell-dependent bronchial hyperresponsiveness and eosinophilic inflammation partly via IFN-γ. *J. Immunol.* **166**:207-217

184. **Tang, C., Inman, M. D., van Rooijen, N., Yang, P., Shen, H., Matsumoto, K. and O'Byrne, P.M.** (2001) Th type 1-stimulating activity of lung macrophages inhibits Th2-mediated allergic airway inflammation by an IFN-γ-dependent mechanism. *J. Immunol.* **166**:1471-1481

185. **Finotto, S., Neurath, M. F., Glickman, J. N., Qin, S., Lehr, H. A., Green, F. H. Y., Ackerman, K., Haley, K., Galle, P. R., Szabo, S. J., Drazen, J. M., De Sanctis, G. T. and Glimcher, L. H.** (2002) Development of spontaneous airway changes consistent with human asthma in mice lacking T-bet. *Science* **295**:336-338

186. **Shi, Z. O.-Q., Fischer, M. J., De Sanctis, G. T., Schuyler, M. R. and Tesfaigzi, Y.** (2002) IFN-γ, but not Fas, mediates reduction of allergen-induced mucous cell metaplasia by inducing apoptosis. *J. Immunol.* **168**:4764-4771

187. **Park, C.-S., Choi, E. N., Kim, J. S., Choi, Y. S., Rhim, T. Y., Chang, H. S. and Chung, I. Y.** (2005) Interferon-γ inhibits in vitro mobilization of eosinophils by interleukin-5. *Int. Arch. Allergy Immunol.* **136**:295-302

188. **Bortolatto, J., Borducchi, É., Rodriguez, D., Keller, A. C., Faquim-Mauro, E., Bortoluci, K. R., Mucida, D., Gomez, E., Christ, A., Schnyder-Candrian, S., Schnyder, B., Ryffel, B. and Russo, M.** (2008) Toll-like receptor 4 agonists adsorbed to aluminium hydroxide adjuvant attenuate ovalbumin-specific allergic airway disease: role of MyD88 adaptor molecule and interleukin-12/interferon-γ axis. *Clin. Exp. Allergy* **In press**

189. **Hansen, G., Berry, G., DeKruyff, R. H. and Umetsu, D. T.** (1999) Allergen-specific Th1 cells fail to counterbalance Th2 cell-induced airway hyperreactivity but cause severe airway inflammation. *J. Clin. Invest.* **103**:175-183

190. **Randolph, D. A., Stephens, R., Carruthers, C. J. and Chaplin, D. D.** (1999) Cooperation between Th1 and Th2 cells in a murine model of eosinophilic airway inflammation. *J. Clin. Invest.* **104**:1021-1029

191. **Koch, M., Witzenrath, M., Reuter, C., Herma, M., Schütte, H., Suttorp, N., Collins, H. and Kaufmann, S. H. E.** (2006) Role of local pulmonary IFN-γ expression in murine allergic airway inflammation *Am. J. Respir. Cell Mol. Biol.* **35**:211-218

192. **Jeon, S. G., Oh, S.-Y., Park, H.-K., Kim, Y.-S., Shim, E.-J., Lee, H.-S., Oh, M.-H., Bang, B., Chun, E.-Y., Kim, S.-H., Gho, Y. S., Zhu, Z., Kim, Y.-Y. and Kim, Y.-K.** (2007) Th2 and Th1 lung inflammation induced by airway allergen sensitization with low and high doses of double-stranded RNA. *J. Allergy Clin. Immunol.* **120**:803-812

193. **Watanabe, N., Wang, Y.-H., Lee, H. K., Ito, T., Wang, Y.-H., Cao, W. and Liu, Y.-J.** (2005) Hassall's corpuscles instruct dendritic cells to induce $CD4^+CD25^+$ regulatory T cells in human thymus. *Nature* **436**:1181-1185

194. **Vukmanovic-Stejic, M., Zhang, Y., Cook, J. E., Fletcher, J. M., McQuaid, A., Masters, J. E., Rustin, M. H. A., Taams, L. S., Beverley, P. C. L., Macallan, D. C. and Akbar, A. N.** (2006) Human $CD4^+CD25^{hi}Foxp3^+$ regulatory T cells are derived by rapid turnover of memory populations in vivo. *J. Clin. Invest.* **116(9)**:2423-2433

195. **Fontenot, J. D., Gavin, M. A. and Rudensky, A. Y.** (2003) Foxp3 programs the development and function of $CD4^+CD25^+$ regulatory T cells. *Nature Immunol.* **4(4)**:330-336

196. **Hori, S., Nomura, T. and Sakaguchi, S.** (2003) Control of regulatory T cell development by the transcription factor Foxp3. *Science* **299**:1057-1061

197. **Liu, Z., Tugulea, S., Cortesini, R. and Suciu-Foca, N.** (1998) Specific suppression of T helper alloreactivity by allo-MHC class I-restricted $CD8^+$ $CD28^-$ T cells. *Int. Immunol.* **10(6)**:775-783

198. **Najafian, N., Chitnis, C., Salama, A. D., Zhu, B., Benou, C., Yuan, X., Clarkson, M. C., Sayegh, M. H. and Khoury, S. J.** (2003) Regulatory functions of $CD8^+$ $CD28^-$ T cells in an autoimmune disease model. *J. Clin. Invest.* **112**:1037-1048

199. **Vignali, D. A. A., Collison, L. W. and Workman, C. J.** (2008) How regulatory T cells work. *Nature Rev. Immunol.* **8**:523-532

200. **Groux, H., O'Garra, A., Bigler, M., Rouleau, M., Antonenko, S., de Vries, J. E. and Roncarolo, M. G.** (1997) A $CD4^+$ T-cell subset inhibits antigen-specific T-cell responses and prevents colitis. *Nature* **389**:737-742

201. **Chen. Y., Inobe, J.-I., Marks, R., Gonnella, P., Kuchroo, V. K. and Weiner, H. L.** (1995) Peripheral deletion of antigen-reactive T cells in oral tolerance. *Nature* **376**:177-180

202. **Bellinghausen, I., Klostermann, B., Knop, J. and Saloga, J.** (2003) Human $CD4^+CD25^+$ T cells derived from the majority of atopic donors are able to suppress Th1 and Th2 cytokine production. *J. Allergy Clin. Immunol.* **111**:862-868

203. **Akdis, M., Verhagen, J., Taylor, A., Karamloo, F., Karagiannidis, C., Crameri, R., Thunberg, S., Deniz, G., Valenta, R., Fiebig, H., Kegel, C., Disch, R., Schmidt-Weber, C. B., Blaser, K. and Akdis, C. A.** (2004) Immune responses in healthy and allergic individuals are characterized by a fine balance between allergen-specific T regulatory 1 and T helper 2 cells. *J. Exp. Med.* **199(11)**:1567-1575

204. **Ling, E. M., Smith, T., Nguyen, X. D., Pridgeon, C., Dallman, M., Arbery, J., Carr, V. A. and Robinson, D. S.** (2004) Relation of CD4+CD25+ regulatory

T-cell suppression of allergen-driven T-cell activation to atopic status and expression of allergic disease. *Lancet* **363**:608-615

205. **Grindebacke, H., Wing, K., Anderson, A.-C., Suri-Payer, E., Rak, S. and Rudin, A.** (2004) Defective suppression of Th2 cytokines by $CD4^+CD25^+$ regulatory T cells in birch allergics during birch pollen season. *Clin. Exp. Allergy* **34**:1364-1372

206. **Karagiannidis, C., Akdis, M., Holopainen, P., Woolley, N. J., Hense, G., Rückert, B., Mantel, P. Y., Menz, G., Akdis, C. A., Blaser, K. and Schmidt-Weber, C. B.** (2004) Glucocorticoids upregulate *FOXP3* expression and regulatory T cells in asthma. *J. Allergy Clin. Immunol.* **114**:1425-1433

207. **Nguyen, X. D. and Robinson, D. S.** (2004) Fluticasone propionate increases $CD4^+CD25^+$ T regulatory cell suppression of allergen-stimulated $CD4^+CD25^-$ T cells by an IL-10-dependent mechanism. *J. Allergy Clin. Immunol.* **114**:296-301

208. **Francis, J. N., Till, S. J. and Durham, S. R.** (2003) Induction of IL-10^+ $CD4^+CD25^+$ T cells by grass pollen immunotherapy. *J. Allergy Clin. Immunol.* **111**:1255-1261

209. **Jutel, M., Akdis, M., Budak, F., Aebischer-Casaulta, C., Wrzyszcz, M., Blaser, K. and Akdis, C. A.** (2003) IL-10 and TGF-β cooperate in the regulatory T cell response to mucosal allergens in normal immunity and specific immunotherapy. *Eur. J. Immunol.* **33**:1205-1214

210. **Lin, Y.-L., Shieh, C. C. and Wang, J.-Y.** (2008) The functional insufficiency of human $CD4^+$ $CD25^{high}$ T-regulatory cells in allergic asthma is subjected to TNF-α modulation. *Allergy* **63**:67-74

211. **Berry, M., Brightling, C., Pavord, I. and Wardlaw, A. J.** (2007) TNF-α in asthma. *Curr. Opin. Pharmacol.* 7:279-282

212. **Mosmann, T. R. and Coffman, R. L.** (1987) Two types of mouse helper T-cell clone. *Immunol Today* **8(7-8)**:223-227

213. **Renauld, J.-C., Kermouni, A., Vink, A., Louahed, J. and Van Snick, J.** (1995) Interleukin-9 and its receptor: involvement in mast cell differentiation and T cell oncogenesis. *J. Leukoc. Biol.* **57**:353-360

214. **McKenzie, A. N. J., Culpepper, J. A., de Waal Malefyt, R., Brière, F., Punnonen, J., Aversa, G., Sato, A., Dang, W., Cocks, B. G., Menon, S., de Vries, J. E., Banchereau, J. and Zurawski, G.** (1993) Interleukin 13, a T-cell-derived cytokine that regulates human monocyte and B-cell function. *Proc. Natl. Acad. Sci. USA* **90**:3735-3739

215. **Robinson, D. S., Bentley, A. M., Hartnell, A., Kay, A. B. and Durham, S. R.** (1993) Activated memory T helper cells in bronchoalveolar lavage fluid from patients with atopic asthma: relation to asthma symptoms, lung function, and bronchial responsiveness. *Thorax* **48**:26-32

216. **Tang, C., Rolland, J. M., Ward, C., Quan, B. and Walters, E. H.** (1997) IL-5 production by bronchoalveolar lavage and peripheral blood mononuclear cells in asthma and atopy. *Eur. Respir. J.* **10**:624-632

217. **Bodey, K. J., Semper, A. E., Redington, A. E., Madden, J., Teran, L. M., Holgate, S. T. and Frew, A. J.** (1999) Cytokine profiles of BAL T cells and T-cell clones obtained from human asthmatic airways after local allergen challenge. *Allergy* **54(10)**:1083-1093

218. **Erpenbeck, V. J., Hagenberg, A., Krentel, H., Discher, M., Braun, A., Hohlfeld, J. M. and Krug, N.** (2006) Regulation of GATA-3, c-maf and T-bet mRNA expression in bronchoalveolar lavage cells and bronchial biopsies after segmental allergen challenge. *Int. Arch, Allergy Immunol.* **139**:306-316

219. **Solley, G. O., Gleich, G. J., Jordon, R. E. and Schroeter, A. L.** (1976) The late phase of the immediate wheal and flare skin reaction. Its dependence upon IgE antibodies. *J. Allergy Clin, Immunol.* **58(2)**:408-20.

220. **Budde, I. K., Lopuhaa, C. E., de Heer, P. G., Langdon, J. M., MacDonald, S. M., van der Zee, J. S. and Aalberse, R. C.** (2002) Lack of correlation between bronchial late allergic reaction to *Dermatophagoides pteronyssinus* and in vitro immunoglobulin E reactivity to histamine-releasing factor derived from mononuclear cells. *Ann. Allergy Asthma Immunol.* **89**:606-612

221. **Haselden, B. M., Kay, A. B. and Larchè, M.** (1999) Immunoglobulin E-independent major histocompatibility complex-restricted T cell peptide epitope-induced late asthmatic reaction. *J. Exp. Med.* **189(12)**:1885-1894

222. **Runa Ali, F., Oldfield, W. L. G., Higashi, N., Larchè, M. and Kay, A. B.** (2004) Late asthmatic reactions induced by inhalation of allergen-derived T cell peptides. *Am. J. Respir. Crit. Care Med.* **169**:20-26

223. **Runa Ali, F., Kay, A. B. and Larchè, M.** (2007) Airway hyperresponsiveness and bronchial mucosal inflammation in T cell peptide-induced asthmatic reactions in atopic subjects. *Thorax* **62**:750-757

224. **Shahid, S. K., Kharitonov, S. A., Wilson, N. M., Bush, A. and Barnes, P. J.** (2002) Increased interleukin-4 and decreased interferon-γ in exhaled breath condensate of children with asthma. *Am. J. Respir. Crit. Care Med.* **165(9)**:1290-1293

225. **Ying, S., Meng, Q., Kay, A. B. and Robinson, D. S.** (2002) Elevated expression of interleukin-9 mRNA in the bronchial mucosa of atopic asthmatics and allergen-induced cutaneous late-phase reaction: relationships to eosinophils, mast cells and T lymphocytes. *Clin. Exp. Allergy* **32**:866-871

226. **Erpenbeck, V. J., Hohlfeld, J. M., Volkmann, B., Hagenberg, A., Geldmacher, H., Braun, A. and Krug, N.** (2003) Segmental allergen challenge in patients with atopic asthma leads to increased IL-9 expression in bronchoalveolar lavage fluid lymphocytes. *J. Allergy Clin. Immunol.* **111(6)**:1319-1327

227. **Humbert, M., Durham, S. R., Kimmitt, P., Powell, N., Assoufi, B., Pfister, R., Menz, G., Kay, A. B. and Corrigan, C. J.** (1997) Elevated expression of messenger ribonucleic acid encoding IL-13 in the bronchial mucosa of atopic and nonatopic subjects with asthma. *J. Allergy Clin. Immunol.* **99(5)**:657-665

228. **Kaplan, M. H., Schindler, U., Smiley, S. T. and Grusby, M. J.** (1996) Stat6 is required for mediating responses to IL-4 and for development of Th2 cells. *Immunity* **4(3)**:313-319

229. **Shimoda, K., van Deursen, J., Sangster, M. Y., Sarawar, S. R., Carson, R. T., Tripp, R. A., Chu, C., Quelle, F. W., Nosaka, T., Vignali, D. A., Doherty, P. C., Grosveld, G., Paul, W. E. and Ihle, J. N.** (1996) Lack of IL-4-induced Th2 response and IgE class switching in mice with disrupted Stat6 gene. *Nature* **380**:630-633

230. **Kuperman, D., Schofield, B., Wills-Karp, M. and Grusby, M. J.** (1998) Signal transducer and activator of transcription factor 6 (Stat6)-deficient mice are protected from antigen-induced airway hyperresponsiveness and mucus production. *J. Exp. Med.* **187(6)**:939-948

231. **Komai, M., Tanaka, H., Masuda, T., Nagao, K., Ishikazi, M., Sawada, M. and Nagai, H.** (2003) Role of Th2 responses in the development of allergen-induced airway remodelling in a murine model of allergic asthma. *Br. J. Pharmacol.* **138**:912-920

232. **Swain, S. L., Weinberg, A. D., English, M. and Huston, G.** (1990) IL-4 directs the development of Th2-like helper effectors. *J. Immunol.* **145**:3796-3806

233. **Abehsira-Amar, O., Gibert, M., Joliy, M., Thèze, J. and Jankovic, D. L.** (1992) IL-4 plays a dominant role in the differential development of Th0 into Th1 and Th2 cells. *J. Immunol.* **148**:3820-3829

234. **Hilton, D. J., Zhang, J.-G., Metcalf, D., Alexander, W. S., Nicola, N. A. and Willson, T. A.** (1996) Cloning and characterization of a binding subunit of the interleukin 13 receptor that is also a component of the interleukin 4 receptor. *Proc. Natl. Acad. Sci. USA* **93**:497-501

235. **Yamaguchi, Y., Hayashi, Y., Sugama, Y., Miura, Y., Kasahara, T., Kitamura, S., Torisu, M., Mita, S., Tominaga, A., Takatsu, K. and Suda, T.** (1988) Highly purified murine interleukin 5 (IL-5) stimulates eosinophil function and prolongs in vitro survival. IL-5 as an eosinophil chemotactic factor. *J. Exp. Med.* **167**:1737-1742

236. **Yamaguchi, Y., Suda, T., Suda, J., Eguchi, M., Miura, Y., Harada, N., Tominaga, N., Tominaga, A. and Takatsu, K.** (1988) Purified interleukin 5 supports the terminal differentiation and proliferation of murine eosinophilic precursors. *J. Exp. Med.* **167**:43-56

237. **Lopez, A. F., Sanderson, C. J., Gamble, J. R., Campbell, H. D., Young, I. G. and Vadas, M. A.** (1988) Recombinant human interleukin 5 is a selective activator of human eosinophil function. *J. Exp. Med.* **167**:219-224

238. **Hogan, S. P., Koskinen, A., Matthaei, K. I., Young, I. G. and Foster, P. S.** (1998) Interleukin-5-producing $CD4^+$ T cells play a pivotal role in aeroallergen-induced eosinophilia, bronchial hyperreactivity, and lung damage in mice. *Am. J. Respir. Crit. Care Med.* **157(1)**:210-218

239. **Matsuzawa, S., Sakashita, K., Kinoshita, T., Ito, S., Yamashita, T. and Koike, K.** (2003) IL-9 enhances the growth of human mast cell progenitors under stimulation with stem cell factor. *J. Immunol.* **170**:3461-3467

240. **Eklund, K. K., Ghildyal, N., Austen, K. F. and Stevens, R. L.** (1993) Induction by IL-9 and suppression by IL-3 and IL-4 of the levels of chromosome 14-derived transcripts that encode late-expressed mouse mast cell proteases. *J. Immunol.* **151(8)**:4266-4273

241. **Vermeer, P. D., Harson, R., Einwalter, L. A., Moninger, T. and Zabner, J.** (2003) Interleukin-9 induces goblet cell hyperplasia during repair of human airway epithelia. *Am. J. Respir. Cell Mol. Biol.* **28(3)**:286-295

242. **Grünig, G., Warnock, M., Wakil, A. E., Venkayya, R., Brombacher, F., Rennick, D. M., Sheppard, D., Mohrs, M., Donaldson, D. D., Locksley, R. M. and Corry, D. B.** (1998) Requirement for IL-13 independently of IL-4 in experimental asthma. *Science* **282**:2261-2263

243. **Wills-Karp, M., Luyimbazi, J., Xu, X., Schofield, B., Neben, T. Y., Karp, C. L. and Donaldson, D. D.** (1998) Interleukin-13: central mediator of allergic asthma. *Science* **282**:2258-2261

244. **Laporte, J. C., Moore, P. E., Baraldo, S., Jouvin, M. H., Church, T. L., Schwartzman, I. N., Panettieri, Jr., R. A., Kinet, J. P. and Shore, S. A.** (2001) Direct effects of interleukin-13 on signaling pathways for physiological responses in cultured human airway smooth muscle cells. *Am. J. Respir. Crit. Care Med.* **164(1)**:141-148

245. **Nathans, D. and Smith, H. O.** (1975) Restriction endonucleases in the analysis and restructuring of DNA molecules. *Annu. Rev. Biochem.* **44**:273-293

246. **Lehman, I. R., Bessman, M. J., Simms, E. S. and Kornberg, A.** (1958) Enzymatic synthesis of deoxyribonucleic acid. I. Preparation of substrates and partial purification of an enzyme from *Escherichia coli. J. Biol. Chem.* **233**:163-170

247. **Wetmur, J. G. and Davidson, N.** (1968) Kinetics of renaturation of DNA. *J. Mol. Biol.* **31**:349-370

248. **Pardue, M. L. and Gall, J. G.** (1969) Molecular hybridization of radioactive DNA to the DNA of cytological preparations. *Proc. Natl. Acad. Sci. USA* **64**:600-604

249. **Mullis, K. B. and Faloona, F. A.** (1987) Specific synthesis of DNA in vitro via a polymerase-catalyzed chain reaction. *Methods Enzymol.* **155**:335-350

250. **Timmis, K., Cabello, F. and Cohen, S. N.** (1974) Utilization of two distinct modes of replication by a hybrid plasmid constructed in vitro from separate replicons. *Proc. Natl. Acad. Sci. USA* **71**:4556-4560

251. **Gottesman, M. M., Hicks, M. L. and Gellert, M.** (1973) Genetics and function of DNA ligase in *Escherichia coli. J. Mol. Biol.* **77(4)**:531-547

252. **Weston, A., Brown, M. G., Perkins, H. R., Saunders, J.R. and Humphreys, G. O.** (1981) Transformation of *Escherichia coli* with plasmid deoxyribonucleic acid: calcium-induced binding of deoxyribonucleic acid to whole cells and to isolated membrane fractions. *J. Bacteriol.* **145(2)**:780-787.

253. **Foster, T. J.** (1983) Plasmid-determined resistance to antimicrobial drugs and toxic metal ions in bacteria. *Microbiol. Rev.* **47(3)**:361-409.

254. **Southern, E. M.** (1992) Genome mapping: cDNA approaches. *Curr. Opin. Genet. Dev.* **2(3)**:412-416.

255. **Dodgson, J. B., Strommer, J. and Engel, J. D.** (1979) Isolation of the chicken beta-globin gene and a linked embryonic beta-like globin gene from a chicken DNA recombinant library. *Cell* **17(4)**:879-887

256. **Lathe, R.** (1985) Synthetic oligonucleotide probes deduced from amino acid sequence data. Theoretical and practical considerations. *J. Mol. Biol.* **183(1)**:1-12.

257. **Sanger, F., Nicklen, S. and Coulson, A. R.** (1977) DNA sequencing with chain-terminating inhibitors. *Proc. Natl. Acad. Sci. USA* **74(12)**:5463–5467

258. **McGinnis, W., Hart, C. P., Gehring, W. J. and Ruddle, F. H.** (1984) Molecular cloning and chromosome mapping of a mouse DNA sequence homologous to homeotic genes of *Drosophila. Cell* **38(3)**:675-680

259. **Collins, F. S.** (1992) Cystic fibrosis: molecular biology and therapeutic implications. *Science* **256(5058)**:774-779

260. **International Human Genome Sequencing Consortium.** (2001) Initial sequencing and analysis of the human genome. *Nature* **409:**860-921

261. **Grover, D., Yang, J., Tavaré, S. and Tower, J.** (2008) Simultaneous tracking of fly movement and gene expression using GFP. *BMC Biotechnol.* **8:**93-102

262. **Meng, A., Tang, H., Ong, B. A., Farrell, M. J. and Lin, S.** (1997) Promoter analysis in living zebrafish embryos identifies a cis-acting motif required for neuronal expression of GATA-2. *Proc. Natl. Acad. Sci. USA* **94(12):**6267–6272

263. **Hemsley, A., Arnheim, N., Toney, M. D., Cortopassi, G. and Galas, D. J.** (1989) A simple method for site-directed mutagenesis using the polymerase chain reaction. *Nucleic Acids Res.* **17(16):**6545–6551

264. **Makrides, S. C.** (1996) Strategies for achieving high-level expression of genes in *Escherichia coli. Microbiol. Rev.* **60(3):**512–538.

265. **Pinkert, C. A., Widera, G., Cowing, C., Heber-Katz, E., Palmiter, R. D., Flavell, R. A. and Brinster, R. L.** (1985) Tissue-specific, inducible and functional expression of the E alpha d MHC class II gene in transgenic mice. *EMBO J.* **4(9):**2225–2230.

266. **Prinzen, C., Trümbach, D., Wurst, W., Endres, K., Postina, R. and Fahrenholz, F.** (2009) Differential gene expression in ADAM10 and mutant ADAM10 transgenic mice. *BMC Genomics* **10:**66-89

267. **Kleinerman, E. S., Daniels, C. A., Polisson, R. P. and Snyderman, R.** (1976) Effect of virus infection on the inflammatory response. Depression of macrophage accumulation in influenza-infected mice. *Am. J. Pathol.* **85:**373-382

268. **Graham, B. S., Perkins, M. D., Wright, P. F. and Karzon, D. T.** (1988) Primary respiratory syncytial virus infection in mice. *J. Med. Virol.* **26:**153-162

269. **Alwan, W. H., Record, F. M. and Openshaw, P. J. M.** (1992) CD4+ T cells clear virus but augment disease in mice infected with respiratory syncytial virus. Comparison with the effects of CD8+ T cells. *Clin. Exp. Immunol.* **88:**527-536

270. **McCullers J. A. and Bartmess, K. C.** (2003) Role of neuraminidase in lethal synergism between influenza virus and Streptococcus pneumoniae. *J. Infect. Dis.***187:**1000–1009

271. **Helegbe, G. K., Huy, N. T., Yanagi, T., Shuaibu, M. N., Yamazaki, A., Kikuchi, M., Yasunami, M. and Hirayama, K.** (2009) Rate of red blood cell destruction varies in different strains of mice infected with *Plasmodium berghei-ANKA* after chronic exposure. *Malar. J.* **8:**91-103

272. **Wynn, T. A., Jankovic, D., Hieny, S., Cheever, A. W. and Sher, A.** (1995) IL-12 enhances vaccine-induced immunity to *Schistosoma mansoni* in mice and decrease T helper 2 cytokine expression, IgE production and tissue eosinophilia. *J. Immunol.* **154:**4701-4709

273. **Bouilleret, V., Ridoux, V., Depaulis, A., Marescaux, C., Nehlig, A. and Le Gal La Salle, G.** (1999) Recurrent seizures and hippocampal sclerosis following intrahippocampal kainate injection in adult mice: electroencephalography, histopathology and synaptic reorganization similar to mesial temporal lobe epilepsy. *Neuroscience* **89:**717–729

274. **Heo, K., Cho, Y.-J., Cho, K.-J., Kim, H.-W., Kim, H.-J., Shin, H. Y., Lee, B. I. and Kim, G. W.** (2006) Minocycline inhibits caspase-dependent and -independent cell death pathways and is neuroprotective against hippocampal damage after treatment with kainic acid in mice. *Neurosci. Letters* **398:**195–200

275. **Lu, M.-O., Zhang, X.-M., Mix, E., Quezada, H. C., Jin, T., Zhu, J. and Adem, A.** (2008) TNF-α receptor 1 deficiency enhances kainic acid–induced hippocampal injury in mice. *J. Neurosci. Res.* **86:**1608–1614

276. **Kuraoka, M., Furuta, T., Matsuwaki, T., Omatsu, T., Ishii, Y., Kyuwa, S. and Yoshikawa, Y.** (2009) Direct experimental occlusion of the distal middle

cerebral artery induces high reproducibility of brain ischemia in mice. *Exp. Anim.* **58(1)**:19-29

277. **Fritz, R. B., Chou, C.-H. J. and McFarlin, D. E.** (1983) Relapsing murine experimental allergic encephalomyelitis induced by myelin basic protein. *J. Immunol.* **130(3)**:1024-1026

278. **Amor, S., Baker, D., Groome, N. and Turk, J, L.** (1993) Identification of a major encephalitogenic epitope of proteolipid protein (residues 56-70) for the induction of experimental allergic encephalomyelitis in Biozzi AB/H and nonobese diabetic mice. *J. Immunol.* **150(12)**:5666-5672

279. **Anderson, M. S. and Bluestone, J. A.** (2005) The NOD mouse: a model of immune dysregulation. *Annu. Rev. Immunol.* **23**:447-485

280. **Madsen, L. S., Andersson, E. C., Jansson, L., Krogsgaard, M., Andersen, C. B., Engberg, J., Strominger, J. L., Svejgaard, A., Hjorth, J. P., Holmdahl, R., Wucherpfennig, K. W. and Fugger, L.** (1999) A humanized model for multiple sclerosis using HLA-DR2 and a human T-cell receptor. *Nature Genet.* **23**:343-347

281. **Quandt, J. A., Baig, M., Yao, K., Kawamura, K., Huh, J., Ludwin, S. K., Bian, H.-J., Bryant, M., Quigley, L., Nagy, Z. A., McFarland, H. F., Muraro, P. A., Martin, R. and Ito, K.** (2004) Unique clinical and pathological features in HLA-DRB1*0401-restricted MBP 111-129-specific humanized TCR transgenic mice. *J. Exp. Med.* **200(2)**:223-234

282. **Ellmerich, S., Takacs, K., Mycko, M., Waldner, H., Wahid, F., Boyton, R. J., Smith, P. A., Amor, S., Baker, D., Hafler, D. A., Kuchroo, V. K. and Altmann, D. M.** (2004) Disease-related epitope spread in a humanized T cell receptor transgenic model of multiple sclerosis. *Eur. J. Immunol.* **34**:1839-1848

283. **Ellmerich, S., Mycko, M., Takacs, K., Waldner, H., Wahid, F. N., Boyton, R. J., King, R. H. M., Smith, P. A., Amor, S., Herlihy, A. H., Hewitt, R. E., Jutton, M., Price, D. A., Hafler, D. A., Kuchroo, V. K. and Altmann, D. M.** (2005) High incidence of spontaneous disease in an HLA-DR15 and TCR transgenic multiple sclerosis model. *J. Immunol.* **174**:1938-1946

284. **Smith, N. and Johnson, F. J.** (2005) Early- and late-phase bronchoconstriction, airway hyper-reactivity and cell influx into the lungs, after 5'-adenosine monophosphate inhalation: comparison with ovalbumin. *Clin. Exp. Allergy* **35(4)**:522-530

285. **Hylkema, M. N., Hoekstra, M. O., Luinge, M. and Timens, W.** (2002) The strength of the OVA-induced airway inflammation in rats is strain dependent. *Clin. Exp. Immunol.* **129(3)**:390-396

286. **Kung, T. T., Jones, H., Adams III, G. K., Umland, S. P., Kreutner, W. Egan, R. W., Chapman, R. W. and Watnick, A. S.** (1994) Characterization of a murine model of allergic pulmonary inflammation. *Int. Arch. Allergy Immunol.* **105(1)**:83-90

287. **Garlisi, C. G., Falcone, A., Hey, J. A., Paster, T. M., Fernandez, X., Rizzo, C. A., Minnicozzi, M., Jones, H., Billah, M. M., Egan, R. W. and Umland, S. P.** (1997) Airway eosinophils, T cells, Th2-type cytokine mRNA, and hyperreactivity in response to aerosol challenge of allergic mice with previously established pulmonary inflammation. *Am. J. Respir. Cell Mol. Biol.* **17**:642-651

288. **Hessel, E. M., Van Oosterhout, A. J. M., Hofstra, C. L., De Bie, J. J., Garssen, J., Van Loveren, H., Verheyen, A. K. C. P., Savelkoul, H. F. J. and Nijkamp, F. P.** (1995) Bronchoconstriction and airway hyperresponsiveness after ovalbumin inhalation in sensitized mice. *Eur. J. Pharmacol.* **293**:401-412

289. **Brewer, J. M., Conacher, M., Hunter, C. A., Mohrs, M., Brombacher, F. and Alexander, J.** (1999) Aluminium hydroxide adjuvant initiates strong antigen-specific Th2 responses in the absence of IL-4- or IL-13-mediated signaling. *J. Immunol.* **163**:6448-6454

290. **di Siquiera, A. L. P., Russo, M., Steil, A. A., Facincone, S., Mariano, M. and Jancar, S.** (1997) A new murine model of pulmonary eosinophilic hypersensitivity: contribution to experimental asthma. *J. Allergy Clin. Immunol.* **100**:383-388

291. **Seymour, B. W. P., Gershwin, L. J. and Coffman, R. L.** (1998) Aerosol-induced immunoglobulin (Ig)-E unresponsiveness to ovalbumin does not require $CD8^+$ or T cell receptor (TCR)-γ/δ^+ T cells or interferon (IFN)-γ in a murine model of allergen sensitization. *J. Exp. Med.* **187(5)**:721-731

292. **Shinagawa, K. and Kojima, M.** (2003) Mouse model of airway remodeling. Strain differences. *Am. J. Respir. Crit. Care Med.* **168**:959-967

293. **Temelkovski, J., Hogan, S. P., Shepherd, D. P., Foster, P. S. and Kumar, R. K.** (1998) An improved murine model of asthma: selective airway inflammation, epithelial lesions and increased methacholine responsiveness following chronic exposure to aerosolised allergen. *Thorax* **53**:849-856

294. **Mojtabavi, N., Dekan, G., Stingl, G. and Epstein, M. M.** (2002) Long-lived Th2 memory in experimental allergic asthma. *J. Immunol.* **169**:4788-4796

295. **Wise, J. T., Baginski, T. J. and Mobley, J. L.** (1999) An adoptive transfer model of allergic lung inflammation in mice is mediated by $CD4^+CD62L^{low}CD25^+$ T cells. *J. Immunol.* **162**:5592-5600

296. **Cohn, L., Homer, R. J., Marinov, A., Rankin, J. and Bottomly, K.** (1997) Induction of airway mucus production by T helper 2 (Th2) cells: a critical role for interleukin 4 in cell recruitment but not mucus production. *J. Exp. Med.* **186(10)**:1737-1747

297. **Murphy, K. M., Heimberger, A. B. and Loh, D. Y.** (1990) Induction by antigen of intrathymic apoptosis of $CD4^+$ $CD8^+$ TCR^{lo} thymocytes in vivo. *Science* **250**:1720-1723

298. **Brusselle, G. G., Kips, J. C., Tavernier, J. H., van der Heyden, J. G., Cuvelier, C. A., Pauwels, R. A. and Bluethmann, H.** (1994) Attenuation of

allergic airway inflammation in IL-4 deficient mice. *Clin. Exp. Allergy* **24(1)**:73-80

299. **Foster, P. S., Hogan, S. P., Ramsay, A. J., Matthaei, K. I. and Young, I. G.** (1996) Interleukin 5 deficiency abolishes eosinophilia, airways hyperreactivity, and lung damage in a mouse asthma model. *J. Exp. Med.* **183**:195-201

300. **Tanaka, H., Nagai, H. and Maeda, Y.** (1998) Effect of anti-IL-4 and anti-IL-5 antibodies on allergic airway hyperresponsiveness in mice. *Life Sci.* **62(13)**:PL169-PL174

301. **McMillan, S. J., Bishop, B., Townsend, M. J., McKenzie, A. N. and Lloyd, C. M.** (2002) The absence of interleukin 9 does not affect the development of allergen-induced pulmonary inflammation nor airway hyperreactivity. *J. Exp. Med.* **195(1)**:51-57

302. **Kung, T. T., Luo, B., Crawley, Y., Garlisi, C. G., Devito, K., Minnicozzi, M., Egan, R. W., Kreutner, W. and Chapman, R. W.** (2001) Effect of anti-mIL-9 antibody on the development of pulmonary inflammation and airway hyperresponsiveness in allergic mice. *Am. J. Respir. Cell Mol. Biol.* **25**:600-605

303. **Nath, P., Leung, S. Y., Williams, A .S., Noble, A., Xie, S., McKenzie, A. N. and Chung, K. F.** (2007) Complete inhibition of allergic airway inflammation and remodelling in quadruple IL-4/5/9/13$^{-/-}$ mice. *Clin. Exp. Allergy* **37(10)**:1427-1435

304. **Lee, J. J., McGarry, M. P., Farmer, S. C., Denzler, K. L., Larson, K. A., Carrigan, P. E., Brenneise, I. E., Horton, M. A., Haczku, A., Gelfand, E. W., Leikauf, G. D. and Lee, N. A.** (1997) Interleukin-5 expression in the lung epithelium of transgenic mice leads to pulmonary changes pathognomonic of asthma. *J. Exp. Med.* **185(12)**:2143-2156

305. **Temann, U. A., Geba, G. P., Rankin, J. A. and Flavell, R. A.** (1998) Expression of interleukin 9 in the lungs of transgenic mice causes airway inflammation, mast cell hyperplasia, and bronchial hyperresponsiveness. *J. Exp. Med.* **188(7)**:1307-1320

306. **Temann, U.-A., Ray, P. and Flavell, R. A.** (2002) Pulmonary overexpression of IL-9 induces Th2 cytokine expression, leading to immune pathology. *J. Clin. Invest.* **109(1)**:29-39

307. **Zhu, Z., Homer, R. J., Wang, Z., Chen, Q., Geba, G. P., Wang, J., Zhang, Y. and Elias, J. A.** (1999) Pulmonary expression of interleukin-13 causes inflammation, mucus hypersecretion, subepithelial fibrosis, physiologic abnormalities, and eotaxin production. *J. Clin. Invest.* **103**:779-788

308. **Meyts, I., Vanoirbeek, J. A., Hens, G., Vanaudenaerde, B. M., Verbinnen, B., Bullens, D. M. A., Overbergh, L., Mathieu, C., Ceuppens, J. L. and Hellings, P. W.** (2008) T-cell mediated late increase in bronchial tone after allergen provocation in a murine asthma model. *Clin. Immunol.* **128**:248-258

309. **McMillan, S. J., Xanthou, G. and Lloyd, C. M.** (2005) Manipulation of allergen-induced airway remodeling by treatment with anti-TGF-β antibody: effect on the Smad signaling pathway. *J. Immunol.* **174**:5774-5780

310. **Alcorn, J. F., Rinaldi, L. M., Jaffe, E. F., van Loon, M., Bates, J. H. T., Janssen-Heininger, Y. M. W. and Irvin, C. G.** (2007) Transforming growth factor-β1 suppresses airway hyperresponsiveness in allergic airway disease. *Am. J. Respir. Crit. Care Med.* **176**:974-982

311. **Cheng, K. C., Lee, K. M., Krug, M. S., Watanabe, T., Suzuki, M., Choe, I. S. and Yoo, T.-J.** (1998) House dust mice-induced sensitivity in mice. *J. Allergy Clin. Immunol.* **101**:51-59

312. **Clarke, A. H., Thomas, W. R., Rolland, J. M., Dow, C. and O'Brien, R. M.** (1999) Murine allergic respiratory responses to the major house dust mite allergen Der p 1. *Int. Arch. Allergy Immunol.* **120**:126-134

313. **Duez, C., Kips, J., Pestel, J., Tournoy, K., Tonnel, A.-B. and Pauwels, R.** (2000) House dust mite-induced airway changes in hu-SCID mice. *Am. J. Respir. Crit. Care Med.* **161**:200-206

314. **Cates, E. C., Fattouh, R., Wattie, J., Inman, M. D., Goncharova, S., Coyle, A. J., Gutierrez-Ramos, J.-C. and Jordana, M.** (2004) Intranasal exposure of mice to house dust mice elicits allergic airway inflammation via a GM-CSF-mediated mechanism. *J. Immunol.* **173**:6384-6392

315. **Johnson, J. R., Wiley, R. E., Fattouh, R., Swirski, F. K., Gajewska, B. U., Coyle, A. J., Gutierrez-Ramos, J.-C., Ellis, R., Inman, M. D. and Jordana, M.** (2004) Continuous exposure to house dust mite elicits chronic airway inflammation and structural remodeling. *Am. J. Respir. Crit. Care Med* **169**:378-385

316. **Southam, D. S., Ellis, R., Wattie, J. and Inman, M. D.** (2007) Components of airway hyperresponsiveness and their associations with inflammation and remodeling in mice. *J. Allergy Clin. Immunol.* **119**:848-854

317. **Rydell-Törmänen, K., Johnson, J. R., Fattouh, R., Jordana, M. and Erjefält, J. S.** (2008) Induction of vascular remodeling in the lung by chronic house dust mite exposure. *Am. J. Respir. Cell Mol. Biol.* **39**:61-67

318. **Fattouh, R., Midence, N. G., Arias, K., Johnson, J. R., Walker, T. D., Goncharova, S., Souza, K. P., Gregory, Jr., R. C., Lonning, S., Gauldie, J. and Jordana, M.** (2008) Transforming growth factor-β regulates house dust mite-induced allergic airway inflammation but not airway remodeling. *Am. J. Respir. Crit. Care Med.* **177**:593-603

319. **Ulrich, K., Hincks, J. S., Walsh, R., Wetterstrand, E. M. C., Fidock, M. D., Sreckovic, S., Lamb, D. L., Douglas, G. J., Yeadon, M., Perros-Huguet, C. and Evans, S. M.** (2008) Anti-inflammatory modulation of chronic airway inflammation in the murine house dust mite model. *Pulm. Pharmacol. Ther.* **21**:637-647

320. **Kim, J., McKinley, L., Natarajan, S., Bolgos, G. L., Siddiqui, J., Copeland, S. and Remick, D. G.** (2006) Anti-tumor necrosis factor-α antibody treatment reduces pulmonary inflammation and methacholine hyper-responsiveness in a murine asthma model induced by house dust. *Clin. Exp. Allergy* **36**:122-132

321. **Adel-Patient, K., Nahori, M.-A., Proust, B., Lapa e Silva, J. R., Créminon, C., Wal, J.-M. and Vargaftig, B. B.** (2003) Elicitation of the allergic reaction in β-lactoglobulin-sensitized Balb/c mice: biochemical and clinical manifestations differ according to the structure of the allergen used for challenge. *Clin. Exp. Allergy* **33**:376-385

322. **Kim, J., Merry, A. C., Nemzek, J. A., Bolgos, G. L., Siddiqui, J. and Remick, D. G.** (2001) Eotaxin represents the principal eosinophil chemoattractant in a novel murine asthma model induced by house dust containing cockroach allergens. *J. Immunol.* **167**:2808-2815

323. **Cates, E. C., Gajewska, B. U., Goncharova, S., Alvarez, D., Fattouh, R., Coyle, A. J., Gutierrez-Ramos, J.-C. and Jordana, M.** (2003) Effect of GM-CSF on immune, inflammatory, and clinical responses to ragweed in a novel mouse model of mucosal sensitization. *J. Allergy Clin. Immunol.* **111**:1076-1086

324. **Hardy, C. L., Kenins, L., Drew, A. C., Rolland, J. M. and O-Hehir, R. E.** (2003) Characterization of a mouse model of allergy to a major occupational latex glove allergen Hev b 5. *Am. J. Respir. Crit. Care Med.* **167**:1393-1399

325. **Robertson, J. M., Jensen, P. E. and Evavold, B. D.** (2000) DO11.10 and OT-II T cells recognize a C-terminal ovalbumin 323-339 epitope. *J. Immunol.* **164**:4706-4712

326. **Lee, S.C., Jaffar, Z. H., Wan, K.-S., Holgate, S. T. and Roberts, K.** (1999) Regulation of pulmonary T cell responses to inhaled antigen: role in Th1- and Th2-mediated inflammation. *J. Immunol.* **162**:6867-6879

327. **Knott, P. G., Gater, P. R. and Bertrand, C. P.** (2000) Airway inflammation driven by antigen-specific resident lung $CD4^+$ T cells in αβ-T cell receptor transgenic mice. *Am. J. Respir. Crit.Care Med.* **161**:1340-1348

328. **Wilder, J. A., Collie, D. D. S., Bice, D. E., Tesfaigzi, Y., Lyons, R. C. and Lipscomb, M. F.** (2001) Ovalbumin aerosols induce airway hyperreactivity in naïve DO11.10 T cell receptor transgenic mice without pulmonary eosinophilia or OVA-specific antibody. *J. Leukoc. Biol.* **69**:538-547

329. **McKinley, L., Alcorn, J. F., Peterson, A., DuPont, R. B., Kapadia, S., Logar, A., Henry, A., Irvin, C. G., Piganelli, J. D., Ray, A. and Kolls, J. K.** (2008) Th17 cells mediate steroid-resistant airway inflammation and airway hyperresponsiveness in mice. *J. Immunol.* **181**:4089-4097

330. **Jarman, E. R., Tan, K. A. L. and Lamb, J. R.** (2005) Transgenic mice expressing the T cell antigen receptor for an immunodominant epitope of a major allergen of house dust mite develop an asthmatic phenotype on exposure of the airways to allergen. *Clin. Exp. Allergy* **35**:960-969

331. **Yssel, H., Johnson, K. E., Schneider, P. V., Wideman, J., Terr, A., Kastelein, R. and de Vries, J. E.** (1992) T cell activation-inducing epitopes of the house dust mite allergen Der p I. Proliferation and lymphokine production patterns by Der p I-specific CD4+ T cell clones. *J. Immunol.* **148(3)**:738-745

332. **van Ree, R., van Leeuwen, W. A., Bulder, I., Bond, J. and Aalberse, R. C.** (1999) Purified natural and recombinant Fel d 1 and cat albumin in in vitro diagnostics for cat allergy. *J. Allergy Clin. Immunol.* **104(6)**:1223-1230

333. **Duffort, O. A., Carreira, J., Nitti, G., Polo, F. and Lombardero, M.** (1991) Studies on the biochemical structure of the major cat allergen Felis domesticus 1. *Mol. Immunol.* **28(4-5)**:301-309

334. **Counsell, C. M., Bond, J. F., Ohman, Jr., J. L., Greenstein, J. L. and Garman, R. D.** (1996) Definition of the human T-cell epitopes of Fel d 1, the major cat allergen of the domestic cat. *J. Allergy Clinn. Immunol,* **98(5 Pt 1)**:884-894

335. **Friedl-Hajek, R., Spangfort, M. D., Schou, C., Breiteneder, H., Yssel, H. and van Neerven, R. J. J.** (1999) Identification of a highly promiscuous and an HLA allele-specific T-cell epitope in the birch major allergen Bet v 1: HLA restriction, epitope mapping and TCR sequence comparisons. *Clin. Exp. Allergy* **29**:478-487

336. **Friedl-Hajek, R., Breiteneder H., Bohle, B., Fischer, G., Ebner, C. and Scheiner, O.** (1998) Conserved sequence motifs of CDR3 loops of TCR specific for two major epitopes of the grass pollen allergen Phl p 1. *Int. Immunol.* **10(11)**:1725-1732

337. **Texier, C., Pouvelle, S., Busson, M., Hervé, M., Charron, D., Ménez, A. and Maillère, B.** (2000) HLA-DR restricted peptide candidates for bee venom immunotherapy. *J. Immunol.* **164(6)**:3177-3184

338. **Oldfield, W. L. G., Kay, A. B. and Larché, M.** (2001) Allergen-derived T cell peptide-induced late asthmatic reactions precede the induction of antigen-specific hyporesponsiveness in atopic allergic asthmatic subjects. *J. Immunol.* **167**:1734-1739

339. **Hoyne, G. F., O'Hehir, R. E., Wraith, D. C., Thomas, W. R. and Lamb, J. R.** (1993) Inhibition of T cell and antibody responses to house dust mite allergen by inhalation of the dominant T cell epitope in naïve and sensitized mice. *J. Exp. Med.* **178(5)**:1783-1788

340. **Runa Ali, F. R., Oldfield, W. L., Higashi, N., Larché, M. and Kay, A. B.** (2003) Late asthmatic reactions induced by inhalation of allergen-derived T cell peptides. *Am. J. Respir. Crit. Care Med.* **169(1)**:20-26

341. **Oldfield, W. L., Larché, M. and Kay, A. B.** (2002) Effect of T-cell peptides derived from Fel d 1 on allergic reactions and cytokine production in patients sensitive to cats: a randomised controlled trial. *Lancet* **360**:47-53

342. **Alexander, C., Tarzi, M., Larché, M. and Kay, A. B.** (2005) The effect of Fel d 1-derived peptides on upper and lower airway outcome measurements in cat-allergic subjects. *Allergy* **60(10)**:1269-1274

343. **Smith, T. R. F., Alexander, C., Kay, A. B., Larché, M. and Robinson, D. S.** (2004) Cat allergen peptide immunotherapy reduces CD4(+) CD25(+) T cells: a double-blind placebo-controlled study. *Allergy* **59(10)**:1097-1101

344. **Alexander, C., Ying, S., Kay, A. B. and Larché, M.** (2005) Fel d 1-derived T cell peptide therapy induces recruitment of CD4+ CD25+; CD4+ interferon-gamma+ T helper type 1 cells to sites of allergen-induced late-phase skin reactions in cat-allergic subjects. *Clin. Exp. Allergy* **35(1)**:52-58

345. **Verhoef, A., Alexander, C., Kay, A. B. and Larché, M.** (2005) T cell epitope immunotherapy induces a $CD4^+$ T cell population with regulatory activity. *PLoS Med.* **2(3) e78**:0253-0261

346. **Kouskoff, V., Signorelli, K., Benoist, C. and Mathis, D.** (1995) Cassette vectors directing expression of T cell receptor genes in transgenic mice. *J. Immunol. Methods* **180**:273-280

347. **Evans, R. L., Lazarus, H., Penta, A. C. and Schlossman, S. F.** (1978) Two functionally distinct subpopulations of human T cells that collaborate in the generation of cytotoxic cells responsible for cell-mediated lympholysis. *J. Immunol.* **120(4)**:1423-1428

348. **Fink, P. J. and Bevan, M. J.** (1978) H-2 antigens of the thymus determine lymphocyte specificity. *J. Exp, Med.* **148(3)**:766-775

349. **Marsh, S. G. E., Albert, E. D., Bodmer, W. F., Bontrop, R. E., Dupont, B., Erlich, H. A., Geraghty, D. E., Hansen, J. A., Hurley, C. K., Mach, B., Mayr, W. R., Parham, P., Petersdorf, E. W., Sasazuki, T., Th, G. M., Schreuder, J. L., Strominger, J. L., Svejgaard, A., Terasaki, P. I. and Trowsdale, J.** (2004) Nomenclature for factors of the HLA system. *Tissue Antigens* **65**:301-369

350. **Erb, P. and Feldmann, M.** (1975) The role of macrophages in the generation of T-helper cells. II. The genetic control of the macrophage-T-cell interaction for helper cell induction with soluble antigens. *J. Exp. Med.* **142(2)**:460-472

351. **Allison, J. P., McIntyre, B. W. and Bloch, D.** (1982) Tumor-specific antigen of murine T-lymphoma defined with monoclonal antibody. *J. Immunol.* **129(5)**:2293-2300

352. **Kappler, J., Kubo, R., Haskins, K., Hannum, C., Marrack, P., Pigeon, M., McIntyre, B., Allison, J. and Trowbridge, I.** (1983) The major histocompatibility complex-restricted antigen receptor on T cells in mouse and man: identification of constant and variable regions. *Cell* **35**:295-302

353. **Hedrick, S. M., Cohen, D. I., Nielsen, E.A. and Davis, M. M.** (1984) Isolation of cDNA clones encoding specific membrane-associated proteins. *Nature* **308**:149-153

354. **Barker, P. E., Royer, H.-D., Ruddle, F. H. and Reinherz, E. L.** (1985) Regional location of T cell receptor gene *Tiα* on human chromosome 14. *J. Exp. Med.* **162**:387-392

355. **Collins, M. K. L., Goodfellow, P. N., Dunne, M. J., Spurr, N. K., Solomon, E. and Owen, M. J.** (1984) A human T-cell antigen receptor β chain gene maps to chromosome 7. *EMBO J.* **3(10)**:2347-2349

356. **Kranz, D. M., Saito, H., Disteche, C. M., Swisshelm, K., Pravtcheva, D., Ruddle, F. H., Eisen, H. N. and Tonegawa, S.** (1985) Chromosomal locations of the murine T-cell receptor α-chain gene and the T-cell γ gene. *Science* **227**:941-945

357. **Lee, N. E., D'Eustachio, P., Pravtcheva, D., Ruddle, F. H., Hedrick, S. M. and Davis, M. M.** (1984) Murine T cell receptor beta chain is encoded on chromosome 6. *J. Exp. Med.* **160(3)**:905-913

358. **Kuhns, M. S., Davis, M. M. and Garcia, K. C.** (2006) Deconstructing the form and function of the TCR/CD3 complex. *Immunity* **24**:133-139

359. **Reinherz, E. L., Kung, P. C., Goldstein, G. and Schlossman, S. F.** (1979) Further characterization of the human inducer T cell subset defined by monoclonal antibody. *J. Immunol.* **123(6)**:2894-2896

360. **Marrack, P., Endres, R., Shimonkevitz, R., Zlotnik, A., Dialynas, D., Fitch, F. and Kappler, J.** (1983) The major histocompatibility complex-restricted antigen receptor on T cells. II. Role of the L3T4 product. *J. Exp. Med.* **158**:1077-1091

361. **Meuer, S. C., Schlossman, S. F. and Reinherz E. L.** (1982) Clonal analysis of human cytotoxic T lymphocytes: $T4^+$ and $T8^+$ effector T cells recognize products of different major histocompatibility complex regions. *Proc. Natl. Acad. Sci. USA* **79**:4395-4399

362. **Garcia, K. C., Scott, C. A., Brunmark, A., Carbone, F. R., Peterson, P. A., Wilson, I. A. and Teyton, L.** (1996) CD8 enhances formation of stable T-cell receptor/MHC class I molecule complexes. *Nature* **384**:577-581

363. **Friedman, S. M., Hunter, S. B., Irigoyen, O. H., Kung, P. C., Goldstein, G. and Chess, L.** (1981) Functional analysis of human T cell subsets defined by monoclonal antibodies. II. Collaborative T-T interactions in the generation of TNP-altered-self-reactive cytotoxic T lymphocytes. *J. Immunol.* **126(5)**:1702-1705

364. **Babbitt, B. P., Allen, P. M., Matsueda, G., Haber, E. and Unanue, E. R.** (1985) Binding of immunogenic peptides to Ia histocompatibility molecules. *Nature* **317**:359-361

365. **Chen, B. P. and Parham, P.** (1989) Direct binding of influenza peptides to class I HLA molecules. *Nature* **337**:743-745

366. **Horton, R., Wilming, L., Rand, V., Lovering, R. C., Bruford, E. A., Khodiyar, V. K., Lush, M. J., Povey, S., Talbot, Jr., C. C., Wright, M. W., Wain, H. M., Trowsdale, J., Ziegler, A. and Beck,** S. (2004) Gene map of the extended human MHC. *Nat Rev Genet.* **5(12)**:889-99

367. **HLA/IMGT database:** http://www.ebi.ac.uk/imgt/hla/stats.html

368. **Cresswell, P., Turner, M. J. and Strominger, J. L.** (1973) Papain-solubilized HL-A antigens from cultured human lymphocytes contain two peptide fragments. *Proc. Natl. Acad. Sci. USA* **70(5)**:1603-1607

369. **Wake, C. T., Long, E. O., Strubin, M., Gross, N., Accolla, R., Carrel, S. and Mach, B.** (1982) Isolation of cDNA clones encoding HLA-DR α chains. *Proc. Natl. Acad. Sci. USA* **79**:6979-6983

370. **Long, E. O., Wake, C. T., Strubin, M., Gross, N., Accolla, R. S., Carrel, S. and Mach, B.** (1982) Isolation of distinct cDNA clones encoding HLA-DR β chains by use of an expression assay. *Proc. Natl. Acad. Sci. USA* **79**:7465-7469

371. **Bjorkman, P. J., Saper, M. A., Samraoui, B., Bennett, W. S., Strominger, J. L. and Wiley, D. C.** (1987) Structure of the human class I histocompatibility antigen, HLA-A2. *Nature* **329**:506-512

372. **Brown, J. H., Jardetzky, T. S., Gorga, J. C., Stern, L. J., Urban, R. G., Strominger, J. L. and Wiley, D. C.** (1993) Three-dimensional structure of the human class II histocompatibility antigen HLA-DR1. *Nature* **364**:33-39

373. **Garboczi, D. N., Ghosh, P., Utz, U., Fan, Q. R., Biddison, W. E. and Wiley, D. C.** (1996) Structure of the complex between human T-cell receptor, viral peptide and HLA-A2. *Nature* **384**:134-141

374. **Stern, L. J., Brown, J. H., Jardetzky, T. S., Gorga, J. S., Urban, R. G., Strominger, J. L. and Wiley, D. C.** (1994) Crystal structure of the human class II MHC protein HLA-DR1 complexed with an influenza virus peptide. *Nature* **368**:215-221

375. **Bjorkman, P. J., Saper, M. A., Samraoui, B., Bennett, W. S., Strominger, J. L. and Wiley, D. C.** (1987) The foreign antigen binding site and T cell recognition regions of class I histocompatibility antigens. *Nature* **329**:512-518

376. **Hennecke, J., Carfi, A. and Wiley, D. C.** (2000) Structure of a covalently stabilized complex of a human αβ T-cell receptor, influenza HA peptide and MHC class II molecule, HLA-DR1 *EMBO J.* **19(21)**:5611-5624

377. **Rudolph, M. G., Stanfield, R. L. and Wilson, I. A.** (2006) How TCRs bind MHCs, peptides, and coreceptors. *Annu. Rev. Immunol.* **24**:419-466

378. **IMGT database:** http://imgt.cines.fr

379. **Sim, B.-C., Zerva, L., Greene, M. I. and Gascoigne, N. R. J.** (1996) Control of MHC restriction by TCR Vα CDR1 and CDR2. *Science* **273**:963-966

380. **Danska, J. S., Livingstone, A. M., Paragas, V., Ishihara, T. and Fathman, C. G.** (1990) The presumptive CDR3 regions of both T cell receptor α and β chains determine T cell specificity for myoglobin peptides. *J. Exp. Med.* **172**:27-33

381. **Lieber, M. R., Hesse, J. E., Mizuuchi, K. and Gellert, M.** (1987) Developmental stage specificity of the lymphoid V(D)J recombination activity. *Genes Dev.* **1(8)**:751-761

382. **Yancopoulos, G. D., Blackwell, T, K., Suh, H., Hood, L. and Alt, F. W.** (1986) Introduced T cell receptor variable region gene segments recombine in pre-B cells: evidence that B and T cells use a common recombinase. *Cell* **44(2)**:251-259

383. **Godfrey, D. I., Kennedy, J., Mombaerts, P., Tonegawa, S. and Zlotnik, A.** (1994) Onset of TCR-β gene rearrangement and role of TCR-β expression during $CD3^-CD4^-CD8^-$ thymocyte differentiation. *J. Immunol.* **152(10)**:4783-4792

384. **Levelt, C. N., Wang, B., Ehrfeld, A., Terhorst, C. and Eichmann, K.** (1995) Regulation of T cell receptor (TCR)-β locus allelic exclusion and initiation of TCR-α locus rearrangement in immature thymocytes by signaling through the CD3 complex. *Eur. J. Immunol.* **25(5)**:1257-1261

385. **Aifantis, I., Buer, J., von Boehmer, H. and Azogui, O.** (1997) Essential role of the pre-T-cell receptor in allelic exclusion of the T cell receptor β locus. *Immunity* 7:601-607

386. **Schatz, D. G., Oettinger, M, A. and Baltimore, D.** (1989) The V(D)J recombination activating gene, RAG-1. *Cell* **59**:1035-1048

387. **Kirch, S. A., Rathbun, G. A. and Oettinger, M. A.** (1998) Dual role of RAG2 in V(D)J recombination: catalysis and regulation of ordered Ig gene assembly. *EMBO J.* **17**:4881-4886

388. **Fugmann, S. D., Villey, I. J., Ptaszek, L. M. and Schatz, D. G.** (2000) Identification of two catalytic residues in RAG1 that define a single active site within the RAG1/RAG2 protein complex. *Mol. Cell* **5(1)**:97-107

389. **Ramsden, D. A., Baetz, K. and Wu, G. E.** (1994) Conservation of sequence in recombination signal sequence spacers. *Nucleic Acids Res.* **22**:1785-1796

390. **van Gent, D. C., Ramsden, D. A. and Gellert, M.** (1995) The RAG1 and RAG2 proteins establish the 12/23 rule in V(D)J recombination. *Cell* **85**:107-113

391. **Eastman, Q. M., Leu, T. M. J. and Schatz, D. G.** (1996) Initiation of V(D)J recombination *in vitro* obeying the 12/23 rule. *Nature* **380**:85-88

392. **Bassing, C. H., Alt, F. W., Hughes, M. M., D'Auteuil, M., Wehrly, T. D., Woodman, B. B., Gärtner, F., White, J. M., Davidson, L. and Sleckman, B. P.** (2000) Recombination signal sequences restrict chromosomal V(D)J recombination beyond the 12/23 rule. *Nature* **405**:583-586

393. **Sleckman, B. P., Bassing, C. H., Hughes, M. M., Okada, A., D'Auteuil, M., Wehrly, T. D., Woodman, B. B., Davidson, L., Chen, J. and Alt, F. W.** (2000) Mechanisms that direct ordered assembly of T cell receptor β locus V, D and J gene segments. *Proc. Natl. Acad. Sci. USA* **97(14)**:7975-7980

394. **McBlane, J. F., van Gent, D. C., Ramsden, D. A., Romeo, C., Cuomo, C. A., Gellert, M. and Oettinger, M. A.** (1995) Cleavage at a V(D)J recombination signal requires only RAG1 and RAG2 proteins and occurs in two steps. *Cell* **83**:387-395

395. **van Gent, D. C., Mizuuchi, K. and Gellert, M.** (1996) Similarities between initiation of V(D)J recombination and retroviral integration. *Science* **271**:1592-1594

396. **Agrawal, A. and Schatz, D. G.** (1997) RAG1 and RAG2 form a stable postcleavage synaptic complex with DNA containing signal ends in V(D)J recombination. *Cell* **89(1)**:43-53

397. **Bassing, C. H., Swat, W. and Alt, F. W.** (2002) The mechanism and regulation of chromosomal V(D)J recombination. *Cell* **109**:S45-S55

398. **Gu, Y., Jin, S., Gao, Y., Weaver, D. T. and Alt, F. W.** (1997) Ku70-deficient embryonic stem cells have increased ionizing radiosensitivity, defective DNA end-binding activity, and inability to support V(D)J recombination. *Proc. Natl. Acad. Sci. USA* **94**:8076-8081

399. **Difilippantonio, M. J., Zhu, J., Chen, H. T., Meffre, E., Nussenzweig, M. C., Max, E. E., Ried, T. and Nussenzweig, A.** (2000) DNA repair protein Ku80 suppresses chromosomal aberrations and malignant transformation. *Nature* **404**:510-514

400. **Gao, Y., Chaudhuri, J., Zhu, C., Davidson, L., Weaver, D. T. and Alt, F. W.** (1998) A targeted DNA-PKcs-null mutation reveals DNA-PK-independent functions for Ku in V(D)J recombination. *Immunity* **9(3)**:367-376

401. **Ma, Y., Pannicke, U., Schwarz, K. and Lieber, M.** (2002) Hairpin opening and overhang processing by an Artemis/DNA-dependent protein kinase complex in nonhomologous end joining and V(D)J recombination. *Cell* **108**:781-794

402. **Landau, N. R., Schatz, D. G., Rosa, M. and Baltimore, D** (1987) Increased frequency of N-region insertion in a murine pre-B-cell line infected with a terminal deoxynucleotidyl transferase retroviral expression vector. *Mol. Cell Biol.* **7(9)**:3237-3243

403. **Gilfillan, S., Dierich, A., Lemeur, M., Benoist, C. and Mathis, D.** (1993) Mice lacking TdT: mature animals with an immature lymphocyte repertoire. *Science* **261**:1175-1178

404. **Hughes, M. M., Yassai, M., Sedy, J. R., Wehrly, T. D., Huang, C. Y., Kanagawa, O., Gorski, J. and Sleckman, B. P.** (2003) T cell receptor CDR3

loop length repertoire is determined primarily by features of the V(D)J recombination reaction. *Eur. J. Immunol.* **33(6)**:1568-1575

405. **Li, Z., Otevrel, T., Gao, Y., Cheng, H. L., Seed, B., Stamato, T. D., Taccioli, G. E. and Alt, F. W.** (1995) The XRCC4 gene encodes a novel protein involved in DNA double-strand break repair and V(D)J recombination. *Cell* **83(7)**:1079-1089

406. **Grawunder, U., Wilm, M., Wu, X., Kulesza, P., Wilson, T. E., Mann, M. and Lieber, M. R.** (1997) Activity of DNA ligase IV stimulated by complex formation with XRCC4 protein in mammalian cells. *Nature* **388**:492-495

407. **Gao, Y., Sun, Y., Frank, K. M., Dikkes, P., Fujiwara, Y., Seidl, K. J., Sekiguchi, J. M., Rathbun, G. A., Swat, W., Wang, J., Bronson, R. T., Malynn, B. A., Bryans, M., Zhu, C., Chaudhuri, J., Davidson, L., Ferrini, R., Stamato, T., Orkin, S. H., Greenberg, M. E. and Alt, F. W.** (1998) A critical role for DNA end-joining proteins in both lymphogenesis and neurogenesis. *Cell* **95**:891-902

408. **Koch, C. A., Agyei, R., Galicia, S., Metalnikov, P., O'Donnell, P., Starostine, A., Weinfeld, M. and Durocher, D.** (2004) Xrcc4 physically links DNA end processing by polynucleotide kinase to DNA ligation by DNA ligase IV. *EMBO J.* **23(19)**:3874-3885

409. **Grawunder, U., Zimmer, D., Fugmann, S., Schwarz, K. and Lieber, M. R.** (1998) DNA ligase IV is essential for V(D)J recombination and DNA double-strand break repair in human precursor lymphocytes. *Mol. Cell* **2**:477-484

410. **Arstila, T. P., Casrouge, A., Baron, V., Even, J., Kanellopoulos, J. and Kourilsky, P.** (1999) A direct estimate of the human αβ T cell receptor diversity. *Science* **286**:958-961

411. **Casrouge, A., Beaudoing, E., Dalle, S., Pannetier, C., Kanellopoulos, J. and Kourilsky, P.** (2000) Size estimate of the αβ TCR repertoire of naïve mouse splenocytes. *J. Immunol.* **164**:5782-5787

412. **Lind, E. F., Prockop, S. E., Porritt, H. E. and Petrie, H. T** (2001) Mapping precursor movement through the postnatal thymus reveals specific microenvironments supporting defined stages of early lymphoid development. *J. Exp. Med.* **194(2)**:127-134

413. **Lepault, F., Coffman, R. L. and Weissman, I. L.** (1983) Characteristics of thymus-homing bone marrow cells. *J. Immunol.* **131(1)**:64-69

414. **Lesley, J., Hyman, R. and Schulte, R.** (1985) Evidence that the Pgp-1 glycoprotein is expressed on thymus-homing progenitor cells of the thymus. *Cell. Immunol.* **91**:397-403

415. **Bluestone, J. A., Pardoll, D., Sharrow, S. O. and Fowlkes, B. J.** (1987) Characterization of murine thymocytes with CD3-associated T-cell receptor structures. *Nature* **326**:82-84

416. **Godfrey, D. I., Kennedy, J., Suda, T. and Zlotnik, A.** (1993) A developmental pathway involving four phenotypically distinct subsets of $CD3^-CD4^-CD8^-$ triple-negative adult mouse thymocytes defined by CD44 and CD25 expression. *J. Immunol.* **150**:4244-4252

417. **Mombaerts, P., Iacomini, J., Johnson, R. S., Herrup, K., Tonegawa, S. and Papaioannou, V. E.** (1992) RAG-1-deficient mice have no mature B and T lymphocytes. *Cell* **68(5)**:869-877

418. **Shinkai, Y., Rathbun, G., Lam, K. P., Oltz, E. M., Stewart, V., Mendelsohn, M., Charron, J., Datta, M., Young, F., Stall, A. M. and Alt, F. W.** (1992) RAG-2-deficient mice lack mature lymphocytes owing to inability to initiate V(D)J rearrangement. *Cell* **68(5)**:855-867

419. **Mombaerts, P., Clarke, A. R., Rudnicki, M. A., Iacomini, J., Itohara, S., Lafaille, J. J., Wang, L., Ichikawa, Y., Jaenisch, R., Hooper, M. L. and Tonegawa, S.** (1992) Mutations in T-cell antigen receptor genes α and β block thymocyte development at different stages. *Nature* **360**:225-231

420. **Petrie, H. T., Livak, F., Schatz, D. G., Strasser, A., Crispe, I. N. and Shortman, K.** (1993) Multiple rearrangements in T cell receptor α chain genes maximise the production of useful thymocytes. *J. Exp. Med.* **178**:615-622

421. **Groettrup, M., Ungewiss, K., Azogui, O., Palacios, R., Owen, M. J., Hayday, A.C. and von Boehmer, H.** (1993) A novel disulfide-linked heterodimer on pre-T cells consists of the T cell receptor beta chain and a 33 kd glycoprotein. *Cell* **75(2)**:283-294

422. **Del Porto, P., Bruno, L., Mattei, M.-G., von Boehmer, H. and Saint-Ruf, C.** (1995) Cloning and comparative analysis of the human pre-T-cell receptor α-chain gene. *Proc. Natl. Acad. Sci. USA* **92**:12105-12109

423. **Fehling, H. J., Krotkova, A., Saint-Ruf, C. and von Boehmer, H.** (1995) Crucial role of the pre-T-cell receptor α gene in development of αβ but not γδ T cells. *Nature* **375**:795-798

424. **Borowski, C., Li, X., Aifantis, I., Gounari, F. and von Boehmer, H.** (2004) Pre-TCRα and TCRα are not interchangeable partners of TCRβ during T lymphocyte development. *J. Exp. Med.* **199(5)**:607-615

425. **Lacorazza, H. D., Tuček-Szabo, C., Vasović, L. V., Remus, K. and Nikolich-Žugich, J.** (2001) Premature TCRαβ expression and signaling in early thymocytes impair thymocyte expansion and partially block their development. *J. Immunol.* **166**:3184-3193

426. **Aifantis, I., Borowski, C., Gounari, F., Lacorazza, H. D., Nikolich-Žugich, J. and von Boehmer, H.** (2002) A critical role for the cytoplasmic tail of pTα in T lymphocyte development. *Nat. Immunol.* **3(5)**:483-488

427. **Falk, I., Nerz, G., Haidl, I., Krotkova, A. and Eichmann, K.** (2001) Immature thymocytes that fail to express TCRβ and/or TCRγδ proteins die by apoptotic cell death in the $CD44^-CD25^-$ (DN4) subset. *Eur. J. Immunol.* **31**:3308-3317

428. **Pénit, C., Lucas, B. and Vasseur, F.** (1995) Cell expansion and growth arrest phases during the transition from precursor ($CD4^-8^-$) to immature ($CD4^+8^+$) thymocytes in normal and genetically modified mice. *J. Immunol.* **154**:5103-5113

429. **Shortman, K., Vremec, D. and Egerton, M.** (1991) The kinetics of T cell antigen receptor expression by subgroups of $CD4^+8^+3^{2+}$ thymocytes as post-selection intermediates leading to mature T cells. *J. Exp. Med.* **173**:323-332

430. **Trop, S., Rhodes, M., Wiest, D. L., Hugo, P. and Zúñiga-Pflücker, J. C.** (2000) Competitive displacement of pTα by TCR-α during TCR assembly prevents surface coexpression of pre-TCR and αβ TCR. *J. Immunol.* **165**:5566-5572

431. **Elliott, J. I. and Altmann, D. M.** (1995) Dual T cell receptor alpha chain T cells in autoimmunity. *J. Exp. Med.* **182(4)**:953-959

432. **Starr, T. K., Jameson, S.C. and Hogquist, K. A.** (2003) Positive and negative selection of T cells. *Annu. Rev. Immunol.* **21**:139-176

433. **Kappler, J. W., Roehm, N. and Marrack, P.** (1987) T cell tolerance by clonal elimination in the thymus. *Cell* **49**:273-280

434. **Anderson, G., Owen, J. J. T., Moore, N. C. and Jenkinson, E. J.** (1994) Thymic epithelial cells provide unique signals for positive selection of $CD4^+$ $CD8^+$ thymocytes in vitro. *J. Exp. Med.* **179**:2027-2031

435. **Baldwin, K. K., Trenchak, B. P., Altman, J. D. and Davis, M. M.** (1999) Negative selection of T cells occurs throughout thymic development. *J. Immunol.* **163**:689-698

436. **Goldman, K. P., Park, C.-S., Kim, M., Matzinger, P. and Anderson, C. C.** (2005) Thymic cortical epithelium induces self tolerance. *Eur. J. Immunol.* **35**:709-717

437. **Mamalaki, C., Norton, T., Tanaka, Y., Townsend, A. R., Chandler, P., Simpson, E. and Kioussis, D.** (1992) Thymic depletion and peripheral activation of class I major histocompatibility complex-restricted T cells by soluble peptide in T-cell receptor transgenic mice. *Proc. Natl. Acad. Sci. USA* **89**:11342-11346

438. **Ziljstra, M., Bix, M., Simister, N. E., Loring, J. M., Raulet, D. H. and Jaenisch, R.** (1990) β2-microglobulin deficient mice lack $CD4^-$ $CD8^+$ cytolytic T cells. *Nature* **344**:742-746

439. **Anderson, M. S., Venanzi, E. S., Klein, L., Chen, Z., Berzins, S. P., Turley, S. J., von Boehmer, H., Bronson, R., Dierich, A., Benoist, C. and Mathis, D.** (2002) Projection of an immunological self shadow within the thymus by the Aire protein. *Science* **298**:1395-1401

440. **Derbinski, J., Schulte, A., Kyewski, B. and Klein, L.** (2001) Promiscuous gene expression in medullary thymic epithelial cells mirrors the peripheral self. *Nat. Immunol.* **2(11)**:1032-1039

441. **Ashton-Rickardt, P. G. and Tonegawa, S.** (1994) A differential-avidity model for T-cell selection. *Immunol. Today* **15(8)**:362-366

442. **Germain, R. N.** (2002) T-cell development and the CD4-CD8 lineage decision. *Nat. Rev. Immunol.* **2**:309-322

443. **Singer, A.** (2002) New perspectives on a developmental dilemma: the kinetic signalling model and the importance of signal duration for the CD4/CD8 lineage decision. *Curr. Opin. Immunol.* **14**:207-215

444. **Brugnera, E., Bhandoola, A., Cibotti, R., Yu, Q., Guinter, T. I., Yamashita, Y., Sharrow, S. O. and Singer, A.** (2000) Coreceptor reversal in the thymus: signalled $CD4^+8^+$ thymocytes initially terminate CD8 transcription even when differentiating into $CD8^+$ T cells. *Immunity* **13**:59-71

445. **Chen, W.** (2004) The late stage of T cell development within mouse thymus. *Cell. Mol. Immunol.* **1(1)**:3-11

446. **Choudhuri, K. and van der Merwe, P. A.** (2007) Molecular mechanisms involved in T cell receptor triggering. *Semin. Immunol.* **19**:255-261

447. **Gil, D., Schamel, W.W., Montoya, M., Sanchez-Madrid, F. and Alarcón, B.** (2002) Recruitment of Nck by CD3 epsilon reveals a ligand-induced conformational change essential for T cell receptor signalling and synapse formation. *Cell* **109**:901-912

448. **Aivazian, D., and Stern, L. J.** (2000) Phosphorylation of T cell receptor zeta is regulated by a lipid dependent folding transition. *Nat. Struct. Biol.* 7:1023-1026

449. **Campi, G., Varma, R. and Dustin, M. L.** (2005) Actin and agonist MHC-peptide complex-dependent T cell receptor microclusters as scaffolds for signalling. *J. Exp. Med.* **202**:1031-1036

450. **Irvine, D. J., Purbhoo, M. A., Krogsgaard, M. and Davis, M. M.** (2002) Direct observation of ligand recognition by T cells. *Nature* **419**:845-849

451. **Veillette, A., Bookman, M. A., Horak, E. M. and Bolen, J. B.** (1988) The CD4 and CD8 T cell surface antigens are associated with the internal membrane tyrosine-protein kinase p56lck. *Cell* **55**:301-308

452. **Schilham, M. W., Fung-Leung, W. P., Rahemtulla, A., Kuendig, T., Zhang, L., Potter, J., Miller, R. G., Hengartner, H. and Mak, T. W.** (1993) Alloreactive cytotoxic T cells can develop and function in mice lacking both CD4 and CD8. *Eur. J. Immunol.* **23**:1299-1304

453. **Krogsgaard, M., Li, Q. J., Sumen, C., Huppa, J. B., Huse, M. and Davis, M. M.** (2005) Agonist/endogenous peptide-MHC heterodimers drive T cell activation and sensitivity. *Nature* **434**:238-243

454. **Davis, S. J. and van der Merwe, P. A.** (2006) The kinetic-segregation model: TCR triggering and beyond. *Nat. Immunol.* 7:803-809

455. **Varma, R., Campi, G., Yokosuka, T., Saito, T. and Dustin, M. L.** (2006) T cell receptor-proximal signals are sustained in peripheral microclusters and terminated in the central supramolecular activation cluster. *Immunity* **25**:117-127

456. **Irles, C., Symons, A., Michel, F., Bakker, T. R., van der Merwe, P. A. and Acuto, O.** (2003) CD45 ectodomain controls interaction with GEMs and Lck activity for optimal TCR signalling. *Nat. Immunol.* **4**:189-197

457. **Choudhuri, K., Wiseman, D., Brown, M. H., Gould, K. and van der Merwe, P. A.** (2005) T cell receptor triggering is critically dependent on the dimensions of its peptide-MHC ligand. *Nature* **436**:578-582

458. **Minguet, S., Swamy, M., Alarcón, B., Luescher, I. F. and Schamel, W. W.** (2007) Full activation of the T cell receptor requires both clustering and conformational changes at CD3. *Immunity* **26**:43-54

459. **Monks, C. R., Freiberg, B. A., Kupfer, H., Sciaky, N. and Kupfer, A.** (1998) Three-dimensional segregation of supramolecular activation clusters in T cells. *Nature* **395**:82-86

460. **Isakov, N.** (1997) Immunoreceptor tyrosine-based activation motif (ITAM), a unique modul linking antigen and Fc receptors to their signalling cascades. *J. Leukoc. Biol.* **61**:6-16

461. **Irving, B. A., Chan, A. C. and Weiss, A.** (1993) Functional characterization of a signal transducing motif present in the T cell antigen receptor ζ chain. *J. Exp. Med.* **177**:1093-1103

462. **Chan, A. C., Dalton, M., Johnson, R., Kong, G.-H., Wang, T., Thoma, R. and Kurosaki, T.** (1995) Activation of ZAP-70 kinase activity by phosphorylation of tyrosine 493 is required for lymphocyte antigen receptor function. *EMBO J.* **14**:2499-2508

463. **Zhang, W., Sloan-Lancaster, J., Kitchen, J., Trible, R. P. and Samelson, L. E.** (1998) LAT: the ZAP-70 tyrosine kinase substrate that links T cell receptor to cellular activation. *Cell* **92**:83-92

464. **Zhang, W., Trible, R. P., Zhu. M., Liu, S. K., McGlade, C. J. and Samelson, L. E.** (2000) Association of Grb2, Gads, and phospholipase C-γ1 with phosphorylated LAT tyrosine residues. *J. Biol. Chem.* **275**:23355-23361

465. **Nel, A. E., Gupta, S., Lee, L., Ledbetter, J. A. and Kanner, S. B.** (1995) Ligation of the T-cell antigen receptor (TCR) induces association of hSOS1, ZAP-70, phospholipase C-γ1, and other phosphoproteins with Grb2 and the ζ-chain of the TCR.*J. Biol. Chem.* **270**:18428-18436

466. **Genot, E., Cleverley, S., Henning, S. and Cantrell, D.** (1996) Multiple p21ras effector pathways regulate nuclear factor of activated T cells. *EMBO J.* **15**:3923-3933

467. **Liu, S. K., Fang, N., Koretzky, G. A. and McGlade, C. J.** (1999) The hematopoietic-specific adaptor protein gads functions in T-cell signalling via interactions with the SLP-76 and LAT adaptors. *Curr. Biol.* **9**:67-75

468. **da Silva, A. J., Li. Z., de Vera, C., Canto, E., Findell, P. and Rudd, C. E.** (1997) Cloning of a novel T-cell protein FYB that binds FYN and SH2-domain-containing leukocyte protein 76 and modulates interleukin 2 production. *Proc. Natl. Acad. Sci. USA* **94**:7493-7498

469. **Wilkinson, B., Wang, H. and Rudd, C. E.** (2004) Positive and negative adaptors in T-cell signalling. *Immunology* **111**:368-374

470. **Tuosto, L., Michel, F. and Acuto, O.** (1996) $p95^{vav}$ associates with tyrosine-phosphorylated SLP-76 in antigen-stimulated T cells. *J. Exp. Med.* **184**:1161-1166

471. **Fischer, K.-D., Kong, Y.-Y., Nishina, H., Tedford, K., Marengére, L. E. M., Kozieradzki, I., Sasaki, T., Starr, M., Chan, G., Gardener, S., Nghiem, M. P., Bouchard, D., Barbacid, M., Bernstein, A. and Penninger, J. M.** (1998) Vav is a regulator of cytoskeletal reorganization mediated by the T-cell receptor. *Curr. Biol.* **8**:554-562

472. **Costello, P. S., Walters, A. E., Mee, P. J., Turner, M., Reynolds, L. F., Prisco, A., Sarner, N., Zamoyska, R. and Tybulewicz, V. L. J.** (1999) The Rho-family GTP exchange factor Vav is a critical transducer of T cell receptor signals to the calcium, ERK and NF-κB pathways. *Proc. Natl. Acad. Sci. USA* **96**:3035-3040

473. **Reynolds, L. F., Smyth, L. A., Norton, T., Freshney, N., Downward, J., Kioussis, D. and Tybulewicz, V. L. J.** (2002) Vav1 transduces T cell receptor signals to the activation of phospholipase C-γ1 via phosphoinositide 3-kinase-dependent and -independent pathways. *J. Exp. Med.* **195**:1103-1114

474. **Rebecchi, M. J. and Pentyala, S. N.** (2000) Structure, function, and control of phophoinositide-specific phospholipase C. *Physiol. Rev.* **80**:1291-1335

475. **Liu, K.-Q., Bunnell, S. C., Gurniak, C. B. and Berg, L. J.** (1998) T cell receptor-initiated calcium release is uncoupled from capacitative calcium entry in Itk-deficient T cells. *J. Exp. Med.* **187**:1721-1727

476. **Sun, Z., Arendt, C. W., Ellmeier, W., Schaeffer, E. M., Sunshine, M. J., Gandhi, L., Annes, J., Petrzilka, D., Kupfer, A., Schwartzberg, P. L. and Littman, D. R.** (2000) PKC-θ is required for TCR-induced NK-κB activation in mature but not immature T lymphocytes. *Nature* **404**:402-407

477. **Corado, J., Le Deist, F., Griscelli, C. and Fischer, A.** (1990) Inositol 1,4,5-trisphosphate- and arachidonic acid-induced calcium mobilization in T and B lymphocytes. *Cell. Immunol.* **126**:245-254

478. **Hogan, P.G. and Li, H.** (2005) Calcineurin. *Curr. Biol.* **15**:R442-R443

479. **McCaffrey, P. G., Perrino, B. A., Soderling, T. R. and Rao, A.** (1993) NF-AT_p, a T lymphocyte DNA-binding protein that is a target for calcineurin and immunosuppressive drugs. *J. Biol. Chem.* **268**:3747-3752

480. **Acuto, O., Di Bartolo, V. and Michel, F.** (2008) Tailoring T-cell receptor signals by proximal negative feedback mechanisms. *Nat. Rev. Immunol.* **8**:699-712

481. **Nel. A. E.** (2002) T-cell activation through the antigen receptor. Part 1: Signaling components, signaling pathways, and signal integration at the T-cell antigen receptor synapse. *J. Allergy Clin. Immunol.* **109**:758-770

482. **Bergman, M., Mustelin, T., Oetken, C., Partanen, J., Flint, N. A., Amrein, K. E., Autero, M., Burn, P. and Alitalo, K.** (1992) The human $p50^{csk}$ tyrosine kinase phosphorylates $p56^{lck}$ at Tyr-505 and down regulates its catalytic activity. *EMBO J.* **11**:2919-2924

483. **Davidson, D., Bakinowski, M., Thomas, M. L., Horejsi, V. and Veillette, A.** (2003) Phosphorylation-dependent regulation of T-cell activation by PAG/Cbp, a lipid raft-associated transmembrane adaptor. *Mol. Cell. Biol.* **23**:2017-2028

484. **Cahir McFarland, E. D., Hurley, T. R., Pingel, J. T., Sefton, B. M., Shaw, A. and Thomas, M. L.** (1993) Correlation between Src family member regulation by the protein-tyrosine-phosphatase CD45 and transmembrane signlaing through the T-cell receptor. *Proc. Natl. Acad. Sci USA* **90**:1402-1406

485. **D'Oro, U., Sakaguchi, K., Appella, E. and Ashwell, J. D.** (1996) Mutational analysis of Lck in CD45-negative T cells: dominant role of tyrosine 394 phosphorylation in kinase activity. *Mol. Cell. Biol.* **16**:4996-5003

486. **Blanchard, N. and Hivroz, C.** (2002) The immunological synapse: the more you look the less you know... *Biol. of the Cell* **94**:345-354

487. **Davis, D. M.** (2002) Assembly of the immunological synapse for T cells and NK cells. *Trends Immunol.* **23(7)**:356-363

488. **Stoll, S., Delon, J., Brotz, T. M. and Germain, R. N.** (2002) Dynamic imaging of T cell-dendritic cell interactions in lymph nodes. *Science* **296**:1873-1876

489. **Holdorf, A. D., Lee, K. H., Burack, W. R., Allen, P. M. and Shaw, A. S.** (2002) Regulation of Lck activity by CD4 and CD28 in the immunological synapse. *Nat. Immunol.* **3**:259–264

490. **Blanchard, N., di Bartolo, V. and Hivroz, C.** (2002) In the immune synapse, ZAP-70 controls T cell polarization and recruitment of signaling proteins but not formation of the synaptic pattern. *Immunity* **17**:389-399

491. **Bromley, S. K., Iaboni, A., Davis, S. J., Whitty, A., Green, J. M., Shaw, A. S., Weiss, A. and Dustin, M.L.** (2001) The immunological synapse and CD28–CD80 interactions. *Nat. Immunol.* **2**:1159–1166

492. **Leupin, O., Zaru, R., Laroche, T., Muller, S. and Valitutti, S.** (2000) Exclusion of CD45 from the T-cell receptor signaling area in antigen-stimulated T lymphocytes. *Curr. Biol.* **10**:277-280

493. **Delon, J., Kaibuchi, K. and Germain, R.N.** (2001) Exclusion of CD43 from the immunological synapse is mediated by phosphorylation-regulated relocation of the cytoskeletal adaptor moesin. *Immunity* **15**:691–701

494. **Grakoui, A., Bromley, S. K., Sumen, C., Davis, M. M., Shaw, A. S., Allen, P. M. and Dustin, M. L.** (1999) The immunological synapse: a molecular machine controlling T cell activation. *Science* **285**:221-227

495. **Lee, K. H., Holdorf, A.D., Dustin, M. L., Chan, A. C., Allen, P. M. and Shaw, A. S.** (2002) T cell receptor signalling precedes immunological synapse formation. *Science* **295**:1539-1542

496. **Lee, K. H., Dinner, A.R., Tu, C., Campi, G., Raychaudhuri, S., Varma, R., Sims, T. N., Burack, W. R., Wu, H., Wang, J., Kanagawa, O., Markiewicz, M., Allen, P. M., Dustin, M. L., Chakraborty, A. K. and Shaw, A. S.** (2003) The immunological synapse balances T cell receptor signaling and degradation. *Science* **302**:1218–1222

497. **Hailman, E., Burack, W. R., Shaw, A. S., Dustin, M. L. and Allen, P.M.** (2002) Immature $CD4^+CD8^+$ thymocytes form a multifocal immunological synapse with sustained tyrosine phosphorylation. *Immunity* **16**:839–848

498. **Krummel, M. F., Sjaastad, M. D., Wulfing, C. and Davis, M.M.** (2000) Differential clustering of CD4 and CD3zeta during T cell recognition. *Science* **289**:1349–1352

499. **Campi, G., Varma, R. and Dustin, M.L.** (2005) Actin and agonist MHC-peptide complex-dependent T cell receptor microclusters as scaffolds for signaling. *J. Exp. Med.* **202**:1031–1036

500. **Varma, R., Campi, G., Yokosuka, T., Saito, T. and Dustin, M.L.** (2006) T cell receptor-proximal signals are sustained in peripheral microclusters and terminated in the central supramolecular activation cluster. *Immunity* **25**:117–127

501. **Yokosuka, T., Sakata-Sogawa, K., Kobayashi, W., Hiroshima, M., Hashimoto-Tane, A., Tokunaga, M., Dustin, M. L. and Saito, T.** (2005) Newly generated T cell receptor microclusters initiate and sustain T cell activation by recruitment of Zap70 and SLP-76. *Nat. Immunol.* **6**:1253–1262

502. **Egen, J. G. and Allison, J. P.** (2002) Cytotoxic T lymphocyte antigen-4 accumulation in the immunological synapse is regulated by TCR signal strength. *Immunity* **16**:23–35

503. **Stinchcombe, J. C., Bossi, G., Booth, S. and Griffiths, G. M.** (2001) The immunological synapse of CTL contains a secretory domain and membrane bridges. *Immunity* **15**:751–761

504. **Kupfer, A., Mosmann, T. R. and Kupfer, H.** (1991) Polarized expression of cytokines in cell conjugates of helper T cells and splenic B cells. *Proc. Natl. Acad. Sci. USA* **88**:775-779

505. **Szabo, S. J., Kim, S. T., Costa, G. L., Zhang, X., Fathman, C. G. and Glimcher, L. H.** (2000) A novel transcription factor, T-bet, directs Th1 lineage commitment. *Cell* **100**:655-669

506. **Lighvani, A. A., Frucht, D. M., Jankovic, D., Yamane, H., Aliberti, J., Hissong, B. D., Nguyen, B. V., Gadina, M., Sher, A., Paul, W. E. and O'Shea, J. J.** (2001) T-bet is rapidly induced by interferon-γ in lymphoid and myeloid cells. *Proc. Natl. Acad. Sci. USA* **98**:15137-15142

507. **Kotenko, S. V., Izotova, L. S., Pollack, B. P., Mariano, T. M., Donnelly, R. J., Muthukumaran, G., Cook, J. R., Garotta, G., Silvennoinen, O., Ihle, J. N. and Pestka, S.** (1995) Interaction between the components of the interferon γ receptor complex. *J. Biol. Chem.* **270**:20915-20921

508. **Afkarian, M., Sedy, J. R., Yang, J., Jacobson, N. G., Cereb, N., Yang, S. Y., Murphy, T. L. and Murphy, K. M.** (2002) T-bet is a STAT1-induced regulator of IL-12R expression in naive $CD4^+$ T cells. *Nat. Immunol.* **3**:549-557

509. **Mullen, A. C., High, F. A., Hutchins, A. S., Lee, H. W., Villarino, A. V., Livingston, D. M., Kung, A. L., Cereb, N., Yao, T. P., Yang, S. Y. and Reiner, S. L.** (2001) Role of T-bet in commitment of TH1 cells before IL-12-dependent selection. *Science* **292**:1907-1910

510. **Hsieh, C. S., Macatonia, S. E., Tripp, C. S., Wolf, S. F., O'Garra, A. and Murphy, K. M.** (1993) Development of TH1 $CD4^+$ T cells through IL-12 produced by Listeria-induced macrophages. *Science* **260**:547-549

511. **Macatonia, S. E., Hosken, N. A., Litton, M., Vieira, P., Hsieh, C. S., Culpepper, J. A., Wysocka, M., Trinchieri, G., Murphy, K. M. and O'Garra, A.** (1995) Dendritic cells produce IL-12 and direct the development of Th1 cells from naive $CD4^+$ T cells. *J. Immunol.* **154**:5071-5079

512. **Orange, J. S. and Biron, C. A.** (1996) An absolute and restricted requirement for IL-12 in natural killer cell IFN-γ production and antiviral defense. Studies of natural killer and T cell responses in contrasting viral infections. *J. Immunol.* **156**:1138-1142

513. **Bacon, C. M., McVicar, D. W., Ortaldo, J. R., Rees, R. C., O'Shea, J. J. and Johnston, J. A.** (1995) Interleukin 12 (IL-12) induces tyrosine phosphorylation of JAK2 and TYK2: differential use of Janus family tyrosine kinases by IL-2 and IL-12. *J. Exp. Med.* **181**:399-404

514. **Jacobson, N. G., Szabo, S. J., Weber-Nordt, R. M., Zhong, Z., Schreiber, R. D., Darnell, Jr., J. E. and Murphy, K. M.** (1995) Interleukin 12 signaling in T

helper type 1 (Th1) cells involves tyrosine phosphorylation of signal transducer and activator of transcription (Stat) 3 and Stat4. *J. Exp. Med.* **181**:1755-1762

515. **Seder, R. A., Gazzinelli, R., Sher, A. and Paul, W. E.** (1993) Interleukin 12 acts directly on $CD4^+$ T cells to enhance priming for interferon γ production and diminishes interleukin 4 inhibition of such priming. *Proc. Natl. Acad. Sci. USA* **90**:10188-10192

516. **Yoshimoto, T., Takeda, K., Tanaka, T., Ohkusu, K., Kashiwamura, S.-I., Okamura, H., Akira, S. and Nakanishi, K.** (1998) IL-12 up-regulates IL-18 receptor expression on T cells, Th1 cells, and B cells: synergism with IL-18 for IFN-γ production. *J. Immunol.* **161**:3400-3407

517. **Robinson, D., Shibuya, K., Mui, A., Zonin, F., Murphy, E., Sana, T., Hartley, S, B., Menon, S., Kastelein, R., Bazan, F. and O'Garra, A.** (1997) IGIF does not drive Th1 development but synergizes with IL-12 for interferon-γ production and activates IRAK and NFκB. *Immunity* **7**:571-581

518. **Hibbert, L., Pflanz, S., de Waal Malefyt, R. and Kastelein, R. A.** (2003) IL-27 and IFN-α signal via Stat1 and Stat3 and induce T-bet and IL-12Rβ2 in naive T cells. *J. Interferon Cytokine Res.* **23**:513-522

519. **Zheng, W.-P. and Flavell, R.** (1997) The transcription factor GATA-3 is necessary and sufficient for Th2 cytokine gene expression in CD4 T cells. *Cell* **89**:587-596

520. **Chen, X. H., Patel, B. K. R., Wang, L.-M., Frankel, M., Ellmore, N., Flavell, R. A., LaRochelle, W. J. and Pierce, J. H.** (1997) Jak1 expression is required for mediating interleukin-4-induced tyrosine phosphorylation of insulin receptor substrate and Stat6 signaling molecules. *J. Biol. Chem.* **272**:6556-6560

521. **Malabarba, M. G., Kirken, R. A., Rui, H., Koettnitz, K., Kawamura, M., O'Shea, J. J., Kalthoff, F. S. and Farrar, W. L.** (1995) Activation of JAK3, but not JAK1, is critical to interleukin-4 (IL4) stimulated proliferation and requires a membrane-proximal region of IL4 receptor α. *J. Biol. Chem.* **270**:9630-9637

522. **Zhu, J., Min, B., Hu-Li, J., Watson, C. J., Grinberg, A., Wang, Q., Killeen, N., Urban, Jr., J. F., Guo, L. and Paul, W. E.** (2004) Conditional deletion of Gata3 shows its essential function in T(H)1-T(H)2 responses. *Nat. Immunol.* **5**:1157-1165

523. **Ouyang, W., Löhning, M., Gao, Z., Assenmacher, M., Ranganath, S., Radbruch, A. and Murphy, K. M.** (2000) Stat6-independent GATA-3 autoactivation directs IL-4-independent Th2 development and commitment. *Immunity* **12**:27-37

524. **Bjerke, T., Gaustadnes, M., Nielsen, S., Nielsen, L. P., Schiøtz, P. O., Rudiger, N., Reimert, C. M., Dahl, R., Christensen, I. and Poulsen, L. K.** (1996) Human blood eosinophils produce and secrete interleukin 4. *Respir. Med.* **90**:272-277

525. **Ho, I. C., Hodge, M. R., Rooney, J. W. and Glimcher, L. H.** (1996) The proto-oncogene c-maf is responsible for tissue-specific expression of interleukin-4. *Cell* **85**:973-983

526. **Kim, J. I., Ho, I.-C., Grusby, M. J. and Glimcher, L. H.** (1999) The transcription factor c-Maf controls the production of interleukin-4 but not other Th2 cytokines. *Immunity* **10**:745-751

527. **Zhu, J., Cote-Sierra, J., Guo, L. and Paul, W. E.** (2003) Stat5 activation plays a critical role in Th2 differentiation. *Immunity* **19**:739-748

528. **Cote-Sierra, J., Foucras, G., Guo, L., Chiodetti, L., Young, H. A., Hu-Li, J., Zhu, J. and Paul, W. E.** (2004) Interleukin 2 plays a central role in Th2 differentiation. *Proc. Natl. Acad. Sci. USA* **101**:3880-3885

529. **Agarwal, S., Avni, O. and Rao, A.** (2000) Cell-type-restricted binding of the transcription factor NFAT to a distal IL-4 enhancer in vivo. *Immunity* **12**:643-652

530. **Ivanov, I. I., McKenzie, B. S., Zhou, L., Tadokoro, C. E., Lepelley, A., Lafaille, J. J., Cua, D. J. and Littman, D. R.** (2006) The orphan nuclear receptor RORγt directs the differentiation of proinflammatory IL-17$^+$ T helper cells. *Cell* **126**:1121-1133

531. **Veldhoen, M., Hocking, R. J., Atkins, C. J., Locksley, R. M. and Stockinger, B.** (2006) TGF-β in the context of an inflammatory cytokine milieu supports de novo differentiation of IL-17-producing T cells. *Immunity* **24**:179-189

532. **Bettelli, E., Carrier, Y., Gao, W., Korn, T., Strom, T. B., Oukka, M., Weiner, H. L. and Kuchroo, V. K.** (2006) Reciprocal developmental pathways for the generation of pathogenic effector TH17 and regulatory T cells. *Nature* **441**: 235-238

533. **Annunziato, F., Cosmi, L., Liotta, F., Maggi, E. and Romagnani, S.** (2008) The phenotype of human Th17 cells and their precursors, the cytokines that mediate their differentiation and the role of Th17 cells in inflammation. *Int. Immunol.* **20**: 1361-1368

534. **Nishihara, M., Ogura, H., Ueda, N., Tsuruoka, M., Kitabayashi, C., Tsuji, F., Aono, H., Ishihara, K., Huseby, E., Betz, U. A. K., Murakami, M. and Hirano, T.** (2007) IL-6-gp130-STAT3 in T cells directs the development of IL-17$^+$ T_h with a minimum effect on that of Treg in the steady state. *Int. Immunol.* **19**:695-702

535. **Stritesky, G. L., Yeh, N. and Kaplan, M. H.** (2008) IL-23 promotes maintenance but not commitment to the Th17 lineage. *J. Immunol.* **181**:5948-5955

536. **Gajewski, T. F. and Fitch, F. W.** (1988) Anti-proliferative effect of IFN-γ in immune regulation. I. IFN-γ inhibits the proliferation of Th2 but not Th1 murine helper T lymphocytes. *J. Immunol.* **140**:4245-4252

537. **Manetti, R., Parronchi, P., Giudizi, M. G., Piccinni, M. P., Maggi, E., Trinchieri, G. and Romagnani, S.** (1993) Natural killer cell stimulatory factor (interleukin 12 [IL-12]) induces helper T type 1 (Th1)-specific immune responses and inhibits the development of IL-4-producing Th cells. *J. Exp. Med.* **177**:1199-1204

538. **Usui, T., Preiss, J. C., Kanno, Y., Yao, Z. J., Bream, J. H., O'Shea, J. J. and Strober, W.** (2006) T-bet regulates Th1 responses through essential effects on GATA-3 function rather than on *IFNG* gene acetylation and transcription. *J. Exp. Med.* **203**:755-766

539. **Powrie, F., Menon, S. and Coffman, R. L.** (1993) Interleukin-4 and interleukin-10 synergize to inhibit cell-mediated immunity in vivo. *Eur. J. Immunol.* **23**:2223-2229

540. **Ferber, I. A., Lee, H.-J., Zonin, F., Heath, V., Mui, A., Arai, N. and O'Garra, A.** (1999) GATA-3 significantly downregulates IFN-γ production from developing Th1 cells in addition to inducing IL-4 and IL-5 levels. *Clin. Immunol.* **91**:134-144

541. **Maldonado, R. A., Irvine, D. J., Schreiber, R. and Glimcher, L. H.** (2004) A role for the immunological synapse in lineage commitment of CD4 lymphocytes. *Nature* **431**:527-532

542. **Maldonado, R. A., Soriano, M. A., Perdomo, L. C., Sigrist, K., Irvine, D. J., Decker, T. and Glimcher, L. H.** (2009) Control of T helper cell differentiation through cytokine receptor inclusion in the immunological synapse. *J. Exp. Med.* **206:**877-892

543. **Svetic, A., Jian, Y. C., Lu, P., Finkelman, F. D. and Gause, W. C.** (1993) *Brucella abortus* induces a novel cytokine gene expression pattern characterised by elevated IL-10 and IFN-γ in $CD4^+$ T cells. *Int. Immunol.* **5**:877-883

544. **Noben-Trauth, N., Kropf, P. and Müller, I.** (1996) Susceptibility to Leishmania major infection in interleukin-4-deficient mice. *Science* **271**:987-990

545. **McKenzie, G. J., Emson, C. L., Bell, S. E., Anderson, S., Fallon, P., Zurawski, G., Murray, R., Grencia, R. and McKenzie, A. N. J.** (1998) Impaired development of Th2 cells in IL-13-deficient mice. *Immunity* **9**:423-432

546. **Seder, R. A., Germain, R. N., Linsley, P. S. and Paul, W. E.** (1994) CD28-mediated costimulation of interleukin 2 (IL-2) production plays a critical role in T cell priming for IL-4 and interferon γ production. *J. Exp. Med.* **179**:299-304

547. **Kapsenberg, M. L., Hilkens, C. M. U., Wierenga, E. A. and Kalinski, P.** (1999) The paradigm of type 1 and type 2 antigen-presenting cells. Implications for atopic allergy. *Clin. Exp. Allergy* **29(s2)**:33-36

548. **Mazzoni, A. and Segal, D. M.** (2004) Controlling the Toll road to dendritic cell polarization. *J. Leukoc. Biol.* **75**:721-730

549. **de Jong, E. C., Vieira, P. L., Kalinski, P., Schuitemaker, J. H. N., Tanaka, Y., Wierenga, E. A., Yazdanbakhsh, M. and Kapsenberg, M. L.** (2002) Microbial compounds selectively induce Th1 cell-promoting or Th2 cell-promoting dendritic cells in vitro with diverse Th cell-polarizing signals. *J. Immunol.* **168**:1704-1709

550. **Pulendran, B., Kumar, P., Cutler, C. W., Mohamadzadeh, M., Van Dyke, T. and Banchereau, J.** (2001) Lipopolysaccharides from distinct pathogens induce different classes of immune responses. *J. Immunol.* **167**:5067-5076

551. **Manickasingham, S. P., Edwards, A. D., Schulz, O. and Reis e Sousa, C.** (2003) The ability of murine dendritic cell subsets to direct T helper cell differentiation is dependent on microbial signals. *Eur. J. Immunol.* **33**:101-107

552. **Hayes, M. P., Wang, J. and Norcross, M. A.** (1995) Regulation of interleukin-12 expression in human monocytes: selective priming by interferon-gamma of lipopolysaccharide-inducible p35 and p40 genes. *Blood* **86**:646-650

553. **Kalinski, P., Hilkens, C. M. U., Snijders, A., Snijdewint, F. G. M. and Kapsenberg, M. L.** (1997) IL-12-deficient dendritic cells, generated in the presence of prostaglandin E_2, promote type 2 cytokine production in maturing human naïve T helper cells. *J. Immunol.* **159**:28-35

554. **Iwasaki, A. and Kelsall, B. L.** (1999) Freshly isolated Peyer's patch, but not spleen, dendritic cells produce interleukin 10 and induce differentiation of T helper type 2 cells. *J. Exp. Med.* **190**:229-239

555. **Constant, S. L., Lee, K. S. and Bottomly, K.** (2000) Site of antigen delivery can influence T cell priming: pulmonary environment promotes preferential Th2-type differentiation. *Eur. J. Immunol.* **30**:840-847

556. **Tao, X., Constant, S., Jorritsma, P. and Bottomly, K.** (1997) Strength of TCR signal determined the costimulatory requirements for Th1 and Th2 $CD4^+$ T cell differentiation. *J. Immunol.* **159**:5956-5963

557. **Lenschow, D. J., Herold, K. C., Rhee, L., Patel, B., Koons, A., Qin, H.-Y., Fuchs, E., Singh, B., Thompson, C. B. And Bluestone, J. A.** (1997) CD28/B7 regulation of Th1 and Th2 subsets in the development of autoimmune diabetes. *Immunity* **5**:285-293

558. **Kuchroo, V. K., Das, M. P., Brown, J. A., Ranger, A. M., Zamvil, S. S., Sobel, R. A., Weiner, H. L., Nabavi, N. and Glimcher, L. H.** (1995) B7-1 and B7-2 costimulatory molecules activate differentially the Th1/Th2 developmental pathways: application to autoimmune disease therapy. *Cell* **80**:707-718

559. **Freeman, G. J., Boussiotis, V. A., Anumanthan, A., Bernstein, G. M., Ke, X.-Y., Rennert, P. D., Gray, G. S., Gribben, J. G. and Nadler, L. M.** (1995) B7-1 and B7-2 do not deliver identical costimulatory signals, since B7-2 but not B7-1 preferentially costimulates the initial production of IL-4. *Immunity* **2**:523-532

560. **Elloso, M. M. and Scott, P.** (1999) Expression and contribution of B7-1 (CD80) and B7-2 (CD86) in the early immune response to Leishmania major infection. *J. Immunol.* **162**:6708-6715

561. **Ekkens, M. J., Liu, Z., Liu, Q., Foster, A., Whitmire, J., Pesce, J., Sharpe, A. H., Urban, J. F. and Gause, W. C.** (2002) Memory Th2 effector cells can develop in the absence of B7-1/B7-2, CD28 interactions, and effector Th cells after priming with an intestinal nematode parasite. *J. Immunol.* **168**:6344-6351

562. **Odobasic, D., Leech, M. T., Xue, J. R. and Holdsworth, S. R.** (2008) Distinct in vivo roles of CD80 and CD86 in the effector T-cell responses inducing antigen-induced arthritis. *Immunology* **124**:503-513

563. **Flynn, S., Toellner, K.-M., Raykundalia, C., Goodall, M. and lane, P.** (1998) CD4 T cell cytokine differentiation: the B cell activation molecule, OX40 ligand, instructs CD4 T cells to express interleukin 4 and upregulates expression of the chemokine receptor, Blr-1. *J. Exp. Med.* **188**:297-304

564. **McAdam, A. J., Chang, T. T., Lumelsky, A. E., Greenfield, E. A., Boussiotis, V. A., Duke-Cohan, J. S., Chernova, T., Malenkovich, N., Jabs, C., Kuchroo, V. K., Ling, V., Collins, M., Sharpe, A. H. and Freeman, G. J.** (2000) Mouse inducible costimulatory molecule (ICOS) expression in enhanced by CD28 costimulation and regulates differentiation of $CD4^+$ T cells. *J. Immunol.* **165**:5035-5040

565. **Brown, D. R., Moskowitz, N. H., Killeen, N. and Reiner, S. L.** (1997) A role for CD4 in peripheral T cell differentiation. *J. Exp. Med.* **186**:101-107

566. **Goedert, S., Germann, T., Hoehn, P., Koelsch, S., Palm, N., Rüde, E. and Schmitt, E.** (1996) Th1 development of naive $CD4^+$ T cells is inhibited by co-activation with anti-CD4 monoclonal antibodies. *J. Immunol.* **157**:566-573

567. **Salomon, B. And Bluestone, J. A.** (1996) LFA-1 interaction with ICAM-1 and ICAM-2 regulates Th2 cytokine production. *J. Immunol.* **161**:5138-5142

568. **Rogers, P. R. and Croft, M.** (2000) CD28, Ox-40, LFA-1, and CD4 modulation of Th1/Th2 differentiation is directly dependent on the dose of antigen. *J. Immunol.* **164**:2955-2963

569. **Chaturvedi, P., Yu, Q., Southwood, S., Sette, A. and Singh, B.** (1996) Peptide analogs with different affinities for MHC alter the cytokine profile of T helper cells. *Int. Immunol.* **8**:745-755

570. **Pfeiffer, C., Stein, J., Southwood, S., Ketelaar, H., Sette, A. and Bottomly, K.** (1995) Altered peptide ligands can control CD4 T lymphocyte differentiation in vivo. *J. Exp. Med.* **181**:1569-1574

571. **Secrist, H., DeKruyff, R. H. and Umetsu, D. T.** (1995) Interleukin 4 production by $CD4^+$ T cells from allergic individuals is modulated by antigen concentration and antigen-presenting cell type. *J. Exp. Med.* **181**:1081-1089

572. **Constant, S., Pfeiffer, C., Woodard, A., Pasqualini, T. and Bottomly, K.** (1995) Extent of T cell receptor ligation can determine the functional differentiation of naïve $CD4^+$ T cells. *J. Exp. Med.* **182**:1591-1596

573. **Hosken, N. A., Shibuya, K., Heath, A. W., Murphy, K. M. and O'Garra, A.** (1995) The effect of antigen dose on $CD4^+$ T helper cell phenotype in a T cell receptor-αβ-transgenic model. *J. Exp. Med.* **182**:1579-1584

574. **Constant, S. L. and Bottomly, K.** (1997) Induction of Th1 and Th2 $CD4^+$ T cell responses: the alternative approaches. *Annu. Rev. Immunol.* **15**:297-322

575. **Boutin, Y., Leitenberg, D., Tao, X. and Bottomly, K.** (1997) Distinct biochemical signals characterize agonist- and altered peptide ligand-induced differentiation of naive $CD4^+$ T cells into Th1 and Th2 subsets. *J. Immunol.* **159**:5802-5809

576. **Brogdon, J. L., Leitenberg, D. and Bottomly, K.** (2002) The potency of TCR signalling differentially regulates NFATc/p activity and early IL-4 transcription in naive $CD4^+$ T cells. *J. Immunol.* **168**:3825-3832

577. **Iezzi, G., Karjaleinen, K. and Lanzavecchia, A.** (1998) The duration of antigenic stimulation determines the fate of naive and effector T cells. *Immunity* **8**:89-95

578. **Iezzi, G., Scotet, E., Scheidegger, D. and Lanzavecchia, A.** (1999) The interplay between the duration of TCR and cytokine signalling determines T cell polarization. *Eur. J. Immunol.* **29**:4092-4101

579. **Corr, M., Slanetz, A. E., Boyd, L. F., Jelonek, M. T., Khilko, S., al-Ramadi, B. K., Kim, Y. S., Maher, S. E., Bothwell, A. L. and Margulies, D. H.** (1994) T cell receptor-MHC class I peptide interactions: affinity, kinetics, and specificity. *Science* **265**:946-949

580. **Lyons, D. S., Lieberman, S. A., Hampl, J., Boniface, J. J., Chien, Y., Berg, L. J. and Davis, M. M.** (1996) A TCR binds to antagonist ligands with lower affinities and faster dissociation rates than to agonists. *Immunity* **5**:53-61

581. **Valitutti, S., Müller, S., Cella, M., Padovan, E. and Lanzavecchia, A.** (1995) Serial triggering of many T-cell receptors by a few peptide-MHC complexes. *Nature* **375**:148-151

582. **Valitutti, S. and Lanzavecchia, A.** (1997) Serial triggering of TCRs: a basis for the sensitivity and specificity of antigen recognition. *Immunol. Today* **18**:299-304

583. **McKeithan, T. W.** (1995) Kinetic proofreading in T-cell receptor signal transduction. *Proc. Natl. Acad. Sci. USA* **92**:5042-5046

584. **Kalergis, A. M., Boucheron, N., Doucey, M.-A., Palmieri, E., Goyarts, E. C., Vegh, Z., Luescher, I. F. and Nathenson, S. G.** (2001) Efficient T cell activation requires an optimal dwell-time of interaction between the TCR and the pMHC complex. *Nat. Immunol.* **2**:229-234

585. **Kjer-Nielsen, L., Clements, C. S., Purcell, A. W., Brooks, A. G., Whisstock, J. C., Burrows, S. R., McCluskey, J. and Rossjohn, J.** (2003) A structural basis for the selection of dominant αβ T cell receptors in antiviral immunity. *Immunity* **18**:53-64

586. **Moss, P. A. H. and Bell, J. I.** (1995) Sequence analysis of the human αβ T-cell receptor CDR3 region. *Immunogenetics* **42**:10-18

587. **Jorgensen, J. L., Esser, U., de St. Groth, B. F., Reay, P. A. and Davis, M. M.** (1992) Mapping T-cell receptor-peptide contacts by variant peptide immunization of single-chain transgenics. *Nature* **355**:224-230

588. **Lee, P. U. Y., Churchill, H. R. O., Daniels, M., Jameson, S. C. and Kranz, D. M.** (2000) Role of 2C T cell receptor residues in the binding of self- and allo-major histocompatibility complexes. *J. Exp. Med.* **191**:1355-1364

589. **Borg, N. A., Ely, L. K., Beddoe, T., Macdonald, W. A., Reid, H. H., Clements, C. S., Purcell, A. W., Kjer-Nielsen, L., Miles, J. J., Burrows, S. R., McCluskey, J. and Rossjohn, J.** (2005) The CDR3 regions of an immunodominant T cell receptor dictate the 'energetic landscape' of peptide-MHC recognition. *Nat. Immunol.* **6**:171-180

590. **Holler, P. D., Holman, P. O., Shusta, E. V., O'Herrin, S., Wittrup, K. D. and Kranz, D. M.** (2000) *In vitro* evolution of a T cell receptor with high affinity for peptide/MHC. *Proc. Natl. Acad. Sci. USA* **97**:5387-5392

591. **Manning, T. C., Parke, E. A., Teyton, L. and Kranz, D. M.** (1999) Effects of complementarity determining region mutations on the affinity of an α/β T cell receptor: measuring the energy associated with CD4/CD8 repertoire skewing. *J. Exp. Med.* **189**:461-470

592. **Chlewicki, L. K., Holler, P. D., Monti, B. C., Clutter, M. R. and Kranz, D. M.** (2005) High-affinity, peptide-specific T cell receptors can be generated by mutations in CDR1, CDR2 or CDR3. *J. Mol. Biol.* **346**:223-239

593. **Cose, S. C., Kelly, J. M. and Carbone, F. R.** (1995) Characterization of a diverse primary herpes simplex virus type 1 gB-specific cytotoxic T-cell response showing a preferential Vβ bias. *J. Virol.* **69**:5849-5852

594. **Wucherpfennig, K. W., Zhang, J., Witek, C., Matsui, M., Modabber, Y., Ota, K. and Hafler, D. A.** (1994) Clonal expansion and persistence of human T cells for an immunodominant myelin basis protein peptide. *J. Immunol.* **152**:5581-5592

595. **Hodges, E., Dasmahapatra, J., Smith, J. L., Quin, C. T., Lanham, S., Krishna, M. T., Holgate, S. T. and Frew, A. J.** (1998) T cell receptor (TCR) Vβ gene usage in bronchoalveolar lavage and peripheral blood T cells from asthmatic and normal subjects. *Clin. Exp. Immunol.* **112**:363-374

596. **Umibe, T., Kita, Y., Nakao, A., Nakajima, H., Fukuda, T., Yoshida, S., Sakamaki, T., Saito, Y. And Iwamoto, I.** (2000) Clonal expansion of T cells

infiltrating in the airways of non-atopic asthmatics. *Clin. Exp. Immunol.* **119**:390-397

597. **McHeyzer-Williams, L. J., Panus, J. F., Mikszta, J. A. and McHeyzer-Williams, M. G.** (1999) Evolution of antigen-specific T cell receptors in vivo: preimmune and antigen-driven selection of preferred complementarity-determining region 3 (CDR3) motifs. *J. Exp. Med.* **189**:1823-1837

598. **Maryanski, J. L., Jongeneel, C. V., Bucher, P., Casanova, J.-L. and Walker, P. R.** (1996) Single-cell PCR analysis of TCR repertoires selected by antigen in vivo: a high magnitude CD8 response is comprised of very few clones. *Immunity* **4**:47-55

599. **Blander, J. M., Sant'Angelo, D. B., Bottomly, K. and Janeway, Jr., C. A.** (2000) Alteration at a single amino acid residue in the T cell receptor α chain complementarity determining region 2 changes the differentiation of naive CD4 T cells in response to antigen from T helper cell type 1 (Th1) to Th2. *J. Exp. Med.* **191**:2065-2074

600. **Das, M. P., Nicholson, L. B., Greer, J. M. and Kuchroo, V. K.** (1997) Autopathogenic T helper cell type 1 (Th1) and protective Th2 clones differ in their recognition of the autoantigenic peptide of myelin proteolipid protein. *J. Exp. Med.* **186**:867-876

601. **Boyton, R. J., Zaccai, N., Jones, E. Y. and Altmann, D. M.** (2002) CD4 T cells selected by antigen under Th2 polarizing conditions favor an elongated TCRα chain complementarity-determining region 3. *J. Immunol.* **168(3)**:1018-1027

602. **Shastri, N., Gammon, G., Miller, A. and Sercarz, E. E.** (1986) Ia molecule-associated selectivity in T cell recognition of a 23-amino-acid peptide of lysozyme. *J. Exp. Med.* **164**:882-896

603. **Kinsella, T. M. and Nolan, G. P.** (1996) Episomal vectors rapidly and stably produce high-titer recombinant retrovirus. *Human Gene Therapy* **7**:1405-1413

604. **Riviére, I., Brose, K. and Mulligan, R. C.** (1995) Effects of retroviral vector design on expression of human adenosine deaminase in murine bone marrow transplant recipients engrafted with genetically modified cells. *Proc. Natl. Acad. Sci USA* **92**:6733-6737

605. **Annenkov, A. and Chernajovsky, Y.** (2000) Engineering mouse T lymphocytes specific to type II collagen by transduction with a chimeric receptor consisting of a single chain Fv and TCR zeta. *Gene Therapy* **7**:714-722

606. **Mycko, M. P., Waldner, H., Anderson, D. E., Bourcier, K. D., Wucherpfennig, K. W., Kuchroo, V. K. and Hafler, D. A.** (2004) Cross-reactive TCR responses to self antigens presented by different MHC class II molecules. *J. Immunol.* **173**:1689-1698

607. **Curtis, J. L., Byrd, P. K., Wanrock, M. L. and Kaltreider, H. B.** (1991) Requirement of CD4-positive T cells for cellular recruitment to the lungs of

mice in response to a particulate intratracheal antigen. *J. Clin. Invest.* **88(4)**:1244-1254

608. **Papapetropoulos, A., Simoes, D. C., Xanthou, G., Roussos, C. and Gratziou, C.** (2006) Soluble guanylyl cyclase expression is reduced in allergic asthma. *Am. J. Physiol. Lung Cell Mol. Physiol.* **290(1)**:L179-L184

609. **Henwood, J., Loveridge, J., Bell, J. I. and Gaston, J. S. H.** (1993) Restricted T cell receptor expression by human T cell clones specific for mycobacterial 65-kDa heat-shock protein: selective *in vivo* expansion of T cells bearing defined receptors. *Eur. J. Immunol.* **23**:1256-1265

610. **Monod, M. Y., Giudicelli, V., Chaume, D. and Lefranc, M.-P.** (2004) IMGT/JunctionAnalysis: the first tool for the analysis of the immunoglobulin and T cell receptor complex V-J and V-D-J JUNCTIONs. *Bioinformatics* **20 Suppl 1**:I379-I385

611. **Lorens, J. B., Sousa, C., Bennett, M. K., Molineaux, S. M. and Payan, D. G.** (2001) The use of retroviruses as pharmaceutical tools for target discovery and validation in the field of functional genomics. *Curr. Opin. Biotech.* **12**:613-621

612. **Pasare, C., Mukherjee, P., Verhoef, A., Bansal, P., Mendiratta, S. K., George, A., Lamb, J. R., Rath, S. and Bal, V.** (2001) T cells in mice expressing a transgenic human TCRβ chain get positively selected but cannot be activated in the periphery by signalling through TCR. *Int. Immunol.* **13**:53-62

613. **Pear, W. S., Nolan, G. P., Scott, M. L. and Baltimore, D.** (1993) Production of high-titer helper-free retroviruses by transient transfection. *Proc. Natl. Acad. Sci. USA* **90(18)**:8392-8396

614. **Heemskerk, M. H. M., Blom, B., Nolan, G., Stegmann, A. P. A., Bakker, A. Q., Weijer, K., Res, P. C. M. and Spits, H.** (1997) Inhibition of T cell and promotion of natural killer cell development by the dominant negative helix loop helix factor Id3. *J. Exp. Med.* **186(9)**:1597-1602

615. **Wang, H., Moon, E.-Y., Azouz, A., Wu, X., Smith, A., Schneider, H., Hogg, N. and Rudd, C.** (2003) SKAP-55 regulates integrin adhesion and formation of T cell-APC conjugates. *Nat. Immunol.* **4(4)**:366-374

616. **Costa, G. L., Sandora, M. R., Nakajima, N., Nguyen, E. V., Taylor-Edwards, C., Slavin, A. J., Contag, C. H., Fathman, C. G. and Benson, J. M.** (2001) Adoptive immunotherapy of experimental autoimmune encephalomyelitis via T cell delivery of the IL-12 p40 subunit. *J. Immunol.* **167**:2379-2387

617. **Kalams, S. A., Johnson, R.P., Trocha, A. K., Dynan, M. J., Ngo, H. S., D'Aquila, R. T., Kurnik, J. T. and Walker, B. D.** (1994) Longitudinal analysis of T cell receptor (TCR) gene usage by human immunodeficiency virus 1 envelope-specific cytotoxic T lymphocyte clones reveals a limited TCR repertoire. *J. Exp. Med.* **179**:1261-1271

618. **Maini, M. K., Gudgeon, N., Wedderburn, L. R., Rickinson, A. B. and Beverley, P. C. L.** (2000) Clonal expansions in acute EBV infection are detectable in the CD8 and not the CD4 subset and persist with a variable CD45 phenotype. *J. Immunol.* **165**:5729-5737

619. **Kedzierska, K., Day, E. B., Pi, J., Heard, S. H., Doherty, P. C., Turner, S. J. and Perlman, S.** (2006) Quantification of repertoire diversity of influenza-specific epitopes with predominant public or private TCR usage. *J. Immunol.* **177**:6705-6712

620. **Kou, Z. C., Puhr, J. S., Rojas, M., McCormack, W. T., Goodenow, M. M. and Sleasman, J. W.** (2000) T-cell receptor Vβ repertoire CDR3 length diversity differs within CD45RA and CD45RO T-cell subsets in healthy and human immunodeficiency virus-infected children. *Clin. Diag. Lab. Immunol.* 7:953-959

621. **Roglic, M., MacPhee, R. D., Duncan, S. R., Sattler, F. R. and Theofilopoulos, A. N.** (1997) T cell receptor (TCR) BV gene repertoires and clonal expansions of CD4 cells in patients with HIV infections. *Clin. Exp. Immunol.* **197**:21-30

622. **Marsh, J. C. W. and Gordon-Smith, E. C.** (2004) Insights into the autoimmune nature of aplastic anaemia. *Lancet* **364**:308-309

623. **Risitano, A. M., Maciejewski, J. P., Green, S., Plasilova, M., Zeng, W. and Young, N. S.** (2004) In-vivo dominant immune responses in aplastic anaemia: molecular tracking of putatively pathogenetic T-cell clones by TCRβ-CDR3 sequencing. *Lancet* **364**:355-364

624. **Zeng, W., Maciejewski, J. P., Chen, G. and Young, N. S.** (2001) Limited heterogeneity of T cell receptor BV usage in aplastic anaemia. *J. Clin. Invest.* **108**:765-773

625. **Babbe, H., Roers, A., Waisman, A., Lassmann, H., Goebels, N., Hohlfeld, R., Friese, M., Schröder, R., Deckert, M., Schmidt, S., Ravid, R. and Rajewsky, K.** (2000) Clonal expansions of $CD8^+$ T cells dominate the T cell infiltrate in active multiple sclerosis lesions as shown by micromanipulation and single cell polymerase chain reaction. *J. Exp. Med.* **192**:393-404

626. **Quinn, A., McInerney, M., Huffman, D., McInerney, B., Mayo, S., Haskins, K. and Sercarz, E.** (2006) T cells to a dominant epitope of GAD65 express a public CDR3 motif. *Int. Immunol.* **18**:967-979

627. **Takahama, H., Masuko-hongo, K., Tanaka, A., Kawa, Y., Ohta, N., Yamamoto, K., Mizoguchi, M., Nishioka, K. and Kato, T.** (2002) T-cell clonotypes specific for *Dermatophagoides pteronyssinus* in the skin lesions of patients with atopic dermatitis. *Hum. Immunol.* **63**:558-566

628. **Bakakos, P., Smith, J. L., Warner, J. O., Vance, G., Moss, C. T., Hodges, E., Lanham, S. and Howell, W. M.** (2001) Modification of T-cell receptor Vβ repertoire in response to allergen stimulation in peanut allergy. *J. Allergy Clin. Immunol.* **107**:1089-1094

629. **Kircher, M. F., Haeusler, T., Nickel, R., Lamb, J. R., Renz, H. and Beyer, K.** (2002) Vβ18.1$^+$ and Vα2.3$^+$ T-cell subsets are associated with house dust mite allergy in human subjects. *J. Allergy Clin. Immunol.* **109**:517-523

630. **Beyer, K., Häusler, T., Kircher, M., Nickel, R., Wahn, U. and Renz, H.** (1999) Specific Vβ T cell subsets are associated with cat and birch pollen allergy in humans. *J. Immunol.* **162**:1186-1191

631. **Sekine, T., Kato, T., Masuko-Hongo, K., Nakamura, H., Yoshino, S., Nishioka, K. and Yamamoto, K.** (1999) Type II collagen is a target antigen of clonally expanded T cells in the synovium of patients with rheumatoid arthritis. *Ann. Rheum. Dis.* **58**:446-450

632. **Sun, J., Link, H., Olsson, T., Xiao, B. G., Andersson, G. Ekre, H. P., Linington, C. and Diener, P.** (1991) T and B cell responses to myelin-oligodendrocyte glycoprotein in multiple sclerosis. *J. Immunol.* **146**:1490-1495

633. **Kedzierska, K., Turner, S. J. and Doherty, P. C.** (2004) Conserved T cell receptor usage in primary and recall responses to an immunodominant influenza virus nucleoprotein epitope. *Proc. Natl. Acad. Sci. USA* **101**:4942-4947

634. **Menezes, J. S., van den Elzen, P., Thornes, J., Huffman, D., Droin, N. M., Maverakis, E. and Sercarz, E. E.** (2007) A public T cell clonotype within a heterogeneous autoreactive repertoire is dominant in driving EAE. *J. Clin. Invest.* **117**:2176-2185

635. **Turner, S. J., Kedzierska, K., Komodromou, H., La Gruta, N. L., Dunstone, M. A., Webb, A. I., Webby, R., Walden, H., Xie, W., McCluskey, J., Purcell, A. W., Rossjohn, J. and Doherty, P. C.** (2005) Lack of prominent peptide-major histocompatibility complex features limits repertoire diversity in virus-specific CD8$^+$ T cell populations. *Nat. Immunol.* **6**:382-389

636. **Jones, E. Y.** (2005) Favorite flavors of surfaces. *Nat. Immunol.* **6**:365-367

637. **Miles, J. J., Elhassen, D., Borg, N. A., Silins, S. L., Tynan, F. E., Burrows, J. M., Purcell, A. W., Kjer-Nielsen, L., Rossjohn, J., Burrows, S. R. and McCluskey, J.** (2005) CTL recognition of a bulged viral peptide involves biased TCR selection. *J. Immunol.* **175**:3826-3834

638. **Venturi, V., Kedzierska, K., Price, D. A., Doherty, P. C., Douek, D. C., Turner, S. J. and Davenport, M. P.** (2006) Sharing of T cell receptors in antigen-specific responses is driven by convergent recombination. *Proc. Natl. Aca. Sci. USA* **103**:18691-18696

639. **Venturi, V., Price, D. A., Douek, D. C. and Davenport, M. P.** (2008) The molecular basis for public T-cell responses? *Nat. Rev. Immunol.* **8**:231-238

640. **Altman, J. D., Moss, P. A. H., Goulder, P. J. R., Barouch, D. H., McHeyzer-Williams, M. G., Bell, J. I., McMichael, A. J. and Davis, M. M.** (1996) Phenotypic analysis of antigen-specific T lymphocytes. *Science* **274**:94-96

641. **Smith, E. A. and Corn, R. M.** (2003) Surface Plasmon resonance imaging as a tool to monitor biomolecular interactions in an array based format. *Appl. Spectrosc.* **57**:320A-332A

642. **Suzuki, T., Aizawa, S. and Ikeda, H.** (2001) Expression of receptor for ecotropic murine leukemia virus on hematopoietic cells. *Arch. Virol.* **146**:507-519

643. **Miller, A. D. and Chen, F.** (1996) Retrovirus packaging cells based on 10A1 murine leukemia virus for production of vectors that use multiple receptors for cell entry. *J. Virol.* **70**:5564-5571

644. **Blüthmann, H., Kisielow, P., Uematsu, Y., Malissen, M., Krimpenfort, P., Berns, A., von Boehmer, H. and Steinmetz, M.** (1988) T-cell-specific deletion of T-cell receptor transgenes allows functional rearrangement of endogenous α and β genes. *Nature* **334**:156-159

645. **O'Brien, D. P., Baecher-Allen, C. M., Burns, Jr., R. P., Shastri, N. and Barth, R. K.** (1997) Elimination of T-cell-receptor β-chain diversity in transgenic mice restricts antigen-specific but not alloreactive responses. *Immunology* **91**:375-382

646. **Perkins, D. L., Wang, Y., Fruman, D., Seidman, J. G. and Rimm, I. J.** (1991) Immunodominance is altered in T cell receptor (β-chain) transgenic mice without the generation of a hole in the repertoire. *J. Immunol.* **146**:2960-2964

647. **Perry, S. S., Wang, H., Pierce, L. J., Yang, A. M., Tsai, S. and Spangrude, G. J.** (2004) L-selectin defines a bone marrow analog to the thymic early T-lineage progenitor. *Blood* **103(8)**:2990-2996

648. **Yamashita, I., Nagata, T., Tada, T. and Nakayama, T.** (1993) CD69 cell surface expression identifies developing thymocytes which audition for T cell antigen receptor-mediated positive selection. *Int. Immunol.* **5(9)**:1139-1150

649. **McCarty, N., Shinohara, M. L., Lu, L. and Cantor, H.** (2004) Detailed analysis of gene expression during development of T cell lineages in the thymus. *Proc. Natl. Acad. Sci. USA* **101**:9339-9344

650. **Fine, J. S. and Kruisbeek, A. M.** (1991) The role of LFA-1/ICAM-1 interactions during murine T lymphocyte development. *J. Immunol.* **147(9)**:2852-2859

651. **Hutloff, A., Dittrich, A. M., Beier, K. C., Eljaschewitsch, B., Kraft, R., Anagnostopoulos, I. and Kroczek, R. A.** (1999) ICOS is an inducible T-cell co-stimulator structurally and functionally related to CD28. *Nature* **397**:263-266

652. **Gramaglia, I., Weinberg, A. D., Lemon, M. and Croft, M.** (1998) Ox-40 ligand: a potent costimulatory molecule for sustaining primary CD4 T cell responses. *J. Immunol.* **161**:6510-6517

653. **Mages, H. W., Hutloff, A., Heuck, C., Büchner, K., Himmelbauer, H., Oliveri, F. and Kroczek, R. A.** (2000) Molecular cloning and characterization

of murine ICOS and identification of B7h as ICOS ligand. *Eur. J. Immunol.* **30(4)**:1040-1047

654. **Tian, T., Zhang, J., Gao, L., Qian, X. P. and Chen, W. F.** (2005) Heterogeneity within medullary-type TCR$\alpha\beta^+$ $CD3^+$ $CD4^-$ $CD8^+$ thymocytes in normal mouse thymus. *Int. Immunol.* **13(3)**:313-320

655. **Hara, T., Jung, L. K. L., Bjorndahl, J. M. and Fu, S. M.** (1986) Human T cell activation. III. Rapid induction of a phosphorylated 28 kD/32kD disulfide linked early activation antigen (EA-1) by 12-*O*-tetradecanoyl phorbol-13-acetate, mitogens, and antigens. *J. Exp. Med.* **164:**1988–2005

656. **Anderson, G., Hare, K. J., Platt, N. and Jenkinson, E. J.** (1997) Discrimination between maintenance- and differentiation-inducing signals during initial and intermediate stages of positive selection. *Eur. J. Immunol.* **27(8)**:1838-1842

657. **Sheard, M., Sugaya, K., Furuta, M., Tsuda, S. and Takahama, Y.** (1996) Heterogeneous expression of recombination activating genes and surface CD5 in $CD3^{low}$ $CD4^+$ $CD8^+$ thymocytes. *Scand. J. Immunol.* **43(6)**:619-625

658. **Boyd, A. W., Wawryk, S. O., Burns, G.F. and Fecondo, J.V.** (1988) Intercellular adhesion molecule 1 (ICAM-I) has a central role in cell-cell contact mediated immune mechanism. *Proc. Natl. Acad. Sci USA* **85**: 3095–3099

659. **Uchiyama, T., Broder, S. and Waldmann, T. A.** (1981) A monoclonal antibody (anti-Tac) reactive with activated and functionally mature human T cells. I. Production of anti-Tac monoclonal antibody and distribution of Tac (+) cells. *J. Immunol.* **126**:1393-1397

660. **Uchiyama, T., Nelson, D. L., Fleisher, T. A. and Waldmann, T. A.** (1981) A monoclonal antibody (anti-Tac) reactive with activated and functionally mature human T cells. II. Expression of Tac antigen on activated cytotoxic killer T cells, suppressor cells, and on one of two types of helper T cells. *J. Immunol.* **126**:1398-1403

661. **D'Cruz, L. M. and Klein, L.** (2005) Development and function of agonist-induced $CD25^+$ $Foxp3^+$ regulatory T cells in the absence of interleukin 2 signaling. *Nat. Immunol.* **6(11)**:1152-1159

662. **Haynes, B. F., Telen, M. J., Hale, L. P. and Denning, S. M.** (1989) CD44 - a molecule involved in leukocyte adherence and T-cell activation. *Immunol. Today* **10(12)**:423-428

663. **DeGrendele, H. C., Kosfiszer, M., Estess, P. and Siegelman, M. H.** (1997) CD44 activation and associated primary adhesion is inducible via T cell receptor stimulation. *J. Immunol.* **159**:2549-2553

664. **Jung, T. M. and Dailey, M. O.** (1990) Rapid modulation of homing receptors ($gp90^{MEL-14}$) induced by activators of protein kinase C. *J. Immunol.* **144**:3130-3136

665. **Mascarell, L. and Truffa-Bachi, P.** (2004) T lymphocyte activation initiates the degradation of the CD62L encoding mRNA and increases the transcription of the corresponding gene. *Immunol. Lett.* **94**:115-122

666. **Stuber, E. and Strober, W.** (1996) The T cell-B cell interaction via OX40-OX40L is necessary for the T-cell dependent humoral immune response. *J. Exp. Med.* **183**:979-989

667. **Gramaglia, I., Jember, A., Pippig, S. D., Weinberg, A. D., Killeen, N. and Croft, M.** (2000) The OX40 costimulatory receptor determines the development of CD4 memory by regulating primary clonal expansion. *J. Immunol.* **165**:3043-3050

668. **Barends, M., van Oosten, M., de Rond, C. G. H., Dormans, J. A. M. A., Osterhaus, A. D. M. E., Neijens, H. J. and Kimman, T. G.** (2004) Timing of infection and prior immunization with respiratory syncytial virus (RSV) in RSV-enhanced allergic inflammation. *J. Infect. Dis.* **189**:1866-1872

669. **Le, A. V., Cho, J. Y., Miller, M., McElwain, S., Golgotiu, K. and Broide, D.H.** (2007) Inhibition of allergen-induced airway remodeling in Smad 3-deficient mice. *J. Immunol.* **178**:7310-7316

670. **McMillan, S.J., Xanthou, G. and Lloyd, C. M.** (2005) Manipulation of allergen induced airway remodeling by treatment with anti-TGF-beta antibody: effect of the Smad signaling pathway. *J. Immunol.* **174**:5774-5780

671. **Lee, C. G., Link, H., Baluk, P., Homer, R. J., Chapoval, S., Bhandari, V., Kang, M. H., Cohn, L., Kim, Y. K., McDonald, D. M. and Elias, J. A.** (2004) Vascular endothelial growth factor (VEGF) induces remodeling and enhances TH2-mediated sensitization and inflammation in the lung. *Nat. Med.* **10**:1095-1103

672. **Chen, K., Huang, J., Gong, W., Iribarren, P., Dunlop, N. M. and Wang, J. M.** (2007) Toll-like receptors in inflammation, infection and cancer. *Int. Immunopharmacol.* 7:1271-1285

673. **Veldhoen, M., Uyttenhove, C., van Snick, J., Helmby, H., Westendorf, A., Buer, J., Martin, B., Wilhelm, C. and Stockinger, B.** (2008) Transforming growth factor-β 'reprograms' the differentiation of T helper 2 cells and promotes an interleukin 9-producing subset. *Nat. Immunol.* **In press**

674. **Yoshimura, T., Matsushima, K., Tanaka, S., Robinson, E. A., Appella, E., Oppenheim, J. J. and Leonard, E. J.** (1987) Purification of a human monocyte-derived neutrophil chemotactic factor that has peptide sequence similarity to other host defense cytokines. *Proc. Natl. Acad. Sci. USA* **84**:9233-9237

675. **Hall, F. C., Visconti, K. C., Ahmad, R. C., Parry, S. L., Miltenburg, A. M., McConnell, H. M., Mellins, E. D. and Sønderstrup, G.** (2003) Cytokines elicited by T cell epitopes from a synovial autoantigen: altered peptide ligands can reduce interferon-γ and interleukin-10 production. *Arthritis Rheum.* **48**:2375-2385

676. **Boots, A. M., Hubers, H., Kouwijzer, M., den Hoed-van Zandbrink, L., Westrek-Esselink, B. M., van Doorn, C., Stenger, R., Bos, E. S., van Lierop, M. J., Verheijden, G. F., Timmers, C. M. and van Staveren, C. J.** (2007) Identification of an altered peptide ligand based on the endogenously presented, rheumatoid arthritis-associated, human cartilage glycoprotein-$39_{(263-275)}$ epitope: an MHC anchor variant peptide for immune modulation. *Arthritis Res. Ther.* **9**:R71

677. **Aruna, B. V., Ben-David, H., Sela, M. and Mozes, E.** (2006) A dual altered peptide ligand down-regulates myasthenogenic T cell responses and reverses experimental autoimmune myasthenia gravis via up-regulation of Fas-FasL-mediated apoptosis. *Immunology* **118**:413-424

678. **Leech, M. D., Chung, C. Y., Culshaw, A. and Anderton, S. M.** (2007) Peptide-based immunotherapy of experimental autoimmune encephalomyelitis without anaphylaxis. *Eur. J. Immunol.* **37**:3576-3581

679. **Lahn, M., Kanehiro, A., Hahn, Y. S., Wands, J. M., Aydintug, M. K., O'Brien, R. L., Gelfand, E. W. and Born, W. K.** (2004) Aerosolized anti-T-cell-receptor antibodies are effective against airway inflammation and hyperreactivity. *Int. Arch. Allergy Immunol.* **134**:49-55

Appendix 1 - Stock solutions and buffers

TAE buffer

- 40 mM Tris-acetate (Tris-base, Sigma, T1503, acetic acid, Sigma 45726)
- 1 mM EDTA, pH 8.0 (Sigma, E4884)

6X loading buffer

- 40% sucrose (Sigma, S7903)
- 0.25% bromophenol blue (Sigma, B8026)

Tetracycline (Sigma, T3258)

- 5 mg/ml stock solution, prepared in 100% ethanol
- Working concentration – 50 μg/ml

Chloramphenicol (Sigma, C0378)

- 34 mg/ml stock solution, prepared in 100% ethanol
- Working concentration – 25 μg/ml

Solution A for competent cells

- 100 μM $CaCl_2$ (Sigma, C3881)
- 10 mM $MgCl_2$ (Sigma, M8266)
- 400 μM MES (Sigma, M3671)

Solution B for competent cells

- 10 mM $CaCl_2$ (Sigma, C3881)
- 2 mM $MgCl_2$ (Sigma, M8266)
- 800 μM MES (Sigma, M3671)
- 5% glycerol (Sigma, G5516)

Ampicillin (Sigma, A9518)

- 50 mg/ml stock solution, prepared in deionised water
- Working concentration – 50 μg/ml

Tail digestion buffer

- 50 mM Tris-hydrochloride (Sigma, T3253)
- 100 mM EDTA (ethylene diammine tetrasodium acetate) (Sigma, ED-500)
- 100 mM sodium chloride (Sigma, S7653)
- 1% sodium dodecyl sulphate (Sigma, L6026)

Sodium dodecyl sulphate (Sigma, L3490)

- 10% stock solution (w/v), prepared in deionised water

Complete growth medium – RPMI-1640

- RPMI-1640 medium (Invitrogen, 31870-074)
- 10% heat-inactivated foetal calf serum (Globepharm)
- 2 mM L-glutamine (Invitrogen, 25030-012)
- 100 U/ml penicillin/100 µg/ml streptomycin (Invitrogen, 15140-122)
- 50 µM β-mercaptoethanol (2-ME) (Sigma, M7522), prepared in sterile PBS

FACS buffer

- 1x PBS (Invitrogen, 10010-056)
- 10% heat-inactivated foetal calf serum (Globepharm)

Depurination solution for Southern analysis

- 0.2 M hydrochloric acid (Sigma, H9892), diluted in dH_2O

Denaturation buffer for Southern analysis

- 1.5 M sodium chloride (Sigma, S7653)
- 0.5 M sodium hydroxide (Sigma, S8045)
- diluted in dH_2O

Neutralisation buffer for Southern analysis

- 1.5 M sodium chloride (Sigma, S7653)
- 0.5 M Tris-base (Sigma, T1503)
- pH 7.5, diluted in dH_2O

20x SSC

- 3 M sodium chloride (Sigma, S7653)
- 0.3 M sodium citrate (Sigma, C3434)
- pH 7.0, diluted in dH_2O

DNA dilution buffer

- 50 µg/ml salmon sperm DNA Roche, 11 585 614 910), prepared in TE buffer
- pH 8.0

TE buffer

- 10 mM Tris-HCl (Sigma, T3253)
- 1 mM EDTA (Sigma, ED-500), pH 8.0

Maleic acid buffer

- 0.1 M maleic acid (Sigma, M0375)
- 0.15 M sodium chloride (Sigma, C3434)
- pH 7.5, diluted in dH_2O

Maleic acid washing buffer

- maleic acid buffer
- 0.3% Tween 20 (Sigma, P1379)

DIG-detection buffer for Southern analysis

- 0.1 M Tris-HCl (Sigma, T3253)
- 0.1 M sodium chloride (Sigma, C3434)
- pH 9.5, diluted in dH_2O

Complete growth medium – DMEM

- Dulbecco's Modified Eagle's Medium (Invitrogen, 11960-044)
- 10% heat-inactivated foetal calf serum (Globepharm)
- 2 mM L-glutamine (Invitrogen, 25030-012)
- 100 U/ml penicillin/100 μg/ml streptomycin (Invitrogen, 15140-122)

DMEM-HAT medium

- complete growth medium – DMEM
- 30 μM hypoxanthine (Sigma, H9377)
- 1 μM aminopterin (Sigma, A3411)
- 20 μM thymidine (Sigma, T1895)

Aminopterin (Sigma, A3411)

- 5 μM stock solution, prepared in 1x PBS (Invitrogen, 10010-056), 0.2 μm filtered

Thymidine (Sigma, T1895)

- 1 mM stock solution, prepared in 1x PBS (Invitrogen, 10010-056), 0.2 μm filtered, 500x working concentration

Hypoxanthine (Sigma, H9377)

- 1.5 mM stock solution, prepared in 1x PBS (Invitrogen, 10010-056), 0.2 μm filtered, 500x working concentration

DMEM-HT medium

- complete growth medium - DMEM
- 30 μM hypoxanthine (Sigma, T1895)
- 20 μM thymidine (Sigma, T1895)

Chloroquine (Sigma, C6628)

- 25 mM stock solution, prepared in 1x PBS (Invitrogen, 10010-056), 0.2 μm filtered

Calcium chloride (Sigma, C3881)

- 2 M stock solution, prepared in deionised water, 0.2 μm filtered

HEPES-buffered saline (2x)

- 50 mM 4-(2-hydroxyethyl)-1-piperazineethanesulfonic acid (HEPES) (Gibco, 15630-056)
- 10 mM potassium chloride (Sigma, P9333)
- 12 mM D-(+)-glucose (Sigma, G7528)
- 280 mM sodium chloride (Sigma, C3434)
- 1.5 mM sodium phosphate (dibasic sodium orthophosphate, Sigma, S7907)

Polybrene (hexadimethrine bromide, Sigma, H9268)

- 4 mg/ml stock solution, prepared in 1x PBS (Invitrogen, 10010-056), 0.2 μm filtered

Complete HL-1 medium

- HL-1 serum-free medium (Lonza, 77201)
- 2 mM L-glutamine (Invitrogen, 25030-012)
- 50 U/ml penicillin/50 µg/ml streptomycin (Invitrogen, 15140-122)

Collagenase type D (Roche, 11 088 858 001)

- 30 mg/ml stock solution, prepared in 1x PBS (Invitrogen, 10010-056)
- Working concentration – 0.15 mg/ml

DNase I (Roche, 11 284 932 001)

- 5 mg/ml stock solution, prepared in 1x PBS (Invitrogen, 10010-056)
- Working concentration – 25 µg/ml

Phosphate buffered saline, 1x (for ELISAs)

- 5 tablets of PBS (Sigma, P4417) dissolved in 1 l deionised water gives:
- 27 mM potassium chloride
- 137 mM sodium chloride
- 10 mM phosphate buffer

ELISA wash buffer (all ELISAs)

- 0.05% Tween 20 (Sigma, P1379) in 1x PBS

ELISA blocking buffer and diluent (for IgE ELISA)

- 10% heat-inactivated foetal calf serum in PBS (Globepharm)

ELISA blocking buffer (for all other ELISAs)

- 1% bovine serum albumin (w/v) (Sigma, A7906)
- 5% sucrose (w/v) (Sigma, S7903)
- 0.05% sodium azide (v/v) (Sigma, S8032)
- 1x PBS

Sodium azide (Sigma, S032)

- 5% stock solution (w/v), prepared in deionised water

ELISA diluent (for all other ELISAs)

- 1% bovine serum albumin (Sigma, A7906) (w/v), in 1x PBS

ELISA stop solution (all ELISAs)

- 1 M sulphuric acid (Sigma, 435589)

1% Eosin Y solution

- 10 g eosin powder (VWR, 341973R) in 1 l tap water

1% periodic acid

- 1 g periodic acid (Sigma, P5463) in 100 ml deionised water

Appendix 2 – PCR conditions and primers and restriction enzymes for TCR CDR3 analysis in the HLA-DR1-restricted human T-cell lines grown in response to peptide 4 of Fel d 1

PCR conditions and primers

	Primer sequence (5'→3')	Product size (bp)	Annealing temp. (°C)	$[MgCl_2]$, mM
Human TCRα anchor PCR				
Anchor polyC primer	(f) CTATCTAGAGAGCTCGCGGCCGCCC CCCCCCCCCC	300-700	50/60*	1.5
3' Cα primer	(r) GATAGATCTTAGAGTCTCTCAGC			
Human TCRβ anchor PCR				
Anchor polyC primer	(f) CTATCTAGAGAGCTCGCGGCCGCCC CCCCCCCCCC	300-700	50/60*	1.5
3' Cβ primer	(r) CGCGAATTCAGATCTCTGCTTCTGATG			

* = reaction conditions for these PCRs are quite atypical. Reactions comprised of an initial denaturing step (95°C for 5 minutes), followed by 28 cycles of denaturation - 95°C for 1 minute, annealing - 50°C for 45 seconds, then 60°C for 15 seconds and elongation - 72°C for 10 minutes, and finished with a final elongation step (72°C for 10 minutes).

Primer sequences and PCR conditions as outlined in reference 609.

Restriction enzyme used to identify *E.coli* clones containing TCR chain inserts

Enzyme	Buffer	Incubation temp. (°C)	Restriction site (5'→3')	Enzyme source
EcoRI	4-CORE H (Promega)	37	G↓AATTC	Promega (R6011)

Promega buffer – 4-CORE H composition (1x):

- 90 mM Tris-HCl
- 10 mM $MgCl_2$
- 50 mM NaCl
- pH 7.5 (37°C)

Sequencing primer

Primer name	Primer sequence (5'→3')	Primer concentration (nM)
M13 forward	GTAAAACGACGGCCAG	10

Primer designed by a postdoctoral researcher in the Boyton laboratory.

Appendix 3 – PCR conditions, primers and linkers used in MFG cloning strategies

PCR conditions and primers

	Primer sequence (5'→3')	Product size (bp)	Annealing temp. (°C)	[$MgCl_2$], mM
MFG (TCR CIR010α chain)				
TRAV8-4NotI	(f) GCGGCCGCATGCTCCTGCTGCTCGTCCCAGTGC	878	64	1.5
TRAC1noNotI #	(r) CTCAGCTGGACCACAGCCGC			
MFG (TCR CIR010αmCα)				
A3.CIR010αVJNotI	(f) GCGGCCGCATGCTCCTGCTGCTCGTCCC	439	65	1.5
A3.CIR010αVJCPstI	(r) GCTGGTACACTGCAGGATCAGGGTTC			
A2.CIR010mCαPstI	(f) CAGAACCTGCAGTGTACCAG	422	60	1.5
A2.CIR010mCαNotI	(r) GCGGCCGCCTCAACTGGACCACAGCCTC			
MFG (TCR 010β mCβ)				
A5.CIR010βVJNotI	(f) GCGGCCGCATGAGCATCGGGCTCCTGTGC	414	63.5	1.5
A5.CIR010βVJHindIII	(r) GAAAGCTTCAGTGCCCGACGCC			
A4.CIR010mCβPpuMI	(f) AGGACCTGAGAAATGTGACTCC	530	53	1.5
A4.CIR010mCβNotI	(r) GCGGCCGCTTCATGAATTCTTTCTTTTG			
MFG (TCR A10(2) β chain)				
CβmutationClaI	(f) CCCTCGGATCGATTTTCTGCTG	700	60	2.0
CβmutationEcoRI	(r) GAATTCGGCTTACCGGTCAGGAATTTTTTTTC TTGACCATGGC			
MFG (TCR D3(3) β chain)				
CβmutationBstXI	(f) CCAGTACTTTGGGCCAGGCAC	577	60	1.5
CβmutationEcoRI	(r) GAATTCGGCTTACCGGTCAGGAATTTTTTTTC TTGACCATGGC			

Linkers

Cloning step	Linker name	Linker sequence (5'→3')
To insert an additional NotI site into pBluescriptII	NotIPBSlinkertop	TCGAGATGCCATTCATTGGACTATAAC TGACTGTTACATCGCGGCCGCAT
	NotIPBSlinkerbottom	CGATGCGGCCGCGATGTAACAGTCAG TTATAGTCCAATGAATGGCATC
To insert an additional NotI site into MFG	NcoINotIMFGlinkertop	CATGGCGGCCGCACTTTCGGATCTATG CTCGTAGCCATTGCGGCCGCGTC
	NcoINotIMFGlinkerbottom	CATGGACGCGGCCGCAATGGCTACGA GCATAGATCCGAAAGTGCGGCCGC
To allow linkage of CIR010β VJ region with a murine Cβ region	CIR010βHindIIIJCPpuMIlinkertop	AGCTTTCTTTGGACAAGGCACCAGACT CACAGTTGTAGAGGTCCTC
	CIR010βHindIIIJCPpuMIlinkerbotto	TCGAGAGGACCTCTACAACTGTGAGTC TGGTGCCTTGTCCAAAGAA

Primers and conditions used for orienting TCR sequences in MFG

	Primer sequence (5'→3')	Product size (bp) – correct orientation	Product size (bp) – incorrect orientation	Annealing temp. (°C)	[$MgCl_2$], mM
MFG (TCR 010α chain)					
TRAV8-4NotI	(f) GCGGCCGCATGCTCCTG CTGCTCGTCCCAGTGC	938	0	61	1.5
MFGreverse	(r) CTGGACCACTGATATCC TGTC				
TRAV8-4NotI	(f) GCGGCCGCATGCTCCTG CTGCTCGTCCCAGTGC	0	958	61	1.5
MFGforward	(r) AGTAGACGGCATCGCA GCTTG				
MFG (TCR 010αmCα)					
CIR010αVJNotI	(f) GCGGCCGCATGCTCCT GCTGCTCGTCCC	887	0	66	1.5
MFGreverse	(r) CTGGACCACTGATATC CTGTC				
CIR010αVJNotI	(f) GCGGCCGCATGCTCCTG CTGCTCGTCCC	0	907	67	1.5
MFGforward	(r) AGTAGACGGCATCGCA GCTTG				
MFG (TCR 010βmCβ)					
CIR010βVJNotI	(f) GCGGCCGCATGAGCA TCGGGCTCCTGTGC	1004	0	66	1.5
MFGreverse	(r) CTGGACCACTGATATC CTGTC				
CIR010βVJNotI	(f) GCGGCCGCATGAGCA TCGGGCTCCTGTGC	0	1024	67	1.5
MFGforward	(r) AGTAGACGGCATCGC AGCTTG				
MFG (TCR A10(2) α 5-D4 α chain)					
TRAV5-D4 *	(f) ATGAAAACATATGCTC CTAC	962	0	59	1.5
MFGreverse	(r) CTGGACCACTGATATC CTGTC				
TRAV5-D4 *	(f) ATGAAAACATATGCTC CTAC	0	982	60	1.5
MFGforward	(r) AGTAGACGGCATCGCA GCTTG				
MFG (TCR A10(2) α 7-D3 and D3(3) α chains)					
TRAV7-D3/4 *	(f) ATGAAATCCTTGAGTG TTTC	957 (7-D3) 965 (D3)	0	63	1.5
MFGreverse	(r) CTGGACCACTGATATC CTGTC				
TRAV7-D3/4 *	(f) ATGAAATCCTTGAGTG TTTC	0	977 (7-D3) 985 (D3)	65	1.5
MFGforward	(r) AGTAGACGGCATCGC AGCTTG				

	Primer sequence (5'→3')	Product size (bp) – correct orientation	Product size (bp) – incorrect orientation	Annealing temp. (°C)	$[MgCl_2]$, mM
MFG (TCR A10(2) β chain)					
TRBV14F *	(f) ATGGGCACCAGGCTTC TTGGCTG	1072	0	64	1.5
MFGreverse	(r) CTGGACCACTGATATCC TGTC				
TRBV14F *	(f) ATGGGCACCAGGCTTCT TGGCTG	0	1092	66	1.5
MFGforward	(r) AGTAGACGGCATCGCA GCTTG				
MFG (TCR D3(3) β chain)					
TRBV2F *	(f) ATGGGCTCCATTTTCCT CAGTTGCCT	1059	0	62	1.5
MFGreverse	(r) CTGGACCACTGATATCC TGTC				
TRBV2F *	(f) ATGGGCTCCATTTTCCT CAGTTGCCT	0	1079	63	1.5
MFGforward	(r) AGTAGACGGCATCGCA GCTTG				

Sequencing primers

Primer name	Primer sequence (5'→3')	Primer concentration (nM)
All sequences amplified by high-fidelity PCR and cloned into TA cloning vector pCR2.1		
M13 forward *	(f) GTAAAACGACGGCCAG	10
M13 reverse *	(r) CAGGAAACAGCTATGAC	10
All final constructs (i.e. MFG (TCR chain)		
MFGforward	(f) AGTAGACGGCATCGCAGCTTG	10
MFGreverse	(r) CTGGACCACTGATATCCTGTC	10

Primers and conditions used for detecting TCR genes in transduced BW7 lines

Primer name	Primer sequence (5'→3')	Product size (bp)	Annealing temp. (°C)	$MgCl_2$, [mM]
Detection of D3(3) and A10(2) 7-D3 TCRα genes in BW7				
TRAV 7D3f *	(f) ATGAAATCCTTGAGTGTTTC	~500	54	1.5
NJ109 *	(r) CAGGAAACAGCTATGAC			

Primers marked with an asterisk (*) were designed by postdoctoral researchers in the Boyton laboratory. I designed all other primers and linkers. The primer marked # was redesigned as the no PCR product could be obtained using the original primer which had an additional restriction site added to it. This site was removed in the resdesigned primer.

Appendix 4 – PCR conditions, primers and linkers used in pTcass cloning strategies

PCR conditions and primers

	Primer sequence (5'→3')	Product size (bp)	Annealing temp. (°C)	[$MgCl_2$], mM
pTα (TCR CIR010α VJ-intron)				
CIR010pTαXmaI	(f) CCCGGGATGCTCCTGCTGCTCGTCCCAG	375	63	1.5
CIR010pTαHindIII	(r)GCCAGTTCCAAAGATAAGCTTGTTTGTAGC			
pTβ (TCR CIR010β VJ-intron)				
CIR010pTβXhoI	(f) CTCGAGATGAGCATCGGGCTCCTGTGC	375	64	1.5
CIR010pTβHindIII	(r) GAAAGCTTCAGTGCCCGACGCC			
pTα (TCR A10(2) α 5-D4 VJ-intron)				
B2.A105D4αVJXmaI	(f) CCCGGGATGAAAACATATGCTCCTAC	512	60	1.5
NJ109 *	(r) CGGCACATTGATTTGGGAGTC			
B1.A105D4αJiBstXI	(f) TTCTGGGACTTACCAGAGGTTTG	109	55	1.5
B1.A105D4αJiSacII	(r) CCGCGGCAAATGCTATATTAGAGAAC			
pTα (TCR A10(2) α 7-D3 VJ-intron)				
B4.A107D3αVJXmaI	(f) CCCGGGATGAAATCCTTGAGTGTTTC	367	55	1.5
B4.A107D3αVJSacI	(r) CAAATATCAGAGCTCTGCCTCC			
B3.A107D3αJiSacI	(f) GGCAGAGCTCTGATATTTGG	89	57	1.5
B3.A107D3αJiSacII	(r) CCGCGGCGGGCGTCATAATCACCAGC			
pTβ (TCR A10(2) β VJ-intron)				
B6.A10βVJXhoI	(f) CTCGAGATGGGCACCAGGCTTCTTGGC	397	65	1.5
B6.A10βVJXmaI	(r) CCTGGTCCCGGGACCGAAGTAC			
B5.A10βJiXmaI	(f) CTTCGGTCCCGGGACCAGGCTC	88	65	1.5
B5.A10βJiSacII	(r) CCGCGGCCAAACTACTCCAGGGACCCAG			
pTα (TCR D3(3) α VJ-intron)				
C2.D3αVJXmaI	(f) CCCGGGATGAAATCCTTGAGTGTTTC	397	57	1.5
C2.D3αVJKpnI	(r) CAGATACTCTGGTACCAAGACCG			
C1.D3αJiKpnI	(f) CGGTCTTGGTACCAGAGTATCTG	87	61	1.5
C1.D3αJiSacII	(r) CCGCGGCCCTCACCCCAGCTCATCCC			
pTβ (TCR D3(3) β VJ-intron)				
C4.D3βVJXhoI	(f) CTCGAGATGGGCTCCATTTTCCTCAG	394	63	1.5
C4.D3βVJBstXI	(r) CGAGTGCCGGGCCCAAAGTACTGG			
C3.D3βJiBstXIf1	(f) CACCCAGTACTTTGGGCCAGG	120	63	1.5
C3.D3βJiSacIIr1	(r) CCGCGGTGACTCCCAGAGAAACCCGG			

Linkers

Construct and cloning step	Linker name	Linker sequence (5'→3')
pTα (TCR CIR010α VJ-intron) – to insert the J-intron region of the TCR α sequence into pBluescriptII	TCRCIR010αJ-intronpTαcasstop	AGCTTATCTTTGGAACTGGCACTCTG CTTGCTGTCCAGCCAAGTACGTAAGT AGTGGCATGTGTCAGGTGGATTCTGT GTCCATGGCAAGTCCGCGGC
	TCRCIR010αJ-intronpTαcassbottom	TCGAGCCGCGGACTTGCCATGGACA CAGAATCCACCTGACACATGCCACT ACTTACGTACTTGGCTGGACAGCAA GCAGAGTGCCAGTTCCAAAGATA

pTβ (TCR CIR010β VJ-intron) – to insert the J-intron region of the TCR β sequence into pBluescriptII	TCRCIR010βJ-intronpTβcasstop	AGCTTTCTTTGGACAAGGCACCAGA CTCACAGTTGTAGGTAAGACATTTTT CAGGTTCTTTTGCAGATCCGTCACAG GGAAACCGCGGG
	TCRCIR010βJ-intronpTβcassbottom	TCGACCCGCGGTTTCCCTGTGACGGA TCTGCAAAAGAACCTGAAAAATGTC TTACCTACAACTGTGAGTCTGGTGCC TTGTCCAAAGAA

Sequencing primers

Primer name	Primer sequence (5'→3')	Primer concentration (nM)
All sequences amplified by high-fidelity PCR and cloned into TA cloning vector pCR2.1		
M13 forward *	(f) GTAAAACGACGGCCAG	10
M13 reverse *	(r) CAGGAAACAGCTATGAC	10
Final construct - pTα (TCR CIR010 α VJ-intron)		
CIR010pTαXmaI	(f) CCCGGGATGCTCCTGCTGCTCGTCCCAG	10
CIR010pTαHindIII	(r) GCCAGTTCCAAAGATAAGCTTGTTTGTAGC	10
Final construct – pTβ (TCR CIR010 β VJ-intron)		
CIR010pTβXhoI	(f) CTCGAGATGAGCATCGGGCTCCTGTGC	10
CIR010pTβHindIII	(r) GAAAGCTTCAGTGCCCGACGCC	10
Final construct - pTα (TCR A10(2) α 5-D4 VJ-intron)		
A105D4αVJXmaI	(f) CCCGGGATGAAAACATATGCTCCTAC	10
A105D4αJiSacII	(r) CCGCGGCAAATGCTATATTAGAGAAC	10
Final construct - pTα (TCR A10(2) α 7-D3 VJ-intron)		
A107D3αVJXmaI	(f) CCCGGGATGAAATCCTTGAGTGTTTC	10
A107D3αJiSacII	(r) CCGCGGCGGGCGTCATAATCACCAGC	10
Final construct – pTβ (TCR A10(2) β VJ-intron)		
A10βVJXhoI	(f) CTCGAGATGGGCACCAGGCTTCTTGGC	10
A10βJiSacII	(r) CCGCGGCCAAACTACTCCAGGGACCCAG	10
Final construct - pTα (TCR D3(3) α VJ-intron)		
D3αVJXmaI	(f) CCCGGGATGAAATCCTTGAGTGTTTC	10
D3αJiSacII	(r) CCGCGGCCCTCACCCCAGCTCATCCC	10
Final construct – pTβ (TCR D3(3) β VJ-intron)		
D3βVJXhoI	(f) CTCGAGATGGGCTCCATTTTCCTCAG	10
D3βJiSacIIr1	(r) CCGCGGTGACTCCCAGAGAAACCCGG	10

Primers marked with an asterisk (*) were designed by postdoctoral researchers in the Boyton laboratory. I designed all other primers and linkers. Primer NJ109 was used in place of a primer which I designed but which did not produce a PCR product upon use in a reaction.

Appendix 5 – restriction enzymes and digests used in MFG and pTcass cloning strategies

Single restriction enzyme digests

Enzyme	Buffer	Incubation temp. (°C)	Restriction site (5'→3')	Enzyme source
BamHI	4-CORE E (Promega)	37	G↓GATCC	Promega (R6021)
BstXI	SuRE/Cut H (Roche)	45	CCA(N)$_5$↓NTGG	Roche (111 177 770 01)
ClaI	4-CORE C (Promega)	37	AT↓CGAT	Promega (R6551)
EcoRI	4-CORE H (Promega) REact 3 (Invitrogen)	37	G↓AATTC	Promega (R6011) Invitrogen (15202-013)
HindIII	4-CORE E (Promega)	37	A↓AGCTT	Promega (R6041)
KpnI	4-CORE J (Promega)	37	GGTAC↓C	Promega (R6341)
NcoI	4-CORE D (Promega)	37	C↓CATGG	Promega (R6513)
NotI	4-CORE D (Promega)	37	GC↓GGCCGC	Promega (R6431)
SacI	4-CORE J (Promega)	37	GAGCT↓C	Promega (R6061)

Double restriction enzyme digests

Enzymes	Buffer	Incubation temp. (°C)	Restriction sites (5'→3')	Enzyme sources
ApaI/ PpuMI	NE Buffer 4 (New England Biolabs)	37	GGGCC↓C	Promega (R6361)
			RG↓GWCCY	New England Biolabs (R0506)
BamHI/ BstXI	4-CORE E (Promega)	37	G↓GATCC	Promega (R6021)
			CCA(N)$_5$↓NTGG	Promega (R6471)
BamHI/ HindIII	4-CORE E (Promega)	37	G↓GATCC ↓	Promega (R6021)
			A↓AGCTT	Promega (R6041)
BamHI/ PstI	4-CORE H (Promega)	37	G↓GATCC	Promega (R6021)
			CTGCA↓G	Promega (R6111)
BstXI/ XbaI	4-CORE D (Promega)	37	CCA(N)$_5$↓NTGG	Promega (R6471)
			T↓CTAGA	Promega (R6181)
ClaI/ XhoI	4-CORE C (Promega)	37	AT↓CGAT	Promega (R6551)
			C↓TCGAG	Promega (R6161)
EcoRI/ KpnI	4-CORE Multicore (Promega)	37	G↓AATTC	Promega (R6011)
			GGTAC↓C	Promega (R6341)
EcoRI/ PstI	4-CORE H (Promega)	37	G↓AATTC	Promega (R6011)
			CTGCA↓G	Promega (R6111)
EcoRV/ HindIII	4-CORE Multicore (Promega)	37	GAT↓ATC	Promega (R6351)
			A↓AGCTT	Promega (R6041)
HindIII/ PstI	4-CORE H (Promega)	37	A↓AGCTT	Promega (R6041)
			CTGCA↓G	Promega (R6111)
HindIII/ SalI	4-CORE C (Promega)	37	A↓AGCTT	Promega (R6041)
			G↓TCGAC	Promega (R6051)
HindIII/ XhoI	4-CORE B (Promega)	37	A↓AGCTT	Promega (R6041)
			C↓TCGAG	Promega (R6161)
KpnI/ XmaI	4-CORE Multicore (Promega)	37	GGTAC↓C	Promega (R6341)
			C↓CCGGG	Promega (R6491)
SacI/ SpeI	4-CORE E (Promega)	37	GAGCT↓C	Promega (R6061)
			A↓CTAGT	Promega (R6591)
SacII/ XhoI	4-CORE H (Promega)	37	CCGC↓GG	Promega (R6221)
			C↓TCGAG	Promega (R6161)
SacII/ XmaI	4-CORE A (Promega)	37	CCGC↓GG	Promega (R6221)
			C↓CCGGG	Promega (R6491)
XbaI/ XmaI	4-CORE B (Promega)	37	T↓CTAGA	Promega (R6181)
			C↓CCGGG	Promega (R6491)

Buffer compositions (1x)

Promega buffers – 4-CORE

Buffer A:

- 6 mM Tris-HCl
- 6 mM $MgCl_2$
- 6 mM NaCl
- 1 mM DTT
- pH 7.5 (37°C)

Buffer B:

- 6 mM Tris-HCl
- 6 mM $MgCl_2$
- 50 mM NaCl
- 1 mM DTT
- pH 7.5 (37°C)

Buffer C:

- 10 mM Tris-HCl
- 10 mM $MgCl_2$
- 50 mM NaCl
- 1 mM DTT
- pH 7.9 (37°C)

Buffer D:

- 6 mM Tris-HCl
- 6 mM $MgCl_2$
- 150 mM NaCl
- 1 mM DTT
- pH 7.9 (37°C)

Buffer E:

- 6 mM Tris-HCl
- 6 mM $MgCl_2$
- 100 mM NaCl
- 1 mM DTT
- pH 7.5 (37°C)

Buffer H:

- 90 mM Tris-HCl
- 10 mM $MgCl_2$
- 50 mM NaCl
- pH 7.5 (37°C)

Buffer J:

- 10 mM Tris-HCl
- 10 mM $MgCl_2$
- 50 mM KCl
- 1 mM DTT
- pH 7.5 (37°C)

Multi-core buffer:

- 25 mM Tris-acetate
- 10 mM Mg-acetate
- 100 mM K-acetate
- 1 mM DTT
- pH 7.5 (37°C)

Roche buffers – SuRE/Cut

Buffer H:

- 50 mM Tris-HCl
- 10 mM $MgCl_2$
- 100 mM NaCl
- 1 mM DTE
- pH 7.5 (25°C)

New England Biolabs buffers

Buffer 4:

- 20 mM Tris-acetate
- 50 mM K-acetate
- 10 mM Na-acetate
- 1 mM DTT
- pH 7.9 (25°C)

Appendix 6 – PCR conditions and primers, fluorescently-labelled FACS antibodies and restriction enzymes for Southern hybridisations used in genotyping the P4 TCR/DR1/ABO transgenic mouse lines

PCR conditions and primers

	Primer sequence (5'→3')	Product size (bp)	Annealing temp. (°C)	[$MgCl_2$], mM
RBP (housekeeping gene)				
RBPWT1 *	(f) GTTCTTAACCTGTTGGTCGGAACC	500	55	1.5
RBPWT2 *	(r) GCTTGAGGCTTGATGTTCTGTATTGC			
HLA-DR1α				
HumanDR1αF #	(f) CTCCAAGCCCTCTCCCAGAG	150	55	1.5
HumanDR1αR #	(r) ATGTGCCTTACAGAGGCCCC			
HLA-DR1β				
HumanDR1βF #	(f) TTCAATGGGACGGAGCGGGTG	200	55	1.5
HumanDR1βR #	(r) GAAAGCTTCAGTGCCCGACGCC			
Murine class II knockout				
DR1ABOF #	(f) TCCGCAGGGCATTTCGTGTA	500	60	1.5
DR1ABO-KO3 #	(r) GAGGATCTCGTCGTGACCCA			
TCR P4α chain				
TCRAP4F *	(f) TCTCAATTGCAGTTATGAAG	300	60	2.5
TCRAP4R *	(r) ATGAGCTTGTTTGTAGCACC			
TCR P4β chain				
TCRP4VβF *	(f) CACCTGATCACAGCAACTGG	400	60	1.5
TCRP4βSouthR *	(r) GGTCCACCCTCCGACTCC			
TCR P4α chain (splicing PCR)				
NewP4αF1 *	(f) ACTAGCTATCTTTTGGCTTC	478 – gDNA, 346 – cDNA	56	1.25
NewP4αR1 *	(r) CTGTGATGTTCAGGATGCTG			
TCR P4β chain (splicing PCR)				
TCRP4βSouthF *	(f) GGTCCACCCTCCGACTCC	425 – gDNA, 272 – cDNA	55	1.5
TCRBP4R *	(r) CGAAGTACTGCTCGTATACC			

Fluorescently-labelled antibodies used to identify mouse class II knockout status of P4 TCR/DR1/ABO transgenic mouse lines

	Clone	Source	Cat. no.	Working concentration	Antibody isotype
FITC-conjugated antibodies (FL1 channel)					
Monoclonal anti-mouse CD3e	145-2C11	eBioscience	11-0031	0.5 μg/10^6 cells	Armenian hamster IgG
Monoclonal anti-mouse CD45R	RA3-6B2	AbD Serotec	MCA1258F	1 μg/10^6 cells	Rat IgG2a
PE-conjugated antibodies (FL2 channel)					
Monoclonal anti-mouse CD4	GK1.5	eBioscience	12-0041	0.125 μg/10^6 cells	Rat IgG2b
Monoclonal anti-mouse I-A/I-E (MHC class II)	M5/114.15.2	BD Pharmingen	557000	1 μg/10^6 cells	Rat IgG2b

Restriction enzymes used for Southern analysis of P4 TCR/DR1/ABO transgenic mouse lines

Enzyme	Buffer	Incubation temp. (°C)	Restriction site (5'→3')	Enzyme source
P4 α Southern digest				
HindIII	4-CORE E (Promega)	37	A↓AGCTT	Promega (R6041)
EcoRV	4-CORE D (Promega)	37	GAT↓ATC	Promega (R6351)
P4 β Southern digest				
BamHI	4-CORE E (Promega)	37	G↓GATCC	Promega (R6021)

PCR conditions and primers to produce probes for the P4 TCR Southern analysis

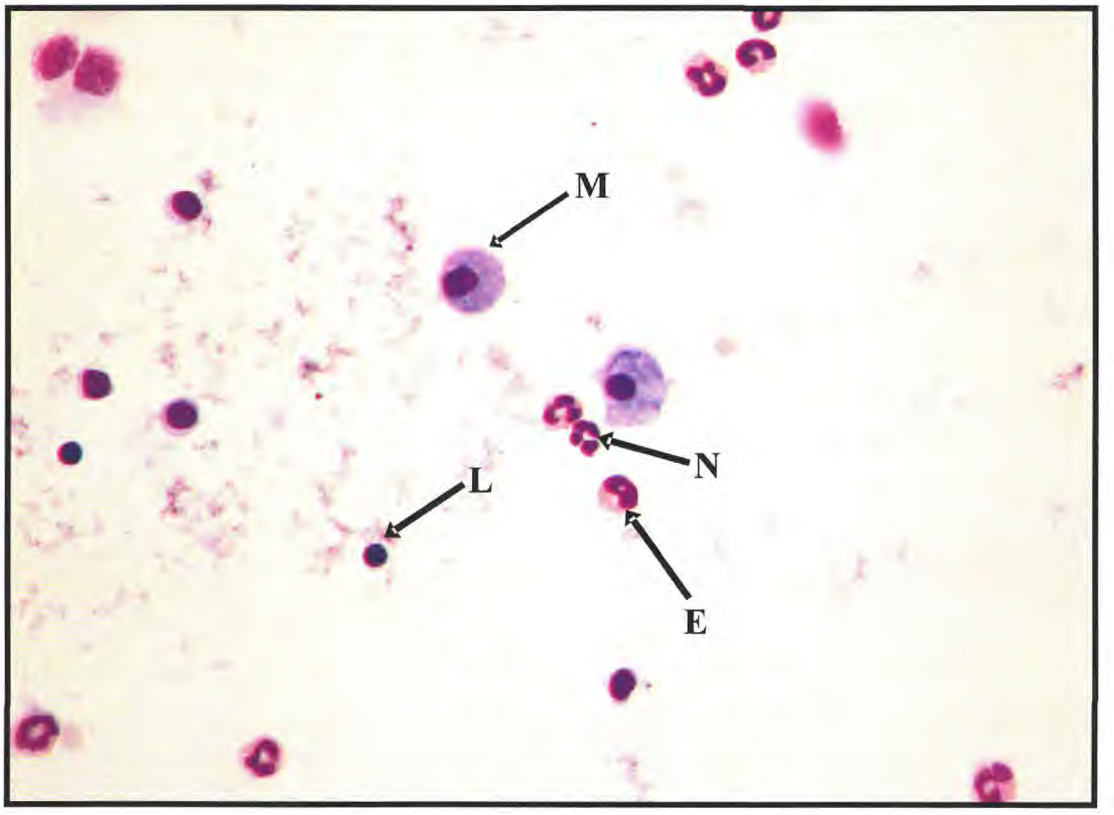
	Primer sequence (5'→3')	Product size (bp)	Annealing temp. (°C)	[$MgCl_2$], mM
P4 α probe				
TCRP4αprobeF	(f) GGATGATGAAGTGTCCACAGG	593	55	1.5
TCRP4αprobeR	(r) TGGACACAGAATCCACCTGA			
P4 β probe				
TCRP4βSouthF	(f) GGTCCACCCTCCGACTCC	646	55	1.5
TCRP4βSouthR	(r) GGTCCACCCTCCGACTCC			

All primers marked * above were designed by researchers in the Boyton laboratory. All primers marked # were designed by Prof. Danny Altmann. I designed all other primers.

Appendix 7 – fluorescently-labelled antibodies used in FACS analysis of potentially-transduced BW7 lines

	Clone	Source	Cat. no.	Working concentration	Antibody isotype
FITC-conjugated antibodies (FL1 channel)					
Monoclonal anti-mouse CD4	GK1.5	eBioscience	11-0041	0.25 μg/10^6 cells	Rat IgG2b
Monoclonal anti-mouse CD3e	145-2C11	eBioscience	11-0031	0.5 μg/10^6 cells	Armenian hamster IgG
Monoclonal anti-mouse TCRβ chain	H57-597	eBioscience	11-5961	0.5 μg/10^6 cells	Armenian hamster IgG
Monoclonal anti-mouse TCR Vβ 4 region	KT4	BD Pharmingen	553365	1 μg/10^6 cells	Rat IgG2b
Monoclonal anti-mouse TCR Vβ13 region	MR12-3	BD Pharmingen	553204	4 μg/10^6 cells	Mouse IgG1
PE-conjugated antibodies (FL2 channel)					
Monoclonal anti-mouse CD4	GK1.5	eBioscience	12-0041	0.125 μg/10^6 cells	Rat IgG2b
Monoclonal anti-mouse TCRβ chain	H57-597	eBioscience	12-5961	0.5 μg/10^6 cells	Rat IgG2b
Propidium iodide staining for cell death (FL2 channel)					
Propidium iodide	n/a	Beckman Coulter	731727	10 μl/10^6 cells	n/a

Appendix 8 – differential cell phenotyping of Wright-Giemsa stained cytospins



Key:

M - macrophage - large cells, dark purple nucleus, with light purple cytoplasm, distinctive 'fried-egg' morphology

N - neutrophil - dark purple, multi-lobed nucleus, cytoplasm does not stain

E - eosinophil - dark purple, multi-lobed nucleus, cytoplasm stains pink

L - lymphocyte - small cells, dark purple nucleus, very little visible cytoplasm

Appendix 9 – antibodies and standards used in ELISAs

Antibodies

	Clone	Source	Cat. no.	Working concentration
Capture antibodies				
Monoclonal rat anti-mouse interleukin-4 antibody	30340.11	R&D Systems	MAB404	2 μg/ml
Monoclonal rat anti-mouse/human interleukin-5 antibody	TRFK5	R&D Systems	MAB405	1 μg/ml
Monoclonal rat anti-mouse interleukin-13 antibody	38213	R&D Systems	MAB413	4 μg/ml
Monoclonal rat anti-mouse interferon-γ antibody	37801, 37875	R&D Systems	MAB785	4 μg/ml
Purified rat anti-mouse immunoglobulin E antibody	R35-72	BD Pharmingen	553413	2 μg/ml
Detection antibodies				
Biotinylated goat anti-mouse interleukin-4 antibody	Lot no. WB05	R&D Systems	BAF404	100 ng/ml
Biotinylated rat anti-mouse interleukin-5 antibody	TRFK4	R&D Systems	BAM705	50 ng/ml
Biotinylated goat anti-mouse interleukin-13 antibody	Lot no. AJP09	R&D Systems	BAF413	100 ng/ml
Biotinylated goat anti mouse interferon-γ antibody	Lot no. XR10	R&D Systems	BAF485	400 ng/ml
Biotin-conjugated rat anti-mouse immunoglobulin E antibody	R35-118	BD Pharmingen	553419	2 μg/ml

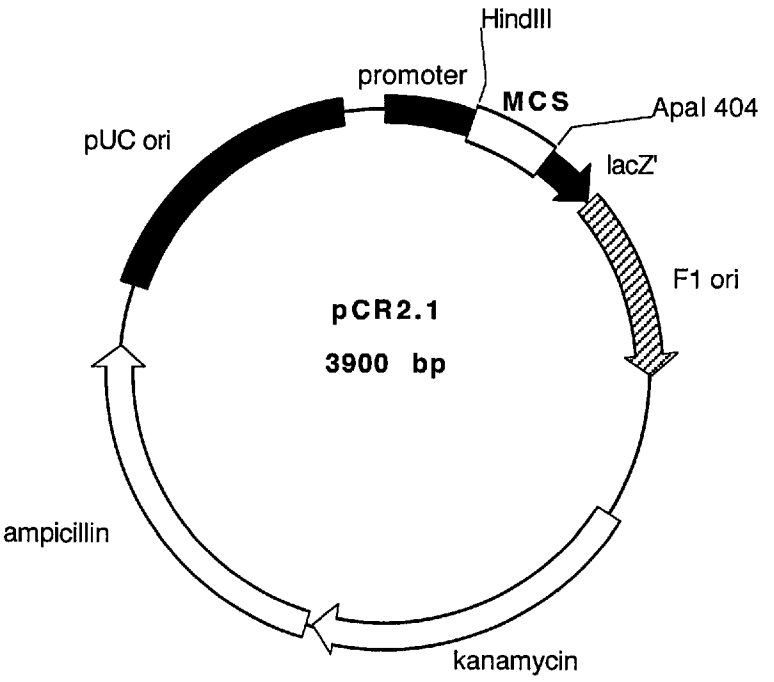
Standards

	Source	Cat. no.	No.of 2-fold dilutions	Starting concentration	Finishing concentration
Recombinant mouse interleukin-4	R&D Systems	404-ML	8	4000 pg/ml	15.6 ng/ml
Recombinant mouse interleukin-5	R&D Systems	405-ML	8	4000 pg/ml	15.6 ng/ml
Recombinant mouse interleukin-13	eBioscience	14-8131	8	4000 pg/ml	15.6 ng/ml
Recombinant mouse interferon-γ	R&D Systems	485-MI	8	4000 pg/ml	15.6 ng/ml
Purified mouse immunoglobulin E, κ (anti-TNP)	BD Pharmingen	557079 (clone C38-2)	7	500 ng/ml	3.9 ng/ml

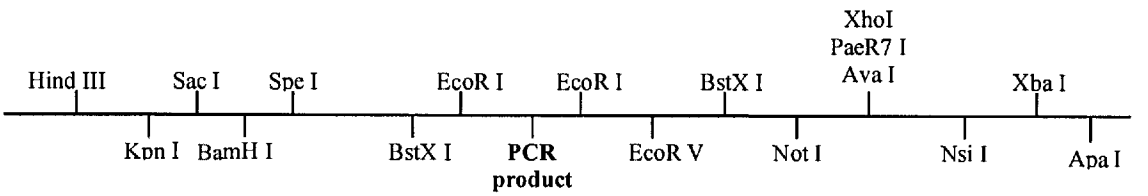
Appendix 10 – fluorescently-labelled antibodies used in FACS analysis of mice from P4 TCR/DR1/ABO transgenic lines 4 and 16

	Clone	Source	Cat. no.	Working concentration	Antibody isotype
FITC-conjugated antibodies (FL1 channel)					
Monoclonal anti-mouse CD4	GK1.5	eBioscience	11-0041	0.25 μg/10^6 cells	Rat IgG2b
Monoclonal anti-mouse CD3e	145-2C11	eBioscience	11-0031	0.5 μg/10^6 cells	Armenian hamster IgG
Monoclonal anti-mouse CD69	H1.2F3	eBioscience	11-0691	0.5 μg/10^6 cells	Armenian hamster IgG
Monoclonal anti-mouse CD25	PC61.5	eBioscience	11-0251	0.25 μg/10^6 cells	Rat IgG1
Monoclonal anti-mouse CD44	IM7	eBioscience	11-0441	0.5 μg/10^6 cells	Rat IgG2b
Monoclonal anti-mouse CD54	YN1/1.7.4	eBioscience	11-0541	1 μg/10^6 cells	Rat IgG2b
Monoclonal anti-mouse CD62L	MEL-14	eBioscience	11-0621	0.5 μg/10^6 cells	Rat IgG2a
Monoclonal anti-mouse OX40	OX-86	AbD Serotec	MCA1420F	1 μg/10^6 cells	Rat IgG1
PE-conjugated antibodies (FL2 channel)					
Monoclonal anti-mouse CD8a	53-6.7	eBioscience	12-0081	0.25 μg/10^6 cells	Rat IgG2a
Monoclonal anti-mouse CD4	GK1.5	eBioscience	12-0041	0.125 μg/10^6 cells	Rat IgG2b
Monoclonal anti-mouse OX40L	RM134L	eBioscience	12-5905	0.5 μg/10^6 cells	Rat IgG2b
Monoclonal anti mouse ICOS	7E.17G9	eBioscience	12-9942	0.25 μg/10^6 cells	Rat IgG2b
PE-Cy5-conjugated antibodies (FL3 channel)					
Monoclonal anti-mouse CD8a	53-6.7	eBioscience	13-0081	0.125 μg/10^6 cells	Rat IgG2a

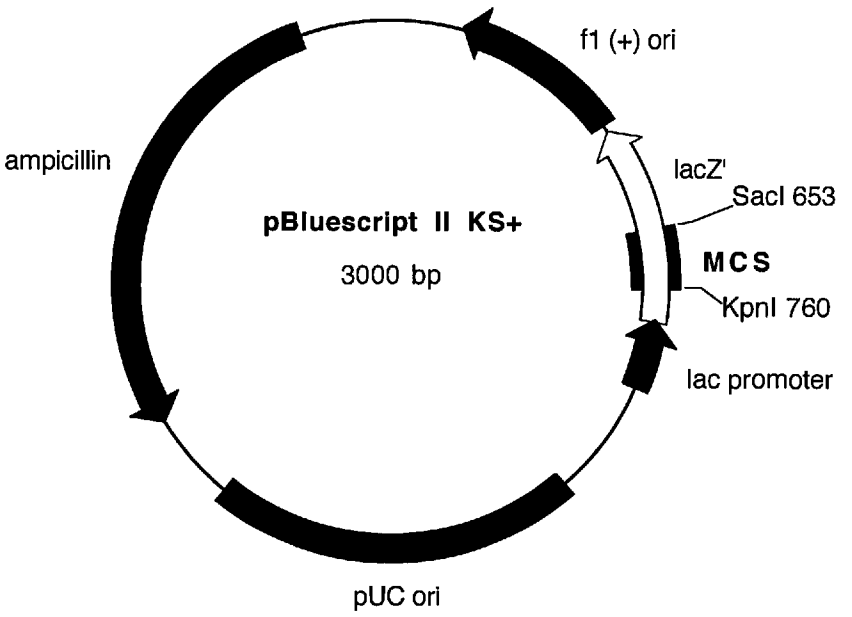
Appendix 11 - pCR®2.1 – vector map and multiple cloning site



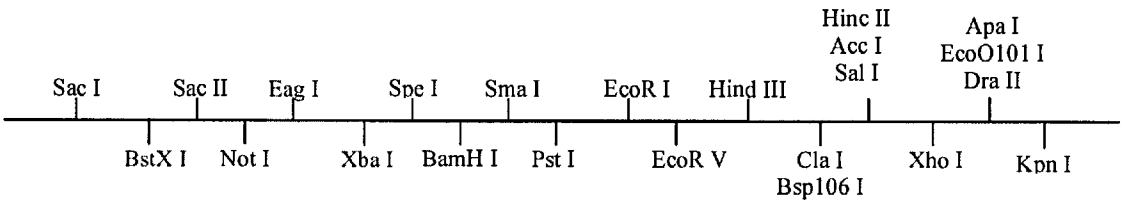
Multiple cloning site:



Appendix 12 - pBluescriptII vector map and multiple cloning site



Multiple cloning site:



Appendix 13 - Amino acid sequence of the TCR α chain (TRAV 5-D4 TRAJ 13 TRAC) from the murine T cell clone A10(2) (chain 5-D4) cloned into retroviral vector MFG

1
ATG AAA ACA TAT GCT CCT ACA TTA TTC ATG TTT CTA TGG CTG CAG CTG GAT GGG ATG AGC CAA
M K T Y A P T L F M F L W L Q L D G M S Q

64
GGC GAG CAG GTG GAG CAG CTT CCT TCC ATC CTG AGA GTC CAG GAG GGA TCC AGT GCC AGC
G E Q V E Q L P S I L R V Q E G S S A S

123
ATC AAC TGC ACT TAT GAG AAC AGT GCC TCC AAC TAC TTC CCT TGG TAT AAG CAA GAA CCT GGA
I N C T Y E N S A S N Y F P W Y K Q E P G

186
GAG AAT CCT AAG CTC ATC ATT GAC ATT CGT TCA AAT ATG GAA AGA AAG CAG ACC CAA GGA CTC
E N P K L I I D I R S N M E R K Q T Q G L

249
ATC GTT TTA CTG GAT AAG AAA GCC AAA CGC TTC TCC CTG CAC ATC ACA GAC ACC CAG CCT GGA
I V L L D K K A K R F S L H I T D T Q P G

312
GAC TCA GCC ATG TAC TTC TGT GCT GCA AAA AAT TCT GGG ACT TAC CAG AGG TTT GGA ACT GGG
D S A M Y F C A A K N S G T Y Q R F G T G

375
ACA AAA CTC CAA GTC GTT CCA AAC ATC CAG AAC CCA GAA CCT GCT GTG TAC CAG TTA AAA GAT
T K L Q V V P N I Q N P E P A V Y Q L K D

438
CCG CGG TCT CAG GAC AGC ACC CTC TGC CTG TTC ACC GAC TTT GAC TCC CAA ATC AAT GTG CCG
P R S Q D S T L C L F T D F D S Q I N V P

501
AAA ACC ATG GAA TCT GGA ACG TTC ATC ACT GAC AAA ACT GTG CTG GAC ATG AAA GCT ATG GAT
K T M E S G T F I T D K T V L D M K A M D

564
TCC AAG AGC AAT GGG GCC ATT GCC TGG AGC AAC CAG ACA AGC TTC ACC TGC CAA GAT ATC TTC
S K S N G A I A W S N Q T S F T C Q D I F

627
AAA GAG ACC AAC GCC ACC TAC CCC AGT TCA GAC GTT CCC TGT GAT GCC ACG TTG ACT GAG AAA
K E T N A T Y P S S D V P C D A T L T E K

690
AGC TTT GAA ACA GAT ATG AAC CTA AAC TTT CAA AAC CTG TCA GTT ATG GGA CTC CGA ATC CTC
S F E T D M N L N F Q N L S V M G L R I L

753 810
CTG CTG AAA GTA GCC GGA TTT AAC CTG CTC ATG ACG CTG AGG CTG TGG TCC AGT TGA
L L K V A G F N L L M T L R L W S S **STOP**

TRAV 5-D4 is highlighted in green, TRAJ 13 in purple and TRAC 1 in turquoise. The CDR3 is highlighted in blue with the coding DNA sequence underlined.

Appendix 14 - Amino acid sequence of the TCR α chain (TRAV 7-D3 TRAJ 15 TRAC) from the murine T cell clone A10(2) (chain 7-D3) cloned into retroviral vector MFG

1
ATG AAA TCC TTG AGT GTT TCC CTA GTG GTC CTG TGG CTC CAG TTA AAC TGG GTG AAC AGC CAG
M K S L S V S L V V L W L Q L N W V N S Q

64
CAG AAG GTG CAG CAG AGC CCA GAA TCC CTC ATT GTC CCA GAG GGA GCC ATG ACC TCT CTC AAC
Q K V Q Q S P E S L I V P E G A M T S L N

127
TGC ACT TTC AGC GAC AGT GCT TCT CAG TAT TTT GCA TGG TAC AGA CAG CAT TCT GGG AAA GCC
C T F S D S A S Q Y F A W Y R Q H S G K A

190
CCC AAG GCA CTG ATG TCC ATC TTC TCC AAT GGT GAA AAA GAA GAA GGC AGA TTC ACA ATT CAC
P K A L M S I F S N G E K E E G R F T I H

253
CTC AAT AAA GCC AGT CTG CAT TTC TCG CTA CAC ATC AGA GAC TCC CAG CCC AGT GAC TCT GCT
L N K A S L H F S L H I R D S Q P S D S A

316
CTC TAC CTC TGT GCA GGA GGG CAG GGA GGC AGA GCT CTG ATA TTT GGA ACA GGA ACC ACG GTA
L Y L C A G G Q G G R A L I F G T G T T V

379
TCA GTC AGC CCC AAC ATC CAG AAC CCA GAA CCT GCT GTG TAC CAG TTA AAA GAT CCG CGG TCT
S V S P N I Q N P E P A V Y Q L K D P R S

442
CAG GAC AGC ACC CTC TGC CTG TTC ACC GAC TTT GAC TCC CAA ATC AAT GTG CCG AAA ACC ATG
Q D S T L C L F T D F D S Q I N V P K T M

505
GAA TCT GGA ACG TTC ATC ACT GAC AAA ACT GTG CTG GAC ATG AAA GCT ATG GAT TCC AAG AGC
E S G T F I T D K T V L D M K A M D S K S

568
AAT GGG GCC ATT GCC TGG AGC AAC CAG ACA AGC TTC ACC TGC CAA GAT ATC TTC AAA GAG ACC
N G A I A W S N Q T S F T C Q D I F K E T

631
AAC GCC ACC TAC CCC AGT TCA GAC GTT CCC TGT GAT GCC ACG TTG ACT GAG AAA AGC TTT GAA
N A T Y P S S D V P C D A T L T E K S F E

694
ACA GAT ATG AAC CTA AAC TTT CAA AAC CTG TCA GTT ATG GGA CTC CGA ATC CTC CTG CTG AAA
T D M N L N F Q N L S V M G L R I L L L K

757 804
GTA GCC GGA TTT AAC CTG CTC ATG ACG CTG AGG CTG TGG TCC AGT TGA
V A G F N L L M T L R L W S S **STOP**

TRAV 7-D3 is highlighted in green, TRAJ 15 in purple and TRAC 1 in turquoise. The CDR3 is highlighted in blue with the coding DNA sequence underlined.

Appendix 15 - Amino acid sequence of the TCR α chain (TRAV 7-D4 TRAJ 26-like TRAC) from the murine T cell clone D3(3) cloned into retroviral vector MFG

1
ATG AAA TCC TTG AGT GTT TCA CTA GTG GTC CTG TGG CTC CAG GTA AAC TGC GTG AGG AGC CAG
M K S L S V S L V V L W L Q V N C V R S Q

64
CAG AAG GTG CAG CAG AGC CCA GAA TCC CTC AGT GTC CCA GAG GGA GGC ATG GCC TCT TTC AAC
Q K V Q Q S P E S L S V P E G G M A S F N

127
TGC ACT TCA AGT GAT CGT AAT TTT CAG TAC TTC TGG TGG TAC AGA CAG CAT TCT GGA GAA GGC
C T S S D R N F Q Y F W W Y R Q H S G E G

190
CCC AAG GCA CTG ATG TCA ATC TTC TCT GAT GGT GAC AAG AAA GAA GGC AGA TTT ACA GCT CAC
P K A L M S I F S D G D K K E G R F T A H

253
CTC AAT AAG GCC AGC CTG CAT GTT TCC CTG CAC ATC AGA GAC TCC CAG CCC AGT GAC TCC GCT
L N K A S L H V S L H I R D S Q P S D S A

316
CTC TAC TTC TGT GCA GCT AGT GCC GTG GAT AAC TAT GCC CAG GGA TTA ACC TTC GGT CTT GGC
L Y F C A A S A V D N Y A Q G L T F G L G

379
ACC AGA GTA TCT GTG TTT CCC TAC ATC CAA AAC CCA GAA CCT GCT GTG TAC CAG TTA AAA GAT
T R V S V F P Y I Q N P E P A V Y Q L K D

442
CCG CGG TCT CAG GAC AGC ACC CTC TGC CTG TTC ACC GAC TTT GAC TCC CAA ATC AAT GTG CCG
P R S Q D S T L C L F T D F D S Q I N V P

505
AAA ACC ATG GAA TCT GGA ACG TTC ATC ACT GAC AAA ACT GTG CTG GAC ATG AAA GCT ATG GAT
K T M E S G T F I T D K T V L D M K A M D

568
TCC AAG AGC AAT GGG GCC ATT GCC TGG AGC AAC CAG ACA AGC TTC ACC TGC CAA GAT ATC TTC
S K S N G A I A W S N Q T S F T C Q D I F

631
AAA GAG ACC AAC GCC ACC TAC CCC AGT TCA GAC GTT CCC TGT GAT GCC ACG TTG ACT GAG AAA
K E T N A T Y P S S D V P C D A T L T E K

694
AGC TTT GAA ACA GAT ATG AAC CTA AAC TTT CAA AAC CTG TCA GTT ATG GGA CTC CGA ATC CTC
S F E T D M N L N F Q N L S V M G L R I L

757 813
CTG CTG AAA GTA GCC GGA TTT AAC CTG CTC ATG ACG CTG AGG CTG TGG TCC AGT TGA
L L K V A G F N L L M T L R L W S S **STOP**

TRAV 7-D4 is highlighted in green, TRAJ 26-like (95% identity) in purple and TRAC 1 in turquoise. The CDR3 is highlighted in blue with the coding DNA sequence underlined.

Appendix 16 - Amino acid sequence of the TCRβ chain (TRBV 14 TRBJ 2-7 TRBC 1) from the murine T cell clone A10(2) cloned into retroviral vector MFG

1
ATG GGC ACC AGG CTT CTT GGC TGG GCA GTG TTC TGT CTC CTT GAC ACA GTA CTG TCT GAA GCT
M G T R L L G W A V F C L L D T V L S E A

64
GGA GTC ACC CAG TCT CCC AGA TAT GCA GTC CTA CAG GAA GGG CAA GCT GTT TCC TTT TGG TGT
G V T Q S P R Y A V L Q E G Q A V S F W C

127
GAC CCT ATT TCT GGA CAT GAT ACC CTT TAC TGG TAT CAG CAG CCC AGA GAC CAG GGG CCC CAG
D P I S G H D T L Y W Y Q Q P R D Q G P Q

190
CTT CTA GTT TAC TTT CGG GAT GAG GCT GTT ATA GAT AAT TCA CAG TTG CCC TCG GAT CGA TTT
L L V Y F R D E A V I D N S Q L P S D R F

253
TCT GCT GTG AGG CCT AAA GGA ACT AAC TCC ACT CTC AAG ATC CAG TCT GCA AAG CAG GGC GAC
S A V R P K G T N S T L K I Q S A K Q G D

316
ACA GCC ACC TAT CTC TGT GCC AGC AGC CCC CTC GAC TGG GGG GAT GAA CAG TAC TTC GGT CCC
T A T Y L C A S S P L D W G D E Q Y F G P

379
GGC ACC AGG CTC ACG GTT TTA GAG GAT CTG AGA AAT GTG ACT CCA CCC AAG GTC TCC TTG TTT
G T R L T V L E D L R N V T P P K V S L F

442
GAG CCA TCA AAA GCC GAG CTG GCA AAC AAA CAA AAG GCT ACC CTC GTG TGC TTG GCC AGG GGC
E P S K A E L A N K Q K A T L V C L A R G

505
TTC TTC CCT GAC CAC GTG GAG CTG AGC TGG TGG GTG AAT GGC AAG GAG GTC CAC AGT GGG GTC
F F P D H V E L S W W V N G K E V H S G V

568
AGC ACG GAC CCT CAG GCC TAC AAG GAG AGC AAT TAT AGC TAC TGC CTG AGC AGC CGC CTG AGG
S T D P Q A Y K E S N Y S Y C L S S R L R

631
GTC TCT GCT ACC TTC TGG CAC AAT CCT CGA AAC CAC TTC CGC TGC CAA GTG CAG TTC CAT GGG
V S A T F W H N P R N H F R C Q V Q F H G

694
CTT TCA GAG GAG GAC AAG TGG CCA GAG GGC TCA CCC AAA CCT GTC ACA CAG AAC ATC AGT GCA
L S E E D K W P E G S P K P V T Q N I S A

757
GAG GCC TGG GGC CGA GCA GAC TGT GGA ATC ACT TCA GCA TCC TAT CAT CAG GGG GTT CTG TCT
E A W G R A D C G I T S A S Y H Q G V L S

820
GCA ACC ATC CTC TAT GAG ATC CTA CTG GGG AAG GCC ACC CTA TAT GCT GTG CTG GTC AGT GGC
A T I L Y E I L L G K A T L Y A V L V S G

883 921
CTG GTG CTG ATG GCC ATG GTC AAG AAA AAA AAT TCC TGA
L V L M A M V K K K N S **STOP**

TRBV 14 is highlighted in green, TRBJ 2-7 in purple and TRBC 1 in turquoise. The CDR3 is highlighted in blue with the coding DNA sequence underlined. The letter underlined in red indicates the base pair that was inserted by site-directed mutagenesis in order to convert the incorrect sequence to the original DNA sequence, thus allowing for correct read-through of the amino acid sequence and correct positioning of the stop codon.

Appendix 17 - Amino acid sequence of the TCRβ chain (TRBV 2 TRBJ 2-5 TRBC 1) from the murine T cell clone D3(3) cloned into retroviral vector MFG

1
ATG GGC TCC ATT TTC CTC AGT TGC CTG GCC GTT TGT CTC CTG GTG GCA GGT CCA GTC GAC CCG
M G S I F L S C L A V C L L V A G P V D P

64
AAA ATT ATC CAG AAA CCA AAA TAT CTG GTG GCA GTC ACA GGG AGC GAA AAA ATC CTG ATA TGC
K I I Q K P K Y L V A V T G S E K I L I C

127
GAA CAG TAT CTA GGC CAC AAT GCT ATG TAT TGG TAT AGA CAA AGT GCT AAG AAG CCT CTA GAG
E Q Y L G H N A M Y W Y R Q S A K K P L E

190
TTC ATG TTT TCC TAC AGC TAT CAA AAA CTT ATG GAC AAT CAG ACT GCC TCA AGT CGC TTC CAA
F M F S Y S Y Q K L M D N Q T A S S R F Q

253
CCT CAA AGT TCA AAG AAA AAC CAT TTA GAC CTT CAG ATC ACA GCT CTA AAG CCT GAT GAC TCG
P Q S S K K N H L D L Q I T A L K P D D S

316
GCC ACA TAC TTC TGT GCC AGC AGC CAA GCC GGG ACT GGA GAA GAC ACC CAG TAC TTT GGG CCA
A T Y F C A S S Q A G T G E D T Q Y F G P

379
GGC ACT CGG CTC CTC GTG TTA GAG GAT CTG AGA AAT GTG ACT CCA CCC AAG GTC TCC TTG TTT
G T R L L V L E D L R N V T P P K V S L F

442
GAG CCA TCA AAA GCC GAG CTG GCA AAC AAA CAA AAG GCT ACC CTC GTG TGC TTG GCC AGG GGC
E P S K A E L A N K Q K A T L V C L A R G

505
TTC TTC CCT GAC CAC GTG GAG CTG AGC TGG TGG GTG AAT GGC AAG GAG GTC CAC AGT GGG GTC
F F P D H V E L S W W V N G K E V H S G V

568
AGC ACG GAC CCT CAG GCC TAC AAG GAG AGC AAT TAT AGC TAC TGC CTG AGC AGC CGC CTG AGG
S T D P Q A Y K E S N Y S Y C L S S R L R

631
GTC TCT GCT ACC TTC TGG CAC AAT CCT CGA AAC CAC TTC CGC TGC CAA GTG CAG TTC CAT GGG
V S A T F W H N P R N H F R C Q V Q F H G

694
CTT TCA GAG GAG GAC AAG TGG CCA GAG GGC TCA CCC AAA CCT GTC ACA CAG AAC ATC AGT GCA
L S E E D K W P E G S P K P V T Q N I S A

757
GAG GCC TGG GGC CGA GCA GAC TGT GGA ATC ACT TCA GCA TCC TAT CAT CAG GGG GTT CTG TCT
E A W G R A D C G I T S A S Y H Q G V L S

820
GCA ACC ATC CTC TAT GAG ATC CTA CTG GGG AAG GCC ACC CTA TAT GCT GTG CTG GTC AGT GGC
A T I L Y E I L L G K A T L Y A V L V S G

883 921
CTG GTG CTG ATG GCC ATG GTC AAG AAA AAA AAT TCC TGA
L V L M A M V K K K N S **STOP**

TRBV 2 is highlighted in green, TRBJ 2-5 in purple and TRBC 1 in turquoise. The CDR3 is highlighted in blue with the coding sequence underlined. The letter underlined in red indicates the base pair inserted by site-directed mutagenesis to convert the incorrect sequence to the original DNA sequence, allowing for correct read-through of the amino acid sequence and correct positioning of the stop codon.

Appendix 18 - Amino acid sequence of the dominant TCR α chain (TRAV 8-4 TRAJ 32 TRAC) from the human T cell line 010 cloned into retroviral vector MFG

1
ATG CTC CTG CTG CTC GTC CCA GTG CTC GAG GTG ATT TTT ACC CTG GGA GGA ACC AGA
M L L L L V P V L E V I F T L G G T R

58
GCC CAG TCG GTG ACC CAG CTT GGC AGC CAC GTC TCT GTC TCT GAG GGA GCC CTG GTT
A Q S V T Q L G S H V S V S E G A L V

115
CTG CTG AGG TGC AAC TAC TCA TCG TCT GTT CCA CCA TAT CTC TTC TGG TAT GTG CAA
L L R C N Y S S S V P P Y L F W Y V Q

172
TAC CCC AAC CAA GGA CTC CAG CTT CTC CTG AAG TAC ACA ACA GGG GCC ACC CTG GTT
Y P N Q G L Q L L L K Y T T G A T L V

229
AAA GGC ATC AAC GGT TTT GAG GCT GAA TTT AAG AAG AGT GAA ACC TCC TTC CAC CTG
K G I N G F E A E F K K S E T S F H L

286
ACG AAA CCC TCA GCC CAT ATG AGC GAC GCG GCT GAG TAC TTC TGT GCC GTG TGG AGT
T K P S A H M S D A A E Y F C A V W S

343
GGT GCT ACA AAC AAG CTC ATC TTT GGA ACT GGC ACT CTG CTT GCT GTC CAG CCA AAT
G A T N K L I F G T G T L L A V Q P N

400
ATC CAG AAC CCT GAC CCT GCC GTG TAC CAG CTG AGA GAC TCT AAA TCC AGT GAC AAG
I Q N P D P A V Y Q L R D S K S S D K

457
TCT GTC TGC CTA TTC ACC GAT TTT GAT TCT CAA ACA AAT GTG TCA CAA AGT AAG GAT
S V C L F T D F D S Q T N V S Q S K D

514
TCT GAT GTG TAT ATC ACA GAC AAA ACT GTG CTA GAC ATG AGG TCT ATG GAC TTC AAG
S D V Y I T D K T V L D M R S M D F K

571
AGC AAC AGT GCT GTG GCC TGG AGC AAC AAA TCT GAC TTT GCA TGT GCA AAC GCC TTC
S N S A V A W S N K S D F A C A N A F

628
AAC AAC AGC ATT ATT CCA GAA GAC ACC TTC TTC CCC AGC CCA GAA AGT TCC TGT GAT
N N S I I P E D T F F P S P E S S C D

685
GTC AAG CTG GTC GAG AAA AGC TTT GAA ACA GAT ACG AAC CTA AAC TTT CAA AAC CTG
V K L V E K S F E T D T N L N F Q N L

742
TCA GTG ATT GGG TTC CGA ATC CTC CTC CTG AAA GTG GCC GGG TTT AAT CTG CTC ATG
S V I G F R I L L L K V A G F N L L M

799 822
ACG CTG CGG CTG TGG TCC AGC TGA
T L R L W S S **STOP**

TRAV 8-4 is highlighted in green, TRAJ 32 in purple and TRAC 1 in turquoise. The CDR3 is highlighted in blue with the coding DNA sequence underlined.

Appendix 19 - Amino acid sequence of the dominant TCR α chain (TRAV 8-4 TRAJ 32) from the human T cell line CIR010 joined to a murine C region (murine TRAC 1) cloned into retroviral vector MFG

1
ATG CTC CTG CTG CTC GTC CCA GTG CTC GAG GTG ATT TTT ACC CTG GGA GGA ACC AGA GCC
M L L L L V P V L E V I F T L G G T R A

61
CAG TCG GTG ACC CAG CTT GGC AGC CAC GTC TCT GTC TCT GAG GGA GCC CTG GTT CTG CTG
Q S V T Q L G S H V S V S E G A L V L L

121
AGG TGC AAC TAC TCA TCG TCT GTT CCA CCA TAT CTC TTC TGG TAT GTG CAA TAC CCC AAC
R C N Y S S S V P P Y L F W Y V Q Y P N

181
CAA GGA CTC CAG CTT CTC CTG AAG TAC ACA ACA GGG GCC ACC CTG GTT AAA GGC ATC AAC
Q G L Q L L L K Y T T G A T L V K G I N

241
GGT TTT GAG GCT GAA TTT AAG AAG AGT GAA ACC TCC TTC CAC CTG ACG AAA CCC TCA GCC
G F E A E F K K S E T S F H L T K P S A

301
CAT ATG AGC GAC GCG GCT GAG TAC TTC TGT GCC GTG TGG AGT GGT GCT ACA AAC AAG CTC
H M S D A A E Y F C A V W S G A T N K L

361 GCC
ATC TTT GGA ACT GGC ACT CTG CTT GCT GTC CAG CCA AAT ATC CAG AAC CCT GAA *CCT GCA*
I F G T G T L L A V Q P N I Q N P E P A

421
*G*TG TAC CAG TTA AAA GAT CCT CGG TCT CAG GAC AGC ACC CTC TGC CTG TTC ACC GAC TTT
V Y Q L K D P R S Q D S T L C L F T D F

481
GAC TCC CAA ATC AAT GTG CCG AAA ACC ATG GAA TCT GGA ACG TTC ATC ACT GAC AAA ACT
D S Q I N V P K T M E S G T F I T D K T

541
GTG CTG GAC ATG AAA GCT ATG GAT TCC AAG AGC AAT GGG GCC ATT GCC TGG AGC AAC CAG
V L D M K A M D S K S N G A I A W S N Q

601
ACA AGC TTC ACC TGC CAA GAT ATC TTC AAA GAG ACC AAC GCC ACC TAC CCC AGT TCA GAC
T S F T C Q D I F K E T N A T Y P S S D

661
GTT CCC TGT GAT GCC ACG TTG ACC GAG AAA AGC TTT GAA ACA GAT ATG AAC CTA AAC TTT
V P C D A T L T E K S F E T D M N L N F

721
CAA AAC CTG TCA GTT ATG GGA CTC CGA ATC CTC CTG CTG AAA GTA GCG GGA TTT AAC CTG
Q N L S V M G L R I L L L K V A G F N L

781 810
CTC ATG ACG CTG AGG CTG TGG TCC AGT TGA
L M T L R L W S S **STOP**

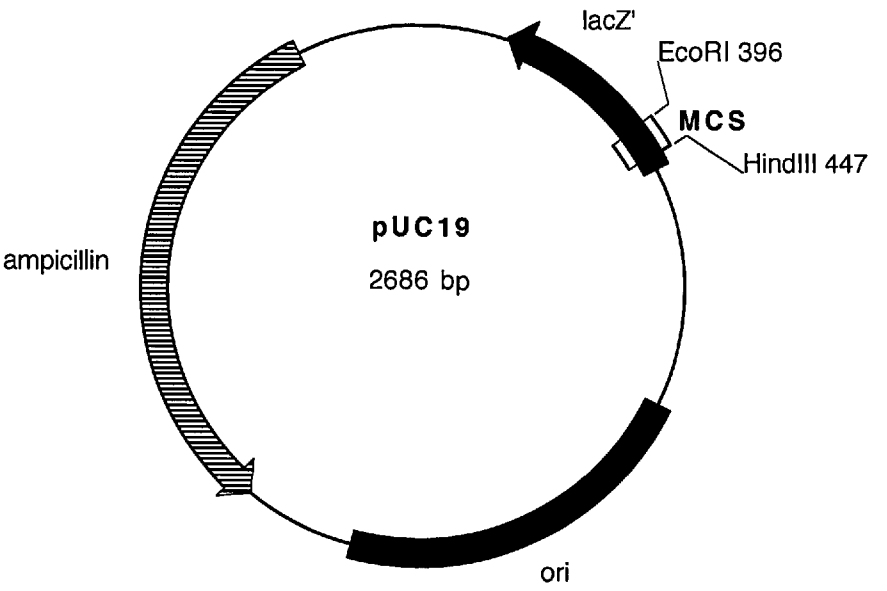
TRAV 8-4 is highlighted in green, TRAJ 32 in purple and murine TRAC 1 in turquoise. The CDR3 is highlighted in blue with the coding DNA sequence underlined. The letters underlined in red indicate the base pair change (C→A) that was required to allow the VJ and C regions to be combined using PstI (site in italics). This did not cause a change in the amino acid sequence of the translated protein (codons GCC and GCA both code for the amino acid alanine).

Appendix 20 - Amino acid sequence of the dominant TCR β chain (TRBV 6-1 TRBJ 1-1) from the human T cell line CIR010 joined to a murine C region (murine TRBC 1) cloned into retroviral vector MFG

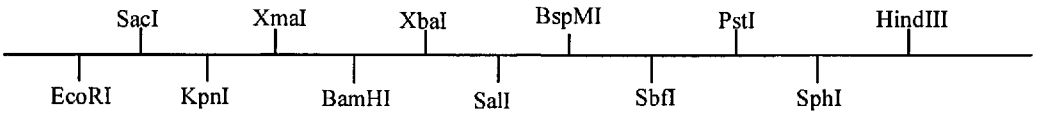
1
ATG AGC ATC GGG CTC CTG TGC TGT GTG GCC TTT TCT CTC CTG TGG GCA AGT CCA GTG AAT
M S I G L L C C V A F S L L W A S P V N
61
GCT GGT GTC ACT CAG ACC CCA AAA TTC CAG GTC CTG AAG ACA GGA CAG AGC ATG ACA CTG
A G V T Q T P K F Q V L K T G Q S M T L
121
CAG TGT GCC CAG GAT ATG AAC CAT AAC TCC ATG TAC TGG TAT CGA CAA GAC CCA GGC ATG
Q C A Q D M N H N S M Y W Y R Q D P G M
181
GGA CTG AGG CTG ATT TAT TAC TCA GCT TCT GAG GGT ACC ACT GAC AAA GGA GAA GTC CCC
G L R L I Y Y S A S E G T T D K G E V P
241
AAT GGC TAC AAT GTC TCC AGA TTA AAC AAA CGG GAG TTC TCG CTC AGG CTG GAG TCG GCT
N G Y N V S R L N K R E F S L R L E S A
301
GCT CCC TCC CAG ACA TCT GTG TAC TTC TGT GCC AGC AGT GAG GCT GGG TGG GGG GCG TCG
A P S Q T S V Y F C A S S E A G W G A S
361 GAT
GGC ACT GAA GCT TTC TTT GGA CAA GGC ACC AGA CTC ACA GTT GTA G*AG GAC CTG* AGA AAT
G T E A F F G Q G T R L T V V E D L R N
421
GTG ACT CCA CCC AAG GTC TCC TTG TTT GAG CCA TCA AAA GCA GAG ATT GCA AAC AAA CAA
V T P P K V S L F E P S K A E I A N K Q
481
AAG GCT ACC CTC GTG TGC TTG GCC AGG GGC TTC TTC CCT GAC CAC GTG GAG CTG AGC TGG
K A T L V C L A R G F F P D H V E L S W
541
TGG GTG AAT GGC AAG GAG GTC CAC AGT GGG GTC AGC ACG GAC CCT CAG GCC TAC AAG GAG
W V N G K E V H S G V S T D P Q A Y K E
601
AGC AAT TAT AGC TAC TGC CTG AGC AGC CGC CTG AGG GTC TCT GCT ACC TTC TGG CAC AAT
S N Y S Y C L S S R L R V S A T F W H N
661
CCT CGC AAC CAC TTC CGC TGC CAA GTG CAG TTC CAT GGG CTT TCA GAG GAG GAC AAG TGG
P R N H F R C Q V Q F H G L S E E D K W
721
CCA GAG GGC TCA CCC AAA CCT GTC ACA CAG AAC ATC AGT GCA GAG GCC TGG GGC CGA GCA
P E G S P K P V T Q N I S A E A W G R A
781
GAC TGT GGG ATT ACC TCA GCA TCC TAT CAA CAA GGG GTC TTG TCT GCC ACC ATC CTC TAT
D C G I T S A S Y Q Q G V L S A T I L Y
841
GAG ATC CTG CTA GGG AAA GCC ACC CTG TAT GCT GTG CTT GTC AGT ACA CTG GTG GTG ATG
E I L L G K A T L Y A V L V S T L V V M
901 927
GCT ATG GTC AAA AGA AAG AAT TCA TGA
A M V K R K N S **STOP**

TRBV 6-1 is highlighted in green, TRBJ 1-1 in purple and murine TRBC 1 in turquoise. The CDR3 is highlighted in blue with the coding DNA sequence underlined. The letters underlined in red indicate the base pair change (C→T) that was required to allow the VJ and C regions to be combined using PpuMI (site in italics). This did not cause a change in the amino acid sequence of the translated protein (codons GAC and GAT both code for the amino acid aspartic acid).

Appendix 21 - pUC19 – vector diagram and multiple cloning site



Multiple cloning site:



Appendix 22 - Amino acid sequence of one of the two TCR α chains (TRAV 5-D4 TRAJ 13) from the murine T cell clone A10(2) cloned into the TCR cassette vector pTαcass

1
ATG AAA ACA TAT GCT CCT ACA TTA TTC ATG TTT CTA TGG CTG CAG CTG GAT GGG ATG AGC
M K T Y A P T L F M F L W L Q L D G M S

61
CAA GGC GAG CAG GTG GAG CAG CTT CCT TCC ATC CTG AGA GTC CAG GAG GGA TCC AGT GCC
Q G E Q V E Q L P S I L R V Q E G S S A

121
AGC ATC AAC TGC ACT TAT GAG AAC AGT GCC TCC AAC TAC TTC CCT TGG TAT AAG CAA GAA
S I N C T Y E N S A S N Y F P W Y K Q E

181
CCT GGA GAG AAT CCT AAG CTC ATC ATT GAC ATT CGT TCA AAT ATG GAA AGA AAG CAG ACC
P G E N P K L I I D I R S N M E R K Q T

241
CAA GGA CTC ATC GTT TTA CTG GAT AAG AAA GCC AAA CGC TTC TCC CTG CAC ATC ACA GAC
Q G L I V L L D K K A K R F S L H I T D

301
ACC CAG CCT GGA GAC TCA GCC ATG TAC TTC TGT GCT GCA AAA AAT TCT GGG ACT TAC CAG
T Q P G D S A M Y F C A A K N S G T Y Q

361
AGG TTT GGA ACT GGG ACA AAA CTC CAA GTC GTT CCA AGT AAG TCC ATG TCT GAA TTG TTC
R F G T G T K L Q V V P

421 447
TCA TGT TGT TCT CTA ATA TAG CAT TTG

TRAV 5-D4 is highlighted in green and TRAJ 13 in purple. The additional intronic sequence required for correct processing of the vector is also shown, untranslated, in turquoise. The CDR3 is highlighted in blue with the coding DNA sequence underlined. Letters shown in red indicate the restriction site (BstXI) used to combine the V-J region with the J-intronic sequence.

Appendix 23 - Amino acid sequence of one of the two TCR α chains (TRAV 7-D3 TRAJ 15) from the murine T cell clone A10(2) cloned into the TCR cassette vector pTαcass

1
ATG AAA TCC TTG AGT GTT TCC CTA GTG GTC CTG TGG CTC CAG TTA AAC TGG GTG AAC AGC
M K S L S V S L V V L W L Q L N W V N S

61
CAG CAG AAG GTG CAG CAG AGC CCA GAA TCC CTC ATT GTC CCA GAG GGA GCC ATG ACC TCT
Q Q K V Q Q S P E S L I V P E G A M T S

121
CTC AAC TGC ACT TTC AGC GAC AGT GCT TCT CAG TAT TTT GCA TGG TAC AGA CAG CAT TCT
L N C T F S D S A S Q Y F A W Y R Q H S

181
GGG AAA GCC CCC AAG GCA CTG ATG TCC ATC TTC TCC AAT GGT GAA AAA GAA GAA GGC AGA
G K A P K A L M S I F S N G E K E E G R

241
TTC ACA ATT CAC CTC AAT AAA GCC AGT CTG CAT TTC TCG CTA CAC ATC AGA GAC TCC CAG
F T I H L N K A S L H F S L H I R D S Q

301
CCC AGT GAC TCT GCT CTC TAC CTC TGT GCA GGA GGG CAG GGA GGC AGA GCT CTG ATA TTT
P S D S A L Y L C A G G Q G G R A L I F

361
GGA ACA GGA ACC ACG GTA TCA GTC AGC CCC AGT AAG TAC CTG ATA GCT GGT GAT TAT GAC
G T G T T V S V S P

421 427
GCC CGC C

TRAV 7-D3 is highlighted in green and TRAJ 15 in purple. The additional intronic sequence required for correct processing of the vector is also shown, untranslated, in turquoise. The CDR3 is highlighted in blue with the coding DNA sequence underlined. Letters shown in red indicate the restriction site (SacI) used to combine the V-J region with the J-intronic sequence.

Appendix 24 - Amino acid sequence of the TCR β chain (TRBV 14 TRBJ 2-7) from the murine T cell clone A10(2) cloned into the TCR cassette vector pTβcass

1
ATG GGC ACC AGG CTT CTT GGC TGG GCA GTG TTC TGT CTC CTT GAC ACA GTA CTG TCT GAA GCT
M G T R L L G W A V F C L L D T V L S E A

64
GGA GTC ACC CAG TCT CCC AGA TAT GCA GTC CTA CAG GAA GGG CAA GCT GTT TCC TTT TGG TGT
G V T Q S P R Y A V L Q E G Q A V S F W C

127
GAC CCT ATT TCT GGA CAT GAT ACC CTT TAC TGG TAT CAG CAG CCC AGA GAC CAG GGG CCC CAG
D P I S G H D T L Y W Y Q Q P R D Q G P Q

190
CTT CTA GTT TAC TTT CGG GAT GAG GCT GTT ATA GAT AAT TCA CAG TTG CCC TCG GAT CGA TTT
L L V Y F R D E A V I D N S Q L P S D R F

253
TCT GCT GTG AGG CCT AAA GGA ACT AAC TCC ACT CTC AAG ATC CAG TCT GCA AAG CAG GGC
S A V R P K G T N S T L K I Q S A K Q G

313
GAC ACA GCC ACC TAT CTC TGT GCC AGC AGC CCC CTC GAC TGG GGG GAT GAA CAG TAC TTC GGT
D T A T Y L C A S S P L D W G D E Q Y F G

376 GGC
CCC GGG ACC AGG CTC ACG GTT TTA GGT AAG ATT CAC ATC TCT CGC TTC CAC CCA AAT TCC TGG
P G T R L T V L

439 456
GTC CCT GGA GTA GTT TGG

TRBV 14 is highlighted in green and TRBJ 2-7 in purple. The additional intronic sequence required for correct processing of the vector is also shown, untranslated, in turquoise. The CDR3 is highlighted in blue with the coding DNA sequence underlined. Letters shown in red and underlined indicate an intentional base pair change to allow combination of the V-J region with the J-intronic sequence using XmaI (site in italics). The base pair change did not alter the amino acid sequence of the translated protein.

Appendix 25 - Amino acid sequence of the TCR α chain (TRAV 7-D4 TRAJ 26-like) from the murine T cell clone D3(3) cloned into the TCR cassette vector pTαcass

1
ATG AAA TCC TTG AGT GTT TCA CTA GTG GTC CTG TGG CTC CAG GTA AAC TGC GTG AGG AGC CAG
M K S L S V S L V V L W L Q V N C V R S Q

64
CAG AAG GTG CAG CAG AGC CCA GAA TCC CTC AGT GTC CCA GAG GGA GGC ATG GCC TCT TTC AAC
Q K V Q Q S P E S L S V P E G G M A S F N

127
TGC ACT TCA AGT GAT CGT AAT TTT CAG TAC TTC TGG TGG TAC AGA CAG CAT TCT GGA GAA GGC
C T S S D R N F Q Y F W W Y R Q H S G E G

190
CCC AAG GCA CTG ATG TCA ATC TTC TCT GAT GGT GAC AAG AAA GAA GGC AGA TTT ACA GCT CAC
P K A L M S I F S D G D K K E G R F T A H

253
CTC AAT AAG GCC AGC CTG CAT GTT TCC CTG CAC ATC AGA GAC TCC CAG CCC AGT GAC TCC GCT
L N K A S L H V S L H I R D S Q P S D S A

316 GGC
CTC TAC TTC TGT GCA GCT AGT GCC GTG GAT AAC TAT GCC CAG GGA TTA ACC TTC GGT CTT *GGT*
L Y F C A A S A V D N Y A Q G L T F G L G

379
ACC AGA GTA TCT GTG TTT CCC TGT AAG TAT ACC TGA GTG AAA GGC TGG TGT GGG GAT GAG CTG
T R V S V F P

442 450
GGG TGA GGG

TRAV 7-D4 is highlighted in green and TRAJ 26-like (95% identity) in purple. The additional intronic sequence required for correct processing of the vector is also shown, untranslated, in turquoise. The CDR3 is highlighted in blue with the coding DNA sequence underlined. Letters shown in red and underlined indicate an intentional base pair change to allow combination of the V-J region with the J-intronic sequence using KpnI (site in italics). The base pair change did not alter the amino acid sequence of the translated protein.

Appendix 26 - Amino acid sequence of the TCR β chain (TRBV 2 TRBJ 2-5) from the murine T cell clone D3(3) cloned into the TCR cassette vector pTβcass

1
ATG GGC TCC ATT TTC CTC AGT TGC CTG GCC GTT TGT CTC CTG GTG GCA GGT CCA GTC GAC CCG
M G S I F L S C L A V C L L V A G P V D P

64
AAA ATT ATC CAG AAA CCA AAA TAT CTG GTG GCA GTC ACA GGG AGC GAA AAA ATC CTG ATA
K I I Q K P K Y L V A V T G S E K I L I

124
TGC GAA CAG TAT CTA GGC CAC AAT GCT ATG TAT TGG TAT AGA CAA AGT GCT AAG AAG CCT
C E Q Y L G H N A M Y W Y R Q S A K K P

184
CTA GAG TTC ATG TTT TCC TAC AGC TAT CAA AAA CTT ATG GAC AAT CAG ACT GCC TCA AGT CGC
L E F M F S Y S Y Q K L M D N Q T A S S R

247
TTC CAA CCT CAA AGT TCA AAG AAA AAC CAT TTA GAC CTT CAG ATC ACA GCT CTA AAG CCT GAT
F Q P Q S S K K N H L D L Q I T A L K P D

310
GAC TCG GCC ACA TAC TTC TGT GCC AGC AGC CAA GCC GGG ACT GGA GAA GAC ACC CAG TAC
D S A T Y F C A S S Q A G T G E D T Q Y

370
TTT GGG CCA GGC ACT CGG CTC CTC GTG TTA GGT GAG CTG GGG CCC CAC GTG CGC GTT CTC AGC
F G P G T R L L V L

433 485
GGG ATT GGG CTG CAG TGG GCG CGG GTC CCT TGG CCG GGT TTC TCT GGG AGT CA

TRBV 2 is highlighted in green and TRBJ 2-5 in purple. The additional intronic sequence required for correct processing of the vector is also shown, untranslated, in turquoise. The CDR3 is highlighted in blue with the coding DNA sequence underlined. Letters shown in red indicate the restriction site (BstXI) used to combine the V-J region with the J-intronic sequence.

Appendix 27 - Amino acid sequence of the dominant TCR α chain (TRAV 8-4 TRAJ 32) from the human T cell line CIR010 cloned into the TCR cassette vector pTαcass

1
ATG CTC CTG CTG CTC GTC CCA GTG CTC GAG GTG ATT TTT ACC CTG GGA GGA ACC AGA GCC
M L L L L V P V L E V I F T L G G T R A

61
CAG TCG GTG ACC CAG CTT GGC AGC CAC GTC TCT GTC TCT GAG GGA GCC CTG GTT CTG CTG
Q S V T Q L G S H V S V S E G A L V L L

121
AGG TGC AAC TAC TCA TCG TCT GTT CCA CCA TAT CTC TTC TGG TAT GTG CAA TAC CCC AAC
R C N Y S S S V P P Y L F W Y V Q Y P N

181
CAA GGA CTC CAG CTT CTC CTG AAG TAC ACA ACA GGG GCC ACC CTG GTT AAA GGC ATC AAC
Q G L Q L L L K Y T T G A T L V K G I N

241
GGT TTT GAG GCT GAA TTT AAG AAG AGT GAA ACC TCC TTC CAC CTG ACG AAA CCC TCA GCC
G F E A E F K K S E T S F H L T K P S A

301 CTC
CAT ATG AGC GAC GCG GCT GAG TAC TTC TGT GCC GTG TGG AGT GGT GCT ACA AAC *AAG CTT*
H M S D A A E Y F C A V W S G A T N K L

361
ATC TTT GGA ACT GGC ACT CTG CTT GCT GTC CAG CCA AGT ACG TAA GTA GTG GCA TGT GTC
I F G T G T L L A V Q P

421 446
AGG TGG ATT CTG TGT CCA TGG CAA GT

TRAV 8-4 is highlighted in green and TRAJ 32 in purple. The additional intronic sequence required for correct processing of the vector is also shown, untranslated, in turquoise. The CDR3 is highlighted in blue with the coding DNA sequence underlined. Letters shown in red and underlined indicate an intentional base pair change to allow combination of the V-J region with the J-intronic sequence using HindIII (site in italics). The base pair change did not alter the amino acid sequence of the translated protein.

Appendix 28 - Amino acid sequence of the dominant TCR β chain (TRBV 6-1 TRBJ 1-1) from the human T cell line CIR010 cloned into the TCR cassette vector pTβcass

1
ATG AGC ATC GGG CTC CTG TGC TGT GTG GCC TTT TCT CTC CTG TGG GCA AGT CCA GTG AAT
M S I G L L C C V A F S L L W A S P V N

61
GCT GGT GTC ACT CAG ACC CCA AAA TTC CAG GTC CTG AAG ACA GGA CAG AGC ATG ACA CTG
A G V T Q T P K F Q V L K T G Q S M T L

121
CAG TGT GCC CAG GAT ATG AAC CAT AAC TCC ATG TAC TGG TAT CGA CAA GAC CCA GGC ATG
Q C A Q D M N H N S M Y W Y R Q D P G M

181
GGA CTG AGG CTG ATT TAT TAC TCA GCT TCT GAG GGT ACC ACT GAC AAA GGA GAA GTC CCC
G L R L I Y Y S A S E G T T D K G E V P

241
AAT GGC TAC AAT GTC TCC AGA TTA AAC AAA CGG GAG TTC TCG CTC AGG CTG GAG TCG GCT
N G Y N V S R L N K R E F S L R L E S A

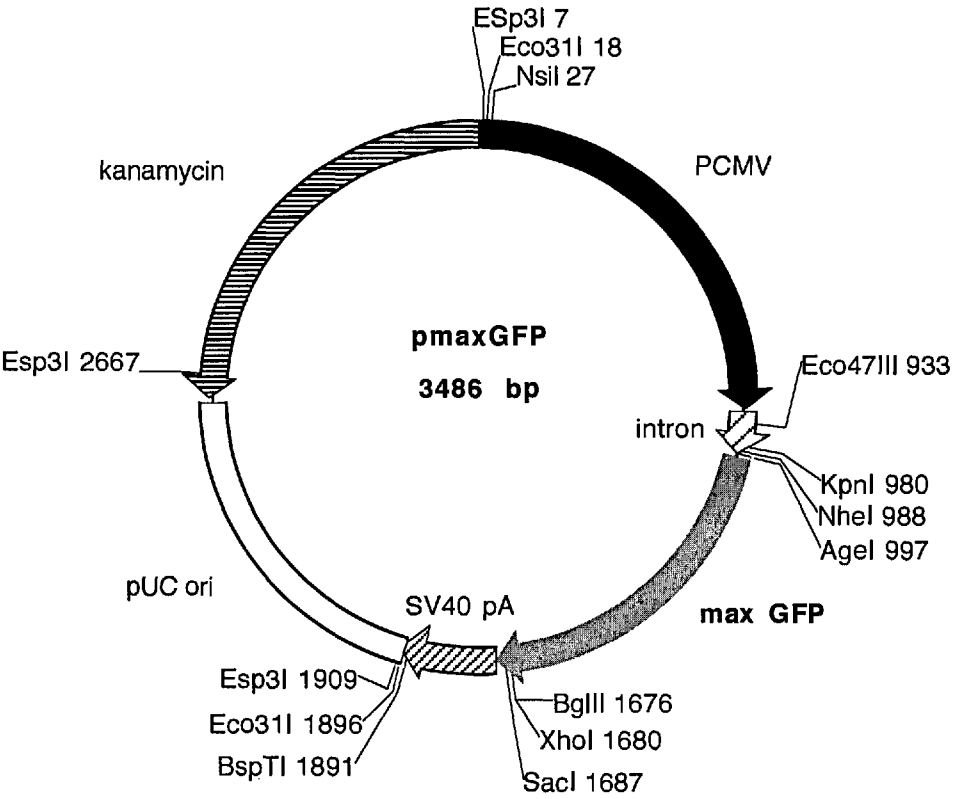
301
GCT CCC TCC CAG ACA TCT GTG TAC TTC TGT GCC AGC AGT GAG GCT GGG TGG GGG GCG TCG
A P S Q T S V Y F C A S S E A G W G A S

361
GGC ACT GAA GCT TTC TTT GGA CAA GGC ACC AGA CTC ACA GTT GTA GGT AAG ACA TTT TTC
G T E A F F G Q G T R L T V V

421 450
AGG TTC TTT TGC AGA TCC GTC ACA GGG AAA

TRBV 6-1 is highlighted in green and TRBJ 1-1 in purple. The additional intronic sequence required for correct processing of the vector is also shown, untranslated, in turquoise. The CDR3 is highlighted in blue with the coding DNA sequence underlined. Letters shown in red indicate the restriction site (HindIII) used to combine the V-J region with the J-intronic sequence.

Appendix 29 - pmaxGFP



The diagram shows the components of the Amaxa system positive control vector pmaxGFP and the target gene GFP, including all promoter regions required for expression of the target gene. The GFP gene in this vector has a fluorescence intensity similar to or slightly higher than that of eGFP.

Appendix 30 - DNA coding sequences for the P4 TCR α and β chains

P4 TCR α chain – TRAV 36-DV7 TRAJ 32 TRAC

ATG ATG AAG TGT CCA CAG GCT TTA CTA GCT ATC TTT TGG CTT CTA CTG AGC
M M K C P Q A L L A I F W L L L S

TGG GTG AGC AGT GAA GAC AAG GTG GTA CAA AGC CCT CTA TGT CTG GTT
W V S S E D K V V Q S P L S L V

GTC CAC GAG GGA GAC ACC GTA ACT CTC AAT TGC AGT TAT GAA GTG ACT
V H E G D T V T L N C S Y E V T

AAC TTT CGA AGC CTA CTA TGG TAC ATG CAG GAA AAG AAA GCT CCC ACA
N F R S L L W Y M Q E K K A P T

TTT CTA TTT ATG CTA ACT TCA AGT GGA ATT GAA AAG AAG TCA GGA AGA
F L F M L T S S G I E K K S G R

CTA AGT AGC ATA TTA GAT AAG AAA GAA CTT TTC AGC ATC CTG AAC ATC
L S S I L D K K E L S S I L N I

ACA GCC ACC CAG ACC GGA GAC TCG GCC ATC TAC CTC TGT GCG GTA TGG
T A T Q T G D S A I Y L C A V W

GCG GGT GCT ACA AAC AAG CTC ATC TTT GGA ACT GGC ACT CTG CTT GCT GTC
A G A T N K L I F G T G T L L A V

CAG CCA AAT ATC CAG AAC CCT GAC CCT GCC GTG TAC CAG CTG AGA GAC
Q P N I Q N P D P A V Y Q L R D

TCT AAA TCC AGT GAC AAG TCT GTC TGC CTA TTC ACC GAT TTT GAT TCT CAA
S K S S D K S V C L F T D F D S Q

ACA AAT GTG TCA CAA AGT AAG GAT TCT GAT GTG TAT ATC ACA GAC AAA
T N V S Q S K D S D V Y I T D K

ACT GTG CTA GAC ATG AGG TCT ATG GAC TTC AAG AGC AAC AGT GCT GTG
T V L D M R S M D F K S N S A V

GCC TGG AGC AAC AAA TCT GAC TTT GCA TGT GCA AAC GCC TTC AAC AAC
A W S N K S D F A C A N A F N N

AGC ATT ATT CCA GAA GAC ACC TTC TTC CCC AGC CCA GAA AGT TCC TGT GAT
S I I P E D T F F P S P E S S C D

GTC AAG CTG GTC GAG AAA AGC TTT GAA ACA GAT ACG AAC CTA AAC TTT
V K L V E K S F E T D T N L N F

CAA AAC CTG TCA GTG ATT GGG TTC CGA ATC CTC CTC CTG AAA GTG GCC
Q N L S V I G F R I L L L K V A

GGG TTT AAT CTG CTC ATG ACG CTG CGG CTG TGG TCC AGC TGA
G F N L L M T L R L W S S •

Key: TRAV 36 DV7
TRAJ 32
TRAC
CDR3

P4 TCR β chain – TRBV 9 TRBJ 2-7 TRBC 2

ATG GGC TTC AGG CTC CTC TGC TGT GTG GCC TTT TGT CTC CTG GGA GCA GGC
M G F R L L C C V A F C L L G A G

CCA GTG GAT TCT GGA GTC ACA CAA ACC CCA AAG CAC CTG ATC ACA GCA
P V D S G V T Q T P K H L I T A

ACT GGA CAG CGA GTG ACG CTG AGA TGC TCC CCT AGG TCT GGA GAC CTC
T G Q R V T L R C S P R S G D L

TCT GTG TAC TGG TAC CAA CAG AGC CTG GAC CAG GGC CTC CAG TTC CTC ATT
S V Y W Y Q Q S L D Q G L Q F L I

CAG TAT TAT AAT GGA GAA GAG AGA GCA AAA GGA AAC ATT CTT GAA CGA
Q Y Y N G E E R A K G N I L E R

TTC TCC GCA CAA CAG TTC CCT GAC TTG CAC TCT GAA CTA AAC CTG AGC TCT
F S A Q Q F P D L H S E L N L S S

CTG GAG CTG GGG GAC TCA GCT TTG TAT TTC TGC CAG GTG CCG GAC AGG
L E L G D S A L Y F C Q V P D R

GGG GTA TAC GAG CAG TAC TTC GGG CCG GGC ACC AGG CTC ACG GTC ACA
G V Y E Q Y F G P G T R L T V T

GAG GAC CTG AAA AAC GTG TTC CCA CCC GAG GTC GCT GTG TTT GAG CCA
E D L K N V F P P E V A V F E P

TCA GAA GCA GAG ATC TCC CAC ACC CAA AAG GCC ACA CTG GTG TGC CTG
S E A E I S H T Q K A T L V C L

GCC ACA GGC TTC TAC CCC GAC CAC GTG GAG CTG AGC TGG TGG GTG AAT
A T G F Y P D H V E L S W W V N

GGG AAG GAG GTG CAC AGT GGG GTC AGC ACA GAC CCG CAG CCC CTC AAG
G K E V H S G V S T D P Q P L K

GAG CAG CCC GCC CTC AAT GAC TCC AGA TAC TGC CTG AGC AGC CGC CTG
E Q P A L N D S R Y C L S S R L

AGG GTC TCG GCC ACC TTC TGG CAG AAC CCC CGC AAC CAC TTC CGC TGT
R V S A T F W Q N P R N H F R C

CAA GTC CAG TTC TAC GGG CTC TCG GAG AAT GAC GAG TGG ACC CAG GAT
Q V Q F Y G L S E N D E W T Q D

AGG GCC AAA CCT GTC ACC CAG ATC GTC AGC GCC GAG GCC TGG GGT AGA
R A K P V T Q I V S A E A W G R

GCA GAC TGT GGC TTC ACC TCC GAG TCT TAC CAG CAA GGG GTC CTG TCT GCC
A D C G F T S E S Y Q Q G V L S A

ACC ATC CTC TAT GAG ATC TTG CTA GGG AAG GCC ACC TTG TAT GCC GTG CTG
T I L Y E I L L G K A T L Y A V L

GTC AGT GCC CTC GTG CTG ATG GCC ATG GTC AAG AGA AAG GAT TTC TGA
V S A L V L M A M V K R K D F •

Key:	TRBV 9	TRAJ 2-7	CDR3
	Non-germline sequence		TRBC 2